

Úa Compendium

G. Hilmar Gudmundsson

University of Northumbria
Newcastle upon Tyne
UK

January 2, 2026

Contents

Introduction	i
Notation and definitions	iii
I General theoretical background for the use of the \tilde{U}ice-flow model	1
1 Key governing equations	3
1.1 Equations of ice flow	3
1.2 Shallow Ice-Stream Approximation (STREAM/SSA)	4
1.3 Shallow Ice Shelf (SHELF/SSA)	6
1.4 Shallow Ice-Sheet (SHEET/SIA)	6
1.5 Recap of typically SIA and SSA scalings	8
1.5.1 BCs for small slopes	10
1.6 Three dimensional formulation, assuming cryostatic vertical stresses	11
1.7 Vertical integration, assuming cryostatic vertical stress state	12
1.7.1 Simplifications of the vertically-integrated system	13
1.7.2 Budd simplification	14
1.7.3 L1L2	14
1.7.4 The Goldberg Variation	15
1.8 Equation of mass conservation	18
1.9 Vertically averaged density and firn density corrections	20
1.10 Vertical velocities	21
1.11 Sliding laws	21
1.11.1 Weertman sliding law (W)	22
1.11.2 Budd sliding law (Generalised Weertman sliding law, W-N)	23
1.11.3 Coulomb (C)	24
1.11.4 Combining Weertman (W) with Coulomb (C)	24
1.12 Ocean and atmospheric drag terms	28
1.12.1 Note on icebergs and detached ice shelves	28
1.13 Effective basal water pressure	30
1.13.1 Hydrology	30
1.14 Flow law	31
1.15 Floating relationships	31
1.15.1 Expressing geometrical variables in terms of ice thickness	32
1.15.2 Calculating b and s given h , S and B	32
1.15.3 Calculating b and h given s , S and B	33
1.16 Stress boundary conditions at an ice front	34
1.16.1 Floating	36
1.16.2 Grounded	36
1.17 Boundary condition at a glacier terminus as a natural boundary condition	36
1.18 STREAM in 1HD	37

2 Finite-element implementation	39
2.1 Function expansions in the FE basis	39
2.2 FE formulation of the diagnostic equations	42
2.3 FE formulation of the transient problem	43
2.3.1 Time integration algorithms	43
2.4 Consistent Streamline-Upwind Petrov-Galerkin (SUPG)	49
2.5 SIA-motivated diffusion	54
2.6 Connection between third order Taylor-Galerkin (TG3) and streamline-upwind Petrov-Galerkin (SUPG)	55
2.7 Implementing fully-implicit forward time integration with respect to velocity and thickness	56
2.7.1 Mass conservation test	56
2.7.2 First-order fully implicit	56
2.7.3 Fully implicit SSTREAM time integration with the θ method	57
2.7.4 Semi-implicit: uv explicit, and h implicit	61
2.8 Transient implicit SSHEET/SIA with the θ method	62
2.8.1 SSHEET with no-flux natural boundary condition	64
2.8.2 Transient SSHEET/SIA with a free-flux natural boundary condition	65
2.9 Method of characteristics	66
2.10 Taylor-Galerkin	67
2.11 Third order implicit Taylor Galerkin (1HD)	68
2.12 Time discretisation of the tracer conservation equation	69
3 Constraints	71
3.1 Nodal constraints assembly	71
3.2 Linear system with multi-linear constraints	72
3.2.1 Pre-eliminating point constraints	73
3.3 Nodal reactions	74
3.4 Non-linear system with non-linear constraints	76
3.5 FE formulation of the Newton-Raphson method with multi-linear constraints	76
3.6 Automated thickness-positivity constraints (active set method)	78
3.6.1 Thickness barrier	79
4 The non-linear FE system its solution	81
4.1 Variational formulation	81
4.2 Non-linear self-adjoint problem	82
4.3 Non-linear non-self-adjoint problem	83
4.4 Constrained self-adjoint problem	84
4.5 Convergence criteria	86
4.5.1 Force residuals	87
4.5.2 Work residuals	87
4.5.3 Increments	88
4.6 Summary of convergence criteria	88
4.7 Minimising the norm of the residuals	89
4.8 Time stepping	94
5 Continuation Methods	97
5.1 Simple analytical solutions involving mass-balance altitude feedback	98
5.2 Weertman's solution for mass-balance elevation feedback on ice caps	98
5.2.1 Stability of the Weertman solution	101
5.2.2 Weertman analysis for shear-deforming ice sheet with no sliding at the base	101
5.3 Vialov solution	103
5.3.1 Note on the stability of the Vialov solution	104
5.4 Simple example of unstable mass-balance feedback	105
5.5 Numerical approach	106
5.5.1 Euler-Newton Continuation	108
5.5.2 Pseudo-Arclength Continuation	108

6 Inverse modelling	111
6.1 Preliminaries	111
6.1.1 Calculating the gradient and the Hessian of the cost function J	113
6.1.2 Calculating the Hessian of the cost function J	116
6.1.3 Brute force finite differences	118
6.2 General inverse methodology	119
6.2.1 Example of Bayesian estimation	121
6.3 Sparse precision matrices	122
6.4 Inversion in $\tilde{U}a$	124
6.5 Objective functions	124
6.6 Misfit functions in $\tilde{U}a$	129
6.7 Regularisation in $\tilde{U}a$	130
6.7.1 Bayesian approach	130
6.7.2 Tikhonov regularisation	133
6.8 Relationships between rate factors corresponding to different values of the stress exponent	133
6.9 Calculating gradients	134
6.9.1 Fix-point method	134
6.9.2 The adjoint method	136
6.9.3 Summarising the first-order adjoint approach	138
6.9.4 Time dependent adjoint	140
6.10 Directional derivative and gradients	141
6.11 Evaluating objective functions and their directional derivatives	142
6.12 Simple example of a gradient calculation of an objective function	144
6.12.1 Direct approach	145
6.12.2 Calculating the elements of the gradient in the FE basis	146
6.13 Velocity inversion using mass equation	147
6.14 Thickness (h) inversion using mass equation	147
6.15 Thickness (h) inversion using momentum equation	152
6.16 B inversion using momentum and mass equation	153
6.17 Inverting for b using a fixed floating mask	154
6.18 Inverting for bedrock elevation B with varying flotation mask	156
6.19 Gradients of objective functions with respect to control variables	157
6.19.1 Gradient calculation in 1HD with respect to C	157
6.19.2 Gradient calculation in 1HD with respect to A	157
6.19.3 Gradient calculation in 1HD with respect to b	158
6.20 Inverting for $\log p$	159
6.21 The form of the adjoint equations for Bayesian approach using Gaussian statistics	160
6.22 Adjoint equations (Bayesian case with constraints on vertical velocity)	160
6.23 Prognostic equations are formally self-adjoint	161
6.24 Covariance kernels	163
7 Calving	165
7.1 Level-set method	165
7.1.1 Numerical implementation	169
7.1.2 Ice calving	174
7.2 Verification test case	174
7.2.1 Thule	178
7.2.2 Thwaites and Pine Island Glacier Calving Experiments	183
7.3 Calving implemented as surface mass-balance term	183
8 Damage	185
8.1 Hayhurst criterion and variants thereof	185
8.2 Some other damage evolution laws	186
8.3 Sainan Sun Damage Model	187
9 Virtual crack closure technique	189
9.1 J and C^* integrals for elastic and viscous fracture	190

10 Further technical FE implementation details	193
10.1 Only the (fully) floating condition as a natural boundary condition	193
10.1.1 Remark	193
10.1.2 FE formulation	194
10.1.3 2HD FE diagnostic equation written in terms of h (suitable for fully coupled approach)	195
10.2 Element integrals	195
10.3 Edge integrals	197
10.3.1 Edge 12	197
10.3.2 Edge 23	198
10.3.3 Edge 32	198
10.4 Various directional derivatives	199
10.4.1 Directional derivative of draft with respect to ice thickness	199
10.4.2 Linearisation of the 2HD forward problem needed for the adjoint method	200
10.5 FE formulation and linearisation for the 1HD Problem	201
10.5.1 Field equations and boundary conditions (1HD)	201
10.6 Linearisation of field equations (1HD)	201
10.6.1 Newton Raphson	202
10.6.2 Connection to Picard iteration	204
10.7 Linearisation in 2HD	205
10.7.1 Drag-term linearisation (2HD)	205
10.7.2 Flow law linearisation (2HD)	207
10.7.3 Field-equation linearisation	209
10.8 Weak form	211
10.9 Thoughts about ice shelf von Neumann BC	213
10.9.1 1d case	213
10.10 Tracer equation with cross-wind diffusion	213
II Some aspects of glacier mechanics, possibly of interest to $\tilde{U}a$ users, but not specifically related to $\tilde{U}a$	215
11 An ice shelf in one horizontal dimension (1HD).	219
11.1 Boundary condition at the calving front	220
11.2 The SSA as an expression of horizontal force balance.	221
11.3 Stresses and strains within a one-dimensional plane-strain ice shelf	222
11.4 Shear stress	223
11.5 Steady-state geometry of a 1HD plane-strain ice shelf	224
11.6 Side-drag dominated ice shelf	227
12 Simple 1d solutions for an ice-stream	229
12.1 Problem definition:	229
12.1.1 One dimensional uniformly inclined slab with periodic BCs	230
12.1.2 Two dimensional uniformly inclined slab with periodic BCs	230
13 Grounding-line dynamics	231
13.1 Ice-Shelf Buttressing	231
13.2 Kinematic expression for GL migration	231
13.3 Geometrical grounding-line migration	233
13.4 Flux at the grounding line	235
13.5 Balance between terms on both side of the grounding line	237
13.6 GL scalings (Schoof)	238
13.7 Grounding-line instability	239
14 Subglacial hydrology	241
14.1 Traditional groundwater theory	242
14.1.1 Simple analytical steady-state solution of the groundwater equation	243
14.1.2 Possible modifications of the groundwater equation for glacier hydrology	245
14.2 Basal water flow in a film of variable thickness	247
14.3 Simplified hydrological model for routing purposes	249

15 Time scales	253
15.1 Alpine glaciers	253
15.2 Marine ice sheets	254
16 The Shallow Ice Approximation (SIA)	255
16.1 Scaling assumptions	255
16.2 Governing equations	256
16.3 Scaling the equations	257
16.4 SIA solutions	258
17 Shallow Ice Stream Approximation (SSTREAM/SSA)	261
17.1 Field equations and boundary conditions	261
17.2 Definition of scales	262
17.3 Scaling the equations	263
17.3.1 Sliding law	264
17.4 The STREAM (zeroth-order) equations	269
17.4.1 Boundary conditions	269
17.4.2 Field equations	270
17.4.3 Vertical integration	270
17.4.4 Tensor of restive stresses	271
17.4.5 Weertman sliding law	272
17.5 The shallow ice shelf approximation (SSHELF)	272
17.5.1 Boundary conditions at the calving front	273
17.5.2 Ice Shelf Buttressing	275
17.6 Scaling the sliding law using SSA/SSTREAM scalings	277
18 Perturbation solutions of the STREAM/SSA	279
18.1 Problem definition	279
18.1.1 Bedrock perturbations	279
18.1.2 Slipperiness perturbations	288
III Appendices	289
A Calculating vertical surface velocity	291
A.1 grounded part	291
A.2 floating part	292
B Integral theorem	293
C Finite-Element equations derived from a minimisation problem	295
D Definition of gradients in terms of directional derivatives and inner products	297

List of Figures

1	Geometrical variables	iv
2	Distribution of integration points with the unit reference triangle and the degree of precision.	x
1.1	MismipPlus results for different sliding laws	26
1.2	Calculating b and h from s , S , and B by minimising J as given in Eq. (1.209) with respect to b	34
1.3	Analytical and numerical flow-line solutions for an unconfined ice shelf	38
1.4	Close up of velocity and surface profiles. The analytical solutions are derived in section 11.5, see for example Eq. (11.43). This numerical solution was obtained using linear elements and automated mesh refinement based on the gradient of the effective strain rate.	38
2.1	Nodal and integration-point evaluations	40
2.2	Amplification factors for different time discretisation methods, for the $dy/dt = -v dy/dx$ equation.	46
2.3	SUPG	51
2.4	Initial ice thickness distribution at $t = 0$. Parameters: $A = 3 \times 10^{-9} \text{ kPa}^{-3}\text{a}^{-1}$, $n = 3$, $C = 0.0125 \text{ kPa}^{-3}$, $m = 3$, $a_s = a_b = 0 \text{ m a}^{-1}$, $\rho = 900 \text{ kg m}^{-3}$	56
2.5	Changes in ice thickness distribution at $t = 10 \text{ yr}$	56
2.6	Boundary conditions for mass-conservation test.	57
2.7	Changes in ice volume over time. As there is no mass added or removed, and velocities along boundaries are set to zero, mass conservation implies that the volume must not change with time.	57
3.1	Example of an iterative solution of $\tilde{\mathbf{A}}$ using the Generalised Minimum Residual Method (gmres). The matrices A and B stem from a uvh solve of the WAIS, with 250,896 number of unknowns. Computationally the solver for non-equilibrated matrix using the ilu(0), pre-conditioner is fastest and reaches the prescribed reduction in relative residual, 10^{-15} , in about 40 sec. However, on same machine, a direct solver solves the same problem to in about 9 sec.	74
3.2	Same example as shown in Fig. 3.1, but now using the ilupt condition with drop tolerance of 10^{-4} . The two iterative solvers using this pre-conditioner now arrive at the prescribed tolerance in about 5 iterations. The non-equilibrated system solve with the ilupt pre-conditioner is fastest, and takes about 14 sec, of which 8 are required for the incomplete LU factorisation, about 1 sec for the nested dissection permutation, and about 5 sec for the gmres iteration.	75
3.3	Positive ice thickness and the active-set method	77
4.1	An example of the variation of r_{Force}^2 and r_{Work}^2 as a function of γ during a line-search. Here the backtracking algorithm selects $\gamma \approx 1/2$. For clarity, the circles show some additional function values not calculated during the line search.	86
4.2	Another example of the variation of r_{Force}^2 and r_{Work}^2 as a function of γ . Here the full Newton step ($\gamma = 1$) was accepted. Also shown are the slopes at $\gamma = 0$ calculated as $2r$ at $\gamma = 0$	86
4.3	An simple backtracking example.	87
4.4	An example of r_{Force}^2 and r_{Work}^2 as a function of Newton-Raphson iteration number.	88

4.5 Example of time stepping an number of non-linear uvh -iterations in a run. Initially the time step is quite small or at 1×10^{-5} yr, and then increases to about 0.1 yr. This example was based on a run including Pine Island and Thwaites glaciers, using automated mesh refinement and unrefinement around the grounding line.	95
5.1 The surface profile of an ice sheet as given by Eqs. (5.8) and (5.10), for $a^+ = 1 \text{ m/yr}$, $a^- = 1 \text{ m/yr}$, $c = 2 \text{ m}^{1/2} \text{ yr}^{1/2}$. Everywhere where $h > h_{\text{ELA}}$ the surface mass balance is equal to a given positive number a^+ . For $h \leq h_{\text{ELA}}$ the surface mass balance is set to $-a^- < 0$. Although the mass balance is therefore spatially constant within the accumulation and the ablation areas, the mass balance is nevertheless a function of the surface elevation.	99
5.2 (a) The change in surface profile with accumulation (a). The length and the thickness decrease with increasing accumulation rate a^+ . (b) The ice thickness h_{ELA} of a steady-state ice sheet as a function of horizontal distance R towards the equilibrium line (the dividing line between accumulation and ablation.) Also plotted is ELA (as determined by the climate). Only for $\text{ELA} = h_{\text{ELA}}$ is a steady-state ice sheet under given climatic conditions possible.	100
5.3 Ice thickness at summit ($H = h(x = 0)$) from Eq. (5.12), and the length (L) from Eq. (5.7) as functions of surface accumulation, a^+ , above the equilibrium line altitude (ELA). Here $\text{ELA} = 2000 \text{ m}$, $a^- = 1 \text{ m/yr}$, and $c = 2 \text{ m}^{1/2} \text{ yr}^{1/2}$. As $a^+ \rightarrow 0$ the ice sheet becomes infinitely thick and infinitely wide.	101
5.4 The Vialov solution, as given by Eq. (5.24), for $l = 1000 \text{ km}$, $n = 3$, $B = 0.01 \text{ m}^{-n} \text{ a}^{-1}$, and $a = 0.5 \text{ m a}^{-1}$	104
5.5 The Vialov solution for $l = 1000 \text{ km}$, $n = 3$, $B = 0.01 \text{ m}^{-3} \text{ a}^{-1}$, $a_G = -0.1 \text{ m a}^{-1}$, and $da/dh = da/dT \times dT/dh = 0.04 \times 0.005 = 2 \times 10^{-4} \text{ yr}^{-1}$	105
6.1 Sensitivities of velocities to changes in A at one node. The full sensitivity matrix ξ was calculated solving Eq. (6.8), providing the sensitivity of all nodal velocities to any nodal A values. The FE mesh had 31,717 nodes and calculating the sensitivities took about 3 min. The examples is for Pine Island Glacier, West Antarctica.	114
6.2 Sensitivities of velocities to changes in C at one node. See Fig. (6.1) for details.	115
6.3 Comparison between an inversion using the Hessian and the LBFGS methods. The function J is the cost function. This example was done for a relatively small problem where calculating the full Hessian using brute-force was feasible, using finite-differences of the gradient as shown in Eq. (6.25).	119
6.4 Example of an estimated A distribution over section of West Antarctica for $n = 3$. Here $\gamma_a = 1$ and $\gamma_s = 100,000$	125
6.5 Example of an estimated C distribution over a section of West Antarctica using the Cornford sliding law with the stress exponent $m = 3$ and the coefficient of kinetic friction $\mu_k = 1/2$. Here $\gamma_a = 1$ and $\gamma_s = 100,000$	126
6.6 Example of an estimated A distribution for Antarctica for $n = 3$. Here $\gamma_a = 1$ and $\gamma_s = 100,000$	127
6.7 Example of an estimated basal slipperiness (C) distribution for Antarctica for Weertman sliding law where $m = 3$. Here $\gamma_a = 1$ and $\gamma_s = 10,000$	127
6.8 Modelled velocities for the A and C distributions in Figs. 6.6 and 6.7.	128
6.9 Modelled basal drag for Cornford sliding law given by Eq. (1.164) for $m = 3$ and $\mu = 1/2$, and perfect hydrological connection, Eq. (1.187), using the A and C distributions shown in Figs. 6.6 and 6.7.	128
6.10 The function $rK_1(r)$ appearing in Eq. (6.39)	130
6.11 Three examples of Matérn realisations for $\rho = 3 \text{ km}$, $\nu = 1$, $d=2$ and $\sigma = 1$	131
6.12 Gradient and Hessian based inversions	136
6.13 Gradient calculation, dJ/dB , done with adjoint and finite differences. This test was done for the Hoffsjökull ice cap in Iceland.	139
6.14 Gradient calculation, dB/dC , done with adjoint and finite differences. This test was done for the Hoffsjökull ice cap in Iceland.	139
6.15 Comparison between adjoint and finite differences gradient calculations. This test was done for the Hoffsjökull ice cap in Iceland.	140
7.1 The $k(x)$ function suggested by Li et al. (2010), and given by Eq. 7.16. This term introduces forward-and-backward diffusion to Eq. (7.15).	169

7.2	The perturbation term \mathcal{P} given by Eq. (7.17) and the corresponding $k(x)$ function given by Eq. (7.18) and the derivative $k'(x)$ used in the Newton-Raphson integration, all shown for $p = 2$ and $q = 2$	169
7.3	Same as Fig. 7.2 but for the Eikonal functional, where $p = 2$ and $q = 1$. In this case the function $k(x)$ is not bounded as $x \rightarrow 0$	170
7.4	Geometric reinitialisation using only crossing points with element edges.	170
7.5	Geometrical re-initialisation using additional points along the level set $\varphi = 0$. The leftmost figure shows the level set function φ after re-initialisation, the middle one the change, $\Delta\varphi$, during the re-initialisation, and the rightmost figure is a zoom-in of the middle figure.	170
7.6	Example of level-set re-initialisation by solving only the non-linear diffusion term. This is the initial level set φ_0	172
7.7	And this is φ_1 after solving for the non-linear diffusion term alone, i.e. $\nabla \cdot (\kappa \nabla \varphi_1) = 0$ using φ_0 as an initial guess.	172
7.8	Same as in Fig. 7.6, but showing the norm of the gradient, $\ \nabla \varphi_0\ $	173
7.9	Same as in Fig. 7.7, but showing the norm of the gradient, $\ \nabla \varphi_1\ $	173
7.10	Removing ice	175
7.11	Removing ice	175
7.12	Geometry and velocities of an one-dimensional unconfined ice shelf	176
7.13	Phase portrait for calving law (6.15) with parameter values same as in Fig. 7.12. The steady-state at $x_c = x_1 = 100$ km is stable, and the one at $x_c = x_2 = 331$ km unstable.	176
7.14	Calculated (coloured thin lines) and analytical (thick black line) calving front positions (left y axis) as a function of time, with the difference between the two shown as dashed lines (right y axis). The difference is too small for the analytical solution (black line) to be fully visible under those representing the numerical solution. The calculations were done for linear (T3), quadratic (T6) and cubic (T10) triangular elements. The element partition was in all three cases the same with the overall element diameters set at 10 km, but with finer division for the first 10 km downstream of the grounding line. The calculations were done for an unconfined ice shelf with the calving rate, c , being a function of ice thickness at the calving front as shown in Fig. 7.12. Initially the calving front is at $x = 200$ km and with time the calving front migrates towards the stable steady state solution at $x = 100$ km (see also Fig. 7.13).	177
7.15	Analytical and numerically modelled calving front positions for an unconfined ice shelf (see) with the calving rate, c , being a function of ice thickness at the calving front as shown in Fig. 7.12. The calving front are initially set at $x_c(t = 0) = 50$ km, $x_c(t = 0) = 100$ km, and $x_c(t = 0) = 50$ km and the numerical solutions are shown as blue, green and magenta lines, respectively. The corresponding analytical solutions are in black. The difference between the analytical and numerical solutions, Δx_c , are shown as dashed lines with the right y -axis as scale. In this particular example, μ was spatially constant and set to $\mu = 1 \times 10^7 \text{ km}^2 \text{ yr}^{-2}$. The resolution of the finite-element mesh was 2 km and the error in the converged solutions about half of that, or 1 km.	178
7.16	Surface and geometry of Thule. This surface geometry is the steady-state solution when starting with zero ice thickness everywhere.	181
7.17	Surface and geometry of Thule. This surface geometry is the steady-state solution when starting with a large initial ice thickness where the initial surface geometry is $s = s_0 \sqrt{(1 - r/R)}$ where $R = 750$ km and $s_0 = 4000$ m, and r is the radial distance from the centre.	181
7.18	Bedrock geometry of Thule	182
7.19	Velocities for steady state Thule Min	182
7.20	Calculated changes in volume above flotation (VAF) for different values of min ice, h_{\min} , thickness downstream of the calving front, as well as automated element deactivation. These experiments were done for a sector WAIS including Pine Island, Thwaites and Pope, Smith and Kohler glaciers. Uniform mesh size of 4.6 km was used. The solid lines showing total VAF loss use the left-hand y axis, and the dashed lines showing difference in calculated VAF with respect to using $h_{\min} = 1$ m use the right-hand y axis.	183

11.1 Left: Stresses within a one-dimensional ice shelf. Horizontal Cauchy stresses are positive at the surface and negative below $z = d/2$ where d is the ice shelf draft. Horizontal and vertical deviatoric stresses are independent of depth, and horizontal deviatoric stresses positive while vertical deviatoric stresses are negative. Parameters: $\rho = 910 \text{ kg m}^{-3}$, $\rho_o = 1030 \text{ kg m}^{-3}$, $h = 100 \text{ m}$	224
11.2 Analytical ice shelf profile. The left hand figure is for an accumulation of $a = 0.3 \text{ m a}^{-1}$, while the figure on the right was made for $a = -1 \text{ m a}^{-1}$. All other parameters are the same in both cases. Parameters: $A = 1.14 \times 10^{-8} \text{ kPa}^{-3} \text{ a}^{-1}$, $n = 3$, $h_{gl} = 2000 \text{ m}$, $u_{gl} = 300 \text{ m a}^{-1}$, $\rho = 910 \text{ kg m}^{-3}$, $\rho_o = 1030 \text{ kg m}^{-3}$. The value for A corresponds to an ice temperature of about -10 degrees Celsius.	225
11.3 Steady-state ice shelf thickness as a function of englacial temperature and surface accumulation. Parameters: $n = 3$, $\rho = 910 \text{ kg m}^{-3}$, $\rho_o = 1030 \text{ kg m}^{-3}$	226
13.1 Geometrical variables: Glacier surface (s), glacier bed (b), ocean surface (S), ocean floor (B), glacier thickness ($h = s - b$)), ocean depth ($H = S - B$), glacier draft ($d = S - b$), glacier freeboard ($f = s - S$).	232
13.2 Example of grounding line migration in response to tidal forcing using the hydrostatic assumption. The curves were calculated using the flow model \dot{U}_a which is a vertically integrated flow model that calculates grounding line positions using the hydrostatic assumption. The blue curve was calculated for a constant surface slope of $ds/dx = -0.001$ and red curve for a constant thickness gradient of $dh/dx = -0.001$. In both cases the bedrock gradient as $dB/dx = -0.01$. The tidal amplitude was 2 m and the tidal period 1 day. To suppress the effects of ice flow, the flow parameters were set to values that made the ice effectively rigid and basal sliding was enforced to be close to zero. The dashed lines show the upper and lower extent of horizontal grounding-line migration as calculated by Eq. (13.5).	234
13.3 Ice flux at a grounding line (red) from Eq. (13.18), and integrated surface mass balance upstream from the grounding line (cyan), for a given bedrock profile (black). Here $A = 1.146 \times 10^{-8} \text{ kPa}^{-3} \text{ a}^{-1}$, $n = 3$, $m = 3$, and $C = 0.8 \times 10^{-3} \text{ kPa}^{-3} \text{ m a}^{-1}$	239
14.1 The solution to Eq. (14.19) for $h_w(x)$ (black line) and $q_w(x)$ (red line) for an unconfined aquifer. Here $h_w(x = l) = 1 \text{ m}$, $a_w = 1 \text{ m yr}^{-1}$, $l = 100 \text{ km}$ and $k = 1 \times 10^4 \text{ m yr kg}^{-1}$	245
14.2 Total water flux across a closed circular boundary. In steady state the flux across the boundary must be equal to the total internal water production within the area enclosed by the boundary. The horizontal dashed line is the analytically calculated correct steady state limit $Q_{\text{int}} = \pi r^2 a_w = 38.4845 \text{ km}^3/\text{yr}$	248
14.3 Calculated steady state water flux vectors. The thick black line is the circle used in Fig. 14.2 to calculate the water flux shown. The red line is the grounding line. Across the grounded area a uniform water flux of $a_w = 10 \text{ m/yr}$ is prescribed. The radius of the flux gate is $r = 35 \text{ km}$ and the total internal water production within that circle is therefore $Q_{\text{int}} = \pi r^2 a_w = 38.4845 \text{ km}^3/\text{yr}$	248
14.4 Geometry.	251
14.5 Velocities.	251
14.6 Flux. The analytical flux value was $Q = 25.502 \text{ km}^3/\text{yr}$ and numerical steady-state value was $Q = 25.560 \text{ km}^3/\text{yr}$	252
17.1 Problem geometry.	262
18.1 The phase speed ($\ \mathbf{v}_p\ $) as a function of wavelength for $\theta=0$. The dashed-dotted curve is based on the shallow-ice-sheet (SSHEET) approximation, the dashed one is based on the shallow-ice-stream (SSTREAM) approximation, and the solid one is a full-system (FS) solution. The surface slope is $\alpha=0.005$ and slip ratio $\bar{C}=30$ and $n = m = 1$. The unit on the y axis is the mean surface velocity of the full-system solution ($\bar{u}=\bar{C}+1=31$).	283
18.2 The x component of the group velocity (u_g) as a function of wavelength for $\theta=0$. Values of mean surface slope and slip ratio are 0.005 and 30, respectively, and $m = n = 1$	283

18.3 The phase speed ($\ \mathbf{v}_p\ $) of the full-system solution as a function of wavelength λ and orientation θ of the sinusoidal perturbations with respect to mean flow direction. The mean surface slope is $\alpha=0.002$ and the slip ratio is $\bar{C}=100$, and $n = m = 1$. The plot has been normalised with the non-dimensional surface velocity $\bar{u}=\bar{C}+1=101$ of the full-system solution.	283
18.4 The shallow-ice-stream phase speed as a function of wavelength λ and orientation θ . As in Fig. 18.3a the mean surface slope is $\alpha=0.002$ and the slip ratio is $\bar{C}=100$, $n = m = 1$, and the plot has been normalised with the non-dimensional surface velocity $\bar{u}=\bar{C}+1=101$ of the full-system solution.	283
18.5 The relaxation time scale (t_r) as a function of wavelength λ . The wavelength is given in units of mean ice thickness (\bar{h}) and t_r is given in years. The mean surface slope is $\alpha=0.002$, the slip ratio is $\bar{C}=999$, and $n = m = 1$. For these values t_r is on the order of 10 years for a fairly wide range of wavelengths. Lowering the slip ratio will reduce the value of t_r . It follows that ice streams will react to sudden changes in basal properties or surface profile by a characteristic time scale of a few years.	284
18.6 Steady-state response of surface topography (Δs) to a perturbation in bed topography (Δb). The surface slope is 0.002, the mean slip ratio $\bar{C}=100$, and $n = m = 1$. Transfer functions based on the shallow-ice-stream approximation (dashed line, Eq. 18.32), the shallow-ice-sheet approximation (dotted line, and a full system solution (solid line) are shown.	284
18.7 (a) The SSTREAM amplitude ratio ($ T_{sb} $) between surface and bed topography (Eq. 18.32). Surface slope is 0.002, the slip ratio $\bar{C}=99$, and $n = m = 1$. λ is the wavelength of the sinusoidal bed topography perturbation and θ is the angle with respect to the x axis, with $\theta=0$ and $\theta=90$ corresponding to transverse and longitudinal undulations in bed topography, respectively.	284
18.7 (b) The FS amplitude ratio between surface and bed topography ($ T_{sb} $). The shape of the same transfer function for the same set of parameters based on the SSTREAM approximation is shown in Fig. 18.7a.	284
18.8 (a) The steady-state amplitude ratio ($ T_{ub} $) between longitudinal surface velocity (Δu) and bed topography (Δb) in the shallow-ice-stream approximation. Surface slope is 0.002, the slip ratio is 99, and $n = m = 1$	285
18.8 (b) The steady-state amplitude ratio ($ T_{ub} $) between longitudinal surface velocity (Δu) and bed topography (Δb). The shape of the same transfer function for the same set of parameters, but based on the shallow-ice-stream approximation, is shown in Fig. 18.8a.	285
18.9 (a) The steady-state amplitude ratio ($ T_{vb} $) between transverse velocity (Δv) and bed topography (Δb) in the shallow-ice-stream approximation. Surface slope is 0.002, the slip ratio is 99 and $n = m = 1$	285
18.8 (b) The steady-state amplitude ratio ($ T_{vb} $) between transverse velocity (Δv) and bed topography (Δb). The shape of the same transfer function for the same set of parameters, but based on the shallow-ice-stream approximation, is shown in Fig. 18.9a.	285
18.9 Steady-state response of surface topography to a perturbation in bed topography for linear and non-linear sliding. All curves are for linear medium ($n=1$). The solid lines are calculated for linear sliding ($m=1$) and the dashed lines for non-linear sliding ($m=3$). The red lines are SSHEET solutions, the blue ones are SSTREAM solutions, and the black line is a FS solution which is only available for $m=1$. Mean surface slope is 0.002 and slip ratio is equal to 100.	286
18.9 Steady-state response of surface topography to a basal slipperiness perturbation. Shown are FS (solid line), SSTREAM (circles), and SSHEET (crosses) transfer amplitudes for both $\bar{C}=1$ and $\bar{C}=10$. In the plot the SSTREAM curves for $\bar{C}=1$ and $\bar{C}=10$ are too similar to be distinguished. The surface slope is 0.002.	286
18.10 Transient surface topography response to a sinusoidal perturbation in bed topography applied at $t=0$. Shown are the amplitude ratios between surface and bed topography ($ T_{sb} $) as a function of wavelength for $\alpha=0.002$, $\theta=0$, $\bar{C}=100$, and $n = m = 1$ for $t=0.001$ (red), $t=0.01$ (blue), and $t=10$ (green).	286

- 18.10 Steady-state response of surface longitudinal (u), transverse (v), and vertical (w) velocity components to a basal slipperiness perturbation. The surface slope is 0.002 and the slip ratio $\bar{C}=10$. The T_{uc} and T_{wc} amplitudes are calculated for slipperiness perturbations aligned transversely to the flow direction ($\theta=0$). For T_{vc} , $\theta=45$ degrees. Of the two y axis the scale to the left is for the horizontal velocity components (T_{uc} and T_{wc}), and the one to the right is the scale for T_{vc} 286
- 18.11 Steady-state response of the surface longitudinal (Δu) velocity component to a basal slipperiness perturbation in the shallow-ice-stream approximation. The surface slope is 0.002 and the slip ratio $\bar{C}=99$ 287
- 18.12(a) Surface topography response to a flow over a Gaussian-shaped bedrock disturbance as given by a FS (lower half of figure) and a SSTREAM solution (upper half of figure). The mean flow direction is from left to right. Surface slope is 3 degrees and mean basal velocity equal to mean deformational velocity ($\bar{C}=1$). The spatial unit is one mean ice thickness (\bar{h}). The Gaussian-shaped bedrock disturbance has a width of $10 \bar{h}$ and it's amplitude is $0.1 \bar{h}$. The problem definition is symmetrical about the x axis ($y=0$) and any deviations in the figure from this symmetry are due to differences in the FS and the SSTREAM solutions. 287
- 18.13(b) Response in surface velocity to a Gaussian-shaped bedrock perturbation. All parameters are equal to those in Fig. 18.12a. The contour lines give horizontal speed and the vectors the horizontal velocities. The velocity unit is mean-deformational velocity (\bar{u}_d). The slip ratio is equal to one, and the mean surface velocity is $2\bar{u}_d$. The upper half of the figure is the SSTREAM solution and the lower half the corresponding FS solution. 287

List of Tables

1	List of variables	v
2	List of main geometrical variables.	vi
1.1	Sliding laws and definitions.	22
2.1	SUPG form function (M) limits for different definitions of τ	53
5.1	List of variables	98
6.1	Notation used in inverse modelling (I)	112
6.2	Notation used in inverse modelling (II)	129
7.1	179

Introduction

$\tilde{U}a$ is a finite-element ice flow model. This document provides some theoretical background information to $\tilde{U}a$. It is not a manual. This is a ‘life’ document, i.e. it is constantly being modified and changed and the current form of the document is in no means final. It contains some general material on glacier mechanics, a bit on the FE method, and lots of some very specific $\tilde{U}a$ related stuff. Most of the material related to glacier mechanics is from a glaciology lectures given at Caltech in 2014, and ETH Zurich prior to that.

Notation and definitions

Typical problem geometry is depicted in Fig. 1 and the main geometrical variables listed in Table 2. Upper and lower glacier surfaces are denoted by s and b , respectively, while the ocean surface and the bedrock are denoted by S and B , respectively. The ice thickness is

$$h = s - b,$$

and is always positive. The ocean depth, or vertical distance from bedrock (B) to the ocean surface (S), is

$$H = S - B,$$

and this quantity can be either positive or negative, depending on location.

The three components of the velocity vector are

$$\mathbf{v} = \begin{pmatrix} u \\ v \\ w \end{pmatrix}$$

but frequently we will just refer to the horizontal velocity components and write

$$\mathbf{v} = \begin{pmatrix} u \\ v \end{pmatrix}$$

and which form is being used should be clear from context.

The maximal ice thickness possible without grounding is denoted by h_f and is

$$h_f := (S - B)\rho_o/\rho, \quad (1)$$

where ρ and ρ_o are the ice and the ocean densities, respectively. The ice grounds if the ice thickness exceeds h_f , that is whenever $h > h_f$. Note that h_f becomes negative for $B > S$, i.e. whenever the bedrock (B) is located above sea level (S). In that case we always have $h > h_f$ for any positive ice thickness h and the ice is always grounded. We also define the positive flotation thickness, h_f^+ , as

$$h_f^+ = h_f \mathcal{H}(h_f), \quad (2)$$

where \mathcal{H} is the Heaviside function, defined as

$$\mathcal{H}(x) = \begin{cases} 0 & \text{for } x < 0 \\ 1/2 & \text{for } x = 0 \\ 1 & \text{for } x > 0 \end{cases}$$

The function $\mathcal{H}(h - h_f)$ (equal to one if grounded, zero if afloat), is needed frequently and we define the grounding/flotation mask \mathcal{G} as

$$\mathcal{G} = \mathcal{H}(h - h_f)$$

Hence

$$\mathcal{G} = \mathcal{H}(h - h_f) = \begin{cases} 0 & \text{over floating areas} \\ 1/2 & \text{at the grounding line} \\ 1 & \text{over grounded areas} \end{cases} \quad (3)$$

The variable \mathcal{G} can be thought of as a ‘grounding’ parameter.

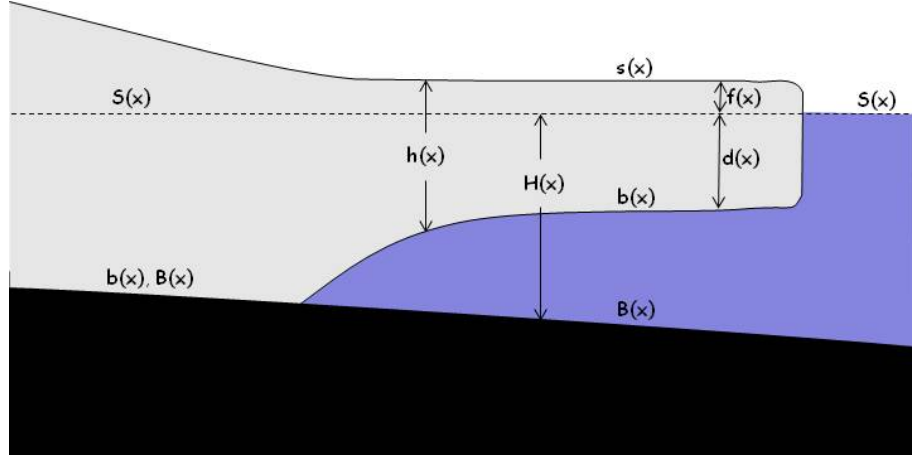


Figure 1: Geometrical variables: Glacier surface (s)), glacier bed (b), ocean surface (S), ocean floor (Basals), glacier thickness ($h = s - b$)), ocean depth ($H = S - B$), glacier draft, $d = S - b$, glacier freeboard $f = s - S$.

The freeboard f , which at the calving front we can also refer to as the subaerial cliff height, is

$$f := s - S,$$

and the draft d , i.e. the submarine ice thickness, is defined as

$$d := \begin{cases} S - b, & \text{if } S > b \\ 0, & \text{otherwise} \end{cases} \quad (4)$$

which can also be written as

$$d = \mathcal{H}(H)(S - b), \quad (5)$$

The ‘positive’ ocean depth H^+ is defined as

$$H^+ := \mathcal{H}(H)H, \quad (6)$$

i.e. $H^+ = H$ if $H > 0$ and zero otherwise.

To distinguish between continuous quantities and discrete quantities we use bold face for the latter. In a finite-element context we might write

$$f(x) = f_q \phi_q(x).$$

Here f is a continuous function, f_q the nodal variables, and ϕ_q the shape/form functions. We sometimes group the nodal variables together into a vector writing

$$\mathbf{f} = [f_1, f_2, \dots, f_N]^T,$$

and then

$$f(x) = \mathbf{f}^T \cdot \boldsymbol{\phi}(x).$$

Note that $f(x)$ and f_q very are different quantities: $f(x)$ is a function, whereas f_q is a scalar and can be thought of as the q th component of the function $f(x)$ in the basis $\{\phi\}$.

If, for a vector \mathbf{f} , we need to refer to the q element of the vector, we write $[\mathbf{f}]_q$, i.e.

$$f_q = [\mathbf{f}]_q.$$

The matrix representation of a continuous operator $L : H_1 \rightarrow H_2$ is written in bold as \mathbf{L} . The elements of the matrix are $L_{pq} = [\mathbf{L}]_{pq}$.

The L^2 inner product is

$$\langle f, g \rangle_{L^2} = \int f(x) g(x) dx,$$

Table 1: List of variables

s	elevation of upper glacier surface
\hat{s}	measurements of the elevation of upper glacier surface
b	elevation of lower glacier surface
\hat{b}	measurements of the elevation of lower glacier surface
S	ocean surface
B	bedrock / ocean floor
$h := s - b$	glacier thickness
$H := S - B$	ocean depth (pos. or neg. depending on location)
$H^+ = \mathcal{H}(H)H$	(positive) ocean depth
$d := \mathcal{H}(H)(S - b)$	glacier draft, i.e. submarine ice thickness (positive by definition)
$f := s - S$	freeboard (always positive)
$\mathcal{G} := \mathcal{H}(h - h_f)$	grounding/flotation mask, 1 if ice grounded, 0 otherwise.
$h_f := \rho_o H / \rho$	flotation thickness (maximal ice thickness without grounding)
$h_f^+ := \rho_o H^+ / \rho$	positive flotation thickness
α	tilt of coordinate system
ρ	ice density
ρ_o	ocean density
$\varrho = \rho(1 - \rho/\rho_o)$	
(u_b, v_b, w_b)	xyz components of basal velocity
(u_s, v_s, w_s)	xyz components of surface velocity
$\tau_{xx}, \tau_{yy}, \tau_{xy}$ etc.	deviatoric stress components
$\sigma_{xx}, \sigma_{yy}, \sigma_{xy}$ etc.	Cauchy stress components
$\dot{\epsilon}_{xx}, \dot{\epsilon}_{yy}, \dot{\epsilon}_{xy}$ etc.	strain rates
g	gravitational acceleration

where f and g are square integrable functions and the l^2 inner product is

$$(\mathbf{f}, \mathbf{g})_{l^2} = \mathbf{f}^T \cdot \mathbf{g} ,$$

where \mathbf{f} and \mathbf{g} are vectors. The inner products define corresponding L^2 and l^2 norms.

The notation used for inner products is currently a bit inconsistent in this compendium, as I use both the round bracket and the angle bracket (bra/ket) notations. Hence, for inner product from $V \rightarrow \mathbb{R}$ all these notations are used

$$(f, g) = \langle f, g \rangle = \langle f | g \rangle ,$$

and they all have the same meaning.

From the definition of an inner product we have the induced norm

$$\|f\|^2 = \langle f | f \rangle .$$

Hence

$$\|f\|_{L^2} = \sqrt{\langle f | f \rangle_{L^2}} = \sqrt{\int f(x) f(x) dx}$$

We often need to linearise various quantities, which we do by calculating directional derivatives. The directional derivative $D_v f$ of a function f of the variable x in the direction v is defined as

$$D_v f(x) = \lim_{\epsilon \rightarrow 0} \frac{d}{d\epsilon} f(x + \epsilon v) . \quad (7)$$

Often we think of v being a small perturbation to x in which case we write

$$D_{\Delta x} f(x) = \lim_{\epsilon \rightarrow 0} \frac{d}{d\epsilon} f(x + \epsilon \Delta x) ,$$

and may then write $Df(x)$ or just δf . In this document I use $D_v f(x)$, $Df(x)[v]$, and $\delta_v f$ to denote the directional derivative.

Table 2: List of main geometrical variables.

symbol	definition
s	upper glacier surface
b	lower glacier surface
S	ocean surface
B	bedrock / ocean floor
$h := s - b$	glacier thickness
$H := S - B$	ocean depth (pos. or neg. depending on location)
$d := \mathcal{H}(H)(S - b)$	glacier, i.e. submarine ice thickness (positive by definition)
$f := s - S$	freeboard (always positive)
$h_f := \rho_w H / \rho$	maximum ice thickness without grounding

As explained in more detail in Appendix D the gradient is defined in terms of the directional derivative for a given inner product as

$$Df(p)[\phi] = \langle \nabla J(p) | \phi \rangle_H , \quad (8)$$

where H is a Hilbert space and $f : H \rightarrow \mathbb{R}$.

Consider the scalar function J of the function $f(x)$

$$J = J(f(x)) .$$

The functional J might, for example, be some cost function that we are interested in minimising with respect to the function $f(x)$. In a typical FE context the function f expanded in a basis $\phi_i(x)$, that is

$$\begin{aligned} f(x) &= f_p \phi_p(x) \\ &= \mathbf{f}^T \cdot \boldsymbol{\phi}(x) \end{aligned}$$

where f_p can be thought of as the nodal values. The directional derivative of J with respect to f_q , i.e. with respect to one of the coefficients (nodal values) in the expansion for $f(x)$, is then

$$\begin{aligned} [\delta J]_q &:= DJ(f(x))[f_q] = \lim_{\epsilon \rightarrow 0} \frac{d}{d\epsilon} J(f_p \phi_p(x) + \epsilon \phi_q(x)) \\ &= \lim_{\epsilon \rightarrow 0} \frac{d}{d\epsilon} J((f_p + \epsilon \delta_{pq}) \phi_p(x)) \end{aligned}$$

We express the vector \mathbf{f} of the nodal values in a basis $\{\mathbf{e}_i\}$ and write $\mathbf{f} = f_q \mathbf{e}_p$ and refer to this as the Euclidean representation. For a given FE mesh and element type i.e. for some given basis $\{\phi_i\}$, we can now think of J either as a function of the vector of nodal values \mathbf{f} , i.e.

$$J = J(\mathbf{f})$$

or

$$J = J(f(x))$$

and we can express the gradient of f with respect to either the Euclidean basis $\{\mathbf{e}_i\}$ or with respect to the basis $\{\phi_i(x)\}$.

Taking the viewpoint that f is a function of nodal values, the directional derivative shown above can be written as

$$DJ(f(x))[f_q] = \lim_{\epsilon \rightarrow 0} \frac{d}{d\epsilon} J(\mathbf{f} + \epsilon \mathbf{e}_q)$$

The directional derivative can be estimated numerically in a FE model through first-order forward finite differences by perturbing the corresponding nodal value as

$$DJ(f(x))[f_q] \approx \frac{J(\mathbf{f} + \epsilon \mathbf{e}_q) - J(\mathbf{f})}{\epsilon} \quad (9)$$

Generally, however, the directional gradient will be calculated more efficiently using the adjoint method, but the above finite-difference approximation can be used to test the correctness of the adjoint implementation.

Using the definition (8) of a gradient, we now give examples of several different gradients \mathbf{g} , $h(x)$, $j(x)$, and $k(x)$ defined as

$$\begin{aligned} DJ(f(x))[f_q] &= \langle \mathbf{g}, \mathbf{e}_q \rangle_{l^2} \\ &= \langle h, \phi_q \rangle_{L^2} \\ &= \langle j, \phi_q \rangle_{H^1} \\ &= \langle \nabla k, \nabla \phi_q \rangle_{L^2} \end{aligned}$$

Note that the inner-product induced norm of the last inner product, $(\langle \nabla \cdot, \nabla \cdot \rangle_{L^2})$ is a semi-norm. We are interested in knowing the relationship between these gradients to each other in a typical FE setting.

We refer to the vector $\mathbf{g} = g_p \mathbf{e}_p$ in the basis $\{\mathbf{e}_i\}$ as the l^2 gradient, and the function $h(x) = h_p \phi_p(x)$ in the basis $\{\phi_i(x)\}$ as the L^2 gradient. The elements of the l^2 and L^2 gradients in the respective basis \mathbf{e}_q and $\phi_q(x)$ are the coefficients h_i and g_i the in the expansions

$$\begin{aligned} h(x, y) &= h_q \phi_q(x, y) \\ \mathbf{g} &= g_q \mathbf{e}_q \\ j(x, y) &= j_q \phi_q(x, y) \\ k(x, y) &= k_q \phi_q(x, y) \end{aligned}$$

where we have set $\Omega = (x, y)$.

The l^2 gradient relates to the directional derivative in a simple way. Each element q of the l^2 gradient vector \mathbf{g} is simply the directional derivative of $J(\mathbf{f})$ in the direction \mathbf{e}_q . This follows from the definition of the l^2 inner product

$$\begin{aligned} DJ(f(x))[f_q] &= \lim_{\epsilon \rightarrow 0} \frac{d}{d\epsilon} J(\mathbf{f} + \epsilon \mathbf{e}_q) \\ &= \langle \mathbf{g}, \mathbf{e}_q \rangle \\ &= \langle g_p \mathbf{e}_p, \mathbf{e}_q \rangle \\ &= g_p \langle \mathbf{e}_p, \mathbf{e}_q \rangle \\ &= g_p \mathbf{e}_p \cdot \mathbf{e}_q \\ &= g_p \delta_{pq} \\ &= g_q . \end{aligned}$$

For the L^2 gradient we find, using the definition of the corresponding L^2 inner product, that

$$\begin{aligned} DJ(f(x))[f_q] &= \lim_{\epsilon \rightarrow 0} \frac{d}{d\epsilon} J(\mathbf{f} + \epsilon \mathbf{e}_q) \\ &= \langle h(x), \phi_q(x) \rangle_{L^2} \\ &= \langle h_p \phi_p(x), \phi_q(x) \rangle_{L^2} \\ &= h_p (\phi_p(x), \phi_q(x))_{L^2} \\ &= h_p M_{pq} \end{aligned}$$

where M_{pq} are the elements of the mass matrix

$$M_{pq} = \langle \phi_p(x), \phi_q(x) \rangle_{L^2} = \int_A \phi_p(x) \phi_q(x) dA$$

also referred to as the Gramian matrix elements of the basis ϕ_i in the inner product space L^2 . Hence the elements g_i and h_i of the l^2 gradient \mathbf{g} and the L^2 gradient $h(x)$, respectively, are related by

$$g_i = M_{ij} h_j$$

or in matrix notation

$$\mathbf{g} = \mathbf{M} \mathbf{h}$$

where again $[\mathbf{h}]_i = h_i$ and the L^2 gradient is $\mathbf{h}(x) = h_p \phi_p(x)$. Since the mass matrix is always invertible we can calculate the L^2 gradient vector \mathbf{h} as

$$\mathbf{h} = \mathbf{M}^{-1} \mathbf{g}$$

where the elements of the l^2 gradient \mathbf{g} are the directional derivatives with respect to the nodal values. Same calculations using the H^1 inner product lead to

$$\mathbf{g} = (\mathbf{M} + \mathbf{D}_{xx} + \mathbf{D}_{yy}) \mathbf{j}$$

where

$$\mathbf{j}(x) = \mathbf{j} \cdot \boldsymbol{\phi}(x)$$

is the H^1 gradient. For the $\|\nabla \cdot\|_{L_2}$ semi-norm we can define the H^1 semi-norm gradient \mathbf{k} as before through

$$\begin{aligned} DJ(f(x))[f_q] &=: \langle k(x), \phi_q(x) \rangle_{H^1} \\ &= \langle \nabla k(x), \nabla \phi_q(x) \rangle_{L^2} \\ &= k_p \langle \nabla \phi_p, \nabla \phi_q \rangle_{L^2} \\ &= \mathbf{k} \mathbf{D} \end{aligned}$$

And in two dimensions the elements of the l^2 and the H^1 semi-norm gradients are related as

$$\mathbf{g} = (\mathbf{D}_{xx} + \mathbf{D}_{yy}) \mathbf{k}$$

Sobolev space of order 1 on Ω denoted by H^1 and defined by

$$H^1(\Omega) = \{f, \partial_x f, \partial_y f \in L^2(\Omega)\}$$

The inner product is

$$\langle f, g \rangle_{H^1} = \int_{\Omega} (fg + \partial_x f \partial_x g + \partial_y f \partial_y g) d\Omega$$

and the resulting inner-product induced norm

$$\begin{aligned} \|f\|_{H^1}^2 &= \int_{\Omega} (f^2 + (\nabla f)^2) d\Omega \\ &= \|f\|_{L^2}^2 + \|\nabla f\|_{L^2}^2 \end{aligned}$$

where f is a real valued function.¹

Alternatively to the finite-differences test given by (9), the correctness of the gradient calculation can be verified

$$J(f(x) + \epsilon d(x)) = J(f(x)) + \epsilon \langle \nabla J, d(x) \rangle + O(\epsilon^2)$$

by calculating the limit

$$\lim_{\epsilon \rightarrow 0} \frac{J(f(x) + \epsilon d(x)) - J(f(x))}{\epsilon \langle \nabla J, d(x) \rangle}$$

¹A common Sobolev-norm notation is

$$\|f\|_{W_p^k(\Omega)} := \left(\sum_{|\alpha| \leq k} \|D^\alpha u\|_{L_p}^p \right)^{1/p}$$

and the Sobolev spaces defined as

$$W_p^k(\Omega) = \left\{ f \in L_1 : \|f\|_{W_p^k} < \infty \right\}$$

And another common notational simplification is to define

$$H^k(\Omega) := W_2^k(\Omega)$$

We have

$$\|f\|_{H^1}^2 = \|f\|_{L_2}^2 + \|\nabla f\|_{L_2}^2$$

and $\|\nabla \cdot\|_{L_2}$ is a semi-norm.

which must be equal to 1 for the gradient estimate to be correct.

For a scalar function f using the l^2 inner product, the first-order Taylor expansion of a scalar function f is here written as

$$f(\mathbf{x} + \mathbf{h}) = f(\mathbf{x}) + (\nabla f)^T \mathbf{h},$$

and similarly for a vector function \mathbf{f} as

$$\mathbf{f}(\mathbf{x} + \mathbf{h}) = \mathbf{f}(\mathbf{x}) + (\nabla \mathbf{f})^T \mathbf{h},$$

which implies that the gradient of a scalar function f is a column vector and the gradient of a vector function \mathbf{f} the matrix²

$$\begin{aligned}\nabla \mathbf{f} &= \begin{pmatrix} \partial_{x_1} f_1 & \partial_{x_1} f_2 & \cdots & \partial_{x_1} f_m \\ \partial_{x_2} f_1 & \partial_{x_2} f_2 & \cdots & \partial_{x_2} f_m \\ \vdots & \vdots & \ddots & \vdots \\ \partial_{x_n} f_1 & \partial_{x_n} f_2 & \cdots & \partial_{x_n} f_m \end{pmatrix} \\ &= \nabla \otimes \mathbf{f}\end{aligned}$$

and also

$$\nabla \mathbf{f}(\mathbf{x}) = \frac{\partial f_i}{\partial x_j} \mathbf{e}_i \otimes \mathbf{e}_j.$$

Using index notation and the summation and comma conventions we can write the Taylor expansion as

$$f_p(\mathbf{x} + \mathbf{h}) = f_p(\mathbf{x}) + f_{p,q} h_q$$

and

$$[\nabla \mathbf{f}]_{pq} = f_{q,p}.$$

The Jakobian matrix \mathbf{K} for a vector function $\mathbf{f} = (f_1, f_2, \dots, f_m)^T$ of the vector $\mathbf{x} = (x_1, x_2, \dots, x_n)^T$ is commonly defined as the $m \times n$ matrix having the elements $[\mathbf{K}]_{ij} = \partial f_i / \partial x_j$. Therefore $\mathbf{K} = (\nabla \mathbf{f})^T$ and the first-order Taylor expansion can be written as

$$\mathbf{f}(\mathbf{x} + \mathbf{h}) = \mathbf{f}(\mathbf{x}) + \mathbf{K} \mathbf{h}.$$

²Sometimes an outer product between two (column) vectors \mathbf{a} and \mathbf{b} is defined as

$$\mathbf{a}\mathbf{b}^T = \mathbf{a} \otimes \mathbf{b}.$$

If we think of the operator ∇ as a (column) vector, then one could argue that a correct notation for the operation of ∇ on \mathbf{f} is, written using the outer product, $\nabla \mathbf{f}^T$.

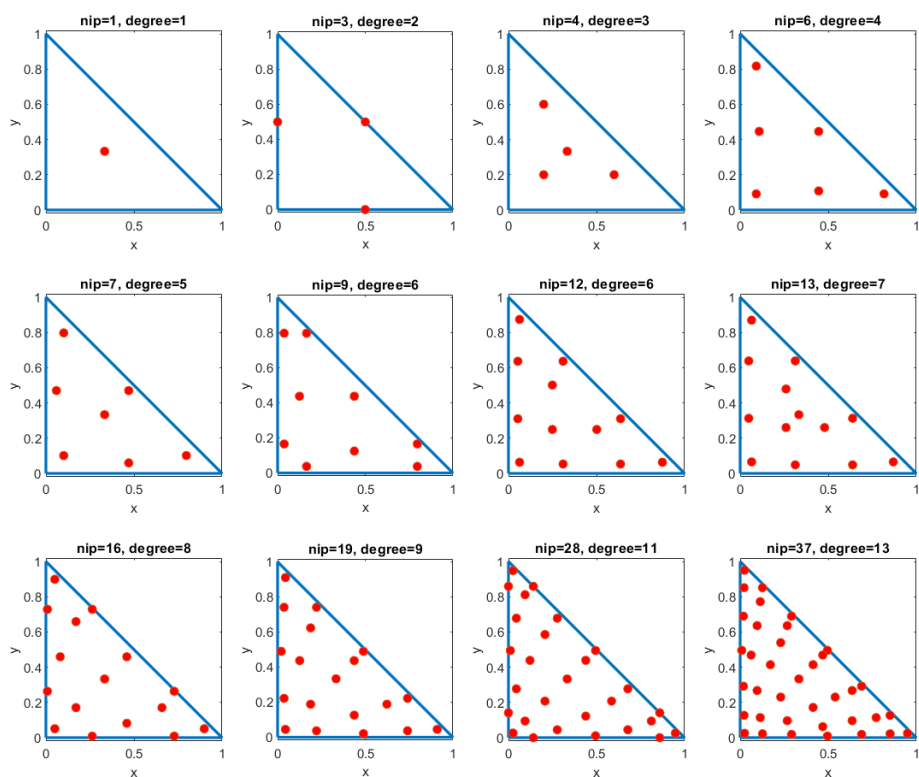


Figure 2: Distribution of integration points with the unit reference triangle and the degree of precision.

Part I

General theoretical background for the use of the $\dot{U}a$ ice-flow model

Chapter 1

Key governing equations

1.1 Equations of ice flow

For reference, we start by recapping the key governing equations of glacier flow which are

$$\dot{\boldsymbol{\epsilon}} = A \tau^{n-1} \boldsymbol{\tau} \quad (\text{constitutive law}) \quad (1.1)$$

$$\mathbf{t}_b = f(\mathbf{v}) \frac{\mathbf{v}_b}{\|\mathbf{v}_b\|} \quad (\text{sliding law}) \quad (1.2)$$

$$\nabla \cdot \boldsymbol{\sigma} + \mathbf{b} = 0 \quad (\text{momentum}) \quad (1.3)$$

$$\nabla \cdot \mathbf{v} = 0 \quad (\text{mass}) \quad (1.4)$$

where the effective stress is

$$\tau = \sqrt{\tau_{pq}\tau_{pq}/2},$$

and $f : \mathbb{R}^3 \rightarrow \mathbb{R}$, is a given scalar function (the sliding law).

The constitutive law can also be written in terms of strain rates as

$$\boldsymbol{\tau} = A^{-1/n} \dot{\boldsymbol{\epsilon}}^{(1-n)/n} \dot{\boldsymbol{\epsilon}}, \quad (1.5)$$

where

$$\dot{\boldsymbol{\epsilon}} = \sqrt{\dot{\epsilon}_{pq}\dot{\epsilon}_{pq}/2},$$

is the effective strain rate, or in an implicit form as

$$\boldsymbol{\tau} = A^{-1} \tau^{1-n} \dot{\boldsymbol{\epsilon}}. \quad (1.6)$$

Sometimes the constitutive law is written on the form

$$\tau_{ij} = 2\eta \dot{\epsilon}_{ij} \quad (1.7)$$

where η is the effective viscosity given by

$$\eta = \frac{1}{2} A^{-1/n} \dot{\epsilon}^{(1-n)/n} \quad (1.8)$$

$$= \frac{\tau^{1-n}}{2A}. \quad (1.9)$$

The relationship between the elements, σ_{pq} , of the Cauchy stress tensor and the deviatoric stress components, τ_{pq} , and the pressure, p , is

$$\boldsymbol{\sigma} = \boldsymbol{\tau} - p\mathbf{1}$$

that is

$$\begin{pmatrix} \sigma_{xx} & \sigma_{xy} & \sigma_{xz} \\ \sigma_{xy} & \sigma_{yy} & \sigma_{yz} \\ \sigma_{xz} & \sigma_{yz} & \sigma_{zz} \end{pmatrix} = \begin{pmatrix} \tau_{xx} - p & \tau_{xy} & \tau_{xz} \\ \tau_{xy} & \tau_{yy} - p & \tau_{yz} \\ \tau_{xz} & \tau_{yz} & \tau_{zz} - p \end{pmatrix}, \quad (1.10)$$

and the elements of the strain-rate tensor are related to the velocity components as follow:

$$\dot{\epsilon} = \begin{pmatrix} \dot{\epsilon}_{xx} & \dot{\epsilon}_{xy} & \dot{\epsilon}_{xz} \\ \dot{\epsilon}_{xy} & \dot{\epsilon}_{yy} & \dot{\epsilon}_{yz} \\ \dot{\epsilon}_{xz} & \dot{\epsilon}_{yz} & \dot{\epsilon}_{zz} \end{pmatrix} = \begin{pmatrix} \frac{\partial u}{\partial x} & \frac{1}{2} \left(\frac{\partial u}{\partial y} + \frac{\partial v}{\partial x} \right) & \frac{1}{2} \left(\frac{\partial u}{\partial z} + \frac{\partial w}{\partial x} \right) \\ \frac{1}{2} \left(\frac{\partial u}{\partial y} + \frac{\partial v}{\partial x} \right) & \frac{\partial v}{\partial y} & \frac{1}{2} \left(\frac{\partial v}{\partial z} + \frac{\partial w}{\partial y} \right) \\ \frac{1}{2} \left(\frac{\partial u}{\partial z} + \frac{\partial w}{\partial x} \right) & \frac{1}{2} \left(\frac{\partial v}{\partial z} + \frac{\partial w}{\partial y} \right) & \frac{\partial w}{\partial z} \end{pmatrix}. \quad (1.11)$$

Written out, the three components of the momentum equation, (1.3), are

$$\partial_x \sigma_{xx} + \partial_y \tau_{xy} + \partial_z \tau_{xz} = 0, \quad (1.12)$$

$$\partial_x \tau_{xy} + \partial_y \sigma_{yy} + \partial_z \tau_{yz} = 0, \quad (1.13)$$

$$\partial_x \tau_{xz} + \partial_y \tau_{yz} + \partial_z \sigma_{zz} = \rho g, \quad (1.14)$$

or equally as

$$\partial_x \tau_{xx} + \partial_y \tau_{xy} + \partial_z \tau_{xz} = \partial_x p, \quad (1.15)$$

$$\partial_x \tau_{xy} + \partial_y \tau_{yy} + \partial_z \tau_{yz} = \partial_y p, \quad (1.16)$$

$$\partial_x \tau_{xz} + \partial_y \tau_{yz} + \partial_z \tau_{zz} = \partial_z p + \rho g, \quad (1.17)$$

where we have assumed a coordinate system where the z axis is oriented upwards, that is against the direction of the gravity vector.

1.2 Shallow Ice-Stream Approximation (SSTREAM/SSA)

The shallow ice-stream (SSTREAM/SSA/Shelfy) equations are

$$\partial_x(h(2\tau_{xx} + \tau_{yy})) + \partial_y(h\tau_{xy}) - t_{bx} = (\rho gh\partial_x s + \frac{1}{2}h^2g\partial_x\rho)\cos\alpha - \rho gh\sin\alpha \quad (1.18)$$

$$\partial_y(h(2\tau_{yy} + \tau_{xx})) + \partial_x(h\tau_{xy}) - t_{by} = (\rho gh\partial_y s + \frac{1}{2}h^2g\partial_y\rho)\cos\alpha \quad (1.19)$$

where α is the tilt of the coordinate system with respect to the gravity vector, and the shallow ice-stream approximation for the effective stress, τ , is

$$\tau = \tau^{\text{SSA}} = \sqrt{\tau_{xx}^2 + \tau_{yy}^2 + \tau_{xx}\tau_{yy} + \tau_{xy}^2}. \quad (1.20)$$

These equations can also be written in terms of velocities as

$$\partial_x(4h\eta\partial_x u + 2h\eta\partial_y v) + \partial_y(h\eta(\partial_x v + \partial_y u)) - \beta^2 u = (\rho gh\partial_x s + \frac{1}{2}h^2g\partial_x\rho)\cos\alpha - \rho g\sin\alpha, \quad (1.21)$$

$$\partial_y(4h\eta\partial_y v + 2h\eta\partial_x u) + \partial_x(h\eta(\partial_y u + \partial_x v)) - \beta^2 v = (\rho gh\partial_y s + \frac{1}{2}h^2g\partial_y\rho)\cos\alpha. \quad (1.22)$$

where we have written the sliding law as

$$t_{bx} = \beta^2 u, \quad (1.23)$$

$$t_{by} = \beta^2 v, \quad (1.24)$$

and used the constitutive law on the form

$$\dot{\epsilon}_{ij} = \frac{1}{2\eta} \tau_{ij} \quad (1.25)$$

where

$$\eta = \frac{1}{2} A^{-1/n} \dot{\epsilon}^{(1-n)/n},$$

and where in the SSA the effective strain rate, $\dot{\epsilon}$, is given by

$$\dot{\epsilon} = \dot{\epsilon}^{\text{SSA}} = \sqrt{(\partial_x u)^2 + (\partial_y v)^2 + \partial_x u \partial_y v + (\partial_x v + \partial_y u)^2/4}.$$

Defining the *resistive stress tensor* as

$$\mathbf{R} = \begin{pmatrix} 2\tau_{xx} + \tau_{yy} & \tau_{xy} \\ \tau_{xy} & 2\tau_{yy} + \tau_{xx} \end{pmatrix} \quad (1.26)$$

and

$$\nabla_{xy} = (\partial_x, \partial_y)$$

the SSA field equations can be written in a compact form as

$$\nabla_{xy} \cdot (h \mathbf{R}) - \mathbf{t}_{bh} = \rho g h \nabla_{xy} s + \frac{1}{2} g h^2 \nabla_{xy} \rho, \quad (1.27)$$

for $\alpha = 0$, where

$$\mathbf{t}_{bh} = \begin{pmatrix} t_{bx} \\ t_{by} \end{pmatrix}$$

is the horizontal part of the basal stress vector (basal traction)

$$\mathbf{t}_b = \boldsymbol{\sigma} \hat{\mathbf{n}} - (\hat{\mathbf{n}} \cdot \boldsymbol{\sigma} \hat{\mathbf{n}}) \hat{\mathbf{n}},$$

with $\hat{\mathbf{n}}$ being a unit normal vector to the bed pointing into the ice.

As shown in section 1.17 we have

$$g \rho h \partial_x s + \frac{1}{2} g h^2 \partial_x \rho = \frac{g}{2} \partial_x (\rho h^2 - \rho_o d^2) + g(\rho h - \rho_o d) \partial_x b, \quad (1.28)$$

and also

$$g(\rho h - \rho_o d) \partial_x b = \mathcal{G} g(\rho h - \rho_o H^+) \partial_x B. \quad (1.29)$$

We can therefore also write the field equations as

$$\nabla_{xy} \cdot (h \mathbf{R}) - \mathbf{t}_{bh} = \frac{g}{2} \nabla_{xy} (\rho h^2 - \rho_o d^2) + g(\rho h - \rho_o d) \nabla_{xy} b, \quad (1.30)$$

or

$$\nabla_{xy} \cdot (h \mathbf{R}) - \mathbf{t}_{bh} = \frac{g}{2} \nabla_{xy} (\rho h^2 - \rho_o d^2) + \mathcal{G} g(\rho h - \rho_o H^+) \nabla_{xy} B. \quad (1.31)$$

again for $\alpha = 0$. Note that where the ice is afloat the right hand sides of Eqs. (1.30) and (1.31) are equal to zero.

We will also show (see section 1.16) that the stress boundary condition at both grounded and floating ice edges can be written as

$$h \mathbf{R} \cdot \hat{\mathbf{n}}_{xy} = \frac{g}{2} (\rho h^2 - \rho_o d^2) \hat{\mathbf{n}}_{xy}. \quad (1.32)$$

where

$$\hat{\mathbf{n}}_{xy} = (n_x, n_y, 0)^T,$$

is a unit normal pointing horizontally outward from the ice front.

Note that it is the horizontal component of the basal traction that enters the field equations. We will sometimes just write \mathbf{t}_b instead of \mathbf{t}_{bh} which is a slight abuse of notation, and strictly speaking incorrect.

In $\tilde{\mathbf{U}}$ the form of the STREAM equations is therefore (written for non-tilted coordinate system):

$$\partial_x (h(2\tau_{xx} + \tau_{yy})) + \partial_y (h\tau_{xy}) - t_{bx} = \frac{1}{2} g \partial_x (\rho h^2 - \rho_o d^2) + g \mathcal{H}(h - h_f)(\rho h - \rho_o H^+) \partial_x B \quad (1.224)$$

$$\partial_y (h(2\tau_{yy} + \tau_{xx})) + \partial_x (h\tau_{xy}) - t_{by} = \frac{1}{2} g \partial_y (\rho h^2 - \rho_o d^2) + g \mathcal{H}(h - h_f)(\rho h - \rho_o H^+) \partial_y B \quad (1.225)$$

And written in terms of the velocity components:

$$\begin{aligned} \partial_x (h\eta(4\partial_x u + 2\partial_y v)) + \partial_y (h\eta(\partial_y u + \partial_x v)) - t_{bx} = \\ \frac{1}{2} g \partial_x (\rho h^2 - \rho_o d^2) + g \mathcal{H}(h - h_f)(\rho h - \rho_o H^+) \partial_x B \end{aligned} \quad (1.226)$$

$$\begin{aligned} \partial_y (h\eta(4\partial_y v + 2\partial_x u)) + \partial_x (h\eta(\partial_x v + \partial_y u)) - t_{by} = \\ \frac{1}{2} g \partial_y (\rho h^2 - \rho_o d^2) + g \mathcal{H}(h - h_f)(\rho h - \rho_o H^+) \partial_y B \end{aligned} \quad (1.227)$$

Here the draft d , is

$$d = \mathcal{H}(h_f - h)\rho h/\rho_o + \mathcal{H}(h - h_f)H^+ \quad (1.203)$$

and the positive ocean 'thickness' H^+ is

$$H^+ := \mathcal{H}(H)H, \quad (1.33)$$

i.e. $H^+ = H$ if $H > 0$ and zero otherwise. The variable h_f is the flotation thickness (maximal ice thickness without grounding)

$$h_f := H\rho_o/\rho, \quad (1)$$

where ρ and ρ_o are the ice and the ocean densities, respectively. The function $\mathcal{H}(x)$ is the Heaviside step function, i.e. $\mathcal{H}(x) = 1$ for $x > 0$ and $\mathcal{H}(x) = 0$ for $x < 0$ and $\mathcal{H}(0) = 1/2$. The ice thickness h is $h = s - b$ where s is the upper and b the lower ice surfaces. The ocean 'thickness' H is $H = S - B$ where S is the ocean surface and B the ocean floor.

1.3 Shallow Ice Shelf (SSHELF/SSA)

The shallow ice shelf approximation is simply the shallow ice stress approximation with the drag term dropped. Since

$$s = S + h(1 - \rho/\rho_o)$$

we have over a floating ice shelf

$$\rho gh\nabla_{xy} s = \frac{1}{2}\varrho g\nabla_{xy} h^2$$

where

$$\varrho = \rho(1 - \rho/\rho_o), \quad (1.34)$$

and the momentum equations have the form

$$\nabla_{xy} \cdot (h \mathbf{R}) = \frac{1}{2}\varrho g\nabla_{xy} h^2 + \frac{1}{2}gh^2\nabla_{xy} \rho, \quad (1.35)$$

or if we skip the spatial density gradient

$$\nabla_{xy} \cdot \left(\mathbf{R} - \frac{1}{2}\varrho g \begin{pmatrix} h & 0 \\ 0 & h \end{pmatrix} \right) = 0 \quad (1.36)$$

1.4 Shallow Ice-Sheet (SSHEET/SIA)

In the shallow ice-sheet approximation, the stress balance is

$$\mathbf{t}_b = \mathbf{t}_b^{\text{SIA}} = -\rho gh\nabla_{xy} s, \quad (1.37)$$

and the pressure and the stresses are

$$\begin{aligned} -p(z) &= \sigma_{zz}(z) = -\rho g(s - z), \\ \tau_{xz}(z) &= -\rho g(s - z)\partial_x s, \\ \tau_{yz}(z) &= -\rho g(s - z)\partial_y s, \end{aligned}$$

and the effective stress therefore

$$\begin{aligned} \tau(z) &= \tau_{\text{SIA}} = \sqrt{\tau_{xz}^2(z) + \tau_{yz}^2(z)}, \\ &= \rho g(s - z)\sqrt{(\partial_x s)^2 + (\partial_y s)^2}. \end{aligned}$$

The flow law

$$\dot{\epsilon}_{ij} = A(T)\tau^{n-1}\tau_{ij}, \quad (1.7.5)$$

implies

$$\begin{aligned} \partial_z u &= 2A\tau^{n-1}\tau_{xz} \\ &= -2A\left(\rho g(s - z)\sqrt{(\partial_x s)^2 + (\partial_y s)^2}\right)^{n-1}\rho g(s - z)\partial_x s \end{aligned}$$

Integrating, and assuming A does not vary with depth, we find

$$\begin{aligned}\mathbf{v} &= -2A(\rho g)^n ((\partial_x s)^2 + (\partial_y s)^2)^{(n-1)/2} \nabla_{xy} s \int_b^z (s - z')^n dz' + \mathbf{v}_b \\ &= -\frac{2A}{n+1}(\rho g)^n \|\nabla_{xy} s\|^{n-1} (h^{n+1} - (s - z)^{n+1}) \nabla_{xy} s + \mathbf{v}_b \\ &= -\frac{2A}{(n+1)h^n}(\rho g h)^n \|\nabla_{xy} s\|^{n-1} (h^{n+1} - (s - z)^{n+1}) \nabla_{xy} s + \mathbf{v}_b \\ &= -\frac{2A}{(n+1)h^n}(\rho g h)^n \|\nabla_{xy} s\|^{n-1} (h^{n+1} - (s - z)^{n+1}) \nabla_{xy} s + \mathbf{v}_b \\ &= \frac{2A}{(n+1)h^n} (h^{n+1} - (s - z)^{n+1}) \|\mathbf{t}_b^{\text{SIA}}\|^{n-1} \mathbf{t}_b^{\text{SIA}} + \mathbf{v}_b\end{aligned}$$

that is

$$\mathbf{v}_d(z) = \frac{2A}{(n+1)h^n} (h^{n+1} - (s - z)^{n+1}) \|\mathbf{t}_b^{\text{SIA}}\|^{n-1} \mathbf{t}_b^{\text{SIA}} \quad (1.38)$$

where

$$\|\nabla_{xy} s\| = \sqrt{(\partial_x s)^2 + (\partial_y s)^2}.$$

and $\mathbf{t}_b^{\text{SIA}}$ is given by Eq. (1.37). For a sliding law on the form

$$\mathbf{v}_b = C \|\mathbf{t}_b^{\text{SIA}}\|^{m-1} \mathbf{t}_b^{\text{SIA}},$$

the basal velocity, \mathbf{v}_b , is

$$\mathbf{v}_b = -C(\rho g h)^m \|\nabla_{xy} s\|^{m-1} \nabla_{xy} s.$$

or

$$\begin{aligned}\mathbf{v} &= \mathbf{v}_d + \mathbf{v}_b \\ &= \frac{2A}{(n+1)h^n} (h^{n+1} - (s - z)^{n+1}) \|\mathbf{t}_b^{\text{SIA}}\|^{n-1} \mathbf{t}_b^{\text{SIA}} + C \|\mathbf{t}_b^{\text{SIA}}\|^{m-1} \mathbf{t}_b^{\text{SIA}}.\end{aligned} \quad (1.39)$$

The deformational velocity, \mathbf{v}_d , can also be written as

$$\mathbf{v}_d(z) = -E \|\nabla_{xy} s\|^{n-1} (h^{n+1} - (s - z)^{n+1}) \nabla_{xy} s, \quad (1.40)$$

where

$$E = \frac{2A}{n+1}(\rho g)^n.$$

The vertically integrated flux

$$\mathbf{q} = \int_b^s \rho \mathbf{v} dz,$$

is then

$$\mathbf{q}_d = \int_b^s \rho \mathbf{v}_d dz = -\frac{2\rho A}{n+2} (\rho g h \|\nabla_{xy} s\|)^{n-1} (\rho g h \nabla_{xy} s) h^2 \quad (1.41)$$

$$= \frac{2\rho A}{n+2} \|\mathbf{t}_b^{\text{SIA}}\|^{n-1} \mathbf{t}_b^{\text{SIA}} h^2, \quad (1.42)$$

and

$$\mathbf{q}_b = \int_b^s \rho \mathbf{v}_b dz = -C \rho h (\rho g h)^m \|\nabla_{xy} s\|^{m-1} \nabla_{xy} s \quad (1.43)$$

$$= C \rho h \|\mathbf{t}_b^{\text{SIA}}\|^{m-1} \mathbf{t}_b^{\text{SIA}}, \quad (1.44)$$

hence

$$\begin{aligned}\mathbf{q} &= \mathbf{q}_d + \mathbf{q}_b \\ &= \frac{2\rho A}{n+2} \|\mathbf{t}_b^{\text{SIA}}\|^{n-1} \mathbf{t}_b^{\text{SIA}} h^2 + C \rho h \|\mathbf{t}_b^{\text{SIA}}\|^{m-1} \mathbf{t}_b^{\text{SIA}},\end{aligned} \quad (1.45)$$

where \mathbf{t}_b is given by Eq. (1.37), and where we have assumed that A and ρ are independent of depth.

We can also write \mathbf{q}_d as

$$\mathbf{q}_d = -D\rho \|\nabla_{xy} s\|^{n-1} h^{n+2} \nabla_{xy} s, \quad (1.46)$$

where

$$D = \frac{2A}{n+2} (\rho g)^n. \quad (1.47)$$

The flux can also be written in terms of the deformational and basal velocities as

$$\begin{aligned} \mathbf{q} &= \mathbf{q}_d + \mathbf{q}_b \\ &= \rho h (F \mathbf{v}_d(z=s) + \mathbf{v}_b), \end{aligned}$$

with

$$F = \frac{n+1}{n+2}.$$

In the SIA/SSTREAM approximation the driving stress, $-\rho gh\partial_x s$, is always equal to the basal traction. This is because the impact of horizontal stress gradients on the force balance is not included.

The ice-thickness evolution is then calculated by solving the vertically integrated mass-conservation equation, derived in section 1.8, or

$$\rho \partial_t h + \nabla_{xy} \cdot \mathbf{q} = \rho a. \quad (1.121)$$

Because \mathbf{q} can be written explicitly in terms of h as given by (1.46), we simply solve for the thickness evolution h directly and then calculate the velocities, should those be required, afterwards using (1.40).

1.5 Recap of typically SIA and SSA scalings

The shallow ice-sheet (SIA/SSHEET) and the shallow ice-stream (SSA/SSTREAM) equations are derived in Chapters 16 and 17, respectively. Baral (1999) provides a useful overview over asymptotic theories of large-scale glacier flow. Here, we give a short overview over the main assumptions.

Both the shallow ice-sheet (SIA/SSHEET) and the shallow ice-stream (SSA/SSTREAM) are shallow-ice approximations, that is they assume $[z]/[x] = \varepsilon \ll 1$. For the mass conservation, $v_{p,p} = 0$, to be invariant, we then must have $[w]/[u] = \varepsilon$. For the kinematic boundary conditions to be invariant, we must scale time as $[t] = [x]/[u]$.

In both SIA and SSA the strain-rate tensor is, in terms of velocities, given by

$$\dot{\boldsymbol{\epsilon}} = \begin{pmatrix} \frac{\partial u}{\partial x} & \frac{1}{2} \left(\frac{\partial u}{\partial y} + \frac{\partial v}{\partial x} \right) & \frac{1}{2} \left(\frac{1}{\varepsilon} \frac{\partial u}{\partial z} + \varepsilon \frac{\partial w}{\partial x} \right) \\ \frac{1}{2} \left(\frac{\partial u}{\partial y} + \frac{\partial v}{\partial x} \right) & \frac{\partial v}{\partial y} & \frac{1}{2} \left(\frac{1}{\varepsilon} \frac{\partial v}{\partial z} + \varepsilon \frac{\partial w}{\partial y} \right) \\ \frac{1}{2} \left(\frac{1}{\varepsilon} \frac{\partial u}{\partial z} + \varepsilon \frac{\partial w}{\partial x} \right) & \frac{1}{2} \left(\frac{1}{\varepsilon} \frac{\partial v}{\partial z} + \varepsilon \frac{\partial w}{\partial y} \right) & \frac{\partial w}{\partial z} \end{pmatrix} \quad (1.48)$$

Although shallow ice-stream (SSA) stresses are usually scaled using the shallowness ratio ε , there is no reason to expect the deviatoric stresses to, for example, go to zero as $\varepsilon \rightarrow 0$ (e.g. horizontal deviatoric stresses in an ice shelf do not become smaller as the ice shelf gets longer and wider).

SSA stress scalings:

$$\boldsymbol{\tau}_{\text{SSA}} = [\sigma] \begin{pmatrix} \tau_{xx} & \tau_{xy} & \delta\tau_{xz} \\ \tau_{xy} & \tau_{yy} & \delta\tau_{yz} \\ \delta\tau_{xz} & \delta\tau_{yz} & \tau_{zz} \end{pmatrix} \quad (1.49)$$

On the other hand, the deviatoric SIA stresses should go to zero as $\varepsilon \rightarrow 0$, and the horizontal deviatoric stresses to be smaller than the vertical shear stresses. One way of expressing this is to write

$$\boldsymbol{\tau}_{\text{SIA}} = \varepsilon[\sigma] \begin{pmatrix} \varepsilon\tau_{xx} & \varepsilon\tau_{xy} & \tau_{xz} \\ \varepsilon\tau_{xy} & \varepsilon\tau_{yy} & \tau_{yz} \\ \tau_{xz} & \tau_{yz} & \varepsilon\tau_{zz} \end{pmatrix} \quad (1.50)$$

In both SIA and SSA, $[p] = [\sigma] = \rho g[z]$. Note that since $[p] = [\sigma] = \rho g[z]$, we have $[\rho g] = [p]/[z] = [p]/(\varepsilon[x])$. The effective stress, τ , is zeroth-order in SSA, but of first order, $O(\varepsilon)$, in SIA. It is actually not very usefully to discuss these orders without referring to the balances that the STREAM and SHEET assume, and, as discussed below, STREAM balances horizontal deviatoric stresses and horizontal velocity gradients, while SHEET balances vertical shear deformation and vertical shear stresses.

The scaled shallow ice-stream (SSTREAM/SSA) momentum equations are

$$\partial_x \tau_{xx} + \partial_y \tau_{xy} + \partial_z \tau_{xz} = \partial_x p , \quad (1.51)$$

$$\partial_x \tau_{xy} + \partial_y \tau_{yy} + \partial_z \sigma_{yz} = \partial_y p , \quad (1.52)$$

$$\delta^2 \partial_x \tau_{xz} + \delta^2 \partial_y \tau_{yz} + \partial_z \tau_{zz} = \partial_z p + \rho g . \quad (1.53)$$

Note that the vertical shear stresses enter the momentum balance at leading order, and that the SSA pressure, p , is not hydrostatic.

The scaled shallow ice-sheet (SSHEET/SIA) momentum equations are

$$\varepsilon^2 \partial_x \tau_{xx} + \varepsilon^2 \partial_y \tau_{xy} + \frac{\varepsilon}{\varepsilon} \partial_z \tau_{xz} = \partial_x p , \quad (1.54)$$

$$\varepsilon^2 \partial_x \tau_{xy} + \varepsilon^2 \partial_y \tau_{yy} + \frac{\varepsilon}{\varepsilon} \partial_z \sigma_{yz} = \partial_y p , \quad (1.55)$$

$$\varepsilon \partial_x \tau_{xz} + \varepsilon \partial_y \tau_{yz} + \frac{\varepsilon^2}{\varepsilon} \partial_z \tau_{zz} = \frac{1}{\varepsilon} \partial_z p + \frac{1}{\varepsilon} \rho g . \quad (1.56)$$

Note that the vertical shear stresses are the only leading order terms in the horizontal momentum balance, and that the SIA pressure, p , is hydrostatic.

In the shallow ice stream approximation (SSTREAM/SSA) we balance horizontal deviatoric stresses and horizontal strain rates, were

$$\frac{[u]}{[x]} \frac{\partial u}{\partial x} = A[\sigma]^n \tau_{xx} \quad (\text{SSA } xz\text{-term})$$

and we get the balance we aim at for

$$\frac{[u]}{[x]} = A[\sigma]^n \quad (\text{SSA balance})$$

Physically, this implies horizontal velocity gradients, $[u]/[x]$, are controlled by horizontal deviatoric stresses, noticing that in the SSA scalings above $[\tau] = [\sigma]$. For the xz term in the constitutive relationship we then obtain

$$\frac{[u]}{[x]} \frac{1}{2} \left(\frac{1}{\varepsilon} \frac{\partial u}{\partial z} + \varepsilon \frac{\partial w}{\partial x} \right) = A[\sigma]^n \delta \tau_{xz} \quad (\text{SSA } xz\text{-term})$$

or

$$\frac{1}{2} \left(\frac{\partial u}{\partial z} + \varepsilon^2 \frac{\partial w}{\partial x} \right) = \varepsilon \delta \tau_{xz} \quad (\text{SSA } xz\text{-term})$$

Traditionally, in the SSA approximation we set $\delta = \varepsilon$, in which case we must conclude that $\partial u / \partial z = O(\varepsilon^2)$, and the horizontal velocity therefore independent of depth.

In the shallow ice-sheet approximation (SIA) we aim at balancing the vertical shearing of the ice with vertical shear stresses, were

$$\frac{[u]}{[x]} \left(\frac{1}{\varepsilon} \frac{\partial u}{\partial z} + \varepsilon \frac{\partial w}{\partial x} \right) = A[\sigma]^n \varepsilon^n \tau_{xz} \quad (\text{SIA } xz\text{-term})$$

and the SIA balance therefore is

$$\frac{[u]}{[x]} = A[\sigma]^n \varepsilon^{n+1} \quad (\text{SIA balance})$$

or

$$[u] = A[\tau]^n [z] .$$

The physical picture here is that of thin-film flow controlled by shearing across the thickness of the layer. For the SIA xx term of the constitutive relationships, we find that

$$\frac{[u]}{[x]} \frac{\partial u}{\partial x} = A \varepsilon^n [\sigma]^n \varepsilon^2 \tau_{xx} \quad (\text{SIA } xx\text{-term})$$

or

$$\frac{[u]}{A[x][\sigma]^n \varepsilon^{n+1}} \frac{\partial u}{\partial x} = \varepsilon \tau_{xx}$$

and therefore $\partial u / \partial x = O(\varepsilon)$.

The effective SSA and SIA strain rates are

$$\dot{\epsilon}_{\text{SSA}} = \sqrt{(\partial_x u_b)^2 + (\partial_y v_b)^2 + \partial_x u_b \partial_y v_b + (\partial_x v_b + \partial_y u_b)^2 / 4} \quad (1.57)$$

and

$$\dot{\epsilon}_{\text{SIA}} = \sqrt{(\partial_z u_d)^2 + (\partial_z v_d)^2} \quad (1.58)$$

The SIA velocities are calculated by first observing that $p = \rho g(s - z)$, using Eq. (1.56), and therefore $\tau_{xz} = \rho g(s - z) \partial_x s$ from Eq. (1.54), and then use the flow law together with Eq. (1.58) to calculate the deformational velocity components (u_d and v_d) as a function of depth. This is a reasonable approximation if the horizontal deviatoric stresses are small.

1.5.1 BCs for small slopes

Typically, ice-flow approximations assume small slopes and/or small aspect ratios, i.e. $\varepsilon = [z]/[x] \ll 1$. As shown in Chapter 17 the stress conditions at the surface $\sigma \hat{n} = \mathbf{0}$ are to second order in ε

$$-\sigma_{xx} \partial_x s - \tau_{xy} \partial_y s + \tau_{xz} = 0, \quad (1.58)$$

$$-\tau_{xy} \partial_x s - \sigma_{yy} \partial_y s + \tau_{yz} = 0, \quad (1.59)$$

$$\sigma_{zz} = 0, \quad (1.60)$$

for $z = s(x, y)$. Using

$$\sigma_{xx} = 2\tau_{xx} + \tau_{yy} + \sigma_{zz}, \quad (1.54)$$

together with (1.60), and therefore

$$\sigma_{xx} = 2\tau_{xx} + \tau_{yy} \quad (\text{at } z = s(x, y)).$$

We can also write the upper-surface stress conditions, Eqs. (1.58) and (1.59), as

$$-(2\tau_{xx} + \tau_{yy}) \partial_x s - \tau_{xy} \partial_y s + \tau_{xz} = 0, \quad (1.59)$$

$$-\tau_{xy} \partial_x s - (2\tau_{yy} + \tau_{xx}) \partial_y s + \tau_{yz} = 0, \quad (1.60)$$

for $z = s(x, y)$, or in terms of velocities, as

$$0 = \partial_x s (4\partial_x u + 2\partial_y v) + \partial_y s (\partial_x v + \partial_y u) - \partial_z u, \quad (1.61)$$

$$0 = \partial_y s (4\partial_y v + 2\partial_x u) + \partial_x s (\partial_x u + \partial_y v) - \partial_z v. \quad (1.62)$$

for $z = b(x, y)$, where we have used $\tau_{pq} = 2\eta(v_{p,q} + v_{q,p})$ and $\partial_x w$ and $\partial_y w$ being of second order, or smaller.

At the lower surface, $z = b(x, y)$, we have the sliding law

$$u_b = C \|t_b\|^{m-1} t_{bx}, \quad (1.744)$$

$$v_b = C \|t_b\|^{m-1} t_{by}, \quad (1.745)$$

where, to second order

$$t_{bx} = \partial_x b (\sigma_{zz} - \sigma_{xx}) - \partial_y b \tau_{xy} + \tau_{xz}, \quad (1.741)$$

$$t_{by} = \partial_y b (\sigma_{zz} - \sigma_{yy}) - \partial_x b \tau_{xy} + \tau_{yz}, \quad (1.742)$$

for $z = b(x, y)$. Again using

$$\sigma_{xx} = 2\tau_{xx} + \tau_{yy} + \sigma_{zz}, \quad (1.54)$$

we can also write the basal boundary conditions, Eqs. (1.741) and (1.742), as

$$t_{bx} = -\partial_x b (2\tau_{xx} + \tau_{yy}) - \partial_y b \tau_{xy} + \tau_{xz}, \quad (1.63)$$

$$t_{by} = -\partial_y b (2\tau_{yy} + \tau_{xx}) - \partial_x b \tau_{xy} + \tau_{xz}. \quad (1.64)$$

for $z = b(x, y)$, or in terms of the velocities as

$$t_{bx} = -\eta(\partial_x b(4\partial_x u + 2\partial_y v) - \partial_y b(\partial_x v + \partial_y u) + \partial_z u) , \quad (1.65)$$

$$t_{by} = -\eta(\partial_y b(4\partial_y v + 2\partial_x u) - \partial_x b(\partial_x u + \partial_y v) + \partial_z v) , \quad (1.66)$$

for $z = b(x, y)$, where we have used $\tau_{pq} = 2\eta\dot{\epsilon}_{pq}$ and $\partial_x w$ and $\partial_y w$ being of second order, or smaller.

These small-slope BCs are used in both SIA and SSA, but in the case of SIA where horizontal deviatoric stresses are small, they simplify to

$$\tau_{xz} = 0,$$

$$\tau_{yz} = 0,$$

$$\sigma_{zz} = 0,$$

for $z = s(x, y)$, and

$$t_{bx} = \tau_{xz} ,$$

$$t_{by} = \tau_{yz} ,$$

at $z = b(x, y)$.

1.6 Three dimensional formulation, assuming cryostatic vertical stresses

Alternatively to vertically integrated formulations, and as a possible path towards a hybrid formulation, we can include the effect of horizontal stresses on the vertical shear stresses using the full form of the x and y momentum balance, while assuming that $\partial_x \tau_{xz} + \partial_y \tau_{yz}$ are small compared to $\partial_z \sigma_{zz}$ (i.e. the second-order δ terms in Eq. (1.53) dropped), that is

$$\partial_x \sigma_{xx} + \partial_y \tau_{xy} + \partial_z \tau_{xz} = 0 , \quad (1.12)$$

$$\partial_x \tau_{xy} + \partial_y \sigma_{yy} + \partial_z \tau_{yz} = 0 , \quad (1.13)$$

$$\partial_z \sigma_{zz} = \rho g . \quad (1.67)$$

and therefore

$$\sigma_{zz} = -\rho g(s - z) . \quad (1.68)$$

Hence, the pressure is non-hydrostatic and the vertical stresses, σ_{zz} , are lithostatic/cryostatic. Note that using

$$\sigma_{xx} = 2\tau_{xx} + \tau_{yy} + \sigma_{zz} , \quad (17.54)$$

and (1.68), the system (1.12) and (1.13) can be written as

$$\partial_x(2\tau_{xx} + \tau_{yy}) + \partial_y \tau_{xy} + \partial_z \tau_{xz} = \rho g \partial_x s , \quad (1.69)$$

$$\partial_y(2\tau_{yy} + \tau_{xx}) + \partial_x \tau_{xy} + \partial_z \tau_{yz} = \rho g \partial_y s , \quad (1.70)$$

or equivalently using

$$\tau_{ij} = 2\eta\dot{\epsilon}_{ij} , \quad (1.7)$$

as

$$\partial_x(2\eta(2\partial_x u + \partial_y v)) + \partial_y(\eta(\partial_x v + \partial_y u)) + \partial_z(\eta\partial_z u) = \rho g \partial_x s , \quad (1.71)$$

$$\partial_y(2\eta(2\partial_y v + \partial_x u)) + \partial_x(\eta(\partial_x v + \partial_y u)) + \partial_z(\eta\partial_z v) = \rho g \partial_y s . \quad (1.72)$$

where we have also simplified the strain-rate tensor by dropping $\partial_x w$ and $\partial_y w$ (see 1.48). The resulting system, which is fully three-dimensional, is usually referred to as the Blatter-Pattyn model (Blatter, 1995; Pattyn, 2003), and is sometimes used together with the stress boundary conditions for small slopes (Eqs. 17.38, 17.39, 17.40, 17.44 and 17.45). The original derivation of the Blatter-Pattyn system by Blatter (1995), is arguably somewhat inconsistent as the terms $\partial_x \tau_{xz}$ and $\partial_y \tau_{yz}$ appear to be dropped without a full justification, however Dukowicz et al. (2010, 2011) shows that this is required for the dissipation rate to be positive.

1.7 Vertical integration, assuming cryostatic vertical stress state

Integrating the x component of the momentum equations, Eq. (1.12), over the depth from $z = b$ to $z = s$, and changing the order of differentiation and integration gives

$$\begin{aligned} 0 &= \partial_x \int_b^s \sigma_{xx} dz + \partial_y \int_b^s \tau_{xy} dz \\ &\quad - \sigma_{xx}(s) \partial_x s - \tau_{xy}(s) \partial_y s + \tau_{xz}(s) \\ &\quad + \sigma_{xx}(b) \partial_x b + \tau_{xy}(b) \partial_y b - \tau_{xz}(b) \end{aligned} \quad (1.73)$$

The second line is identically zero due to the small-amplitude boundary condition Eq. (17.38), and the third line can be written as $-t_{bx} + \partial_x b \sigma_{zz}(b)$, giving

$$0 = \partial_x \int_b^s \sigma_{xx} dz + \partial_y \int_b^s \tau_{xy} dz - t_{bx} + \partial_x b \sigma_{zz}(b). \quad (1.74)$$

Using (17.54)

$$\sigma_{xx} = 2\tau_{xx} + \tau_{yy} + \sigma_{zz}, \quad (1.75)$$

the (1.73) term, involving vertical integration over σ_{xx} , can be written (see also page 271) as

$$\int_b^s \sigma_{xx} dz = \int_b^s (2\tau_{xx} + \tau_{yy}) dz + \sigma_{zz}(b) (\partial_x s - \partial_x b)$$

and Eq. (1.74), hence, becomes

$$\partial_x \int_b^s (2\tau_{xx} + \tau_{yy}) dz + \partial_y \int_b^s \tau_{xy} dz - t_{bx} = \rho g h \partial_x s \quad (1.75)$$

$$\partial_y \int_b^s (2\tau_{yy} + \tau_{xx}) dz + \partial_x \int_b^s \tau_{xy} dz - t_{by} = \rho g h \partial_y s \quad (1.76)$$

where we have used $\sigma_{zz}(z = b) = -\rho g h$, and where have added the corresponding equation for the y direction.

Equations (1.75) and (1.76) have a long history in glaciology. These same equations are, for example, Eqs. (14) and (15) in Van Der Veen and Whillans (1989)¹ and these equations, or simple variants thereof, can be found in Kamb and Echelmeyer (1986); Echelmeyer et al. (1986) and various other papers and books before that.² Eqs. (1.75) and (1.76) are usually solved as functions of velocities, with velocities and pressure being the primitive variables, and, generally, solving Eqs. (1.75) and (1.76) will involve a vertical integration.³ Similar ideas, but arguably more general as the $\partial_z \tau_{xz}$ terms are included, are found in Budd (1969) and Budd (1970), see for example Eq. 20 in Budd (1970) and Eq. 10 in Nye (1969).

Evaluating the integrals in Eqs. (1.75) and (1.76) for non-Newtonian media such as ice, requires knowing the effective viscosity (or the effective strain rates) as a function of depth, and that in turns requires knowledge of the vertical shear stresses (or the vertical shear strain rates). Hence, although τ_{xz} and τ_{yx} , (or $\dot{\epsilon}_{xz}$ $\dot{\epsilon}_{yz}$) do not appear explicitly in Eqs. (1.75) and (1.76), these equations can not be solved without knowing the vertical shear stresses. Here we can use an iterative procedure where, once we have solved Eqs. (1.75) and (1.76) using an initial guess for τ_{xz} and τ_{yz} , we re-calculate the vertical shear stresses, τ_{xz} and τ_{yz} , using again the the momentum equations, that is

$$\partial_x \sigma_{xx} + \partial_y \tau_{xy} + \partial_z \tau_{xz} = 0, \quad (1.49)$$

¹Although Van Der Veen and Whillans (1989) appear to be wrong to state that this equation is exact and can be arrived at without any approximations. The approximations are: a) $\partial_x \tau_{xz}$ and $\partial_y \tau_{yz}$ small compared to $\partial_z \tau_{zz}$ and therefore $\sigma_{zz} = \rho g(s - z)$, and b) small-slopes in the kinematic boundary conditions.

²In the shallow ice-stream approximation, where τ_{xx} , τ_{yy} and τ_{xy} are all independent of depth, equation (1.75) simplifies to

$$\begin{aligned} \partial_x (2h\tau_{xx} + h\tau_{yy}) + \partial_y (h\tau_{xy}) - t_{bx} &= \rho g h \partial_x s, \\ \partial_y (2h\tau_{yy} + h\tau_{xx}) + \partial_x (h\tau_{xy}) - t_{by} &= \rho g h \partial_y s, \end{aligned}$$

which is Eq. (1.18) for $\alpha = 0$ and $\partial_x \rho = 0$. In the case of the shallow ice-sheet approximation, Eqs. (1.75) and (1.76) simply become

$$t_b = -\rho g h \nabla_{xy} s,$$

which is Eq. (1.37).

³For the SSTREAM, the integration can be done analytically, and is in fact trivial, as all terms are independent of depth, and in the SSHEET approximation, no integration is required because all related terms are identically zero.

giving

$$\begin{aligned}\partial_z \tau_{xz} &= -\partial_x \sigma_{xx} - \partial_y \tau_{xy} && \text{(from 17.49)} \\ &= -\partial_x (2\tau_{xx} + \tau_{yy} + \sigma_{zz}) - \partial_y \tau_{xy} && \text{(using 17.54)} \\ &= -\rho g \partial_x s - \partial_x (2\tau_{xx} + \tau_{yy}) - \partial_y \tau_{xy}\end{aligned}\quad (1.77)$$

and then integrating

$$\tau_{xz}(z) = -\rho g(s-z) \partial_x s - \int_b^z (\partial_x (2\tau_{xx} + \tau_{yy}) + \partial_y \tau_{xy}) dz + K \quad (1.78)$$

where K needs to be determined from the boundary conditions. We find a similar equation for τ_{yz} . The vertical velocity profile is then obtained by integrating

$$u(z) = 2 \int_b^z A \tau^{n-1} \tau_{xz} dz + u_b \quad (1.79)$$

where

$$\tau(z) = \sqrt{\tau_{xx}^2 + \tau_{yy}^2 + \tau_{xx} \tau_{yy} + \tau_{xy}^2 + \tau_{xz}^2(z) + \tau_{yz}^2(z)}. \quad (1.80)$$

Again, while this procedure has here been described in terms of the stresses, this system would typically be written down, and solved, in terms of the velocities using the flow law on the form

$$\tau_{ij} = A^{-1/n} \dot{\epsilon}^{(1-n)/n} \dot{\epsilon}_{ij}, \quad (1.188)$$

where

$$\dot{\epsilon} = \sqrt{(\partial_x u)^2 + (\partial_y v)^2 + \partial_x u \partial_y v + (\partial_x v + \partial_y u)^2/4 + (\partial_z u)^2/4 + (\partial_z v)^2/4}. \quad (1.81)$$

To my knowledge the above procedure of exactly solving Eq. (1.75) and (1.76) is almost never used. Rather, typically some additional simplifications are made to make the vertical integration involved less onerous (examples provided below).

1.7.1 Simplifications of the vertically-integrated system

Various suggestions have been made on how best to simplify, or get rid of altogether, the vertical integration in Eq. (1.75) and (1.76), and/or the additional vertical integration of the vertical shear stress, (1.78), and velocity, (1.79). To simplify the notation I here just write out the equations for the flow-line case, where $\tau_{yy} = \tau_{xy} = 0$, and Eq (1.75) reduces to

$$2 \partial_x \int_b^s \tau_{xx} dz - t_{bx} = \rho g h \partial_x s \quad (1.82)$$

This equation is generally solved in terms of the velocity and we can assume that we have a sliding law relating the basal traction to basal velocity, that is

$$t_{bx} = f(u_b)$$

where f is some given function (the sliding law). The most logical approach would then presumably be to use the constitutive law, Eq. (1.5), to write τ_{xx} in terms of the velocities as

$$\begin{aligned}\tau_{xx} &= A^{-1/n} \dot{\epsilon}^{(1-n)/n} \dot{\epsilon}_{xx} \\ &= \frac{1}{2} A^{-1/n} ((\partial_x u)^2 + (\partial_z u)^2/4)^{(1-n)/(2n)} \partial_x u\end{aligned}$$

insert this expression into Eq. (1.82) and evaluate the integral in terms of the unknown $u(x, z)$. This would give a value for t_{bx} .

However, several papers in the past have here used the implicit form of the flow law

$$\tau_{xx} = A^{-1} \tau^{n-1} \dot{\epsilon}_{xx}, \quad (1.6)$$

i.e. with the elements of the deviatoric stress tensor on both sides, and where here the effective stress is

$$\tau = \sqrt{(\tau_{xx}^2 + \tau_{xz}^2)},$$

that is

$$\tau_{xx} = A^{-1} (\tau_{xx}^2 + \tau_{xz}^2)^{(1-n)/2} \partial_x u, \quad (1.83)$$

resulting in an implicit equation for τ_{xx} in terms of u and τ_{xz} .

1.7.2 Budd simplification

One simplification, which I believe might originally be due to Budd (1970), is simply to assume that $\tau_{xz}(z) = \rho g(h - z)\partial_x s$, in which case Eq. (1.83) reads

$$\tau_{xx}(z) = A^{-1}(\tau_{xx}^2 + (\rho g(h - z)\partial_x s)^2)^{(1-n)/2}\partial_x u \quad (1.84)$$

which can solved for $\tau_{xx}(z)$ for a given $\partial_x u$. Knowing τ_{xx} as a function of depth, then allows us to solve (1.82) for t_{bx} . If we use a sliding law on the form $t_{bx} = f(u_b)u_b$, we would solve for u_b in this step. There is now no need to do the integration in (1.78) as we have already assumed τ_{xz} is known as a function of depth, and we then calculate the velocities through vertical integration using (1.79) and u_b we calculated previously when solving (1.82). This could be solved using an iterative procedure where, once we have (re) calculated $u(x, z)$ using (1.79), then re-solve Eq. (1.84) for τ_{xx} using our new estimate of $u(x, z)$.

1.7.3 L1L2

Another approach, which most likely was originally presented by Hindmarsh (2004) and then further explored by Schoof and Hindmarsh (2010), is to approximate (1.83) as

$$\tau_{xx} = A^{-1} (\tau_{xx}^2 + \tau_{xz}^2(b))^{(1-n)/2} \partial_x u_b \quad (1.85)$$

where, similar to Budd (1970), it is assumed that

$$\tau_{xz}(z = b) = \tau_{xz}^{\text{SIA}}(z = b) = \rho g h \partial_x s .$$

Thus, when calculating the effective stress, τ , the vertical shear stress, τ_{xz} , is evaluated at the base assuming SIA force balance, and the horizontal velocity gradient is similarly approximated by its value at the base. This assumption greatly (over) simplifies the solution procedure as τ_{xx} is now independent of depth. To summarise, using this approximation, we solve Eq. (1.82), which we write on on the form

$$4\partial_x \int_b^s \eta \partial_x u_b dz - f(u_b)u_b = \rho g h \partial_x s , \quad (1.86)$$

for the basal velocity, u_b , where have used

$$\tau_{xx} = 2\eta \partial_x u_b ,$$

where the effective viscosity, η , is now a solution to the implicit equation

$$2\eta = A^{-1} (4\eta^2(\partial_x u_b)^2 + (\rho g h \partial_x s)^2)^{(1-n)/2} , \quad (1.87)$$

which follows from (1.85). Note that if A is independent of depth, η is independent of depth as well and the vertical integration in (1.86) is trivial and we have

$$4\partial_x (h\eta \partial_x u_b) - f(u_b)u_b = \rho g h \partial_x s , \quad (1.88)$$

which is formally identical to the SSA/SSTREAM equations, the only difference being that the effective viscosity is now determined by solving Eq. (1.87), rather than as $\eta = \frac{1}{2}A^{-1/n}|\partial_x u_b|^{1-1/n}$.

We then determine τ_{xz} as a function of depth, using (1.78), which now reads

$$\begin{aligned} \tau_{xz}(z) &= -\rho g(s - z)\partial_x s - 2 \int_b^z \partial_x \tau_{xx} dz , \\ &= -\rho g(s - z)\partial_x s - 2(z - b)\partial_x \tau_{xx} \end{aligned}$$

because we have assumed that $\tau_{xz}(z = b) = \rho g h \partial_x s$, and therefore the integration constant K in Eq. (1.78) equal to zero, and because all horizontal stresses are independent of depth, or rather, where we simply chose to use the values at the bed. We then calculate the deformational velocity using (1.79), which here has the form

$$u(z) = 2 \int_b^z A \tau^{n-1} \tau_{xz} dz + u_b , \quad (1.89)$$

where, as in Eq. (1.80), the effective stress is given by

$$\tau(z) = \sqrt{\tau_{xx}^2 + \tau_{xz}^2(z)} . \quad (1.90)$$

It appears that at least in some implementations of the L1L2 method, the deformational velocity, $u_d(z) = u(z) - u_b$, is however not included (Cornford et al., 2013).

1.7.4 The Goldberg Variation

Goldberg (2011) suggested another variation, where we solve directly for the mean vertically averaged horizontal velocities, \bar{u} and \bar{v} . He writes (Eqs. 20 and 21 in Goldberg (2011))

$$h^{-1}\partial_x(2\bar{\eta}h(2\partial_x\bar{u}+\partial_y\bar{v}))+h^{-1}\partial_y(\bar{\eta}h(\partial_x\bar{v}+\partial_y\bar{u}))+\partial_z(\eta\partial_zu)=\rho g\partial_xs, \quad (1.91)$$

$$h^{-1}\partial_y(2\bar{\eta}h(2\partial_y\bar{v}+\partial_x\bar{u}))+h^{-1}\partial_x(\bar{\eta}h(p_x\bar{v}+\partial_u\bar{u}))+\partial_z(\eta\partial_zv)=\rho g\partial_ys, \quad (1.92)$$

which he derives from a variational principle, where $\bar{\eta}$ is the vertical average

$$\bar{\eta}=\frac{1}{h}\int_b^s\eta(z)dz,$$

of

$$\eta=\frac{1}{2A^{1/n}}\left((\partial_x\bar{u})^2+(\partial_y\bar{v})^2+\partial_x\bar{u}\partial_y\bar{v}+(\partial_x\bar{v}+\partial_y\bar{u})^2/4+(\partial_zu_d)^2/4+(\partial_zv_d)^2/4\right)^{\frac{1-n}{2n}}.$$

Note that in Eqs. (1.91) and (1.92) all variables in all terms, except $\partial_z(\eta\partial_zu)$ and $\partial_z(\eta\partial_zv)$, have been replaced by the vertically-integrated counterparts. The advantage of this formulation/ansatz is that it can now easily be vertically integrated, and using the same manipulations of the $\partial_z\tau_{xz}$ and $\partial_z\tau_{yz}$ terms as above in section 1.7 we arrive at

$$\partial_x(2h\bar{\eta}(\partial_x\bar{u}+\partial_y\bar{v}))+\partial_y(h\eta(\partial_x\bar{v}+\partial_y\bar{u}))-\beta^2u_b=\rho gh\partial_xs, \quad (1.93)$$

$$\partial_y(2h\bar{\eta}(\partial_y\bar{v}+\partial_x\bar{u}))+\partial_x(h\eta(\partial_y\bar{u}+\partial_x\bar{v}))-\beta^2v_b=\rho gh\partial_ys. \quad (1.94)$$

One of the consequences of this formulation is that from comparing Eq. (1.93) with Eq. (1.91), we must conclude that

$$-\beta^2u_b=h\partial_z(\eta\partial_zu), \quad (1.95)$$

that is

$$-\beta^2u_b=\partial_z\tau_{xz}, \quad (1.96)$$

using $\tau_{xz}=\eta\partial_zu$. The left-hand side of (1.96) is independent of z , so the implication must be that $\eta\partial_zu$ is too and that τ_{xz} is therefore a linear function of depth. This is plausible and strictly true in both the SSA and the SIA limits.

Integrating (1.95)

$$-\int_z^s\beta^2u_bdz'=h\int_z^s\partial_z(\eta\partial_zu)dz',$$

gives

$$\begin{aligned}-\beta^2u_b(s-z)&=h\eta(s)\partial_zu|_s-h\eta(z)\partial_zu|_z \\ &=h\tau_{xz}(s)-h\tau_{xz}(z)\end{aligned}$$

If $\tau_{xz}(s)=0$, then

$$\eta\partial_zu=\beta^2u_b(s-z)/h, \quad (1.97)$$

giving a very simple expression for the vertical shear stress, τ_{xz} , where τ_{xz} varies linearly with depth, and is equal to zero at the upper surface and equal to β^2u_b at the lower surface.⁴

Integrating (1.97)

$$\int_b^z\partial_zudz'=\frac{\beta^2u_b}{h}\int_b^z\frac{s-z'}{\eta(z')}dz',$$

gives

$$u(z)-u_b=\frac{\beta^2u_b}{h}\int_b^z\frac{s-z'}{\eta(z')}dz',$$

⁴However, the stress conditions at the surface, $\sigma\hat{n}=\mathbf{0}$, are (to second order in ε)

$$-\sigma_{xx}\partial_xs-\tau_{xy}\partial_ys+\tau_{xz}=0, \quad (17.38)$$

$$-\tau_{xy}\partial_xs-\sigma_{yy}\partial_ys+\tau_{yz}=0, \quad (17.39)$$

$$\sigma_{zz}=0, \quad (17.40)$$

for $z=s(x,y)$, and therefore it is incorrect to assume $\tau_{xz}(s)=0$ as Goldberg (2011) appears to do in his Eq. (31). However, Goldberg (2011) writes the upper stress BCs as $\partial_zu=0$ and $\partial_zv=0$, i.e. assumes that $\tau_{xz}(s)=\tau_{yz}(s)=0$ (his Eq. (22)). So in his derivation everything is consistent, but the questions remains why he assumes $\tau_{xz}(s)=\tau_{yz}(s)=0$. He also appears to make a similar simplification for the basal stress BCs (his Eq. (23)).

or

$$u(z) = u_b \left(1 + \frac{\beta^2}{h} \int_b^z \frac{s - z'}{\eta(z')} dz' \right). \quad (1.98)$$

We can integrate both sides once again to determine the mean velocity

$$\bar{u} = \frac{1}{h} \int_b^s u(z') dz'$$

and arrive at

$$\bar{u} = u_b \left(1 + \frac{\beta^2}{h^2} \int_s^b \int_b^z \frac{s - z'}{\eta(z')} dz' dz \right).$$

This provides us with a relationship between the mean vertically average velocity, \bar{u} , and the basal velocity, u_b , and we can now replace u_b and v_b in Eqs. (1.93) and (1.94) with \bar{u} and \bar{v} , respectively, by simply redefining β^2 accordingly. We therefore solve exactly the same equations as we would solve in the SSA, the only change being that the effective viscosity is calculated somewhat differently. In the Goldberg Variation, the effect of τ_{xz} and τ_{yz} terms on the effective stress and the effective viscosity are included, whereas in the SSA these terms are dropped.

From (1.98) it might appear that $u(z)$ will be zero for $u_b = 0$. However, this is not correct as in that limit the basal boundary condition must be modified. We can do this easily by simply replacing the product $\beta^2 u_b$ with $\tau_{xz}(b)$. Note, however, that it appears strictly speaking incorrect, or at least somewhat inaccurate, to do so as this implies $t_{bx} = \tau_{xz}(b)$, which while generally correct in the SIA limit, is only correct in the SSA limit for almost flat lower surfaces. But that would imply variations in basal topography slopes to be smaller than $[z]/[x]$, which seems unnecessarily restrictive.

Alternative approach #1

When deriving Eq. (1.75) and (1.76), no assumptions were made about the vertical shear stresses τ_{xz} and τ_{yz} . We can see from (1.51) and (1.52), that in the shallow ice-stream approximation τ_{xz} and τ_{yz} are linear functions of depth, and the same holds of course for the shallow ice-sheet approximation where they are identically equal to zero.

We solve the SSA equations, without any modifications,

$$\partial_x(h(2\tau_{xx} + \tau_{yy})) + \partial_y(h\tau_{xy}) - t_{bx} = \rho gh\partial_x s \quad (1.99)$$

$$\partial_y(h(2\tau_{yy} + \tau_{xx})) + \partial_x(h\tau_{xy}) - t_{by} = \rho gh\partial_y s \quad (1.100)$$

with

$$t_{bx} = f(\mathbf{v})u_b \quad (1.101)$$

$$t_{by} = f(\mathbf{v})v_b \quad (1.102)$$

where $f : \mathbb{R}^3 \rightarrow \mathbb{R}$, is a given scalar function. Solving the SSA equations gives the basal sliding velocity, \mathbf{v}_b . We then determine the vertical shear stress distribution by assuming a linear variation with depth, and where the upper and lower surface shear stresses are given by the SSA solution, that is

$$\tau_{xz}(z = s) = (2\tau_{xx} + \tau_{yy})\partial_x s + \tau_{xy}\partial_y s, \quad (1.103)$$

$$\tau_{yz}(z = s) = \tau_{xy}\partial_x s + (2\tau_{yy} + \tau_{xx})\partial_y s, \quad (1.104)$$

at $z = s(x, y)$, (see 1.59 and 1.60), and (see 1.63 and 1.64)

$$\tau_{xz}(z = b) = t_{bx} + \partial_x b(2\tau_{xx} + \tau_{yy}) + \partial_y b\tau_{xy}, \quad (1.105)$$

$$\tau_{yz}(z = b) = t_{by} + \partial_y b(2\tau_{yy} + \tau_{xx}) + \partial_x b\tau_{xy}. \quad (1.106)$$

for $z = b(x, y)$.

Linear vertical shear stress variation with depth

$$\tau_{xz}(z) = \tau_{xz}^s + (\tau_{xz}^b - \tau_{xz}^s)(s - z)/h$$

$$\tau_{yz}(z) = \tau_{yz}^s + (\tau_{yz}^b - \tau_{yz}^s)(s - z)/h$$

and

$$\tau(z) = \tau_{SIA} = \sqrt{\tau_{xz}^2(z) + \tau_{yz}^2(z)}$$

$$\partial_z u = 2A\tau^{n-1} \tau_{xz} .$$

$$u = 2A \int_b^z \tau(z')^{n-1} \tau_{xz}(z') dz' + u_b$$

$$q = 2\rho \int_b^s \int_b^z A\tau(z')^{n-1} \tau_{xz}(z') dz' dz + \rho h u_b$$

Alternative approach #2

We solve the SSA equations, without any modifications,

$$\partial_x(h(2\tau_{xx} + \tau_{yy})) + \partial_y(h\tau_{xy}) - t_{bx} = \rho gh\partial_x s \quad (1.107)$$

$$\partial_y(h(2\tau_{yy} + \tau_{xx})) + \partial_x(h\tau_{xy}) - t_{by} = \rho gh\partial_y s \quad (1.108)$$

and the SSA expression for the effective stress,

$$\tau = \tau_{SSA} = \tau \sqrt{\tau_{xx}^2 + \tau_{yy}^2 + \tau_{xx}\tau_{yy} + \tau_{xy}^2} . \quad (1.109)$$

with

$$t_{bx} = f(\mathbf{v})u_b \quad (1.110)$$

$$t_{by} = f(\mathbf{v})v_b \quad (1.111)$$

where $f : \mathbb{R}^3 \rightarrow \mathbb{R}$, is a given scalar function (mapping into the scalar field of real numbers), and where This gives us the basal velocity, \mathbf{v}_b .

The small amplitude boundary conditions give

$$\tau_{xz}(z = s) = \partial_x s (2\tau_{xx} + \tau_{yy}) + \partial_y s \tau_{xy} , \quad (1.112)$$

$$\tau_{yz}(z = s) = \partial_y s (2\tau_{yy} + \tau_{xx}) + \partial_x s \tau_{xy} , \quad (1.113)$$

$$\tau_{xz}(z = b) = t_{bx} + \partial_x b (2\tau_{xx} + \tau_{yy}) + \partial_y b \tau_{xy} , \quad (1.114)$$

$$\tau_{yz}(z = b) = t_{by} + \partial_y b (2\tau_{yy} + \tau_{xx}) + \partial_x b \tau_{xy} . \quad (1.115)$$

We now make the approximation,

$$\tau_{xz}(z) = t_{bx} (s - z)/h , \quad (1.116)$$

$$\tau_{yz}(z) = t_{by} (s - z)/h \quad (1.117)$$

i.e. we make the approximations, both correct in the SIA limit, that $\tau_{xz}(z = s) = 0$ and $\tau_{xz}(z = b) = t_{bx}$, and that the variation in vertical shear stresses with depth is linear, correct in both the SIA and the SSA limits. We then further consider the SIA limit where

$$\tau(z) = \tau_{SSA}(z) = \sqrt{\tau_{xz}^2 + \tau_{yz}^2} \quad (1.118)$$

which we can also write as

$$\tau_{SIA} = \sqrt{t_{bx}^2 + t_{by}^2} (s - z)/h$$

In this limit, the flow law

$$\dot{\epsilon}_{ij} = A(T) \tau_{SIA}^{n-1} \tau_{ij} , \quad (1.7.5)$$

implies

$$\begin{aligned} \partial_z u &= 2A\tau_{SSA}^{n-1} \tau_{xz} \\ &= 2A ((\tau_{xz}^b)^2 + (\tau_{yz}^b)^2)^{(n-1)/2} \tau_{xz} ((s - z)/h)^n \end{aligned}$$

Integrating, and assuming A does not vary with depth, we then arrive at

$$\begin{aligned}\mathbf{v} &= \frac{2A}{h^n} ((\tau_{xz}^b)^2 + (\tau_{yz}^b)^2)^{(n-1)/2} \mathbf{t}_b^{\text{SSA}} \int_b^z (s - z')^n dz' + \mathbf{v}_b \\ &= \frac{2A}{(n+1)h^n} ((\tau_{xz}^b)^2 + (\tau_{yz}^b)^2)^{(n-1)/2} \mathbf{t}_b^{\text{SSA}} [-(s - z')^{n+1}]_b^z + \mathbf{v}_b \\ &= \frac{2A}{(n+1)h^n} \|\mathbf{t}_b^{\text{SSA}}\|^{(n-1)/2} \mathbf{t}_b^{\text{SSA}} (h^{n+1} - (s - z)^{n+1}) + \mathbf{v}_b\end{aligned}$$

that is

$$\begin{aligned}\mathbf{v} &= \mathbf{v}_d + \mathbf{v}_b \\ &= \frac{2A}{(n+1)h^n} (h^{n+1} - (s - z)^{n+1}) \|\mathbf{t}_b\|^{n-1} \mathbf{t}_b + \mathbf{v}_b^{\text{SSA}}\end{aligned}$$

To summarise, the velocity and the vertically integrated flux are, hence,

$$\mathbf{v} = \frac{2A}{(n+1)h^n} (h^{n+1} - (s - z)^{n+1}) \|\mathbf{t}_b\|^{n-1} \mathbf{t}_b + \mathbf{v}_b \quad (1.119)$$

$$\mathbf{q} = \frac{2\rho A}{n+2} \|\mathbf{t}_b\|^{n-1} \mathbf{t}_b h^2 + \rho \mathbf{v}_b h, \quad (1.120)$$

where basal drag, \mathbf{t}_b , and the basal velocity, \mathbf{v}_b , are determined by solving the unmodified SSA system (1.107) and (1.108), and where the effective stress is given by Eq. (1.109). Anticipating that in the SIA limit the shear stresses dominate horizontal deviatoric stresses, we have approximated the effective stress by Eq. (1.118) when calculating the SIA contribution, allowing for an analytical vertical integration.

The resulting velocities and fluxes are correct in both the SIA and the SSA limits. In the SSA limit — where horizontal deviatoric stresses are large compared to vertical shear stresses but the vertical shear stresses appear in the stress balance at leading order — we have the limit $\|\mathbf{t}_b\| \rightarrow 0$, and therefore the SSA solutions for the velocity $\mathbf{v} = \mathbf{v}_b$ and the ice flux, $\mathbf{q} = \rho \mathbf{v} h$. In the SIA limit, where horizontal deviatoric stresses can be ignored, Eqs. (1.99) and (1.100) imply $\mathbf{t}_b = \rho g h \nabla s$ which agrees with the SIA expression (1.37) and the velocity and vertically integrated flux is identical to (1.38) and (1.42), respectively.

1.8 Equation of mass conservation

The prognostic equation

$$\rho \partial_t h + \nabla_{xy} \cdot \mathbf{q} = \rho a, \quad (1.121)$$

where

$$a = a_s + a_b, \quad (1.122)$$

is a vertically-integrated expression of mass conservation. The mass balance term, a , has the units distance per time, and the mass flux, ρa , the SI units $\text{kg}/(\text{m}^2 \text{sec})$, i.e. mass per area per time. If the mass balance, a , is available as water equivalent per time, then a will need to be multiplied by the ratio between the density of water and the density of the ice at a given location. That is, the a provided needs to be multiplied by the dimensionless ratio $1000/\rho$, assuming ρ is in SI units.

We will now derive Eq. (1.121) using the local form of the mass-conservation equation⁵ and the kinematic boundary conditions at the upper and lower surfaces. The local form of the mass-conservation equation is

$$\nabla \cdot (\rho \mathbf{v}) + \partial_t \rho = 0, \quad (1.123)$$

⁵Assuming

$$\left| \frac{D\rho}{Dt} \right| \ll \rho \nabla \cdot \mathbf{v}$$

we have

$$\begin{aligned}\nabla \cdot (\rho \mathbf{v}) + \partial_t \rho &= \nabla \cdot \mathbf{v} + \frac{D\rho}{Dt} \\ &\approx \nabla \cdot \mathbf{v}\end{aligned}$$

and the local form is

$$\nabla \cdot \mathbf{v} = 0.$$

and the kinematic boundary conditions at the upper and lower surface are

$$\partial_t s + u_s \partial_x s + v_s \partial_y s - w_s = a_s \quad \text{at} \quad z = s, \quad (1.124)$$

$$\partial_t b + u_b \partial_x b + v_b \partial_y b - w_b = -a_b \quad \text{at} \quad z = b. \quad (1.125)$$

Note the sign convention for a_s and a_b used in (1.124) and (1.125). *Mass flux into the ice is defined positive irrespective over which surface it takes place. Surface accumulation is positive, melting always negative.*

The horizontal ice flux is defined as

$$\mathbf{q}_{xy} = \int_b^s \rho \mathbf{v}_{xy},$$

although we will not always write the subscripts xy and frequently simply write instead

$$\mathbf{q} = \int_b^s \rho \mathbf{v}.$$

Focusing on the flow-line case for the moment we find that

$$\begin{aligned} \partial_x q_x &= \partial_x \int_b^s (\rho u) dz \\ &= \int_b^s \partial_x(\rho u) dz + \rho u_s \partial_x s - \rho u_b \partial_x b \\ &= - \int_b^s (\partial_z(\rho w) + \partial_t \rho) dz + \rho u_s \partial_x s - \rho u_b \partial_x b \\ &= -\rho w_s + \rho w_b - h \partial_t \rho + \rho u_s \partial_x s - \rho u_b \partial_x b \\ &= -h \partial_t \rho - \rho w_s + \rho u_s \partial_x s + \rho w_b - \rho u_b \partial_x b \\ &= -h \partial_t \rho + \rho a_s - \rho \partial_t s + \rho a_b + \rho \partial_t b \\ &= -h \partial_t \rho + \rho a - \rho \partial_t h \end{aligned}$$

or

$$\partial_x q_x = -\partial_t(\rho h) + \rho a. \quad (1.126)$$

where again

$$a = a_s + a_b, \quad (1.122)$$

and therefore, once the y component has been added

$$\partial_t(\rho h) + \nabla_{xy} \cdot \mathbf{q} = \rho a. \quad (1.127)$$

In deriving (1.127) we used

$$\partial_x(\rho u) + \partial_y(\rho v) = -\partial_z(\rho w) + \partial_t \rho$$

which follows from the general form of the local mass conservation equation, Eq. (1.123). However, when inserting the integration limits, we assumed same value for ρ at both the upper and lower boundaries. If ρ varies vertically, we must use the corresponding density values at the upper and lower surface when evaluating the limits of the integral.

In most modelling work of large ice masses it is assumed that the density ρ is uniform in space and does not vary with time. In $\tilde{U}a$ we relax this condition somewhat and only assume that the density at a given location does not change with time, i.e.

$$\partial_t \rho = 0,$$

but allow the density to vary in the horizontal ($\partial_x \rho$ and $\partial_y \rho$ are not assumed to be equal to zero, but $\partial_z \rho = 0$) and (1.127) therefore reads

$$\rho \partial_t h + \nabla \cdot \mathbf{q} = \rho a \quad (1.121)$$

or

$$\rho \partial_t h + \partial_x(\rho h u) + \partial_y(\rho h v) = \rho a \quad (1.128)$$

for a velocity and density fields that only vary horizontally and not with depth.

Eq. (1.121) is the form of the mass continuity equation used in $\tilde{U}a$. The effect of horizontal gradients in (vertically integrated) density are also included in the momentum equations (1.27). The implications of horizontal density gradients on ice flow are explored in Schelpe and Gudmundsson (2023).

1.9 Vertically averaged density and firn density corrections

\hat{U}_a uses for the density the vertically averaged value, that is

$$\rho_{\hat{U}_a} := \bar{\rho} = \frac{1}{h} \int_b^s \rho(z) dz .$$

Sometimes a two layer model consisting of an ice layer and a firn layer, is used for the thickness $h = s - b$. Let F be the thickness of the firn layer and ρ_f the density of that firn layer, then the vertically averaged ice density can be calculated as

$$\begin{aligned} \bar{\rho} &= \frac{1}{h} \int_b^s \rho(z) dz \\ &= \frac{1}{h} \left(\int_b^{s-F} \rho_i dz + \int_{s-F}^s \rho_f dz \right) \\ &= \frac{1}{h} ((h - F)\rho_i + I) \\ &= \frac{1}{h} (\rho_i h - (\rho_i F - I)) \end{aligned} \quad (1.129)$$

where I denotes the integral

$$I := \int_{s-F}^s \rho_f dz .$$

The “firn air content”, δ , is sometimes defined as

$$\begin{aligned} \delta &= \frac{1}{\rho_i} \int_{s-F}^s (\rho_i - \rho_f) dz \\ &= \frac{1}{\rho_i} (\rho_i F - I) \end{aligned}$$

(note that δ has the units distance), or

$$\rho_i F - I = \rho_i \delta . \quad (1.130)$$

Inserting (1.130) into (1.129) shows that the vertically averaged density ($\bar{\rho}$) is related to ice thickness (h), ice density (ρ_i) and air content (δ) through

$$\begin{aligned} \bar{\rho} &= \frac{1}{h} (h\rho_i - \delta\rho_i) \\ &= (1 - \delta/h)\rho_i . \end{aligned} \quad (1.131)$$

In some other numerical models the density is kept constant, often set equal to the density of ice, and instead the ice thickness modified by subtracting the firn air content, δ , from the ice thickness h . Hence, those models would then use for the ice thickness $h' = h - \delta$. This is, for example, the assumption made in the *BedMachine* data compilation (Morlighem et al., 2020). In BedMachine the flotation condition can be thought of as being

$$((s - \delta) - b)\rho_i + \delta \rho_{air} = (S - b)\rho_o , \quad (1.132)$$

but as the air density, ρ_{air} , is small compared to ice and ocean densities, the approximation $\rho_{air} \approx 0$ is made, and the flotation condition then reads

$$(s - \delta - b)\rho_i = (S - b)\rho_o \quad (\text{BedMachine}) , \quad (1.133)$$

whereas in \hat{U}_a it is

$$(s - b)\bar{\rho} = (S - b)\rho_o \quad (\hat{U}_a) , \quad (1.134)$$

with $\bar{\rho}$ given by Eq. (1.131). Both formulations result in an identical flotation condition, that is both Eqs. (1.133) and (1.134)

$$\begin{aligned} (S - b)\rho_o &= (s - b)\bar{\rho} && (\hat{U}_a) \\ &= h(1 - \delta/h)\rho_i \\ &= (h - \delta)\rho_i \\ &= h'\rho_o && (\text{BedMachine}) \\ &= (S - b)\rho_o \end{aligned}$$

so at the grounding line where $b = B$,

$$h \bar{\rho} = h' \rho_i = H \rho_o$$

but the ice thicknesses used different, i.e. h and $h' = h - \delta$.

1.10 Vertical velocities

Note that

$$w_s = u_s \partial_x s + w_b - u_b \partial_x b - \frac{1}{\rho} \partial_x q_x - \frac{h}{\rho} \partial_t \rho$$

or

$$w_s = u_s \partial_x s + \partial_t b + a_b - \frac{1}{\rho} \partial_x q_x - \frac{h}{\rho} \partial_t \rho$$

which can be used to calculate vertical velocities. If the bed elevation does not change with time and if furthermore $\partial_t \rho = 0$, we have the special case

$$w_s = u_s \partial_x s + a_b - \frac{1}{\rho} \partial_x q_x$$

1.11 Sliding laws

Basal drag is often assumed to be a function of velocity, i.e. Robin type boundary condition, and written as

$$\mathbf{t}_b = f(u, v, h) \frac{\mathbf{v}_b}{\|\mathbf{v}_b\|},$$

where f is some given function, \mathbf{v}_b is the tangential basal velocity, i.e. the basal sliding velocity

$$\mathbf{v}_b = \mathbf{v} - (\hat{\mathbf{n}}^T \cdot \mathbf{v}) \hat{\mathbf{n}}, \quad (1.135)$$

$$= \mathbf{T}\mathbf{v}, \quad (1.136)$$

and \mathbf{t}_b is the tangential component of the basal traction

$$\mathbf{t}_b = -\mathbf{T}(\boldsymbol{\sigma} \hat{\mathbf{n}}), \quad (1.137)$$

where

$$\mathbf{T} = \mathbf{1} - \hat{\mathbf{n}} \otimes \hat{\mathbf{n}}, \quad (1.138)$$

is the tangential operator⁶. We refer to \mathbf{t}_b as *basal shear traction*. Note that the shear traction is, in general, not equal to basal shear stress. The basal drag caused by ice flow only acts over the grounded parts, a fact which we can express as

$$\mathbf{t}_b = \mathcal{G}\mathbf{f}(\mathbf{v}_b),$$

where \mathcal{G} is the grounding/flotation mask defined as

$$\mathcal{G} := \mathcal{H}(h - h_f).$$

All formulations in use assume that the tangential component of the basal drag vector points in the same direction as the basal component of the basal velocity, that is

$$\mathbf{t}_b = \|\mathbf{t}_b\| \frac{\mathbf{v}_b}{\|\mathbf{v}_b\|}. \quad (1.139)$$

⁶This can be seen as follows:

$$\begin{aligned} \mathbf{v}_b &= \mathbf{v} - (\mathbf{v}^T \cdot \hat{\mathbf{n}}) \hat{\mathbf{n}} \\ &= (\mathbf{1} - \hat{\mathbf{n}} \otimes \hat{\mathbf{n}})\mathbf{v} \\ &= \mathbf{T}\mathbf{v} \end{aligned}$$

where \mathbf{v}_b is the bed tangential component of \mathbf{v} and we have used the identity $(\hat{\mathbf{n}} \otimes \hat{\mathbf{n}})\mathbf{v} = (\mathbf{v}^T \cdot \hat{\mathbf{n}})\hat{\mathbf{n}}$. One can also define the normal operator \mathbf{N} as

$$\mathbf{N} = \hat{\mathbf{n}} \otimes \hat{\mathbf{n}},$$

and we have

$$\boldsymbol{\sigma} = \mathbf{N}\boldsymbol{\sigma} + \mathbf{T}\boldsymbol{\sigma}.$$

In general, given a unit vector $\hat{\mathbf{n}}$, the orthogonal projection onto the subspace spanned by $\hat{\mathbf{n}}$ is $\hat{\mathbf{n}} \otimes \hat{\mathbf{n}}$.

Table 1.1: Sliding laws and definitions.

Name	Abbreviation	Definition	Parameters
Weertman	W	$\mathbf{t}_b = \mathcal{G} \beta^2 \mathbf{v}_b$	$C \ m$
Coulomb	C	$\mathbf{t}_b = \mu_k N \frac{\mathbf{v}_b}{\ \mathbf{v}_b\ }$	μ_k
Budd	W-N	$\mathbf{t}_b = \mathcal{G} N^{q/m} \beta^2 \mathbf{v}_b$	$C \ m \ q$
Tsai	minCW	$\mathbf{t}_b = \min(\mathcal{G} \beta^2 \ \mathbf{v}_b\ , \mathbf{v}_b, \mu_k N) \frac{\mathbf{v}_b}{\ \mathbf{v}_b\ }$	$C \ m \ \mu_k$
Cornford	rCwm	$\mathbf{t}_b = \frac{\mathcal{G} \beta^2 \ \mathbf{v}_b\ \mu_k N}{((\mu_k N)^m + (\mathcal{G} \beta^2 \ \mathbf{v}_b\)^m)^{1/m}} \frac{\mathbf{v}_b}{\ \mathbf{v}_b\ }$	$C \ m \ \mu_k$
Umbi	rCW	$\mathbf{t}_b = \frac{\mathcal{G} \beta^2 \ \mathbf{v}_b\ \mu_k N}{\mu_k N + \mathcal{G} \beta^2 \ \mathbf{v}_b\ } \frac{\mathbf{v}_b}{\ \mathbf{v}_b\ }$	$C \ m \ \mu_k$
Zeroth-order hydrology	N0	$N = \mathcal{G} g \rho (h - h_f^+)$	

When combined with the zeroth-order hydrology the abbreviations are: W, C, W-N0, minCW-N0, rCwm-N0 , and rCW-N0. The variable β^2 is defined as

$$\beta^2 = C^{-1/m} \|\mathbf{v}_b\|^{1/m-1}$$

and hence, depends on the parameters C and m .

1.11.1 Weertman sliding law (W)

The power-law type Weertman sliding law is

$$\mathbf{T}\sigma\hat{\mathbf{n}} + C^{-1/m} \|\mathbf{T}\mathbf{v}\|^{1/m-1} \mathbf{T}\mathbf{v} = 0, \quad \text{for } z = B(x, y)$$

where the tangential operator is

$$\mathbf{T} = \mathbf{1} - \hat{\mathbf{n}} \otimes \hat{\mathbf{n}}, \quad (1.138)$$

with $\hat{\mathbf{n}}$ being a unit vector normal to the bed profile. The tangential basal sliding velocity, \mathbf{v}_b , is

$$\mathbf{v}_b = \mathbf{T}\mathbf{v}, \quad (1.136)$$

and the tangential component of the basal traction

$$\mathbf{t}_b = -\mathbf{T}(\sigma\hat{\mathbf{n}}). \quad (1.137)$$

Different formulations of the Weertman sliding law are

$$\mathbf{t}_b = \mathcal{G} C^{-1/m} \|\mathbf{v}_b\|^{1/m-1} \mathbf{v}_b, \quad (1.140)$$

$$\mathbf{t}_b = \mathcal{G} C^{-1/m} \|\mathbf{v}_b\|^{1/m} \frac{\mathbf{v}_b}{\|\mathbf{v}_b\|}, \quad (1.141)$$

$$\mathbf{t}_b = \mathcal{G} \beta^2 \mathbf{v}_b, \quad (1.142)$$

$$\|\mathbf{t}_b\| = \mathcal{G} \beta^2 \|\mathbf{v}_b\|, \quad (1.143)$$

where β^2 is defined as,

$$\beta^2 = C^{-1/m} \|\mathbf{v}_b\|^{1/m-1}, \quad (1.144)$$

and⁷

$$\mathbf{v}_b = \mathcal{G}^m C \|\mathbf{t}_b\|^{m-1} \mathbf{t}_b, \quad (1.145)$$

$$\|\mathbf{v}_b\| = \mathcal{G}^m C \|\mathbf{t}_b\|^m, \quad (1.146)$$

In \dot{U} the power-law sliding law is given as

$$\begin{pmatrix} t_{bx} \\ t_{by} \end{pmatrix} = \mathcal{G} \beta^2 \begin{pmatrix} u_b \\ v_b \end{pmatrix}$$

⁷Since

$$\mathcal{G} = \mathcal{G}^m,$$

for any power m we do not strictly need to include the stress exponent m in any equations involving \mathcal{G} . However if we use an approximation to Heaviside function \mathcal{H} in the definition of \mathcal{G} given by Eq. (3), then this stress exponent should be included.

with

$$\beta^2 = (C + C_0)^{-1/m} (u_b^2 + v_b^2 + u_o^2)^{(1-m)/2m},$$

and where C_0 and u_0 are some (small) regularisation parameters.

The basal slipperiness C has the physical dimensions of velocity divided by stress to the power m . It can be useful to think of C as the ratio

$$C = \frac{C_v}{C_\tau^m}$$

where C_v has the dimensions of velocity and C_τ the dimensions of stress. We can then write (1.140) and (1.145) as

$$\mathbf{t}_b = \mathcal{G} C_\tau \left(\frac{\|\mathbf{v}_b\|}{C_v} \right)^{1/m} \frac{\mathbf{v}_b}{\|\mathbf{v}_b\|} \quad (1.147)$$

$$\mathbf{v}_b = C_v \left(\frac{\|\mathbf{t}_b\|}{\mathcal{G} C_\tau} \right)^m \frac{\mathbf{t}_b}{\|\mathbf{t}_b\|} \quad (1.148)$$

Weertman sliding law limits

If we now consider the limit $m \rightarrow +\infty$ we see from Eq. (1.145) that $\|\mathbf{t}_b\| \rightarrow C_\tau$ over the grounded areas (where $\mathcal{G} = 1$) for the velocity to remain finite. With increasing m , the basal velocity \mathbf{v}_b becomes increasingly sensitive to basal shear traction, and in the limit $m \rightarrow +\infty$ the velocity can be considered to become infinitely sensitive to basal shear traction. For $m \rightarrow +\infty$, $1/m \rightarrow 0$ and inserting $1/m = 0$ into Eq. (1.147) gives

$$\mathbf{t}_b = C_\tau \frac{\mathbf{v}_b}{\|\mathbf{v}_b\|} \quad \text{for } m \rightarrow +\infty.$$

Hence, the basal shear traction is in this limit equal to C_τ , and C_τ can be considered to be a yield stress. In this particular limit it therefore arguably better to recast the 'sliding' law as

$$\mathbf{t}_b = \tau^* \frac{\mathbf{v}_b}{\|\mathbf{v}_b\|} \quad \text{for } m \rightarrow +\infty,$$

where $\tau^* = C_\tau$ is a yield stress, and the 'sliding law' is now simply a stress condition for the basal shear traction and τ^* a property of the bed (e.g. till) that is determined by some other physical principle. Using this viewpoint, in the limit $m \rightarrow +\infty$ the parameter C_v has no effect on the solution, but can be calculated afterwards from the velocity. The basal sliding law does not impose any direct constraints on the basal sliding velocity, i.e. for given basal shear traction, the basal velocity can have any value. The basal velocity can still be calculated by solving the SSTREAM/SSA equations provided the velocity is set to a value somewhere along the boundary by the boundary conditions (In this limit the SSTREAM field equations only provide constraints on the gradients of velocities). In the SIA equations the velocity can not be determined using the momentum equation (as by definition there is no direct functional relationship between velocity and basal shear traction), and must be determined from other consideration (such as mass conservation).

Considering the opposite limit where $m \rightarrow 0$, we see from Eq. (1.147) that now it is the basal shear traction that becomes infinitely sensitive to basal velocity, or conversely, the basal velocity becomes in this limit independent of basal shear traction. From Eq. (1.145), we find

$$\mathbf{v}_b = C_v \frac{\mathbf{t}_b}{\|\mathbf{t}_b\|} \quad \text{for } m \rightarrow 0.$$

This is a limit which is (I find) difficult to understand in physical terms. The basal velocity is now no longer a function of the stress state and must be determined by some other physical principle. What physical conditions at the bed would force the basal sliding velocity to obtain some particular value independently of the state of stress?

Note that the limits $m \rightarrow +\infty$ and $m \rightarrow 0$ are fundamentally different. In the former the basal shear traction is fixed, in the latter the basal velocity.

1.11.2 Budd sliding law (Generalised Weertman sliding law, W-N)

The Budd sliding law is

$$\mathbf{t}_b = \mathcal{G} N^{q/m} C^{-1/m} \|\mathbf{v}_b\|^{1/m-1} \mathbf{v}_b. \quad (1.149)$$

where $N = p - p_w$, is the effective pressure. This sliding relationship can also be written as

$$\mathbf{t}_b = \mathcal{G} N^{q/m} \beta^2 \mathbf{v}_b, \quad (1.150)$$

$$\mathbf{v}_b = \frac{C}{\mathcal{G}^m N^q} \|\mathbf{t}_b\|^{m-1} \mathbf{t}_b, \quad (1.151)$$

$$\|\mathbf{v}_b\| = \frac{C}{\mathcal{G}^m N^q} \|\mathbf{t}_b\|^m, \quad (1.152)$$

$$\|\mathbf{t}_b\| = \mathcal{G} \left(\frac{N^q}{C} \right)^{1/m} \|\mathbf{v}_b\|^m. \quad (1.153)$$

where β^2 is again defined by

$$\beta^2 = C^{-1/m} \|\mathbf{v}_b\|^{1/m-1}. \quad (7.28)$$

If one assumes perfect hydrological connection with the ocean (see section 1.13.1), Budd sliding law takes the form

$$\mathbf{t}_b = \mathcal{G} \left(\rho g (h - h_f^+) \right)^{q/m} C^{-1/m} \|\mathbf{v}_b\|^{1/m-1} \mathbf{v}_b, \quad (1.154)$$

$$= \mathcal{G} \left(\rho g (h - h_f^+) \right)^{q/m} \beta^2 \mathbf{v}_b, \quad (1.155)$$

It follows that $N = 0$ where $h = h_f = H\rho_o/\rho$ and therefore $\mathbf{t}_b = \mathbf{0}$ at the grounding line.

1.11.3 Coulomb (C)

The Coulomb friction law is

$$\mathbf{t}_b = \mu_k N \frac{\mathbf{v}_b}{\|\mathbf{v}_b\|}, \quad (\text{Coulomb}) \quad (1.156)$$

where N is the effective pressure the and coefficient of kinetic friction, μ_k , an empirical property. The effective pressure, N , has the same units as the basal drag, \mathbf{t}_b , or Pascal per square-meter, and μ_k is dimensionless.⁸

1.11.4 Combining Weertman (W) with Coulomb (C)

Budd sliding law ensures that basal drag goes to zero as the grounding line is approached. But there are many other ways of ensuring that $\|\mathbf{t}_b\| \rightarrow 0$ as $N \rightarrow 0$, for example by combining Weertman sliding and the Coulomb friction laws:

$$\mathbf{t}_b = \mathcal{G} \beta^2 \mathbf{v}_b, \quad (\text{Weertman}) \quad (1.147)$$

$$\mathbf{t}_b = \mu_k N \frac{\mathbf{v}_b}{\|\mathbf{v}_b\|}, \quad (\text{Coulomb}) \quad (1.156)$$

with

$$\beta^2 = C^{-1/m} \|\mathbf{v}_b\|^{1/m-1}. \quad (7.28)$$

and of regularising the Coulomb friction law, see for example Schoof (2010). Two of those various approaches of combining Weertman and Coulomb type sliding laws, are the *Minimum Value* and the *Reciprocal Sum* approaches.

⁸Weertman sliding law is

$$\mathbf{t}_b = \mathcal{G} C^{-1/m} \|\mathbf{v}_b\|^{1/m} \frac{\mathbf{v}_b}{\|\mathbf{v}_p\|}$$

and therefore

$$\mu_k N = \mathcal{G} C^{-1/m} \|\mathbf{v}_b\|^{1/m},$$

and, if C has been determined, it is tempting to calculate N using

$$N = \mathcal{G} \mu_k^{-1} C^{-1/m} \|\mathbf{v}_b\|^{1/m}.$$

However, there is no guarantee that this will produce a physically plausible effective pressure distribution. For example, for any finite-valued inverted C distribution, N calculated in this manner will not go to zero as the grounding line is approached from above.

Minimum Value (Tsai, minCW)

Here the idea is that basal drag is limited by these two processes acting independently, and the process giving the lower value at a given location is the one to use at that location (Tsai et al., 2015). So calculate both

$$\|\mathbf{t}_b\| = \mathcal{G} \beta^2 \|\mathbf{v}_b\| \quad (\text{Weertman}) \quad (1.157)$$

$$\|\mathbf{t}_b\| = \mu_k N \quad (\text{Coulomb}) \quad (1.158)$$

and at each location use the law producing the lower value of the two. Hence,

$$\mathbf{t}_b = \min(\mathcal{G} \beta^2 \|\mathbf{v}_b\|, \mu_k N) \frac{\mathbf{v}_b}{\|\mathbf{v}_b\|} \quad (\text{Tsai}) \quad (1.159)$$

Again, assuming perfect hydrological connection, the effective pressure can be approximated close to the grounding line using Eq. (1.187).

Reciprocal Sum (rCW, rCWm)

Another option of combining Weertman and Coulomb drag laws is to use a reciprocal sum of the two, i.e.

$$\frac{1}{\|\mathbf{t}_b\|} = \frac{1}{\|\mathbf{t}_b^W\|} + \frac{1}{\|\mathbf{t}_b^C\|},$$

or

$$\|\mathbf{t}_b\| = \frac{1}{\frac{1}{\|\mathbf{t}_b^W\|} + \frac{1}{\|\mathbf{t}_b^C\|}},$$

where again

$$\|\mathbf{t}_b^W\| = \mathcal{G} \beta^2 \|\mathbf{v}_b\|, \quad (1.143)$$

$$\|\mathbf{t}_b^C\| = \mu_k N \quad (1.158)$$

giving⁹,

$$\begin{aligned} \|\mathbf{t}_b\| &= \frac{1}{1/\|\mathbf{t}_b^W\| + 1/\|\mathbf{t}_b^C\|} \\ &= \frac{\|\mathbf{t}_b^C\| \|\mathbf{t}_b^W\|}{\|\mathbf{t}_b^W\| + \|\mathbf{t}_b^C\|} \\ &= \mathcal{G} \frac{\mu_k N \beta^2 \|\mathbf{v}_b\|}{\mu_k N + \mathcal{G} \beta^2 \|\mathbf{v}_b\|}. \end{aligned} \quad (1.160)$$

By looking at the limits where either the Coulomb or Weertman drag becomes small compared to the other, we see that this idea is similar to the *minimum value* idea above, i.e. that these two processes act independently, and the basal drag is at each location effectively determined by the process giving the lower drag of the two.

Note that the grounding/floating mask \mathcal{G} in the numerator is arguably redundant as $\mathcal{G}N = N$, but we keep it here to get the right limits as $N \rightarrow +\infty$. The basal drag vector is then calculated as

$$\begin{aligned} \mathbf{t}_b &= \|\mathbf{t}_b\| \frac{\mathbf{v}_b}{\|\mathbf{v}_b\|} \\ &= \frac{\mu_k N \mathcal{G} \beta^2 \|\mathbf{v}_b\|}{\mu_k N + \mathcal{G} \beta^2 \|\mathbf{v}_b\|} \frac{\mathbf{v}_b}{\|\mathbf{v}_b\|} \end{aligned} \quad (1.161)$$

$$= \mathcal{G} \frac{\mu_k N}{\mu_k N + \mathcal{G} \beta^2 \|\mathbf{v}_b\|} \beta^2 \mathbf{v}_b. \quad (1.162)$$

⁹Formally this appears similar to Schoof's suggestion which, apart from some stress exponents, is

$$\|\mathbf{t}_b\| = \frac{\mu_k N \|\mathbf{v}_b\|}{\lambda A N + \|\mathbf{v}_b\|}$$

and we get Eq. (1.160) if we set $\lambda A = \mu_k / \beta^2$, but the physical interpretation is very different.

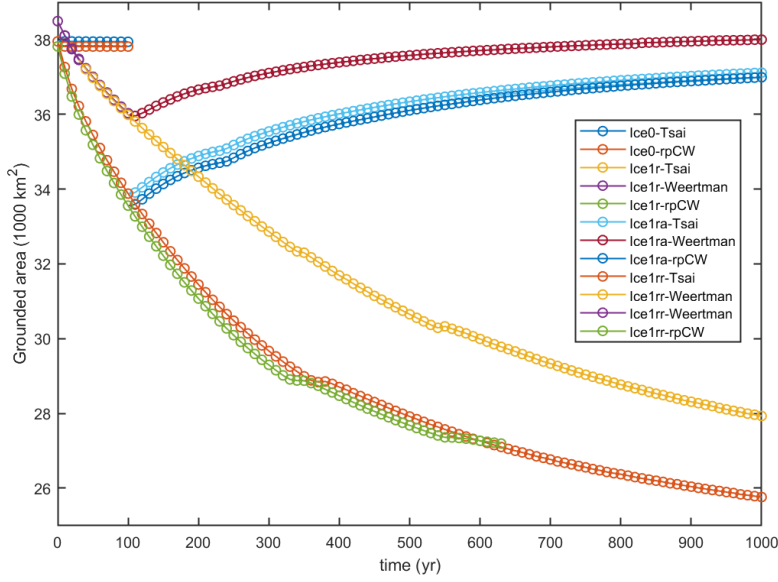


Figure 1.1: MismipPlus: Grounded area as function of time for different sliding laws. Description of the experimental setup is given in [Asay-Davis et al. \(2016\)](#) and recent inter-comparison results are presented in [Cornford et al. \(2020\)](#).

This gives the limits

$$\begin{aligned} \|\mathbf{t}_b\| &= \mathcal{G} \beta^2 \|\mathbf{v}_b\| \quad \text{for } N \rightarrow +\infty && \text{(Weertman)} \\ \|\mathbf{t}_b\| &= \mu_k N \quad \text{for } N \rightarrow 0 && \text{(Coulomb)} \\ \|\mathbf{t}_b\| &= \mu_k N \quad \text{for } \|\mathbf{v}_b\| \rightarrow +\infty && \text{(Coulomb)} \\ \|\mathbf{t}_b\| &= \mathcal{G} \beta^2 \|\mathbf{v}_b\| \quad \text{for } \|\mathbf{v}_b\| \rightarrow 0 && \text{(Weertman)} \end{aligned}$$

Cornford's reciprocal power weighting (rCWm)

In [Asay-Davis et al. \(2016\)](#), Cornford suggests combining the Weertman and Coulomb sliding laws using the reciprocal sum with each term raised to the power m , or as

$$\frac{1}{\|\mathbf{t}_b\|^m} = \frac{1}{\|\mathbf{t}_b^W\|^m} + \frac{1}{\|\mathbf{t}_b^C\|^m},$$

giving

$$\begin{aligned} \|\mathbf{t}_b\| &= \frac{1}{(1/\|\mathbf{t}_b^W\|^m + 1/\|\mathbf{t}_b^C\|^m)^{1/m}} \\ &= \frac{\|\mathbf{t}_b^C\| \|\mathbf{t}_b^W\|}{(\|\mathbf{t}_b^C\|^m + \|\mathbf{t}_b^W\|^m)^{1/m}} \\ &= \frac{\mu_k N \mathcal{G} \beta^2 \|\mathbf{v}_b\|}{((\mu_k N)^m + (\mathcal{G} \beta^2 \|\mathbf{v}_b\|)^m)^{1/m}}. \end{aligned} \tag{1.163}$$

Thus

$$\mathbf{t}_b = \frac{\mu_k N \mathcal{G} \beta^2 \|\mathbf{v}_b\|}{((\mu_k N)^m + (\mathcal{G} \beta^2 \|\mathbf{v}_b\|)^m)^{1/m}} \frac{\mathbf{v}_b}{\|\mathbf{v}_b\|}. \tag{1.164}$$

While expression (1.164) is not identical to Eq. (1.161) it clearly reflects the same idea, i.e. to combine Weertman and Coulomb laws in a gradual and continuous manner, and it gives the same limits, i.e.

$$\begin{aligned} \|\mathbf{t}_b\| &= \mathcal{G} \beta^2 \|\mathbf{v}_b\| \quad \text{for } N \rightarrow +\infty && \text{(Weertman)} \\ \|\mathbf{t}_b\| &= \mu_k N \quad \text{for } N \rightarrow 0 && \text{(Coulomb)} \\ \|\mathbf{t}_b\| &= \mu_k N \quad \text{for } \|\mathbf{v}_b\| \rightarrow +\infty && \text{(Coulomb)} \\ \|\mathbf{t}_b\| &= \mathcal{G} \beta^2 \|\mathbf{v}_b\| \quad \text{for } \|\mathbf{v}_b\| \rightarrow 0 && \text{(Weertman)} \end{aligned}$$

Different notations for the rCWM sliding law in the literature

In Asay-Davis et al. (2016), Eq. 11, the sliding law (1.164) is written as

$$\mathbf{t}_b = \frac{\beta_C^2 \|\mathbf{v}_b\|^{1/m-1} \alpha_C^2 N}{(\beta_C^{2m} \|\mathbf{v}_b\| + (\alpha_C^2 N)^m)^{1/m}} \mathbf{v}_b , \quad (\text{Eq. 11 in Assay-Davis, 2016})$$

where

$$\alpha_C^2 = \mu_k \quad (1.165)$$

$$\beta_C^2 \|\mathbf{v}_b\|^{1/m-1} = \mathcal{G} \beta^2 \quad (1.166)$$

and therefore

$$\begin{aligned} \mathbf{t}_b &= \frac{\beta_C^2 \|\mathbf{v}_b\|^{1/m-1} \alpha_C^2 N}{(\beta_C^{2m} \|\mathbf{v}_b\| + (\alpha_C^2 N)^m)^{1/m}} \mathbf{v}_b \\ &= \frac{\mu_k N \mathcal{G} \beta^2 \|\mathbf{v}_b\|}{((\mu_k N)^m + (\mathcal{G} \beta^2 \|\mathbf{v}_b\|)^m)^{1/m}} \frac{\mathbf{v}_b}{\|\mathbf{v}_b\|} \end{aligned} \quad (1.167)$$

showing that (1.164) and Eq. 11 in Asay-Davis et al. (2016) are identical once we have made the notational substitutions (1.165) and (1.166). Note that the β^2 in Asay-Davis et al. (2016) is not the same as β^2 used here, and for that reason I have used β_C^2 where Asay-Davis et al. (2016) use β^2 .

Joughin's regularised Coulomb-Weertman sliding (rCWM)

In Joughin et al. (2019), Joughin suggest using

$$\mathbf{t}_b = \mathcal{G} C^{-1/m} \left(\frac{\|\mathbf{v}_b\|}{\|\mathbf{v}_b\| + v_0} \right)^{1/m} \frac{\mathbf{v}_b}{\|\mathbf{v}_b\|} \quad (1.168)$$

where v_0 is a new parameters. In Joughin et al. (2019), the value of $v_0 = 300 \text{ m a}^{-1}$ and $m = 3$ was used.

This law includes both Weertman and Coulomb laws as separate limits. For $v_0 \gg \|\mathbf{v}_b\|$ we can write $(\|\mathbf{v}_b\| + v_0) \approx v_0$ and (1.168) can now be approximated as

$$\mathbf{t}_b \approx \mathcal{G} (C v_0)^{-1/m} \|\mathbf{v}_b\|^{1/m} \frac{\mathbf{v}_b}{\|\mathbf{v}_b\|} \quad (1.169)$$

which is Weertman sliding law (1.141) where

$$C_{\text{Weertman}} = C v_0 .$$

For $v_0 \ll \|\mathbf{v}_b\|$ we can write $(\|\mathbf{v}_b\| + v_0) \approx \|\mathbf{v}_b\|$ and (1.168) can now be approximated as

$$\mathbf{t}_b \approx \mathcal{G} C^{-1/m} \frac{\mathbf{v}_b}{\|\mathbf{v}_b\|} \quad (1.170)$$

which is Coulomb friction law (1.156) where

$$\mu_k N = \mathcal{G} C^{-1/m} .$$

However, since C is here a constant, or some spatially variable field determined through model inversion, the basal drag will not automatically go to zero as the grounding line is approached and $N \rightarrow 0$. In fact,

it appears somewhat questionable to equate this limit with the Coulomb friction law, as the basal drag is not limited, or in any manner affected, by the effective basal pressure. Rather, the limit is reached whenever the basal speed is significantly larger than v_0 , irrespective of the state of normal stresses between the basal ice and the substrate.

To obtain the same C field in the limit $v_0 \rightarrow +\infty$ as for the Weertman sliding law, write

$$\mathbf{t}_b = \mathcal{G} C^{-1/m} v_0^{1/m} \left(\frac{\|\mathbf{v}_b\|}{\|\mathbf{v}_b\| + v_0} \right)^{1/m} \frac{\mathbf{v}_b}{\|\mathbf{v}_b\|} \quad (1.171)$$

1.12 Ocean and atmospheric drag terms

To simulate the drag exerted on the ice by the ocean and the atmosphere, corresponding drag terms can be added. For ocean drag term we add

$$\mathbf{t}_b^o = (1 - \mathcal{G}) C_o^{-1/m_o} \|\mathbf{v}_b - \mathbf{v}_o\|^{1/m_o - 1} (\mathbf{v}_b - \mathbf{v}_o),$$

where \mathbf{v}_o is the velocity of the ocean current, and \mathcal{G} is the floating/grounding mask (see Table 1).

The sea-ice literature suggest $m_o = 1/2$, i.e.

$$\mathbf{t}_b^o = (1 - \mathcal{G}) C_o^{-2} \|\mathbf{v}_b - \mathbf{v}_o\| (\mathbf{v}_b - \mathbf{v}_o),$$

and defines

$$D_o = C_o^{-2},$$

where

$$D_o = \rho_o c_o,$$

and typically $c_o = 0.0055$ (no units). Hence

$$C_o = \frac{1}{\sqrt{D_o}} = \frac{1}{\sqrt{\rho_o c_o}} \approx 0.4 \quad (\text{units: } \sqrt{(\text{m/s})/\text{Pa}}).$$

The total drag is a sum of that due to basal sliding and ocean currents, or

$$\mathbf{t}_b = \mathcal{G} \beta^2 \mathbf{v}_b + (1 - \mathcal{G}) \beta_o^2 (\mathbf{v}_b - \mathbf{v}_o).$$

where apparently the literature seems to suggest

$$\beta_o^2 = \rho_o c_o \|\mathbf{v}_b - \mathbf{v}_o\|.$$

Ocean current can have speeds on the order of $0.05 \text{ m s}^{-1} = 1500 \text{ km/yr}$, or at least three orders of magnitudes greater than typical ice flow speeds. The ocean drag, $\|\mathbf{t}_b^o\|$, is then about

$$\|\mathbf{t}_b^o\| = \rho_o c_o v_o^2 = 1000 \times 0.0055 \times 0.05^2 = 10^{-5} \text{ Pa}.$$

In comparison the driving stress term for an ice shelf with slope 10^{-5} is

$$\frac{1}{2} \rho g \partial_x h^2 = 1000 \times 10 \times 100 \times 10^{-5} = 10 \text{ Pa}.$$

This term however, can be even smaller if the thickness gradient is sufficiently small.

By applying ocean drag detached ice shelves (tabular ice bergs) can be included in the computational domain as otherwise the system would be singular.

1.12.1 Note on icebergs and detached ice shelves.

Following Wagner et al. (2017) the momentum equation for an (undeformable, point-like) ice berg can be written on the form

$$\rho \frac{d\mathbf{v}}{dt} + \rho \mathbf{k} \times \mathbf{v} = \mathbf{t}_p + \mathbf{t}_b^o + \mathbf{t}_b^a \quad (1.172)$$

where \mathbf{t}_p is the ocean pressure gradient, and $\rho \mathbf{k} \times \mathbf{v}$ is due to Coriolis force.

Assuming geostrophic flow, the ocean pressure gradient, which will be closely related to the ocean surface slopes, can be approximated from ocean velocity as

$$\mathbf{t}_p = \rho f \mathbf{k} \times \mathbf{v}_o ,$$

and the ocean pressure term can be combined with the Coriolis term to give

$$\rho \frac{d\mathbf{v}}{dt} + \rho \mathbf{k} \times (\mathbf{v} - \mathbf{v}_o) = \mathbf{t}_b^o + \mathbf{t}_b^a . \quad (1.173)$$

The movement of a deformable ice berg can be described using the SSA equations, with the drag being produced by the action of winds and ocean currents, by adding the Coriolis force to Eq. (1.18) and (1.19) giving

$$-\rho f h v + \partial_x(h(2\tau_{xx} + \tau_{yy})) + \partial_y(h\tau_{xy}) - t_{bx} = \frac{1}{2} \varrho g \partial_x h^2 \quad (1.174)$$

$$\rho f h u + \partial_y(h(2\tau_{yy} + \tau_{xx})) + \partial_x(h\tau_{xy}) - t_{by} = \frac{1}{2} \varrho g \partial_y h^2 \quad (1.175)$$

where f is the Coriolis parameter (units per time),

$$f = 2\Omega \sin \varphi \quad (1.176)$$

where φ is the latitude, and Ω the rotational rate of the Earth, i.e. $\Omega T = 2\pi$ where $T = 24\text{ hr} = 7.2921 \times 10^{-5} \text{ rad s}^{-1} = 2301 \text{ rad yr}^{-1}$.

At a latitude of 70 degrees south, $f = 2\Omega \sin \varphi \approx 6.8 \times 10^{-5} \text{ rad/s}$, and for an ice-berg, drifting with the velocity $0.05 \text{ m/s} = 1500 \text{ km/yr}$, the term $\rho f h v$ is on the order of

$$\rho f h v = 1000 \times 6.8 \times 10^{-5} \times 100 \times 0.05 \approx 0.3 \text{ Pa}$$

To gain some insight into the solutions of Eq. (1.174) and (1.175), consider a one-dimensional flat ice berg, ignoring the Coriolis terms for the time being. We arrive at (see also Eq. (1.229))

$$2\partial_x \left(A^{-1/n} h (\partial_x u)^{1/n} \right) - \rho_o c_o |u - u_o| (u - u_0) = 0 \quad (1.177)$$

or

$$\frac{2}{n} A^{-1/n} h (\partial_x u)^{1/n-1} \partial_{xx}^2 u - \rho_o c_o |u - u_o| (u - u_0) = 0 \quad (1.178)$$

We see that the velocity of ice must now vary spatially because $u = u_0$ is not a solution to (1.178). Nevertheless, we can expect the velocity of the ice berg to be close to that of the ocean.

If the balance is between Coriolis and ocean-induced drag, and we ignore all internal ice deformation of the ice berg, the Eq. (1.174) and (1.175) read

$$-\rho f h (v - v_o) = \rho_o c_o \| \mathbf{v} - \mathbf{v}_o \| (u - u_0) \quad (1.179)$$

$$\rho f h (u - u_o) = \rho_o c_o \| \mathbf{v} - \mathbf{v}_o \| (v - v_0) \quad (1.180)$$

and the solution is simply

$$\mathbf{v} = \mathbf{v}_o .$$

Hence, the ice berg moves at the same speed and in the same direction as the ocean current. If the balance is between Coriolis and wind-induced drag, on the other hand, and we again ignore all internal ice deformation of the ice berg, the Eq. (1.174) and (1.175) reduce to

$$-\rho f h (v - v_o) = \rho_a c_a \| \mathbf{v} - \mathbf{v}_a \| (u - u_a) \quad (1.181)$$

$$\rho f h (u - u_o) = \rho_a c_a \| \mathbf{v} - \mathbf{v}_a \| (v - v_a) \quad (1.182)$$

Assuming that wind speeds are much larger than the speed of the ice berg we then have

$$v = v_o + \gamma \| \mathbf{v}_a \| u_a \quad (1.183)$$

$$u = u_o - \gamma \| \mathbf{v}_a \| v_a \quad (1.184)$$

where

$$\gamma = \frac{\rho_a c_a}{\rho f h} .$$

The effect of the wind is, hence, to cause the ice berg to move with a velocity at 90 degrees to the wind direction.

1.13 Effective basal water pressure

1.13.1 Hydrology

The *First Law of Observational Subglacial Hydrology* is that if you drill a hole in a warm-based glacier and measure the subglacial water pressure, that pressure will tend to be at or close to the ice overburden pressure. This observation can be expressed as either relative or absolute terms as (relative)

$$\frac{N}{\rho gh} < \gamma_w \quad (1.185)$$

where γ_w is small compared to unity, e.g.

$$\gamma_w \lesssim 0.1$$

or (absolute)

$$N < \Gamma_w$$

where Γ_w is a dimensional number based on observations, e.g. $\Gamma_w \lesssim 1 \text{ kPa}$.

Perfect hydrological connection

It is sometimes assumed that the sub-glacial pressure in the vicinity of the grounding line equals the ocean pressure, in which case

$$N = g(\rho h - \rho_o H^+) \quad (1.186)$$

$$= g\rho(h - h_f^+) . \quad (1.187)$$

where H^+ is the positive ocean depth and h_f^+ the positive flotation thickness defined by Eqs. (1.33) and (2), respectively. It follows that

$$\frac{dN}{dh} = \begin{cases} \rho g & \text{if } h \geq h_f \\ 0 & \text{if } h < h_f \end{cases}$$

when $h \geq h_f$, and this might seem rather unrealistic if $h \gg h_f$.

Note that the assumption of perfect hydrological implies

$$\begin{aligned} \gamma_w &= \frac{\rho g(h - h_f^+)}{\rho gh} \\ &= 1 - h_f^+/h \end{aligned}$$

clearly violating the relative formulation of the first law of observational subglacial hydrology (Eq. 1.185) whenever $h_f^+ < (1 - \gamma_w)h$.

Rosier hydrology

The Rosier hydrology, defined as

$$N = \min \left(\rho g(h - h_f^+), \gamma_w \rho gh \right)$$

where

$$\gamma_w = (e\pi)^{-1} \approx 0.117$$

is one approach to satisfy the first law in its relative form.¹⁰ For the Rosier hydrology

$$\frac{dN}{dh} = \begin{cases} \gamma_w \rho g & \text{if } h > h_f / (1 - \gamma_w) \\ \rho g & \text{if } h_f \leq h \leq h_f / (1 - \gamma_w) \\ 0 & \text{if } h < h_f \end{cases}$$

¹⁰The exact mathematical expression for γ_w is based on unpublished work by S. Rosier.

Passive hydrology

The *passive hydrology* model is motivated by the absolute formulation of the first law. It does not predict the exact value of N at all, but states that the effective pressure is independent of ice thickness, i.e.

$$\frac{\partial N}{\partial h} = 0.$$

It can be argued that currently many (most?) ice-sheet models implicitly assume the hydrology to be passive in this sense.

1.14 Flow law

Glen's flow law is

$$\dot{\epsilon}_{ij} = A \tau^{n-1} \tau_{ij},$$

where

$$\tau = \sqrt{\tau_{ij} \tau_{ij}/2}$$

The flow law can also be written as

$$\tau_{ij} = A^{-1/n} \dot{\epsilon}^{(1-n)/n} \dot{\epsilon}_{ij}, \quad (1.188)$$

where

$$\dot{\epsilon} = \sqrt{\dot{\epsilon}_{ij} \dot{\epsilon}_{ij}/2}$$

which in the Shallow Ice Stream Approximation takes the form

$$\dot{\epsilon} = \sqrt{(\dot{\epsilon}_{xx})^2 + (\dot{\epsilon}_{yy})^2 + \dot{\epsilon}_{xx} \dot{\epsilon}_{yy} + (\dot{\epsilon}_{xy})^2} \quad (1.189)$$

$$= ((\partial_x u)^2 + (\partial_y v)^2 + \partial_x u \partial_y v + (\partial_x v + \partial_y u)^2/4)^{1/2} \quad (1.190)$$

If we write

$$\tau_{ij} = 2\eta \dot{\epsilon}_{ij}$$

then η is the effective viscosity given by

$$\eta = \frac{1}{2} A^{-1/n} \dot{\epsilon}^{(1-n)/n} \quad (1.18)$$

or

$$\eta = \frac{1}{2} A^{-1/n} ((\partial_x u)^2 + (\partial_y v)^2 + \partial_x u \partial_y v + (\partial_x v + \partial_y u)^2/4)^{(1-n)/2n} \quad (1.191)$$

1.15 Floating relationships

For a given bedrock geometry B and ocean surface S the ice is floating provided $h < h_f$ where

$$h_f := \rho_o H / \rho, \quad (1.192)$$

and for $h \geq h_f$ the glacier is grounded.

Where the ice is afloat, we have the floating condition

$$\begin{aligned} \rho g (s - b) &= \rho_o g (S - b), \\ \rho g h &= \rho_o g d. \end{aligned}$$

Following relations are obtained by rearranging this floating condition,

$$h = \rho_o d / \rho = \frac{s - S}{1 - \rho / \rho_o} = \frac{\rho_o}{\rho} (S - b), \quad (1.193)$$

$$b = \frac{\rho_o S - \rho s}{\rho_o - \rho} = S - \frac{\rho}{\rho_o} h, \quad (1.194)$$

$$s = S + (1 - \rho / \rho_o) h = (1 - \rho_o / \rho) b + \frac{\rho_o}{\rho} S, \quad (1.195)$$

$$f := s - S = (1 - \rho / \rho_o) h. \quad (1.196)$$

Furthermore, if $\partial_x S = 0$, and ρ is spatially constant, then the slopes of the upper and the lower boundary are related through

$$b \partial_x s - s \partial_x b = S \partial_x h, \quad (1.197)$$

and also

$$\partial_x s = (1 - \rho/\rho_o) \partial_x h.$$

At the grounding line we have

$$\begin{aligned} h &= h_f, \\ d &= H, \end{aligned}$$

where h_f is defined by Eq. (1.192).

1.15.1 Expressing geometrical variables in terms of ice thickness

For a fully implicit treatment, i.e. implicit with respect both velocity and geometry, is advantageous to be able to express geometrical variables such as s , b , and d in terms of ice thickness h .

It is easy to see that

$$s = \mathcal{H}(h - h_f) (h + B) + \mathcal{H}(h_f - h) (S + (1 - \rho/\rho_o) h), \quad (1.198)$$

$$b = \mathcal{H}(h - h_f) B + \mathcal{H}(h_f - h) (S - \rho h/\rho_o), \quad (1.199)$$

and that

$$d := \mathcal{H}(H)(S - b) \quad (1.200)$$

$$= \mathcal{H}(H) [\mathcal{H}(h_f - h) \rho h / \rho_o + \mathcal{H}(h - h_f) H], \quad (1.201)$$

i.e.

$$d = \begin{cases} H, & \text{if } h > h_f \text{ and } H > 0 \\ \rho h / \rho_o, & \text{if } h < h_f \text{ and } H > 0 \\ 0, & \text{if } H < 0 \end{cases}$$

The draft is always $0 \leq d \leq \rho h / \rho_o$.

Eq. (1.201) can be simplified a bit further by noticing that if $H > 0$ then $\mathcal{H}(H)\mathcal{H}(h_f - h) = \mathcal{H}(h_f - h)$. On the other hand if $H < 0$ then $\mathcal{H}(H) = 0$ but so is $\mathcal{H}(h_f - h)$ because if $H = S - B < 0$ then $h_f = \frac{\rho_o}{\rho}(S - B) < 0$ and since h is always positive we have $\mathcal{H}(h_f - h) = 0$, i.e.

$$\mathcal{H}(H)\mathcal{H}(h_f - h) = \mathcal{H}(h_f - h),$$

and d can therefore be written as a function of h as

$$d = \mathcal{H}(h_f - h) \rho h / \rho_o + \mathcal{H}(H)\mathcal{H}(h - h_f) H. \quad (1.202)$$

or as

$$d = \mathcal{H}(h_f - h) \rho h / \rho_o + \mathcal{H}(h - h_f) H^+. \quad (1.203)$$

using

$$H^+ := \mathcal{H}(H) H.$$

1.15.2 Calculating b and s given h , S and B

If we think of S , B , and h as independent variables, i.e.

$$\begin{aligned} s &= s(h, S, B, \rho, \rho_o) \\ b &= b(h, S, B, \rho, \rho_o) \end{aligned}$$

then s and b are given by

$$\begin{aligned} s &= \mathcal{G}(B + h) + (1 - \mathcal{G}) ((1 - \rho_o/\rho)b + \rho_o S / \rho), \\ &= \mathcal{G}(B + h) + (1 - \mathcal{G}) \left(b + \frac{\rho_o}{\rho}(S - b) \right), \\ b &= \mathcal{G}B + (1 - \mathcal{G})(S - \rho h / \rho_o), \end{aligned}$$

valid both over the grounded and the floating sections. where again the grounding/flotation mask \mathcal{G} is defined as

$$\mathcal{G} := \mathcal{H}(h - h_f),$$

with

$$h_f := \rho_o(S - B)/\rho.$$

Here s and b are explicit functions of h because for h and S and B given, the flotation/grounding mask \mathcal{G} is already determined.

In numerical calculations, it may sometimes be desired to use a smooth and continuous approximation of the Heaviside step function.¹¹ However, any smooth approximation of the Heaviside step function will inescapably imply that the upper and lower surfaces are not in a perfect point-wise agreement with flotation/grounding conditions. In particular, we can have the situation where the lower ice surface b is lower than the bedrock B . To see this note that the condition $b \geq B$ implies

$$\begin{aligned} b - B &= B(\mathcal{G} - 1) + (1 - \mathcal{G})(S - \rho h/\rho_o) \\ &= (S - B)(1 - \mathcal{G}) - (1 - \mathcal{G})\rho h/\rho_o \\ &= H(1 - \mathcal{G}) - (1 - \mathcal{G})\rho h/\rho_o \\ &= (H - \rho h/\rho_o)(1 - \mathcal{G}) \\ &\geq 0 \end{aligned}$$

or

$$(\rho_o H/\rho - h)\mathcal{H}(\rho_o H/\rho - h) \geq 0$$

or simply

$$x\mathcal{H}(x) \geq 0.$$

Whenever $\mathcal{H}(x)$ is an exact step function, this inequality is clearly fulfilled for any x . If, however, $\mathcal{H}(x)$ is approximated by some smooth function this is no longer the case. For example, if $\mathcal{H}(-\epsilon) = \delta > 0$ where ϵ and δ are some arbitrarily small positive numbers, then $x\mathcal{H}(x) < 0$ for $x = -\epsilon$ and therefore $b < B$. One can argue that for any sensible approximation of the Heaviside step function, we must have $\mathcal{H}(x) \geq 1/2$ for $x \geq 0$. Assuming this, then at the grounding line where $h = h_f$, we have $\mathcal{G} = 1/2$ and therefore

$$\begin{aligned} b &= B/2 + (S - \rho h_f/\rho_o)/2 \\ &= B/2 + (S - (S - B))/2 \\ &= B \end{aligned}$$

and downstream of the grounding line $b > B$. However, upstream of the grounding line any approximation of the Heaviside step function unavoidably implies that we may encounter a situation where numerically $b < B$. This can be seen to be a consequence of b being partly determined by flotation conditions upstream of the grounding line despite h there being greater than flotation thickness h_f .

1.15.3 Calculating b and h given s , S and B

The lower glacier surface (b) and the ice thickness (h) can be calculated from the upper glacier surface (s), the ocean surface (S) and the bedrock (B) as

$$b = \max \left\{ B, \frac{\rho s - \rho_o S}{\rho - \rho_o} \right\}, \quad (1.204)$$

$$h = s - b. \quad (1.205)$$

Hence, b should never be lower than the bedrock, B , or the flotation limit for the lower surface. Again as discussed above, this is potentially violated if flotation mask is calculated using a (slightly) smoothed step function (as is done in \tilde{U}_a). For that reason this problem is a bit more complicated, and in \tilde{U}_a it is solved implicitly as follows. We write

$$\begin{aligned} b &= b(s, S, B, \rho, \rho_o), \\ h &= h(s, S, B, \rho, \rho_o), \end{aligned}$$

¹¹This is, for example, needed to achieve second-order convergence in the NR iteration.

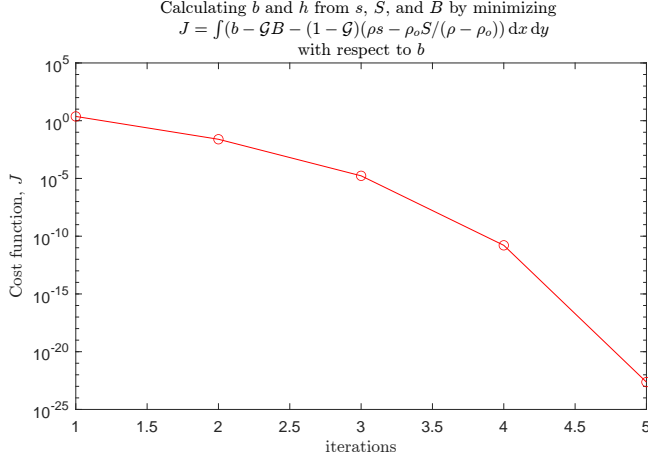


Figure 1.2: Calculating b and h from s , S , and B by minimising J as given in Eq. (1.209) with respect to b .

as

$$b = \mathcal{G} B + (1 - \mathcal{G}) \frac{\rho s - \rho_o S}{\rho - \rho_o}, \quad (1.206)$$

$$h = \mathcal{G} (s - B) + (1 - \mathcal{G}) \frac{s - S}{1 - \rho/\rho_o}, \quad (1.207)$$

where

$$\mathcal{G} = \mathcal{H}(h - \rho_o(S - B)/\rho). \quad (1.208)$$

The system (1.206) to (1.208) is non-linear because \mathcal{G} depends on h . Finding b given s , S and B is equivalent to solving the equation

$$F_b(b) = 0,$$

where the function F_b is defined as

$$F_b(b) := b - \mathcal{G} B - (1 - \mathcal{G}) \frac{\rho s - \rho_o S}{\rho - \rho_o},$$

and \mathcal{G} and h are defined in terms of b through Eqs. (1.206) and (1.207).

We can calculate b from s , S and B given ρ and ρ_o by minimising the cost function J defined as

$$J = \frac{1}{2} \|F_b\|_{l^2}^2 = \frac{1}{2} \mathbf{F}_b \cdot \mathbf{F}_b \quad (1.209)$$

with respect to b using the NR method as follows: For given s , S , B , ρ and ρ_o , and an initial guess for b and h repeat:

$$\begin{aligned} \mathcal{G} &= \mathcal{H}(h - \rho_o(S - B)/\rho) \\ F_b &= b - \mathcal{G} B - (1 - \mathcal{G})(\rho s - \rho_o S)/(\rho - \rho_o) \\ \partial F_b / \partial b &= 1 + \delta(h - h_f) (B - (\rho s - \rho_o S)/(\rho - \rho_o)) \\ (\partial F_b / \partial b) \Delta b &= -F_b \\ b &= b + \Delta b \\ h &= s - b \end{aligned}$$

until $\|J\| < \epsilon$. An initial guess for b and h is provided by Eqs. (1.204) and (1.205).

1.16 Stress boundary conditions at an ice front

We consider the case of an ice front in contact with water of a given depth. The treatment is general and includes the cases of zero water depth, i.e. glacier terminating on land, and a floating ice front, i.e. a glacier terminating in an ocean.

At the calving front the jump condition is

$$\boldsymbol{\sigma} \cdot \hat{\mathbf{n}}_{xy} = -p_o \hat{\mathbf{n}}_n.$$

where p_o is the hydrostatic ocean pressure, and

$$\hat{\mathbf{n}}_{xy} = (n_x, n_y, 0)^T,$$

is a unit normal pointing horizontally outward from the ice front. The vertically integrated form of this stress condition is

$$\int_b^s (\sigma_{xx} n_x + \sigma_{xy} n_y) dz = - \int_b^S p_o n_x dz \quad \text{on } \Gamma_2 \quad (1.210)$$

$$\int_b^s (\sigma_{xy} n_x + \sigma_{yy} n_y) dz = - \int_b^S p_o n_y dz \quad \text{on } \Gamma_2 \quad (1.211)$$

If the draft d at the ice front is zero, i.e. if the ice front is fully grounded, then $S < b$, the right hand sides of (1.210) and (1.211) are to be set to zero.

Using

$$\sigma_{xx} = 2\tau_{xx} + \tau_{yy} + \sigma_{zz},$$

and with

$$\sigma_{zz} = -\rho g(s - z),$$

(where we have set $\alpha = 0$), it follows that

$$\begin{aligned} \int_b^s \sigma_{xx} dz &= \int_b^s (2\tau_{xx} + \tau_{yy}) dz - \int_b^s \rho g(s - z) dx \\ &= h(2\tau_{xx} + \tau_{yy}) - \frac{\rho g}{2} h^2. \end{aligned}$$

The x component of the vertically integrated ocean pressure acting on the calving front is

$$\begin{aligned} - \int_b^S p_o n_x dz &= - \int_b^S \rho_o g(S - z) n_x dz \\ &= - \frac{1}{2} \rho_o g (S - b)^2 \\ &= - \frac{1}{2} \rho_o g d^2. \end{aligned}$$

Boundary conditions (1.210) and (1.211) can therefore be written as

$$h(2\tau_{xx} + \tau_{yy}) n_x + h\tau_{xy} n_y = \frac{g}{2} (\rho h^2 - \rho_o d^2) n_x, \quad (1.212)$$

$$h(2\tau_{yy} + \tau_{xx}) n_y + h\tau_{xy} n_x = \frac{g}{2} (\rho h^2 - \rho_o d^2) n_y, \quad (1.213)$$

or more compactly as

$$\mathbf{R} \cdot \hat{\mathbf{n}}_{xy} = \frac{g}{2h} (\rho h^2 - \rho_o d^2) \hat{\mathbf{n}}_{xy}. \quad (1.214)$$

where the resistive stress tensor, \mathbf{R} , is

$$\mathbf{R} = \begin{pmatrix} 2\tau_{xx} + \tau_{yy} & \tau_{xy} \\ \tau_{xy} & 2\tau_{yy} + \tau_{xx} \end{pmatrix} \quad (1.26)$$

Boundary condition (1.214) is valid for both grounded and floating ice edges.

1.16.1 Floating

In the particular case where the calving front is afloat, $\rho h = \rho_o d$ boundary conditions (1.212) and (1.213) simplify to

$$h(2\tau_{xx} + \tau_{yy})n_x + h\tau_{xy}n_y = \frac{1}{2}\varrho gh^2 n_x \quad (1.215)$$

$$h(2\tau_{yy} + \tau_{xx})n_y + h\tau_{xy}n_x = \frac{1}{2}\varrho gh^2 n_y \quad (1.216)$$

where

$$\varrho := \rho(1 - \rho/\rho_o),$$

Written in terms of the velocity components the boundary conditions along a floating ice front are:

$$\eta h(4\partial_x u + 2\partial_y v)n_x + \eta h(\partial_x v + \partial_y u)n_y = \frac{\varrho gh^2}{2}n_x, \quad (1.217)$$

$$\eta h(\partial_x v + \partial_y u)n_x + \eta h(4\partial_y v + 2\partial_x u)n_y = \frac{\varrho gh^2}{2}n_y. \quad (1.218)$$

1.16.2 Grounded

On the other hand if the ice terminates on land then $d = 0$ and

$$h(2\tau_{xx} + \tau_{yy})n_x + h\tau_{xy}n_y = \frac{g}{2}\rho h^2 n_x, \quad (1.219)$$

$$h(2\tau_{yy} + \tau_{xx})n_y + h\tau_{xy}n_x = \frac{g}{2}\rho h^2 n_y. \quad (1.220)$$

1.17 Boundary condition at a glacier terminus as a natural boundary condition

For solving (1.18) and (1.19) it is advantageous to modify the equations in such a way that the boundary conditions (1.212) and (1.213) become the ‘natural’ boundary conditions. Furthermore, for an implicit time integration with respect to both velocities, grounding-line position, and ice thickness, it is of advantage to write all evolving geometrical variables (s, b) in terms of the ice thickness h .

The key idea is to rewrite (assuming $\alpha = 0$) the Eqs. (1.18) and (1.19) as

$$\partial_x(h(2\tau_{xx} + \tau_{yy})) + \partial_y(h\tau_{xy}) - t_{bx} = \frac{1}{2}g\partial_x(\rho h^2 - \rho_o d^2) + g(\rho h - \rho_o d)\partial_x b, \quad (1.221)$$

$$\partial_y(h(2\tau_{yy} + \tau_{xx})) + \partial_x(h\tau_{xy}) - t_{by} = \frac{1}{2}g\partial_y(\rho h^2 - \rho_o d^2) + g(\rho h - \rho_o d)\partial_y b, \quad (1.222)$$

(note the d term is not missing a $\mathcal{H}(H)$ because d is automatically zero whenever $\mathcal{H}(H) = 0$.) where it has been used that $\partial_x \rho_o = \partial_y \rho_o = 0$ and $\partial_x S = \partial_y S = 0$. Note that in Eqs. (1.221) and (1.222) the second terms on the right hand sides are automatically zero where the ice is afloat and that this formulation can also be used if the ice density varies in the horizontal.

The equality of the right-hand terms in (1.18) and (1.221) (for $\alpha = 0$) follows from

$$\begin{aligned} \frac{1}{2}g\partial_x(\rho h^2 - \rho_o d^2) + g(\rho h - \rho_o d)\partial_x b &= \frac{1}{2}gh^2\partial_x\rho + g(\rho h\partial_x h - \rho_o d\partial_x d) + g(\rho h - \rho_o d)\partial_x b \\ &= \frac{1}{2}gh^2\partial_x\rho + g(\rho h\partial_x(s - b) - \rho_o d\partial_x d) + g(\rho h - \rho_o d)\partial_x b \\ &= \frac{1}{2}gh^2\partial_x\rho + g(\rho h\partial_x s - \rho_o d\partial_x d) - g\rho_o d\partial_x b \\ &= \frac{1}{2}gh^2\partial_x\rho + g(\rho h\partial_x s - \rho_o d\partial_x(\mathcal{H}(H)(S - b))) - g\rho_o d\partial_x b \\ &= \frac{1}{2}gh^2\partial_x\rho + g\rho h\partial_x s - g\rho_o d(S - b)\partial_x \mathcal{H}(H) \end{aligned}$$

and the last term is (in an integrated sense) zero

$$\begin{aligned} \int g\rho_o d(S - b)\partial_x \mathcal{H}(H) dx &= \int g\rho_o d(S - b) \partial_H \mathcal{H}(H) \partial_x H dx \\ &= \int g\rho_o d(S - b) \delta(H) \partial_x H dx \\ &= g\rho_o d(S - b) \quad (\text{for } x \text{ where } H = 0) \\ &= 0 \end{aligned}$$

where the last step follows from the fact that where $H = 0$, we have $S = b$, because if $H = 0$, then $h_f = \rho H / \rho_o = 0$, and hence $h \geq h_f$ because h is never negative. Where $H = 0$ the ice is therefore grounded, and $B = b$ and therefore $S - b = S - B = H = 0$, so $S = b$.

Hence

$$g\rho h \partial_x s + \frac{1}{2}gh^2 \partial_x \rho = \frac{1}{2}g\partial_x(\rho h^2 - \rho_o d^2) + g(\rho h - \rho_o d)\partial_x b. \quad (1.223)$$

Because $\rho_o d \leq \rho h$, with the equality sign fulfilled where the ice is afloat, the second terms on the right-hand sides of Eqs. (1.221) and (1.222) are positive where the ice is both partly and fully grounded, and zero where it is afloat. Therefore

$$\begin{aligned} g(\rho h - \rho_o d)\partial_x b &= \mathcal{H}(h - h_f)g(\rho h - \rho_o d)\partial_x b \\ &= \mathcal{H}(h - h_f)g(\rho h - \rho_o d)\partial_x B \\ &= \mathcal{H}(h - h_f)g(\rho h - \rho_o H^+)\partial_x B \end{aligned}$$

where we used

$$d = \mathcal{H}(h_f - h)\rho h / \rho_o + \mathcal{H}(h - h_f)H^+, \quad (1.203)$$

and hence

$$\mathcal{H}(h - h_f)d = \mathcal{H}^2(h - h_f)H^+,$$

again in an integrated sense (i.e. when evaluated under an integral).

The basal drag terms are also zero where the ice is afloat and the system can therefore be written as

$$\partial_x(h(2\tau_{xx} + \tau_{yy})) + \partial_y(h\tau_{xy}) - t_{bx} = \frac{1}{2}g\partial_x(\rho h^2 - \rho_o d^2) + g\mathcal{H}(h - h_f)(\rho h - \rho_o H^+)\partial_x B \quad (1.224)$$

$$\partial_y(h(2\tau_{yy} + \tau_{xx})) + \partial_x(h\tau_{xy}) - t_{by} = \frac{1}{2}g\partial_y(\rho h^2 - \rho_o d^2) + g\mathcal{H}(h - h_f)(\rho h - \rho_o H^+)\partial_y B \quad (1.225)$$

This suggests how the boundary condition (1.214) can form the natural boundary condition of our FE formulation. This can be achieved by including in the corresponding boundary integral the first terms on the left and right-hand sides of (1.224) and (1.225). The details are given in Section 2.2.

Written in terms of the velocity components:

$$\begin{aligned} \partial_x(h\eta(4\partial_x u + 2\partial_y v)) + \partial_y(h\eta(\partial_y u + \partial_x v)) - t_{bx} &= \\ \frac{1}{2}g\partial_x(\rho h^2 - \rho_o d^2) + g\mathcal{H}(h - h_f)(\rho h - \rho_o H^+)\partial_x B & \end{aligned} \quad (1.226)$$

$$\begin{aligned} \partial_y(h\eta(4\partial_y v + 2\partial_x u)) + \partial_x(h\eta(\partial_x v + \partial_y u)) - t_{by} &= \\ \frac{1}{2}g\partial_y(\rho h^2 - \rho_o d^2) + g\mathcal{H}(h - h_f)(\rho h - \rho_o H^+)\partial_y B & \end{aligned} \quad (1.227)$$

1.18 SSTREAM in 1HD

In one horizontal dimension (1HD), i.e. in the flow-line case, the SSTREAM equation becomes

$$4\partial_x(h\eta\partial_x u) - t_{bx} = \frac{1}{2}g\partial_x(\rho h^2 - \rho_o d^2) + g\mathcal{H}(h - h_f)(\rho h - \rho_o H^+)\partial_x B$$

with

$$\eta = \frac{1}{2}A^{-1/n}\dot{\epsilon}^{(1-n)/n} = \frac{1}{2}A^{-1/n}\|\partial_x u\|^{(1-n)/n}$$

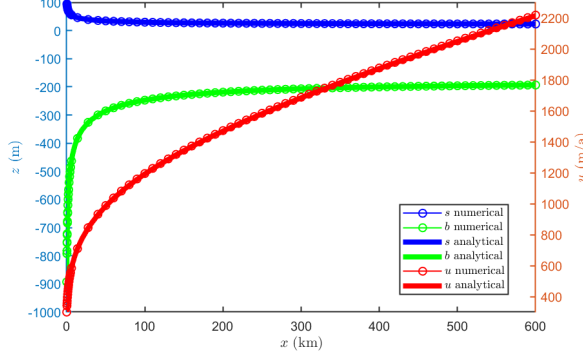


Figure 1.3: Comparison between analytical and numerical solutions for a one-dimensional ice shelf. Parameters: $A = 1.14 \times 10^{-8} \text{ kPa}^{-3} \text{a}^{-1}$, $n = 3$, $h_{gl} = 1000 \text{ m}$, $u_{gl} = 300 \text{ m/a}$, $\rho = 910 \text{ kg m}^{-3}$, $\rho_o = 1030 \text{ kg m}^{-3}$. The value for A corresponds to an ice temperature of about -10 degrees Celsius.

if we use Glen's flow law, and with

$$t_{bx} = \mathcal{H}(h - h_f) C^{-1/m} |u|^{1/m-1} u$$

if we use Weertman sliding law, where d is the draft

$$d = \mathcal{H}(H)(S - b).$$

Inserting Glen's flow law we get

$$2\partial_x(A^{-1/n} h |\partial_x u|^{(1-n)/n} \partial_x u) - t_{bx} = \frac{1}{2} g \partial_x(\rho h^2 - \rho_o d^2) + g \mathcal{H}(h - h_f)(\rho h - \rho_o H^+) \partial_x B \quad (1.228)$$

and if we can assume that $u > 0$ and $\partial_x u > 0$ then the SSTREAM equation is

$$2\partial_x \left(A^{-1/n} h (\partial_x u)^{1/n} \right) - \mathcal{H}(h - h_f) C^{-1/m} u^{1/m} = \rho g h \partial_x s + \frac{1}{2} g h^2 \partial_x \rho \quad (1.229)$$

Eq. (1.229) is a common way of writing down the SSTREAM/SSA equation in 1HD.

If the ice is afloat, in which case $\mathcal{H}(h - h_f) = 1$, and basal drag can be ignored we have

$$2\partial_x(A^{-1/n} h (\partial_x u)^{(1-n)/n} \partial_x u) = \frac{1}{2} g \partial_x(\rho h^2 - \rho_o d^2)$$

which we can integrate to

$$A^{-1/n} h (\partial_x u)^{(1-n)/n} \partial_x u = \frac{1}{4} g (\rho h^2 - \rho_o d^2),$$

where we have used the boundary condition at the calving front to show the integration constant is zero. This can be rearranged to

$$\dot{\epsilon}_{xx} = A \left(\frac{g(\rho h^2 - \rho_o d^2)}{4h} \right)^n,$$

and

$$h \tau_{xx} = \frac{1}{4} g(\rho h^2 - \rho_o d^2).$$

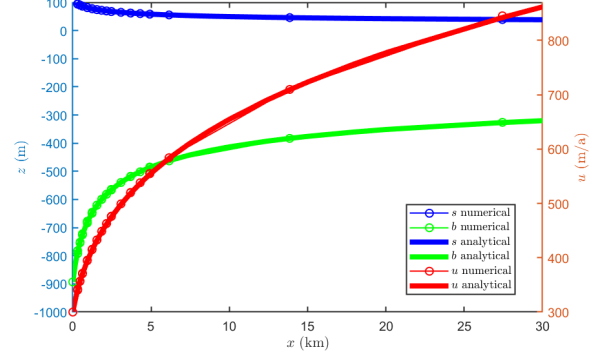


Figure 1.4: Close up of velocity and surface profiles. The analytical solutions are derived in section 11.5, see for example Eq. (11.43). This numerical solution was obtained using linear elements and automated mesh refinement based on the gradient of the effective strain rate.

Chapter 2

Finite-element implementation

The general idea behind finite elements is to expand all functions in a given basis, $\{\phi_p \mid p = 1 \dots n\}$, insert those into the equations, $\mathcal{L}(x) = 0$, to be solved, and then form the algebraic system

$$\langle \mathcal{L}(x) | \phi_q \rangle = 0$$

for $q = 1 \dots n$.

2.1 Function expansions in the FE basis

Generally, when solving for example the non-linear system

$$\mathcal{L} = \partial_x (a(x, f(x)) \partial_x f(x)) + b(x, f(x)) f(x) = g(x, f(x))$$

for the unknown $f(x)$ and the given functions $g(x, f(x))$, $a(x, f(x))$ and $b(x, f(x))$, we expand $f(x)$ as

$$f(x) = f_p \phi_p(x)$$

and solve

$$\langle \mathcal{L}(x, f(x)) | \phi_q \rangle = 0 \quad \text{for } q = 1 \dots n$$

for f_p , where $p = 1 \dots n$. The basis functions, $\phi_q(x)$, have the property that

$$\phi_p(x_q) = \delta_{pq}$$

where x_q are the nodal coordinates. Hence,

$$f(x_q) = f_p \phi_p(x_q) = f_q$$

so f_q is the values of $f(x)$ at the nodal point q with the coordinate x_q .

There are several different options of expanding the functions a , b and g , which in general can be expected to be functions of f for non-linear problems. One approach is to evaluate the functions on the nodal points

$$\begin{aligned} a_p &:= a(x_p, f(x_p)) \\ b_p &:= b(x_p, f(x_p)) \\ g_p &:= g(x_p, f(x_p)) \end{aligned}$$

and then expand as, for example.

$$a(x) = a_p \phi_p(x)$$

Another approach would be to evaluate $a(x, f(x))$ at the integration points. This approach must be used if the functions a , b and g depend on the derivative of $f(x)$, which can only be evaluated within the element, for example at the integration points.

For example, assume we have the two functions $f(x)$ and $h(x)$, and the function $g(x)$ where

$$g(x) = f(h(x)) .$$

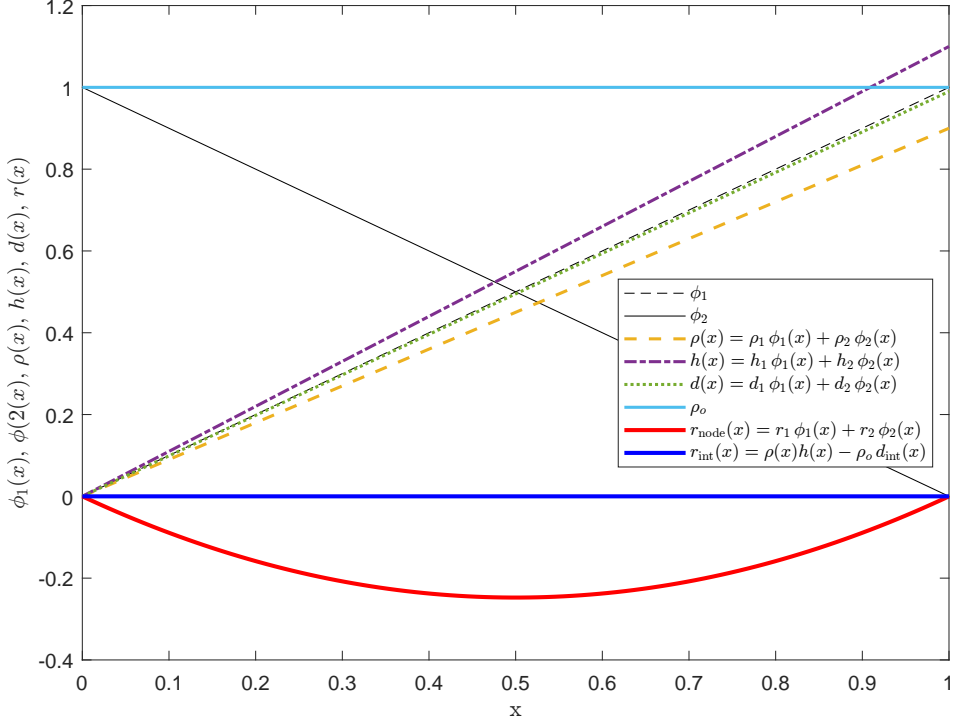


Figure 2.1: Comparison between nodal and integration-point evaluations.

What are the values of $g(x)$ at the integration points x_{int} ? Assuming $f(x)$ and $h(x)$ are expanded in terms of their known nodal values as

$$\begin{aligned} f(x) &= f_p \phi_p(x) \\ h(x) &= h_p \phi_p(x) \end{aligned}$$

then we have two options for expanding $g(x)$, i.e. the nodal-point and the integration-point approach.

Using the nodal-point approach, we write

$$\begin{aligned} g(x) &= g_p \phi_p(x) \\ &= g(f(h_p)) \phi_p(x) \end{aligned}$$

i.e. we evaluate $g(x) = f(h(x))$ at the nodes, giving us the nodal values of $g(x)$ as

$$g_p = f(h_p)$$

and then we expand $g(x)$ as $g(x) = g_p \phi_p(x)$. This gives us the integration-point values for $g(x)$ as

$$g(x_{\text{int}}) = g(f(h_p)) \phi_p(x_{\text{int}})$$

Alternatively, using the integration-point approach, we evaluate the function $g(x)$ at the integration as

$$g(x_{\text{int}}) = g(f(h_{\text{int}}))$$

Generally, those two modes of evaluation integration-point values of a composite function do not agree, that is

$$\underbrace{g(f(h_p)) \phi_p(x_{\text{int}})}_{\text{nodal}} \neq \underbrace{g(f(h_{\text{int}}))}_{\text{integration-point}}$$

As an example, assume $\phi_1(x) = x$ and $\phi_2(x) = 1 - x$, over the interval $0 \leq x \leq 1$, and we expand the functions $\rho(x)$ and $h(x)$ as

$$\begin{aligned} \rho(x) &= \rho_1 \phi_1(x) + \rho_2 \phi_2(x) \\ h(x) &= h_1 \phi_1(x) + h_2 \phi_2(x) \end{aligned}$$

We would like to select $d(x)$ such that

$$\rho(x)h(x) - \rho_o d(x) = 0$$

for $\rho(x)$, $h(x)$ and ρ_o , given, i.e. we must have

$$d(x) = \rho(x)h(x)/\rho_o .$$

Using the nodal-point evaluation for $d(x)$ we first write

$$d_{\text{node}}(x) = d_1\phi_1(x) + d_2\phi_2(x)$$

and solve for d_1 and d_2 by writing the residual

$$r(x) := \rho(x)h(x) - \rho_o d(x)$$

and setting $r(x_j) = 0$ at nodal points, which here are $x_1 = 0$ and $x_2 = 1$. Since

$$\phi_i(x_j) = \delta_{ij}$$

we find that

$$\begin{aligned} d_1 &= \rho_1 h_1 / \rho_o \\ d_2 &= \rho_2 h_2 / \rho_o \end{aligned}$$

The residual r , using the nodal evaluation for $d(x)$, is therefore

$$\begin{aligned} r_{\text{node}}(x) &= (\rho_1\phi_1(x) + \rho_2\phi_2(x))(h_1\phi_1(x) + h_2\phi_2(x)) - \rho_o d_{\text{node}} \\ &= (\rho_1\phi_1(x) + \rho_2\phi_2(x))(h_1\phi_1(x) + h_2\phi_2(x)) - \rho_o(d_1\phi_1(x) + d_2\phi_2(x)) \end{aligned}$$

This residual will be zero at the nodal points where $x = x_p$, but not necessarily zero for all values of x .

Alternatively, we can calculate $d(x)$ at any given location as $d(x) = \rho(x)h(x)/\rho_o$, i.e.

$$d_{\text{int}}(x) = \frac{1}{\rho_o}(\rho_1\phi_1(x) + \rho_2\phi_2(x))(h_1\phi_1(x) + h_2\phi_2(x))$$

Now the residual function, using the integration-point evaluation for $d(x)$, becomes

$$\begin{aligned} r_{\text{int}}(x) &= (\rho_1\phi_1(x) + \rho_2\phi_2(x))(h_1\phi_1(x) + h_2\phi_2(x)) - \rho_o d_{\text{int}}(x) \\ &= (\rho_1\phi_1(x) + \rho_2\phi_2(x))(h_1\phi_1(x) + h_2\phi_2(x)) - (\rho_1\phi_1(x) + \rho_2\phi_2(x))(h_1\phi_1(x) + h_2\phi_2(x)) \end{aligned}$$

which clearly is zero for all values of x . This situation is depicted in Fig. (2.1), for $\rho_1 = 0.9$, $\rho_2 = 0$, $h_1 = 1.1$, $h_2 = 0$, and $\rho_o = 1$. As can be seen, the nodal residual is zero at the nodes, but not at all values within the element.

As a further example consider the basal drag term in 1HD written as

$$t_{bx} = \mathcal{H}(h - h_f)\beta^2(u) u$$

where

$$h_f = \rho_o H / \rho$$

or

$$b(x, u(x)) = \mathcal{H}(h(x) - h_f(x))\beta^2(u(x), x)$$

or, when evaluated at nodes,

$$b(x) = b_p \phi_p(x)$$

where

$$b_p = \mathcal{H}(h(x_p) - h_f(x_p))\beta^2(u_p, x_p)$$

2.2 FE formulation of the diagnostic equations

In the FE method the inner product of the field equations with a test function is formed. The inner product is

$$\langle \phi | \theta \rangle = \iint_{\Omega} \phi \theta \, dx \, dy$$

where ϕ and θ are some functions. One form of Green's theorem states that

$$\iint_{\Omega} \phi \partial_x \theta \, dx \, dy = - \iint_{\Omega} \partial_x \phi \theta \, dx \, dy + \oint_{\Gamma} \phi \theta n_x \, d\Gamma$$

As shown above, the SSA/SSTREAM momentum equations are

$$\partial_x(h(2\tau_{xx} + \tau_{yy})) + \partial_y(h\tau_{xy}) - t_{bx} = \frac{1}{2}g\partial_x(\rho h^2 - \rho_o d^2) + g\mathcal{H}(h - h_f)(\rho h - \rho_o H^+) \partial_x B \quad (1.224)$$

$$\partial_y(h(2\tau_{yy} + \tau_{xx})) + \partial_x(h\tau_{xy}) - t_{by} = \frac{1}{2}g\partial_y(\rho h^2 - \rho_o d^2) + g\mathcal{H}(h - h_f)(\rho h - \rho_o H^+) \partial_y B \quad (1.225)$$

where the (positive) ocean depth is

$$\begin{aligned} H^+ &:= \mathcal{H}(H)H \\ &= \mathcal{H}(H)(S - B) \end{aligned} \quad (1.33)$$

i.e. $H^+ = H$ if $H > 0$ and zero otherwise, and the draft is

$$d = \mathcal{H}(H)(S - b). \quad (5)$$

Applying the Green's theorem on the stress terms and the first term on the right-hand side of Eq. (1.224), i.e. x direction, leads to

$$\begin{aligned} 0 &= \iint_{\Omega} \left(h(2\tau_{xx} + \tau_{yy}) \partial_x \phi + h\tau_{xy} \partial_y \phi + t_{bx} \phi \right. \\ &\quad \left. - \frac{1}{2}g(\rho h^2 - \rho_o d^2) \partial_x \phi \right. \\ &\quad \left. + \phi g \mathcal{H}(h - h_f)(\rho h - \rho_o H^+) \partial_x B \right) dx \, dy \\ &\quad - \oint_{\Gamma} \left(h(2\tau_{xx} + \tau_{yy}) \phi n_x + h\tau_{xy} \phi n_y - \frac{1}{2}g(\rho h^2 - \rho_o d^2) \phi n_x \right) d\Gamma \end{aligned}$$

Performing the same calculation of the y direction results in boundary terms that are identically equal to zero for the boundary condition (1.214). The natural boundary condition is therefore exactly (1.214) and covers not only the case of a fully floating ice front, but that of a grounded and partially grounded ice fronts as well. Using Eq. (1.201) the draft (d) appearing the equations above can be written in terms of the ice thickness (h). This formulation is therefore well suited as a starting point for a linearisation around h required for a fully implicit solution of transient flow.

Expressing the SSA (SSTREAM) momentum equation ins terms of the velocity components u and v leads to

$$\begin{aligned} 0 &= \iint_{\Omega} \left(h\eta(4\partial_x u + 2\partial_y v) \partial_x \phi + h\eta(\partial_y u + \partial_x v) \partial_y \phi + \mathcal{H}(h - h_f)\beta^2 u \phi \right. \\ &\quad \left. - \frac{1}{2}g(\rho h^2 - \rho_o d^2) \partial_x \phi + \phi g \mathcal{H}(h - h_f)(\rho h - \rho_o H^+) \partial_x B \right) dx \, dy \\ &\quad - \oint_{\Gamma} \left(h\eta(4\partial_x u + 2\partial_y v) \phi n_x + h\eta(\partial_y u + \partial_x v) \phi n_y - \frac{1}{2}g(\rho h^2 - \rho_o d^2) N \right) n_x d\Gamma \quad (2.1) \\ 0 &= \iint_{\Omega} \left(h\eta(4\partial_y v + 2\partial_x u) \partial_y \phi + h\eta(\partial_x v + \partial_y u) \partial_x \phi + \mathcal{H}(h - h_f)\beta^2 v \phi \right. \\ &\quad \left. - \frac{1}{2}g(\rho h^2 - \rho_o d^2) \partial_y \phi + \phi g \mathcal{H}(h - h_f)(\rho h - \rho_o H^+) \partial_y B \right) dx \, dy \\ &\quad - \oint_{\Gamma} \left(h\eta(4\partial_y v + 2\partial_x u) \phi n_y + h\eta(\partial_x v + \partial_y u) \phi n_x - \frac{1}{2}g(\rho h^2 - \rho_o d^2) N \right) n_y d\Gamma \quad (2.2) \end{aligned}$$

where the corresponding expression in y direction has been added.

2.3 FE formulation of the transient problem

$\hat{U}a$ allows for implicit time integration with respect to both geometry, grounding-line migration, and velocity. This approach is not limited by the CFL condition and is unconditionally stable allowing for arbitrarily large times steps irrespective of spatial discretisation. The time step is only limited by the convergence radius of the Newton-Raphson method¹.

The recommended option in a transient run is to use an implicit fractional-step θ scheme combined with the consistent streamline-upwind Petrov-Galerkin method (SUPG). This is the default option.

In $\hat{U}a$ a semi-implicit approach (implicit with respect to geometry, explicit with respect to velocity) is also implemented. Unless memory is a limiting factor, the fully implicit approach is always preferable to the semi-implicit (staggered) approach.

Experience shows the θ method to give good results when used in a combination with a fully implicit forward time integration. For a semi-implicit approach a third-order Taylor Galerkin (TG3) is a better approach.

In 2HD both θ and TG3 have been implemented for both staggered and implicit approach. (The 1HD fully implicit was only done using the θ method and not using TG3.) Using TG3 in 1HD staggered approach resulted in a great improvement over the θ method. It appears that in the implicit approach there is no great advantage of using TG3 over the θ method.

There is no separate diffusion term added to the prognostic equations in $\hat{U}a$, and no shock-stabilisation term either. Even just using the fully implicit approach without SUPG generally gives good results. But using SUPG is nevertheless recommended, especially for problems involving grounding line migration.

2.3.1 Time integration algorithms

Consider the transient problem

$$\frac{dy}{dt} = f(y)$$

where f is a known function, and $y = y(t)$. A large number of time-discretisation methods have been proposed.

The θ method

The (generalised) trapezoidal method, often referred to as the θ method, is

$$\frac{y^1 - y^0}{\Delta t} = \theta f(y^1) + (1 - \theta)f(y^0) \quad \theta \in [0, 1] \quad (2.3)$$

where $y^0 = y(t_0)$ and $y^1 = y(t_1)$ with $t_1 = t_0 + \Delta t$. For $\theta = 0$ we have the explicit forward Euler method, for $\theta = 1$ the implicit backward Euler method, and for $\theta = 1/2$ the implicit Crank-Nicolson method.

Selection of method and parameters is problem dependent. Forward Euler should, for example, never be used for hyperbolic equations as it is unconditionally unstable for all wave-numbers. To see this consider the linear hyperbolic equation

$$y_t = -v y_x$$

for $v > 0$, and the finite-difference discretisation on a regular grid for $f(y) = -vy_x$ and $\theta = 0$ in Eq. (2.3) gives

$$\begin{aligned} \frac{y_i^1 - y_i^0}{\Delta t} &= f(y_i^0) \\ &= -v \frac{dy_i^0}{dx} \\ &= -v \frac{y_{j+1}^0 - y_{j-1}^0}{2 \Delta x} \end{aligned}$$

or

$$y_j^1 = y_j^0 - \frac{\xi}{2} (y_{j+1}^0 - y_{j-1}^0)$$

¹Joseph Raphson published his method 50 years earlier than Newton in his book *Analysis Aequationum Universalis*, Raphson (1702)

where $\xi := v \Delta t / \Delta x$ is the Courant number (or the Courant-Friedrichs-Lowy number). Von Neumann stability analysis with

$$\begin{aligned} y_j^1 &= Y_k^1 e^{ikx_j} \\ y_j^0 &= Y_k^0 e^{ikx_j} \\ y_{j+1}^0 &= Y_k^0 e^{ik(x_j + \Delta x)} \\ y_{j-1}^0 &= Y_k^0 e^{ik(x_j - \Delta x)} \end{aligned}$$

gives for the forward Euler method

$$\begin{aligned} Y_k^1 e^{ikx_j} &= Y_k^0 e^{ikx_j} - \frac{\xi}{2} (Y_k^0 e^{ik(x_j + \Delta x)} - Y_k^0 e^{ik(x_j - \Delta x)}) \\ &= Y_k^0 e^{ikx_j} \left(1 - \frac{\xi}{2} (e^{ik\Delta x} - e^{-ik\Delta x}) \right) \\ &= Y_k^0 e^{ikx_j} (1 - i\xi \sin(k\Delta x)) \end{aligned}$$

or the amplification factor r as

$$r := \frac{Y_k^1}{Y_k^0} = 1 - i\xi \sin(k\Delta x)$$

and since $|r| > 0$ for all wave-numbers k and all time steps Δt , the method is always unconditionally unstable.

For backward Euler, where $\theta = 1$, with

$$y_j^1 = y_j^0 - \frac{\xi}{2} (y_{j+1}^1 - y_{j-1}^1)$$

we find

$$\frac{Y_k^1}{Y_k^0} = \frac{1}{1 + i\xi \sin(k\Delta x)}$$

which is unconditionally stable.

In the generalised trapezoidal method, or the θ method, we write

$$\frac{y_i^1 - y_i^0}{\Delta t} = -a \left(\theta \frac{y_{j+1}^1 - y_{j-1}^1}{2 \Delta x} + (1 - \theta) \frac{y_{j+1}^0 - y_{j-1}^0}{2 \Delta x} \right)$$

that is

$$y_i^1 - y_i^0 = -\frac{\xi}{2} (\theta (y_{j+1}^1 - y_{j-1}^1) + (1 - \theta) (y_{j+1}^0 - y_{j-1}^0))$$

And stability analysis gives

$$\begin{aligned} Y_k^1 e^{ikx_j} - Y_k^0 e^{ikx_j} &= -\frac{\xi}{2} (\theta (Y_k^1 e^{ik(x_j + \Delta x)} - Y_k^1 e^{ik(x_j - \Delta x)}) + (1 - \theta) (Y_k^0 e^{ik(x_j + \Delta x)} - Y_k^0 e^{ik(x_j - \Delta x)})) \\ Y_k^1 - Y_k^0 &= -\frac{\xi}{2} (\theta (Y_k^1 e^{ik\Delta x} - Y_k^1 e^{-ik\Delta x}) + (1 - \theta) (Y_k^0 e^{ik\Delta x} - Y_k^0 e^{-ik\Delta x})) \\ Y_k^1 - Y_k^0 &= -\frac{\xi}{2} (\theta Y_k^1 (e^{ik\Delta x} - e^{-ik\Delta x}) + (1 - \theta) Y_k^0 (e^{ik\Delta x} - e^{-ik\Delta x})) \\ Y_k^1 - Y_k^0 &= -i\xi (\theta Y_k^1 (\sin(k\Delta x)) + (1 - \theta) Y_k^0 \sin(k\Delta x))) \end{aligned}$$

or

$$Y_k^1 (1 + i\xi (\theta (\sin(k\Delta x))) = Y_k^0 (1 - i\xi (1 - \theta) \sin(k\Delta x)))$$

that is

$$r = \frac{Y_k^1}{Y_k^0} = \frac{1 - i\xi (1 - \theta) \sin(k\Delta x)}{1 + i\xi \theta \sin(k\Delta x)}$$

For $\theta = 1/2$ the method is A stable but not L stable. For $\theta = 1$ the methods is A and L stable, but somewhat dissipative.

Explicit Euler with upwinding

Apparently, some ice-flow model use forward Euler with upwinding. For the test equation

$$y_t = -v y_x$$

for $a > 0$, finite-difference discretisation with upwinding on a regular grid gives

$$\begin{aligned} \frac{y_i^1 - y_i^0}{\Delta t} &= f(y_i^0) \\ &= -a \frac{dy_i^0}{dx} \\ &= -a \frac{y_j^0 - y_{j-1}^0}{\Delta x} \end{aligned}$$

or

$$y_j^1 = y_j^0 - \xi(y_j^0 - y_{j-1}^0)$$

where $\xi := a \Delta t / \Delta x$ is the Courant number (or the Courant-Friedrichs-Lowy number). Von Neumann stability analysis with

$$\begin{aligned} y_j^1 &= Y_k^1 e^{ikx_j} \\ y_j^0 &= Y_k^0 e^{ikx_j} \\ y_{j-1}^0 &= Y_k^0 e^{ik(x_j - \Delta x)} \\ y_j^0 &= Y_k^0 e^{ikx_j} \end{aligned}$$

gives for the forward Euler method gives for the forward Euler method

$$\begin{aligned} Y_k^1 e^{ikx_j} &= Y_k^0 e^{ikx_j} - \xi(Y_k^0 e^{ikx_j} - Y_k^0 e^{ik(x_j - \Delta x)}) \\ &= Y_k^0 e^{ikx_j} (1 + \xi(e^{ik\Delta x} - 1)) \end{aligned}$$

or the complex amplification factor r as

$$r := \frac{Y_k^1}{Y_k^0} = 1 + \xi (e^{ik\Delta x} - 1)$$

where again

$$\xi := \frac{v \Delta t}{\Delta x}.$$

The method is stable for $\xi < 1$, but causes severe damping of amplitudes with time for even relatively small ξ values (see Fig. 2.2) as compared to the other stable methods.

TR-BDR2

The TR-BDF2 method (Bank et al., 1985) is a two stage method consisting of a fractional trapezoidal (TR) stage followed by a second order backward difference formula (BDF2) stage, i.e.

$$\begin{aligned} \frac{y^\gamma - y^0}{\gamma \Delta t} &= \frac{1}{2} f(y^\gamma) + \frac{1}{2} f(y^0) \\ y^1 - \frac{1}{\gamma(2-\gamma)} y^\gamma + \frac{(1-\gamma)^2}{\gamma(2-\gamma)} y^0 &= \frac{1-\gamma}{2-\gamma} \Delta t f(y^1) \end{aligned}$$

where $\gamma \in (0, 1)$, or as

$$y^\gamma = y^0 + \frac{\gamma \Delta t}{2} (f(y^\gamma) + f(y^0)) \quad (2.4)$$

$$y^1 = \frac{1}{2-\gamma} \left(\frac{1}{\gamma} y^\gamma + \frac{(1-\gamma)^2}{\gamma} y^0 + (1-\gamma) \Delta t f(y^1) \right) \quad (2.5)$$

While this method involves two stages, it is a one-step method as only the solution at the previous time step is required. Note that if we set $\gamma = 1$ we obtain the trapezoidal method, i.e. the θ method for

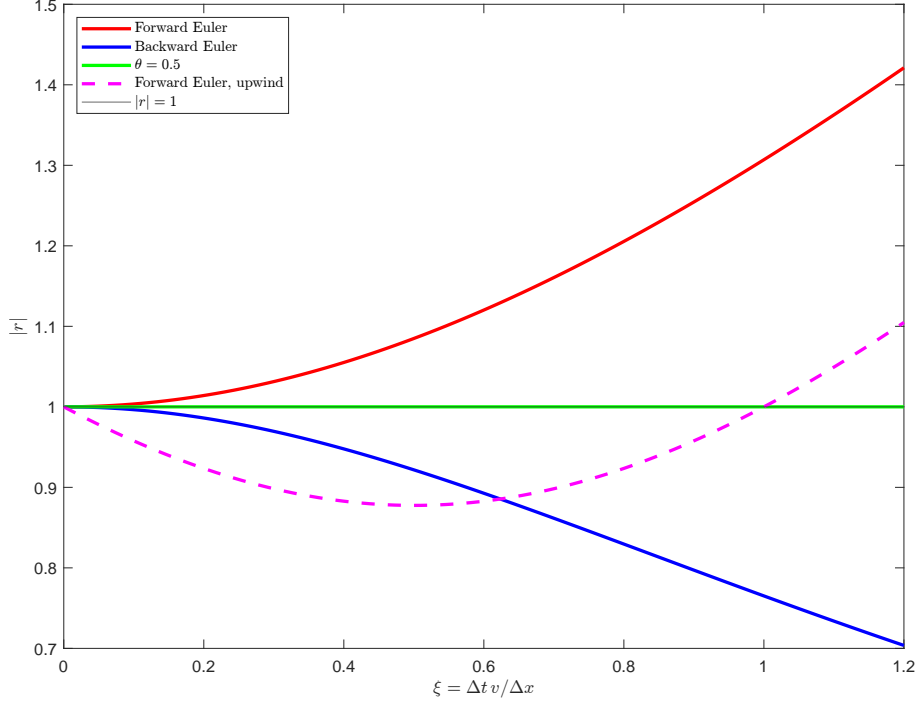


Figure 2.2: Amplification factors for different time discretisation methods, for the $dy/dt = -v dy/dx$ equation.

$\theta = 1/2$. Often the TR-BDF2 method is used with $\gamma = 1/2$ or $\gamma = 2 - \sqrt{2}$. The $\gamma = 2 - \sqrt{2}$ gives the largest stability region and a proportional Jacobian, as we have

$$\frac{\gamma}{2} = \frac{1 - \gamma}{2 - \gamma}$$

for $\gamma = 2 - \sqrt{2}$. The TR-BDF2 method is both A and L stable (Bank et al., 1985; Hosea and Shampine, 1996; Carciopolo, 2015), whereas the trapezoidal method for $\theta = 1/2$ is only A stable, and this is sometimes reflected in oscillations not being damped over time (Dharmaraja, 2007). The TR-BDF2 is a popular time-discretisation methods and used in various FE codes (e.g. Bathe, 2007).

For

$$y_t = f(y) ,$$

the first phase, i.e. the TR part of the TR-BDF2 methods Eq. (2.4) is

$$y^\gamma = y^0 + \frac{\gamma \Delta t}{2} (f(y^\gamma) + f(y^0)) .$$

Using Newton-Raphson method we write

$$y_{i+1}^\gamma = y_i^\gamma + \Delta y ,$$

and

$$\begin{aligned} f(y_{i+1}^\gamma) &= f(y_i^\gamma + \Delta y) \\ &= f(y_i^\gamma) + \partial_y f(y_i^\gamma) \Delta y \end{aligned}$$

where the Jacobian is

$$J_i^\gamma := \partial_y f(y_i^\gamma) ,$$

leading to

$$y_i^\gamma + \Delta y = y^0 + \frac{\gamma \Delta t}{2} (f(y_i^\gamma) + J_i^\gamma \Delta y + f(y^0)) . \quad (2.6)$$

The Newton-Raphson iterations, thus, consist in repeatedly solving

$$\left(\mathbf{1} - \frac{1}{2}\gamma \Delta t J_i^\gamma \right) \Delta y = y^0 - y_i^\gamma + \frac{1}{2}\gamma \Delta t (f(y_i^\gamma) + f(y^0)) \quad (2.7)$$

$$y_i^\gamma \leftarrow y_i^\gamma + \Delta y \quad (2.8)$$

until either $\|\Delta y\| < \epsilon$ or

$$\|y^0 - y_i^\gamma + \frac{1}{2}\gamma \Delta t (f(y_i^\gamma) + f(y^0))\| < \delta$$

where ϵ and δ are some prescribed tolerances.

The second phase, i.e. the BDF2 part of the TR-BDF2 methods Eq. (2.5) is

$$y^1 = \frac{1}{2-\gamma} \left(\frac{1}{\gamma} y^\gamma + \frac{(1-\gamma)^2}{\gamma} y^0 + (1-\gamma) \Delta t f(y^1) \right)$$

Here y^1 is the unknown and y^0 and y^γ are known. Again using the Newton-Raphson method we write

$$y_{i+1}^1 = y_i^1 + \Delta y$$

and

$$\begin{aligned} y_i^1 + \Delta y &= \frac{1}{2-\gamma} \left(\frac{1}{\gamma} y^\gamma + \frac{(1-\gamma)^2}{\gamma} y^0 + (1-\gamma) \Delta t f(y_i^1 + \Delta y) \right) \\ y_i^1 + \Delta y &= \frac{1}{2-\gamma} \left(\frac{1}{\gamma} y^\gamma + \frac{(1-\gamma)^2}{\gamma} y^0 + (1-\gamma) \Delta t (f(y_i^1) + J_i^1 \Delta y) \right) \end{aligned}$$

or

$$\left(\mathbf{1} - \frac{1-\gamma}{2-\gamma} \Delta t J_i^1 \right) \Delta y = -y_i^1 + \frac{1}{2-\gamma} \left(\frac{1}{\gamma} y^\gamma + \frac{(1-\gamma)^2}{\gamma} y^0 + (1-\gamma) \Delta t f(y_i^1) \right) \quad (2.9)$$

$$y_i^1 \leftarrow y_i^1 + \Delta y \quad (2.10)$$

As mentioned above, we get identical left-hand sides of Eqs. (2.7) and (2.9) for $\gamma = 2 - \sqrt{2}$.

Third order implicit Taylor Galerkin (TG3)

This method is also referred to as fourth-order Crank-Nicolson time-stepping.

First expand h at time step 1 and 0 using third order Taylor expansion as

$$h_1 = h_0 + \Delta t \partial_t h_0 + \frac{(\Delta t)^2}{2} \partial_{tt}^2 h_0 + \frac{(\Delta t)^3}{6} \partial_{ttt}^3 h_0,$$

$$h_0 = h_1 - \Delta t \partial_t h_1 + \frac{(\Delta t)^2}{2} \partial_{tt}^2 h_1 - \frac{(\Delta t)^3}{6} \partial_{ttt}^3 h_1,$$

adding and simplifying gives

$$\frac{1}{\Delta t} (h_1 - h_0) = \frac{1}{2} (\partial_t h_0 + \partial_t h_1) + \frac{\Delta t}{4} (\partial_{tt}^2 h_0 - \partial_{tt}^2 h_1) + \frac{(\Delta t)^2}{12} (\partial_{ttt}^3 h_0 + \partial_{ttt}^3 h_1) \quad (2.11)$$

Note that including only the first term of the Taylor expansion is equal to using the θ method with $\theta = 1/2$.

Then replace the third-order derivative is expressed through finite differences giving

$$\begin{aligned} \frac{1}{\Delta t} (h_1 - h_0) &= \frac{1}{2} (\partial_t h_0 + \partial_t h_1) + \frac{\Delta t}{4} (\partial_{tt}^2 h_0 - \partial_{tt}^2 h_1) + \frac{(\Delta t)^2}{12\Delta t} (\partial_{tt}^2 (h_1 - h_0) + \partial_{tt}^2 (h_1 - h_0)) \\ &= \frac{1}{2} (\partial_t h_0 + \partial_t h_1) + \frac{\Delta t}{4} (\partial_{tt}^2 h_0 - \partial_{tt}^2 h_1) + \frac{\Delta t}{6} \partial_{tt}^2 (h_1 - h_0) \end{aligned}$$

i.e.

$$h_1 - h_0 = \frac{\Delta t}{2} (\partial_t h_0 + \partial_t h_1) + \frac{(\Delta t)^2}{12} (\partial_{tt}^2 h_0 - \partial_{tt}^2 h_1) \quad (2.12)$$

At this stage we can use the differential equation, i.e.

$$\frac{dy}{dt} = f(y)$$

to express time derivatives in terms of $f(y)$.

For example if we have an equation on the form

$$\frac{dh}{dt} = a - \nabla \cdot \mathbf{q}(h(t), \mathbf{v}(t))$$

we find

$$\begin{aligned}\rho \partial_{tt}^2 h &= \rho \partial_t a - \nabla_{xy} \cdot \partial_t \mathbf{q} \\ &= \rho \partial_t a - \nabla_{xy} \cdot (\partial_h \mathbf{q} \partial_t h + (\nabla_{uv} \mathbf{q}) \cdot \partial_t \mathbf{v}) \\ &= \rho \partial_t a - \nabla_{xy} \cdot (\partial_h \mathbf{q} (\rho a - \nabla_{xy} \cdot \mathbf{q}) / \rho + (\nabla_{uv} \mathbf{q}) \cdot \partial_t \mathbf{v})\end{aligned}$$

or

$$\rho \partial_{tt}^2 h = \rho \partial_t a - \nabla_{xy} \cdot (\partial_h \mathbf{q} (\rho a - \nabla_{xy} \cdot \mathbf{q}) / \rho + (\nabla_{uv} \mathbf{q}) \cdot \partial_t \mathbf{v}) \quad (2.13)$$

where $\nabla_{uv} := (\partial_u, \partial_v)$ is the *horizontal velocity gradient operator*.

Third-order Taylor-Galerkin (TG3) for SSHEET/SSA

Using (2.13) in the SSHEET/SIA approximation where

$$\mathbf{q} = \mathbf{v}(h),$$

we find that

$$\rho \partial_{tt}^2 h = \rho \partial_t a - \nabla_{xy} \cdot (\partial_h \mathbf{q} (\rho a - \nabla_{xy} \cdot \mathbf{q})).$$

TG3 for SSTREAM/SSA

Using (2.13) in the SSTREAM/SSA approximation where $\mathbf{q} = \rho h \mathbf{v}$ we find²

$$\rho \partial_{tt}^2 h = \rho \partial_t a - \nabla_{xy} \cdot (\mathbf{v} (\rho a - \nabla_{xy} \cdot \mathbf{q}) + \rho h \partial_t \mathbf{v}) \quad (2.15)$$

The Third-Order-Taylor-Galerkin (TG3) method is obtained by inserting Eqs. (1.128) and (2.15) into Eq. (2.12) leading to

$$\begin{aligned}\langle \rho(h_1 - h_0), N \rangle &= \frac{\Delta t}{2} (\langle \rho a_0 - \nabla_{xy} \cdot \mathbf{q}_0 | N \rangle + \langle \rho a_1 - \nabla_{xy} \cdot \mathbf{q}_1 | N \rangle) \\ &\quad + \frac{1}{2} \frac{\Delta t^2}{6} (\langle \rho a_0 - \nabla_{xy} \cdot \mathbf{q}_0 | \mathbf{v}_0 \cdot \nabla_{xy} N \rangle - \langle \rho a_1 - \nabla_{xy} \cdot \mathbf{q}_1 | \mathbf{v}_1 \cdot \nabla_{xy} N \rangle)\end{aligned} \quad (2.16)$$

(where a few terms involving $\partial_t u$ and $\partial_t a$ have been omitted as well as the boundary terms, see below). This from is suitable as a starting point of a fully implicit approach, i.e. where both thickness and velocity is solved for implicitly. Note that the higher-order terms (i.e. those of second and third order) in the implicit TG3 method for $t = t_0$ and $t_1 = t_0 + \Delta t$ have opposite signs. In steady-state they will therefore cancel each other out.

In more detail the TG3 system is as follows (missing ρ in a number of places):

$$\begin{aligned}0 &= \frac{1}{\Delta t} (h_1 - h_0) \\ &\quad - \frac{1}{2} (a_0 - \partial_x(q_{x0}) - \partial_y(q_{y0}) + a_1 - \partial_x(q_{x1}) - \partial_y(q_{y1})) \\ &\quad - \frac{\Delta t}{12} (\partial_t a_0 - \partial_x(h_0 \partial_t u_0 + u_0(a_0 - \partial_x(q_{x0}) - \partial_y(q_{y0}))) - \partial_y(h_0 \partial_t v_0 + v_0(a_0 - \partial_x(q_{x0}) - \partial_y(q_{y0})))) \\ &\quad + \frac{\Delta t}{12} (\partial_t a_1 - \partial_x(h_1 \partial_t u_1 + u_1(a_1 - \partial_x(q_{x1}) - \partial_y(q_{y1}))) - \partial_y(h_1 \partial_t v_1 + v_1(a_1 - \partial_x(q_{x1}) - \partial_y(q_{y1}))))\end{aligned} \quad (2.17)$$

²This expression can also be derived operating on each component as follows

$$\begin{aligned}\partial_{tt}^2 h &= \partial_t a - \partial_{tx}^2(hu) - \partial_{ty}^2(hv) \\ &= \partial_t a - \partial_x(h \partial_t u + u \partial_t h) - \partial_y(h \partial_t v + v \partial_t h)\end{aligned}$$

leading to

$$\partial_{tt}^2 h = \partial_t a - \partial_x(h \partial_t u + u(a - \partial_x(hu) - \partial_y(hv))) - \partial_y(h \partial_t v + v(a - \partial_x(hu) - \partial_y(hv))) \quad (2.14)$$

which is identical to Eq. (2.15).

For (2.17) corresponding Galerkin system is

$$\begin{aligned}
0 = & \int (h_1 - h_0 - \frac{\Delta t}{2}(a_0 - \partial_x(q_{x0}) - \partial_y(q_{0y}) + a_1 - \partial_x(q_{x1}) - \partial_y(q_{y1}))) N dA \\
& - \frac{\Delta t^2}{12} \int (\partial_t a_0 N + (h_0 \partial_t u_0 + u_0(a_0 - \partial_x(q_{x0}) - \partial_y(q_{0y}))) \partial_x N \\
& \quad + (h_0 \partial_t v_0 + v_0(a_0 - \partial_x(q_{x0}) - \partial_y(q_{0y}))) \partial_y N) dA \\
& + \frac{\Delta t^2}{12} \int (\partial_t a_1 N + (h_1 \partial_t u_1 + u_1(a_1 - \partial_x(q_{x1}) - \partial_y(q_{y1}))) \partial_x N \\
& \quad + (h_1 \partial_t v_1 + v_1(a_1 - \partial_x(q_{x1}) - \partial_y(q_{y1}))) \partial_y N) dA \\
& + \frac{\Delta t^2}{12} \oint ((h_0 \partial_t u_0 + u_0(a_0 - \partial_x(q_{x0}) - \partial_y(q_{0y}))) n_x \\
& \quad + (h_0 \partial_t v_0 + v_0(a_0 - \partial_x(q_{x0}) - \partial_y(q_{0y}))) n_y) N d\gamma \\
& - \frac{\Delta t^2}{12} \oint ((h_1 \partial_t u_1 + u_1(a_1 - \partial_x(q_{x1}) - \partial_y(q_{y1}))) n_x \\
& \quad + (h_1 \partial_t v_1 + v_1(a_1 - \partial_x(q_{x1}) - \partial_y(q_{y1}))) n_y) N d\gamma
\end{aligned} \tag{2.18}$$

where the second order spatial derivatives have been eliminated through partial integration.

The boundary term can be written as

$$\begin{aligned}
& \frac{\Delta t^2}{12} \oint ((h_0 \partial_t u_0 + u_0(a_0 - \partial_x(q_{x0}) - \partial_y(q_{0y}))) n_x \\
& \quad + (h_0 \partial_t v_0 + v_0(a_0 - \partial_x(q_{x0}) - \partial_y(q_{0y}))) n_y) N d\gamma \\
& - \frac{\Delta t^2}{12} \oint ((h_1 \partial_t u_1 + u_1(a_1 - \partial_x(q_{x1}) - \partial_y(q_{y1}))) n_x \\
& \quad + (h_1 \partial_t v_1 + v_1(a_1 - \partial_x(q_{x1}) - \partial_y(q_{y1}))) n_y) N d\gamma \\
& = \frac{\Delta t^2}{12} \oint ((h_0 \partial_t u_0 + u_0 \partial_t h_0) n_x + (h_0 \partial_t v_0 + v_0 \partial_t h_0) n_y) N d\gamma \\
& - \frac{\Delta t^2}{12} \oint ((h_1 \partial_t u_1 + u_1 \partial_t h_1) n_x + (h_1 \partial_t v_1 + v_1 \partial_t h_1) n_y) N d\gamma \\
& = \frac{\Delta t^2}{12} \oint (\partial_t(q_{x0}) n_x + \partial_t(q_{0y}) n_y) N d\gamma - \frac{\Delta t^2}{12} \oint (\partial_t(q_{x1}) n_x + \partial_t(h_1 v_1) n_y) N d\gamma \\
& = \frac{\Delta t^2}{12} \oint \partial_t(h_0 \mathbf{v}_0 - h_1 \mathbf{v}_1) \cdot \mathbf{n} N d\gamma
\end{aligned}$$

showing that it disappears if $\partial_t q = 0$ over the boundary. Experience suggests that this boundary term can be ignored.

2.4 Consistent Streamline-Upwind Petrov-Galerkin (SUPG)

The standard SUPG is of the form

$$\langle \rho \partial_t h + \nabla \mathbf{q} - \rho a | N + M \rangle = 0 \tag{2.19}$$

where M is a perturbation to the test-function space. In the literature various forms for M have been suggested. One such form is

$$M = \tau \mathbf{v} \cdot \nabla N$$

where τ is a parameter with the dimension of time [Jia and Esmaily \(2023\)](#). Note that in (2.19) the added term is applied to all terms, including time derivative. This is sometimes referred to as a 'consistent' weighting. The extra terms are interpreted element-wise, as

$$\langle \rho \partial_t h + \nabla \mathbf{q} - \rho a | N \rangle + \beta \sum_e \langle \rho \partial_t h + \nabla q - \rho a | \tau \mathbf{v} \cdot \nabla N \rangle = 0$$

The extra term, which is considered as a correction term, is zero for an exact solution in the classical sense. There is no one single accepted/optimal way of selecting τ , and in the literature various definition has been proposed, e.g. [Manzan, M; Oñate \(2000\)](#).

The SUPG was initially introduced for equations on the form

$$\partial_t h + \mathbf{v} \cdot \nabla h - \nabla \cdot k \nabla h + g = 0$$

and in this case, and for linear elements and regular grids, the optimal value for τ is

$$\tau = \frac{l}{2\|\mathbf{v}\|} \left(\coth \text{Pe} - \frac{1}{\text{Pe}} \right). \quad (2.20)$$

where the Péclet number is

$$\text{Pe} = \|\mathbf{v}\| l / (2k)$$

with k the diffusivity and l is a measure of the (local) element size. In the limiting case where $k \rightarrow 0$, the equation becomes hyperbolic, $\text{Pe} \rightarrow +\infty$, and τ simply becomes

$$\tau = \frac{l}{2\|\mathbf{v}\|}$$

and perturbation term to the test function has the form

$$M = \frac{l}{2\|\mathbf{v}\|} \mathbf{v} \cdot \nabla N$$

If on the other hand $\text{Pe} \rightarrow 0$ then (2.20) leads to

$$\tau = \frac{l}{2\|\mathbf{v}\|} \frac{\text{Pe}}{3} = \frac{l}{2\|\mathbf{v}\|} \frac{\|\mathbf{v}\| l}{6k} = \frac{l^2}{12k}$$

in which case

$$M = \frac{l^2}{12k} \mathbf{v} \cdot \nabla N.$$

It is somewhat unclear how best to estimate the Péclet number for the mass conservation equation

$$\rho \partial_t h + u \partial_x h + h \partial_x u = \rho a$$

But if we consider the problem of grounded ice with flow mainly due to Weertman type sliding, where

$$u = -C(\rho gh)^m |\partial_x h|^{m-1} \partial_x h$$

assuming flat bed. Inserting gives a diffusion term on the form

$$-hC(\rho gh)^m m (\partial_x h)^{m-1} \partial_{xx}^2 h$$

or

$$k = mCh(\rho gh)^m (\partial_x h)^{m-1}$$

which has the units of velocity times distance. Using the sliding law, we write

$$k = \frac{muh}{|\partial_x h|}$$

suggesting that the element Péclet number is

$$\begin{aligned} \text{Pe} &= \frac{\|\mathbf{v}\| l}{2k} \\ &\approx \frac{\|\nabla h\| l}{2mh} \\ &\approx \frac{10^{-3}}{1000} l \end{aligned}$$

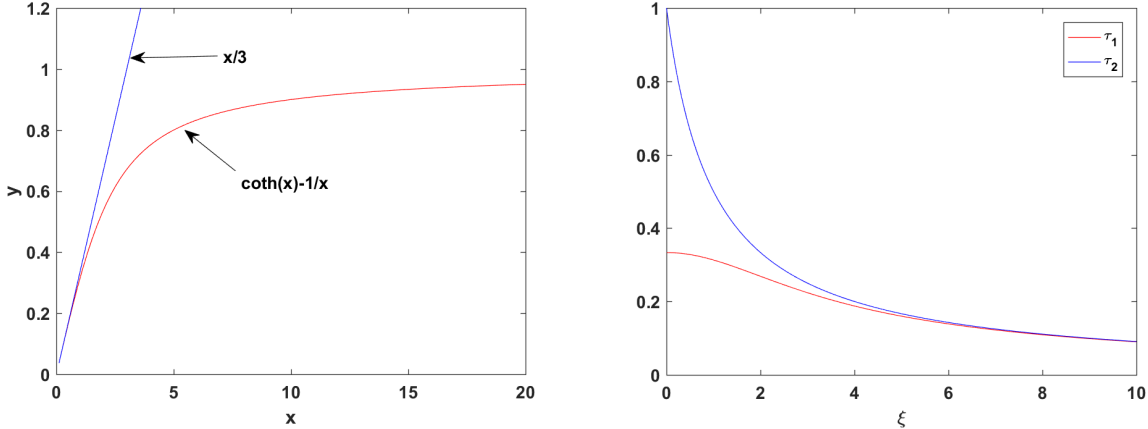


Figure 2.3: SUPG

where l is in the units meters. So for almost all element sizes $\text{Pe} \ll 1$. This suggests using

$$\begin{aligned}\tau &= \frac{l^2}{12k} \\ &\propto \frac{\|\nabla h\|}{12mh} \frac{l^2}{\|\mathbf{v}\|}\end{aligned}$$

The value of τ given by (2.20) does not depend on Δt . For transient problems with high Péclet number it has been suggested using

$$\tau = \tau_t$$

where

$$\tau_t := \Delta t/2 \quad (2.21)$$

as well as

$$\tau = \tau_s$$

where

$$\tau_s := \frac{l}{2\|\mathbf{v}\|} \quad (2.22)$$

The first definition (τ_t) is a temporal criterion while the second (τ_s) is a spatial criterion. The first form is often used in transient situations where diffusion is small and the problem either hyperbolic or close to being hyperbolic. The second form is often used for convection diffusion problems involving temperature such as $\mathbf{v} \cdot \nabla T - \nabla(k\nabla T) + f = 0$ (no time dependency).

A guidance as to how to select τ is looking at some specific limits. The SUPG correction term should vanish if $\Delta t \rightarrow 0$, if $l \rightarrow 0$, and also if $\|\mathbf{v}\| \rightarrow 0$. A smart choice could then be

$$\tau = \tau_1$$

where

$$\tau_1 := \tau_s \kappa \quad (2.23)$$

$$= \frac{l}{2\|\mathbf{v}\|} \kappa \quad (2.24)$$

with

$$\kappa = \coth \xi - \frac{1}{\xi} \quad (2.25)$$

and where

$$\xi = \frac{\|\mathbf{v}\|}{l} \Delta t \quad (2.26)$$

$$= \frac{1}{2\tau_s} 2\tau_t \quad (2.27)$$

$$= \frac{\tau_t}{\tau_s} \quad (2.28)$$

is the element Courant number and l is a characteristic local element size. We can also write τ_1 as

$$\begin{aligned}\tau_1 &:= \frac{l}{2\|\mathbf{v}\|} \kappa \\ &= \frac{\Delta t}{2} \frac{1}{\xi} \left(\coth(\xi) - \frac{1}{\xi} \right) \\ &= \frac{l}{2\|\mathbf{v}\|} \left(\coth\left(\frac{\|\mathbf{v}\|\Delta t}{l}\right) - \frac{l}{\|\mathbf{v}\|\Delta t} \right).\end{aligned}$$

For $\xi \ll 1$ we have $\kappa \sim \xi/3$, and

$$\tau_1 = \frac{l}{2\|\mathbf{v}\|} \frac{\|\mathbf{v}\|\Delta t}{3l} = \Delta t/6$$

hence

$$M = \frac{\Delta t}{6} \mathbf{v} \cdot \nabla N$$

showing that for $\tau = \tau_1$ the SUPG correction term does indeed go to zero as either $\Delta t \rightarrow 0$ and $\|\mathbf{v}\| \rightarrow 0$. Furthermore, if $l \rightarrow 0$ then $\kappa \rightarrow 1$ and $\tau_1 \rightarrow 0$, so all the above listed limits are obtained with $\tau = \tau_1$ given by (2.24).

In summary, for $\tau = \tau_1$ given by (2.24) the SUPG perturbation term is

$$M = \frac{l\kappa}{2\|\mathbf{v}\|} \mathbf{v} \cdot \nabla N$$

and the following limits are obtained

$$\begin{aligned}M &\rightarrow 0 \quad \text{when } \Delta t \rightarrow 0 \\ M &\rightarrow 0 \quad \text{when } \|\mathbf{v}\| \rightarrow 0 \\ M &\rightarrow 0 \quad \text{when } l \rightarrow 0\end{aligned}\tag{2.29}$$

$$M \rightarrow \frac{l}{2\|\mathbf{v}\|} \frac{\mathbf{v}}{\|\mathbf{v}\|} \cdot \nabla N \quad \text{when } \Delta t \rightarrow \infty\tag{2.29}$$

$$M \rightarrow \frac{l}{2\|\mathbf{v}\|} \frac{\mathbf{v}}{\|\mathbf{v}\|} \cdot \nabla N \quad \text{when } \|\mathbf{v}\| \rightarrow \infty\tag{2.30}$$

$$M \rightarrow \frac{\Delta t}{6} \mathbf{v} \cdot \nabla N \quad \text{when } l \rightarrow \infty\tag{2.31}$$

In the literature it is shown that (2.29) and (2.30) is the optimal choice in the convective limit, i.e. for large element Courant numbers. Limit (2.31) can be justified using Taylor-Galerkin approach (see below). The local element size, l , can be defined in a number of similar ways leading to different numerical pre-factors to τ and ξ . The exact functional relationship between κ and ξ is also not uniquely defined.

Another option of creating a smooth transition between the temporal and spatial criteria 2.21 and 2.22 is to select τ as

$$\tau = \tau_2$$

where

$$\tau_2 := \left(\frac{1}{\tau_t} + \frac{1}{\tau_s} \right)^{-1}\tag{2.32}$$

which can also be written as

$$\tau_2 = \frac{1}{2} \frac{\Delta t}{1 + \xi}\tag{2.33}$$

Expression (2.33) gives the limits

$$\begin{aligned}M &\rightarrow 0 \quad \text{when } \Delta t \rightarrow 0 \\ M &\rightarrow 0 \quad \text{when } \|\mathbf{v}\| \rightarrow 0 \\ M &\rightarrow 0 \quad \text{when } l \rightarrow 0 \\ M &\rightarrow \frac{l}{2\|\mathbf{v}\|} \frac{\mathbf{v}}{\|\mathbf{v}\|} \cdot \nabla N \quad \text{when } \Delta t \rightarrow \infty \\ M &\rightarrow \frac{l}{2\|\mathbf{v}\|} \frac{\mathbf{v}}{\|\mathbf{v}\|} \cdot \nabla N \quad \text{when } \|\mathbf{v}\| \rightarrow \infty \\ M &\rightarrow \frac{\Delta t}{2} \mathbf{v} \cdot \nabla N \quad \text{when } l \rightarrow \infty\end{aligned}\tag{2.34}$$

Table 2.1: SUPG form function (M) limits for different definitions of τ

	$\Delta t \rightarrow 0$	$\ \mathbf{v}\ \rightarrow 0$	$l \rightarrow 0$	$\Delta t \rightarrow \infty$	$\ \mathbf{v}\ \rightarrow \infty$	$l \rightarrow \infty$	$\xi \rightarrow \infty$
$M = \tau_1 \mathbf{v} \cdot \nabla N$	0	0	0	$\frac{l}{2} \frac{\mathbf{v}}{\ \mathbf{v}\ } \cdot \nabla N$	$\frac{l}{2} \frac{\mathbf{v}}{\ \mathbf{v}\ } \cdot \nabla N$	$\frac{\Delta t}{6} \mathbf{v} \cdot \nabla N$	0
$M = \tau_2 \mathbf{v} \cdot \nabla N$	0	0	0	$\frac{l}{2} \frac{\mathbf{v}}{\ \mathbf{v}\ } \cdot \nabla N$	$\frac{l}{2} \frac{\mathbf{v}}{\ \mathbf{v}\ } \cdot \nabla N$	$\frac{\Delta t}{2} \mathbf{v} \cdot \nabla N$	0
$M = \tau_t \mathbf{v} \cdot \nabla N$	0	0	$\frac{\Delta t}{2} \mathbf{v} \cdot \nabla N$	∞	∞	$\frac{\Delta t}{2} \mathbf{v} \cdot \nabla N$	
$M = \tau_s \mathbf{v} \cdot \nabla N$	$\frac{l}{2\ \mathbf{v}\ } \mathbf{v} \cdot \nabla N$	0	0	$\frac{l}{2} \frac{\mathbf{v}}{\ \mathbf{v}\ } \cdot \nabla N$	$\frac{l}{2} \frac{\mathbf{v}}{\ \mathbf{v}\ } \cdot \nabla N$	∞	

Apart from a different numerical factor in the last limit, all limits are the same as obtained using definition (2.24).

These two above listed options for τ can also be written as

$$\tau_1 = \frac{\Delta t}{2} \frac{1}{\xi} (\coth \xi - 1/\xi) \quad (2.35)$$

$$\tau_2 = \frac{\Delta t}{2} \frac{1}{1+\xi} \quad (2.36)$$

and they are shown in Fig. 2.3b as functions of ξ for $\Delta t/2 = 1$. Only for $\|\mathbf{v}\| \Delta t < 2l$ is there any significant difference, and the difference is never larger than a factor 3 obtained in the limit $\xi \rightarrow 0$. It appears unlikely that there will be any significant resulting differences between selecting $\tau = \tau_1$ or $\tau = \tau_2$ (see (2.35) and (2.36)). Currently the SUPG implementation in $\tilde{U}a$ uses $\tau = \tau_1$.

Implementing SUPG implicitly using the θ method leads to

$$0 = \langle \rho(h_1 - h_0)/\Delta t + (1-\theta)(\nabla_{xy} \cdot \mathbf{q}_0 - a_0) + \theta(\nabla_{xy} \cdot \mathbf{q}_1 - a_1) | N \rangle \\ + \beta \langle \rho(h_1 - h_0)/\Delta t + (1-\theta)(\nabla_{xy} \cdot \mathbf{q}_0 - a_0) + \theta(\nabla_{xy} \cdot \mathbf{q}_1 - a_1) | \tau ((1-\theta)\mathbf{v}_0 + \theta\mathbf{v}_1) \cdot \nabla_{xy} N \rangle$$

Here the correction/perturbation to the test-function space is a weighted average over the values at the beginning and the end of the time step. This adds another source of non-linearity to the problem. Experience showed this to reduce the radius of convergence considerably and to increase grumpiness on a personal level. Former can be avoided by using the value of perturbation term at the beginning of the time step, i.e.

$$0 = \langle \rho(h_1 - h_0)/\Delta t + (1-\theta)(\nabla_{xy} \cdot \mathbf{q}_0 - a_0) + \theta(\nabla_{xy} \cdot \mathbf{q}_1 - a_1) | N \rangle \\ + \beta \langle \rho(h_1 - h_0)/\Delta t + \nabla_{xy} \cdot \mathbf{q}_0 - a_0 | \tau \mathbf{v}_0 \cdot \nabla_{xy} N \rangle$$

In summary, these options for τ are

$$\begin{aligned} \tau_s &:= \frac{l}{2\|\mathbf{v}\|}, \\ \tau_t &:= \Delta t/2 \\ \tau_1 &:= \tau_s \kappa = \frac{l}{2\|\mathbf{v}\|} \kappa, \\ \tau_2 &:= \left(\frac{1}{\tau_t} + \frac{1}{\tau_s} \right)^{-1} = \frac{\Delta t}{2(1+\xi)}, \end{aligned}$$

with

$$\begin{aligned} \kappa &= \coth \xi - \frac{1}{\xi} \\ \xi &= \frac{\|\mathbf{v}\|}{l} \Delta t, \end{aligned}$$

where the SUPG term is

$$M = \tau \mathbf{v} \cdot \nabla N.$$

These stabilisation methods are usually motivated by considering the convection-diffusion-reaction equation

$$\partial_t h + \mathbf{u} \cdot \nabla h - \epsilon \nabla^2 h + ch = f$$

with the weak form

$$a(h, \phi) = (f, \phi)$$

The SUPG stabilisation term is then

$$\tau \langle \mathbf{u} \cdot \nabla h, \mathbf{u} \cdot \nabla \phi \rangle$$

where, for example,

$$\tau = \tau_0 \min \left\{ \frac{l}{\|\mathbf{v}\|}, \frac{l^2}{\epsilon} \right\}$$

The mass conservation equation

$$\rho \partial_t h + u \partial_x h + h \partial_x u = \rho a$$

If we consider the problem of grounded ice with flow mainly due to Weertman type sliding, where

$$u = -C(\rho gh)^m |\partial_x h|^{m-1} \partial_x h$$

assuming flat bed. Inserting gives a diffusion term on the form

$$-h C(\rho gh)^m m (\partial_x h)^{m-1} \partial_{xx}^2 h$$

or

$$\epsilon = m Ch(\rho gh)^m (\partial_x h)^{m-1}$$

which has the units of velocity times distance. Using the sliding law, we write

$$\epsilon = hu \frac{m}{|\partial_x h|}$$

and as expected the diffusion term goes to infinity for zero surface slopes. We therefore have

$$\begin{aligned} \tau &= \tau_0 \min \left\{ \frac{l}{\|\mathbf{v}\|}, \frac{l^2}{\epsilon} \right\} \\ &= \tau_0 \min \left\{ \frac{l}{\|\mathbf{v}\|}, \frac{l^2 \|\nabla h\|}{\|\mathbf{v}\| mh} \right\} \\ &= \tau_0 \frac{l}{\|\mathbf{v}\|} \min \left\{ 1, \frac{l \|\nabla h\|}{h m} \right\} \end{aligned}$$

2.5 SIA-motivated diffusion

$$\mathbf{q} = \mathbf{q}^b + \mathbf{q}^d$$

where

$$\mathbf{q}^b = \mathbf{v} h$$

and

$$\mathbf{q}^d = \rho D h^{n+2} \|\nabla_{xy} s\|^{n-1} \nabla s$$

where

$$D = \frac{2A}{n+2} (\rho g)^n$$

$$s = (h + B)\mathcal{H}(h - h_f) + (1 - \mathcal{H}(h - h_f))(S + (1 - \rho/\rho_o) h)$$

and therefore (almost)

$$\partial_x s = (\partial_x h + \partial_x B)\mathcal{H}(h - h_f) + (1 - \mathcal{H}(h - h_f))(S + (1 - \rho/\rho_o) \partial_x h)$$

This motivates adding a SIA based diffusion term

$$-D \langle \|\nabla_{xy} s\|^{n-1} h^{n+2} \nabla s \mid \nabla_{xy} N \rangle$$

However, this is (currently) not done in *Ua*.

In 1HD the SIA form of the continuity equation can be written as

$$\rho \partial_t s + \partial_x (k \partial_x s) = \rho a$$

with

$$k := \frac{2\rho A (\rho g)^n}{n+2} \|\partial_x s\|^{n-1} h^{n+2}$$

suggesting a Peclet number

$$\text{Pe} = \frac{uL}{k}$$

2.6 Connection between third order Taylor-Galerkin (TG3) and streamline-upwind Petrov-Galerkin (SUPG)

In the context of SUPG, the TG3 system given by (2.16) can be thought of as also introducing extra weighting term beside the standard N term. But those additional weighting terms are only applied to the source term (a) and the spatial term, and not to the time-derivative term. Furthermore, as mentioned above in a steady-state these extra weighting terms cancel each other out.

It is instructive to consider as well the case where a second-order forward Taylor expansion

$$h_1 = h_0 + \Delta t \partial_t h_0 + \frac{(\Delta t)^2}{2} \partial_{tt}^2 h_0 \quad (2.37)$$

is used instead of the centred expansion given by Eq. (2.12). Inserting (1.128) and (2.15) into (2.37) gives

$$0 = h_1 - h_0 - \Delta t (a - \nabla_{xy} \cdot \mathbf{q}) - \frac{(\Delta t)^2}{2} (\partial_t a - \nabla_{xy} \cdot (\mathbf{v}(a - \nabla_{xy} \cdot \mathbf{q}) + h \partial_t \mathbf{v}))$$

The Galerkin system is

$$\begin{aligned} \langle \rho(h_1 - h_0), N \rangle &= \Delta t \langle \rho a - \nabla_{xy} \cdot \mathbf{q}, N \rangle \\ &\quad + \frac{(\Delta t)^2}{2} \langle \rho \partial_t a, N \rangle - \frac{(\Delta t)^2}{2} \langle \rho h \partial_t \mathbf{v}, N \rangle \\ &\quad + \frac{(\Delta t)^2}{2} \langle \rho a - \nabla_{xy} \cdot \mathbf{q} \mid \mathbf{v} \cdot \nabla_{xy} N \rangle \end{aligned}$$

where a partial integration has been used to get rid of second order derivatives (not writing the boundary terms). The last term is similar to what in some other ad-hoc methods is introduced as a stabilisation term. This term only acts in the direction of flow and is zero transverse to the flow direction. In the above expression all terms are to be evaluated at the beginning of the interval. This approach is usually referred to as the second-order explicit Taylor-Galerkin (TG2e) method. If we evaluate all terms by taking the mean value over the time interval, we get an implicit method, but now the second-order terms do not cancel out in steady-state, and the resulting method is quite similar to the streamline-upwind Petrov-Galerkin.

Dropping the time derivatives of a and \mathbf{v} , we can rewrite the above system as

$$\langle \rho(h_1 - h_0)/\Delta t, N \rangle = \langle \rho a - \nabla_{xy} \cdot \mathbf{q}, N + \frac{1}{2} \Delta t \mathbf{v} \cdot \nabla_{xy} N \rangle$$

showing that the TG2e results in an ‘inconsistent’ weighting with $\tau = \Delta t$ and $\beta = 1/2$.

Comparing 2.16 with (2.19), TG3 can be interpreted as a some sort of Petrov-Galerkin method where only the spatial terms and the source terms are multiplied by a modified test function. In TG3 the modified test function is

$$N + \frac{\Delta t}{6} \mathbf{v} \cdot \nabla_{xy} N, \quad (2.38)$$

wheres in SUPG it has the form

$$N + \beta \tau \mathbf{v} \cdot \nabla_{xy} N. \quad (2.39)$$

The weighting is done inconsistently in TG3, i.e. not over the time-derivative. Apart for the inconsistent weighting used in TG3, the SUPG is equal to TG3 provided the two adjustable parameters β and τ are selected as $\beta = 1/6$ and $\tau = \Delta t$.

The TG3 methods follows automatically from a third-order Taylor expansion and involves no adjustable parameters. The SUPG is in essence a heuristic method.

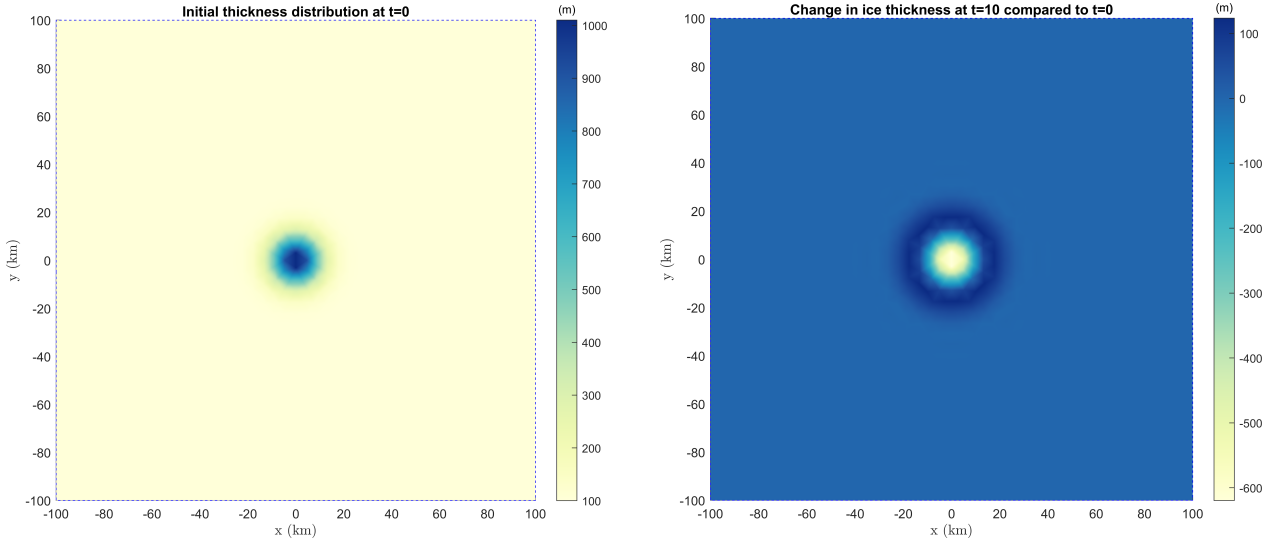


Figure 2.4: Initial ice thickness distribution at $t = 0$. Parameters: $A = 3 \times 10^{-9} \text{ kPa}^{-3} \text{ a}^{-1}$, $n = 3$, $C = 0.0125 \text{ kPa}^{-3}$, $m = 3$, $a_s = a_b = 0 \text{ m a}^{-1}$, $\rho = 900 \text{ kg m}^{-3}$.

Figure 2.5: Changes in ice thickness distribution at $t = 10 \text{ yr}$.

2.7 Implementing fully-implicit forward time integration with respect to velocity and thickness

In a fully implicit approach using the Newton-Raphson iteration the unknowns at time-step 1 are written in incremental form as

$$\begin{aligned} u_1^{i+1} &= \Delta u + u_1^i, \\ v_1^{i+1} &= \Delta v + v_1^i, \\ h_1^{i+1} &= \Delta h + h_1^i, \end{aligned}$$

where u_1^{i+1} is the estimate for u_1 at Newton-Raphson iteration step i . (Note that $\Delta h \neq h_1 - h_0$ and that $\Delta h \rightarrow 0$ with increasing i .)

2.7.1 Mass conservation test

Figures (2.4) to (2.7) show the results of a mass-conservation test. The bedrock is flat with $b = B = 0$, and the surface is a Gaussian peak on the form

$$s(x, y, t = 0) = \Delta s_0 e^{-(x/\sigma)^2 - (y/\sigma)^2} + s_0$$

with $\Delta s_0 = 1000 \text{ m}$, $\sigma = 10,000 \text{ m}$, and $s_0 = 100 \text{ m}$. Using the SSA flow approximation the problem was solved implicitly with respect to velocities and thickness using linear elements. As the Fig. (2.7) shows, mass is conserved to a high degree of accuracy.

2.7.2 First-order fully implicit

Taking only the first-order Taylor terms from (2.18), and only considering the x components for the time being, gives

$$\begin{aligned} 0 &= \frac{\rho}{\Delta t} (\Delta h + h_1^i - h_0) \\ &\quad - \frac{1}{2} (\rho(a_0 + a_1) - \partial_x(\rho u_0 h_0) - \partial_x(\rho(\Delta h + h_1^i)(\Delta u + u_1^i))) \end{aligned}$$

2.7. IMPLEMENTING FULLY-IMPLICIT FORWARD TIME INTEGRATION WITH RESPECT TO VELOCITY AND THICKNESS

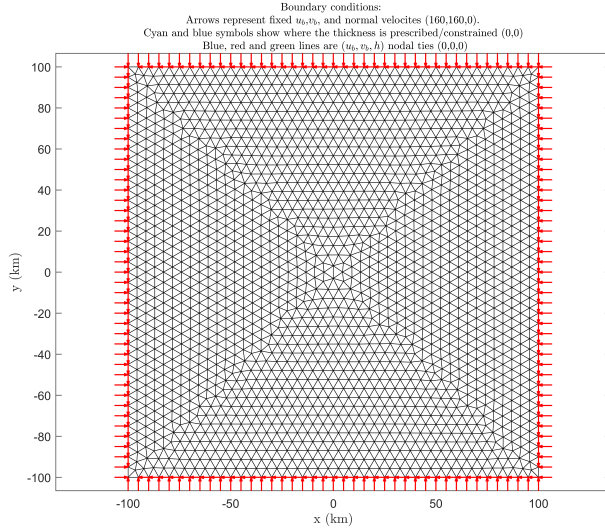


Figure 2.6: Boundary conditions for mass conservation test.

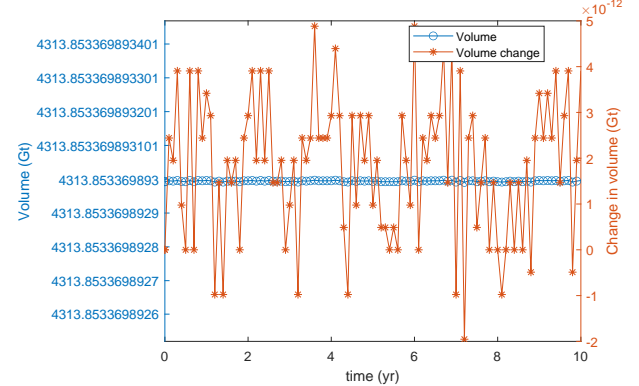


Figure 2.7: Changes in ice volume over time. As there is no mass added or removed, and velocities along boundaries are set to zero, mass conservation implies that the volume must not change with time.

If the specific mass balance is a function of thickness, i.e.

$$a = a(h)$$

then an additional term must be added to the matrix on the left-hand side, and the right-hand side terms must be evaluated within the NR loop every time that the thickness is updated. The first-order equation is then

$$\begin{aligned} 0 &= \frac{\rho}{\Delta t}(\Delta h + h_1^i - h_0) \\ &\quad - \frac{1}{2}(\rho(a_0(h_0) + a_1(h_1) + \partial_h a_1|_{h_1} \Delta h) - \partial_x(q_{x0}) - \partial_x((\Delta h + h_1^i))(\Delta u + u_1^i)) \end{aligned}$$

Ignoring second-order terms and taking the terms involving the unknown Δh to the left-hand side leads to

$$\begin{aligned} \rho \frac{\Delta h}{\Delta t} + \frac{1}{2}(\partial_x(\rho u_1^i \Delta h + \rho h_1^i \Delta u) + \partial_y(\rho v_1^i \Delta h + \rho h_1^i \Delta v) - \rho \partial_h a|_{h_1} \Delta h) \\ = \frac{\rho}{2}(a_0 + a_1) - \frac{\rho}{\Delta t}(h_1^i - h_0) - \frac{1}{2}(\partial_x(q_{x0}) + \partial_x(\rho h_1^i u_1^i) + \partial_y(q_{0y}) + \partial_y(\rho h_1^i v_1^i)) \end{aligned} \quad (2.40)$$

where the corresponding y terms have been added.

2.7.3 Fully implicit SSTREAM time integration with the θ method

$$\begin{aligned} \mathcal{F}_x &= 0 && x \text{ Momentum} \\ \mathcal{F}_y &= 0 && y \text{ Momentum} \\ \mathcal{M} &= 0 && \text{Mass} \end{aligned}$$

$$K^{uu} \Delta \mathbf{u} := Dr_x(\mathbf{u}_1^i, \mathbf{v}_1^i, \mathbf{h}_1^i)[\Delta \mathbf{u}]$$

In a fully implicit NR iteration we arrive at a block system with the structure

$$\begin{bmatrix} K^{\mathcal{F}_x u} & K^{\mathcal{F}_x v} & K^{\mathcal{F}_x h} \\ K^{\mathcal{F}_y u} & K^{\mathcal{F}_y v} & K^{\mathcal{F}_y h} \\ K^{\mathcal{M} u} & K^{\mathcal{M} v} & K^{\mathcal{M} h} \end{bmatrix} \begin{bmatrix} \Delta \mathbf{u} \\ \Delta \mathbf{v} \\ \Delta \mathbf{h} \end{bmatrix} = \begin{bmatrix} r_{\mathcal{F}_x} \\ r_{\mathcal{F}_y} \\ r_{\mathcal{M}} \end{bmatrix} \quad (2.41)$$

We go from time step $t = t_0$ to $t = t_1$ and solve for the unknown values for \mathbf{u} , \mathbf{v} , and \mathbf{h} , at $t = t_1$ (\mathbf{u}_1 , \mathbf{v}_1 , and \mathbf{h}_1) given their respective values at $t = t_0$ (\mathbf{u}_0 , \mathbf{v}_0 , and \mathbf{h}_0).

$$\begin{aligned}\mathbf{u}_1^{i+1} &= \mathbf{u}_1^i + \Delta\mathbf{u} \\ \mathbf{v}_1^{i+1} &= \mathbf{v}_1^i + \Delta\mathbf{v} \\ \mathbf{h}_1^{i+1} &= \mathbf{h}_1^i + \Delta\mathbf{h}\end{aligned}$$

Note that the increment in velocity and thickness have different physical units. In a transient run it might be better to solve for

$$\Delta\dot{\mathbf{h}} := \Delta\mathbf{h}/\Delta t$$

and consider the system

$$\begin{bmatrix} K^{\mathcal{F}_x u} & K^{\mathcal{F}_x v} & K^{\mathcal{F}_x h} \Delta t \\ K^{\mathcal{F}_y u} & K^{\mathcal{F}_y v} & K^{\mathcal{F}_y h} \Delta t \\ K^{\mathcal{M} u} & K^{\mathcal{M} v} & K^{\mathcal{M} h} \Delta t \end{bmatrix} \begin{bmatrix} \Delta\mathbf{u} \\ \Delta\mathbf{v} \\ \Delta\mathbf{h} \end{bmatrix} = \begin{bmatrix} \mathbf{r}_{\mathcal{F}_x} \\ \mathbf{r}_{\mathcal{F}_y} \\ \mathbf{r}_{\mathcal{M}} \end{bmatrix} \quad (2.42)$$

and

$$\mathbf{h}_1^{i+1} = \mathbf{h}_1^i + \Delta\dot{\mathbf{h}} \Delta t$$

For notational simplicity we omit the i superscript and it is to be understood that the values of η , β^2 , h , u , and v are the estimated values at iteration i .

At element level the matrices are

$$\begin{aligned}[K^{\mathcal{F}_x u}]_{pq} &= \int_{\Omega} \left\{ 4\eta h \partial_x N_p \partial_x N_q + h\eta \partial_y N_p \partial_y N_q + \mathcal{H}(h - h_f) \beta^2 N_p N_q \right. \\ &\quad + h D_{eu} (4\partial_x u + 2\partial_y v) \partial_x N_p + h D_{eu} (\partial_x v + \partial_y u) \partial_y N_p \\ &\quad \left. + D_b u u N_p N_q \right\} dx dy\end{aligned}$$

$$\begin{aligned}[K^{\mathcal{F}_y v}]_{pq} &= \int_{\Omega} \left\{ 4\eta h \partial_y N_p \partial_y N_q + h\eta \partial_x N_p \partial_x N_q + \mathcal{H}(h - h_f) \beta^2 N_p N_q \right. \\ &\quad + h D_{ev} (4\partial_y v + 2\partial_x u) \partial_y N_p + h D_{ev} (\partial_x v + \partial_y u) \partial_x N_p \\ &\quad \left. + D_b v v N_p N_q \right\} dx dy\end{aligned}$$

$$\begin{aligned}[K^{\mathcal{F}_x v}]_{pq} &= \int_{\Omega} \left\{ h\eta (2\partial_x N_p \partial_y N_q + \partial_y N_p \partial_x N_q) \right. \\ &\quad + h D_{ev} (4\partial_x u + 2\partial_y v) \partial_x N_p + h D_{ev} (\partial_x v + \partial_y u) \partial_y N_p \\ &\quad \left. + D_b u v N_p N_q \right\} dx dy\end{aligned}$$

$$\begin{aligned}[K^{\mathcal{F}_y u}]_{pq} &= \int_{\Omega} \left\{ h\eta (2\partial_y N_p \partial_x N_q + \partial_x N_p \partial_y N_q) \right. \\ &\quad + h D_{eu} (4\partial_y v + 2\partial_x u) \partial_y N_p + h D_{eu} (\partial_x v + \partial_y u) \partial_x N_p \\ &\quad \left. + D_b v u N_p N_q \right\} dx dy\end{aligned}$$

(floating only (original version))

$$\begin{aligned}[K^{xh}]_{pq} &= \int_{\Omega} \left\{ \eta (4\partial_x u + 2\partial_y v) \partial_x N_p N_q + \eta (\partial_y u + \partial_x v) \partial_y N_p N_q \right. \\ &\quad + \delta(h - h_f) \beta^2 u N_p N_q \\ &\quad + \rho g (\mathcal{H}(h - h_f) + h \delta(h - h_f)) ((\rho/\rho_o \partial_x h - \partial_x H) \cos \alpha - \sin \alpha) N_p N_q \\ &\quad + \frac{\rho^2 g}{\rho_o} h \mathcal{H}(h - h_f) \cos \alpha N_p \partial_x N_q \\ &\quad \left. - \varrho g h \cos \alpha \partial_x N_p N_q \right\} dx dy\end{aligned}$$

)

(floating only (corrected July 2011)

$$\begin{aligned} [\mathbf{K}^{\mathcal{F}_x h}]_{pq} = & \int_{\Omega} \left\{ \eta(4\partial_x u + 2\partial_y v)\partial_x N_p N_q + \eta(\partial_y u + \partial_x v)\partial_y N_p N_q \right. \\ & + \delta(h - h_f)\beta^2 u N_p N_q \\ & + \rho g \mathcal{H}(h - h_f) ((\rho/\rho_o \partial_x h - \partial_x H) \cos \alpha - \sin \alpha) N_p N_q \\ & + \frac{\rho^2 g}{\rho_o} h \mathcal{H}(h - h_f) \cos \alpha N_p \partial_x N_q \\ & + \frac{\rho^2}{\rho_o} \delta(h - h_f) \cos \alpha h \partial_x h N_p N_q \\ & \left. - \varrho g h \cos \alpha \partial_x N_p N_q \right\} dx dy \end{aligned}$$

)

(general case

$$\begin{aligned} [\mathbf{K}^{\mathcal{F}_x h}]_{pq} = & \int_{\Omega} \left\{ \eta(4\partial_x u + 2\partial_y v)\partial_x N_p N_q + \eta(\partial_y u + \partial_x v)\partial_y N_p N_q \right. \\ & + \delta(h - h_f)\beta^2 u N_p N_q \\ & + \rho g \mathcal{H}(h - h_f) \partial_x B \cos \alpha N_p N_q - \rho g \sin \alpha N_p N_q \\ & \left. - \rho g h \left(1 - \frac{\rho}{\rho_o} \mathcal{H}(h_f - h) \right) \cos \alpha \partial_x N_p N_q \right\} \end{aligned}$$

)

(floating only version:

$$\begin{aligned} [\mathbf{K}^{\mathcal{F}_y h}]_{pq} = & \int_{\Omega} \left\{ \eta(4\partial_y v + 2\partial_x u)\partial_y N_p N_q + \eta(\partial_x v + \partial_y u)\partial_x N_p N_q \right. \\ & + \delta(h - h_f)\beta^2 v N_p N_q \\ & + \rho g (\mathcal{H}(h - h_f) + h \delta(h - h_f)) (\rho/\rho_o \partial_y h - \partial_y H) \cos \alpha N_p N_q \\ & + \frac{\rho^2 g}{\rho_o} h \mathcal{H}(h - h_f) \cos \alpha N_p \partial_y N_q \\ & \left. - \varrho g h \cos \alpha \partial_y N_p N_q \right\} dx dy \end{aligned}$$

)

(general case

$$\begin{aligned} [\mathbf{K}^{\mathcal{F}_y h}]_{pq} = & \int_{\Omega} \left\{ \eta(4\partial_y v + 2\partial_x u)\partial_y N_p N_q + \eta(\partial_x v + \partial_y u)\partial_x N_p N_q \right. \\ & + \delta(h - h_f)\beta^2 v N_p N_q \\ & + \rho g (\mathcal{H}(h - h_f) + h \delta(h - h_f)) (\rho/\rho_o \partial_y h - \partial_y H) \cos \alpha N_p N_q \\ & + \frac{\rho^2 g}{\rho_o} h \mathcal{H}(h - h_f) \cos \alpha N_p \partial_y N_q \\ & \left. - \varrho g h \cos \alpha \partial_y N_p N_q \right\} dx dy \end{aligned}$$

)

$$[\mathbf{K}^{\mathcal{M}u}]_{pq} = \theta(\partial_x h N_q + h \partial_x N_q) N_p$$

$$[\mathbf{K}^{\mathcal{M}v}]_{pq} = \theta(\partial_y h N_q + h \partial_y N_q) N_p$$

$$[\mathbf{K}^{\mathcal{M}h}]_{pq} = (N_q/\Delta t + \theta(\partial_x u N_q + u \partial_x N_q + \partial_y v N_q + v \partial_y N_q)) N_p$$

In the equations the quantities D_{eu} , D_{ev} , E , and D_b , which arise because of the linearisation of η and β^2 , are given by

$$D_{eu} = E((2\partial_x u + \partial_y v)\partial_x N_q + \frac{1}{2}(\partial_x v + \partial_y u)\partial_y N_q) \quad (2.43)$$

$$D_{ev} = E((2\partial_y v + \partial_x u)\partial_y N_q + \frac{1}{2}(\partial_x v + \partial_y u)\partial_x N_q) \quad (2.44)$$

$$(2.45)$$

$$E = \frac{1-n}{4n} A^{-1/n} \dot{\epsilon}^{(1-3n)/n}$$

$$D_b := (1/m - 1) C^{-1/m} \|v\|^{(1-3m)/m}$$

Third-order Taylor-Galerkin fully implicit

The terms in

$$\begin{aligned} \frac{\Delta t^2}{12} & \int (\partial_t a_1 N + (h_1 \partial_t u_1 + u_1(a_1 - \partial_x(q_{x1}) - \partial_y(q_{y1}))) \partial_x N \\ & + (h_1 \partial_t v_1 + v_1(a_1 - \partial_x(q_{x1}) - \partial_y(q_{y1}))) \partial_y N) dA \end{aligned} \quad (2.46)$$

from (2.18), need to be linearised. Starting with

$$h_1 \partial_t u_1 + u_1(a_1 - \partial_x(q_{x1}) - \partial_y(q_{y1}))$$

and inserting $h^{i+1} = \Delta h + h_1^i$ etc. gives

$$(\Delta h + h_1^i) \partial_t (\Delta u + u_1^i) + (\Delta u + u_1^i)(a_1 - \partial_x((\Delta h + h_1^i)(\Delta u + u_1^i)) - \partial_y((\Delta h + h_1^i)(\Delta v + v_1^i)))$$

and first ignoring only some second-order terms

$$\partial_t u_1^i \Delta h + h_1^i \partial_t \Delta u + h_1^i \partial_t u_1^i + (a_1 \Delta u + u_1^i a_1) - (\Delta u + u_1^i)(\partial_x(u_1^i \Delta h + h_1^i \Delta u + h_1^i u_1^i) + \partial_y(v_1 \Delta h + h_1^i \Delta v + h_1^i v_1^i))$$

and then ignoring the remaining second-order terms

$$\begin{aligned} ((u_1^i - u_0)/\Delta t)(\Delta h + h_1^i) + a_1 \Delta u + u_1^i a_1 \\ - u_1^i (\partial_x(u_1^i \Delta h + h_1^i \Delta u + h_1^i u_1^i) + \partial_y(v_1 \Delta h + h_1^i \Delta v + h_1^i v_1^i)) \\ - (\partial_x(h_1^i u_1^i) + \partial_y(h_1^i v_1^i)) \Delta u \end{aligned}$$

where $\partial_t u_1^i = (u_1^i - u_0)/\Delta t$ and $\partial_t \Delta u$ has been set to zero. Now shifting the unknowns over to the left-hand side

$$\begin{aligned} & \partial_t u_1^i \Delta h + a_1 \Delta u \\ & - u_1^i (\partial_x(u_1^i \Delta h + h_1^i \Delta u) + \partial_y(v_1 \Delta h + h_1^i \Delta v)) \\ & - (\partial_x(h_1^i u_1^i) + \partial_y(h_1^i v_1^i)) \Delta u \\ & = u_1^i (\partial_x(h_1^i u_1^i) + \partial_y(h_1^i v_1^i)) - u_1^i a_1 - \partial_t u_1^i h_1^i \end{aligned}$$

and adding the y terms

$$\begin{aligned} & (\partial_t u_1^i \partial_x N + \partial_t v_1^i \partial_y N) \Delta h + a_1 (\partial_x N \Delta u + \partial_y N \Delta v) \\ & - (u_1^i \partial_x N + v_1^i \partial_y N) (\partial_x(u_1^i \Delta h + h_1^i \Delta u) + \partial_y(v_1 \Delta h + h_1^i \Delta v)) \\ & - (\partial_x(h_1^i u_1^i) + \partial_y(h_1^i v_1^i)) (\partial_x N \Delta u + \partial_y N \Delta v) \\ & = (\partial_x N u_1^i + \partial_y N v_1^i) (\partial_x(h_1^i u_1^i) + \partial_y(h_1^i v_1^i)) - a_1 (\partial_x N u_1^i + \partial_y N v_1^i) - (\partial_t u_1^i \partial_x N + \partial_t v_1^i \partial_y N) h_1^i \end{aligned}$$

Then adding the remaining higher-order Taylor terms in (2.18), involving fields from time-step zero, to the right-hand side gives

$$\begin{aligned}
 & (\partial_t u_1^i \partial_x N + \partial_t v_1^i \partial_y N) \Delta h \\
 & + (\partial_x N \Delta u + \partial_y N \Delta v) (a_1 - \partial_x(h_1^i u_1^i) + \partial_y(h_1^i v_1^i)) \\
 & - (\partial_x N u_1^i + \partial_y N v_1^i) (\partial_x(u_1^i \Delta h + h_1^i \Delta u) + \partial_y(v_1^i \Delta h + h_1^i \Delta v)) \\
 & = \partial_t(a_0 - a_1)N \\
 & - (u_1^i \partial_x N + v_1^i \partial_y N) (a_1 - \partial_x(h_1^i u_1^i) + \partial_y(h_1^i v_1^i)) - h_1^i (\partial_t u_1^i \partial_x N + \partial_t v_1^i \partial_y N) \\
 & + (u_0 \partial_x N + v_0 \partial_y N) (a_0 - \partial_x(q_{x0}) + \partial_y(q_{0y})) + h_0 (\partial_t u_0 \partial_x N + \partial_t v_0 \partial_y N)
 \end{aligned}$$

Now adding first-order Taylor terms from (2.40) to the expression above

$$\begin{aligned}
 & \Delta h N + \frac{\Delta t}{2} (\partial_x(u_1^i \Delta h + h_1^i \Delta u) + \partial_y(v_1^i \Delta h + h_1^i \Delta v)) N \\
 & + \gamma(\partial_t u_1^i \partial_x N + \partial_t v_1^i \partial_y N) \Delta h \\
 & + \gamma(\partial_x N \Delta u + \partial_y N \Delta v) (a_1 - \partial_x(h_1^i u_1^i) + \partial_y(h_1^i v_1^i)) \\
 & - \gamma(\partial_x N u_1^i + \partial_y N v_1^i) (\partial_x(u_1^i \Delta h + h_1^i \Delta u) + \partial_y(v_1^i \Delta h + h_1^i \Delta v)) \\
 & = \left(h_0 - h_1^i + \frac{\Delta t}{2}(a_0 + a_1) - \frac{\Delta t}{2}(\partial_x(q_{x0}) + \partial_x(h_1^i u_1^i) + \partial_y(q_{0y}) + \partial_y(h_1^i v_1^i)) \right) N \\
 & + \gamma \partial_t(a_0 - a_1)N \\
 & - \gamma(u_1^i \partial_x N + v_1^i \partial_y N) (a_1 - \partial_x(h_1^i u_1^i) + \partial_y(h_1^i v_1^i)) - \gamma h_1^i (\partial_t u_1^i \partial_x N + \partial_t v_1^i \partial_y N) \\
 & + \gamma(u_0 \partial_x N + v_0 \partial_y N) (a_0 - \partial_x(q_{x0}) + \partial_y(q_{0y})) + \gamma h_0 (\partial_t u_0 \partial_x N + \partial_t v_0 \partial_y N)
 \end{aligned}$$

which can also be written as

$$\begin{aligned}
 & \Delta h N + (\kappa N - \gamma(\partial_x N u_1^i + \partial_y N v_1^i)) (\partial_x(u_1^i \Delta h + h_1^i \Delta u) + \partial_y(v_1^i \Delta h + h_1^i \Delta v)) \\
 & + \gamma(\partial_t u_1^i \partial_x N + \partial_t v_1^i \partial_y N) \Delta h \\
 & + \gamma(\partial_x N \Delta u + \partial_y N \Delta v) (a_1 - \partial_x(h_1^i u_1^i) - \partial_y(h_1^i v_1^i)) \\
 & = (h_0 - h_1^i) N \\
 & + (\kappa N + \gamma(u_0 \partial_x N + v_0 \partial_y N)) (a_0 - \partial_x(q_{x0}) - \partial_y(q_{0y})) \\
 & + (\kappa N - \gamma(u_1^i \partial_x N + v_1^i \partial_y N)) (a_1 - \partial_x(h_1^i u_1^i) - \partial_y(h_1^i v_1^i)) \\
 & + \gamma \partial_t(a_0 - a_1)N \\
 & - \gamma h_1^i (\partial_t u_1^i \partial_x N + \partial_t v_1^i \partial_y N) \\
 & + \gamma h_0 (\partial_t u_0 \partial_x N + \partial_t v_0 \partial_y N)
 \end{aligned}$$

where

$$\gamma = \frac{(\Delta t)^2}{12}$$

and

$$\kappa = \frac{\Delta}{2}$$

2.7.4 Semi-implicit: uv explicit, and h implicit

In the semi-implicit approach h_1 is treated as the unknown while h_0 , u_1 , v_1 , h_0 , v_0 are assumed to be known.

Taking the unknown h_1 in (2.18) to the left-hand side gives

$$\begin{aligned}
& \int \left(h_1 + \frac{\Delta t}{2} (\partial_x(q_{x1}) + \partial_y(q_{y1})) \right) N dA \\
& + \frac{\Delta t^2}{12} \int ((h_1 \partial_t u_1 - u_1 (\partial_x(q_{x1}) + \partial_y(q_{y1}))) \partial_x N + (h_1 \partial_t v_1 - v_1 (\partial_x(q_{x1}) + \partial_y(q_{y1}))) \partial_y N) dA \\
& - \frac{\Delta t^2}{12} \oint ((h_1 \partial_t u_1 - u_1 (\partial_x(q_{x1}) + \partial_y(q_{y1}))) n_x + (h_1 \partial_t v_1 - v_1 (\partial_x(q_{x1}) + \partial_y(q_{y1}))) n_y) N d\gamma \\
& = \int \left(h_0 + \frac{\Delta t}{2} (a_0 + a_1 - \partial_x(q_{x0}) - \partial_y(q_{0y})) \right) N dA \\
& + \frac{\Delta t^2}{12} \int (\partial_t(a_0 - a_1) N + (h_0 \partial_t u_0 - u_1 a_1 + u_0 (a_0 - \partial_x(q_{x0}) - \partial_y(q_{0y}))) \partial_x N \\
& \quad + (h_0 \partial_t v_0 - v_1 a_1 + v_0 (a_0 - \partial_x(q_{x0}) - \partial_y(q_{0y}))) \partial_y N) dA \\
& - \frac{\Delta t^2}{12} \oint ((h_0 \partial_t u_0 - u_1 a_1 + u_0 (a_0 - \partial_x(q_{x0}) - \partial_y(q_{0y}))) n_x \\
& \quad + (h_0 \partial_t v_0 - v_1 a_1 + v_0 (a_0 - \partial_x(q_{x0}) - \partial_y(q_{0y}))) n_y) N d\gamma
\end{aligned}$$

2.8 Transient implicit SSHEET/SIA with the θ method

In the SIA/SSHEET approximation the ice-thickness evolution is found by solving

$$\rho \partial_t h + \nabla_{xy} \cdot \mathbf{q} = \rho a . \quad (1.121)$$

where

$$\mathbf{q} = -\rho D \|\nabla_{xy} s\|^{(n-1)} h^{n+2} \nabla_{xy} s + \rho \mathbf{v}_b h \quad (1.46)$$

with

$$D = \frac{2A}{n+2} (\rho g)^n , \quad (1.47)$$

and all parameters are listed in section 1.4, or using Weertman sliding law

$$\begin{aligned}
\mathbf{q} &= \mathbf{q}_d + \mathbf{q}_b \\
&= -\frac{2\rho A}{n+2} (\rho g h)^n h^2 \|\nabla_{xy} s\|^{n-1} \nabla_{xy} s - C \rho h (\rho g h)^m \|\nabla_{xy} s\|^{m-1} \nabla_{xy} s
\end{aligned} \quad (2.47)$$

$$= \frac{2\rho A}{n+2} \|\mathbf{t}_b^{\text{SIA}}\|^{n-1} \mathbf{t}_b^{\text{SIA}} h^2 + C \rho h \|\mathbf{t}_b^{\text{SIA}}\|^{m-1} \mathbf{t}_b^{\text{SIA}}, \quad (1.45)$$

where \mathbf{t}_b is

$$\mathbf{t}_b = \mathbf{t}_b^{\text{SIA}} = -\rho g h \nabla_{xy} s , \quad (1.37)$$

and where we have assumed that A and ρ are independent of depth.

An implicit method is used where h_0 and h_1 are the ice thicknesses at the beginning and the end of the time step, respectively. The non-linear system

$$F(h, t) = \rho \partial_t h + \nabla_{xy} \cdot \mathbf{q} - \rho a = 0 , \quad (2.48)$$

is solved implicitly with respect to ice thickness using NR, and we write

$$\begin{aligned}
h^{i+1} &= h^i + \Delta h \\
s^{i+1} &= s^i + \Delta h
\end{aligned}$$

where i is the number of the non-linear iteration step. Provided the method converges, Δh goes to zero with increasing i . In the following we simply write h instead of h^i . Using the θ method we arrive at

$$\int_{\mathcal{A}} \phi (h + \Delta h - h_0) d\mathcal{A} = -(1-\theta) \Delta t \int_{\mathcal{A}} \phi (\nabla_{xy} \cdot \mathbf{q}_0 - a_0) d\mathcal{A} - \theta \Delta t \int_{\mathcal{A}} \phi (\nabla_{xy} \cdot \mathbf{q}_1 (h + \Delta h) - a_1) d\mathcal{A} \quad (2.49)$$

To solve the above equation for Δh using the NR method, where we repeatedly solve the system,

$$\delta_h F \Delta h = -F(h)$$

until $\Delta h \rightarrow 0$, or within some prescribed tolerance (see section 4.5), and we need to know the perturbation in F due to perturbation in thickness, i.e. $\delta_h F$. The only non-linear term is the flux term, and the simplest way of perturbing $q(h)$ with respect to h is to find

$$\delta_h q = \lim_{\epsilon \rightarrow 0} \frac{d}{d\epsilon} q(h + \epsilon \delta h),$$

where in FE context we would typically select

$$\delta h = \phi.$$

As using SSHEET for floating ice shelves is somewhat questionable we here only consider the case of grounded ice³.

Deformational Flux Contribution:

Where grounded the deformational flux x component is

$$[q_d]_x(h) = -\rho D ((\partial_x h + \partial_x B)^2 + (\partial_y h + \partial_y B)^2)^{(n-1)/2} h^{n+2} \partial_x s,$$

and

$$\Delta s = \Delta h,$$

with

$$D = \frac{2A}{n+2} (\rho g)^n \quad (1.47)$$

Therefore

$$\begin{aligned} \delta_h q_{dx} &= \lim_{\epsilon \rightarrow 0} \frac{d}{d\epsilon} q_x(h + \epsilon \Delta h) \\ &= - \lim_{\epsilon \rightarrow 0} \frac{d}{d\epsilon} \rho D (\partial_x(s + \epsilon \Delta h)^2 + \partial_y(s + \epsilon \Delta h)^2)^{(n-1)/2} (h + \epsilon \Delta h)^{n+2} \partial_x(s + \epsilon \Delta h) \\ &= -\rho D \|\nabla_{xy}s\|^{n-1} h^{n+2} \partial_x \Delta h \\ &\quad - \rho D(n+2) \|\nabla_{xy}s\|^{n-1} h^{n+1} \partial_x s \Delta h \\ &\quad - \rho D(n-1) \|\nabla_{xy}s\|^{n-3} h^{n+2} (\partial_x s \partial_x \Delta h + \partial_y s \partial_y \Delta h) \partial_x s \end{aligned}$$

The first term of the final expression shown above is the perturbation in flux due to increase in slope, the second one the perturbation due to increase in thickness. The third term is non-linear terms that vanishes for $n = 1$. This third term represents changes flux caused by a change in effective viscosity due to perturbations in slope. This third terms shows that a change in slope in y direction gives rise to an increase in flux in x direction.

As expected, for a negative unperturbed surface slope ($\partial_x s < 0$), both a positive perturbation in thickness ($\Delta h > 0$), and an increase in (negative) surface slope ($\partial_x \Delta h < 0$), result in a positive perturbation in flux ($\delta q_x > 0$).

Basal Sliding Flux Contribution:

Similarly, linearising the basal sliding flux contribution,

$$[q_b]_x(h) = -\rho \mathcal{D} ((\partial_x h + \partial_x B)^2 + (\partial_y h + \partial_y B)^2)^{(m-1)/2} h^{m+1} \partial_x s,$$

where

$$\mathcal{D} = C(\rho g)^m \quad (2.50)$$

³In general the surface is related to the ice thickness and bed through

$$s = (h + B)\mathcal{H}(h - h_f) + (S + (1 - \rho/\rho_o)h)\mathcal{H}(h_f - h).$$

we arrive at

$$\begin{aligned}
\delta_h q_{dx} &= \lim_{\epsilon \rightarrow 0} \frac{d}{d\epsilon} q_x(h + \epsilon \Delta h) \\
&= - \lim_{\epsilon \rightarrow 0} \frac{d}{d\epsilon} \rho D (\partial_x(s + \epsilon \Delta h)^2 + \partial_y(s + \epsilon \Delta h)^2)^{(m-1)/2} (h + \epsilon \Delta h)^{m+1} \partial_x(s + \epsilon \Delta h) \\
&= -\rho \mathcal{D} \|\nabla_{xy}s\|^{m-1} h^{m+1} \partial_x \Delta h \\
&\quad - \rho \mathcal{D} (m+1) \|\nabla_{xy}s\|^{m-1} h^m \partial_x s \Delta h \\
&\quad - \rho \mathcal{D} (m-1) \|\nabla_{xy}s\|^{n-3} h^{m+1} (\partial_x s \partial_x \Delta h + \partial_y s \partial_y \Delta h) \partial_x s
\end{aligned}$$

2.8.1 SSHEET with no-flux natural boundary condition

Using a variant of Gauss theorem given by Eq. (B.3) we write (2.49) on the form

$$\int_{\Omega} \phi \nabla_{xy} \cdot \mathbf{q} d\Omega = \oint_{\partial\Omega} \phi \mathbf{q} \cdot \hat{\mathbf{n}} d\Gamma - \int_{\Omega} \nabla_{xy} \phi \cdot \mathbf{q} d\Omega \quad (2.51)$$

Applying (2.51) on (linearised) (2.49) and assuming that $\mathbf{q} \cdot \hat{\mathbf{n}} = 0$ on $\partial\Omega$, i.e. ice flux across the boundary is zero (homogeneous Neumann boundary condition), gives

$$\begin{aligned}
\int_{\Omega} (h + \Delta h - h_0) \phi d\Omega &= (1 - \theta) \Delta t \int \mathbf{q}_0 \cdot \nabla_{xy} \phi d\Omega \\
&\quad + \theta \Delta t \int \mathbf{q}_1^i \cdot \nabla_{xy} \phi d\Omega \\
&\quad + \theta \Delta t \int \Delta \mathbf{q} \cdot \nabla_{xy} \phi d\Omega
\end{aligned}$$

or

$$\begin{aligned}
\int_{\Omega} \Delta h \phi d\Omega - \theta \Delta t \int_{\Omega} \Delta \mathbf{q} \cdot \nabla_{xy} \phi d\Omega \\
&= - \int_{\Omega} (h - h_0) \phi d\Omega \\
&\quad + (1 - \theta) \Delta t \int_{\Omega} \mathbf{q}_0 \cdot \nabla_{xy} \phi d\Omega \\
&\quad + \theta \Delta t \int_{\Omega} \mathbf{q}_1^i \cdot \nabla_{xy} \phi d\Omega
\end{aligned}$$

where $\mathbf{q}^{i+1} = \mathbf{q}^i + \Delta \mathbf{q}$ is the NR iteration, with

$$\begin{aligned}
\Delta_h q_x &= \lim_{\epsilon \rightarrow 0} \frac{d}{d\epsilon} q_x(h + \epsilon \Delta h) \\
&= - D(n-1) \|\nabla_{xy}s\|^{n-3} (\partial_x s \partial_x \Delta h + \partial_y s \partial_y \Delta h) h^{n+2} \partial_x s \\
&\quad - D(n+2) \|\nabla_{xy}s\|^{n-1} h^{n+1} \partial_x s \Delta h \\
&\quad - D \|\nabla_{xy}s\|^{n-1} h^{n+2} \partial_x \Delta h
\end{aligned}$$

Collecting terms, and writing s and h instead of s^{i+1} and h^{i+1} , respectively, and s_0 and h_0 instead of s^i and h^i , gives

$$\begin{aligned} & \int N_p N_q \Delta h_q d\Omega \\ & + \theta \Delta t \int D(n+2) \|\nabla_{xy} s\|^{n-1} h^{n+1} (\partial_x N_p \partial_x s + \partial_y N_p \partial_y s) N_q \Delta h_q d\Omega \\ & + \theta \Delta t \int D \|\nabla_{xy} s\|^{n-1} h^{n+2} (\partial_x N_p \partial_x N_q + \partial_y N_p \partial_y N_q) \Delta h_q d\Omega \\ & + \theta \Delta t \int D(n-1) h^{n+2} \|\nabla_{xy} s\|^{n-3} (\partial_x N_p \partial_x s + \partial_y N_p \partial_y s) (\partial_x s \partial_x N_q + \partial_y s \partial_y N_q) \Delta h_q d\Omega \\ & = \int (h_0 - h) N_p d\Omega \\ & + (1-\theta) \Delta t \int (q_{x0} \partial_x N_p + q_{y0} \partial_y N_p) d\Omega \\ & + \theta \Delta t \int (q_{x1} \partial_x N_p + q_{y1} \partial_y N_p) d\Omega \end{aligned}$$

where

$$\begin{aligned} q_{x0} &= D \|\nabla_{xy} s_0\|^{(n-1)} h_0^{n+2} \partial_x s_0 \\ q_{y0} &= D \|\nabla_{xy} s_0\|^{(n-1)} h_0^{n+2} \partial_y s_0 \\ q_{x1} &= D \|\nabla_{xy} s_1\|^{(n-1)} h_1^{n+2} \partial_x s_1 \\ q_{y1} &= D \|\nabla_{xy} s_1\|^{(n-1)} h_1^{n+2} \partial_y s_1 \end{aligned}$$

and

$$D = \frac{2A(\rho g)^n}{n+2}$$

2.8.2 Transient SSHEET/SIA with a free-flux natural boundary condition

To arrive at a formulation where free flux is the natural boundary condition we express the flux in terms of the deformational velocity as[‘]

$$\mathbf{q} = F h \mathbf{v}_d$$

For a ‘free-flux’ boundary condition this is the flux at the in and outflow boundaries.
We solve

$$\int_{\Omega} u_d \phi \Omega = \int_{\Omega} E |\nabla_{xy} s|^{n-1} h^{n+1} \partial_x s d\Omega \quad (2.52)$$

$$\int_{\Omega} v_d \phi \Omega = \int_{\Omega} E |\nabla_{xy} s|^{n-1} h^{n+1} \partial_y s d\Omega \quad (2.53)$$

$$\int_{\Omega} (h_1 - h_0) \phi \Omega = -(1-\theta) \Delta t \int_{\Omega} F \phi \nabla_{xy} \cdot h_0 \mathbf{v}_{d0} \Omega - \theta \Delta t \int_{\Omega} F \phi \nabla_{xy} \cdot h \mathbf{v}_{d1} d\Omega \quad (2.54)$$

for u_d , v_d , and h as unknowns. Writing this as a coupled system with u_d , v_d , and h all as unknowns gives a system of first order differential equations, rather than one second order equation. This eliminates the need to get rid of a second spatial derivative and the natural boundary conditions now corresponds to a ‘free-flux’ condition.

NR with

$$\begin{aligned} u^{i+1} &= u^i + \Delta u \\ v^{i+1} &= v^i + \Delta v \\ h^{i+1} &= h^i + \Delta h \\ s^{i+1} &= s^i + \Delta h \end{aligned}$$

and linearising gives

$$\begin{aligned} u + \Delta u &= E \|\nabla_{xy}s\|^{n-1} h^{n+1} \partial_x s \\ &\quad + E(n-1) \|\nabla_{xy}s\|^{n-3} h^{n+1} \partial_x s (\partial_x s \partial_x \Delta h + \partial_y s \partial_y \Delta h) \\ &\quad + E(n+1) \|\nabla_{xy}s\|^{n-1} h^n \partial_x s \Delta h \\ &\quad + E \|\nabla_{xy}s\|^{n-1} h^{n+1} \partial_x \Delta h \end{aligned}$$

Taking the Δ terms to one side

$$\begin{aligned} &- \Delta u_q \\ &+ E(n-1) \|\nabla_{xy}s\|^{n-3} h^{n+1} \partial_x s (\partial_x s \partial_x \Delta h + \partial_y s \partial_y \Delta h) \\ &+ E(n+1) \|\nabla_{xy}s\|^{n-1} h^n \partial_x s \Delta h \\ &+ E \|\nabla_{xy}s\|^{n-1} h^{n+1} \partial_x \Delta h \\ &= u - E \|\nabla_{xy}s\|^{n-1} h^{n+1} \partial_x s \end{aligned}$$

Galerkin, u term:

$$\begin{aligned} &- \langle N_p, N_q \rangle \Delta u_q \\ &+ (n-1) \langle N_p | E \|\nabla_{xy}s\|^{n-3} h^{n+1} \partial_x s (\partial_x s \partial_x N_q + \partial_y s \partial_y N_q) \rangle \Delta h_q \\ &+ (n+1) \langle N_p | E \|\nabla_{xy}s\|^{n-1} h^n \partial_x s N_q \rangle \Delta h_q \\ &+ \langle N_p | E \|\nabla_{xy}s\|^{n-1} h^{n+1} \partial_x N_q \rangle \Delta h_q \\ &= \langle N_p, u - E \|\nabla_{xy}s\|^{n-1} h^{n+1} \partial_x s \rangle \end{aligned}$$

The corresponding v term is obtained by replacing u with v and derivatives with respect to x by derivatives with respect to y ,

Galerkin q term:

$$\begin{aligned} &\langle N_p | N_q \rangle \Delta h_q + \Delta t \theta F \langle N_p | \partial_x u N_q + u \partial_x N_q + \partial_y v N_q + v \partial_y N_q \rangle \Delta h_q \\ &\quad + \Delta t \theta F \langle N_p | \partial_x h N_q + h \partial_x N_q \rangle \Delta u_q \\ &\quad + \Delta t \theta F \langle N_p | \partial_y h N_q + h \partial_y N_q \rangle \Delta v_q \\ &= \Delta t \langle N_p | (1-\theta) a_0 + \theta a_1 \rangle \\ &\quad - \langle N_p | (h - h_0) \rangle \\ &\quad - \Delta t F \langle N_p, ((1-\theta)(\partial_x(h_0 u_0) + \partial_y(h_0 u_0)) + \theta(\partial_x(hu) + \partial_y(hv))) \rangle \end{aligned}$$

2.9 Method of characteristics

Think of

$$\partial_t h + \partial_x(uh) = a$$

as

$$D_t h + h \partial_x u = a$$

with

$$D_t h = \partial_t h + u \partial_x h$$

Along the characteristics I have

$$D_t h = \lim_{\Delta t \rightarrow 0} \frac{1}{\Delta t} (h(x, t) - h(x - u \Delta t | t - \Delta t))$$

and if I just write

$$h(x - u \Delta t | t - \Delta t) = h(x, t - \Delta t) - d_x h(x, t - \Delta t) u \Delta t$$

and take the limit I (of course) just get

$$\partial_t h + \partial_x(uh) = a$$

again.

The question seem to me to be about how to approximate the variation along the characteristic. If I write

$$h(x - u \Delta t | t - \Delta t) = h_0 - d_x h_0 u \Delta t + \frac{1}{2} d_{xx}^2 h_0 (u \Delta t)^2$$

where h_0 is evaluated at x and at $t - \Delta t$, I get a ‘correction’ term and the discretised version is

$$\frac{1}{\Delta t} (h_1 - h_0 + d_x h_0 u \Delta t + \frac{1}{2} d_{xx}^2 h_0 (u \Delta t)^2) + h d_x u = a$$

It is a bit unclear in the above expression at what time to evaluate u . I could go for the average value over the time step, but I will only know it at the previous time step anyhow.

One way of interpreting the above equation is

$$\frac{1}{\Delta t} (h_1 - h_0) + d_x h u + \frac{1}{2} u^2 \Delta t d_{xx}^2 h + h d_x u = a$$

and then evaluate all terms at some time within the time step, i.e. the θ method. The above equation can be written as

$$\frac{1}{\Delta t} (h_1 - h_0) + \partial_x(hu) + \frac{\Delta t}{2} u^2 \partial_{xx}^2 h = a$$

In combination with the θ method I get

$$\frac{1}{\Delta t} (h_1 - h_0) = \theta \left(a_1 - \partial_x(q_{x1}) - \frac{1}{2} u_1 \Delta t \partial_{xx}^2(u_1 h_1) \right) + (1 - \theta) \left(a_0 - \partial_x(q_{x0}) - \frac{1}{2} u_0 \Delta t \partial_{xx}^2(u_0 h_0) \right)$$

(did not write the a correction term)

2.10 Taylor-Galerkin

We have

$$\partial_t h + \partial_x(uh) = a$$

we write

$$h_1 = h_0 + \Delta t \partial_t h_0 + \frac{(\Delta t)^2}{2} \partial_{tt}^2 h_0$$

which is a second-order accurate Euler method.

Inserting we get

$$\begin{aligned} h_1 &= h_0 + \Delta t(a - \partial_x(hu)) + \frac{(\Delta t)^2}{2} \partial_t(a - \partial_x(uh)) \\ &= h_0 + \Delta t(a - \partial_x(hu)) + \frac{(\Delta t)^2}{2} (\partial_t a - \partial_{xt}^2(uh)) \\ &= h_0 + \Delta t(a - \partial_x(hu)) + \frac{(\Delta t)^2}{2} (\partial_t a - \partial_x(\partial_h(uh) \partial_t h)) \\ &= h_0 + \Delta t(a - \partial_x(hu)) + \frac{(\Delta t)^2}{2} (\partial_t a - \partial_x(u \partial_t h)) \\ &= h_0 + \Delta t(a - \partial_x(hu)) + \frac{(\Delta t)^2}{2} (\partial_t a - \partial_x(u(a - \partial_x(uh)))) \end{aligned}$$

or

$$\frac{1}{\Delta t} (h_1 - h_0) = a - \partial_x(hu) - \frac{\Delta t}{2} \partial_x(u(a - \partial_x(uh))) + \frac{\Delta t}{2} \partial_t a \quad (2.55)$$

All the therms of the right-hand side of (2.55) refer to time step 0. I get the implicit theta method if I evaluate the right-hand side at both 1 and 0 and weight with θ .

After a partial integration we get a correction term

$$\langle \frac{1}{2} \Delta t \partial_x u | a - \partial_x(uh) \rangle$$

2.11 Third order implicit Taylor Galerkin (1HD)

A better justification for evaluation at both time step 1 and 0 comes from writing

$$h_1 = h_0 + \Delta t \partial_t h_0 + \frac{(\Delta t)^2}{2} \partial_{tt}^2 h_0,$$

$$h_0 = h_1 - \Delta t \partial_t h_1 + \frac{(\Delta t)^2}{2} \partial_{tt}^2 h_1,$$

adding

$$2(h_1 - h_0) = \Delta t (\partial_t h_0 + \partial_t h_1) + \frac{(\Delta t)^2}{2} (\partial_{tt}^2 h_0 - \partial_{tt}^2 h_1)$$

and simplifying gives

$$\frac{1}{\Delta t} (h_1 - h_0) = \frac{1}{2} (\partial_t h_0 + \partial_t h_1) + \frac{\Delta t}{4} (\partial_{tt}^2 h_0 - \partial_{tt}^2 h_1) \quad (2.56)$$

Now use

$$\partial_t h = a - \partial_x(hu)$$

and

$$\begin{aligned} \partial_{tt}^2 h &= \partial_t a - \partial_{tx}^2(hu) \\ &= \partial_t a - \partial_t(h\partial_x u + u\partial_x h) \\ &= \partial_t a - (\partial_x h\partial_t u + h\partial_{xt}^2 u + \partial_t h\partial_x u + u\partial_{xt}^2 h) \\ &= \partial_t a - (\partial_x h\partial_t u + h\partial_{xt}^2 u + \partial_x u(a - \partial_x(hu)) + u\partial_x(a - \partial_x(hu))) \\ &= \partial_t a - (\partial_x h\partial_t u + h\partial_{xt}^2 u + \partial_x u(a - \partial_x(hu)) + u\partial_x(a - \partial_x(hu))) \\ &= \partial_t a - \partial_x h\partial_t u - h\partial_{xt}^2 u - \partial_x(u(a - \partial_x(hu))) \end{aligned}$$

or

$$\partial_{tt}^2 h = \partial_t a - \partial_x(h\partial_t u + ua - u\partial_x(uh)) \quad (2.57)$$

Inserting (2.57) into (2.11) gives

$$\begin{aligned} 0 &= Lh \\ &= \frac{1}{\Delta t} (h_1 - h_0) \\ &- \frac{1}{2} (a_0 - \partial_x(q_{x0}) + a_1 - \partial_x(q_{x1})) \\ &- \frac{\Delta t}{4} (\partial_t a_0 - \partial_x(h_0 \partial_t u_0 + u_0(a_0 - \partial_x(q_{x0}))) - \partial_t a_1 + \partial_x(h_1 \partial_t u_1 + u_1(a_1 - \partial_x(q_{x1})))) \end{aligned}$$

Galerkin

$$\langle Lh_1 | N_p \rangle = 0$$

with $u_1 = N_q u_q$, etc. I used partial integration to get rid of second order spatial derivatives

$$\begin{aligned} 0 &= \langle Lu | N_q \rangle \\ &= \frac{1}{\Delta t} \int (h_1 - h_0) N_q dx \\ &- \frac{1}{2} \int (a_0 - \partial_x(q_{x0}) + a_1 - \partial_x(q_{x1})) N_q dx \\ &- \frac{\Delta t}{4} \int (\partial_t a_0 - \partial_t a_1) N_q dx \\ &- \frac{\Delta t}{4} \int (h_0 \partial_t u_0 + u_0 a_0 - u_0 \partial_x(q_{x0})) - h_1 \partial_t u_1 - u_1 a_1 + u_1 \partial_x(q_{x1})) \partial_x N_q dx \\ &- \frac{\Delta t}{4} (-h_0 \partial_t u_0 - u_0(a_0 - \partial_x(q_{x0})) + h_1 \partial_t u_1 + u_1(a_1 - \partial_x(q_{x1}))) N_q|_{x_l}^{x_r} \end{aligned}$$

The unknown is h_1

$$\begin{aligned}
& \int (h_1 + \frac{\Delta t}{2} \partial_x(q_{x1})) N_q dx \\
&+ \frac{(\Delta t)^2}{4} \int (h_1 \partial_t u_1 - u_1 \partial_x(q_{x1})) \partial_x N_q dx + \frac{(\Delta t)^2}{4} (u_1 \partial_x(q_{x1}) - h_1 \partial_t u_1) N_q|_{x_l}^{x_r} \\
&= \int (h_0 + \frac{\Delta t}{2} (a_1 + a_0 - \partial_x(q_{x0}))) N_q dx \\
&+ \frac{(\Delta t)^2}{4} \int \partial_t (a_0 + a_1) N_q dx \\
&+ \frac{(\Delta t)^2}{4} \int (u_0 a_0 - u_1 a_1 + h_0 \partial_t u_0 - u_0 \partial_x(q_{x0})) \partial_x N_q dx \\
&+ \frac{(\Delta t)^2}{4} (u_1 a_1 - u_0 a_0 - h_0 \partial_t u_0 + u_0 \partial_x(q_{x0})) N_q|_{x_l}^{x_r}
\end{aligned}$$

Writing out the product terms

$$\begin{aligned}
& \int (h_1 + \frac{\Delta t}{2} (h_1 \partial_x u_1 + u_1 \partial_x h_1)) N_q dx \\
&+ \frac{(\Delta t)^2}{4} \int (\partial_t u_1 h_1 - u_1 (h_1 \partial_x u_1 + u_1 \partial_x h_1)) \partial_x N_q dx \\
&+ \frac{(\Delta t)^2}{4} (u_1 (h_1 \partial_x u_1 + u_1 \partial_x h_1) - h_1 \partial_t u_1) N_q|_{x_l}^{x_r} \\
&= \int (h_0 + \frac{\Delta t}{2} (a_1 + a_0 - (h_0 \partial_x u_0 + u_0 \partial_x h_0))) N_q dx \\
&+ \frac{(\Delta t)^2}{4} \int \partial_t (a_0 + a_1) N_q dx \\
&+ \frac{(\Delta t)^2}{4} \int (u_0 a_0 - u_1 a_1 + h_0 \partial_t u_0 - u_0 (h_0 \partial_x u_0 + u_0 \partial_x h_0)) \partial_x N_q dx \\
&+ \frac{(\Delta t)^2}{4} (u_1 a_1 - u_0 a_0 - h_0 \partial_t u_0 + u_0 (h_0 \partial_x u_0 + u_0 \partial_x h_0)) N_q|_{x_l}^{x_r}
\end{aligned}$$

Taking this up to third order

$$\frac{1}{\Delta t} (h_1 - h_0) = \frac{1}{2} (\partial_t h_0 + \partial_t h_1) + \frac{\Delta t}{4} (\partial_{tt}^2 h_0 - \partial_{tt}^2 h_1) + \frac{(\Delta t)^2}{12} (\partial_{ttt}^3 h_0 + \partial_{ttt}^3 h_1)$$

is easy, if we simply approximate the time derivative in the third-order term through finite differences.

$$\begin{aligned}
\frac{1}{\Delta t} (h_1 - h_0) &= \frac{1}{2} (\partial_t h_0 + \partial_t h_1) + \frac{\Delta t}{4} (\partial_{tt}^2 h_0 - \partial_{tt}^2 h_1) + \frac{(\Delta t)^2}{12 \Delta t} (\partial_{ttt}^3 (h_1 - h_0) + \partial_{ttt}^3 (h_1 - h_0)) \\
&= \frac{1}{2} (\partial_t h_0 + \partial_t h_1) + \frac{\Delta t}{4} (\partial_{tt}^2 h_0 - \partial_{tt}^2 h_1) + \frac{\Delta t}{6} \partial_{tt}^2 (h_1 - h_0) \\
&= \frac{1}{2} (\partial_t h_0 + \partial_t h_1) + \frac{\Delta t}{12} \partial_{tt}^2 h_0 - \frac{\Delta t}{12} \partial_{tt}^2 h_1
\end{aligned}$$

The only thing that changes is the numerical factor of the second-order term. However this is now correct to third order.

2.12 Time discretisation of the tracer conservation equation

Consider the advection-diffusion equation

$$\frac{\partial c}{\partial t} + \nabla(c\mathbf{v}) - \nabla \cdot (\kappa \nabla c) = a$$

with the boundary conditions

$$\nabla c \cdot \hat{n} = 0 \text{ at } \Gamma_N$$

and

$$c = g \quad \text{at} \quad \Gamma_D$$

at different parts of the boundary. We will first consider the linear case where the velocity \mathbf{v} and the diffusivity, κ , are independent of c , but functions of space.

Finite element formulation

$$\left\langle \frac{\partial c}{\partial t} + \nabla \cdot (c\mathbf{v}) - \nabla \cdot (\kappa \nabla c) - a \middle| N \right\rangle$$

Greens theorem

$$\langle \partial_t c | N \rangle + \langle \nabla \cdot (c\mathbf{v}) | N \rangle + \langle \kappa \nabla c | \nabla N \rangle - \langle a | N \rangle - \int_{\Gamma} \nabla c \cdot \hat{\mathbf{n}} N d\Gamma = 0$$

The FE assembly of the terms, not including the time derivative, results in

$$\begin{aligned} \langle \nabla \cdot (c\mathbf{v}) | N \rangle &= \mathbf{A}\mathbf{c} \\ \langle \kappa \nabla c | \nabla N \rangle &= \mathbf{D}\mathbf{c} \\ \langle a | N \rangle &= \mathbf{B} \end{aligned}$$

Those matrices are evaluated at some time t , and they are in the general non-linear case, also functions of c .

We can write the resulting system as

$$\langle \partial_t c | N \rangle = \mathbf{B}(c) - (\mathbf{A}(c) + \mathbf{D}(c)) \mathbf{c}$$

Chapter 3

Constraints

In \tilde{U} all essential boundary conditions, and various other constraints on the solution, are enforced using the Lagrange multiplier method. Any multi-linear constraint can be written on the form

$$\mathbf{L}\mathbf{f} - \mathbf{c} = \mathbf{0},$$

where $\mathbf{f} \in \mathbb{R}^n$ is a nodal vector for the variable $f(x)$, $\mathbf{c} \in \mathbb{R}^m$ is a vector of m prescribed values, and $\mathbf{L} \in \mathbb{R}^{m \times n}$ is the *multi-linear constraint* (MLC) matrix on the form

$$\mathbf{L} = \begin{pmatrix} a_{1,1} & a_{1,2} & \cdots & a_{1,n} \\ a_{2,1} & a_{2,2} & \cdots & a_{2,n} \\ \vdots & \vdots & \ddots & \vdots \\ a_{m,1} & a_{m,2} & \cdots & a_{m,n} \end{pmatrix}$$

where m is the number of constraints and n the number of nodal values.

If we, for example, want to enforce the ice thickness at node 1 to be equal to 1, the MLC matrix $\mathbf{L} \in \mathbb{R}^{1 \times n}$ has the form

$$\mathbf{L} = (1 \ 0 \ \cdots \ 0)$$

and $\mathbf{c} \in \mathbb{R}^{n \times 1}$ is

$$\mathbf{c} = (1)$$

These types of constraints are referred to as *point constraints*. When implemented using the method of Lagrange multipliers, the Lagrange variable may not have a clear physical interpretation in a given FE basis.

3.1 Nodal constraints assembly

Instead of applying point constraints as above, one can introduce the constraints

Single nodal constraint is

$$f(x_q) = \tilde{f}(x_q)$$

where x_q is a nodal point location of node q and $\tilde{f}(x_q)$ is the prescribed value.

$$\begin{aligned} \langle \lambda, f(x_q) - \tilde{f}(x_q) \rangle &= \langle \lambda_p \phi_p(x), ((f_q - \tilde{f}_q) \phi_q(x)) \rangle \\ &= \lambda_i \langle \phi_i(x), \phi_q(x) \rangle (f_q - \tilde{f}_q) \\ &= \lambda_i M_{iq} (f_q - \tilde{f}_q) \\ &= \lambda_i M_{ij} \delta_{jq} (f_q - \tilde{f}_q) \end{aligned}$$

for $p = 1, N$ and q fixed. or

$$\langle \lambda, f(x_q) - \tilde{f}(x_q) \rangle = \boldsymbol{\lambda} \mathbf{M}_q (f_q - \tilde{f}_q)$$

or also

$$\langle \lambda, f(x_q) - \tilde{f}(x_q) \rangle = \boldsymbol{\lambda}^T \mathbf{M} \mathbf{L}^T (f_q - \tilde{f}_q)$$

where \mathbf{L} is $n \times 1$. And more generally for m number of constraints

$$\langle \lambda, f(x_q) - \tilde{f}(x_q) \rangle = \underbrace{\lambda^T}_{1 \times n} \underbrace{\mathbf{M}}_{n \times n} \underbrace{\mathbf{L}^T}_{n \times m} (\underbrace{\mathbf{L}}_{m \times n} \underbrace{\mathbf{f}}_n - \underbrace{\mathbf{c}}_m)$$

If we only solve for the active Lagrange multiplies, the number of which will be equal to the number m of constraints, we can arrive at

$$\langle \lambda, f(x_q) - \tilde{f}(x_q) \rangle = \underbrace{\lambda^T}_{1 \times m} \underbrace{\mathbf{L}}_{m \times n} \underbrace{\mathbf{M}}_{n \times n} \underbrace{\mathbf{L}^T}_{n \times m} (\underbrace{\mathbf{L}}_{m \times n} \underbrace{\mathbf{f}}_n - \underbrace{\mathbf{c}}_m)$$

and the system to solve is then

$$\mathbf{LML}^T \mathbf{Lf} = \mathbf{LML}^T \mathbf{c}$$

or simply

$$\mathbf{Lf} = \mathbf{c}$$

which is the same system as the one we solve when applying point constraints. So these two approaches are identical. However, the values of the Lagrange multipliers will not be identical for those two approaches. See section 3.3 for further discussion.

3.2 Linear system with multi-linear constraints

Consider a quadratic minimisation problem

$$\min_{\mathbf{x}} I(\mathbf{x}) = \frac{1}{2} \mathbf{x}^T \mathbf{Ax} - \mathbf{bx},$$

subject to the multi-linear set of constraints

$$\mathbf{Lx} - \mathbf{c} = 0.$$

Using the method of Lagrange multipliers, we write

$$\min_{\mathbf{x}} J(\mathbf{x}) := \frac{1}{2} \mathbf{x}^T \mathbf{Ax} - \mathbf{bx} + \boldsymbol{\lambda}^T \cdot (\mathbf{Lx} - \mathbf{c}).$$

Taking the derivatives with respect to \mathbf{x} and $\boldsymbol{\lambda}$ and setting to zero gives the system

$$\begin{bmatrix} \mathbf{A} & \mathbf{L}^T \\ \mathbf{L} & 0 \end{bmatrix} \begin{bmatrix} \mathbf{x} \\ \boldsymbol{\lambda} \end{bmatrix} = \begin{bmatrix} \mathbf{b} \\ \mathbf{c} \end{bmatrix}. \quad (3.1)$$

Here $\mathbf{A} \in \mathbb{R}^{n \times n}$ and $\mathbf{L} \in \mathbb{R}^{p \times n}$ where p are the number of constraints. There are various approaches suggested in the literature to solving the system (3.1) such as the full-space, range-space, null-space approaches.

The *range-space* approach is to use the first equation of (3.1) to arrive at

$$\mathbf{Lx} + \mathbf{LA}^{-1} \mathbf{L}^T \boldsymbol{\lambda} = \mathbf{LA}^{-1} \mathbf{b}.$$

Then insert the second equation of (3.1) giving

$$\mathbf{LA}^{-1} \mathbf{L}^T \boldsymbol{\lambda} = \mathbf{LA}^{-1} \mathbf{b} - \mathbf{c},$$

which can be solved for $\boldsymbol{\lambda}$, and then solve for \mathbf{x} using the first equation equation of (3.1) as

$$\mathbf{Ax} = \mathbf{b} - \mathbf{L}^T \boldsymbol{\lambda}.$$

The *null-space* approach is to find a matrix $\mathbf{Z} \in \mathbb{R}^{n \times (n-p)}$ whose columns form a basis for the null space of \mathbf{L} so that

$$\mathbf{LZ} = \mathbf{0}$$

Let $\hat{\mathbf{x}} \in \mathbb{R}^n$ be a particular solution for the second equation such that

$$\mathbf{L}\hat{\mathbf{x}} = \mathbf{c}$$

After some manipulations we arrive at the null-space method for solving (3.1) which can be summarised as:

- Find \mathbf{Z} so that $\mathbf{L}\mathbf{Z} = \mathbf{0}$.
- Find $\hat{\mathbf{x}}$ so that $\mathbf{L}\hat{\mathbf{x}} = \mathbf{c}$.
- Solve $\mathbf{Z}^T \mathbf{A} \mathbf{Z} \mathbf{z} = \mathbf{Z}^T (\mathbf{b} - \mathbf{A}\hat{\mathbf{x}})$
- Set $\mathbf{x} = \mathbf{Z}\mathbf{z} + \hat{\mathbf{x}}$
- Solve $\mathbf{L}^T \boldsymbol{\lambda} = \mathbf{b} - \mathbf{A}\mathbf{x}$

The matrix $\mathbf{Z}^T \mathbf{A} \mathbf{Z}$ is $(n-p) \times n \times n \times n \times n \times (n-p) = (n-p) \times (n-p)$. Therefore if the number of constraints (p) is significantly large compared to n , $n-p$ is small and this method becomes attractive. However, the matrix $\mathbf{Z}^T \mathbf{A} \mathbf{Z}$ is usually dense.

3.2.1 Pre-eliminating point constraints

The system (3.1) has the size $(n+p) \times (n+p)$ where n is the total number of degrees of freedom and p the number of (point) restraints. In some cases it is fairly easy to pre-eliminate the constraints and so arrive at a reduced system of the size $n \times n$.

The system (3.1) is

$$\mathbf{A}\mathbf{x} + \mathbf{L}^T \boldsymbol{\lambda} = \mathbf{b} \quad (3.2)$$

$$\mathbf{L}\mathbf{x} = \mathbf{c} \quad (3.3)$$

Here the matrix $\mathbf{A} \in \mathbb{R}^{n \times n}$ and has rank n , while the matrix $\mathbf{L} \in \mathbb{R}^{p \times n}$ with $p \leq n$ and has rank p . The products $\mathbf{L}^T \mathbf{L} \in \mathbb{R}^{n \times n}$ and $\mathbf{L}\mathbf{L}^T \in \mathbb{R}^{p \times p}$ both have rank p . The matrix $\mathbf{L}\mathbf{L}^T$ is invertible but $\mathbf{L}^T \mathbf{L}$ is not.

We consider the particular, but in this context not uncommon, case when

$$\mathbf{L}\mathbf{L}^T = \mathbf{I}_{pp}. \quad (3.4)$$

This assumption is not particularly restrictive¹ and allows us to determine $\boldsymbol{\lambda}$ knowing \mathbf{x} using Eq. (3.2) as follows

$$\begin{aligned} \mathbf{L}^T \boldsymbol{\lambda} &= (\mathbf{b} - \mathbf{A}\mathbf{x}) \\ \implies \mathbf{L}\mathbf{L}^T \boldsymbol{\lambda} &= \mathbf{L}(\mathbf{b} - \mathbf{A}\mathbf{x}) \\ \implies \boldsymbol{\lambda} &= \mathbf{L}(\mathbf{b} - \mathbf{A}\mathbf{x}). \end{aligned}$$

And furthermore again using Eq. (3.2)

$$\begin{aligned} \mathbf{A}\mathbf{x} &= \mathbf{b} - \mathbf{L}^T \boldsymbol{\lambda} \\ \implies \mathbf{A}\mathbf{x} &= \mathbf{b} - \mathbf{L}^T \mathbf{L}(\mathbf{b} - \mathbf{A}\mathbf{x}) \\ \implies \mathbf{A}\mathbf{x} - \mathbf{L}^T \mathbf{L}\mathbf{A}\mathbf{x} &= \mathbf{b} - \mathbf{L}^T \mathbf{L}\mathbf{b} \\ \implies (\mathbf{I}_{nn} - \mathbf{L}^T \mathbf{L})\mathbf{A}\mathbf{x} &= (\mathbf{I}_{nn} - \mathbf{L}^T \mathbf{L})\mathbf{b} \end{aligned}$$

or

$$\mathbf{Q}\mathbf{A}\mathbf{x} = \mathbf{Q}\mathbf{b}, \quad (3.5)$$

where the matrix $\mathbf{Q} \in \mathbb{R}^{n \times n}$ defined as

$$\mathbf{Q} = \mathbf{I}_{nn} - \mathbf{L}^T \mathbf{L}.$$

Multiplying with \mathbf{Q} has the effect of ‘killing off’ the first p equations. Pre-multiply both sides of Eq. (3.3) to obtain

$$\mathbf{L}^T \mathbf{L} = \mathbf{L}^T \mathbf{c},$$

¹Provided a node appears in one constraint only, \mathbf{L} can always be scaled so that $\mathbf{L}\mathbf{L}^T$ equals \mathbf{I}_{pp} . For example if

$$\mathbf{L} = \begin{pmatrix} 1 & 10 & 0 & -2 & 0 & 0 & 0 \\ 0 & 0 & 2 & 0 & 0 & 0 & 0 \\ 0 & 0 & 0 & 0 & 5 & 0 & 0 \\ 0 & 0 & 0 & 0 & 0 & 1 & -1 \end{pmatrix}$$

Then scaling each line of \mathbf{L} so that the square root of the sum of the squares of the elements of that line is equal to unity results in $\mathbf{L}\mathbf{L}^T = \mathbf{I}_{44}$.

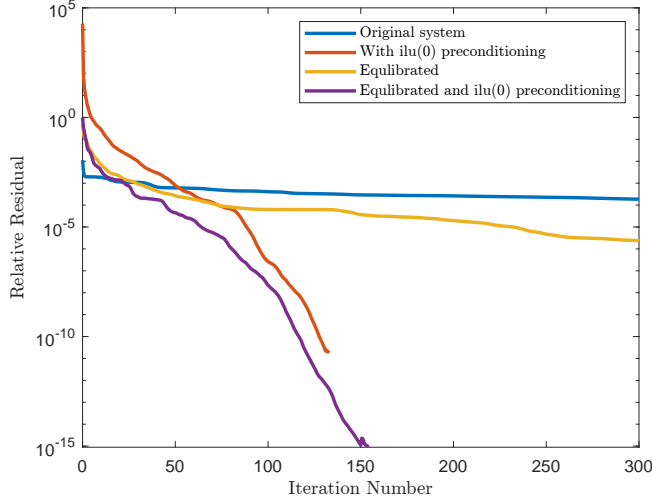


Figure 3.1: Example of an iterative solution of $\tilde{\mathbf{A}}$ using the Generalised Minimum Residual Method (gmres). The matrices A and B stem from a uvh solve of the WAIS, with 250,896 number of unknowns. Computationally the solver for non-equilibrated matrix using the $ilu(0)$, pre-conditioner is fastest and reaches the prescribed reduction in relative residual, 10^{-15} , in about 40 sec. However, on same machine, a direct solver solves the same problem to in about 9 sec.

and adding to Eq. (3.5) gives

$$(\mathbf{Q}\mathbf{A} + \mathbf{L}^T \mathbf{L})\mathbf{x} = \mathbf{Q}\mathbf{b} + \mathbf{L}^T \mathbf{c},$$

and as

$$\tilde{\mathbf{A}} := \mathbf{Q}\mathbf{A} + \mathbf{L}^T \mathbf{L},$$

is clearly full rank, we can now solve for \mathbf{x} as

$$\mathbf{x} = \tilde{\mathbf{A}}^{-1}(\mathbf{Q}\mathbf{b} + \mathbf{L}^T \mathbf{c}), \quad (3.6)$$

and then calculate $\boldsymbol{\lambda}$ from

$$\boldsymbol{\lambda} = \mathbf{L}(\mathbf{b} - \mathbf{A}\mathbf{x}). \quad (3.7)$$

A drawback of this approach is that even when the original matrix \mathbf{A} is symmetrical, $\tilde{\mathbf{A}}$ is generally asymmetrical. While the system can be made symmetrical, in practice doing so in $\tilde{\mathbf{A}}$ is of limited value as most of the calculations tend to be done using implicit time stepping where \mathbf{A} is already non-symmetrical.

Currently (August 2019) this is the approach² used in $\tilde{\mathbf{U}}$ when matrix \mathbf{A} is asymmetrical, i.e. the system (3.1) is then solved using Eqs. (3.6) and (3.7) provided Eq. (3.4) holds.

3.3 Nodal reactions

I define *effective nodal reactions*, \mathbf{R} , as

$$\mathbf{R} = \mathbf{b} - \mathbf{A}\mathbf{x} = \mathbf{L}^T \boldsymbol{\lambda}.$$

The effective nodal reactions are defined for all degrees of freedom and for all nodes, i.e. not only for the degrees of freedom and nodes for which BCs are applied to. Clearly the vector \mathbf{R} does not represent nodal values in the FE basis. To project \mathbf{R} into the FE basis we need to solve

$$\langle [\mathbf{R}^*]_p N_p, N_q \rangle = [\mathbf{R}]_q,$$

for components of what I refer to as the *physical nodal reactions*, \mathbf{R}^* . We see that

$$\mathbf{R}^* = \mathbf{M}^{-1} \mathbf{R},$$

or

$$\mathbf{R}^* = \mathbf{M}^{-1} \mathbf{L}^T \boldsymbol{\lambda}.$$

²Presumably this approach will have been derived earlier in the literature, but I have not seen this approach described anywhere.

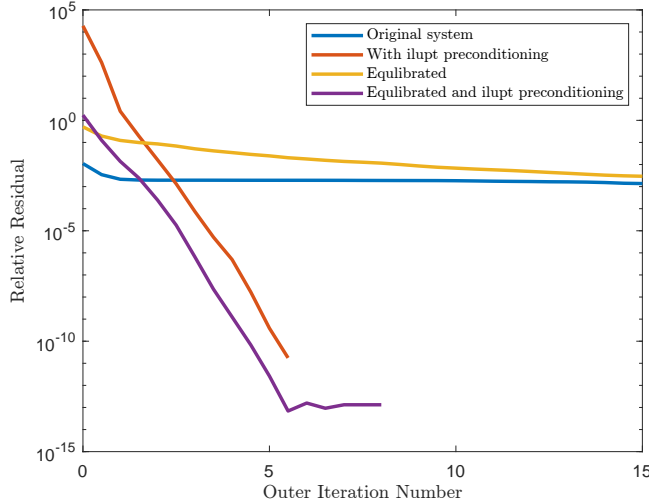


Figure 3.2: Same example as shown in Fig. 3.1, but now using the ilupt conditioner with drop tolerance of 10^{-4} . The two iterative solvers using this pre-conditioner now arrive at the prescribed tolerance in about 5 iterations. The non-equilibrated system solve with the ilupt pre-conditioner is fastest, and takes about 14 sec, of which 8 are required for the incomplete LU factorisation, about 1 sec for the nested dissection permutation, and about 5 sec for the gmres iteration.

Assuming

$$\mathbf{L}\mathbf{L}^T = \mathbf{I}_{pp}. \quad (3.4)$$

we now write the system

$$\begin{aligned} \mathbf{A}\mathbf{x} + \mathbf{L}^T\boldsymbol{\lambda} &= \mathbf{b} \\ \mathbf{L}\mathbf{x} &= \mathbf{c} \end{aligned}$$

as

$$\begin{aligned} \mathbf{A}\mathbf{x} + (\mathbf{L}\mathbf{M})^T\boldsymbol{\lambda}^* &= \mathbf{b} \\ \mathbf{L}\mathbf{M}\mathbf{x} &= \mathbf{L}\mathbf{M}\mathbf{L}^T\mathbf{c} \end{aligned}$$

in which case

$$(\mathbf{L}\mathbf{M})^T\boldsymbol{\lambda}^* = \mathbf{L}^T\boldsymbol{\lambda}$$

or

$$\mathbf{L}^T\boldsymbol{\lambda}^* = \mathbf{M}^{-1}\mathbf{L}^T\boldsymbol{\lambda}$$

hence

$$\mathbf{R}^* = \mathbf{L}^T\boldsymbol{\lambda}^*$$

The above reformulation requires all links to be homogeneous. Dirichlet BCs can be non-homogeneous.

Alternatively, re-write this as

$$\begin{aligned} \mathbf{A}\mathbf{x} + (\mathbf{L}\mathbf{M}\mathbf{L}^T\mathbf{L})^T\boldsymbol{\lambda}^* &= \mathbf{b} \\ \mathbf{L}\mathbf{M}\mathbf{L}^T\mathbf{L}\mathbf{x} &= \mathbf{L}\mathbf{M}\mathbf{L}^T\mathbf{c} \end{aligned}$$

where

$$\mathbf{L}^T\boldsymbol{\lambda} = (\mathbf{L}\mathbf{M}\mathbf{L}^T\mathbf{L})^T\boldsymbol{\lambda}^*,$$

hence

$$\boldsymbol{\lambda}' = (\mathbf{L}\mathbf{L}^T)^{-1}\mathbf{M}^{-1}(\mathbf{L}\mathbf{L}^T)^{-1}\mathbf{L}^T\boldsymbol{\lambda}.$$

We find that

$$\boldsymbol{\lambda}' = (\mathbf{L}\mathbf{L}^T)^{-1}\mathbf{L}\mathbf{R}^*$$

Note that for m linear independent constraints, the matrix $\mathbf{L} \in \mathbb{R}^{m \times n}$ has the rank m . The product $\mathbf{L}\mathbf{L}^T$ is in $\mathbb{R}^{m \times m}$ and

$$\text{rank}(\mathbf{L}\mathbf{L}^T) = \text{rank}(\mathbf{L}^T\mathbf{L}) = \text{rank}(\mathbf{L}) = m$$

and therefore the symmetric matrix $(\mathbf{L}\mathbf{L}^T) \in \mathbb{R}^{m \times m}$ is full rank and its inverse exists. However, $(\mathbf{L}^T\mathbf{L}) \in \mathbb{R}^{n \times n}$ is not full rank and therefore not invertible.

3.4 Non-linear system with non-linear constraints

If we have a non-linear minimisation problem

$$\min_{\mathbf{x}} I(\mathbf{x})$$

and non-linear set of constraints $\mathbf{l}(\mathbf{x}) = 0$, we minimise the extended cost function

$$I(\mathbf{x}) + \langle \lambda(\mathbf{x}) \mid \mathbf{l}(\mathbf{x}) \rangle,$$

or once we have discretised the problem,

$$I(\mathbf{x}) + \boldsymbol{\lambda}^T \mathbf{l}.$$

A stable equilibrium point is a minimum with respect to \mathbf{x} and a maximum with respect to λ . Setting the derivatives with respect to \mathbf{x} and $\boldsymbol{\lambda}$ to zero leads to

$$\begin{aligned} \partial_{\mathbf{x}} I(\mathbf{x}) + \boldsymbol{\lambda}^T \partial_{\mathbf{x}} \mathbf{l}(\mathbf{x}) &= \mathbf{0} \\ \mathbf{l}(\mathbf{x}) &= \mathbf{0} \end{aligned}$$

If this non-linear system is again solved using Newton-Raphson method then we use first-order Taylor expansion and write

$$\begin{aligned} \partial_{\mathbf{x}} I(\mathbf{x}) &= \partial_{\mathbf{x}} I_0 + \boldsymbol{\lambda}_0^T \partial_{\mathbf{x}} \mathbf{l}_0 + \partial_{\mathbf{x}\mathbf{x}}^2 I_0 \Delta \mathbf{x} + \boldsymbol{\lambda}_0 \partial_{\mathbf{x}\mathbf{x}} \mathbf{l}_0 \Delta \mathbf{x} + \partial_{\mathbf{x}} \mathbf{l}_0^T \Delta \boldsymbol{\lambda} \\ \mathbf{l}(\mathbf{x}) &= \mathbf{l}(\mathbf{x}_0) + \partial_{\mathbf{x}} \mathbf{l} \Delta \mathbf{x} \end{aligned}$$

and repeatedly solve

$$\begin{bmatrix} \mathbf{H} + \partial_{\mathbf{x}\mathbf{x}}^2 \mathbf{l} \boldsymbol{\lambda}_0 & \partial_{\mathbf{x}} \mathbf{l}^T \\ \partial_{\mathbf{x}} \mathbf{l} & \mathbf{0} \end{bmatrix} \begin{bmatrix} \Delta \mathbf{x} \\ \Delta \boldsymbol{\lambda} \end{bmatrix} = \begin{bmatrix} -\partial_{\mathbf{x}} I_0 - \partial_{\mathbf{x}} \mathbf{l}^T \boldsymbol{\lambda}_0 \\ -\mathbf{l}_0 \end{bmatrix} \quad (3.8)$$

where again $\mathbf{H} = \partial_{\mathbf{x}\mathbf{x}} I(\mathbf{x})$ is the Hessian matrix.

If the constraints are linear, we can write

$$\mathbf{l} = \mathbf{L}\mathbf{x} - \mathbf{c} = \mathbf{0}$$

in which case

$$\partial_{\mathbf{x}} \mathbf{l} = \mathbf{L} \quad \text{and} \quad \partial_{\mathbf{x}\mathbf{x}}^2 \mathbf{l} = \mathbf{0}$$

and the system to be solved is

$$\begin{bmatrix} \mathbf{H} & \mathbf{L}^T \\ \mathbf{L} & \mathbf{0} \end{bmatrix} \begin{bmatrix} \mathbf{x} \\ \boldsymbol{\lambda} \end{bmatrix} = \begin{bmatrix} -\partial_{\mathbf{x}} I_0 - \partial_{\mathbf{x}} \mathbf{l}^T \boldsymbol{\lambda}_0 \\ -\mathbf{L}\mathbf{x}_0 + \mathbf{c} \end{bmatrix}$$

3.5 FE formulation of the Newton-Raphson method with multi-linear constraints

We solve

$$\langle f(u), N_p \rangle = 0 \quad \text{subject to} \quad g_q(u) = 0 \quad \text{where } q = 1 \dots N$$

Assume there is a scalar $I(u)$ such that $\langle f(u), N_p \rangle$ is derivative of I with respect to u_p , then minimising

$$I(u) + \langle \lambda, g(u) \rangle$$

gives, with $u = N_p u_p$ and $\lambda = N_p \lambda_p$

$$\langle f(u), N_q \rangle + \langle \lambda, \partial g / \partial u N_q \rangle = 0 \quad (3.9)$$

$$\langle N_q, g(u) \rangle = 0 \quad (3.10)$$

In general, the $\langle f(u), N_q \rangle$ system can be expected to be non-linear. Assuming for the moment the constraints $g(u) = 0$ are linear ($g_q = A_{qr} u_r - b_q = 0$), and the resulting system is solved using the Newton-Raphson method, gives

$$\langle f(u_0), N_q \rangle + \langle \partial f / \partial u \Delta u, N_q \rangle + \langle \lambda, \partial g / \partial u N_q \rangle = 0 \quad (3.11)$$

$$\langle N_q, \partial g / \partial u (u_0 + \Delta u) - b \rangle = 0 \quad (3.12)$$

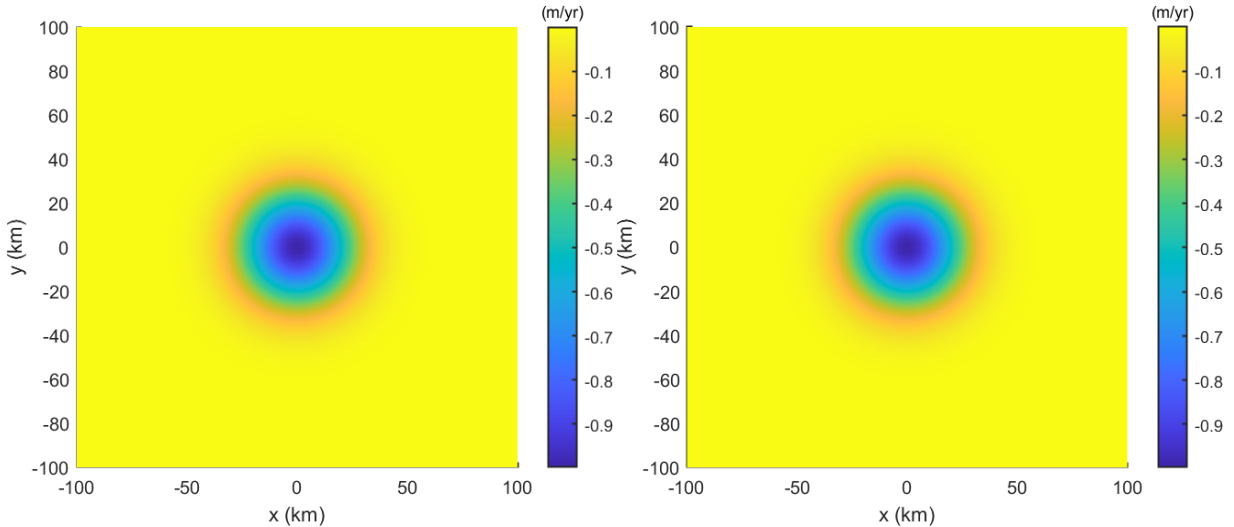


Figure 3.3: Active set method, as described in section 3.6, used to ensure positive ice thicknesses. To the left are the thickness reactions as calculated by \hat{U}_a for a situation where ice thicknesses are zero everywhere, and using the surface-mass balance distribution shown in the right-hand side panel. The ice geometry is a simple horizontal slab. Hence, surface velocities are everywhere equal to zero. The active set method is here used to ensure that despite non-zero melt being applied over an area where the thickness is everywhere zero, the ice thickness does not become negative. Note that the (nodal) thickness reactions need to be pre-multiplied by the mass matrix and divided by the ice density for them to become ‘mesh independent’ and comparable to the surface mass balance. As is evident from comparing the two panels, the active set method creates a fictitious mass balance distribution that exactly counteracts the applied mass balance. Consequently, the ice thickness remains zero everywhere despite non-zero melt being applied along the upper surface.

or

$$\langle f(u_0), N_q \rangle + \langle \partial f / \partial u N_p | N_q \rangle \Delta u_p + \langle N_p, \partial g / \partial u N_q \rangle \lambda_p = 0 \quad (3.13)$$

$$\langle N_q, \partial g / \partial u N_p \rangle u_{0p} + \langle N_q | \partial g / \partial u N_p \rangle \Delta u_p - \langle N_q, N_p \rangle b_p = 0 \quad (3.14)$$

$$\begin{bmatrix} \mathbf{K} & \mathbf{L}^T \\ \mathbf{L} & 0 \end{bmatrix} \begin{bmatrix} \Delta \mathbf{u} \\ \boldsymbol{\lambda} \end{bmatrix} = \begin{bmatrix} -\mathbf{f}(u_0) \\ \mathbf{S}\mathbf{b} - \mathbf{L}\mathbf{u}_0 \end{bmatrix}$$

where

$$f_q := \langle f(u_0), N_q \rangle$$

and

$$S_{qp} := \langle N_q, N_p \rangle$$

and

$$L_{pq} = \langle N_p, \partial g / \partial u N_q \rangle$$

or if $\boldsymbol{\lambda} = \Delta \boldsymbol{\lambda} + \boldsymbol{\lambda}_0$,

$$\begin{bmatrix} \mathbf{K} & \mathbf{L}^T \\ \mathbf{L} & 0 \end{bmatrix} \begin{bmatrix} \Delta \mathbf{u} \\ \Delta \boldsymbol{\lambda} \end{bmatrix} = \begin{bmatrix} -\mathbf{f}(u_0) - \mathbf{L}^T \boldsymbol{\lambda}_0 \\ \mathbf{S}\mathbf{b} - \mathbf{L}\mathbf{u}_0 \end{bmatrix}$$

If the constraints can be written as $A\mathbf{u} - \mathbf{b} = 0$ then

$$L_{pq} = \langle N_p, A_{pq} N_q \rangle$$

(no summation implied). If the form functions are delta functions then, $\mathbf{S} = \mathbf{1}$ and $\mathbf{L} = \mathbf{A}$.

3.6 Automated thickness-positivity constraints (active set method)

Assuming the existence of a potential P the problem can be written as a constraint minimisation problem

$$\begin{aligned} & \min_{\mathbf{h}, \mathbf{v}} P(\mathbf{h}, \mathbf{v}) \\ & \text{s.t. } h(x, y) \geq 0 \quad \text{on } \Omega \end{aligned}$$

The Lagrangian

$$\mathcal{L}P + \int_{\Omega} \lambda(x, y) h(x, y) d\Omega$$

Karush-Kuhn-Tucker conditions are

$$D_{\mathbf{h}} \mathcal{L}(\mathbf{h}, \boldsymbol{\lambda}) = 0 \quad (3.15)$$

$$\lambda_q \leq 0 \quad (3.16)$$

$$h_q \geq 0 \quad (3.17)$$

$$\boldsymbol{\lambda}^T \cdot \mathbf{h} = 0 \quad (3.18)$$

$$(3.19)$$

The condition $\boldsymbol{\lambda}^T \cdot \mathbf{h} = 0$ is the complementary condition, if thickness is positive then the corresponding $\boldsymbol{\lambda}$ nodal values must be zero, and where λ is negative the thickness must be zero.

If the system of field equations can not be derived from a minimum energy principle, as is the case here, the KKT conditions are introduced into the weak form.

Selecting the correct active set is a non-trivial problem and identifying it can be time consuming.

The thickness constraint is

$$h(x, y) = h_p \phi_p(x, y) \geq 0,$$

everywhere, or in the FE context

$$\langle h | \xi_q \rangle = 0 \quad \text{for } i = 1 \dots n ,$$

where n is the number of test functions (here equal to the number of nodes). We can also write this as

$$\mathbf{M}\mathbf{h} \geq \mathbf{0}$$

where $[\mathbf{M}]_{ij} = \int_{\Omega} \phi_i(x, y) \xi_j(x, y) d\Omega$ and \mathbf{h} the vector of nodal thickness values. In the Galerkin method we use $\phi_q = \xi_q$. We solve the resulting inequality problem using a simple iterative procedure usually referred to as the active-set method. The active set, \mathbb{A} , is the set of nodes for which the equality constraint $h_p = 0$ is applied at current iteration. These nodes are referred to as active, while the remaining nodes where $h_p > 0$ are considered inactive. At a given iteration we solve the resulting (equality) constrained problem using the method of Lagrange multipliers and then update the active set as described below. Over the active set we have the equality constraint

$$\begin{aligned} 0 &= \int_{\Omega} \sum_{q \in \mathbb{A}} h_q \phi_q(x, y) \xi_p(x, y) d\Omega \\ &= \int_{\Omega} L_{qr} h_r \phi_q \xi_p d\Omega \quad \text{for } p = 1 \dots n , \end{aligned}$$

where r ranges from 1 to n and $L_{qr} = 1$ if node r is active in the constraint $q \in \mathbb{A}$, and zero otherwise. We can also write the above equation as

$$\mathbf{L}\mathbf{M}\mathbf{h} = \mathbf{0} .$$

In addition to the active-set equality equations we have the field equations, which in this particular case are the conservation equations for momentum and mass, written in discretised form as

$$\mathbf{F}(\mathbf{x}) = \mathbf{0} .$$

These are linearised as

$$\mathbf{K}\Delta\mathbf{x} = -\mathbf{F}(\mathbf{x}_0) ,$$

where \mathbf{K} is the directional derivative of \mathbf{F} , and solved using the Newton-Raphson method. We thus arrive at the KKT system

$$\begin{bmatrix} \mathbf{K} & \mathbf{M}^T \mathbf{L}^T \\ \mathbf{L} \mathbf{M} & \mathbf{0} \end{bmatrix} \begin{bmatrix} \Delta \mathbf{h} \\ \Delta \boldsymbol{\lambda}^* \end{bmatrix} = \begin{bmatrix} -\mathbf{F}(\mathbf{x}_0) - \mathbf{L} \mathbf{M} \boldsymbol{\lambda}_0^* \\ -\mathbf{L} \mathbf{M} \mathbf{h}_0 \end{bmatrix}. \quad (3.20)$$

Physically, $\boldsymbol{\lambda}^*$ can be thought of as the thickness, increment, or additional mass influx per time unit, required to ensure positive thickness. At any given active-set iteration the active set is therefore updated based on the sign of λ_q^* at node q . Those nodes for which λ_q^* is negative become inactive and are taken out of the active set, nodes where λ_q^* is positive are kept in the active set, and previously inactive nodes where h_q becomes negative are added to the active set. The iteration is continued until no further changes to the active set are required. Occasionally, the active set becomes cyclic, and the iteration then terminates with all cyclic nodes included in the active set.

As commonly done in numerical models, linear multi-points constraints are implemented in $\tilde{\mathbf{U}}_a$ as $\mathbf{L}\mathbf{x} = \mathbf{c}$ where \mathbf{L} is the where $\mathbf{L} \in \mathbb{R}^{p \times n}$ is an arbitrary MPCs matrix, where p is the number of linear nodal constraints and n the total degrees of freedom. When combined with Newton-Raphson method, this results in a KKT-type matrix system

$$\begin{bmatrix} \mathbf{K} & \mathbf{L}^T \\ \mathbf{L} & \mathbf{0} \end{bmatrix} \begin{bmatrix} \Delta \mathbf{x} \\ \Delta \boldsymbol{\lambda} \end{bmatrix} = \begin{bmatrix} -\mathbf{F}(\mathbf{x}_0) - \mathbf{L} \boldsymbol{\lambda}_0 \\ -\mathbf{L} \mathbf{c}_0 \end{bmatrix}. \quad (3.21)$$

Note that when solving implicitly for velocities and thickness, as done in $\tilde{\mathbf{U}}_a$, $\Delta \mathbf{x}$ stands for both velocity components and thickness, i.e.

$$\Delta \mathbf{x} = \begin{pmatrix} \Delta \mathbf{u} \\ \Delta \mathbf{v} \\ \Delta \mathbf{h} \end{pmatrix}.$$

The key difference between systems (3.20) and (3.21) is the inclusion of the mass matrix \mathbf{M} in the former. Rather than modifying the commonly used framework (3.21) for implementing MPCs in finite elements to include the mass matrix \mathbf{M} , we now solve (3.21) and then calculate $\boldsymbol{\lambda}^*$ afterwards from the solution of that system as

$$\boldsymbol{\lambda}^* = (\mathbf{L} \mathbf{L}^T)^{-1} \mathbf{L} \mathbf{M}^{-T} \mathbf{L}^T \boldsymbol{\lambda}. \quad (3.22)$$

Both $\boldsymbol{\lambda}^*$ and $\boldsymbol{\lambda}$ are in \mathbb{R}^p while $\mathbf{M}^{-T} \mathbf{L}^T \boldsymbol{\lambda}$ is in \mathbb{R}^n . Note that if each of the columns of $\mathbf{L} \in \mathbb{R}^{p \times n}$ have exactly one non-zero entry and that entry is equal to unity, as will be the case if \mathbf{L} is a thickness constraint, then $\mathbf{L} \mathbf{L}^T$ is a $p \times p$ unity matrix irrespective of how the thickness constraints have been labelled when constructing \mathbf{L} . It is easy to see³ that $\boldsymbol{\lambda}^*$ is indeed identical to solution for $\boldsymbol{\lambda}$ of the KKT-system including the mass matrix, i.e. Eq. (3.20). However, only $\boldsymbol{\lambda}^*$ obtained by solving Eq. (3.20) has the physical interpretation mentioned above, i.e. it is the thickness increment required at a given node in the active set A to enforce thickness positivity. Hence, updating the active set must be based on the sign of $\boldsymbol{\lambda}^*$ and not on the sign of $\boldsymbol{\lambda}$. For linear elements all the entries of the mass matrix \mathbf{M} are positive by construction and therefore, in that particular case, the active set update can be based on either λ_q or λ_q^* . However, for higher order elements, e.g. quadratic or cubic, using $\boldsymbol{\lambda}$ instead of $\boldsymbol{\lambda}^*$ will, in general, result in an incorrect active-set update.

The active-set is updated after each NR iteration, and the active-set update continued until convergence. In transient runs, only one or two updates are typically required. Updating the active set within the Newton loop was tried but did not result in any computational gains.

3.6.1 Thickness barrier

$$\begin{aligned} I &= \gamma_h \lambda_h e^{-(h-h_{\min})/\lambda_h} \\ \partial_h I &= -\gamma_h e^{-(h-h_{\min})/\lambda_h} \\ \partial_{hh}^2 I &= \frac{\gamma_h}{\lambda_h} e^{-(h-h_{\min})/\lambda_h} \end{aligned}$$

³Consider

$$\begin{aligned} \mathbf{F}\mathbf{x} + \mathbf{L}^T \boldsymbol{\lambda} &= 0 \\ \mathbf{F}\mathbf{x} + \mathbf{M} \mathbf{L}^T \boldsymbol{\lambda}^* &= 0 \end{aligned}$$

from which (3.22) follows.

If the problem were self-adjoint then this amounts to adding a term to the prognostic equations, i.e.

$$\partial_t h + \nabla_{xy} \cdot \mathbf{q}_h + \partial_h I = a$$

or

$$\partial_t h + \nabla_{xy} \cdot \mathbf{q}_{xy} = a - \partial_h I$$

which shows that the method is equivalent to adding a fictitious mass-balance term. For $\gamma_h = 1$, $\lambda = 1$, $h_{\min} = 0$ and $h = 100$ the numerical value is about 10^{-44} and about 10^{-5} for $h = 1$.

If $a = 0$ and $\mathbf{v}_h = 0$

$$\partial_t h = -\partial_h I = \gamma_h e^{-(h-h_{\min})/\lambda_h}$$

and γ_h has the units length per time and can be thought of as the fictitious mass balance at $h = h_{\min}$.

Solving

$$\partial_t h + \nabla_{xy} \cdot \mathbf{q}_h - \gamma_h e^{-(h-h_{\min})/\lambda_h} = a$$

implicitly using NR with respect to h where

$$h_{n+1} = h_{n+1}^i + \Delta h$$

is h at time step $n+1$ and i is the NR iteration number, gives

$$\frac{1}{\Delta t}(\Delta h + h_{n+1}^i - h_n) - \frac{1}{2} \left(\gamma_h e^{-(h_{n+1}^i - h_{\min})/\lambda_h} - \frac{\gamma_h}{\lambda_h} e^{-(h_{n+1}^i - h_{\min})/\lambda_h} \Delta h + \gamma_h e^{-(h_n - h_{\min})/\lambda_h} \right) = 0$$

where I have omitted writing the flux and the accumulation terms, i.e.

$$\left(\frac{1}{\Delta t} + \frac{1}{2} \frac{\gamma_h}{\lambda_h} e^{-(h_{n+1}^i - h_{\min})/\lambda_h} \right) \Delta h = -\frac{1}{\Delta t}(h_{n+1}^i - h_n) + \frac{\gamma_h}{2} \left(e^{-(h_{n+1}^i - h_{\min})/\lambda_h} + \gamma_h e^{-(h_n - h_{\min})/\lambda_h} \right)$$

Chapter 4

The non-linear FE system its solution

4.1 Variational formulation

As shown in Appendix C, for an elliptic PDE

$$\mathcal{L}u = f \quad (\text{Ignoring BCs in this example})$$

the unique solution u minimises the functional

$$J(u) = \frac{1}{2} \int_{\Omega} u \mathcal{L}u \, d\Omega - \int_{\Omega} f u \, d\Omega ,$$

provided \mathcal{L} is linear, self-adjoint, i.e.

$$\int_{\Omega} v \mathcal{L}u \, d\Omega = \int_{\Omega} u \mathcal{L}v \, d\Omega ,$$

and positive definite:

$$\int_{\Omega} u \mathcal{L}u \geq 0 .$$

The resulting system for u is

$$\frac{1}{2} \int_{\Omega} \mathcal{L}u \delta u \, d\Omega - \int_{\Omega} f \delta u \, d\Omega = 0 ,$$

and this is the system solved in the finite element method. The discrete form is

$$\mathbf{A}\mathbf{u} = \mathbf{f}$$

where $[A]_{ij} = a_{ij}$ and $F_j = l_j$ and $a_{ij} = a(\phi_i, \xi_k)$, $l_j = l(\xi_j)$ with

$$a_{ij} = \int_{\Omega} \phi_i \mathcal{L} \xi_j \, d\Omega$$

Note that in the FE method tend to construct the system $\mathbf{A}\mathbf{u} = \mathbf{f}$ directly as a weighted residuals problem, i.e.

$$\int_{\Omega} (\mathcal{L}u - f) \phi_i \, d\Omega = 0 .$$

If the PDE is self-adjoint and positive-definite, can we interpret the discrete system $\mathbf{A}\mathbf{u} = \mathbf{f}$ as resulting from a minimisation problem. If \mathbf{A} is positive-definite we can work backwards from the discretised problem and interpret $\mathbf{A}\mathbf{u} = \mathbf{f}$ as the solution to

$$\min_{\mathbf{u}} \left\{ \frac{1}{2} \mathbf{u}^T \cdot \mathbf{A} \mathbf{u} - \mathbf{f}^T \cdot \mathbf{u} \right\} .$$

4.2 Non-linear self-adjoint problem

If the operator is self-adjoint and positive definite the resulting non-linear problem is a convex optimisation problem. We solve

$$\min_{\mathbf{x}} J(\mathbf{x}) , \quad (4.1)$$

where $J : \mathbf{R}^n \rightarrow \mathbf{R}$. If, as we here assume, the problem is convex and differentiable we can in principle solve

$$\nabla J(\mathbf{x}) = 0 . \quad (4.2)$$

For a convex function J , the two problems (4.1) and (4.2) are equivalent. The function J is convex on a convex set if and only if the Hessian is positive semi-definite.

For either solving a non-linear problem, or a non-linear convex optimisation problem, the method of choice is the Newton-Raphson method (Boyd and Vandenberghe, 2004). We expand

$$J(\mathbf{x}) = J(\mathbf{x}_0) + \nabla J(\mathbf{x}_0) \Delta \mathbf{x} + \frac{1}{2} \Delta \mathbf{x}^T \nabla^2 J(\mathbf{x}_0) \Delta \mathbf{x} + O(\|\delta \mathbf{x}^3\|)$$

where $\Delta \mathbf{x} = \mathbf{x} - \mathbf{x}_0$, and solve for

$$\min_{\mathbf{x}} \left\{ \nabla J(\mathbf{x}_0) \Delta \mathbf{x} + \frac{1}{2} \Delta \mathbf{x}^T \nabla^2 J(\mathbf{x}_0) \Delta \mathbf{x} \right\}$$

resulting in the Newton system

$$\nabla^2 J(\mathbf{x}_0) \Delta \mathbf{x} = -\nabla J(\mathbf{x}_0) ,$$

and the Newton update

$$\mathbf{x}_{k+1} = \mathbf{x}_k + \mathbf{d}_k ,$$

where

$$\mathbf{d}_k = -(\mathbf{H}_k)^{-1} \nabla J(\mathbf{x}_k) ,$$

is the Newton step, and

$$\hat{\mathbf{d}}_k = \mathbf{d}_k / \|\mathbf{d}_k\| ,$$

is the Newton direction, and

$$\mathbf{H}_k := \nabla^2 J(\mathbf{x}_k) ,$$

is the Hessian matrix

However, unless the function $J(\mathbf{x})$ can be approximated reasonably well locally around \mathbf{x}_0 as a quadratic function there is no guarantee that $J(\mathbf{x}_{k+1}) \leq J(\mathbf{x}_k)$ where $\mathbf{x}_{k+1} = \mathbf{x}_k + \mathbf{d}_k$. Should this happen, we solve the line-search sub-problem

$$\min_{\gamma} \{J(\mathbf{x}_k + \gamma \mathbf{d}_k)\} ,$$

with $0 < \gamma < 1$. This line-search sub-problem has a local minima for some γ within the bounds $0 \leq \gamma < 1$ provided \mathbf{d}_k is a direction of descent. For \mathbf{d}_k to be a direction of descent requires

$$\nabla J(\mathbf{x}_k)^T \cdot \mathbf{d}_k < 0 . \quad (4.3)$$

From

$$\nabla J(\mathbf{x}_k)^T \cdot \mathbf{d}_k = -\nabla J(\mathbf{x}_k)^T \mathbf{H}_k^{-1} \nabla J(\mathbf{x}_k) ,$$

we see that

$$\nabla J(\mathbf{x}_k)^T \cdot \mathbf{d}_k < 0 , \quad (4.4)$$

is indeed fulfilled, provided \mathbf{H}_k^{-1} is positive definite.

At the minimum of its quadratic approximation $J(x)$ has the value

$$\begin{aligned} J(\mathbf{x}) &\approx J(\mathbf{x}_k) + \nabla J(\mathbf{x}_k) \Delta \mathbf{x} + \frac{1}{2} \Delta \mathbf{x}^T \mathbf{H}_k \Delta \mathbf{x} \\ &= J(\mathbf{x}_k) - \nabla J(\mathbf{x}_k) (\mathbf{H}_k)^{-1} \nabla J(\mathbf{x}_k) + \frac{1}{2} ((\mathbf{H}_k)^{-1} \nabla J(\mathbf{x}_k))^T \mathbf{H}_k (\mathbf{H}_k)^{-1} \nabla J(\mathbf{x}_k) \\ &= J(\mathbf{x}_k) - \frac{1}{2} \nabla J(\mathbf{x}_k) (\mathbf{H}_k)^{-1} \nabla J(\mathbf{x}_k) . \end{aligned}$$

This motivates the definition of the *Newton decrement* D_k as

$$D_k := \sqrt{\nabla J(\mathbf{x}_k) (\mathbf{H}_k)^{-1} \nabla J(\mathbf{x}_k)} ,$$

and $D_k^2/2$ is an approximate bound on the sub-optimality gap at iteration k . Having solved the Newton system, i.e. $\mathbf{d}_k = -(\mathbf{H}_k)^{-1} \nabla J(\mathbf{x}_k)$, we can calculate the Newton increment as

$$D_k^2 = -\nabla J(\mathbf{x}_k) \cdot \mathbf{d}_k.$$

Positive definiteness of $\nabla^2 J$ implies $D > 0$. We can also write the Newton decrement as

$$\begin{aligned} D &= \sqrt{\nabla J(\mathbf{x}_k)^T (\mathbf{H}_k)^{-1} \nabla J(\mathbf{x}_k)} \\ &= (\nabla J^T \mathbf{H}^{-T} \mathbf{H}^T \mathbf{H}^{-1} \nabla J) \\ &= ((\nabla \mathbf{H}^{-1} \nabla J)^T \mathbf{H}^T \mathbf{H}^{-1} \nabla J) \\ &= (\mathbf{d}^T \mathbf{H} \mathbf{d})^{1/2} \\ &= \|\mathbf{d}\|_{\mathbf{H}} \end{aligned}$$

showing that the Newton decrement is the norm of the Newton step in the Hessian norm. The line search problem is finding γ so that

$$\begin{aligned} \frac{d}{d\gamma} J(\mathbf{x} + \gamma \mathbf{d}) &= \nabla J(\mathbf{x}) \cdot \mathbf{d} \\ &= -\nabla J(\mathbf{x}) (\mathbf{H})^{-1} \nabla J(\mathbf{x}) \\ &= -D^2 . \end{aligned}$$

Again we see that if \mathbf{H} is positive definite, the slope at $\gamma = 0$ is negative.

For a self-adjoint problem the Newton's increment is a natural candidate for a stopping criterion, i.e. quit iteration if $D^2/2 \leq \epsilon$, where ϵ is some prescribed sub-optimality tolerance.

4.3 Non-linear non-self-adjoint problem

For a non-self-adjoint differential operator no (scalar) cost function can be defined in a similar way as for the self-adjoint case.

Now the Newton-Raphson system is

$$\mathbf{K} \mathbf{d} = -\mathbf{R} ,$$

where

$$\mathbf{K} = \frac{\partial \mathbf{R}}{\partial \mathbf{d}} ,$$

is the Jakobian. We can also write this as

$$R_{p,q} d_q = -R_p .$$

The vector \mathbf{R} are the nodal residuals and \mathbf{d} the increments during each NR iteration. Provided the system converges, both approach zeros as the iteration progresses. In FE, common convergence criteria are based on

$\ \mathbf{R}\ $	Force Residuals
$\ \mathbf{d}\ $	Displacements
$-\mathbf{R} \cdot \mathbf{d}$	Work Residuals

For self-adjoint problem where $\mathbf{R} = \nabla J$ and $\mathbf{K} = \mathbf{H}$, the work and the Newton decrement criteria

$$\begin{aligned} D^2 &= -\mathbf{R} \cdot \mathbf{d} \\ &= \mathbf{R} \cdot \mathbf{K}^{-1} \mathbf{R} \\ &= \nabla J \cdot \mathbf{H}^{-1} \nabla J \\ &\geq 0 \end{aligned}$$

are identical. However, for a non-self adjoint problem D^2 can be negative as well as positive. Instead of minimising D^2 we find the solution where the increment, \mathbf{d} is normal to the residual force \mathbf{R} , i.e. we minimise

$$D^2 = |\mathbf{R} \cdot \mathbf{d}| .$$

This corresponds to a minimum in the work function, for example because either force and/or displacement increments are small, if the force increments are orthogonal to displacement increments.

4.4 Constrained self-adjoint problem

Again if the problem is self-adjoint there exist a scalar function J such that $\nabla J = \mathbf{R}$ and $H = \nabla^2 J$. Now consider the constraint optimisation problem

$$\begin{aligned} \min_{\mathbf{x}} \quad & J(\mathbf{x}) \\ \text{s.t.} \quad & L\mathbf{x} = \mathbf{c} \end{aligned}$$

where $H \in \mathbb{R}^{n \times n}$, $L \in \mathbb{R}^{p \times n}$, $\mathbf{x} \in \mathbb{R}^n$ and $\mathbf{c} \in \mathbb{R}^p$,

A solution \mathbf{x}^* is optimal if and only if there exist a $\boldsymbol{\lambda}$ such that

$$\begin{aligned} \nabla J(\mathbf{x}^*) + L^T \boldsymbol{\lambda} &= \mathbf{0} \\ L\mathbf{x}^* &= \mathbf{c} \end{aligned}$$

where $\mathbf{R} = \nabla J$ (Boyd and Vandenberghe, 2004). Second-order expansion

$$\begin{aligned} \nabla J(\mathbf{x} + \Delta\mathbf{x}) + L^T \boldsymbol{\lambda} &\approx \nabla J(\mathbf{x}) + \nabla^2 J \Delta\mathbf{x} + L^T (\boldsymbol{\lambda} + \Delta\boldsymbol{\lambda}) = 0 \\ L(\mathbf{x} + \Delta\mathbf{x}) &= \mathbf{c} \end{aligned}$$

and solving for the minimum of the quadratic term, gives the KKT system

$$\left[\begin{array}{cc} H & L^T \\ L & 0 \end{array} \right] \left[\begin{array}{c} \Delta\mathbf{x} \\ \Delta\boldsymbol{\lambda} \end{array} \right] = - \left[\begin{array}{c} \mathbf{R}(\mathbf{x}_0) + L^T \boldsymbol{\lambda}_0 \\ L\mathbf{x}_0 - \mathbf{c} \end{array} \right] \quad (4.5)$$

where $H = \nabla^2 J$ is the Hessian matrix. The $\Delta\mathbf{x}$ and $\Delta\boldsymbol{\lambda}$ are referred to as the primal and the dual steps, respectively. The quantity

$$\|\mathbf{R}(\mathbf{x}_0) + L^T \boldsymbol{\lambda}_0\|$$

is sometimes referred to as *first-order optimality measure*.

The matrix on the left-hand side of (4.5) is the gradient of the right hand side with respect to \mathbf{x} and $\boldsymbol{\lambda}$. That is, if we define

$$\tilde{H} := \left[\begin{array}{cc} H & L^T \\ L & 0 \end{array} \right] \quad (4.6)$$

and

$$\tilde{\mathbf{x}} := \left[\begin{array}{c} \mathbf{x} \\ \boldsymbol{\lambda} \end{array} \right] \quad (4.7)$$

and

$$\tilde{\mathbf{R}} := \left[\begin{array}{c} \mathbf{R}(\mathbf{x}_0) + L^T \boldsymbol{\lambda}_0 \\ L\mathbf{x}_0 - \mathbf{c} \end{array} \right] \quad (4.8)$$

then

$$\tilde{H} = \nabla_{\tilde{\mathbf{x}}} \tilde{\mathbf{R}} .$$

We also have

$$H = \nabla_{\mathbf{x}} \mathbf{R} .$$

The corresponding quadratic model

$$Q = \tilde{\mathbf{x}}^T \cdot \tilde{\mathbf{R}} + \frac{1}{2} \tilde{\mathbf{x}} \cdot (\tilde{H} \tilde{\mathbf{x}})$$

is

$$Q(\Delta\mathbf{x}, \Delta\boldsymbol{\lambda}) = (\mathbf{R}_0 + L^T \boldsymbol{\lambda}_0)^T \cdot \Delta\mathbf{x} + (L\mathbf{x}_0 - \mathbf{c})^T \cdot \Delta\boldsymbol{\lambda} \quad (4.9)$$

$$+ \frac{1}{2} \Delta\mathbf{x}^T (H\Delta\mathbf{x} + L^T \Delta\boldsymbol{\lambda}) + \frac{1}{2} \Delta\boldsymbol{\lambda}^T L \Delta\mathbf{x}_0 \quad (4.10)$$

Note that since the constraints are linear, they are fulfilled exactly at each iteration.¹ The second equation, i.e. the condition $L\Delta\mathbf{x} = \mathbf{c} - L\mathbf{x}_0$ ensures that the Newton step $\Delta\mathbf{x}$ is always a feasible direction. It follows that if \mathbf{x}_0 is a feasible point, i.e. if $L(\mathbf{x}_0) = \mathbf{c}$, and if $\Delta\mathbf{x}$ is in the null space of L , i.e. $L\Delta\mathbf{x} = \mathbf{0}$, then every point $\mathbf{x}_0 + \gamma\Delta\mathbf{x}$ for any γ is also a feasible point because

$$\begin{aligned} L(\mathbf{x}_0 + \gamma\Delta\mathbf{x}) &= L(\mathbf{x}_0) + L\gamma\Delta\mathbf{x} \\ &= \mathbf{c} + \gamma L\Delta\mathbf{x} \\ &= \mathbf{c}. \end{aligned}$$

Hence, when conducting a line search the constraints are automatically fulfilled *provided the starting point for the NR iteration does so*, and there is no need to re-solve the KKT system during the line search. Also, even if the starting point does not fulfil the constraints, the constraints will still be fulfilled *once a full Newton step has been taken at least once during the iteration*.

When the constraints are linear, we can ensure that they are fulfilled exactly at each iteration, and therefore for the final solution, even if the initial starting point does not and we never take a full Newton step, by simply not solving for the Lagrange multiplier, $\boldsymbol{\lambda}$, not in an incremental form as done in (4.5), but rather as

$$\begin{bmatrix} H & L^T \\ L & 0 \end{bmatrix} \begin{bmatrix} \Delta\mathbf{x} \\ \boldsymbol{\lambda} \end{bmatrix} = - \begin{bmatrix} \mathbf{R}(\mathbf{x}_0) \\ L\mathbf{x}_0 - \mathbf{c} \end{bmatrix}. \quad (4.11)$$

If the constraints are non-linear, the solution will, in general, not fulfil the constraints unless at least one of the following is true: 1) the iteration converges, 2) a full Newton step is taken at least once during the iteration, or 3) the starting point of the iteration fulfils the constraints, i.e. the initial iterate is a feasible solution. In $\text{U}\ddot{\text{a}}$ it is always ensured that the initial iterate is feasible.

The Newton step, \mathbf{d} ,

$$\mathbf{d} = \Delta\mathbf{x}$$

is defined as a solution $\Delta\mathbf{x}$ to the two KKT equations

$$\begin{aligned} H\Delta\mathbf{x} + L^T \boldsymbol{\lambda} &= -\mathbf{R}(\mathbf{x}_0) \\ L\Delta\mathbf{x} &= \mathbf{0} \end{aligned}$$

or

$$\begin{aligned} \Delta\mathbf{x} &= -H^{-1}(\mathbf{R} + L^T(\boldsymbol{\lambda}_0 + \Delta\boldsymbol{\lambda})) \\ &= -H^{-1}(\nabla J + L^T \boldsymbol{\lambda}). \end{aligned}$$

Taking the full Newton step, the reduction in J at each iteration is therefore

$$\begin{aligned} J(x) - J(\mathbf{x}_k) &= \nabla J(\mathbf{x}_k)^T \Delta\mathbf{x} + \frac{1}{2} \Delta\mathbf{x}^T H_k \Delta\mathbf{x} \\ &= \nabla J^T H^{-1}(-\nabla J - L^T \boldsymbol{\lambda}) + \frac{1}{2} (H^{-1}(-\nabla J - L^T \boldsymbol{\lambda}))^T H_k H^{-1}(-\nabla J - L^T \boldsymbol{\lambda}) \\ &= \nabla J^T H^{-1}(-\nabla J - L^T \boldsymbol{\lambda}) + \frac{1}{2} (-\nabla J - L^T \boldsymbol{\lambda})^T H^{-1}(-\nabla J - L^T \boldsymbol{\lambda}) \\ &= -\nabla J^T H^{-1} \nabla J - \nabla J H^{-1} L^T \boldsymbol{\lambda} + \frac{1}{2} (-\nabla J - L^T \boldsymbol{\lambda})^T H^{-1}(-\nabla J - L^T \boldsymbol{\lambda}) \\ &= -\nabla J^T H^{-1} \nabla J - \nabla J H^{-1} L^T \boldsymbol{\lambda} \\ &\quad + \frac{1}{2} (\nabla J^T H^{-1} \nabla J + (L^T \boldsymbol{\lambda})^T H^{-1} L^T \boldsymbol{\lambda} + \nabla J H^{-1} L^T \boldsymbol{\lambda} + (L^T \boldsymbol{\lambda})^T H^{-1} \nabla J) \\ &= -\frac{1}{2} (\nabla J^T + (L^T \boldsymbol{\lambda})^T) H^{-1} (\nabla J^T + L^T \boldsymbol{\lambda}) \\ &\quad - \nabla J H^{-1} L^T \boldsymbol{\lambda} + \frac{1}{2} (\nabla J^T H^{-1} L^T \boldsymbol{\lambda} + (L^T \boldsymbol{\lambda})^T H^{-1} \nabla J) \end{aligned}$$

¹We could, in fact, start the iteration with $\mathbf{x} = \mathbf{x}_0$ where \mathbf{x}_0 is a particular solution of $L\mathbf{x}_0 = \mathbf{c}$ and then insist that any addition to x is in the null-space of L , i.e. $L\Delta\mathbf{x} = \mathbf{0}$.

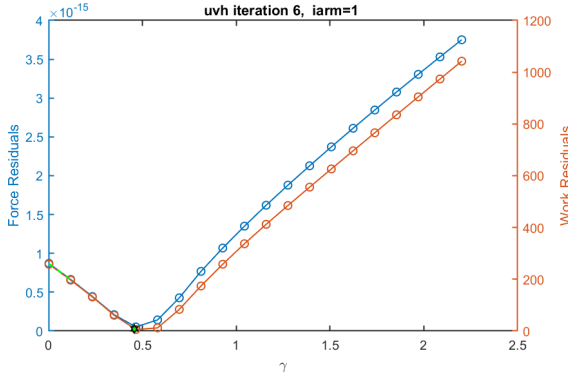


Figure 4.1: An example of the variation of r_{Force}^2 and r_{Work}^2 as a function of γ during a line-search. Here the backtracking algorithm selects $\gamma \approx 1/2$. For clarity, the circles show some additional function values not calculated during the line search.

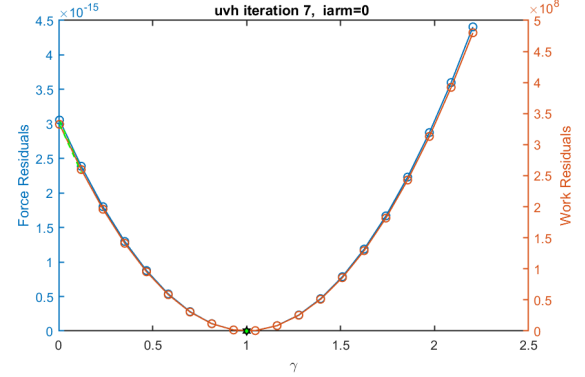


Figure 4.2: Another example of the variation of r_{Force}^2 and r_{Work}^2 as a function of γ . Here the full Newton step ($\gamma = 1$) was accepted. Also shown are the slopes at $\gamma = 0$ calculated as $2r$ at $\gamma = 0$.

The last line equals zero if H symmetrical, hence as in the unconstrained case the Newton decrement is a measure of sub-optimality, i.e.

$$\begin{aligned} J(x) - J(\mathbf{x}_k) &= -\frac{1}{2}(\nabla J^T + (L^T \boldsymbol{\lambda})^T) H^{-1}(\nabla J + L^T \boldsymbol{\lambda}) \\ &= -D^2/2 \end{aligned}$$

where Newton decrement D is

$$\begin{aligned} D^2 &= (\nabla J + (L^T \boldsymbol{\lambda})^T) \cdot \Delta \mathbf{x} \\ &= (\nabla J + L^T \boldsymbol{\lambda})^T H^{-1}(\nabla J + L^T \boldsymbol{\lambda}) \\ &= (\nabla J + L^T \boldsymbol{\lambda})^T H^{-1} H H^{-1}(\nabla J + L^T \boldsymbol{\lambda}) \\ &= (\nabla J + L^T \boldsymbol{\lambda})^T H^{-T} H H^{-1}(\nabla J + L^T \boldsymbol{\lambda}) \\ &= (H^{-1}(\nabla J + L^T \boldsymbol{\lambda}))^T H H^{-1}(\nabla J + L^T \boldsymbol{\lambda}) \\ &= \mathbf{d}^T H \mathbf{d} \end{aligned}$$

When conducting a line search we find, similarly to the unconstrained case, that

$$\begin{aligned} \frac{d}{d\gamma} J(\mathbf{x} + \gamma \mathbf{d}) &= \nabla J(\mathbf{x}) \cdot \mathbf{d} \\ &= \mathbf{R}^T \cdot \mathbf{d} \\ &= -(H \mathbf{d} + L^T \boldsymbol{\lambda})^T \cdot \mathbf{d} \\ &= -\mathbf{d}^T \cdot H^T \mathbf{d} - \boldsymbol{\lambda}^T L \cdot \mathbf{d} \\ &= -\mathbf{d}^T \cdot H^T \mathbf{d} - \boldsymbol{\lambda}^T (\mathbf{c} - L \mathbf{x}_0) \\ &= -D^2 + (L \mathbf{x}_0 - \mathbf{c})^T \cdot \boldsymbol{\lambda}. \end{aligned}$$

Thus if H is symmetrical and positive definite, and furthermore \mathbf{x}_0 a feasible point, then the slope at $\gamma = 0$ is negative. However, the Newton direction at an infeasible point is not necessarily a decent direction for J . This point, and other similar are also discussed in [Boyd and Vandenberghe \(2004\)](#).

4.5 Convergence criteria

If the Newton-Raphson method converges then $\Delta \mathbf{x} \rightarrow 0$ and $\Delta \boldsymbol{\lambda} \rightarrow 0$. This suggests defining a convergence criteria in terms of the norm of $\Delta \mathbf{x}$ and $\Delta \boldsymbol{\lambda}$, i.e. in terms of the size of the update to the solution. Another convergence criteria is the norm of the force residuals \mathbf{R} or the size of the Newton increment $\mathbf{R} \cdot \mathbf{d}$ (work residuals). The primary convergence criteria in \tilde{U}_{a} is the size of the force residuals. It is

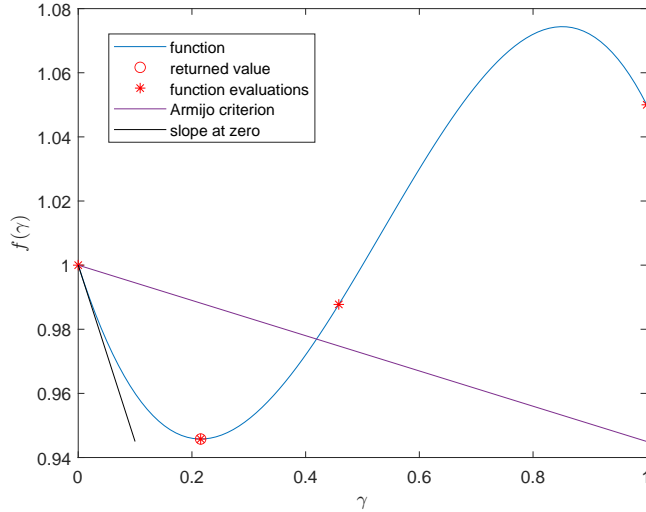


Figure 4.3: An simple backtracking example.

possibly to define a convergence criteria based on force residuals, work residuals and increments, and some combinations thereof. Defining a convergence criteria in terms of increments can be quite problematic as smallness of increments does not imply convergence.

4.5.1 Force residuals

Writing the residual vector \mathbf{R} as

$$\mathbf{R} = \mathbf{T}(\mathbf{x}) - \mathbf{F},$$

where \mathbf{T} and \mathbf{F} are the internal and the external nodal forces, respectively facilitates the definition of a normalised *force residuals* as

$$r^2 := \frac{(\mathbf{R} + L^T \boldsymbol{\lambda})^T (\mathbf{R} + L^T \boldsymbol{\lambda}) + (\mathbf{c} - L\mathbf{x})^T (\mathbf{c} - L\mathbf{x})}{\mathbf{F}^T \mathbf{F}} \quad (4.12)$$

$$= \frac{(\mathbf{R} + L^T \boldsymbol{\lambda})^T (\mathbf{R} + L^T \boldsymbol{\lambda})}{\mathbf{F}^T \mathbf{F}}, \quad (4.13)$$

where in (4.13) it has been assumed that $\mathbf{c} - L\mathbf{x} = \mathbf{0}$ at each iteration. If the Newton step is started from a feasible point, then the Newton direction is a decent direction of (4.13). However if the point is infeasible, (4.12) must be used.

If at some iteration a full Newton step can be taken, the iterate becomes feasible and as all subsequent steps are in the null space of L , all following iterates will be feasible as well.

At start of an iteration using as start values $\mathbf{x} = \mathbf{0}$ and $\boldsymbol{\lambda} = 0$, the internal forces are all zero, $\mathbf{T} = \mathbf{0}$, and hence $r = 1$. The iteration is continued until r drops below a prescribed tolerance. By default this tolerance is

$$r^2 < 10^{-15}.$$

4.5.2 Work residuals

The *work residuals* are defined in terms of the Newton decrement as

$$r := -(\mathbf{R} + L^T \boldsymbol{\lambda})^T \cdot \mathbf{d}$$

where \mathbf{d} is the (full) Newton step.

$$\mathbf{d} = -H^{-1}(\mathbf{R} + L^T \boldsymbol{\lambda}).$$

The actual minimisation is based on the value r^2 which is always positive.

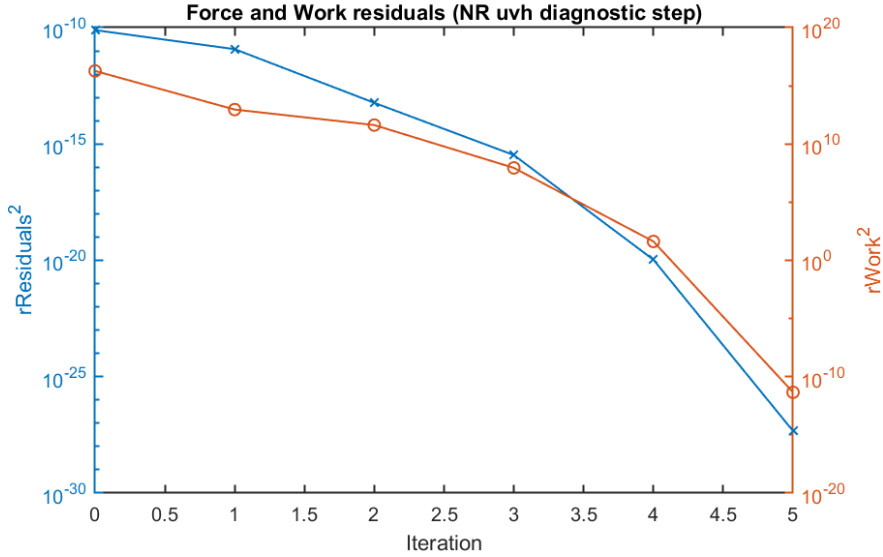


Figure 4.4: An example of r_{Force}^2 and r_{Work}^2 as a function of Newton-Raphson iteration number.

4.5.3 Increments

Using increments as a convergence criteria is not recommended and in $\tilde{U}\alpha$ not implemented for all cases. Where implemented the increments are defined as

$$\Delta = \sqrt{\frac{1}{2\mathcal{A}} \int \left(\frac{\Delta x}{|x| + x_0} \right)^2 d\mathcal{A}},$$

where

$$\mathcal{A} = \int d\mathcal{A},$$

and x_0 is a regularisation parameter. So for example when solving for velocities the size of the velocity increments is defined as

$$\Delta_{uv} = \sqrt{\frac{1}{2\mathcal{A}} \int \left(\left(\frac{\Delta u}{|u| + u_0} \right)^2 + \left(\frac{\Delta v}{|v| + u_0} \right)^2 \right) d\mathcal{A}}.$$

where u_0 is some small constant with the dimension velocity.

4.6 Summary of convergence criteria

Ignoring constraints and possible additional normalisation, the three convergence criteria are:

$$\begin{aligned} r_{\text{Force}}^2 &:= \mathbf{R}^T \cdot \mathbf{R} \\ r_{\text{Work}}^2 &:= (\mathbf{R}^T \cdot \mathbf{d})^2 \\ &= (\mathbf{R}^T \cdot H^{-1} \mathbf{R})^2 \\ r_{\text{Displacements}}^2 &:= \mathbf{d} \cdot \mathbf{d} \end{aligned}$$

Note that since H is not guaranteed to be positive definite, $(\mathbf{R}^T \cdot H^{-1} \mathbf{R})$ is not necessarily positive and we can not define a corresponding inner product as we could in the self-adjoint positive-definite case considered above. The work criteria is the only one independent of coordinates (affine invariance).

The Newton step is a direction of decent if Eq. (4.3) is fulfilled for those cost functions. We have already seen that the Newton step is a direction of decent if the problem is self-adjoint and positive

definite (see Eq. 4.4). For J_{Force} we find

$$\begin{aligned}\nabla r_{\text{Force}}^2 \cdot \mathbf{d} &= (R_p R_p)_{,q} d_q \\ &= (R_p R_{p,q} + R_{p,q} R_p) d_q \\ &= 2R_p R_{p,q} d_q \\ &= -2R_p R_p \\ &= -2r_{\text{Force}}^2 \\ &\leq 0,\end{aligned}$$

or in vector notation as

$$\begin{aligned}\nabla r_{\text{Force}}^2 \cdot \mathbf{d} &= \nabla(\mathbf{R}^T \cdot \mathbf{R}) \cdot \mathbf{d} \\ &= 2\mathbf{R}^T \cdot (\nabla \mathbf{R} \mathbf{d}) \\ &= 2\mathbf{R}^T \cdot (H\mathbf{d}) \\ &= -2\mathbf{R}^T \cdot \mathbf{R} \\ &= -2r_{\text{Force}}^2\end{aligned}$$

and similarly for J_{Work}

$$\begin{aligned}\nabla r_{\text{Work}}^2 \cdot \mathbf{d} &= (R_p d_p R_s d_s)_{,q} d_q \\ &= (R_{p,q} d_p R_s d_s + R_p d_p R_{s,q} d_s) d_q \\ &= (R_{p,q} d_p R_s d_s + R_s d_s R_{p,q} d_p) d_q \\ &= 2R_{p,q} d_p R_s d_s d_q \\ &= 2R_{p,q} d_q d_p R_s d_s \\ &= -2R_p d_p R_s d_s \\ &= -2r_{\text{Work}}^2 \\ &\leq 0,\end{aligned}$$

so the Newton step is a direction of descent for both r_{Force}^2 and r_{Work}^2 . Same calculations show that when conducting a line search, the slopes at $\gamma = 0$ are

$$\begin{aligned}\frac{d}{d\gamma} r_{\text{Force}}^2(\mathbf{x} + \gamma\mathbf{d}) \Big|_{\gamma=0} &= \nabla r_{\text{Force}}^2 \cdot \mathbf{d} \\ &= -2r_{\text{Force}}^2(\mathbf{x}),\end{aligned}$$

and

$$\begin{aligned}\frac{d}{d\gamma} r_{\text{Work}}^2(\mathbf{x} + \gamma\mathbf{d}) \Big|_{\gamma=0} &= \nabla r_{\text{Work}}^2 \cdot \mathbf{d} \\ &= -2r_{\text{Work}}^2(\mathbf{x}).\end{aligned}$$

In \hat{U} a the letter r is used for these costs functions to avoid confusion with the inverse cost function denoted with J . The cost functions can also be written as inner products as

$$\begin{aligned}r_{\text{Force}}^2 &= r_{\text{Force}}^2 = \mathbf{R}^T \mathbf{R} = \langle \mathbf{R} | \mathbf{R} \rangle_{l^2} \\ r_{\text{Work}}^2 &= r_{\text{Work}}^2 = \mathbf{R}^T H^{-1} \mathbf{R} = \langle \mathbf{R} | \mathbf{R} \rangle_{H^{-1}} \\ &= \mathbf{R}^T H^{-T} H H^{-1} \mathbf{R} = \langle \mathbf{d} | \mathbf{d} \rangle_H \quad (\text{if symmetric and positive definite}) \\ r_{\text{Displacements}}^2 &= r_{\text{Displacements}}^2 = \langle \mathbf{d} | \mathbf{d} \rangle_{L^2}\end{aligned}$$

4.7 Minimising the norm of the residuals

The cost function is defined as the square of the residuals, i.e.

$$r^2 := \|\mathbf{R}\|_2^2 = \mathbf{R}^T \cdot \mathbf{R} = (\nabla J)^T \cdot \nabla J$$

and we wish to minimise r^2 . This done iteratively and we aim to find an update $\Delta\mathbf{x}$ to our current estimate \mathbf{x}_0 such that

$$r^2(\mathbf{x}_0 + \Delta\mathbf{x}) < r^2(\mathbf{x}_0) .$$

We do this by iteratively solving a linearised minimisation problem around \mathbf{x}_0

$$\min_{\Delta\mathbf{x}} r^2(\mathbf{x} + \Delta\mathbf{x})$$

as a function of $\Delta\mathbf{x}$. Taking the step $\Delta\mathbf{x}$ from \mathbf{x}_0 to $\mathbf{x} + \Delta\mathbf{x}$ the variation in r^2 is to first order in $\Delta\mathbf{x}$

$$\begin{aligned} r^2(\mathbf{x}_0 + \Delta\mathbf{x}) &= (\mathbf{R}(\mathbf{x}_0 + \Delta\mathbf{x}))^T \cdot (\mathbf{R}(\mathbf{x}_0 + \Delta\mathbf{x})) \\ &\approx (\mathbf{R}_0 + \nabla\mathbf{R}\Delta\mathbf{x})^T \cdot (\mathbf{R}_0 + \nabla\mathbf{R}\Delta\mathbf{x}) \\ &= (\mathbf{R}_0 + H\Delta\mathbf{x})^T \cdot (\mathbf{R}_0 + H\Delta\mathbf{x}) \\ &= \mathbf{R}_0^T \cdot \mathbf{R}_0^T + (\Delta\mathbf{x}^T \cdot H^T \mathbf{R}_0 + \mathbf{R}_0^T \cdot H\Delta\mathbf{x}) + \Delta\mathbf{x}^T \cdot H^T H\Delta\mathbf{x} \\ &= \mathbf{R}_0^T \cdot \mathbf{R}_0^T + 2\mathbf{R}_0^T \cdot H\Delta\mathbf{x} + \Delta\mathbf{x}^T \cdot H^T H\Delta\mathbf{x} \end{aligned} \quad (4.14)$$

or

$$r^2(\mathbf{x}_0 + \Delta\mathbf{x}) \approx r_0^2 + 2\mathbf{R}_0^T \cdot H\Delta\mathbf{x} + \Delta\mathbf{x}^T \cdot H^T H\Delta\mathbf{x}$$

where

$$H = \nabla\mathbf{R}_0$$

and, where we have observed the identity

$$\begin{aligned} \Delta\mathbf{x}^T \cdot H^T \mathbf{R}_0 &= (H^T \mathbf{R})^T \cdot (\Delta\mathbf{x}_0^T)^T \\ &= \mathbf{R}_0^T \nabla\mathbf{R}_0 \cdot \Delta\mathbf{x} . \end{aligned}$$

Note that the linearised minimisation problem (see Eq. 4.14) can be written as

$$\min_{\Delta\mathbf{x}} = \|\mathbf{R}_0 + \nabla\mathbf{R}_0 \Delta\mathbf{x}\|_2^2 ,$$

which is a type of a least-squares problem, subject to some possible additional constraints on the solution vector $\Delta\mathbf{x}$. The quadratic approximation, $Q(\Delta\mathbf{x})$, to r^2 is

$$Q(\Delta\mathbf{x}) = 2\mathbf{R}_0^T \cdot \nabla\mathbf{R}_0 \Delta\mathbf{x} + \Delta\mathbf{x}^T \cdot (\nabla\mathbf{R}_0)^T \nabla\mathbf{R}_0 \Delta\mathbf{x} \quad (4.15)$$

that is

$$r^2(\mathbf{x}_0 + \Delta\mathbf{x}) \approx r_0^2 + Q(\Delta\mathbf{x})$$

A general quadratic minimisation problem is on the form

$$\min_{\mathbf{x}} \frac{1}{2} \mathbf{x}^T B \mathbf{x} + \mathbf{g}^T \mathbf{x} \quad (4.16)$$

and by comparing Eq. (4.15) and (4.16) we see that here

$$B = 2\gamma^2 (\nabla\mathbf{R}_0)^T \nabla\mathbf{R}_0$$

and

$$\mathbf{g} = 2\gamma (\nabla\mathbf{R}_0)^T \mathbf{R}_0$$

If this problem is unconstrained, the solution to is obviously the the full Newton step (see below), however if we limit the step size $\|\Delta\mathbf{x}\| < \Delta$ as, for example, done in trust-region algorithms, the solution is not this simple.

Unconstrained minimisation of $Q(\Delta\mathbf{x})$, as given by Eq. (4.15) by setting the gradient to zero, leads to

$$\nabla Q = 2H^T \mathbf{R}_0 + 2H^T H \Delta\mathbf{x} = 0$$

or

$$H^T H \Delta\mathbf{x} = -H^T \mathbf{R}_0$$

or simply

$$H \Delta\mathbf{x} = -\mathbf{R}_0 \quad (4.17)$$

provided H^{-T} exists, which is the (full) Newton step. Thus, the two unconstrained problems

$$\begin{aligned} H\Delta\mathbf{x} &= -\mathbf{R}_0 \\ 2H^T H\Delta\mathbf{x} &= -2H^T \mathbf{R}_0 \end{aligned}$$

are mathematically identical.

Minimising Q subject to the linear constraints $L\mathbf{x} - \mathbf{c} = 0$ gives the system

$$\mathcal{L} = Q(\Delta\mathbf{x}) + \boldsymbol{\lambda}^T(L(\mathbf{x}_0 + \Delta\mathbf{x}) - \mathbf{c})$$

which we minimise with respect to $\Delta\mathbf{x}$ and $\boldsymbol{\lambda}$ giving

$$\begin{aligned} 2H^T \mathbf{R}_0 + 2H^T H\Delta\mathbf{x} + (\boldsymbol{\lambda} + \Delta\boldsymbol{\lambda})^T L &= 0 \\ L\Delta\mathbf{x} &= -(L\mathbf{x}_0 - \mathbf{c}) \end{aligned}$$

that is

$$\begin{bmatrix} 2H^T H & L^T \\ L & 0 \end{bmatrix} \begin{bmatrix} \Delta\mathbf{x} \\ \Delta\boldsymbol{\lambda} \end{bmatrix} = -\begin{bmatrix} 2H^T \mathbf{R}(\mathbf{x}_0) + L^T \boldsymbol{\lambda}_0 \\ L\mathbf{x}_0 - \mathbf{c} \end{bmatrix}. \quad (4.18)$$

We can pre-multiply (4.18) on both sides with

$$\begin{bmatrix} \frac{1}{2}H^{-T} & 0_{np} \\ 0_{pn} & 1_{pp} \end{bmatrix}$$

where $H \in \mathbb{R}^{n \times n}$, $L \in \mathbb{R}^{p \times n}$, $\mathbf{x} \in \mathbb{R}^n$ and $\mathbf{c} \in \mathbb{R}^p$, arriving at

$$\begin{bmatrix} H & \frac{1}{2}H^{-T}L^T \\ L & 0 \end{bmatrix} \begin{bmatrix} \Delta\mathbf{x} \\ \Delta\boldsymbol{\lambda} \end{bmatrix} = -\begin{bmatrix} \mathbf{R}(\mathbf{x}_0) + \frac{1}{2}H^{-T}L^T\boldsymbol{\lambda}_0 \\ L\mathbf{x}_0 - \mathbf{c} \end{bmatrix}. \quad (4.19)$$

This (constrained) system is not identical to the previous Newton system (4.5), which is

$$\begin{bmatrix} H & L^T \\ L & 0 \end{bmatrix} \begin{bmatrix} \Delta\mathbf{x} \\ \Delta\boldsymbol{\lambda} \end{bmatrix} = -\begin{bmatrix} \mathbf{R}(\mathbf{x}_0) + L^T\boldsymbol{\lambda}_0 \\ L\mathbf{x}_0 - \mathbf{c} \end{bmatrix} \quad (4.5)$$

even when H^{-T} exists, unless all constraints are inactive and $\boldsymbol{\lambda} = \mathbf{0}$. However, it appears that this only affects the solution for $\boldsymbol{\lambda}$ and the systems can be made identical by redefining $\boldsymbol{\lambda}$ accordingly.

Line Searches

In a line search we minimise r^2 along some given direction \mathbf{d} , and write

$$\mathbf{x} = \mathbf{x}_0 + \gamma\mathbf{d}$$

where γ is a new step-size parameter. Assuming the cost function r^2 is defined as

$$R^2 = \mathbf{R}^T \cdot \mathbf{R} \quad (4.20)$$

and we have

$$H = \nabla \mathbf{R} \quad (4.21)$$

we, thus, now solve the minimisation problem

$$\min_{\gamma} r^2(\mathbf{x}_0 + \gamma\mathbf{d})$$

for \mathbf{d} fixed, were

$$R^2(\mathbf{x}_0 + \gamma\mathbf{d}) \approx R_0^2 + 2\gamma\mathbf{R}_0^T \cdot H\mathbf{d} + \gamma^2\mathbf{d}^T \cdot H^T H\mathbf{d}.$$

In general, neither the search direction \mathbf{d} nor the step size γ need to be specified, and this function could be minimise with respect to both the (scalar) step size γ , and the search direction \mathbf{d} , e.g.

$$\min_{\gamma, \mathbf{d}} R^2(\mathbf{x}_0 + \gamma\mathbf{d})$$

subject to, for example, $\gamma\|\mathbf{d}\| < \Delta$, where Δ is the trust-radius. However, in line-search algorithm we solve this minimisation problem with respect to γ alone.

The slope at $\gamma = 0$ is

$$\partial_\gamma R^2(\mathbf{x}_0) \Big|_{\gamma=0} = 2\mathbf{R}_0^T \cdot H\mathbf{d}. \quad (4.22)$$

And the minimum as a function of γ , for a given search direction \mathbf{d} , is found where

$$\mathbf{R}_0^T \cdot H\mathbf{d} + \gamma \mathbf{d}^T \cdot H^T H\mathbf{d} = 0$$

or at

$$\gamma = -\frac{\mathbf{R}_0^T \cdot H\mathbf{d}}{\mathbf{d}^T \cdot H^T H\mathbf{d}} \quad (4.23)$$

$$= -\frac{\mathbf{R}_0^T \cdot H\mathbf{d}}{\|H\mathbf{d}\|^2} \quad (4.24)$$

For the search direction \mathbf{d} to be a direction of descent, we require the slope to be negative and the step size positive. From (4.22) and (4.24) we see that the slope is guaranteed to be negative and the step size positive if, for example:

- we select the steepest descent direction with $\mathbf{d} = -\mathbf{R}_0$ provided that additionally H is positive definite,
- and for the Newton direction where $\mathbf{d} = -H^{-1}\mathbf{R}_0$.

There are many other options of selecting a search direction.

Eqs. (4.22) and (4.23) are general in the sense that they only depend on the linearised minimisation problem itself, and are valid for any search direction \mathbf{d} , and are also correct for constrained problems. The only assumptions made are that Eq. (4.20) defines the function to be minimised, and that relation (4.21) holds.

Cost function base on first-order optimality

The minimum of the cost function $R^2 := \|\mathbf{R}\|^2$ is likely to depend on the constraints and the slope in the search direction will not always be equal to zero at the min.

Alternative cost function is

$$r^2 = (2H^T \mathbf{R} + L^T \boldsymbol{\lambda})^T \cdot (2H^T \mathbf{R} + L^T \boldsymbol{\lambda}) + (L\mathbf{x} - \mathbf{c})^T \cdot (L\mathbf{x} - \mathbf{c}) \quad (4.25)$$

which is the square of the right-hand side of the system

$$\begin{bmatrix} 2H^T H & L^T \\ L & 0 \end{bmatrix} \begin{bmatrix} \Delta\mathbf{x} \\ \Delta\boldsymbol{\lambda} \end{bmatrix} = - \begin{bmatrix} 2H^T \mathbf{R}(\mathbf{x}_0) + L^T \boldsymbol{\lambda}_0 \\ L\mathbf{x}_0 - \mathbf{c} \end{bmatrix}. \quad (4.18)$$

To first order

$$\begin{aligned} r^2(x + \gamma\Delta\mathbf{x}, \boldsymbol{\lambda} + \gamma\Delta\boldsymbol{\lambda}) &= r_0^2 + 2\gamma(2H^T \mathbf{R} + L^T \boldsymbol{\lambda})^T(2H^T H \Delta\mathbf{x} + L^T \Delta\boldsymbol{\lambda}) + 2(L\mathbf{x} - \mathbf{c})L\gamma\Delta\mathbf{x} \\ &= r_0^2 - 2\gamma(2H^T \mathbf{R} + L^T \boldsymbol{\lambda})^T(2H^T \mathbf{R} + L^T \boldsymbol{\lambda}) + 2\gamma(L\mathbf{x} - \mathbf{c})^T \cdot (L\mathbf{x} - \mathbf{c}) \\ &= r_0^2 - 2\gamma r_0^2 \end{aligned}$$

where the change in H with x has been ignored, i.e. $H = H_0$. Ignoring the variation in H with respect to x does introduce an error, and the estimate for the slope at $\gamma = 0$ is no longer exact. This error is introduced here, because the cost function depends explicitly on H . This error is not, for example, introduced in the estimate (4.22).

Line search in Newton direction

In a Newton line search we solve the minimisation problem

$$\min_\gamma r^2(\mathbf{x} + \gamma\mathbf{d})$$

with

$$r^2 := \mathbf{R}^T \cdot \mathbf{R} = (\nabla J)^T \cdot \nabla J \quad (4.26)$$

and where \mathbf{d} is the Newton step

$$H\mathbf{d} = -\mathbf{R}_0 . \quad (4.27)$$

Proceeding as before (see page 90), we find

$$\begin{aligned} r^2(\mathbf{x}_0 + \Delta\mathbf{x}) &= (\mathbf{R}(\mathbf{x}_0 + \Delta\mathbf{x}))^T \cdot (\mathbf{R}(\mathbf{x}_0 + \Delta\mathbf{x})) \\ &\approx (\mathbf{R}_0 + \nabla\mathbf{R}\Delta\mathbf{x})^T \cdot (\mathbf{R}_0 + \nabla\mathbf{R}\Delta\mathbf{x}) \\ &= (\mathbf{R}_0 + H\Delta\mathbf{x})^T \cdot (\mathbf{R}_0 + H\Delta\mathbf{x}) \\ &= (\mathbf{R}_0 + H\gamma\mathbf{d})^T \cdot (\mathbf{R}_0 + H\gamma\mathbf{d}) \\ &= (\mathbf{R}_0 - \gamma\mathbf{R}_0)^T \cdot (\mathbf{R}_0 - \gamma\mathbf{R}_0) \\ &= (1 - 2\gamma + \gamma^2)\mathbf{R}_0^T \cdot \mathbf{R}_0 \\ &= (1 - 2\gamma + \gamma^2)r^2(\mathbf{x}_0) . \end{aligned}$$

The minimum is evidently found at $\gamma = 1$, and the slope of r^2 at $\gamma = 0$ is equal to $-2r_0^2$. Note that the minimum value of this quadratic approximation is always, by construction, $r^2 = 0$ at $\gamma = 1$. This holds when $H\mathbf{d} = -\mathbf{R}_0$, and will also hold for the solution of the KKT system in the more general constrained case, provided we then use the solution of the KKT system as the (feasible) search direction.

We could also have inserted $H\mathbf{d} = -\mathbf{R}_0$ into Eqs. (4.22) and (4.23) and arrived at the same answer.

Line search in the M modified steepest-descent direction

For the M -modified negative steepest-descent direction, we solve

$$M\mathbf{s} = -\mathbf{R} ,$$

where M is the mass matrix. The direction is therefore

$$\mathbf{s} = -M^{-1}\nabla J = -M^{-1}\mathbf{R} .$$

As before we minimise

$$\min_{\gamma} r^2(\mathbf{x} + \gamma\mathbf{s})$$

and the cost function is again the square of the residuals, i.e.

$$r^2 := \mathbf{R}^T \cdot \mathbf{R} = (\nabla J)^T \cdot \nabla J ,$$

but now $\mathbf{d} = \mathbf{s}$ where \mathbf{s} is the M-step

$$M\mathbf{s} = -\mathbf{R}_0$$

Proceeding as before (see page 90), but now taking the step $\Delta\mathbf{x} = \gamma\mathbf{s}$ from \mathbf{x}_0 the variation in r^2 is to first order in $\Delta\mathbf{x}$

$$\begin{aligned} r^2(\mathbf{x}_0 + \Delta\mathbf{x}) &= (\mathbf{R}(\mathbf{x}_0 + \Delta\mathbf{x}))^T \cdot (\mathbf{R}(\mathbf{x}_0 + \Delta\mathbf{x})) \\ &\approx (\mathbf{R}_0 + \nabla\mathbf{R}\Delta\mathbf{x})^T \cdot (\mathbf{R}_0 + \nabla\mathbf{R}\Delta\mathbf{x}) \\ &= (\mathbf{R}_0 + H\Delta\mathbf{x})^T \cdot (\mathbf{R}_0 + H\Delta\mathbf{x}) \\ &= (\mathbf{R}_0 + H\gamma\mathbf{s})^T \cdot (\mathbf{R}_0 + H\gamma\mathbf{s}) \\ &= \mathbf{R}_0^T \cdot \mathbf{R}_0^T - \gamma(\mathbf{s}^T \cdot H^T \mathbf{R}_0 + \mathbf{R}_0^T \cdot H\mathbf{s}) + \gamma^2\mathbf{s}^T \cdot H^T H\mathbf{s} \\ &= r_0^2 - 2\gamma\mathbf{R}_0^T \cdot H\mathbf{s} + \gamma^2\mathbf{s}^T \cdot H^T H\mathbf{s} \end{aligned}$$

or

$$r^2(\mathbf{x}_0 + \gamma\mathbf{s}) \approx r^2(\mathbf{x}_0) + \mathbf{s}^T \cdot B\mathbf{s}$$

where

$$B := \gamma^2 H^T H - \gamma((H^T \mathbf{R}_0)^T + H^T \mathbf{R}_0)$$

The slope at $\gamma = 0$ is

$$\begin{aligned} \partial_{\gamma} r^2|_{\gamma=0} &= -2\mathbf{R}_0^T \cdot H\mathbf{s} \\ &= -\mathbf{R}_0^T \cdot (M^{-1}H^T \mathbf{R}_0) + \mathbf{R}_0^T H M^{-1} \mathbf{R}_0 \\ &= -\mathbf{R}_0^T \cdot (M^{-1}H^T + H M^{-1}) \mathbf{R}_0 \\ &= -2\mathbf{R}_0^T H M^{-1} \mathbf{R}_0 \end{aligned}$$

which is same as Eq. (4.22), and thus negative in the search direction \mathbf{s} provided

$$HM^{-1} \succ 0 ,$$

and the minimum along this search direction is at

$$-\mathbf{s}^T \cdot H^T \mathbf{R} - \mathbf{R}^T \cdot H \mathbf{s} + 2\gamma \mathbf{s}^T H^T H \mathbf{s} = 0$$

or at

$$\gamma = \frac{\mathbf{R}^T \cdot H \mathbf{s}}{(H \mathbf{s})^T \cdot (H \mathbf{s})} .$$

which is same as Eq. (4.23).

Cauchy point: minimum in the direction of steepest descent

For the steepest-decent direction, we 'solve'

$$I\mathbf{d} = -\mathbf{R} ,$$

where I is the identity matrix. The search direction is therefore

$$\mathbf{d} = -\nabla J = -\mathbf{R} .$$

As before we minimise

$$\min_{\gamma} r^2(\mathbf{x} + \gamma \mathbf{d})$$

and the cost function is again the square of the residuals, i.e.

$$r^2 := \mathbf{R}^T \cdot \mathbf{R} = (\nabla J)^T \cdot \nabla J ,$$

but now $\mathbf{d} = -\mathbf{R}$. We proceed as on page 90, and find that the slope at $\gamma = 0$ is

$$\begin{aligned} \partial_{\gamma} r^2 \Big|_{\gamma=0} &= -\mathbf{R}_0^T \cdot (H^T + H) \mathbf{R}_0 \\ &= -2\mathbf{R}_0^T H \mathbf{R}_0 \quad \text{if } H = H^T \end{aligned}$$

and thus negative in the steepest descent direction provided

$$(H^T + H) \succ 0$$

and the minimum of the quadratic model along the steepest descent direction is

$$-\mathbf{R}^T \cdot H^T \mathbf{R} - \mathbf{R}^T \cdot H \mathbf{R} + 2\gamma \mathbf{R}^T H^T H \mathbf{R} = 0$$

or at

$$\gamma = \frac{\mathbf{R}^T \cdot (H^T + H) \mathbf{R}}{2(H \mathbf{R})^T \cdot (H \mathbf{R})} .$$

Here $\gamma > 0$ provided $(H^T + H) \succ 0$.

4.8 Time stepping

Úa uses a simple automated time-stepping algorithm that is based on the number of non-linear iterations per time step. The idea is to keep the time step small enough to stay in the second-order convergence regime of the Newton method, while not making it so small that almost no iterations are needed. Usually the time step is chosen so that the number of iteration is on average close to 3 to 5.

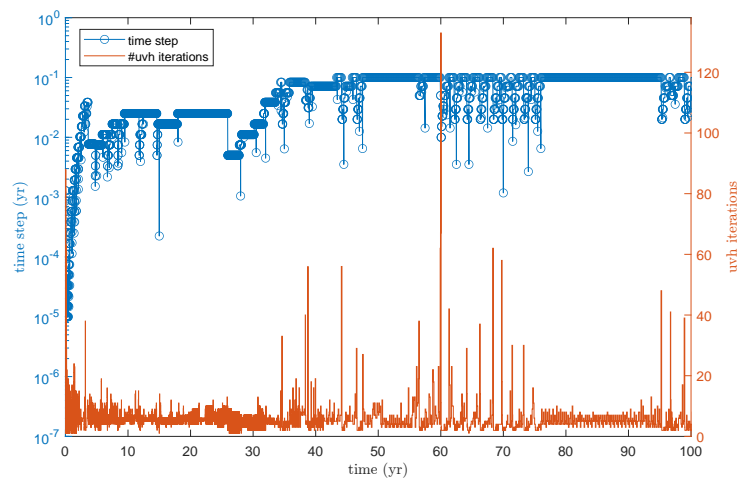


Figure 4.5: Example of time stepping an number of non-linear *uvh*-iterations in a run. Initially the time step is quite small or at 1×10^{-5} yr, and then increases to about 0.1 yr. This example was based on a run including Pine Island and Thwaites glaciers, using automated mesh refinement and unrefinement around the grounding line.

Chapter 5

Continuation Methods

For

$$\frac{dh}{dt} = G(h(\lambda), \lambda)$$

consider the stability of the equilibrium point

$$0 = G(h(\lambda), \lambda)$$

for some given value λ . Perturbation by Δh and Taylor expansion:

$$\begin{aligned}\frac{d(h + \Delta h)}{dt} &= G(h(\lambda) + \Delta h, \lambda) \\ \frac{dh}{dt} + \frac{\Delta h}{dt} &= G(h) + G_h \Delta h + O((\delta h)^2) \\ 0 + \frac{\Delta h}{dt} &= 0 + G_h \Delta h\end{aligned}$$

that is

$$\frac{d\Delta h}{dt} = G_h \Delta h \quad (5.1)$$

and the solution is

$$\Delta h(t) = \Delta h(t = t_0) e^{G_h(t - t_0)}$$

Generally, in a numerical context Eq. (5.1) can be expected to have the form

$$\mathbf{A} \dot{\mathbf{h}} = \mathbf{G}(\mathbf{h}) \quad (5.2)$$

and the fixed-point problem is

$$\mathbf{0} = \mathbf{G}(\mathbf{h}_0) \quad (5.3)$$

Same argument as above then leads to

$$\mathbf{A} \delta \dot{\mathbf{h}} = \mathbf{G}_h \delta \mathbf{h} \quad (\text{linearised system})$$

We look for solutions to

$$\mathbf{A} \delta \dot{\mathbf{h}} = \mathbf{G}_h \delta \mathbf{h} \quad (5.4)$$

on the form

$$\delta \mathbf{h}(t) = \mathbf{x} e^{\mu t}$$

for which

$$\delta \dot{\mathbf{h}}(t) = \mu \mathbf{x} e^{\mu t}$$

and inserting into Eq. (5.4) gives

$$\mathbf{A} \mu \mathbf{x} e^{\mu t} = \mathbf{G}_h \mathbf{x} e^{\mu t}$$

resulting in the generalized eigenvalue problem

$$\mathbf{G}_h \mathbf{x} = \mu \mathbf{A} \mathbf{x} \quad (5.5)$$

and, hence, the stability of the fix-point \mathbf{h}_0 , i.e. the solution to Eq. (5.3), depends of the eigenvalues, μ , of the system (5.5).

Generally, when solving finding the steady-state solution, it is unlikely to be unstable. It certainly will not be unstable if we solve the fix-point problem using a pseudo-time stepping approach. Therefore, we are unlikely to encounter eigenvalues with a positive real part. More generally we expect to possibly find a critical eigenvalue having a zero real part. If it is real (i.e. both real and imaginary parts are zero) and the corresponding critical eigenvector is symmetric, the system encounters a turning point, and if it is imaginary the system undergoes a Hopf bifurcation and starts to oscillate periodically [Salinger et al. \(2002\)](#).

In \tilde{U} the system (2.48) is solved using the NR method and both \mathbf{A} and the \mathbf{G}_h derivative therefore available.

$$F(h, t) = \rho \partial_t h + \nabla_{xy} \cdot \mathbf{q} - \rho a = 0 , \quad (2.48)$$

is solved implicitly with respect to ice thickness using NR, and FE formulation gives

$$\begin{aligned} A_{pq} &= \langle \rho \phi_p, \phi_q \rangle \\ G_q &= \langle \rho a(h), \phi_q \rangle - \langle \mathbf{q}, \nabla \phi_q \rangle \end{aligned}$$

5.1 Simple analytical solutions involving mass-balance altitude feedback

5.2 Weertman's solution for mass-balance elevation feedback on ice caps

One of the first papers to consider the consequences of a feedback between surface mass balance and surface elevation were the papers by Böðvarsson (1955) and [Weertman \(1961\)](#). Here we follow the treatment given in [Weertman \(1961\)](#).

Assume an ice sheet with a constant accumulation a^+ over the accumulation area, and a constant ablation a^- over the ablation area (how realistic is this?).

The ice sheet rests on a flat bed. The thickness is given by $h(x)$ and the equilibrium altitude is h_{ELA} . Where $h > h_{\text{ELA}}$ the accumulation rate is $a^+ > 0$, where $h < h_{\text{ELA}}$ the rate is $-a^- < 0$, where both a^+ and a^- are positive numbers. Although the mass balance is spatially constant over the accumulation and the ablation area, the respective areas are not fixed. The mass balance is therefore a function of the ice sheet geometry.

$$a(h(x)) = \begin{cases} a^+ & \text{where } h(x) > \text{ELA} \\ -a^- & \text{where } h(x) \leq \text{ELA} \end{cases}$$

Note that both a^+ and a^- are positive numbers. The horizontal distance from the centre towards the location x where the ice thickness is equal to ELA is denoted with R , that is by definition of the variable R we have

$$h(R) = \text{ELA} .$$

Table 5.1: List of variables

symbol		units
$a(x)$	surface mass balance distribution	(m/a)
a^+	accumulation rate above the ELA	(m/a)
a^-	ablation rate below the ELA	(m/a)
b	bedrock elevation	(m)
ELA	equilibrium line altitude	(m)
$h(x)$	ice thickness	(m)
h_{ELA}	ice thickness at $x = R$	(m)
R	horizontal distance from the centre of the ice sheet to where $h = h_{\text{ELA}}$	(m)
$s(x)$	surface elevation	(m)
L	(half) width of the ice sheet	(m)

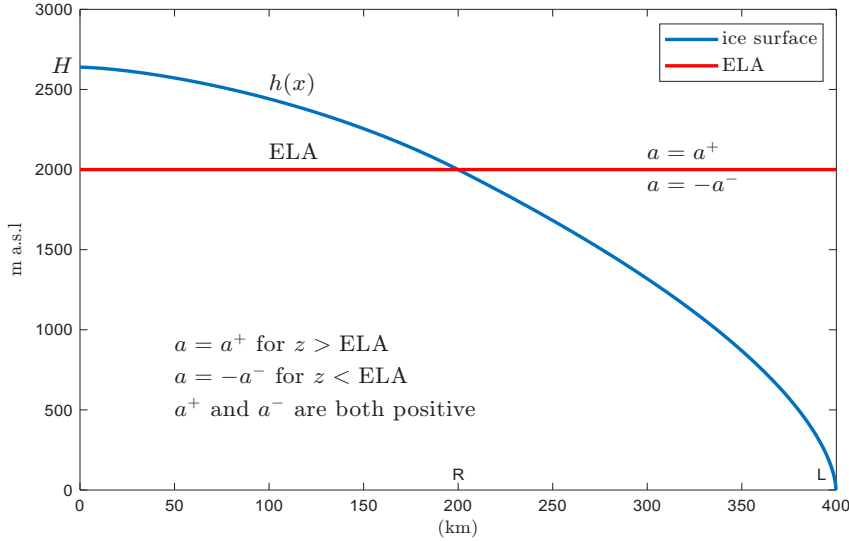


Figure 5.1: The surface profile of an ice sheet as given by Eqs. (5.8) and (5.10), for $a^+ = 1 \text{ m/yr}$, $a^- = 1 \text{ m/yr}$, $c = 2 \text{ m}^{1/2} \text{ yr}^{1/2}$. Everywhere where $h > h_{\text{ELA}}$ the surface mass balance is equal to a given positive number a^+ . For $h \leq h_{\text{ELA}}$ the surface mass balance is set to $-a^- < 0$. Although the mass balance is therefore spatially constant within the accumulation and the ablation areas, the mass balance is nevertheless a function of the surface elevation.

Our objective is to calculate the steady-state geometry as a function of distance x , for a given the accumulation (a^+) and ablation (a^-) and the equilibrium-line altitude (ELA). Symbols are listed in Table 1.

The total length of the ice cap is L and in equilibrium the integrated surface mass balance must be equal to zero, that is

$$a^+R - a^-(L - R) = 0 \quad (5.6)$$

or

$$L = (1 + a^+/a^-)R. \quad (5.7)$$

The vertically integrated mass-conservation equation is

$$\partial_t h + \partial_x q = a,$$

and we look for steady-state solutions where $\partial_t h = 0$. Integrating gives

$$q(x) = \int_0^x a(x) dx,$$

where $a(x)$ is the surface mass balance distribution. We write

$$q(x) = U(x) h(x),$$

where $U = B\tau^m$ is the depth average velocity, τ is the driving stress,

$$\tau = -\rho g h dh/dx,$$

with ρ the ice density, and g the gravitational acceleration. In the original paper Weertman sets $m = 2$ and we will use that value here (In 5.2.2 we repeat some of the calculations for a more general case). Therefore

$$B(\rho g)^2 h^3 (dh/dx)^2 = - \int_0^x a(x') dx',$$

For $x \leq R$ we find

$$B(\rho g)^2 h^3 (dh/dx)^2 = -a^+ x,$$

which we can write as

$$B^{1/2} \rho g h^{3/2} dh = -(a^+ x)^{1/2} dx.$$

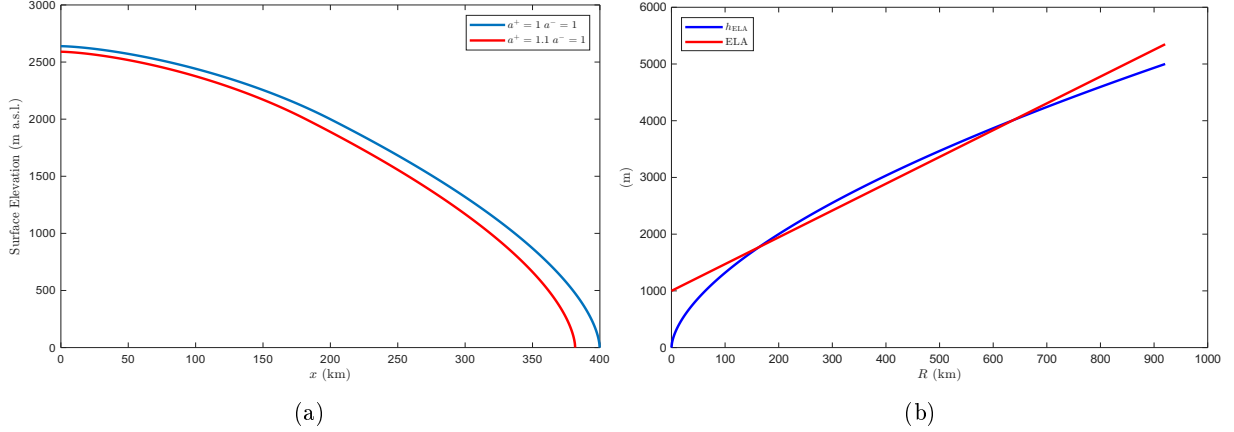


Figure 5.2: (a) The change in surface profile with accumulation (a). The length and the thickness decrease with increasing accumulation rate a^+ . (b) The ice thickness h_{ELA} of a steady-state ice sheet as a function of horizontal distance R towards the equilibrium line (the dividing line between accumulation and ablation.) Also plotted is ELA (as determined by the climate). Only for $\text{ELA} = h_{\text{ELA}}$ is a steady-state ice sheet under given climatic conditions possible.

Integrating

$$\frac{2}{5}B^{1/2}\rho gh^{5/2} = -\frac{2}{3a}(a^+x)^{3/2} + K$$

where K is an integration constant. Inserting $x = 0$ and writing $H = h(x = 0)$ for the thickness at the centre we arrive at

$$h^{5/2}(x) = H^{5/2} - \frac{c}{a^+}(a^+x)^{3/2} \quad \text{for } 0 \leq x \leq R \quad (5.8)$$

where

$$c = \frac{5}{3B^{1/2}\rho g}. \quad (5.9)$$

Similar considerations for $R \leq x \leq L$ lead to

$$h^{5/2}(x) = h_{\text{ELA}}^{5/2} + \frac{c}{a^-} \left((a^+R - a^-(x-R))^{3/2} - (a^+R)^{3/2} \right) \quad \text{for } R \leq x \leq L \quad (5.10)$$

where we determined the integration constant by setting $x = R$ using $h(R) = h_{\text{ELA}}$.

Inserting $x = L$ where $h = 0$ into Eq. (5.10) and using $a^+R - a^-(L-R) = 0$ (which is Eq. (5.6) above), we obtain

$$0 = h_{\text{ELA}}^{5/3} - (c/a^-)(a^+R)^{5/3},$$

or

$$R = \frac{1}{a^+}(a^-/c)^{2/3}h_{\text{ELA}}^{5/3}. \quad (5.11)$$

We can now insert $x = R$ where $h = h_{\text{ELA}}$ into Eq. (5.8) using the above expression for R and we find that

$$H = (1 + a^-/a^+)^{2/5}h_{\text{ELA}}, \quad (5.12)$$

A further expression for L in terms of the ELA, accumulation, and c is obtained by inserting (5.11) into (5.7) giving

$$L = \frac{1}{a^-}(1 + a^-/a^+)^{1/3}(a^-/c)^{2/3}h_{\text{ELA}}^{5/3}. \quad (5.13)$$

Summarising, we have found the following steady-state solution:

$$h(x) = \begin{cases} ((1 + a^-/a^+)h_{\text{ELA}}^{5/2} - \frac{c}{a^+}(a^+x)^{3/2})^{2/5}, & \text{for } 0 \leq x \leq R \\ h_{\text{ELA}}^{5/2} + \frac{c}{a^-} \left((a^+R - a^-(x-R))^{3/2} - (a^+R)^{3/2} \right), & \text{for } R \leq x \leq L \end{cases} \quad (5.14)$$

where R and L are given by Eqs. (5.11) and (5.13), respectively, and c by Eq. (5.9).

Ice sheet profiles for two different values of a^+ are shown in Fig. 5.2a. Values of all other variables are the same for both curves. Both profiles reflect steady-state conditions. Note that an increase in mean

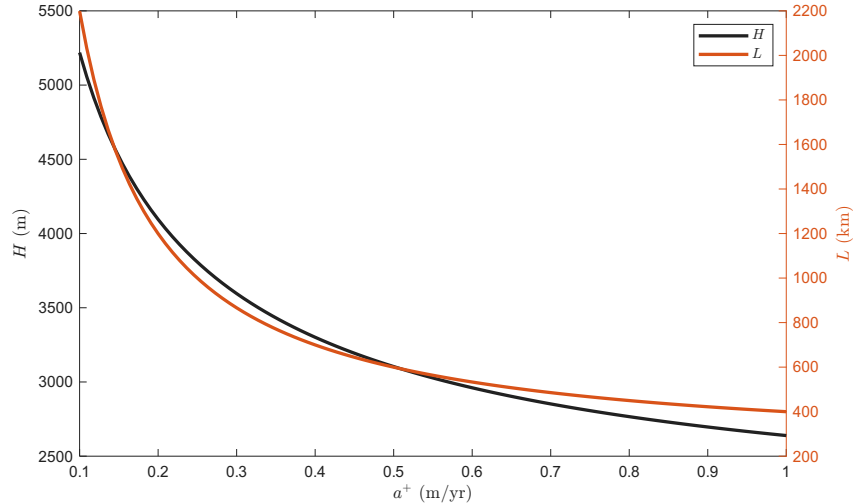


Figure 5.3: Ice thickness at summit ($H = h(x = 0)$) from Eq. (5.12), and the length (L) from Eq. (5.7) as functions of surface accumulation, a^+ , above the equilibrium line altitude (ELA). Here ELA = 2000 m, $a^- = 1 \text{ m/yr}$, and $c = 2 \text{ m}^{1/2} \text{ yr}^{1/2}$. As $a^+ \rightarrow 0$ the ice sheet becomes infinitely thick and infinitely wide.

accumulation is compensated by a reduction in accumulation area, i.e. R becomes smaller with increasing a , leading to an overall decrease in length.

One of the rather surprising aspects of the solution is that both L and H decrease with increasing accumulation rate a^+ , and raising h_{ELA} increases the thickness H and the length L . This aspect of the solution is depicted in Fig. 5.3, showing H and L as functions of a^+ . As $a^+ \rightarrow +0$ the ice sheet becomes infinitely thick and infinitely wide.

5.2.1 Stability of the Weertman solution

Above we have determined the ice thickness distribution, $h(x)$ for a given ELA. We can also consider the dimensions of an ice sheet, e.g. R , as given, and then calculate the thickness of the ice sheet at $x = R$. We denote this ice-dynamical value for ELA with h_{ELA} , while the climatological equilibrium line altitude is as before ELA, i.e. we define

$$h_{\text{ELA}} := h(x = R) \quad \text{for given } R, c, a^+, a^-$$

The ice sheet can only be in a steady state for a given R provided $h_{\text{ELA}} = \text{ELA}$. We find h_{ELA} by inverting Eq. (5.11) and expressing h_{ELA} as a function of R for a given c, a^+, a^- as

$$h_{\text{ELA}} = (a^+ R)^{3/5} (c/a^-)^{2/5}. \quad (5.15)$$

We can think of h_{ELA} as the ELA that the ice sheet requires for a given R, c, a^+ and a^- for it to be in a steady state.

Fig. 5.2b shows h_{ELA} as a function of R as given by Eq. (5.11). In Fig. (5.2b) we assume that the climatological ELA, as a function of R , is given by the straight line. In that case there are two possible steady states. Consider the solution to the right. If we perturb the size of the ice sheet around that solution by increasing R , then $h_{\text{ELA}} < \text{ELA}$, and the actual ELA is now higher than required for steady-state, and the ice sheet will shrink. This solution is therefore stable. The solution on the left is unstable. An ice sheet with a radius slightly larger than the solution to the left, will grow towards the solution to the right. Note that if h_{ELA} does not vary with R (horizontal line) there is only one solution possible and that solution is unstable. In that case there are only two possible solutions. Either the world is ice free, or the earth surface is covered with an infinitely thick ice sheet.

5.2.2 Weertman analysis for shear-deforming ice sheet with no sliding at the base

Weertman did his analysis for a ‘sliding’ ice sheet. His analysis can easily be redone for the, arguably a bit more realistic, case where the motion is due to ice deformation.

For an ice sheet where all the forward motion is due to ice deformation (as opposed to basal sliding) the ice vertically integrated ice flux is

$$q(x) = Bh^{n+2}|dh/dx|^n ,$$

where

$$B = \frac{2A}{n+2}(\rho g)^n .$$

Here A and n are parameters in the ice-flow law, and h is the ice thickness. It is assumed that the ice sheets rests on a flat bed ($b = 0$). The ice centre ice thickness, at $x = 0$ is H , the total length is L , and at the distance $x = R$ the ice thickness is equal to the height of the equilibrium line, that is

$$\begin{aligned} h(x=0) &= H , \\ h(x=R) &= h_{\text{ELA}} , \\ h(x=L) &= 0 . \end{aligned}$$

Further, following Weertman we assume constant accumulation a^+ in the accumulation area where $h > h_{\text{ELA}}$, and a constant ablation a^- in the ablation area where $h \leq h_{\text{ELA}}$. The horizontal distance from the centre of the ice sheet towards the equilibrium line is R and the total length of the ice sheet is L . Overall mass conservation implies at

$$a^+R - a^-(L-R) = 0$$

or that

$$L = (1 + a^+/a^-)R. \quad (5.16)$$

For $0 \leq x \leq R$ the vertically integrated flux is

$$q(x) = a^+x .$$

In steady-state the ice flux must at each location exactly balance the upstream integrated surface mass balance, giving the condition

$$B^{1/n}h^{(n+2)/n} dh/dx = -(a^+x)^{1/n}$$

where we introduce the minus sign because we expect that $dh/dx < 0$ for $x > 0$.

Separating variables and integrating on both sides

$$B^{1/n} \int_H^h (h')^{(n+2)/n} dh' = - \int_0^x (a^+x')^{1/n} dx'$$

gives

$$\frac{nB^{1/n}}{2(n+1)} \left(h^{2(n+1)/n} - H^{2(n+1)/n} \right) = - \frac{n}{a^+(n+1)} (a^+x)^{(n+1)/n}$$

or

$$h^{2(n+1)/n} = H^{2(n+1)/n} - \frac{2}{a^+B^{1/n}} (a^+x)^{(n+1)/n} , \quad (5.17)$$

valid for $0 \leq x \leq R$. We know that at $x = R$, $h(x = R) = h_{\text{ELA}}$ so we also have

$$h_{\text{ELA}}^{2(n+1)/n} = H^{2(n+1)/n} - \frac{2}{a^+B^{1/n}} (a^+R)^{(n+1)/n} . \quad (5.18)$$

Now considering the region $R \leq x \leq L$ for which

$$q(x) = a^+R - a^-(x-R) ,$$

and using the expression for vertically integrated flux

$$q(x) = Bh^{n+2}|dh/dx|^n ,$$

balance between vertically integrated ice flux and total upstream surface accumulation/ablation implies

$$B^{1/n}h^{n+2}dh/dx = -(a^+R - a^-(x-R))^{1/n} .$$

Again, separating variables and integrating gives

$$B^{1/n} \int_{h_{\text{ELA}}}^h (h')^{(n+2)/n} dh' = - \int_R^x (a^+ R - a^- (x' - R))^{1/n} dx'$$

or

$$h_{\text{ELA}}^{2(n+1)/n} = h_{\text{ELA}}^{2(n+1)/n} - \frac{2}{a^- B^{1/n}} \left((a^+ R)^{(n+1)/n} - (a^+ R - a^- (x - R))^{(n+1)/n} \right) \quad (5.19)$$

Inserting $x = L$ where $h = 0$ into the above expression

$$h_{\text{ELA}}^{2(n+1)/n} = \frac{2}{a^- B^{1/n}} \left((a^+ R)^{(n+1)/n} - (a^+ R - a^- (L - R))^{(n+1)/n} \right)$$

and using

$$a^+ R - a^- (L - R) = 0,$$

which follows from mass-balance considerations, gives

$$h_{\text{ELA}}^{2(n+1)/n} = \frac{2(a^+ R)^{(n+1)/n}}{a^- B^{1/n}} \quad (5.20)$$

or

$$R = \frac{1}{a^+} B^{1/(n+1)} (a^- / 2)^{\frac{n}{n+1}} h_{\text{ELA}}^2, \quad (5.21)$$

We write Eq. (5.20) as

$$h_{\text{ELA}}^{2(n+1)/n} = \frac{a^+}{a^-} \frac{2(a^+ R)^{(n+1)/n}}{a^+ B^{1/n}},$$

insert into (5.18), and arrive at

$$H = (1 + a^- / a^+)^{n/(2n+2)} h_{\text{ELA}}, \quad (5.22)$$

giving us the centre ice thickness in terms of the mass balance and the ELA. Together, equations (5.16), (5.21) and (5.22) give us the length, L , the horizontal distance from the centre were the ice thickness is equal to the ELA, and the centre thickness, H , of the ice cap. The thickness, H , at the centre only depends on the stress exponent n and not on B . We see that for a given ELA, the ice thickness and the length decrease with increasing surface accumulation in the accumulation area (a^+). Analysing the above solutions shows that they exhibit the same type of instability as discussed in [Weertman \(1961\)](#).

5.3 Vialov solution

We will now derive a solution for the profile of an ice cap where the mass balance is constant across the surface, and where the total length, l , of the ice cap is fixed, i.e. not allowed to evolve. This same solution is found and derived in various other branches of earth sciences and is, for example, used in similar form in studies of ground water flow. The solution is often referred to as the *Vialov solution*.

In contrast to the Weertman solution shown above, the surface mass balance is now some constant, a , that does not vary with distance and is not a function of surface elevation. The ice cap has the total prescribed width $2l$ is situated on a flat bed ($b = 0$). The ice cap is symmetrical around $x = 0$, and extends from $-l$ to l . The width of the ice sheet is fixed. The accumulation rate $a > 0$ is constant everywhere, and the ice flux is

$$q(x) = Bh^{n+2} |\partial h / \partial x|^{n-1} \partial_x h,$$

where B and n are some rheological parameters, and h is the ice thickness.

It is possibly somewhat surprising that it is possible to find a solution for an ice cap of fixed length where the surface mass balance is always positive. Clearly the total integrated surface mass balance is here $2al > 0$ and it is, at first, unclear how one can find a steady state solution for an ice cap without an ablation area. Putting these reservation to the side we continue and attempt to find a steady-state solution as follows.

Steady state implies $\partial_x q = a$ and therefore for $x \geq 0$ and a constant

$$q(x) = ax$$

where we have used that $q(0) = 0$ because of symmetry around $x = 0$. Therefore,

$$q(x) = ax = Bh^{n+2}(x) \left| \frac{dh(x)}{dx} \right|^n$$

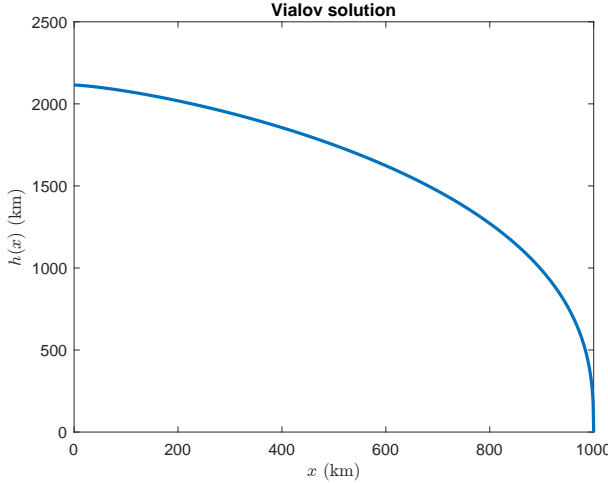


Figure 5.4: The Vialov solution, as given by Eq. (5.24), for $l = 1000$ km, $n = 3$, $B = 0.01 \text{ m}^{-n} \text{ a}^{-1}$, and $a = 0.5 \text{ m a}^{-1}$.

for $x \geq 0$. Separation of variables

$$ax = Bh^{n+2}h(x) |dh/dx|^{n-1} dh/dx$$

or

$$(ax)^{1/n} dx = -B^{1/n} h^{(n+2)/n} dh$$

where we have assumed that $dh/dx < 0$ for $x > 0$.

Integrating on both sides with respect to x and h gives

$$h^{2(1+n)/n} = -2(a/B)^{1/n} x^{(n+1)/n} + K,$$

And the integration constant is then determined by the boundary conditions $h(l) = 0$ and this gives the solution for the ice thickness distribution as

$$h^{2(1+n)/n} = 2(a/B)^{1/n} \left(l^{(n+1)/n} - |x|^{(n+1)/n} \right), \quad (5.23)$$

or

$$h(x) = h_0 \left(1 - |x/l|^{(n+1)/n} \right)^{n/(2+2n)}. \quad (5.24)$$

where

$$h_0 = h(x=0) = 2^{n/(2+2n)} (a/B)^{1/(2+2n)} l^{1/2} \quad (5.25)$$

the the surface elevation at centre where $x = 0$.

Note that for $n = 3$, we have $h_0 = K a^{1/8}$, and B has the units distance $^{-n}$ time $^{-1}$.

The Vialov solution is obtained for a fixed ice cap length l and the surface accumulation a is constant, and positive across the whole length of the ice cap. The ice cap length can, hence, not grow or shrink in response to changes in accumulation.

5.3.1 Note on the stability of the Vialov solution

Similarly as done for the Weertman solution above, we can now imagine a situation where the accumulation depends on some aspects of the ice sheet geometry. For example as

$$a = a_G + \gamma h_0 \quad (5.26)$$

where $a_G = a(h = 0)$ is the mass balance and the ground level, and

$$\gamma = \frac{da}{dh}$$

is the mass-balance gradient. The (spatially constant) surface mass balance is now dependent on the surface elevation at the summit. While this is arguably a somewhat contrived and physically unrealistic

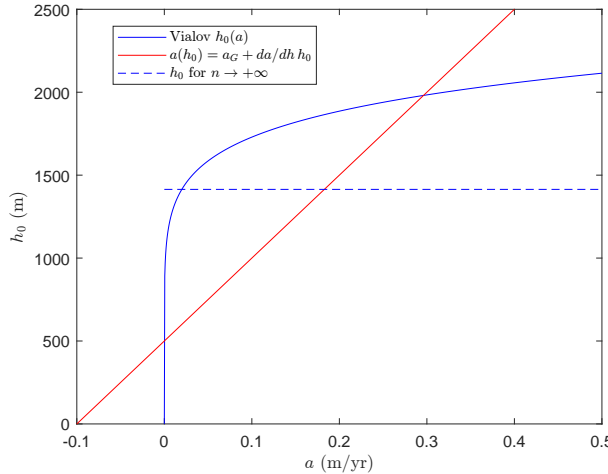


Figure 5.5: The Vialov solution for $l = 1000$ km, $n = 3$, $B = 0.01 \text{ m}^{-3} \text{ a}^{-1}$, $a_G = -0.1 \text{ m a}^{-1}$, and $da/dh = da/dT \times dT/dh = 0.04 \times 0.005 = 2 \times 10^{-4} \text{ yr}^{-1}$.

specification for the mass balance, now the possible solutions are now obtained for those surface mass balance values, a , where the summit height, as given by Eq. (5.26),

$$h_0 = (a - a_G)/\gamma$$

equals h_0 as given by the Vialov solution, Eq. (5.25). In Fig. 5.5 these are the two intersections between the blue (Vialov solution) and the red curve. Of those two solutions one of is stable (the one to the right) and the other unstable (the one to the left).

The blue curve in Fig. 5.5, represents the summit height, h_0 , as a function of the (spatially constant) accumulation, a . As the figure shows, h_0 is initially a sharply increasing function of the surface mass balance, a . In the limiting case $n \rightarrow +\infty$ we have

$$\lim_{n \rightarrow +\infty} h_0 \sqrt{2l}$$

and the ice thickness becomes independent of the accumulation rate (dashed blue line in Fig. 5.5). In this limit, i.e. $n \rightarrow +\infty$ no unstable solution is therefore found. And, as Fig. 5.5 suggests, for $n = 3$ the unstable solution is found for rather small accumulation rate values.

The stability of the Vialov solution is quite different from that of the more general Weertman solution. For spatially constant accumulation rate, a stable Vialov profile is always possible but not for the Weertman solution. The key difference is that for the Vialov solution the surface accumulation can have any given (positive) value for any fixed length l . All the accumulated surface mass balance will always be lost through an equally large ice flux at the terminus. Note that the surface mass balance used in deriving the Vialov solution was assumed independent of elevation, spatially constant, and the surface mass balance gradient is zero. It could therefore be argued that the Vialov solution is not well suited for studying feedbacks between surface elevation and mass balance.

5.4 Simple example of unstable mass-balance feedback

For example for the mass-conservation equation

$$\rho \partial_t h = \rho a - \nabla \cdot (\rho \mathbf{q})$$

for system with the mass-altitude feedback

$$a = \lambda h(x) + \gamma$$

and ρ spatially constant, we have

$$\partial_t h = \lambda h(x, t) + \gamma - \nabla \cdot \mathbf{q}$$

hence

$$G(h(\lambda), \lambda) = \lambda h + \gamma - \nabla \cdot \mathbf{q}$$

Considering SIA in 1D with all motion due to basal sliding and using Weertman sliding law, where

$$q = -Dh^{m+1}|\partial_x s|^{m-1}\partial_x s$$

where D is related to the typically C used when writing Weertman sliding law as

$$D = (\rho g)^m C$$

results in

$$G(h(\lambda), \lambda) = \lambda h + \gamma + D\partial_x(h^{m+1}|\partial_x h|^{m-1})\partial_x h$$

assuming flat bed. At the equilibrium point, where $\partial_t h = G(h, \lambda) = 0$, we must have

$$0 = \lambda h + \gamma + D\partial_x(h^{m+2}(\partial_x h)^m)$$

Solving this is presumably only possibly numerically, but if we for the moment consider the case for which $\lambda = 0$, we have

$$\gamma = -D\partial_x(h^{m+1}|\partial_x h|^{m-1})\partial_x h$$

This can easily be solved, by first integrating both sides with respect to x ,

$$\gamma x = -Dh^{m+1}(\partial_x h)^m$$

Where we have set $q(x = 0) = 0$. Rearranging and separating variables with $\partial_x h < 0$

$$\int (\gamma x)^{1/m} dx = D \int h^{(m+1)/m} dh$$

We set $h(x = l) = 0$ implying that

$$(\gamma x)^{\frac{m+1}{m}} = \frac{m+1}{m+2} D h^{\frac{2m+1}{m}} + (\gamma l)^{\frac{m+1}{m}}$$

or

$$h(x) = h_0 \left(1 - |x/l|^{\frac{m+1}{m}}\right)^{\frac{m}{2m+1}}$$

where

$$h_0 = h(x = 0) = \left(\frac{m+1}{m+2} D\right)^{-\frac{m}{2m+1}} (\gamma l)^{\frac{m+1}{2m+1}}.$$

If we, on the other hand, assume all motion due to internal deformation where

$$q(x) = B h^{n+2} |\partial_h h / dx|^n,$$

with

$$B = \frac{2A}{n+1} (\rho g)^n.$$

and were A and n are parameters in the ice-flow law, same arguments lead to

$$h(x) = h_0 \left(1 - |x/l|^{(n+1)/n}\right)^{n/(2+2n)}. \quad (5.27)$$

where

$$h_0 = h(x = 0) = 2^{n/(2+2n)} (a/B)^{1/(2+2n)} l^{1/2}$$

5.5 Numerical approach

Considering the more general equilibrium SIA problem,

$$\begin{aligned} \frac{ds}{dt} &= G(h(\lambda), \lambda) \\ &= \rho(\lambda(s - B) + \gamma) - D \partial_x (\rho(s - B)^{n+2} |\partial_x s|^{n-1} \partial_x s) \\ &= 0 \end{aligned}$$

which follows from Eq. (1.46), and where

$$D = \frac{2A}{n+2}(\rho g)^n .$$

FE formulation

$$\begin{aligned} & \langle F, \phi_p \rangle = 0 \\ & \langle \rho(\lambda h + \gamma) - D \partial_x (\rho h^{n+2} |\partial_x s|^{n-1} \partial_x s), \phi_p \rangle = 0 \\ & \langle \rho(\lambda(s+B) + \gamma), \phi_p \rangle + \langle D \rho(s+B)^{n+2} |\partial_x s|^{n-1} \partial_x s, \partial_x \phi_p \rangle = 0 \\ & \langle \rho(\lambda B + \gamma), \phi_p \rangle + \langle \rho(\lambda \phi_q + \gamma), \phi_p \rangle s_q + \langle D \rho(s+B)^{n+2} |\partial_x s|^{n-1} \partial_x \phi_q, \partial_x \phi_p \rangle s_q = 0 \\ & \langle \rho \lambda \phi_q, \phi_p \rangle s_q + \langle D \rho(s+B)^{n+2} |\partial_x s|^{n-1} \partial_x \phi_q, \partial_x \phi_p \rangle s_q = - \langle \rho(\lambda B + \gamma), \phi_p \rangle \\ & (\langle \rho \lambda \phi_q, \phi_p \rangle + \langle D \rho(s+B)^{n+2} |\partial_x s|^{n-1} \partial_x \phi_q, \partial_x \phi_p \rangle) s_q = - \langle \rho(\lambda B + \gamma), \phi_p \rangle \end{aligned}$$

where we have used partial integration of the second-order term (free-flux boundary condition) and Picard formulation.

$$\begin{aligned} \langle \rho \dot{h}, \phi_p \rangle &= \langle \rho \lambda h - \nabla \cdot (\rho \mathbf{v}), \phi_p \rangle \\ \langle \rho \phi_q, \phi_p \rangle \dot{h}_q &= \langle \rho \lambda h - \nabla \cdot (\rho \mathbf{v}), \phi_p \rangle \end{aligned}$$

and hence

$$\begin{aligned} \mathbf{A} &= \langle \rho \phi_q, \phi_p \rangle \\ \mathbf{G} &= \langle \rho \lambda h - \nabla \cdot (\rho \mathbf{v}), \phi_p \rangle \\ \mathbf{G}_h &= \langle \rho \lambda \phi_q, \phi_p \rangle \end{aligned}$$

And (5.5) reads

$$\lambda \rho \langle \phi_q, \phi_p \rangle \mathbf{\Lambda} = \rho \lambda \langle \phi_q, \phi_p \rangle \mathbf{\Lambda}$$

or

$$\sigma = \lambda$$

and the system is unstable for $\lambda > 0$.

Saddle-Node Bifurcation: Consider

$$\dot{h} = \alpha(h - h^*)^2 - \lambda .$$

For $\lambda > 0$ we have two steady state solutions

$$h_0 = \pm \sqrt{\lambda/\alpha} + h^* .$$

Linearisation of the continuous problem around the steady-state solutions results in

$$\begin{aligned} \partial_t \delta h &= 2\alpha(h_0 - h^*)\delta h \\ &= \pm 2\alpha\sqrt{\lambda/\alpha}\delta h \end{aligned}$$

so one solution is stable and the other one unstable. The saddle-node (fold) bifurcation happens at $\lambda = 0$.

Pitchfork Bifurcation:

Consider

$$\dot{h} = (h - h^*)^3 - \lambda(h - h^*) .$$

The three solutions to $\dot{h} = 0$ are:

$$\begin{aligned} h_0 &= h^* \\ h_0 &= \pm \sqrt{\lambda} + h^* \end{aligned}$$

Linearisation of the continuous problem around the steady-state solutions results in

$$\begin{aligned}\partial_t \delta h &= (3(h_0 - h^*)^2 - \lambda)\delta h \\ &= \begin{cases} 2\lambda \delta h \\ -\lambda \delta h \\ 2\lambda \delta h \end{cases}\end{aligned}$$

So for $\lambda > 0$, the $h = h^*$ solution is stable and the other two both unstable.

5.5.1 Euler-Newton Continuation

For a known solution

$$G(h_0(\lambda_0), \lambda_0) = 0$$

we search for another nearby solution for $\lambda = \lambda_1$ where λ_1 is in some way close to λ_0 .

Solve for the slope $h_\lambda := \partial_\lambda h$

$$\frac{\partial F}{\partial h} \frac{\partial h}{\partial \lambda} + \frac{\partial F}{\partial \lambda} = 0$$

A forward Euler predictor step gives

$$h_1^0 = h_0 + h_\lambda(\lambda_1 - \lambda_0)$$

where h_1^0 is now our initial guess for h_1 , and then we solve the Newton-Raphson system

$$G_h \Delta h^i = -G(h_1^i, \lambda)$$

where

$$\Delta h^i = h_1^{i+1} - h_1^i$$

This fails if the Jakobian $G_h := \partial_h F$ becomes singular.

5.5.2 Pseudo-Arclength Continuation

Parameterise the solution as a function of the arc-length, s

$$G(h(s), \lambda(s)) = 0 \quad (5.28)$$

Again taking the total derivative

$$\frac{\partial F}{\partial h} \frac{\partial h}{\partial s} + \frac{\partial F}{\partial \lambda} \frac{\partial \lambda}{\partial s} = 0 \quad (5.29)$$

we solve for the slopes

$$\begin{aligned}h_s &= \frac{\partial h}{\partial s} \\ \lambda_s &= \frac{\partial \lambda}{\partial s}\end{aligned}$$

where we now need some additional second equation. This is provided by the arclength condition

$$\|h_s\|^2 + |\lambda_s|^2 = 1 \quad (5.30)$$

We require the projection of vector representing the change in the solution

$$(h(s) - h(s_0), \lambda(s) - \lambda(s_0))$$

onto the tangent (the direction vector) to the solution branch in h, λ space

$$(h_s, \lambda_s) \quad (\text{the direction vector})$$

to be equal to $s - s_0$, that is

$$N := (h_s, \lambda_s) \cdot (h(s) - h(s_0), \lambda(s) - \lambda(s_0)) - (s - s_0) = 0 \quad (5.31)$$

Eq. (5.31) is a linearisation of the arc-length equation (5.30).

The Newton-Raphson system of Eqs. (5.28) and (5.31) is now

$$\begin{pmatrix} G_h & G_\lambda \\ N_h & N_\lambda \end{pmatrix} \begin{pmatrix} \Delta h^i \\ \Delta \lambda^i \end{pmatrix} = - \begin{pmatrix} F(h_1^i, \lambda_1^i) \\ N(h_1^i, \lambda_1^i) \end{pmatrix} \quad (5.32)$$

or in discretized form and using (5.31)

$$\begin{pmatrix} G_h & G_\lambda \\ \mathbf{h}_s^T & \lambda_s \end{pmatrix} \begin{pmatrix} \Delta \mathbf{h}^i \\ \Delta \lambda^i \end{pmatrix} = - \begin{pmatrix} \mathbf{G}(\mathbf{h}_1^i, \lambda_1^i) \\ (\mathbf{h}_1^i - \mathbf{h}_0) \cdot \mathbf{h}_s + (\lambda_1^i - \lambda_0) \lambda_s - (s - s_0) \end{pmatrix}$$

with

$$\begin{aligned} \Delta \mathbf{h}^i &= \mathbf{h}_1^{i+1} - \mathbf{h}_1^i \\ \Delta \lambda^i &= \lambda_1^{i+1} - \lambda_1^i \end{aligned}$$

and $\|\Delta \mathbf{h}^i\|$ and $\Delta \lambda^0$ both going to zero with i increasing. This system can be solved even when G_h is singular. See further in, for example, [Chan and Keller \(1982\)](#); [Rheinboldt \(1988\)](#); [Cliffe et al. \(2000\)](#).

As stated above, the direction vector, $(\mathbf{h}_s, \lambda_s)$, must satisfy Eq. (5.29) and (5.30), i.e.

$$\mathbf{G}_h \mathbf{h}_s + \mathbf{G}_\lambda \lambda_s = 0 \quad (5.33)$$

$$\|\mathbf{h}_s\|^2 + |\lambda_s|^2 = ds^2 \quad (5.34)$$

As shown in [Rheinboldt \(1988\)](#), if \mathbf{G}_h is non-singular we can first solve

$$\mathbf{G}_h \phi = -\mathbf{G}_\lambda$$

then set

$$\mathbf{h}_s = a\phi \quad \text{and} \quad \lambda_s = a$$

where a is some scalar, inserting back into Eq. (5.33) we find

$$a\mathbf{G}_h \phi + \mathbf{G}_\lambda a = -a\mathbf{G}_\lambda + \mathbf{G}_\lambda a = 0$$

showing that this is a solution to Eq. (5.33). Inserting into Eq. (5.34) gives

$$a^2 \|\phi\|^2 + a^2 = 1,$$

or

$$a = \pm \frac{1}{\sqrt{1 + \|\phi\|^2}}.$$

We select the sign by assuring that the angle between the new and the old direction vectors is less than $\pi/2$, i.e.

$$(\mathbf{h}_s^1, \lambda_1^1) \cdot (\mathbf{h}_s^0, \lambda_s^0) > 0.$$

As suggested by [Doedel \(2013\)](#), the direction vector, $(\mathbf{h}_s, \lambda_s)$, can also be calculated as

$$\begin{pmatrix} \mathbf{G}_h & \mathbf{G}_\lambda \\ \mathbf{h}_{0s} & \lambda_{0s} \end{pmatrix} \begin{pmatrix} \mathbf{h}_s \\ \lambda_s \end{pmatrix} = \begin{pmatrix} \mathbf{0} \\ 1 \end{pmatrix} \quad (5.35)$$

which is (5.29) and (5.30) approximated, and then rescale the direction vector afterwards. The first Newton iterate is $(\mathbf{h}_0, \lambda_0) + \gamma(\mathbf{h}_s, \lambda_s)$ where γ is some scalar.

Pseudo-Arclength Continuation: Alternative notation

By lumping $h \in \mathbb{R}^n$ and $\lambda \in \mathbb{R}$ into one variable, the notation can be simplified, see for example [Kuznetsov \(1998\)](#).

Find $y \in \mathbb{R}^{n+1}$ subject to

$$F(y) = 0, \quad \mathbb{R}^{n+1} \rightarrow \mathbb{R}^n$$

We assume we already have a solution

$$F(y_0) = 0$$

and a vector z_0 in the null space of G_y where

$$G_u z_0 = 0 .$$

Clearly such a vector must exist as F is at most of rank n .

We then find a new predicted solution

$$y_1^p = y_0 + \Delta s z_0$$

and then correct this predictor step using the Newton iteration

$$G_y(y_{k+1} - y_k) = -F(y_k) \quad (5.36)$$

$$z_k^T \cdot (y_{k+1} - y_1^p) = 0 \quad (5.37)$$

and once converged, find the new tangent by solving

$$\begin{pmatrix} G_y \\ z_k^T \end{pmatrix} (z_{k+1}) = \begin{pmatrix} 0 \\ 1 \end{pmatrix} \quad (5.38)$$

Here Eq. (5.38) is same as Eq. (5.35), and (5.36) almost the same as (5.32). In (5.37) constraint is used

$$\langle z_0, y_{k+1} - y_1^p \rangle = \langle z_k^T, y_{k+1} - y_0 \rangle + \Delta s$$

var her

Chapter 6

Inverse modelling

We denote the control and the state variables by p and q , respectively. The 'state variable' (q) is any variable calculated by the model, such as velocity, rates of elevation change, etc. The 'control' variable (p) is any model input variable required by the model to calculate the state variables (e.g. A and C , B , etc.).

We write the forward model as

$$F(q(p), p) = 0,$$

where p are model parameters and q the state variable.

A 'forward calculation' consists in finding a solution q to the above equation for some parameters p . Roughly speaking, an 'inverse problem' is the opposite problem of finding p given q . Inverse problems encountered in geophysics typically have at least vigintillion¹ and one possible solutions. However, some of those might be more likely than others. Selecting the more likely one out of the vigintillion and one possible ones is commonly done by introducing some constraints on p .

We consider the problem of minimising an objective function J with respect to p . Typically the objective function J can be thought of as a sum of two terms

$$J(q(p), p) = I(q(p)) + R(p),$$

where I is a misfit term and R a regularisation term.

When inverting for the (distributed) model parameter p we refer to it as the control variable to distinguish it from any other model parameters.

6.1 Preliminaries

Assume we want to solve the minimisation problem

$$\min_{p \in P, q \in U} J(q(p), p)$$

subject to forward model

$$F(q(p), p) = 0.$$

The objective function is

$$J : U \times P \rightarrow \mathbb{R},$$

and the forward model, i.e. the state equation

$$F : U \times P \rightarrow \mathbb{W},$$

the model control parameter space P (also referred to as control space), the state space U and the image space W are Banach spaces. We want to determine the sensitivity of cost function J with respect to the (distributed) control parameter p , i.e. we would like to calculate the directional derivative

$$DJ(p)[\phi] = \langle \nabla_p J | \phi \rangle,$$

as well as determine the gradient $\nabla_p J$, for a given inner product.

¹1 Vigintillion = 10^{63} .

Table 6.1: Notation used in inverse modelling (I)

$F(q(p), p) = 0$	state equation
$q = f(p)$	forward model
p	model parameters, control variable (design variable), e.g. A, B, C
q	state variable, e.g. $u, v, \partial_t h$
p_{prior} and \tilde{p}	<i>a priori</i> estimates of model parameters
q_{meas} and \hat{q}	estimates of the state variable (measurements)
$J = I + R$	objective function
R	regularisation term
I	misfit term
$\mathcal{L} = I + R + \langle \lambda F(q(p), p) \rangle$	Lagrangian or the 'extended' objective function.
K	covariance matrix
$\mathcal{A} = \int d\mathcal{A}$	domain area

If

$$F(q(p), p) = 0, \quad (6.1)$$

for the parameter values p , then the total derivative of F with respect to p is also zero, that is

$$d_p F = \partial_p F + \partial_q F \partial_p q = 0. \quad (6.2)$$

Similarly, the total second derivative of the forward model with respect to p must also be zero, i.e.

$$0 = \frac{d^2 F}{dp dp} = \frac{\partial^2 F}{\partial p \partial p} + \frac{\partial^2 F}{\partial p \partial q} \frac{\partial q}{\partial p} + \frac{\partial^2 F}{\partial q \partial q} \frac{\partial q}{\partial p} \frac{\partial q}{\partial p} + \frac{\partial F}{\partial q} \frac{d^2 q}{\partial p \partial p} \quad (6.3)$$

When minimising the cost function $J(q(p), p)$ with respect to the parameters p we would like to have as much information about how J varies with respect to p as possible. Large scale optimisation is almost impossible unless we know the derivative dJ/dp , and ideally we would also like to calculate the Hessian, or at least be able to construct some approximation to the Hessian.

The total derivative of the cost function J with respect to the model parameters p is

$$d_p J = \frac{\partial J}{\partial p} + \frac{\partial J}{\partial q} \frac{\partial q}{\partial p}, \quad (6.4)$$

and the Hessian is

$$\begin{aligned} H &:= \frac{d^2 J}{dp dp} \\ &= \frac{d}{dp} \left(\frac{\partial J(q(p), p)}{\partial p} + \frac{\partial J(q(p), p)}{\partial q} \frac{\partial q}{\partial p} \right) \\ &= \frac{\partial^2 J}{\partial p \partial q} \frac{\partial q}{\partial p} + \frac{\partial^2 J}{\partial p \partial p} + \frac{d}{dp} \left(\frac{\partial J}{\partial q} \frac{\partial q}{\partial p} \right) \\ &= \frac{\partial^2 J}{\partial p \partial q} \frac{\partial q}{\partial p} + \frac{\partial^2 J}{\partial p \partial p} + \frac{d}{dp} \left(\frac{\partial J}{\partial q} \right) \frac{\partial q}{\partial p} + \frac{\partial J}{\partial q} \frac{d}{dp} \left(\frac{\partial q}{\partial p} \right) \\ &= \frac{\partial^2 J}{\partial p \partial q} \frac{\partial q}{\partial p} + \frac{\partial^2 J}{\partial p \partial p} + \left(\frac{\partial^2 J}{\partial p \partial q} + \frac{\partial^2 J}{\partial q \partial q} \frac{\partial q}{\partial p} \right) \frac{\partial q}{\partial p} + \frac{\partial J}{\partial q} \frac{\partial^2 q}{\partial p \partial p} \\ &= \frac{\partial^2 J}{\partial p \partial q} \frac{\partial q}{\partial p} + \frac{\partial^2 J}{\partial p \partial p} + \frac{\partial^2 J}{\partial p \partial q} \frac{\partial q}{\partial p} + \frac{\partial^2 J}{\partial q \partial q} \frac{\partial q}{\partial p} \frac{\partial q}{\partial p} + \frac{\partial J}{\partial q} \frac{\partial^2 q}{\partial p \partial p} \end{aligned} \quad (6.5)$$

that is

$$H = \frac{\partial^2 J}{\partial p \partial q} \frac{\partial q}{\partial p} + \frac{\partial^2 J}{\partial p \partial p} + \frac{\partial^2 J}{\partial p \partial q} \frac{\partial q}{\partial p} + \frac{\partial^2 J}{\partial q \partial q} \frac{\partial q}{\partial p} \frac{\partial q}{\partial p} + \frac{\partial J}{\partial q} \frac{\partial^2 q}{\partial p \partial p} \quad (6.6)$$

The question is if, and how, we can calculate these quantities efficiently.

Some of the quantities appearing in the derivative of the costs function J , i.e. Eq. (6.3) and the Hessian H , i.e. Eq. (6.6) are easier to calculate than others. For example all partial derivatives of J should be

easy to calculate as the function J is known and will often be some relatively simple expression. But calculating

$$\frac{\partial q}{\partial p},$$

needed if the derivative is calculated using Eq. (6.2), and

$$\frac{\partial^2 q}{\partial p \partial p},$$

needed if the Hessian is calculated using Eq. (6.6) is computationally expensive. However, it turns out that there are ways of calculating the gradient and the Hessian without having to estimate these quantities.

6.1.1 Calculating the gradient and the Hessian of the cost function J

As described above, an inverse problem can be expressed as a constrained minimisation problem. Ideally, when minimising a scalar function $J(q(p), p)$ with respect to p , we would like to know the gradient and the Hessian of J . There are various ways of calculating the gradient and the Hessian

Direct approach (sensitivity approach)

Directly determining the derivatives of the cost function

$$J = J(q(p), p)$$

leads to

$$d_p J = \frac{\partial J}{\partial p} + \frac{\partial J}{\partial q} \frac{\partial q}{\partial p} \quad (6.4)$$

This requires calculating the sensitivity matrix $\partial_p q$. From (6.2) we see that we can determine the sensitivities

$$\xi := \frac{\partial q}{\partial p} \quad (6.7)$$

by solving the system

$$\frac{\partial F}{\partial q} \xi = -\frac{\partial F}{\partial p} \quad (6.8)$$

We can then insert ξ into Eq. (6.4) and calculate the total derivative of the cost function J as

$$d_p J = \frac{\partial J}{\partial p} + \frac{\partial J}{\partial q} \xi. \quad (6.9)$$

Once discretised, the sensitivities $\xi = \partial_p q$ is a matrix with $n_q \times n_p$ entries, and $\partial_q F$ is a matrix with $n_q \times n_q$ entries, and $\partial_p F$ a matrix with $n_q \times n_p$ entries. Calculating ξ therefore requires repeated solves for n_p right-hand sides for each sensitivity vector, i.e. for each column of ξ . Examples of the use of this approach to calculate the sensitivities of velocities to A and C are provided in Figs. (6.1) and (6.2).

First-order adjoint

In the adjoint method we add the forward model to the functional J giving us the augmented first-order cost function

$$\mathcal{L}_1(q(p), p, \lambda) = J(q(p), p) + \lambda^* F(q(p), q) \quad (6.10)$$

We find

$$d_p \mathcal{L}_1 = \frac{\partial J}{\partial p} + \frac{\partial J}{\partial q} \frac{\partial q}{\partial p} + \lambda^* (\partial_p F + \partial_q F \partial_p q) \quad (6.11)$$

which we could also have written down directly by simply adding up Eq. (6.4) and (6.2). Rearranging leads to

$$\begin{aligned} d_p \mathcal{L}_1 &= \frac{\partial J}{\partial p} + \lambda^* \partial_p J + \partial_q J \partial_p q + \lambda^* \partial_q F \partial_p q \\ &= \partial_p J + \lambda^* \partial_p F + \partial_q J \xi + (\partial_q F)^* \lambda \xi \\ &= \partial_p J + \lambda^* \partial_p F + (\partial_q J + (\partial_q F)^* \lambda) \xi \end{aligned} \quad (6.12)$$

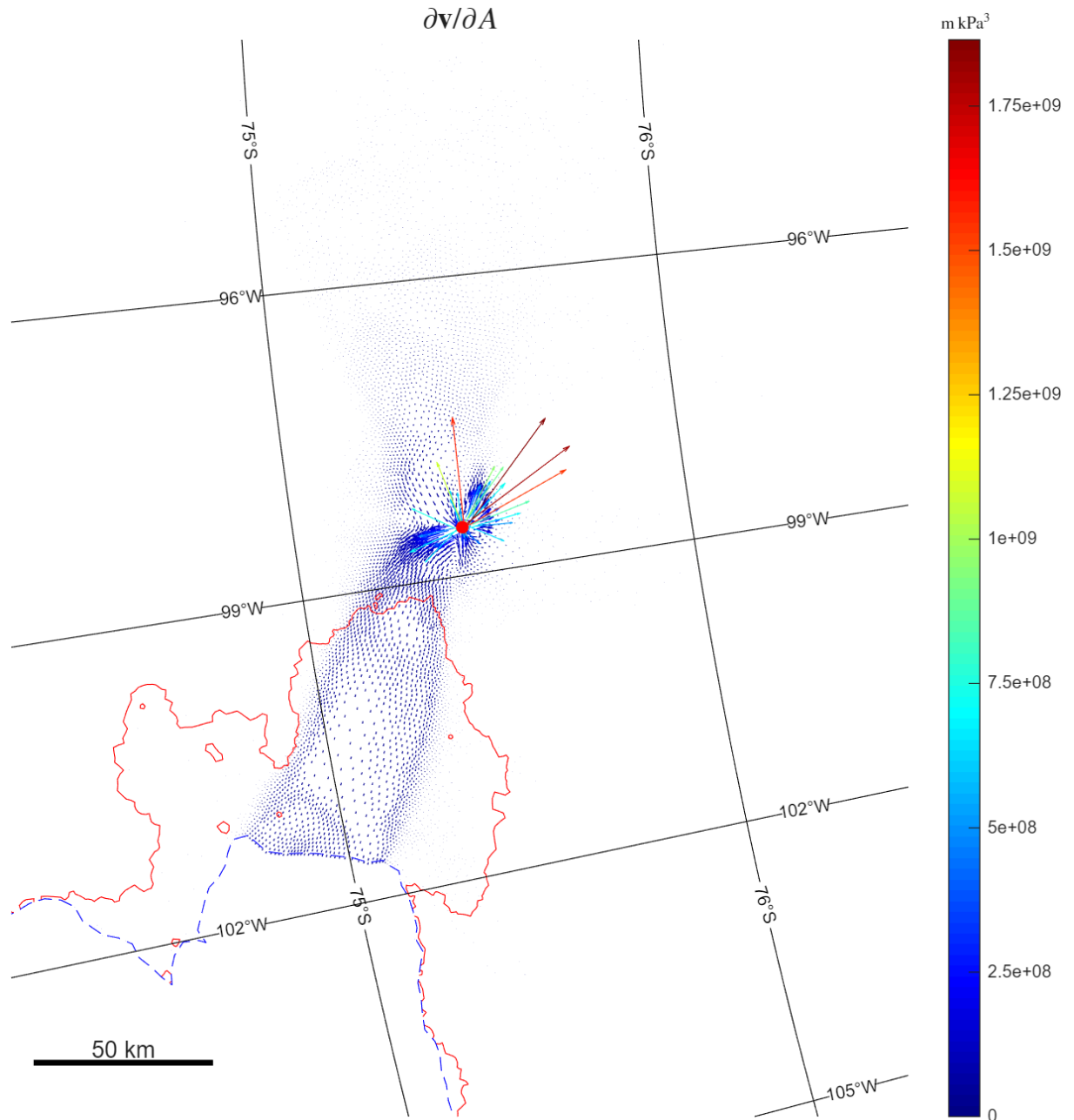


Figure 6.1: Sensitivities of velocities to changes in A at one node. The full sensitivity matrix ξ was calculated solving Eq. (6.8), providing the sensitivity of all nodal velocities to any nodal A values. The FE mesh had 31,717 nodes and calculating the sensitivities took about 3 min. The examples is for Pine Island Glacier, West Antarctica.

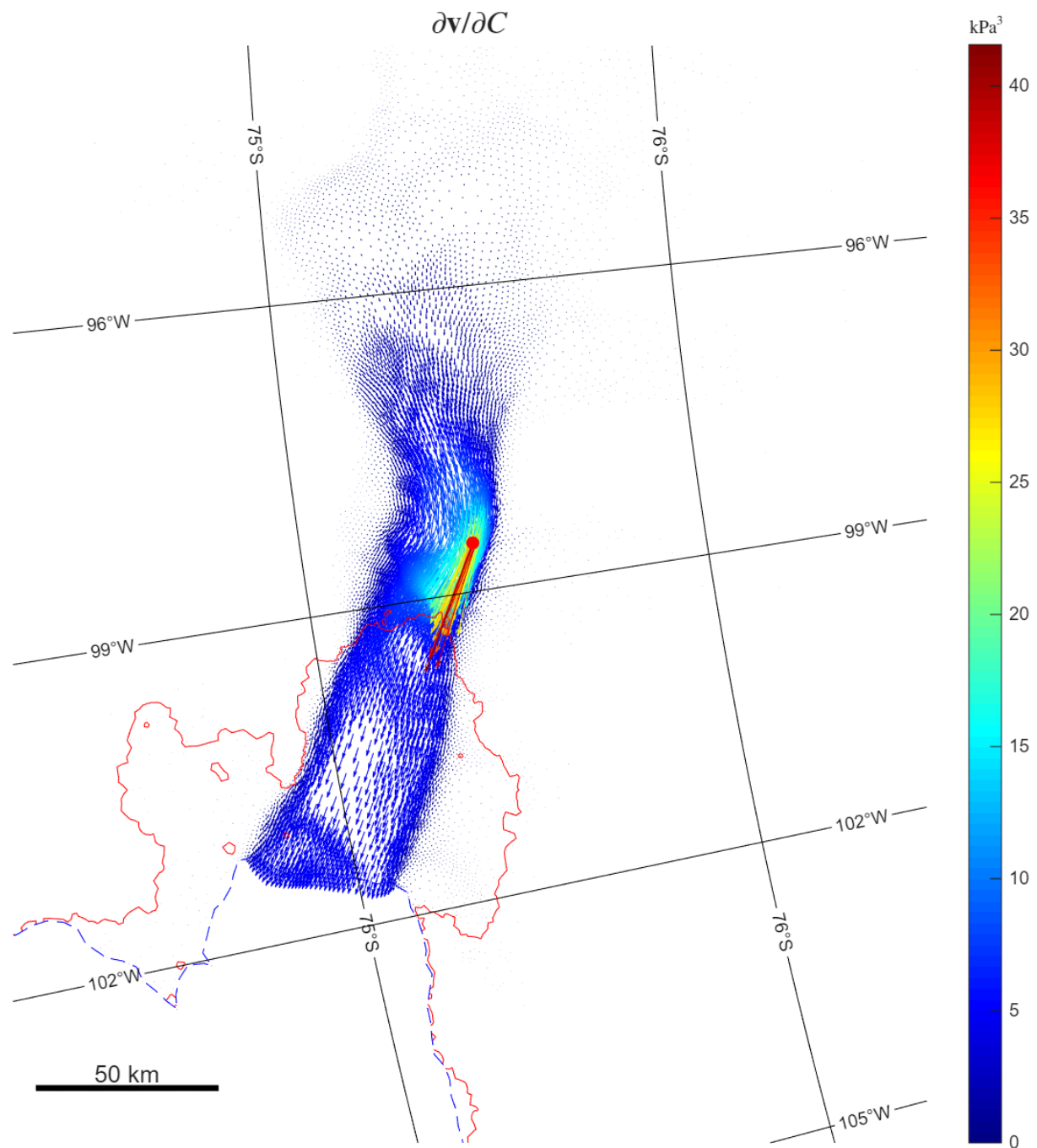


Figure 6.2: Sensitivities of velocities to changes in C at one node. See Fig. (6.1) for details.

Note that the value of λ is, as of yet, undetermined, as the term $\lambda^* F(q(p), q)$ is always zero, irrespective of the value of λ , since $F(q(p), p) = 0$. The key trick is now to set

$$\partial_q J + (\partial_q F)^* \lambda = 0 , \quad (6.13)$$

by solving for λ . Now the second term in (6.12) is zero, and find that now the derivative can be calculated without needing to know ξ as

$$d_p J = \partial_p J + \lambda^* \partial_p F , \quad (6.14)$$

which only requires one solve.

For notational simplicity the formulation above was provided for the discrete version of the problem where F is a vector. When F is a differential operator we must write

$$\mathcal{L}_1(q(p), p, \lambda) = J(q(p), p) + \langle \lambda | F(q(p), q) \rangle , \quad (6.15)$$

and we determine the directional derivative of J with respect to p in some direction ϕ , that is

$$d_p J(p)[\phi] = \lim_{\varepsilon \rightarrow 0} \frac{d}{d\varepsilon} J(p + \varepsilon\phi) \quad (6.16)$$

where $\varepsilon \in \mathbb{R}$ with the gradient defined in terms of the directional derivative for a given inner product using Eq. (8), i.e. as

$$d_p J(p)[\phi] = \langle \nabla_p J | \phi \rangle . \quad (6.17)$$

The details are provided below.

6.1.2 Calculating the Hessian of the cost function J

Direct-Direct

The most straightforward approach to calculate the Hessian is by using Eq. (6.6). This involve determining

$$\frac{\partial q}{\partial p} ,$$

which, as we have discussed above, can be done using Eq. (6.2), but requires n_p solves, and then determine

$$\frac{\partial^2 q}{\partial p \partial p} ,$$

which can be done using Eq. (6.3), but requires on the order of $n_p \times n_p$ solves, although the symmetry of the matrix above, reduces the number of solves to $(n_p + 1) n_p / 2$. The total effort of the direct-direct approach is therefore $n_p + n_p (n_p + 1) / 2$ solves.

Adjoint-Adjoint

We can also calculate second-order derivatives of the cost function with respect to the model parameters, p , using the adjoint method (e.g. Papadimitriou and Giannakoglou, 2008; Pacaud et al., 2022). The key idea is to write the expression for the first-order derivative and again augment this expression with the constraints provided by the state equation

$$F(q(p), p) = 0$$

and now, additionally, by the first-order adjoint equation

$$(\nabla_q F)^* \lambda + \nabla_p J = 0 .$$

The first-order Lagrangian function is

$$\mathcal{L}_1 = J(q(p), p) + \lambda^* F(q(p), p) .$$

Let

$$G = (\nabla_q F)^* \lambda + \nabla_p J ,$$

and define

$$\mathcal{L}_2 = (\nabla_p \mathcal{L}_1)^* w + \mu^* F(q(p), p) + \nu^* G(q(p), p) ,$$

where μ and ν are two additional Lagrange multipliers, and w is a vector. We here interested in the Hessian action, i.e. in the product Hw where w is some vector. Taking derivatives of \mathcal{L}_2 and selecting μ and ν in such a way that term involving $\nabla_q \lambda$ and $\nabla_p \lambda$ are eliminated results in

$$\begin{aligned} \partial_q F \mu &= -(\partial_p F)^* w \\ (\partial_q F)^* \nu &= -(\partial_{pq}^2 J + \partial_{pq}^2 F \lambda) w - (\partial_{qq}^2 J + \partial_{pp}^2 F \lambda) \mu \\ Hw &= (\partial_{pp}^2 J + \partial_{pp}^2 F \lambda) w + (\partial_{pq}^2 J + \partial_{pq}^2 F \lambda) \mu + (\partial_q F)^* \nu \end{aligned}$$

This is the adjoint-adjoint approach for calculating the Hessian. Counting the number of solves in this system we see that the adjoint-adjoint approach requires $1 + 2n_p$ solves.

Direct-Adjoint

For the direct-adjoint approach we add to the Hessian

$$H := \frac{d^2 J}{dp dp} , \quad (6.5)$$

the (zero) term

$$\frac{d^2 F}{dp dp} = 0 \quad (6.18)$$

creating

$$H = \frac{d^2 J}{dp dp} + \Psi \frac{d^2 F}{dp dp} , \quad (6.19)$$

where Ψ is a new adjoint variable, which we are free to define in any suitable way without affecting the value of the Hessian H . We then insert

$$H = \frac{\partial^2 J}{\partial p \partial q} \frac{\partial q}{\partial p} + \frac{\partial^2 J}{\partial p \partial p} + \frac{\partial^2 J}{\partial p \partial q} \frac{\partial q}{\partial p} + \frac{\partial^2 J}{\partial q \partial q} \frac{\partial q}{\partial p} \frac{\partial q}{\partial p} + \frac{\partial J}{\partial q} \frac{\partial^2 q}{\partial p \partial p} \quad (6.6)$$

and

$$\frac{d^2 F}{dp dp} = \frac{\partial^2 F}{\partial p \partial p} + \frac{\partial^2 F}{\partial p \partial q} \frac{\partial q}{\partial p} + \frac{\partial^2 F}{\partial q \partial q} \frac{\partial q}{\partial p} \frac{\partial q}{\partial p} + \frac{\partial F}{\partial q} \frac{\partial^2 q}{\partial p \partial p} \quad (6.3)$$

and in the resulting expression eliminate

$$\frac{\partial^2 q}{\partial p \partial p} ,$$

by setting

$$\left(\frac{\partial F}{\partial q} \right)^* \Psi = -\frac{\partial J}{\partial q} . \quad (6.20)$$

This is the same adjoint-system that we solve in the 1st-order adjoint method. However, we additionally also do need to solve for the forward-model sensitivities, ξ ,

$$\frac{\partial F}{\partial q} \xi = -\frac{\partial F}{\partial p} , \quad (??)$$

which requires n_q solves. It total we need $n_q + 1$ solves, in addition to setting up the resulting system. The adjoint-adjoint approach requires $2n_q + 1$ solves, and the direct-adjoint approach is therefore about twice as efficient in terms of number of matrix solves required.

In a bit more detail, if the discrete forward problem is:

$$\mathbf{F}(\mathbf{q}(\mathbf{p}), \mathbf{p}) = \mathbf{0} \quad (6.21)$$

Then the sensitivity problem is:

$$\frac{\partial F_i}{\partial q_j} \xi_{jk} = -\frac{\partial F_i}{\partial p_k} \quad (6.22)$$

with the entries of the sensitivity matrix, ξ , defined as

$$\xi_{jk} := \frac{\partial q_j}{\partial p_k}. \quad (6.23)$$

The adjoint system is:

$$\left(\frac{\partial F_i}{\partial q_j} \right)^* \Psi_i = -\frac{\partial J}{\partial p_i} \quad (6.24)$$

And once these have been solved, the entries of the Hessian matrix are given by

$$\begin{aligned} H_{ij} &= \frac{\partial^2 J}{\partial p_i \partial p_j} + \Psi_n \frac{\partial^2 F_n}{\partial p_i \partial p_j} + \frac{\partial^2 J}{\partial q_k \partial q_m} \xi_{ki} \xi_{mj} + \Psi_n \frac{\partial^2 F_n}{\partial q_k \partial q_m} \xi_{ki} \xi_{mj} \\ &\quad + \frac{\partial^2 J}{\partial p_i \partial q_k} \xi_{kj} + \Psi_n \frac{\partial^2 F_n}{\partial p_i \partial q_k} \xi_{kj} + \frac{\partial^2 J}{\partial q_k \partial p_j} \xi_{ki} + \Psi_n \frac{\partial^2 F_n}{\partial q_k \partial p_j} \xi_{ki} \end{aligned}$$

There is an option in Úa to use the Hessian, however currently only selected terms in the above expression are evaluated. [Papadimitriou and Giannakoglou \(2008\)](#) provide an example of where omitting some of the above terms does not lead to significant deviations from the Hessian, based on comparison with brute-force finite differences estimate.

6.1.3 Brute force finite differences

Calculating the gradient and the Hessian of J using a brute-force finite differences is computationally infeasible for any large scale minimisation problem. However, for validation purposes it is important to be able to calculate selected elements of the gradient and the Hessian in this manner. This can be used to check the correctness of the adjoint implementation.

Various forward differences approximation can be used. Currently implemented for the gradient estimation are forward first order, forward second order, central second order, and central fourth order finite differences. For the Hessian one can use something like

$$H_{ii} \approx \frac{J(\mathbf{p} + \varepsilon \hat{\mathbf{e}}_i) - 2J(\mathbf{p}) - J(\mathbf{p} - \varepsilon \hat{\mathbf{e}}_i)}{\varepsilon^2}$$

for the diagonal elements, and

$$H_{ij} \approx \frac{J(\mathbf{p} + \varepsilon \hat{\mathbf{e}}_i + \varepsilon \hat{\mathbf{e}}_j) - J(\mathbf{p} + \varepsilon \hat{\mathbf{e}}_i - \varepsilon \hat{\mathbf{e}}_j) - J(\mathbf{p} - \varepsilon \hat{\mathbf{e}}_i + \varepsilon \hat{\mathbf{e}}_j) + J(\mathbf{p} - \varepsilon \hat{\mathbf{e}}_i - \varepsilon \hat{\mathbf{e}}_j)}{4\varepsilon^2}$$

for the off-diagonal elements. This requires a total of $2n_p + 4n_p(n_p - 1)/2 = 2n_p^2$, which for large n_p is generally not feasible.

If the adjoint calculation of the gradient

$$\mathbf{g} = \nabla J$$

is already verified, the Hessian can, for example using centred differences, be approximated using

$$H_{ij} \approx \frac{g_i(\mathbf{p} + \varepsilon \hat{\mathbf{e}}_j) - g_i(\mathbf{p} - \varepsilon \hat{\mathbf{e}}_j)}{2\varepsilon} \quad (6.25)$$

with $i = 1 \dots n_p$ and for each $i, j = i \dots n_p$. The adjoint approach enables us to calculate all the elements g_i , for $i = 1 \dots n_p$, in one forward solve. Therefore we can determine each column of the Hessian matrix in two solves, and the total Hessian in $2n_p$ solves. When solving the Newton system $H \Delta \mathbf{p} = -\mathbf{g}$, using iterative methods such as the conjugate gradient methods (H is symmetric and positive definite), we don't need to know the full Hessian but only the Hessian vector product (HVP), i.e. $H\mathbf{w}$ where \mathbf{w} is some vector. Then we can, for example using forward differences, approximate

$$H\mathbf{w} \approx \frac{\mathbf{g}(\mathbf{p} + \varepsilon \mathbf{w}) - \mathbf{g}(\mathbf{p})}{\varepsilon}$$

for ε sufficiently small.

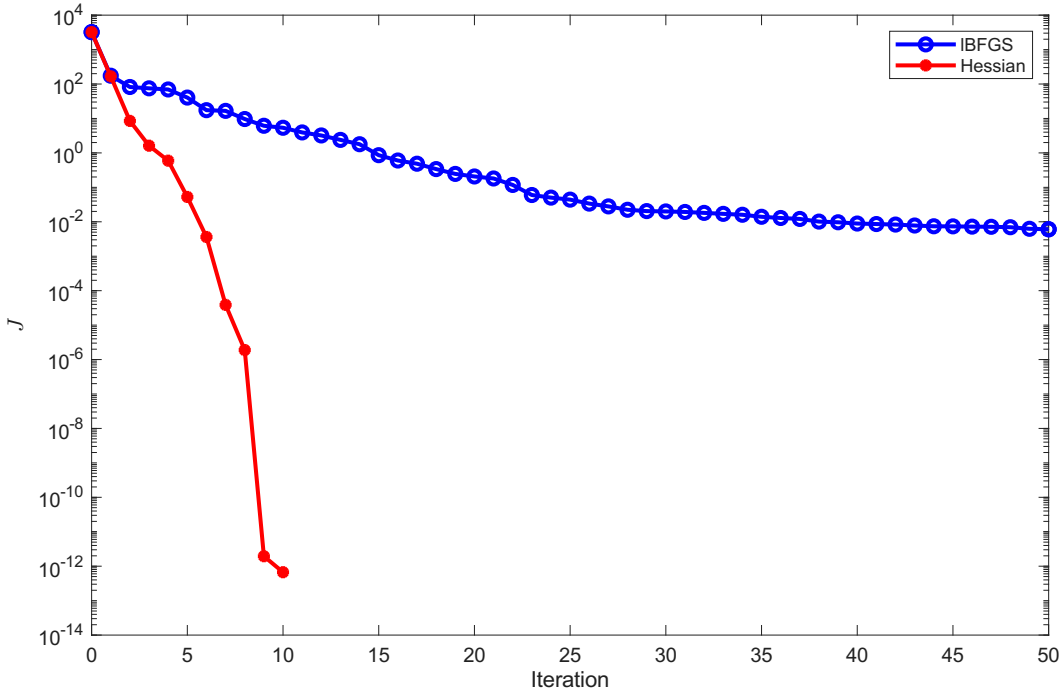


Figure 6.3: Comparison between an inversion using the Hessian and the LBFGS methods. The function J is the cost function. This example was done for a relatively small problem where calculating the full Hessian using brute-force was feasible, using finite-differences of the gradient as shown in Eq. (6.25).

6.2 General inverse methodology

Bayesian framework provides a general methodology for inverse problems. The inverse problem we like to solve is that of determining some model parameters, p , given some measurement data, d . Solving an inverse problem is to determine the conditional distribution

$$P(p|q)$$

that is, we want to determine the probability distribution for our model parameters, p , given our measurement data, q_{meas} , which we can think of as an estimate of q , and where we have a forward model, f , providing a functional relationship between the model parameters and the data

$$q = f(p) .$$

More generally we can write the forward model as

$$q(x, t) = f(x, t_0; p)$$

to stress the fact that the model output is a function of space, x , and variable with time, t . When running a transient model we start the run at $t = t_0$.

If our model is perfect, the measurements error free and we are using the perfectly correct values for all the model parameters p , our model output will match the measurements perfectly. More realistically our data will have some errors and we write

$$\hat{q} = q + \epsilon$$

where \hat{q} are our measurements and q are the (unknown to us) error free data. Similarly, we may have some prior estimates for the model parameters. We can think of these as measurements of p with some associated errors and write

$$\tilde{p} = p + \epsilon$$

where \tilde{p} are our measurements (prior estimates) of the model parameters, and p are the corresponding 'true' values. Finally, the forward model might be inexact and we write

$$\tilde{f} = f + \epsilon$$

where \tilde{f} is the forward model we are using, and f the perfectly correct (and unknown to us) forward model.

Specifying the error structure of \hat{q} and \tilde{p} can be either easy or difficult depending on the situation. Typically ϵ might be assumed to be a Gaussian process with some covariance, i.e. $P(x) = \mathcal{N}(x|\tilde{x}, \Sigma)$, and this now introduces new covariance parameters.

We can think of the inverse model as a *retrieval function* \mathcal{R} which gives us an estimate, \hat{p} , for the model parameters given our measurement data, prior estimates of the model parameters and our description of all associated errors,

$$\hat{p} = \mathcal{R}(f, \hat{q}, \tilde{p}, \mu)$$

Here μ are parameters of our error models. For example if we assume Gaussian normal distribution of errors μ would be a vector with two elements, the elements being the mean and the variance.

The Bayesian theorem

$$P(p|q) = \frac{P(q|p) P(p)}{P(q)} \quad (6.26)$$

is a basic statement about conditional probabilities. Here it allows us to 'invert' the conditional probability $P(q|d)$ and write it in terms of $P(d|p)$ which, given the relation $q = f(p)$, can be done by solving the forward model for a given p .

The Bayesian posterior

$$P(p|q)$$

is the *prior*

$$P(p)$$

multiplied by the the *likelihood* of the evidence

$$P(q|p)$$

and divided by the 'commonness' of the evidence

$$P(q)$$

that is, the *marginal likelihood*, where

$$P(q) = \int_p P(q|p) P(p) dp .$$

The marginal likelihood is a normalising factor in the Bayesian theorem Eq. (6.26) ensuring that $\int_p P(p|q) dp = 1$. (It can be argued that the term marginal likelihood is a misnomer in that it is not defined up to a multiplicative constant as is the case for the likelihood $P(p|q)$, and should more properly be referred to as the marginal probability of the data.)

The essence of the Bayes approach is the *update factor*

$$\frac{P(q|p)}{P(q)} .$$

This is our 'update' of the prior. The prior today is the posterior from yesterday, and the posterior today is the prior from yesterday multiplied by the likelihood of today's evidence, divided by the commonness of that evidence. This update factor can be particularly large if, for example, the overall probability/occurrence of q , (i.e. $P(q)$) is low, but in comparison the probability of obtaining the data q for a given parameter value p (i.e. $P(q|p)$) is high.

Ideally we would like to determine the posterior distribution, $P(x|y)$, but computational limitations might force us to only calculate some of its aspect such as its maximum with respect to x , i.e. the *maximum a posteriori* (MAP) estimate of x .

$$p_{\text{MAP}} = \arg \max_p P(p|q) .$$

If we are only interested in the general shape of $P(p|q)$ as a function of p we do not need to estimate the marginal likelihood, $P(q)$, as it is not dependent of p . Our primary focus is then to determine the likelihood, $P(q|p)$, and the prior, $P(p)$.

6.2.1 Example of Bayesian estimation

To clarify some of the concepts that follow we give a quick summary of Bayesian analysis of a linear model f where

$$f(x) = \sum_1^n f_q \phi_q(x) \quad (6.27)$$

or for any location $x = x^*$

$$f(x_*) = \boldsymbol{\phi}(x_*)^T \mathbf{f}$$

We would like to determine the n coefficients f_q from m available measurements y_q taken at the locations x_q , $q = 1 \dots m$ where

$$y = f(x) + \epsilon$$

and

$$\epsilon \sim \mathcal{N}(0, \sigma^2)$$

hence,

$$\begin{pmatrix} y_1 \\ y_2 \\ \vdots \\ y_m \end{pmatrix} = \begin{pmatrix} \phi_1(x_1) & \phi_2(x_1) & \cdots & \phi_n(x_1) \\ \phi_1(x_2) & \phi_2(x_2) & \cdots & \phi_n(x_2) \\ \vdots & \vdots & \ddots & \vdots \\ \phi_1(x_m) & \phi_2(x_m) & \cdots & \phi_n(x_m) \end{pmatrix} \begin{pmatrix} f_1 \\ f_2 \\ \vdots \\ f_n \end{pmatrix} + \begin{pmatrix} \epsilon \\ \epsilon \\ \vdots \\ \epsilon \end{pmatrix}$$

or

$$\mathbf{y} = \boldsymbol{\Phi} \mathbf{f} + \boldsymbol{\epsilon} \quad (6.28)$$

where \mathbf{y} is the *measurement vector*. Our objective is to determine the vector \mathbf{f} from our measurements \mathbf{y} given our forward model expressed by Eq. (6.28) and $\boldsymbol{\Phi} \in \mathbb{R}^{m \times n}$.

The Bayesian approach to this is to determine

$$P(\mathbf{f}|\mathbf{y}) = \frac{P(\mathbf{y}|\mathbf{f})P(\mathbf{f})}{P(\mathbf{y})}$$

The data errors are assumed to be Gaussian white noise

$$\mathbb{E}[\epsilon(x)\epsilon(x')] = \sigma^2 \delta(x - x')$$

where \mathbb{E} is the expectation operator i.e. $\epsilon \sim \mathcal{N}(0, \sigma^2)$. The *noise model* or the *likelihood* is then

$$P(\mathbf{y}|\mathbf{f}) = \mathcal{N}(\boldsymbol{\Phi} \mathbf{f}, \sigma^2 \mathbf{I})$$

which we can see as follows

$$\begin{aligned} P(\mathbf{y}|\mathbf{f}) &= \prod_{i=1}^n P(y_i|\mathbf{f}) \\ &= \prod_{i=1}^n \frac{1}{\sqrt{2\pi}\sigma} e^{-\frac{(y_i - [\boldsymbol{\Phi}]_{ij}f_j)^2}{2\sigma^2}} \\ &= \frac{1}{\sqrt{2\pi}\sigma} e^{-\frac{\|\mathbf{y} - \boldsymbol{\Phi} \mathbf{f}\|^2}{2\sigma^2}} \\ &= \mathcal{N}(\boldsymbol{\Phi} \mathbf{f} | \sigma^2 \mathbf{I}) \end{aligned}$$

We now need to specify the prior. There are many options available to us. Sometimes a prior is set on the coefficients \mathbf{f} and these are then thought of as 'weights'. This approach is often used in linear regression and then referred to as *ridge regression*. A more common approach in inverse methodology is to set a prior on the function $f(x)$ itself.

Prior on function coefficients (ridge regression)

We put a zero mean Gaussian prior with the covariance matrix K_p on the expansion coefficients \mathbf{f}

$$\mathbf{f} \sim \mathcal{N}(0, K_a)$$

and obtain for

$$\begin{aligned} P(\mathbf{f}|\mathbf{y}) &\propto e^{-\frac{\|\mathbf{y}-\Phi\mathbf{f}\|^2}{2\sigma^2}} e^{-\frac{1}{2}\mathbf{f}^T K_a^{-1} \mathbf{f}} \\ &\propto e^{-\frac{1}{2}(\mathbf{f}-\bar{\mathbf{f}})^T \hat{\mathbf{K}}(\mathbf{f}-\bar{\mathbf{f}})} \end{aligned}$$

where

$$\begin{aligned} \hat{\mathbf{f}} &= \sigma^{-2} (\sigma^{-2} \Phi^T \Phi + K_a^{-1})^{-1} \Phi^T \mathbf{y} \\ \hat{\mathbf{K}} &= (\sigma^{-2} \Phi^T \Phi + K_a^{-1})^{-1} \end{aligned}$$

for the posterior distribution where $\hat{\mathbf{K}}$ is the posterior covariance matrix.

We can generalise these expressions to include the case of a general covariance K_ϵ rather than $K_\epsilon = \sigma^2 \mathbf{1}$ as done above) for the data errors, and non zero mean value for f , i.e.

$$\begin{aligned} \dot{\epsilon} &\sim \mathcal{N}(\mathbf{0}, K_\epsilon) \\ \mathbf{f} &\sim \mathcal{N}(\mathbf{f}_a, K_a) \end{aligned}$$

and obtain²

$$\begin{aligned} \hat{\mathbf{f}} &= \mathbf{f}_a + (\Phi^T K_\epsilon^{-1} \Phi + K_a^{-1})^{-1} \Phi^T K_\epsilon^{-1} (\mathbf{y} - \Phi \mathbf{f}_a) \\ &= \mathbf{f}_a + K_a \Phi^T (\Phi K_a \Phi + K_\epsilon)^{-1} (\mathbf{y} - \Phi \mathbf{f}_a) \\ \hat{\mathbf{K}} &= (\Phi^T K_\epsilon^{-1} \Phi + K_a^{-1})^{-1} \\ &= K_a - K_a \Phi^T (\Phi K_a \Phi^T + K_\epsilon)^{-1} \Phi K_a . \end{aligned}$$

Note that \mathbf{f} , $\hat{\mathbf{f}}$ and \mathbf{f}_a are coefficients or weights in the expansion for $f(x)$ given by Eq. (6.27) and that $f(x)$ at a given location $x = x_*$ is given by

$$f(x_*) = \phi_*^T \mathbf{f}_a + \phi_*^T K_a \Phi^T (\Phi K_a \Phi + K_\epsilon)^{-1} (\mathbf{y} - \Phi \mathbf{f}_a) ,$$

where

$$\phi_* := \phi(x_*) .$$

6.3 Sparse precision matrices

In \tilde{U} the likelihood is assumed to be on the form

$$P(q|p) = \mathcal{N}(p|\hat{p}, \Sigma) := (2\pi)^{-N/2} |\mathbf{Q}_I|^{1/2} e^{-\frac{1}{2}(\hat{\mathbf{q}} - \mathbf{f}(\mathbf{p}))^T \mathbf{Q}_I (\hat{\mathbf{q}} - \mathbf{f}(\mathbf{p}))} , \quad (6.29)$$

where $q = f(p)$ and \hat{q} are measurements of q , and similarly for the prior

$$P(p) = \mathcal{N}(p|\tilde{p}, \Sigma) := (2\pi)^{-N/2} |\mathbf{Q}_R|^{1/2} e^{-\frac{1}{2}(\mathbf{p} - \tilde{\mathbf{p}})^T \mathbf{Q}_R (\mathbf{p} - \tilde{\mathbf{p}})} , \quad (6.30)$$

where the *precision matrices* \mathbf{Q}_I and \mathbf{Q}_R is defined as the inverse of the corresponding covariance matrices, i.e.

$$\mathbf{Q} = \Sigma^{-1} .$$

²Also note that if $\mathbf{f}_a = \mathbf{0}$ and $K_a \rightarrow \infty$ we get the usual least-squares estimate

$$\begin{aligned} \hat{\mathbf{f}} &= (\Phi^T \Phi)^{-1} \Phi^T \mathbf{y} \\ \hat{\mathbf{K}}^{-1} &= \Phi^T K_\epsilon^{-1} \Phi . \end{aligned}$$

These are both Gaussian processes but with different precision matrices.³

Typically the covariance is written as a sum of two terms, uncorrelated noise component and a spatially correlated component. We might for example assume that the only contribution to the covariance of the likelihood $P(y|x)$ are the measurements errors, that is

$$\text{cov}(\hat{q} - f(p)) = \text{cov}(q - \epsilon - q) = \text{cov}(\epsilon)$$

This assumes that the model is perfect, i.e. $\text{cov}(q - f(p)) = 0$. If, on the other hand, the data is perfect but the model is not, the resulting *structural errors* might be expected to be spatially correlated. We now need to select a covariance function which is both flexible enough to describe this correlation realistically, and at the same time results in a sparse precision matrix.

Currently in *Úa*, and as described in more detail in a following section, the precision matrices are specified as a sum of uncorrelated and correlated errors. For uncorrelated errors the precision matrix is

$$\mathbf{Q} = \boldsymbol{\epsilon}^{-1} \mathbf{M} \boldsymbol{\epsilon}^{-1}$$

where \mathbf{M} is the mass matrix. The correlated error component is modelled using a Matérn covariance, where the precision matrix is

$$\mathbf{Q} = \kappa^2 \mathbf{M} + \mathbf{D}. \quad (6.31)$$

Here \mathbf{D} is the stiffness matrix and κ^2 a parameter that can be related to the correlation length. These precision matrices are automatically sparse in the FE basis.

Furthermore, currently in *Úa*, and as is for in large-scale geophysical inverse problems, one does not calculate the distribution

$$P(p|q) \propto P(q|p)P(p)$$

Instead, by taking the negative log we arrive at

$$J = \gamma_1(\hat{q} - f(p))Q_I(\hat{q} - f(p)) + \gamma_2(p - \tilde{p})Q_p(p - \tilde{p})$$

and this cost function J is then minimised with respect to p using a gradient-based optimisation method where the gradient is calculated in a computationally efficient manner using the adjoint method. Here Q_I is the precision matrix of the likely hood, and Q_R the precision matrix for the prior. The two terms above are often referred to as the misfit and the regularisation term, respectively. The MAP estimate is then

$$p_{\text{MAP}} = \arg \max_p J(p)$$

More precisely

$$-\log P(\mathbf{d}|\mathbf{p}) = \frac{N}{2} \log 2\pi + \frac{1}{2} \log |\mathbf{Q}_I| + \frac{1}{2}(\hat{\mathbf{q}} - \mathbf{f}(\mathbf{p}))^T \mathbf{Q}_I (\hat{\mathbf{q}} - \mathbf{f}(\mathbf{p})),$$

and

$$-\log P(\mathbf{p}) = \frac{N}{2} \log 2\pi + \frac{1}{2} \log |\mathbf{Q}_R| + \frac{1}{2}(\tilde{\mathbf{p}} - \mathbf{p})^T \mathbf{Q}_R (\tilde{\mathbf{p}} - \mathbf{p}),$$

or

$$-\log P(\mathbf{p}|\mathbf{d}) = \underbrace{\frac{1}{2}(\hat{\mathbf{q}} - \mathbf{f}(\mathbf{p}))^T \mathbf{Q}_I (\hat{\mathbf{q}} - \mathbf{f}(\mathbf{p}))}_{I} + \underbrace{\frac{1}{2}(\tilde{\mathbf{p}} - \mathbf{p})^T \mathbf{Q}_R (\tilde{\mathbf{p}} - \mathbf{p})}_{R} + \frac{1}{2} \log |\mathbf{Q}_I| + \frac{1}{2} \log |\mathbf{Q}_R| + N \log 2\pi$$

and the cost-function is defined as

$$J = I + R$$

³If we have two estimates of the same quantity each with their own PDF, then the joint PDF is simply the product

$$\begin{aligned} P(\mathbf{f}) &\propto e^{-\frac{1}{2}\mathbf{f}^T \mathbf{K}_1^{-1} \mathbf{f}} e^{-\frac{1}{2}\mathbf{f}^T \mathbf{K}_2^{-1} \mathbf{f}} \\ &= e^{-\frac{1}{2}\mathbf{f}^T (\mathbf{K}_1^{-1} + \mathbf{K}_2^{-1}) \mathbf{f}} \end{aligned}$$

and therefore the joint covariance is

$$\mathbf{K}_{1+2} = (\mathbf{K}_1^{-1} + \mathbf{K}_2^{-1})^{-1}$$

or in terms of precision matrices

$$\mathbf{Q}_{1+2} = \mathbf{Q}_1 + \mathbf{Q}_2$$

so in this context we can simply add precision matrices.

The precision matrices will depend on a number of parameters and we refer to these as *hyper parameters*. We lump all these hyper-parameters into a vector $\boldsymbol{\mu}$

Including the hyper-parameters, the posterior over the model parameters p is

$$P(\mathbf{p}|\mathbf{q}, \boldsymbol{\mu}) = \frac{P(\mathbf{q}|\mathbf{p})P(\mathbf{p}|\boldsymbol{\mu})}{P(\mathbf{q}|\boldsymbol{\mu})}$$

where

$$P(\mathbf{q}|\boldsymbol{\mu}) = \int P(\mathbf{q}|\mathbf{p})P(\mathbf{p}|\boldsymbol{\mu}) d\mathbf{p}$$

is the marginal likelihood or the *evidence*. We can now use Bayes theorem again and write the posterior over the hyper-parameters as

$$P(\boldsymbol{\mu}|\mathbf{q}) = \frac{P(\mathbf{q}|\boldsymbol{\mu})P(\boldsymbol{\mu})}{P(\mathbf{q})}$$

6.4 Inversion in $\tilde{U}a$

Using the inverse capabilities of $\tilde{U}a$ it is possible to invert for A and/or C , and bed geometry (B) using measurements of horizontal surface velocities (u_s, v_s) and/or rates of thickness changes ($\partial_t h$). One can invert jointly for A and C or any combination thereof such as $\log A$ and $\log C$. But currently joint inversion with B are not implemented. When inverting for A and C , regularisation can be applied on A , C or $\log A$ and $\log C$. Again here all combinations are possible, so one can, for example, invert for $\log A$ and $\log C$ with regularisation applied on A and $\log C$, if one so prefers. Typical use involves inverting for $\log A$ and $\log C$ simultaneously with regularisation applied on $\log A$ and $\log C$. When inverting for B , regularisation is applied on B . Note that regularisation is always applied on the difference between p and its prior \tilde{p} , i.e. on $p - \tilde{p}$. In addition, strict limits can put on the range of the control parameter p . One can, for example, but strict upper and lower limits on B at each location.

One can invert for A and C either over nodes or over elements. Typically inversion is done over nodes. Inversion for B is done over nodes only.

The forward model is the SSTREAM momentum equation. Note that if one includes h as measurements, in effect, the mass balance equation is used as well. It is a question of viewpoint if the forward model then includes the mass conservation in addition to the conservation of momentum, or just the momentum equation with the mass conservation used to calculate h as a part of the evaluation of the cost function. Both viewpoints are mathematically equivalent.

6.5 Objective functions

The objective function, J , is a sum of (squared) distances between a) measurements and model outputs (data misfit, I), and b) the parameter values and the priors (regularisation, R), i.e.

$$J = \underbrace{\|q - \hat{q}\|^2}_I + \underbrace{\|p - \tilde{p}\|^2}_R .$$

In $\tilde{U}a$ the objective function J is dimensionless.

Conceptually, and depending on the situation, we might think quite differently about I and R . But these two terms are in some ways also quite similar: Both can be thought of as measures of the distances from model outputs and model parameters to measurements (\hat{q}) of the state variables (q) and measurements (\tilde{p}) of the model parameters (p), respectively.

The data misfit is the distance between model output and measurements and it could, for example, be measured as

$$I(f) = \|f\|^2 = \frac{1}{2\mathcal{A}} \iint f(x, y) \gamma(x, y, x', y') f(x', y') dx dy dx' dy', \quad (6.32)$$

where $\gamma(x, y, x', y')$ is the covariance kernel and \mathcal{A} is the domain area. Defined in this manner, I is dimensionless. In the particular case of uncorrelated fields $\gamma(x, y, x', y') = c \delta(x - x') \delta(y - y')$

$$I = \frac{1}{2\mathcal{A}} \int (f(x, y)/e(x, y))^2 dx dy, \quad (6.33)$$

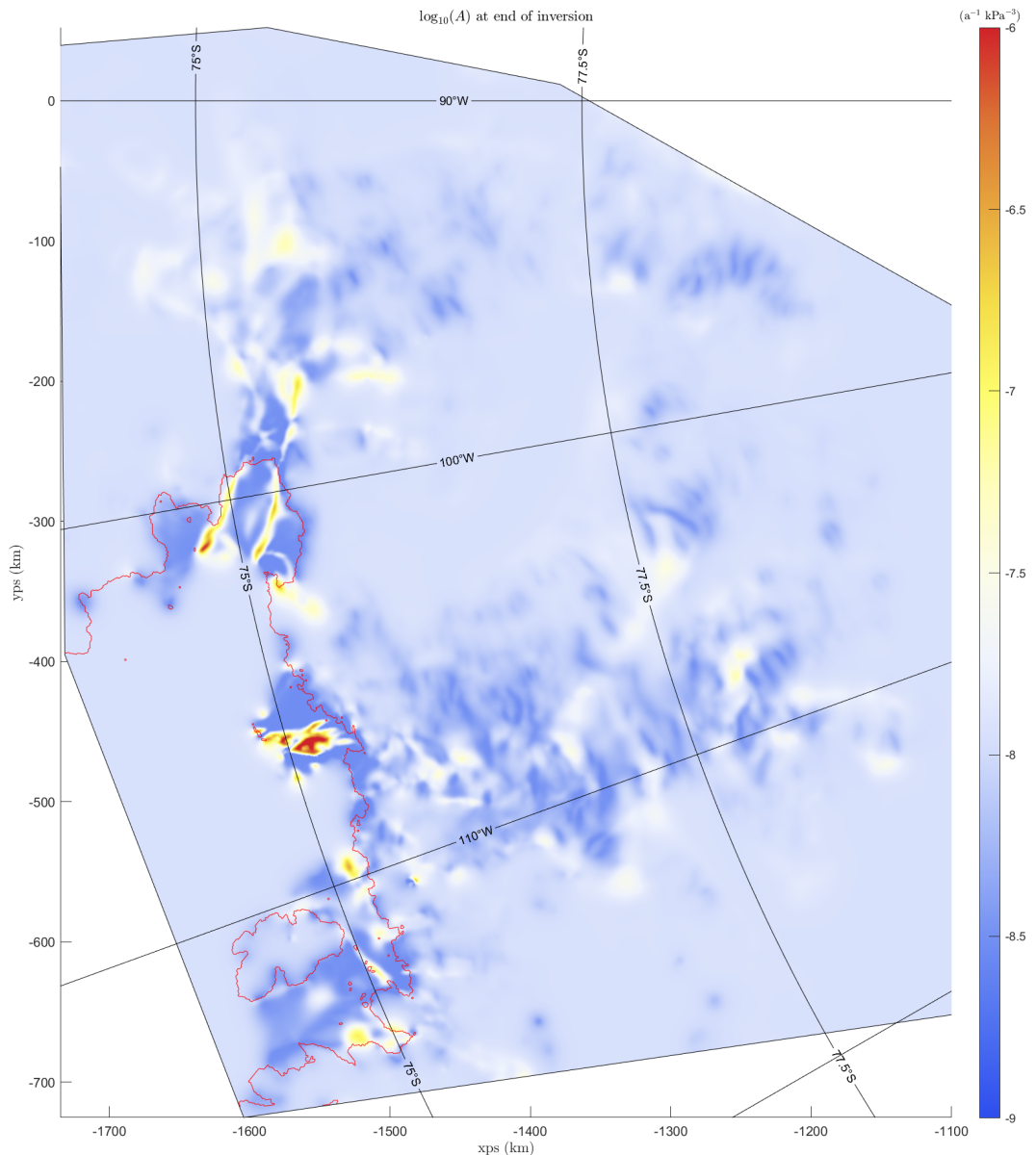


Figure 6.4: Example of an estimated A distribution over section of West Antarctica for $n = 3$. Here $\gamma_a = 1$ and $\gamma_s = 100,000$.

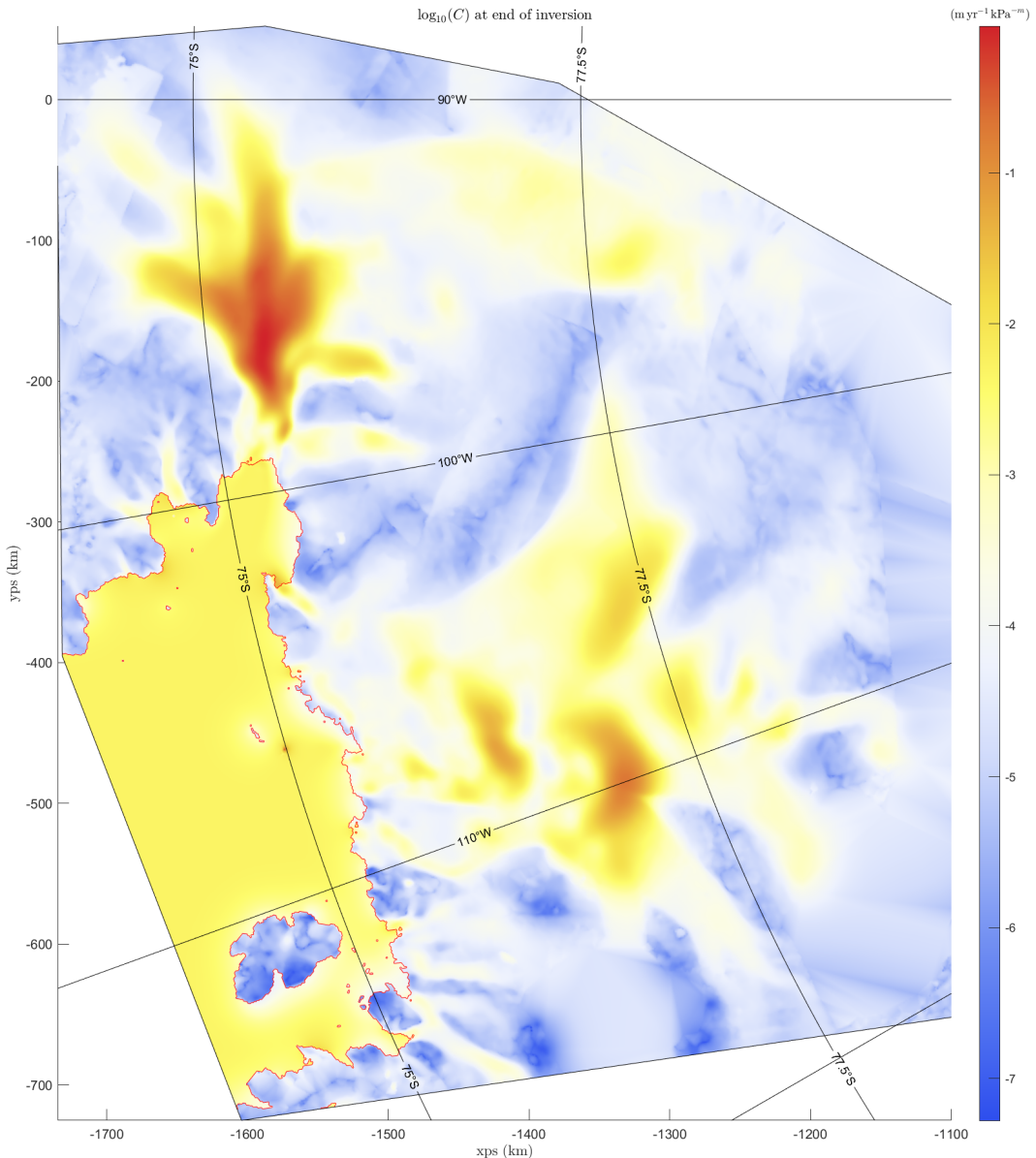


Figure 6.5: Example of an estimated C distribution over a section of West Antarctica using the Cornford sliding law with the stress exponent $m = 3$ and the coefficient of kinetic friction $\mu_k = 1/2$. Here $\gamma_a = 1$ and $\gamma_s = 100,000$.

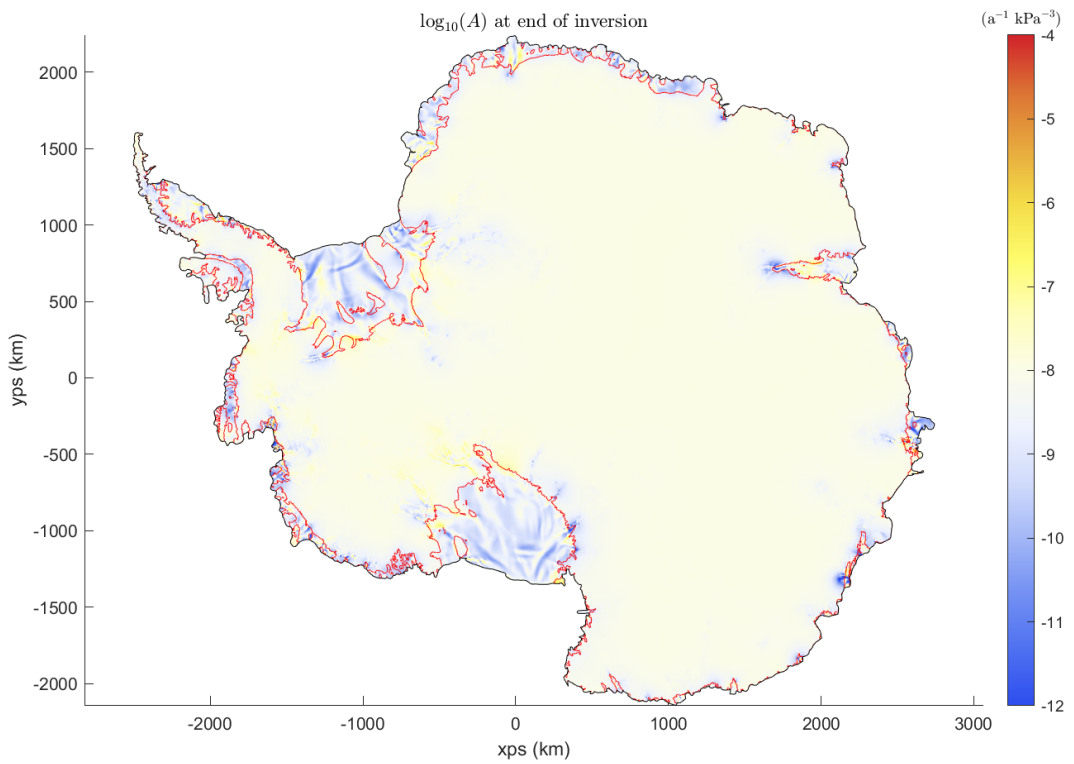


Figure 6.6: Example of an estimated A distribution for Antarctica for $n = 3$. Here $\gamma_a = 1$ and $\gamma_s = 100,000$.

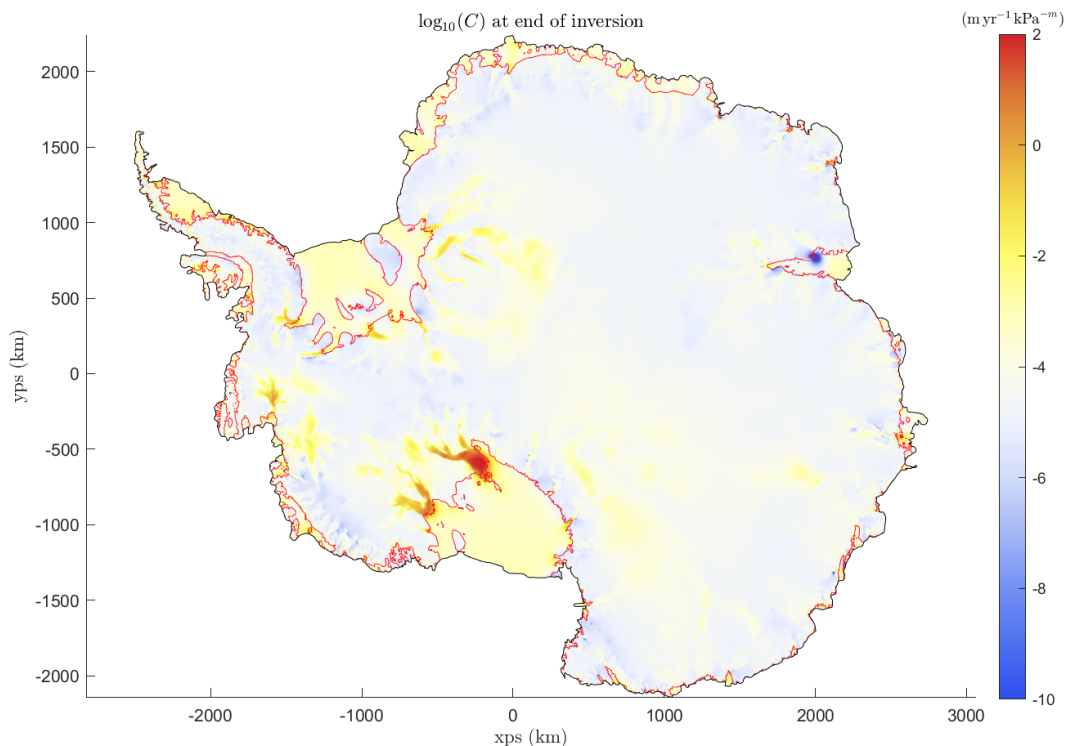


Figure 6.7: Example of an estimated basal slipperiness (C) distribution for Antarctica for Weertman sliding law where $m = 3$. Here $\gamma_a = 1$ and $\gamma_s = 10,000$.

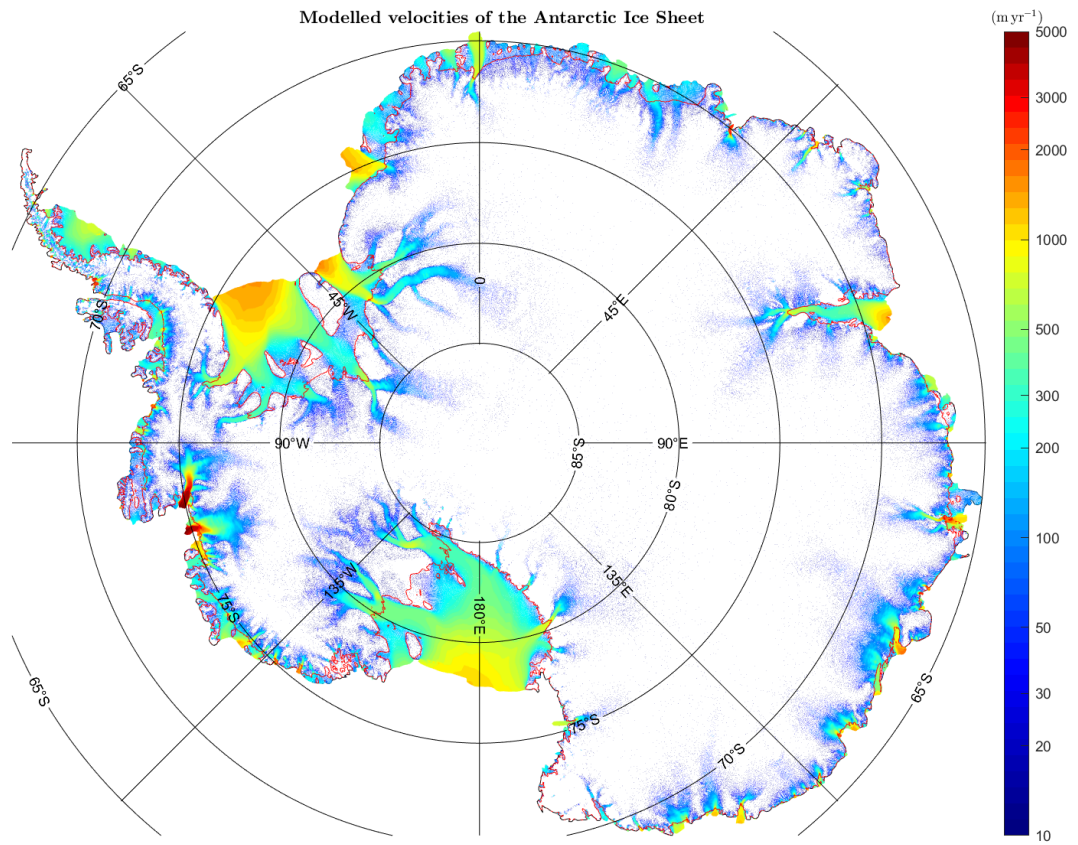


Figure 6.8: Modelled velocities for the A and C distributions in Figs. 6.6 and 6.7.

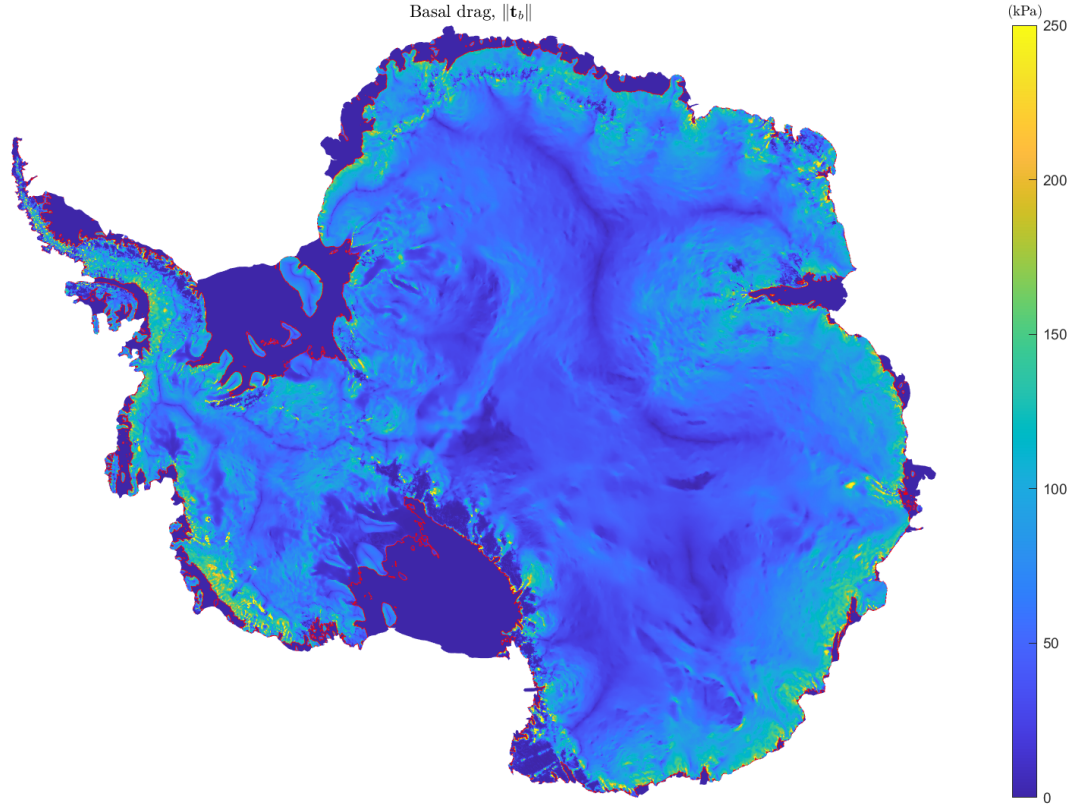


Figure 6.9: Modelled basal drag for Cornford sliding law given by Eq. (1.164) for $m = 3$ and $\mu = 1/2$, and perfect hydrological connection, Eq. (1.187), using the A and C distributions shown in Figs. 6.6 and 6.7.

Table 6.2: Notation used in inverse modelling (II)

Control variables	State variables	Priors	Measurements	Forward model
p	q	\tilde{p}	\hat{q}	$F(q(p), p) = 0$
$A, C, \log A, \log C$	u_s, v_s, \dot{h}	\tilde{A}, \tilde{C}	$\hat{u}_s, \hat{v}_s, \hat{\dot{h}}$	SSTREAM (SSA)
b, B	u_s, v_s, \dot{h}	\tilde{b}, \tilde{B}	$\hat{u}_s, \hat{v}_s, \hat{\dot{h}}$	SSTREAM (SSA)

where $e(x, y) = 1/\sqrt{c}$ are the data errors.

If \hat{q} denotes estimates of q then a typical misfit term might be on the form

$$I = \|q - \hat{q}\|^2 = \frac{1}{2\mathcal{A}} \int ((q - \hat{q})/e_u)^2 d\mathcal{A},$$

where e_u are measurement errors.

In Bayesian context the regularisation term has the same form as $I(f)$ and is a measure of the distance between the system state and the a prior. In a discrete form the misfit term could, for example, be written as

$$R = (\mathbf{p} - \tilde{\mathbf{p}})^T \boldsymbol{\Sigma}^{-1} (\mathbf{p} - \tilde{\mathbf{p}})$$

where $\boldsymbol{\Sigma}$ is a covariance matrix, \mathbf{p} the model parameters, and $\tilde{\mathbf{p}}$ the a prior estimates of those model parameters. Apart from often having only a very limited knowledge of the covariance matrix $\boldsymbol{\Sigma}$, problems with this formulation can, for example, arise if the inverse of $\boldsymbol{\Sigma}$ is not sparse. Practical reasons often influence the form of regularisation term. A pragmatic approach is to select a differential operator having a sparse representation. Preferable such a sparse operator is also the inverse of a ‘reasonable’ covariance matrix.

6.6 Misfit functions in $\dot{U}a$

Currently the misfit function I has the form

$$I = I_u + I_v + I_{\dot{h}}$$

or

$$\begin{aligned} I = & \frac{1}{2\mathcal{A}} \int ((u - u_{\text{meas}})/u_{\text{error}})^2 d\mathcal{A} \\ & + \frac{1}{2\mathcal{A}} \int ((v - v_{\text{meas}})/v_{\text{error}})^2 d\mathcal{A} \\ & + \frac{1}{2\mathcal{A}} \int ((\dot{h} - \dot{h}_{\text{meas}})/\dot{h}_{\text{error}})^2 d\mathcal{A} \end{aligned}$$

where u and v are the horizontal velocity components, and \dot{h} is the rate of thickness change, while

$$\mathcal{A} = \int d\mathcal{A},$$

is the total area.

The rate of thickness change is calculated as

$$\dot{h} = -(a - \partial_x(uh) - \partial_y(vh)),$$

and in the adjoint method the gradient of the cost function with respect to the state variable \mathbf{v} acquires an additional term:

$$2I = \|u - \hat{u}\|^2 + \|\dot{h}_d - (a - \partial_x(uh))\|,$$

or

$$I_{\dot{h}} = \frac{1}{2\mathcal{A}} \int \left((a - \partial_x(uh) - \partial_y(vh) - \dot{h}_{\text{meas}})/\dot{h}_{\text{error}} \right)^2 dx dy,$$

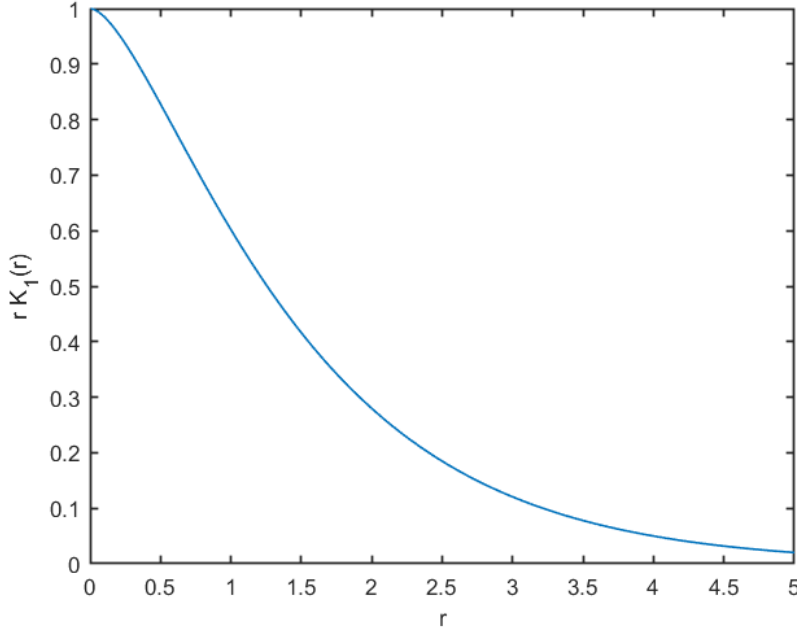


Figure 6.10: The function $rK_1(r)$ appearing in Eq. (6.39)

with the corresponding directional derivative with respect to u and v given by

$$\delta_{uv}I_h = \frac{1}{\mathcal{A}} \int \left((\dot{h} - \dot{h}_{\text{meas}})/\dot{h}_{\text{error}}^2 \right) (\partial_x(h\delta u) + \partial_y(h\delta v)) \, dx \, dy$$

which, like the cost function itself, is dimensionless.

6.7 Regularisation in $\tilde{U}\mathbf{a}$

In $\tilde{U}\mathbf{a}$ the regularisation can be done either using a Bayesian or Tikhonov regularisation.

6.7.1 Bayesian approach

Using this Bayesian formulation, the regularisation term for the (distributed) model parameter p has, has the discretised form

$$R = (\mathbf{p} - \tilde{\mathbf{p}})^T \Sigma_{pp}^{-1} (\mathbf{p} - \tilde{\mathbf{p}}), \quad (6.34)$$

where

$$\Sigma_{pp} = \text{cov}(\mathbf{p}, \mathbf{p})$$

where

$$\text{cov}(f, g) := \mathbb{E}((f - \mathbb{E}(f))(g - \mathbb{E}(g)))$$

where \mathbb{E} is the expectation operator. Generally our prior is here the expected value, and for the model parameter \mathbf{p} , the elements of the covariance matrix are then

$$[\Sigma_{pp}]_{ij} = \mathbb{E}(\mathbf{p}(\mathbf{r}_i) - \tilde{\mathbf{p}}(\mathbf{r}_i), \mathbf{p}(\mathbf{r}_j) - \tilde{\mathbf{p}}(\mathbf{r}_j)).$$

The Bayesian approach has a clear statistical interpretation, but, in general, requires an inversion of the covariance matrix Σ which can be impractical for large problems. In $\tilde{U}\mathbf{a}$ one can specify any covariance matrix Σ but in practice this is not a computationally feasible approach for large problems unless Σ is selected so that it has some computationally advantageous structure. One of the practical difficulties with directly prescribing a covariance matrix in the objective function is that the inverse of the resulting matrix is, in general, not sparse even if the matrix itself is sparse. For that reason the general Bayesian approach in $\tilde{U}\mathbf{a}$, where one specifies Σ directly, can only be used for fairly small problems.

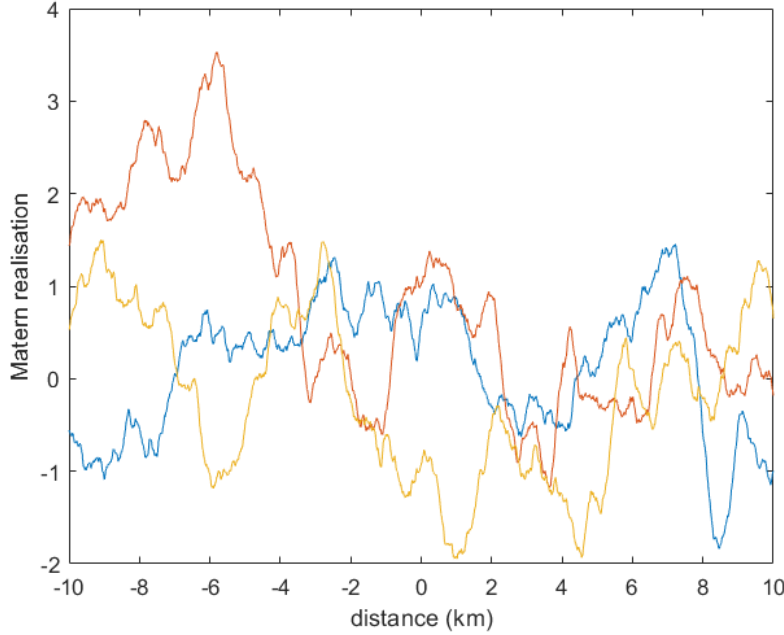


Figure 6.11: Three examples of Matérn realisations for $\rho = 3$ km, $\nu = 1$, $d=2$ and $\sigma = 1$.

A possible alternative approach is to limit the form of the covariance function to a form that allows for the construction of a sparse inverse directly within the FE context. For example consider the discretisation of the (self adjoint) Helmholtz equation

$$\mathcal{L}f(\mathbf{r}) = 0, \quad \mathbf{r} \in \mathbb{R}$$

where

$$\mathcal{L} := \nabla^2 - \kappa^2,$$

f is some scalar function, and k a wave number. This gives the inner-product induced norm

$$\|f\|^2 = \langle \mathcal{L}^{1/2}f | \mathcal{L}^{1/2}f \rangle \tag{6.35}$$

$$= \langle f | \mathcal{L} | f \rangle \tag{6.36}$$

$$= \mathbf{f}^T (\kappa^2 \mathbf{M} + \mathbf{D}) \mathbf{f} \tag{6.37}$$

and hence a precision matrix

$$\mathbf{Q} = \kappa^2 \mathbf{M} + \mathbf{D}, \tag{6.38}$$

which is by construction sparse. Note that minimising $\|f\|$ with respect to f results in the system

$$(\kappa^2 \mathbf{M} + \mathbf{D}) \mathbf{f} = \mathbf{0},$$

so $\|f\|$ is minimised when f is the solution to the Helmholtz equation.

The question is now what the resulting covariance looks like. Consider now a solution to the stochastic partial differential equation (here Helmholtz equation)

$$(\nabla^2 - \kappa^2)f(\mathbf{r}) = \epsilon(\mathbf{r}), \quad \mathbf{r} \in \mathbb{R}$$

where the innovation process $\epsilon(\mathbf{r})$ is a spatial Gaussian white noise. As shown by Whittle (1954), the auto-covariance is then

$$\text{cov}(f(\mathbf{r}_1), f(\mathbf{r}_2)) = \sigma^2 \kappa \|\mathbf{r}_2 - \mathbf{r}_1\| K_1(\kappa \|\mathbf{r}_2 - \mathbf{r}_1\|),$$

where the marginal variance is

$$\sigma^2 = \frac{1}{4\pi\kappa^2}$$

or

$$\text{cov}(f(\mathbf{r}_1), f(\mathbf{r}_2)) = \frac{\|\mathbf{r}_2 - \mathbf{r}_1\|}{4\pi\kappa} K_1(\kappa \|\mathbf{r}_2 - \mathbf{r}_1\|), \quad (6.39)$$

where K_1 is the modified Bessel function of the second kind and order one. Note that

$$\lim_{r \rightarrow 0} r K_1(r) = 1.$$

The shape of the covariance function (6.39) is shown in Fig. 6.10. As pointed out by Whittle (1954) the covariance function is similar to $e^{-\kappa r}$ but differs in that it is flat at the origin and its rate of decay slower.

The covariance shown above is a special case of the Matérn covariance function

$$r(x) = \frac{\sigma^2}{2^{\nu-1}\Gamma(\nu)} (\kappa x)^\nu K_\nu(\kappa x)$$

for $\alpha = 2$ and $\nu = \alpha - d/2 = 1$ for $d = 2$ where d is the number of spatial dimensions. As shown by Whittle (1954), and discussed and explained in great detail by Lindgren et al. (2011), the Matérn covariance function of a Gaussian process is a solution to the linear fractional stochastic partial differential equation

$$(\kappa^2 - \nabla^2)^{\alpha/2} f(x) = g(x), \quad x \in \mathbb{R}^d$$

where the $g(x)$ is a spatial Gaussian process with unit variance. Hence, for the Gaussian probability in Eq. (??) with a Matérn covariance function, the precision matrix in the FE basis is given by Eq. (6.38).

We can easily make this framework more flexible by allowing the coefficients in the Helmholtz equation to vary spatially, i.e. writing

$$\mathcal{L}f = \kappa^2 f - \nabla(a \nabla \cdot f),$$

where a and κ^2 are both functions of space. The FE formulation using

$$\begin{aligned} a(x, y) &= a_q \phi(x, y) \\ \kappa(x, y) &= k_q \phi(x, y) \end{aligned}$$

then gives the Galerkin system

$$\begin{aligned} 0 &= -\langle (\nabla((a_r \nabla \phi_r) f_p \phi_p) + (k_s \phi_s)^2 f_p \phi_p | \phi_q \rangle \\ &= \langle (a_r \phi_r) f_p \nabla \phi_p | \nabla \phi_q \rangle + \langle (k_s \phi_s)^2 f_p \phi_p | \phi_q \rangle \\ &= \langle (a_r \phi_r) \nabla \phi_p | \nabla \phi_q \rangle f_p + \langle (k_s \phi_s)^2 \phi_p | \phi_q \rangle f_p \\ &= [\tilde{\mathbf{D}}]_{pq} f_q - [\tilde{\mathbf{M}}]_{pq} f_p \end{aligned}$$

where the last line defines the elements of the matrices $\tilde{\mathbf{D}}$ and $\tilde{\mathbf{M}}$. Hence

$$\langle f | \mathcal{L} | f \rangle = \mathbf{f}^T (\tilde{\mathbf{D}} + \tilde{\mathbf{M}}) \mathbf{f}$$

In the particular case when $a_q = 1$ and $k_q = \kappa$ for all q , we have $a_q \phi_q = 1$ and $k_q^2 \phi_1 = \kappa$ and $\tilde{\mathbf{M}} = \mathbf{M}$ and $\tilde{\mathbf{D}} = \mathbf{D}$.

We might also imagine a situation where we have 'direct' estimates of the parameter p . For example if we are inverting for the bedrock B (i.e. $p = B$) we might have some 'direct' estimates based on radar soundings, seismic or gravity measurements. We of course quickly get rid of all estimates based on gravity measurements, but we should at least consider the possibility that seismic and radar data may provide

If our prior for p is $P(p)$ before we obtain the data \hat{p} , and $P(\hat{p}|p)$ is the likelihood of the data given p , then updated estimate for p after having seen the data is

$$P(p|\hat{p}) \propto P(\hat{p}|p)P(p)$$

If the measurements are unbiased and uncorrelated, the discretised covariance matrix between the measurements \hat{p} and the p is diagonal and the combined covariance on the form

$$\text{cov}(\hat{p}_i, p_j) = [\Sigma_{BB}]_{ij} + \sigma_i^2 \delta_{ij} \quad (\text{no summation implied})$$

In the finite-element basis this gives us a precision matrix \mathbf{P} on the form

$$\mathbf{P} = \gamma_a \mathbf{M} + \gamma_s (\mathbf{D}_x + \mathbf{D}_y) + \sigma^2 \mathbf{M} \quad (6.40)$$

if the constants γ_a , γ_s , and the measurement error σ are all spatially constant. As shown above, a similar equation is arrived at for spatially variable γ_a , γ_s , and σ .

6.7.2 Tikhonov regularisation

Instead of using the statistical Bayesian framework, one can use the arguably more pragmatic Tikhonov regularisation approach where one, for example, penalises amplitude and/or slope writing

$$R = \gamma_a^2 \|p - \tilde{p}\| + \gamma_s^2 \|\nabla(p - \tilde{p})\|$$

or

$$R = \frac{1}{2\mathcal{A}} \int \left(\gamma_s^2 (\nabla(p - \tilde{p}))^2 + \gamma_a^2 (p - \tilde{p})^2 \right) d\mathcal{A} \quad (6.41)$$

with the s and a subscripts being mnemonics for slope and amplitude, respectively. The parameter γ_a has the inverse dimension of p , and the dimension of γ_s is length times the inverse dimensional of p , i.e.

$$\begin{aligned} [\gamma_a] &= \frac{1}{[p]} \\ [\gamma_s] &= \frac{[l]}{[p]} . \end{aligned}$$

As is presumably already clear from the above expression, this type of Tikhonov regularisation and the Bayesian approach using the Matérn covariance are almost identical and the difference in many ways just a question of semantics.

The inversion can be done directly with respect to the variable p , or with respect to the logarithm of the variable, i.e. $\log_{10} p$. If done with respect to the logarithm of p , the Tikhonov regularisation term has the form

$$\begin{aligned} R &= \frac{1}{2\mathcal{A}} \int \left(\gamma_s^2 (\nabla(\log_{10}(p) - \log_{10}(\tilde{p})))^2 + \gamma_a^2 (\log_{10}(p) - \log_{10}(\tilde{p}))^2 \right) d\mathcal{A} \\ &= \frac{1}{2\mathcal{A}} \int \left(\gamma_s^2 (\nabla \log_{10}(p/\tilde{p}))^2 + \gamma_a^2 \log_{10}^2(p/\tilde{p}) \right) d\mathcal{A} \end{aligned} \quad (6.42)$$

Now γ_a is dimensionless and the dimension of γ_s is length, i.e.

$$\begin{aligned} [\gamma_a] &= [] \\ [\gamma_s] &= [l] . \end{aligned}$$

Derivatives with respect to C and $p = \log_{10} C$ are related through

$$\begin{aligned} \frac{\partial}{\partial p} &= \frac{\partial C}{\partial p} \frac{\partial}{\partial C} \\ &= \ln(10) C \frac{\partial}{\partial C} . \end{aligned}$$

As shown in section 6.11 the Tikhonov approach leads to

$$R = \frac{1}{2} (\mathbf{p} - \tilde{\mathbf{p}})^T (\gamma_a^2 \mathbf{M} + \gamma_s^2 (\mathbf{D}_x + \mathbf{D}_y)) (\mathbf{p} - \tilde{\mathbf{p}}) \quad (6.43)$$

$$= \frac{1}{2} (\mathbf{p} - \tilde{\mathbf{p}})^T \boldsymbol{\Sigma}_{pp}^{-1} (\mathbf{p} - \tilde{\mathbf{p}}) \quad (6.44)$$

where

$$\boldsymbol{\Sigma}_{pp}^{-1} = \frac{1}{2} (\gamma_a^2 \mathbf{M} + \gamma_s^2 (\mathbf{D}_x + \mathbf{D}_y)) \quad (6.45)$$

and \mathbf{M} is the mass matrix and \mathbf{D}_x and \mathbf{D}_y the stiffness matrices. Hence, with the Tikhonov approach we are calculating directly the inverse of a matrix $\boldsymbol{\Sigma}_{pp}$ as (6.45). By construction this inverse will be sparse. However, it is in general not clear if this is an inverse of a covariance matrix. One can, for example, show that for $\gamma_a = 0$ and $\gamma_s \neq 0$, $\boldsymbol{\Sigma}_{pp}$ as defined by Eq. (6.45) is not a covariance matrix.

6.8 Relationships between rate factors corresponding to different values of the stress exponent

Assume we have determined A for $n = 1$. What A distribution should we use as a starting point for an inversion using a different n value?

Generally,

$$\dot{\epsilon}_{ij} = A^{1/n} \dot{\epsilon}^{(n-1)/n} \tau_{ij}$$

and for A_1 with $n = 1$ we have

$$\dot{\epsilon}_{ij} = A_1 \tau_{ij}$$

Let us consider the situation where we have calculated the strain rates and the stresses for a given problem, for $n = 1$. Can we now solve the same problem for some other value of n , for example $n = 3$, and arrive at exactly the same stress and strain-rate distributions by simply suitably modifying the A_n distribution? That is, can we find A such that

$$\dot{\epsilon}_{ij} = A_n^{1/n} \dot{\epsilon}^{(n-1)/n} \tau_{ij}$$

where $\dot{\epsilon}_{ij}$, $\dot{\epsilon}$, and τ_{ij} are fields we obtained by solving the problem for a given A for $n = 1$? We see that by requiring that

$$A_1 = A_n^{1/n} \dot{\epsilon}^{(n-1)/n}$$

or

$$A_n = \dot{\epsilon}^{1-n} A_1^n$$

the functional relationship between $\dot{\epsilon}_{ij}$ and τ_{ij} is the same as before provided $\dot{\epsilon} > 0$ everywhere.

When performing an inversion we might add some prior information on A and in doing so we introduce an explicit dependency of the cost function that we aim to minimise on the variation of the retrieved A with respect to the prior A .

One might possibly argue that the ‘best’ A distribution is the one that has the smallest variance. This could be measured as the variation of the function

$$\text{Var}(A) = \int (A(x) - \bar{A})^2 \, dx$$

If we have done an inversion for $n = 1$ we can then find the ‘best’ A by solving the minimisation problem

$$\min_n \int (A_n(x) - \bar{A}_n)^2 \, dx$$

where

$$A_n(x) = \dot{\epsilon}^{1-n}(x) A_1(x)^n$$

And if we want to limit this optimisation to a particular region we use

$$\min_n \int (A_n(x) - \bar{A}_n)^2 w(x) \, dx$$

where $w(x)$ is a spatial mask selecting the area of interest.

6.9 Calculating gradients

6.9.1 Fix-point method

Derivatives of the objective function are, in general, calculated using the adjoint method (see section 6.9.2). However, it is easy to calculate directly a reasonable approximation to both the derivative and Hessian of the regularisation term (6.41), see Eqs. (6.59), (6.60) and (6.61), with respect to C . For example if we have

$$I = \frac{1}{2\mathcal{A}} \int \left(((u - \tilde{u})/u_{\text{err}})^2 + ((v - \tilde{v})/v_{\text{err}})^2 \right) d\mathcal{A}$$

and we use, for example Weertman sliding law where $u = C\tau^{m-1}\tau_{bx}$ and assume that basal drag does not depend on C , then we find that

$$\begin{aligned}\delta_C I &= D_C I(C, \phi_q) = \lim_{\epsilon \rightarrow 0} \frac{d}{d\epsilon} I(C + \epsilon\phi_q) \\ &= \frac{1}{2\mathcal{A}} \int \left(\left(\frac{(C + \epsilon\phi_q)\tau^{m-1}\tau_{bx} - \tilde{u}}{u_{\text{err}}} \right)^2 + \text{yterm} \right) d\mathcal{A} \\ &= \frac{1}{\mathcal{A}} \int \left(\frac{C\tau^{m-1}\tau_{bx} - \tilde{u}}{u_{\text{err}}} \frac{\tau^{m-1}\tau_{bx}}{u_{\text{err}}} \phi_q + \text{yterm} \right) d\mathcal{A} \\ &= \frac{1}{\mathcal{A}} \int \left(\frac{u - \tilde{u}}{u_{\text{err}}} \frac{u}{u_{\text{err}}} \frac{1}{C} + \text{yterm} \right) \phi_q d\mathcal{A} \\ &= \frac{1}{\mathcal{A}} \int f(x, y) \phi_q(x, y) d\mathcal{A} \\ &= \frac{1}{\mathcal{A}} \int f_p \phi_p \phi_q d\mathcal{A} \\ &= \frac{1}{\mathcal{A}} \mathbf{M} \mathbf{f}\end{aligned}$$

where

$$f(x, y) = \frac{1}{C} \left(\frac{u - \tilde{u}}{u_{\text{err}}} \frac{u}{u_{\text{err}}} + \frac{u - \tilde{v}}{v_{\text{err}}} \frac{v}{v_{\text{err}}} \right)$$

and using

$$\frac{\partial u}{\partial C} = \frac{u}{C}$$

furthermore that

$$\begin{aligned}\delta_{CC}^2 I &= \lim_{\epsilon \rightarrow 0} \frac{d}{d\epsilon} \frac{1}{\mathcal{A}} \int f(C + \epsilon\phi_r) \phi_p \phi_q d\mathcal{A} \\ &= \frac{1}{\mathcal{A}} \int \left((u/u_{\text{err}})^2 + (v/v_{\text{err}})^2 \right) (1/C^2) \phi_r \phi_q d\mathcal{A} \\ &= \frac{1}{\mathcal{A}} \int g(x, y) \phi_r \phi_q d\mathcal{A} \\ &= \frac{1}{\mathcal{A}} \int g_p \phi_p \phi_r \phi_q d\mathcal{A}\end{aligned}$$

where

$$g(x, y) = \left(\left(\frac{u}{u_{\text{err}}} \right)^2 + \left(\frac{v}{v_{\text{err}}} \right)^2 \right) \frac{1}{C^2}$$

We can see that if g were spatially constant, \bar{g} , then

$$\delta_{CC}^2 I = \frac{\bar{g}}{\mathcal{A}} \mathbf{M}$$

(here \bar{g} is a scalar). While this will, in general, not be the true, this does suggest that a rough approximation of the Hessian will be

$$H \approx \frac{1}{\mathcal{A}} \mathcal{O}(u/(\Delta u C^2)) \mathbf{M}$$

where here $\mathcal{O}(u/(\Delta u C^2))$ is a constant and some typical scale.

We also see that the Newton system

$$H \Delta C = -f(C_0) \quad C \rightarrow C_0 + \Delta C$$

leads to

$$\begin{aligned}\Delta C &= -\frac{f(C_0)}{g(C_0)} \\ &= -C \frac{\frac{u - \tilde{u}}{u_{\text{err}}} \frac{u}{u_{\text{err}}} + \frac{v - \tilde{v}}{v_{\text{err}}} \frac{v}{v_{\text{err}}}}{\left(\frac{u}{u_{\text{err}}} \right)^2 + \left(\frac{v}{v_{\text{err}}} \right)^2}\end{aligned}$$

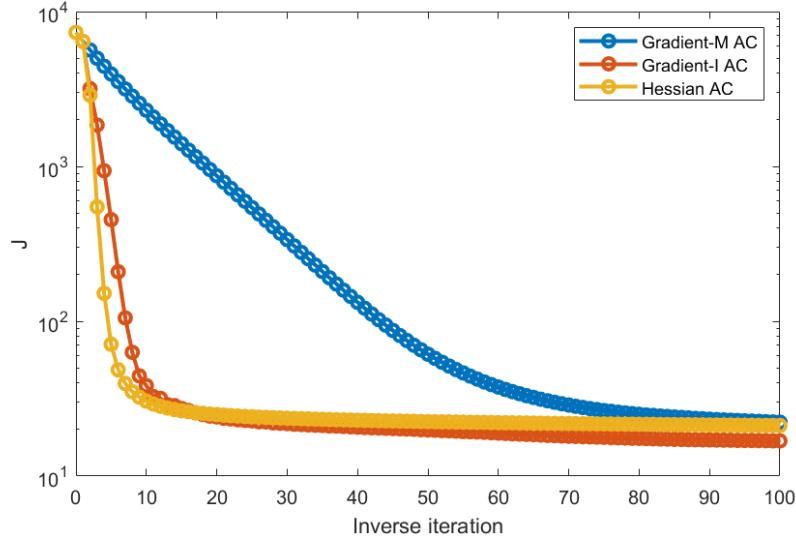


Figure 6.12: An example showing cost function reduction as a function of inverse iterations, when inverting for both A and C using a gradient based approach with l^2 and L^2 gradients, labelled with I and M respectively, and using a Hessian-based inversion where the Hessians of the regularisation terms are exact, and the Hessian of the A and C terms of the misfit are approximated using the fixed-point approach. See section 6.10, for discussion of the l^2 and L^2 gradients.

6.9.2 The adjoint method

The adjoint method is a simple trick to speed up the calculation of gradients of the objective function with respect to the control variables.

Assume we want to solve the minimisation problem

$$\min_{p \in P, q \in U} J(q(p))$$

subject to forward model

$$F(q(p), p) = 0.$$

The objective function is

$$J : U \times P \rightarrow \mathbb{R}$$

and the forward model, i.e. the state equation

$$F : U \times P \rightarrow \mathbb{W}$$

the model control parameter space P (also referred to as control space), the state space U and the image space \mathbb{W} are Banach spaces. We want to determine the sensitivity of cost function J with respect to the (distributed) control parameter p , i.e. we would like to calculate the directional derivative

$$DJ(p)[\phi] = \langle \nabla_p J | \phi \rangle$$

as well as determine the gradient $\nabla_p J$, for a given inner product.

We define the Lagrange function, or the 'extended' objective function, \mathcal{L} as

$$\mathcal{L} = U \times V \times W^* \rightarrow \mathbb{R}$$

as

$$\mathcal{L}(q(p), p, \lambda) = J(q(p), p) + \langle \lambda | F(q(p), p) \rangle_{W^*, W} \quad (6.46)$$

The adjoint variable λ is in the dual of the image space \mathbb{W} .

Equation (6.46) provides no constraints on the adjoint variable λ because the second term is always equal to zero for any value of p . Therefore

$$\mathcal{L}(q(p), p, \lambda) = J(q(p), p)$$

and

$$D_p \mathcal{L}(p)[\phi] = D_\phi J(p) = \langle \nabla_p J \mid \phi \rangle$$

Also note that

$$d_p F = \partial_p F + \partial_q F d_p q = 0.$$

Introducing

$$j(p) = J(q(p), p) = \mathcal{L}(q(p), p, \lambda),$$

we have

$$j'(p) = (\partial q / \partial p)^* \partial \mathcal{L}(q(p), p, \lambda) / \partial q + \partial \mathcal{L}(q(p), p, \lambda) / \partial p, \quad (6.47)$$

Now we chose λ such that

$$\partial \mathcal{L}(q(p), p, \lambda) / \partial q = 0.$$

Hence λ must be a solution to

$$\partial J(q(p), p) / \partial q + (\partial F / \partial q)^* \lambda = 0, \quad (6.48)$$

and then the direction derivative $j'(p)$ is

$$j'(p) = \partial J(q(p), p) / \partial p + (\partial F / \partial p)^* \lambda \quad (6.49)$$

Eq. (6.47) can also be written as

$$\langle j'(p), \phi \rangle_{P^*, P} = \langle \partial_u \mathcal{L} \mid \partial_p q \phi \rangle_{U^*, U} + \langle \partial_p \mathcal{L} \mid \phi \rangle_{P^*, P},$$

and the directional derivative is then

$$\langle \partial_u \mathcal{L}, \partial_p q \phi \rangle_{U^*, U} = 0,$$

for all ϕ .

Another approach: Differentiating Eq. (6.46) with respect to the control variable p we obtain

$$\begin{aligned} D J(p)[\phi] &= D \mathcal{L}(p)[\phi] = \langle \partial_q J \mid d_p q \phi \rangle + \langle \partial_p J, \phi \rangle + \langle \lambda \mid \partial_q F d_p q \phi \rangle + \langle \lambda \mid \partial_p F \phi \rangle + \langle d_p \lambda \mid F \rangle \\ &= \langle \partial_q J \mid d_p q \phi \rangle + \langle (\partial_q F)^* \lambda \mid d_p q \phi \rangle + \langle \lambda \mid \partial_p F \phi \rangle + \langle \partial_p J, \phi \rangle \\ &= \langle \partial_q J + (\partial_q F)^* \lambda \mid d_p q \phi \rangle + \langle \lambda \mid \partial_p F \phi \rangle + \langle \partial_p J, \phi \rangle \end{aligned}$$

where

$$\phi = \delta p.$$

We now use the freedom that λ has not been specified and now determine λ by setting

$$\langle \partial_q J + (\partial_q F)^* \lambda \mid \phi \rangle = 0,$$

and therefore

$$D J(p)[\phi] = \langle (\partial_p F)^* \lambda + \partial_p J \mid \phi \rangle, \quad (6.50)$$

which is identical to (6.49) which we derived earlier using a somewhat different approach.⁴

This now gives us a three-step method for calculating the directional gradient of object function J with respect to p :

1. Solve the state equation, i.e. the forward problem

$$\langle F(q(p), p) \mid \phi \rangle_{W^*, W} = 0,$$

for the state variable q .

This, in general, is a non-linear problem that can be solved iteratively using the Newton-Raphson system, i.e.

$$\langle \partial_q F \Delta q \mid \phi \rangle = -\langle F(q(p), p) \mid \phi \rangle,$$

⁴ Apparently the 'adjoint' method gets its name from the fact that the resulting expression of the derivative of the cost function involves an adjoint of an operator. The adjoint involved is the adjoint of the directional derivative of the forward model F with respect to the control variable p . However, in general there is no need to introduce this adjoint and we can just as well write

$$D J(p)[\phi] = \langle \lambda \mid \partial_p F \phi \rangle + \langle \partial_p J, \phi \rangle.$$

However, when solving for λ we do need the adjoint of the directional derivative of the forward model with respect to q .

and can be written in discrete form as

$$\mathbf{K}\Delta\mathbf{q} = \mathbf{b},$$

where

$$[\mathbf{K}]_{pq} = \langle \partial_{q_p} F \mid \phi_q \rangle,$$

and

$$[\mathbf{b}]_q = -\langle F(q(p), p) \mid \phi_q \rangle.$$

2. Solve the adjoint problem for $\langle \partial_q J + (\partial_q F)^* \lambda \mid \phi \rangle = 0$ for $\lambda \in W^*$, i.e.

$$\langle (\partial_q F)^* \lambda \mid \phi \rangle_{U^*, U} = -\langle \partial_q J \mid \phi \rangle_{U^*, U}$$

for the adjoint variable λ . If the forward tangential model $(\partial_q F)$ is self adjoint, this involves solving

$$\mathbf{K}\lambda = \mathbf{b}$$

3. Calculate the directional derivative of j as

$$DJ(p)[\phi] = \langle j'(p) \mid \phi \rangle_{P^*, P} = \langle (\partial_p F)^* \lambda + \partial_p J \mid \phi \rangle_{P^*, P}$$

In discrete form the derivative can be evaluated as

$$j'(p) = \mathbf{P}\lambda + \mathbf{Q}$$

where

$$[\mathbf{P}]_{ij} = \langle \partial_{p_i} F \mid \phi_j \rangle$$

and

$$[\mathbf{Q}]_i = \langle \partial_p J \mid \phi_i \rangle$$

However, $\langle (\partial_p F)^* \lambda \mid \phi \rangle$ can usually be evaluated directly within the assembly loop without the need of ever forming the matrix \mathbf{P} . Furthermore, the forward model is solved in a weak form and this often involves some manipulations of the $\langle \lambda \mid F \rangle$ term in Eq. (6.46).

Usually the regularisation term is an explicit function of the control variable, i.e.

$$J(F(p, q(p), p) = I(F(p, q(p))) + R(p)$$

and therefore

$$\partial_p J = \partial_p R$$

The adjoint variable λ is the gradient of the objective function with respect to the state variable q

$$\lambda = \nabla_q J$$

In the adjoint method we need to calculate a number of derivatives. These are:

1. The directional derivative of the forward model with respect to the state and control variables, i.e. $\partial_q F$ and $\partial_p F$.
2. The directional derivative of the objective function with respect to the state and control variables, i.e. $\partial_q J$ and $\partial_p J$.

6.9.3 Summarising the first-order adjoint approach

Summarising, and using a somewhat inexact notation, we can calculate the (total) directional derivative $d_p J$ of the objective function J with respect to the control parameters p , as follows:

$$F(q(p), p) = 0 \tag{6.51}$$

$$\partial_q F^* \lambda = \partial_q J \tag{6.52}$$

$$d_p J = \partial_p F^* \lambda + \partial_p J \tag{6.53}$$

A bit more precise notation for the adjoint problem and the calculation of the derivative is

$$\langle \delta_q F^* \mid \lambda \rangle = \delta_q J \tag{6.54}$$

$$d_p J = \langle \delta_p F^* \mid \lambda \rangle + \delta_p J \tag{6.55}$$

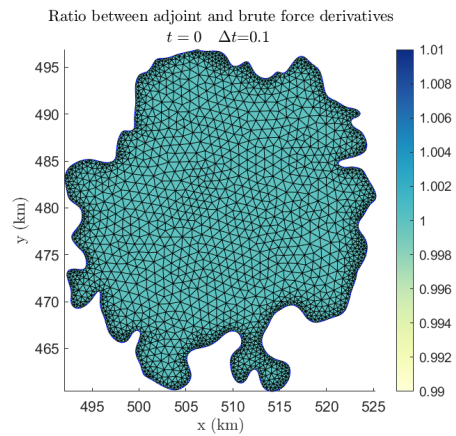


Figure 6.13: Gradient calculation, dJ/dB , done with adjoint and finite differences. This test was done for the Hoffsjökull ice cap in Iceland.

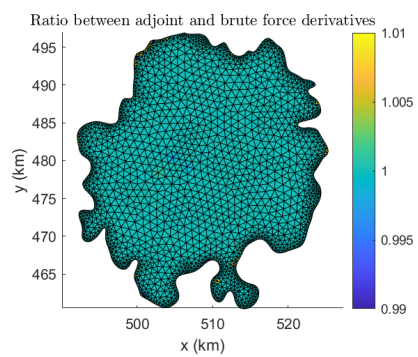


Figure 6.14: Gradient calculation, dB/dC , done with adjoint and finite differences. This test was done for the Hoffsjökull ice cap in Iceland.

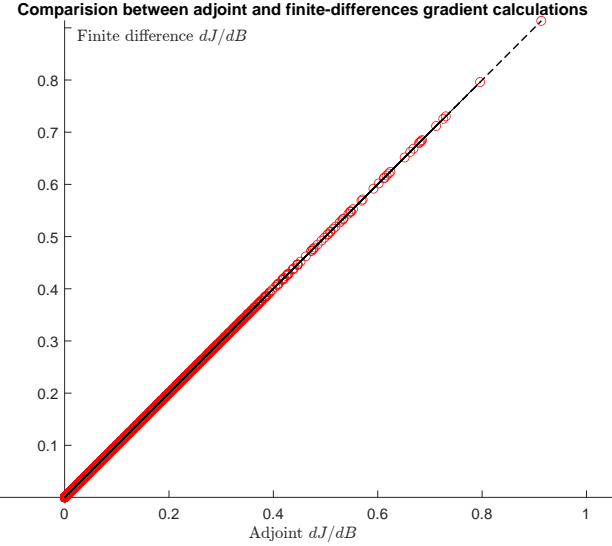


Figure 6.15: Comparison between adjoint and finite differences gradient calculations. This test was done for the Hoffsjökull ice cap in Iceland.

6.9.4 Time dependent adjoint

Consider the situation where the glacier surface s is the observable, with \tilde{s} being the measurement, and the mass balance distribution a is the unknown model parameter, and \tilde{a} the prior.

Minimising

$$J = \frac{1}{2} \int (s(t) - \tilde{s}(t))^2 dt + \frac{1}{2} \int (a(t) - \tilde{a}(t))^2 dt$$

subject to

$$F(s, a) = \partial_t(s - b) + \partial_x q - a = 0$$

with the initial condition

$$s = s_0 \quad \text{at} \quad t = t_0$$

and where, for example, we assume (SIA) that

$$q = -\rho D \| \partial_x s \|^{n-1} h^{q+2} \partial_x s$$

with $D = 2A(\rho g)^n / (n+2)$. In general, the cost function J can be expected to involve a spatial integral too, but for notational simplicity we omit writing it here.

The Lagrangian is

$$\begin{aligned} \mathcal{L} &= J + \int \lambda F dt \\ &= J + \langle \lambda, F \rangle \end{aligned}$$

and the directional derivative of the Lagrangian with respect to δa is

$$\begin{aligned} \delta_a \mathcal{L} &= \frac{\partial J}{\partial a} + \frac{\partial J}{\partial s} \frac{\partial s}{\partial a} + \int \lambda \left(\frac{\partial F}{\partial a} + \frac{\partial F}{\partial s} \frac{\partial s}{\partial a} \right) \delta a dt \\ &= \int (a(t) - \tilde{a}(t)) \delta a dt + \int \frac{\partial J}{\partial s} \frac{\partial s}{\partial a} \delta a dt + \int \lambda \left(\frac{\partial F}{\partial a} + \frac{\partial F}{\partial s} \frac{\partial s}{\partial a} \right) \delta a dt \\ &= \int (a(t) - \tilde{a}(t)) \delta a dt + \int \lambda \frac{\partial F}{\partial a} \delta a dt + \int \lambda \frac{\partial F}{\partial s} \frac{\partial s}{\partial a} \delta a dt + \int \frac{\partial J}{\partial s} \frac{\partial s}{\partial a} \delta a dt \\ &= \int \left(a(t) - \tilde{a}(t) + \lambda \frac{\partial F}{\partial a} \right) \delta a dt + \int \left(\lambda \frac{\partial F}{\partial s} + \frac{\partial J}{\partial s} \right) \frac{\partial s}{\partial a} \delta a dt \end{aligned}$$

Now select λ so that

$$\int \left(\lambda \frac{\partial F}{\partial s} + \frac{\partial J}{\partial s} \right) \delta a dt = 0$$

that is

$$\langle \lambda, \frac{\partial F}{\partial s} \delta a \rangle + \langle \frac{\partial J}{\partial s}, \delta a \rangle = 0$$

or

$$\langle \frac{\partial F^*}{\partial s} \lambda + \frac{\partial J}{\partial s}, \delta a \rangle = 0$$

which is the adjoint equation. The directional derivative (not the gradient!) is then just

$$\delta_a \mathcal{L} = \int \left(a(t) - \tilde{a}(t) + \lambda \frac{\partial F}{\partial a} \right) \delta a \, dt$$

If the initial condition depends on an unknown value of a , we will also need to introduce a Lagrange multiplier relating to that initial conditions. However, here the initial condition $s = s(t_0)$ does not involve a , and no additional Lagrange multiplier is therefore required.

We also need a boundary condition for the adjoint equation. Here the simplest option is to prescribe $\lambda = 0$ at the end of the interval and then solve for λ by integrating backwards, i.e. we solve

$$\int_{t_0}^t \frac{\partial F^*}{\partial s} \lambda \, dt' = - \int_{t_0}^t (s - \tilde{s}) \, dt'$$

with $\lambda(t) = 0$.

6.10 Directional derivative and gradients

Using the adjoint method we can calculate the directional derivative $D_\phi J(p)$ of the cost function J as a function of the model parameter p in the direction ϕ , defined as

$$D_\phi J(p) = \lim_{\epsilon \rightarrow 0} \frac{d}{d\epsilon} J(p + \epsilon\phi) . \quad (6.56)$$

in a computationally effective way (see also Eq. 7). The (distributed) parameter, p , is here a function of (x, y) and can be written as a vector in the basis $\{\phi_i, i = 1 \dots n\}$ as

$$p(x, y) = p_q \phi_q(x, y)$$

and if we group the numbers p_i , for $i = 1 \dots n$, together, they form the elements of the vector \mathbf{p} in the basis $\{\phi_i, i = 1 \dots n\}$. The gradient $\nabla_p J$ is defined through

$$D_\phi J(p) = \langle \nabla_p J | \phi \rangle$$

and this equation must hold for every direction ϕ_i , $i = 1 \dots n$. Our FE inner product is the L^2 inner product

$$\langle f | g \rangle_{L^2} = \int_{\mathcal{A}} f(x, y) g(x, y) \, d\mathcal{A}$$

where \mathcal{A} stands for the area of the computational domain. We would like to determine the components g_i of the gradient vector in the basis $\{\phi_i, i = 1 \dots n\}$ where

$$\nabla_p J = g(x, y) = g_i \phi_i(x, y) .$$

Using the L^2 inner product we thus find that

$$\begin{aligned} D J(p)[\phi_i] &= \langle \nabla_p J | \phi_i \rangle_{L^2} \\ &= \langle g_r \phi_r | \phi_i \rangle_{L^2} \\ &= g_r \langle \phi_r | \phi_i \rangle_{L^2} \\ &= g_r M_{ri} \\ &= g_r M_{ir} \end{aligned}$$

or

$$[D J(p)] = \mathbf{M} \mathbf{g} ,$$

where \mathbf{M} is the mass matrix

$$[\mathbf{M}]_{ij} = \langle \phi_i | \phi_j \rangle ,$$

and \mathbf{g} is the gradient vector and $[\mathbf{g}]_r = g_r$ is the r -th component of that vector in the basis $\{\phi_i\}$, for $i = 1 \dots n$ where n is the number of nodes.

6.11 Evaluating objective functions and their directional derivatives

If ϕ_i are the basis functions then

$$[\mathbf{M}]_{ij} = \langle \phi_i | \phi_j \rangle$$

is the mass matrix (also known as the Gramian matrix), and

$$\begin{aligned} [\mathbf{D}_x]_{ij} &= \langle \nabla_x \phi_i | \nabla_x \phi_j \rangle \\ [\mathbf{D}_y]_{ij} &= \langle \nabla_y \phi_i | \nabla_y \phi_j \rangle \end{aligned}$$

the stiffness matrices.

For

$$I = \frac{1}{2} \|f\|^2 = \frac{1}{2} \int f(x, y) f(x, y) dx dy \quad (6.57)$$

and

$$f(x, y) = f_i \phi_i(x, y)$$

we find

$$\begin{aligned} I &= \frac{1}{2} \|f\|^2 \\ &= \frac{1}{2} \langle f | f \rangle \\ &= \frac{1}{2} \langle f_p \phi_p | f_q \phi_q \rangle \\ &= \frac{1}{2} f_p \langle \phi_p | \phi_q \rangle f_q \\ &= \frac{1}{2} f_p M_{pq} f_q \end{aligned}$$

or

$$I = \frac{1}{2} \mathbf{f} \mathbf{M} \mathbf{f}$$

where

$$[\mathbf{f}]_i = f_i$$

The directional derivative is

$$\begin{aligned} DI(f, \phi_q) &= \lim_{\epsilon \rightarrow 0} \frac{d}{d\epsilon} I(f + \epsilon \phi_q) \\ &= \frac{1}{2} \frac{d}{d\epsilon} \langle f + \epsilon \phi_q | f + \epsilon \phi_q \rangle \\ &= \langle f | \phi_q \rangle \\ &= \langle f_p \phi_p | \phi_q \rangle \\ &= \langle \phi_q | \phi_p \rangle f_p \\ &= M_{qp} f_p \\ &= \mathbf{M} \mathbf{f} \end{aligned}$$

or

$$DI(f, \phi_q) = [\mathbf{M} \mathbf{f}]_q$$

The p component of the directional derivative represents the (linear) rate-of-change in I as the value of f is perturbed by $\epsilon \phi_p$.

We can also write

$$DI(f, \phi_q) = \langle f_p \phi_p | \phi_q \rangle$$

and therefore by the definition of a gradient as

$$\frac{d}{d\epsilon} J(f + \epsilon \delta f)|_{\epsilon=0} = \langle \text{grad}J(f), \delta f \rangle$$

the gradient of I in Eq. (6.57) is f (as it of course should be).

Similarly if

$$I = \frac{1}{2} \langle \nabla f \mid \nabla f \rangle = \frac{1}{2} (\langle \partial_x f, \partial_x f \rangle + \langle \partial_y f, \partial_y f \rangle)$$

then

$$\begin{aligned} I_x &= \frac{1}{2} \langle \partial_x f, \partial_x f \rangle \\ &= \frac{1}{2} \langle f_p \partial_x \phi_p, f_q \partial_x \phi_q \rangle \\ &= \frac{1}{2} f_p \langle \partial_x \phi_p, \partial_x \phi_q \rangle f_q \\ &= \frac{1}{2} \mathbf{f} \mathbf{D}_x \mathbf{f} \end{aligned}$$

and

$$\begin{aligned} DI_x(f, \phi_p) &= \frac{1}{2} \lim_{\epsilon \rightarrow 0} \frac{d}{d\epsilon} \langle \partial_x(f + \epsilon \phi_p) \mid \partial_x(f + \epsilon \phi_p) \rangle \\ &= \langle \partial_x f \mid \partial_x \phi_p \rangle \\ &= \langle f_q \partial_x \phi_q \mid \partial_x \phi_p \rangle \\ &= \langle \partial_x \phi_p \mid \partial_x \phi_q \rangle f_q \\ &= \mathbf{D}_x \mathbf{f} \end{aligned}$$

or

$$DI_x(f, \phi_p) = \mathbf{D}_x \mathbf{f}$$

Summarising, if we have a regularisation term on the form

$$R = \frac{1}{2} \|f\|_{L^2(\Omega)}^2 + \frac{1}{2} \|\nabla f\|_{L^2(\Omega)}^2 \quad (6.58)$$

it can be evaluated knowing the mass and the stiffness matrices as

$$\begin{aligned} R &= \frac{1}{2} \|f\|_{L^2(\Omega)}^2 + \frac{1}{2} \|\nabla f\|_{L^2(\Omega)}^2 \\ &= \frac{1}{2} \mathbf{f} \mathbf{M} \mathbf{f} + \frac{1}{2} \mathbf{f} (\mathbf{D}_x + \mathbf{D}_y) \mathbf{f} \end{aligned}$$

and direction derivative is

$$\frac{d}{d\epsilon} I(f + \epsilon \phi_p) = [\mathbf{M} \mathbf{f} + (\mathbf{D}_x + \mathbf{D}_y) \mathbf{f}]_p$$

And the regularisation term (6.41) can be evaluated similarly as

$$\begin{aligned} R &= \frac{1}{2\mathcal{A}} \int \left(\gamma_s^2 (\nabla(p - \tilde{p}))^2 + \gamma_a^2 (p - \tilde{p})^2 \right) d\mathcal{A} \\ &= \frac{1}{2\mathcal{A}} (\gamma_s^2 (\mathbf{p} - \tilde{\mathbf{p}})^T \mathbf{D} (\mathbf{p} - \tilde{\mathbf{p}}) + \gamma_a^2 (\mathbf{p} - \tilde{\mathbf{p}})^T \mathbf{M} (\mathbf{p} - \tilde{\mathbf{p}})) \\ &= \frac{1}{2\mathcal{A}} (\mathbf{p} - \tilde{\mathbf{p}})^T (\gamma_s^2 \mathbf{D} + \gamma_a^2 \mathbf{M}) (\mathbf{p} - \tilde{\mathbf{p}}) \end{aligned} \quad (6.59)$$

and the directional derivative is

$$d_{\mathbf{p}} R = \frac{1}{\mathcal{A}} (\gamma_s^2 \mathbf{D} + \gamma_a^2 \mathbf{M}) (\mathbf{p} - \tilde{\mathbf{p}}) \quad (6.60)$$

and the Hessian

$$d_{\mathbf{p}\mathbf{p}}^2 R = \frac{1}{\mathcal{A}} (\gamma_s^2 \mathbf{D} + \gamma_a^2 \mathbf{M}) \quad (6.61)$$

6.12 Simple example of a gradient calculation of an objective function

Consider, as an illustration, the problem of inverting for ice thickness (h) using rates of thickness change (\dot{h}) as observations. Here the control variable is h and the field variable \dot{h} . We have measurements \tilde{h} and an *a priori* estimate $\tilde{\tilde{h}}$.

Hence, we have

$$p = h, \quad (6.62)$$

$$q = \dot{h}. \quad (6.63)$$

$$(6.64)$$

The object function J is

$$J = \frac{1}{2\mathcal{A}} \int (\dot{h} - \tilde{h})^2 d\mathcal{A} + \frac{1}{2\mathcal{A}} \int (h - \tilde{\tilde{h}})^2 d\mathcal{A},$$

where the first term is the misfit term and the second one the regularisation term. The extended cost function is

$$\mathcal{L} = J + \langle \lambda, F \rangle$$

where the forward model $F = 0$ is

$$F = \dot{h} - (a - \partial_x(uh))$$

where \dot{h} is the unknown, although using FE we would solve this as

$$\begin{aligned} 0 &= \langle F | \phi_j \rangle = \int (\dot{h} - (a - \partial_x(uh))) \phi_j dA \\ &= \int (\dot{h}_i \phi_i - (a - \partial_x(uh))) \phi_j dA, \end{aligned}$$

for each j , or

$$\int \dot{h}_i \phi_i \phi_j dA = \int (a - \partial_x(uh)) \phi_j dA,$$

that is

$$\dot{\mathbf{h}} = \mathbf{M}^{-1} \mathbf{b},$$

where

$$[\mathbf{M}]_{ij} = \int \phi_i \phi_j dA \quad (6.65)$$

$$[\mathbf{b}]_j = \int (a - \partial_x(uh)) \phi_j dA. \quad (6.66)$$

$$(6.67)$$

and therefore in discrete form the forward model

$$\mathbf{F} = 0.$$

with

$$\mathbf{F} = \mathbf{M} \dot{\mathbf{h}} - \mathbf{b}.$$

We also find that using FE approach that

$$J = \frac{1}{2\mathcal{A}} (\dot{\mathbf{h}} - \tilde{\mathbf{h}})^T \mathbf{M} (\dot{\mathbf{h}} - \tilde{\mathbf{h}}) + \frac{1}{2\mathcal{A}} (\mathbf{h} - \tilde{\tilde{\mathbf{h}}})^T \mathbf{M} (\mathbf{h} - \tilde{\tilde{\mathbf{h}}})$$

The task at hand is to calculate the directional derivative (see Appendix D) of the object function J with respect to the control variable h , i.e.

$$\delta_h J = DJ(h)[\delta h] = \lim_{\epsilon \rightarrow 0} \frac{d}{d\epsilon} J(h + \epsilon \delta h)$$

6.12.1 Direct approach

Since the forward model is so simple we can just take the (total) derivative directly by inserting the forward model F into the objective function J , leading to

$$d_h J = \frac{1}{\mathcal{A}} \int ((a - \partial_x(uh)) - \tilde{h}) \partial_x(u \delta h) d\mathcal{A} + \frac{1}{\mathcal{A}} \int (h - \tilde{h}) \delta h d\mathcal{A}. \quad (6.68)$$

This is the desired directional derivative and one could in principle use this derivative calculated for each perturbation $\delta h = \phi_i$, for $i = 1 \dots n$ where n is the number of nodes, in a gradient-based minimisation method.

First, solve the forward model:

We calculate

$$\partial_q F \Delta q = -F(q) \quad \text{with } q \rightarrow q + \Delta q \text{ and } \Delta q \rightarrow 0,$$

which in this particular case where $q = \dot{h}$ is

$$1 \Delta \dot{h} = -\dot{h}_0 + a - \partial_x(uh_0),$$

since $\partial_{\dot{h}} F = 1$, or

$$\dot{h}_1 = \Delta \dot{h} + \dot{h}_0 = a - \partial_x(uh_o),$$

since this is a linear forward model the NR iteration converges in first iteration.

Of course, as explained above, the FE formulation of the problem leads to

$$\mathbf{M} \Delta \dot{\mathbf{h}} = -(\mathbf{M} \dot{\mathbf{h}} - \mathbf{b})$$

so here $1 = |\phi\rangle\langle\phi| = \mathbf{M}$.

Secondly, solve the adjoint problem:

The adjoint problem is

$$\partial_{\dot{h}} F^* \lambda = \partial_{\dot{h}} J,$$

or

$$1^* \lambda = \frac{1}{\mathcal{A}} \int (\dot{h} - \tilde{h}) \delta \dot{h} d\mathcal{A}.$$

We can ask what the 1 actually stands for in this context, and the answer is that this is the unity operator in the relevant basis, i.e. the inner product between the unit vectors spanning the space, or the Gramian matrix. In the FE context, where the basis functions are ϕ_i , this matrix is the mass matrix $[\mathbf{M}]_{ij} = \langle \phi_i | \phi_j \rangle$.

To see this more clearly let us calculate the directional derivative from the FE formulation of the forward problem while realising that $\partial_{\dot{h}}^* \lambda$ represents an inner product, i.e. we need to evaluate

$$\begin{aligned} \langle \delta_{\dot{h}} F | \lambda \rangle &= \int \delta_{\dot{h}} (\dot{h} - (a - \partial_x(uh))) \lambda d\mathcal{A} \\ &= \int \phi_i \lambda d\mathcal{A} \\ &= \int \phi_i \phi_j \lambda_j d\mathcal{A} \\ &= [\mathbf{M}]_{ij} \lambda_j, \end{aligned}$$

showing that the expression 1λ is, in the FE context, given by $\mathbf{M}\lambda$. Also note that the term $\partial_{\dot{h}} J$ is in fact a directional derivative and, again in FE context, reads

$$\delta_{\dot{h}} = \frac{1}{\mathcal{A}} \int (\dot{h} - \tilde{h}) \phi_j d\mathcal{A}.$$

Hence, the adjoint problem is

$$\mathbf{M}\lambda = \mathbf{l},$$

where

$$[\mathbf{l}]_j = \frac{1}{\mathcal{A}} \int (\dot{\mathbf{h}} - \tilde{\mathbf{h}}) \phi_j d\mathcal{A}.$$

The vector \mathbf{l} is

$$\begin{aligned} \mathbf{l} &= \frac{1}{\mathcal{A}} \int (\dot{\mathbf{h}}_i - \tilde{\mathbf{h}}_i) \phi_i \phi_j d\mathcal{A} \\ &= (\dot{\mathbf{h}}_i - \tilde{\mathbf{h}}_i) \frac{1}{\mathcal{A}} \int \phi_i \phi_j d\mathcal{A} \\ &= \frac{1}{\mathcal{A}} \mathbf{M}(\dot{\mathbf{h}} - \tilde{\mathbf{h}}), \end{aligned}$$

and the adjoint equations therefore simply $\boldsymbol{\lambda} = \frac{1}{\mathcal{A}}(\dot{\mathbf{h}} - \tilde{\mathbf{h}})$.

We can also arrive at the adjoint equation directly from the discrete form of the equations, as derived above, where the forward model and the object function are given by

$$\begin{aligned} \mathbf{F} &= \mathbf{M}\dot{\mathbf{h}} - \mathbf{b}, \\ J &= \frac{1}{2\mathcal{A}}(\dot{\mathbf{h}} - \tilde{\mathbf{h}})^T \mathbf{M}(\dot{\mathbf{h}} - \tilde{\mathbf{h}}) + \frac{1}{2\mathcal{A}}(\mathbf{h} - \tilde{\mathbf{h}})^T \mathbf{M}(\mathbf{h} - \tilde{\mathbf{h}}). \end{aligned}$$

It follows that $\partial_{\dot{\mathbf{h}}} \mathbf{F} = \mathbf{M}$ and $\partial_{\dot{\mathbf{h}}} J = \frac{1}{\mathcal{A}} \mathbf{M}(\dot{\mathbf{h}} - \tilde{\mathbf{h}})$ and the adjoint equation is

$$\mathbf{M}\boldsymbol{\lambda} = \frac{1}{\mathcal{A}} \mathbf{M}(\dot{\mathbf{h}} - \tilde{\mathbf{h}}),$$

and we again arrive at

$$\boldsymbol{\lambda} = \frac{1}{\mathcal{A}}(\dot{\mathbf{h}} - \tilde{\mathbf{h}}).$$

Thirdly, evaluate the directional derivative:

The directional derivative is the given by

$$d_h J = \partial_h F^* \boldsymbol{\lambda} + \partial_h J.$$

We notation in section 6.9.3 was somewhat relaxed, and as F is an operator we need to remember that the first term on the right-hand side is an inner product and we need to evaluate

$$d_h J = \langle \delta_h F^* | \boldsymbol{\lambda} \rangle + \delta_h J,$$

where the δ symbols indicates that these are directional derivative. This leads to

$$\begin{aligned} d_h J &= \int \lambda \partial_x(u \delta h) d\mathcal{A} + \frac{1}{\mathcal{A}} \int (h - \tilde{h}) \delta h d\mathcal{A}, \\ &= \frac{1}{\mathcal{A}} \int (\dot{h} - \tilde{h}) \partial_x(u \delta h) d\mathcal{A} + \frac{1}{\mathcal{A}} \int (h - \tilde{h}) \delta h d\mathcal{A}, \end{aligned}$$

which is same as (6.68).

6.12.2 Calculating the elements of the gradient in the FE basis

Note that if we set $\delta h = \phi$, which is a typical approach and the one used in \tilde{U}_a , this is the derivative with respect to the perturbation in the nodal values, i.e. $\delta h = \phi$. This derivative is clearly intimately related to the FE basis. There is then the separate, but related and quite an important question as to what the *coefficients of the directional derivative* are in a given FE setting. Assuming that all variables are expanded in the same FE basis, i.e. $f(x, y) = f_i \phi_i(x, y)$ where f is any of u , h , \dot{h} and using the definition of the gradient by Eq. (8), we have

$$\begin{aligned} d_h J &= D J(h)[\delta h_i] = \langle \nabla J | \delta h_i \rangle_{L^2} \\ &= \langle \nabla J | \phi_i \rangle_{L^2} \\ &= \langle g(x) | \phi_i(x) \rangle_{L^2} \end{aligned}$$

where we use $\delta h_i = \phi_i$, and in the last expression we denote the gradient ∇J , which is a (dual) vector and a function of space, by $g(x)$. We expand the gradient $\nabla J = g$ in the basis $\{\phi_j(x), j = 1 \dots n\}$ and solve for the coefficients g_i of $g(x)$ in that basis where

$$g(x) = g_j \phi_j(x).$$

Eq. (6.68) therefore leads to

$$\int g_p \phi_p \phi_j d\mathcal{A} = \frac{1}{\mathcal{A}} \int (\dot{h} - \tilde{h}) (\partial_x u \phi_j + u \partial_x \phi_j) d\mathcal{A} + \frac{1}{\mathcal{A}} \int (h - \tilde{h}) \phi_j d\mathcal{A}. \quad (6.69)$$

which we solve for g_i .⁵

Hence, the vector gradient, formed by ordering the coefficients numbers g_i in a vector \mathbf{g} according to nodal numbers, is

$$\mathbf{g} = \mathbf{M}^{-1} \mathbf{k},$$

where

$$[\mathbf{k}]_j = \frac{1}{\mathcal{A}} \int (\dot{h} - \tilde{h}) (\partial_x u \phi_j + u \partial_x \phi_j) d\mathcal{A} + \frac{1}{\mathcal{A}} \int (h - \tilde{h}) \phi_j d\mathcal{A}.$$

6.13 Velocity inversion using mass equation

The thickness equation

$$F := \nabla \cdot (\mathbf{v}h) - a^* = 0 \quad (6.71)$$

provides constraints on the (admissible) velocity field for a given ice thickness.

$$J = \|\mathbf{v} - \check{\mathbf{v}}\| + \langle \lambda | F \rangle$$

or, for example, after linearisation and assembly

$$J = \frac{1}{2}(\mathbf{u} - \check{\mathbf{u}})^T \mathbf{P}_u (\mathbf{u} - \check{\mathbf{u}}) + \frac{1}{2}(\mathbf{v} - \check{\mathbf{v}})^T \mathbf{P}_v (\mathbf{v} - \check{\mathbf{v}}) + \boldsymbol{\lambda}^T \cdot (\mathbf{F}_u \mathbf{u} + \mathbf{F}_v \mathbf{v})$$

where

$$\begin{aligned} \check{\mathbf{v}} & \text{ velocity prior} \\ \check{\mathbf{v}} & \text{ velocity measurements} \end{aligned}$$

Linearisation gives

$$\begin{pmatrix} \mathbf{P}_u & 0 & \mathbf{F}_u^T \\ 0 & \mathbf{P}_v & \mathbf{F}_v^T \\ \mathbf{F}_u & \mathbf{F}_v & 0 \end{pmatrix} \begin{pmatrix} \Delta \mathbf{u} \\ \Delta \mathbf{v} \\ \Delta \boldsymbol{\lambda} \end{pmatrix} = - \begin{pmatrix} \mathbf{P}_u(\mathbf{u} - \check{\mathbf{u}}) - \mathbf{F}_u^T \boldsymbol{\lambda} \\ \mathbf{P}_v(\mathbf{v} - \check{\mathbf{v}}) - \mathbf{F}_v^T \boldsymbol{\lambda} \\ \mathbf{F}(\mathbf{u}) \end{pmatrix}$$

6.14 Thickness (h) inversion using mass equation

Given measurements of velocities, surface mass balance and rates of thickness changes, the vertically integrated mass-conservation equation

$$F := \nabla \cdot (\mathbf{v}h) - a + \partial_t h = 0 \quad (6.70)$$

can be solved for h . Typically we would here consider the case where good estimates of a and $\partial_t h$ are available and we, thus, consider

$$F := \nabla \cdot (\mathbf{v}h) - a^* = 0 \quad (6.71)$$

⁵There appears to be some confusion in the literature regarding this point and sometimes (often, practically always) the expression given for the directional derivative is something like

$$(d_h J)_j = \frac{1}{\mathcal{A}} \int (\dot{h} - \tilde{h}) (\partial_x u \phi_j + u \partial_x \phi_j) d\mathcal{A} + \frac{1}{\mathcal{A}} \int (h - \tilde{h}) \phi_j d\mathcal{A}, \quad (\text{wrong!})$$

and in fact inversion can be successfully done using this derivative. However, this ‘derivative’ will be intimately related to the structure of the FE approximation used, both the basis and the discretisation. This expression for the ‘derivative’ is simply an example of a FE assembly, and it does not represent the values of the coefficients of the derivative in the FE basis. The correct expression is Eq. (6.69).

where

$$a^* = a - \partial_t h .$$

The equation is hyperbolic and information only travels along the characteristics. Anticipating this, we add some cross-wind diffusion and solve

$$\nabla \cdot (\mathbf{v}h) - \nabla \cdot (\boldsymbol{\kappa} \nabla h) = a - \partial_t h$$

with

$$\boldsymbol{\kappa} = \epsilon (\mathbf{1} - \hat{\mathbf{n}} \otimes \hat{\mathbf{n}}) ,$$

where the term $\partial_t h$ is based on measurements and, hence, not considered unknown. See section 10.10 for the solution approach. We initially consider a formulation where the velocities are not updated. After assembly the system can be written on the form

$$\mathbf{F}_h \mathbf{h} = \mathbf{b}$$

where \mathbf{F}_h is the resulting matrix after linearisation of F with respect to h .

This could be solved directly, using the cross-wind diffusion as an effective regularisation. Measurements of h can simply be enforced as boundary conditions, in which case they will be fulfilled exactly. Enforcing the h boundary conditions point-wise, written as

$$\mathbf{L}\mathbf{h} = \mathbf{c}$$

using the method of Lagrange multipliers leads to

$$\begin{bmatrix} \mathbf{F}_h & \mathbf{L}^T \\ \mathbf{L} & \mathbf{0} \end{bmatrix} \begin{bmatrix} \mathbf{h} \\ \boldsymbol{\lambda} \end{bmatrix} = \begin{bmatrix} \mathbf{b} \\ \mathbf{c} \end{bmatrix} . \quad (6.72)$$

Thickness measurements as soft constraints

Alternatively, if we want to introduce the regularisation explicitly, and furthermore not to use measurements as hard constraints, we consider

$$\mathcal{L} = \frac{1}{2}(\mathbf{h} - \check{\mathbf{h}})^T \mathbf{P}_h (\mathbf{h} - \check{\mathbf{h}}) + \frac{1}{2}(\mathbf{h} - \tilde{\mathbf{h}})^T \mathbf{Q} (\mathbf{h} - \tilde{\mathbf{h}}) + \boldsymbol{\lambda}^T (\mathbf{F}_h \mathbf{h} - \mathbf{b})$$

where \mathbf{Q} is a regularisation matrix related to the inverse of the covariance $\text{cov}(h, h)$, for example selected as

$$\mathbf{Q} = \gamma_a \mathbf{M} + \gamma_s \mathbf{D} , \quad (6.38)$$

where \mathbf{M} and \mathbf{D} are the mass and the stiffness matrices, respectively, and \mathbf{P} is the matrix of measurement precision, or the inverse of the error covariance. Here

$$\begin{array}{ll} \tilde{h} & \text{prior} \\ \check{h} & \text{measurements} \end{array}$$

Taking the derivatives of \mathcal{L} with respect to \mathbf{h} and $\boldsymbol{\lambda}$ leads to

$$\begin{aligned} \mathbf{P}_h (\mathbf{h} - \check{\mathbf{h}}) + \mathbf{Q}_h (\mathbf{h} - \tilde{\mathbf{h}}) + \boldsymbol{\lambda}^T \mathbf{F}_h &= \mathbf{0} \\ \mathbf{F}_h \mathbf{h} - \mathbf{b} &= \mathbf{0} \end{aligned}$$

where we have used that both \mathbf{P} and \mathbf{Q} are symmetrical, or

$$\begin{aligned} (\mathbf{P}_h + \mathbf{Q}_h) \mathbf{h} + \mathbf{F}_h^T \boldsymbol{\lambda} &= \mathbf{P} \check{h} + \mathbf{Q} \tilde{h} \\ \mathbf{F}_h \mathbf{h} &= \mathbf{b} \end{aligned}$$

which can be written as

$$\begin{bmatrix} \mathbf{P}_h + \mathbf{Q}_h & \mathbf{F}_h^T \\ \mathbf{F}_h & \mathbf{0} \end{bmatrix} \begin{bmatrix} \mathbf{h} \\ \boldsymbol{\lambda} \end{bmatrix} = \begin{bmatrix} \mathbf{P} \check{h} \\ \mathbf{b} \end{bmatrix} . \quad (6.73)$$

The problem (well one of the problems) with this formulation is that \mathbf{F}_h is full rank and the system

$$\mathbf{F}_h \mathbf{h} = \mathbf{b}$$

uniquely defines \mathbf{h} . Maybe we can provide a bit of flexibility by introducing the forward model as a soft constraint instead

Thickness measurements and forward model as soft constraints

Consider now

$$\mathcal{L} = \frac{1}{2}(\mathbf{h} - \check{\mathbf{h}})^T \mathbf{P}_h (\mathbf{h} - \check{\mathbf{h}}) + \frac{1}{2}(\mathbf{h} - \tilde{\mathbf{h}})^T \mathbf{Q}_{\tilde{h}} (\mathbf{h} - \tilde{\mathbf{h}}) + \frac{1}{2}(\mathbf{F}_h \mathbf{h} - \mathbf{b})^T \mathbf{P}_F (\mathbf{F}_h \mathbf{h} - \mathbf{b})$$

Taking the derivatives of \mathcal{L} with respect to \mathbf{h} leads to

$$\begin{aligned} \mathbf{P}_h (\mathbf{h} - \check{\mathbf{h}}) + \mathbf{Q}_h (\mathbf{h} - \tilde{\mathbf{h}}) + \frac{1}{2} (\mathbf{F}_h^T \mathbf{P}_F (\mathbf{F}_h \mathbf{h} - \mathbf{b}) + (\mathbf{F}_h \mathbf{h} - \mathbf{b})^T \mathbf{P}_F \mathbf{F}_h) \\ \mathbf{P}_h (\mathbf{h} - \check{\mathbf{h}}) + \mathbf{Q}_h (\mathbf{h} - \tilde{\mathbf{h}}) + \mathbf{F}_h^T \mathbf{P}_F \mathbf{F}_h \mathbf{h} - \frac{1}{2} \mathbf{F}_h^T \mathbf{P}_F \mathbf{b} - \frac{1}{2} \mathbf{b}^T \mathbf{P}_F \mathbf{F}_h \end{aligned}$$

or

$$(\mathbf{P}_h + \mathbf{Q}_h + \mathbf{F}_h^T \mathbf{P}_F \mathbf{F}_h) \mathbf{h} = \mathbf{P}_h \check{\mathbf{h}} + \mathbf{Q} \tilde{\mathbf{h}} + \mathbf{F}_h^T \mathbf{P}_F \mathbf{b}$$

We see that if we consider the forward model to be exact, in which case the \mathbf{P}_h goes to infinity, we get

$$\mathbf{F}_h \mathbf{h} = \mathbf{b} \quad (\text{exact forward model})$$

and if the measurements are available everywhere with infinite precision

$$\mathbf{P}_h \mathbf{h} = \mathbf{P}_h \check{\mathbf{h}} \quad (\text{exact measurements})$$

And if the prior is perfect

$$\mathbf{Q}_h \mathbf{h} = \mathbf{Q} \tilde{\mathbf{h}} \quad (\text{exact prior})$$

Link to adjoint formulation of the problem

Using the adjoint approach discussed above where both $p = h$ and $q = h$, we have the augmented function

$$\mathcal{L} = J(h) + \langle \lambda, F(h) \rangle$$

where

$$F(h) = \nabla \cdot (\mathbf{v}h) - \nabla \cdot (\boldsymbol{\kappa} \nabla h) - a + \partial_t h = 0$$

Here the discrete form of the forward problem can be written as

$$\mathbf{K}h = \mathbf{b}$$

The cost function is

$$J = \frac{1}{2}(\mathbf{h} - \check{\mathbf{h}})^T \mathbf{P} (\mathbf{h} - \check{\mathbf{h}}) + \frac{1}{2}(\mathbf{h} - \tilde{\mathbf{h}})^T \mathbf{Q} (\mathbf{h} - \tilde{\mathbf{h}})$$

and therefore

$$J = \frac{1}{2}(\mathbf{h} - \tilde{\mathbf{h}})^T \mathbf{P} (\mathbf{h} - \tilde{\mathbf{h}}) + \frac{1}{2}(\mathbf{h} - \tilde{\mathbf{h}})^T \mathbf{Q} (\mathbf{h} - \tilde{\mathbf{h}}) + \lambda^T (\mathbf{K}h - \mathbf{b})$$

First we solve the forward problem is

$$\langle \phi, F(h) \rangle = 0$$

or

$$\mathbf{K}h = \mathbf{b}$$

for \mathbf{h} . Then solve the adjoint equation

$$\langle \partial_q J + (\partial_q F)^*, \phi \rangle = 0$$

or with $q = h$,

$$\mathbf{K}^T \boldsymbol{\lambda} = -(\mathbf{E} + \mathbf{Q})(\mathbf{h} - \tilde{\mathbf{h}})$$

where we use \mathbf{h} from the forward solve, and then calculate the derivative of the augmented cost function as

$$d_p \mathcal{L} = \langle (\partial_p F)^* \boldsymbol{\lambda} + \partial_p J, \phi \rangle$$

or with $p = h$,

$$d_h \mathcal{L} = \mathbf{K}^T \boldsymbol{\lambda} + (\mathbf{E} + \mathbf{Q})(\tilde{\mathbf{h}} - \mathbf{h})$$

The potential advantage of this adjoint approach is that we do not need to calculate the derivative $d_p q$ (i.e. the sensitivity matrix) which, in general, might be difficult. However, here with $p = q = h$ and we have $d_h h = 1$.

Thickness and velocity measurements as soft constraints

Using the adjoint approach discussed above where we treat \mathbf{v} as a control parameter, and h as the output of forward model, i.e. $p = \mathbf{v}$ and $q = h$,

$$F(h) = \nabla \cdot (\mathbf{v}h) - \nabla \cdot (\kappa \nabla h) - a + \partial_t h = 0$$

Here we consider $\partial_t h$ to be a measured quantity, similarly to a , and write

$$a^* = a - \partial_t h a; .$$

$$\mathcal{L} = \underbrace{\frac{1}{2}\|\mathbf{v} - \tilde{\mathbf{v}}\|^2 + \frac{1}{2}\|h - \tilde{h}\|^2}_{J = \mathcal{I}_v + \mathcal{I}_h + \mathcal{R}} + \underbrace{\mathcal{R}(h) + \langle \lambda | F(h(\mathbf{v})) \rangle}_{=: \mathcal{M}} \quad (6.74)$$

where

$$\frac{1}{2}\|h - \tilde{h}\|^2 = \int_{\mathcal{A}} h(\mathbf{x} - \tilde{h}(\mathbf{x})) \kappa_h(\mathbf{x}', \mathbf{x}') h(\mathbf{x}' - \tilde{h}(\mathbf{x}')) d\mathcal{A}$$

where κ_h is the precision kernel. If data errors are uncorrelated we write $\kappa_h = \delta(\|\mathbf{x} - \mathbf{x}'\|)\epsilon_h^{-2}$ and find

$$\begin{aligned} \mathcal{I}_h &= \frac{1}{2}\|h - \tilde{h}\|^2 \\ &= \frac{1}{2} \int_{\mathcal{A}} \left(h(\mathbf{x}) - \tilde{h}(\mathbf{x}) \right)^2 / \epsilon_h(\mathbf{x})^2 d\mathcal{A} \\ &= \frac{1}{2} \mathbf{h}_\epsilon \mathbf{M} \mathbf{h}_\epsilon \end{aligned}$$

where the nodal residuals are

$$\mathbf{h}^\epsilon = (\mathbf{h} - \tilde{\mathbf{h}}) / \epsilon_h$$

All variables are expanded in the same basis, i.e.

$$h(x, y) = h_i \phi_i(x, y) \quad u(x, y) = u_i \phi_i(x, y) \quad v(x, y) = v_i \phi_i(x, y) \quad \lambda(x, y) = \lambda_i \phi_i(x, y)$$

and hence

$$\delta_j h(x, y) = \phi_j(x, y) \quad \delta_j u(x, y) = \phi_j(x, y) \quad \delta_j v(x, y) = \phi_j(x, y) \quad \delta_j \lambda(x, y) = \phi_j(x, y)$$

The directional derivative of \mathcal{I}_h in the direction δh is

$$\begin{aligned} \delta_h \mathcal{I}_h &= \int_{\mathcal{A}} \left(h - \tilde{h} \right) / \epsilon_h \delta h d\mathcal{A} \\ &= \int_{\mathcal{A}} h_i^\epsilon \phi_i \phi_j d\mathcal{A} \\ &= \left(\int_{\mathcal{A}} \phi_j \phi_i d\mathcal{A} \right) h_i^\epsilon \\ &= \mathbf{M} \mathbf{h}^\epsilon \end{aligned}$$

Similarly

$$\begin{aligned} \mathcal{I}_v &= \frac{1}{2}\|\mathbf{v} - \tilde{\mathbf{v}}\|^2 \\ &= \frac{1}{2}(\mathbf{u}^\epsilon \mathbf{M} \mathbf{v}_\epsilon + \mathbf{v}_\epsilon \mathbf{M} \mathbf{u}_\epsilon) \end{aligned}$$

and

$$\delta_{\mathbf{v}} \mathcal{I}_v = \mathbf{M} \mathbf{u}_\epsilon + \mathbf{M} \mathbf{v}_\epsilon$$

As a regularisation term we use, for example,

$$\begin{aligned} \mathcal{R}(h) &= \frac{1}{2} \int_{\mathcal{A}} (\gamma_a h^2 + \gamma_s ((\partial_x h)^2 + (\partial_y h)^2)) d\mathcal{A} \\ &= \frac{1}{2} \int_{\mathcal{A}} (\gamma_a h^2 + \gamma_s \nabla h \cdot \nabla h) d\mathcal{A} \\ &= \frac{1}{2} \mathbf{h} (\gamma_a \mathbf{M} + \gamma_s (\mathbf{D}_{xx} + \mathbf{D}_{yy})) \mathbf{h} \end{aligned}$$

The directional derivative with respect to h of the regularisation term is

$$\begin{aligned}\delta_h \mathcal{R} &= \int_{\mathcal{A}} (\gamma_a h \delta h + \gamma_s (\partial_x(h + \delta h) + \partial_y(h + \delta h)) d\mathcal{A} \\ &= \gamma_a \langle h | \delta h \rangle + \gamma_s (\langle \partial_x h | \partial_x \delta h \rangle + \langle \partial_y h | \partial_y \delta h \rangle) \\ &= (\gamma_a \mathbf{M} + \gamma_s (\mathbf{D}_{xx} + \mathbf{D}_{yy})) \mathbf{h}\end{aligned}$$

The forward model constraint is

$$\begin{aligned}\delta_\lambda \mathcal{M} &= \delta_\lambda \langle \lambda | F \rangle = \langle \delta \lambda | F \rangle \\ &= \langle \delta \lambda | \nabla \cdot (\mathbf{v} h) - \nabla \cdot (\kappa \nabla h) - a^* \rangle \\ &= \langle \delta \lambda | \nabla \cdot (\mathbf{v} h) - \nabla \cdot (\kappa \nabla h) \rangle - \langle \delta \lambda | a^* \rangle \\ &= \langle \delta \lambda | \partial_x(uh) + \partial_u(vh) \rangle + \kappa (\langle \partial_x \delta \lambda | \partial_x h \rangle + \langle \partial_y \delta \lambda | \partial_y h \rangle) - \langle \delta \lambda | a^* \rangle \\ &= \langle \phi_j | \partial_x(u_p \phi_p h_k \phi_k) + \partial_y(v_p \phi_p h_k \phi_k) \rangle + \kappa (\langle \partial_x \phi_j | h_k \partial_x \phi_k \rangle + \langle \partial_y \phi_j | h_k \partial_y \phi_k \rangle) - \langle \phi_j | a_k^* \phi_k \rangle \\ &= (\langle \phi_j | \partial_x(u_p \phi_p \phi_k) + \partial_y(v_p \phi_p \phi_k) \rangle + \kappa (\langle \partial_x \phi_j | \partial_x \phi_k \rangle + \langle \partial_y \phi_j | \partial_y \phi_k \rangle)) h_k - \langle \phi_j | \phi_k \rangle a_k^* \\ &= \mathbf{K} \mathbf{h} - \mathbf{b}\end{aligned}$$

where

$$\begin{aligned}[\mathbf{K}]_{jk} &= \langle \phi_j | \partial_x(u_p \phi_p \phi_k) + \partial_y(v_p \phi_p \phi_k) \rangle + \kappa (\langle \partial_x \phi_j | \partial_x \phi_k \rangle + \langle \partial_y \phi_j | \partial_y \phi_k \rangle) \\ [\mathbf{b}]_j &= \langle \phi_j | \phi_k \rangle a_k^* = [\mathbf{M} \mathbf{a}^*]_j\end{aligned}$$

Note that we can also write

$$\mathbf{K} = \frac{d}{dh} \langle \delta \lambda | F \rangle = \langle \delta \lambda | d_h F \rangle$$

or

$$[\mathbf{K}]_{ij} = \langle \phi_i | d_{h_j} F \rangle$$

Similarly

$$\begin{aligned}\delta_h \mathcal{M} &= \delta_h \langle \lambda | F \rangle \\ &= \langle \lambda | \nabla \cdot (\mathbf{v} \delta h) - \nabla \cdot (\kappa \nabla \delta h) \rangle \\ &= \langle \lambda | \nabla \cdot (\mathbf{v} \delta h) \rangle + \langle \nabla \lambda | \kappa \nabla \delta h \rangle \\ &= \langle \lambda | \partial_x(u \delta h) + \partial_y(v \delta h) \rangle + \kappa (\langle \partial_x \lambda | \partial_x \delta h \rangle + \langle \partial_y \lambda | \partial_y \delta h \rangle) \\ &= \lambda_j (\langle \phi_j | \partial_x(u_p \phi_p \phi_k) + \partial_y(v_p \phi_p \phi_k) \rangle + \kappa (\langle \partial_x \phi_j | \partial_x \phi_k \rangle + \langle \partial_y \phi_j | \partial_y \phi_k \rangle)) \\ &= \boldsymbol{\lambda}^T \mathbf{K}\end{aligned}$$

And

$$\begin{aligned}\delta_u \mathcal{M} &= \delta_u \langle \lambda | F \rangle \\ &= \langle \lambda | \delta_u F \rangle \\ &= \langle \lambda | \partial_x(\delta_u h) \rangle \\ [\delta_u \mathcal{M}]_p &= \langle \lambda | \partial_x(\delta u_p h_k \phi_k) \rangle \\ &= \langle \lambda_j \phi_j | h_k \partial_x(\phi_p \phi_k) \rangle\end{aligned}$$

If I only solve for \mathbf{h} I get the linear system

$$\begin{aligned}\delta_\lambda \mathcal{L} &= \langle \delta \lambda | F \rangle = \mathbf{K} \mathbf{h} - \mathbf{b} = 0 \\ \delta_h \mathcal{L} &= \langle \lambda | \delta_h F \rangle = \mathbf{M}(\mathbf{h} - \tilde{\mathbf{h}}) \cdot \epsilon_h + (\gamma_a \mathbf{M} + \gamma_s (\mathbf{D}_{xx} + \mathbf{D}_{yy})) \mathbf{h} + \boldsymbol{\lambda}^T \mathbf{K} = 0\end{aligned}$$

which can be written as the KKT system

$$\begin{pmatrix} \mathbf{M} \mathbf{C}_h^{-1} + \gamma_a \mathbf{M} + \gamma_s (\mathbf{D}_{xx} + \mathbf{D}_{yy}) & \mathbf{K}^T \\ \mathbf{K} & 0 \end{pmatrix} \begin{pmatrix} \mathbf{h} \\ \boldsymbol{\lambda} \end{pmatrix} = \begin{pmatrix} \mathbf{M} \mathbf{C}_h^{-1} \tilde{\mathbf{h}} \\ \mathbf{b} \end{pmatrix}$$

$$\delta_\lambda \mathcal{L} = \langle \delta\lambda | F \rangle = \mathbf{K}\mathbf{h} - \mathbf{b} = 0$$

$$\delta_h \mathcal{L} = \langle \lambda | \delta_h F \rangle = \mathbf{M}(\mathbf{h} - \tilde{\mathbf{h}}) ./ \boldsymbol{\epsilon}_h + (\gamma_a \mathbf{M} + \gamma_s (\mathbf{D}_{xx} + \mathbf{D}_{yy})) \mathbf{h} + \boldsymbol{\lambda}^T \mathbf{K} = 0$$

$$\delta_u \mathcal{L} = \langle \lambda | \delta_u F \rangle = \mathbf{M}(\mathbf{u} - \tilde{\mathbf{u}}) ./ \boldsymbol{\epsilon}_u + \boldsymbol{\lambda} = 0$$

The adjoint system is

$$F(h(v), v) = 0 \quad (6.75)$$

$$\partial_h F^* \lambda = -\partial_h J \quad (6.76)$$

$$d_v J = \partial_v F^* \lambda + \partial_v J \quad (6.77)$$

Assuming uncorrelated errors, the misfit (likelihood) terms are

$$\mathcal{I} = \frac{1}{2} \mathbf{h}_\epsilon \mathbf{M} \mathbf{h}_\epsilon$$

The discrete form of the adjoint system is

$$\begin{aligned} \mathbf{K}\mathbf{h} &= \mathbf{b} \\ \mathbf{K}^T \boldsymbol{\lambda} &= -\mathbf{M}(\mathbf{h} - \tilde{\mathbf{h}}) ./ \boldsymbol{\epsilon}_h \end{aligned}$$

and the uv elements of the gradient can then be calculated as

$$\begin{aligned} [\partial_u F^* \lambda]_i &= \langle \partial_x (\phi_i h_j \phi_j), \lambda_r \phi_r \rangle \\ [\partial_v F^* \lambda]_i &= \langle \partial_y (\phi_i h_j \phi_j), \lambda_r \phi_r \rangle \end{aligned}$$

and the $\partial_u J$ and $\partial_v J$ terms added to arrive at $d_v J$.

However since the system is linear and so simple it appears one could also solve this directly. For example if

$$\mathcal{L} = \frac{1}{2} \mathbf{u}_\epsilon \mathbf{M} \mathbf{u}_\epsilon + \frac{1}{2} \mathbf{v}_\epsilon \mathbf{M} \mathbf{v}_\epsilon + \frac{1}{2} \mathbf{h}_\epsilon \mathbf{M} \mathbf{h}_\epsilon + \boldsymbol{\lambda}^T \cdot (\mathbf{K}\mathbf{h} - \mathbf{b}) \quad (6.78)$$

leading to

$$\begin{aligned} \mathbf{K}\mathbf{h} - \mathbf{b} &= \mathbf{0} \\ \mathbf{M}(\mathbf{h} - \tilde{\mathbf{h}}) ./ \boldsymbol{\epsilon}_h + \mathbf{K}^T \boldsymbol{\lambda} &= 0 \\ \mathbf{M}(\mathbf{u} - \tilde{\mathbf{u}}) ./ \boldsymbol{\epsilon}_u + \mathbf{K}_{,\mathbf{u}}^T \mathbf{h} \boldsymbol{\lambda} &= 0 \\ \mathbf{M}(\mathbf{v} - \tilde{\mathbf{v}}) ./ \boldsymbol{\epsilon}_v + \mathbf{K}_{,\mathbf{v}}^T \mathbf{h} \boldsymbol{\lambda} &= 0 \end{aligned}$$

6.15 Thickness (h) inversion using momentum equation

Here $q = v$ and $p = h$, and we have measurements of velocities and ice thicknesses.

$$\begin{aligned} F(v(h), h) &= 0 \\ J(v(h), h) &= \|v - \tilde{v}\| + \|h - \tilde{h}\| \\ \mathcal{L} &= J(v(h), h) + \langle \boldsymbol{\lambda}, F(v(h), h) \rangle \end{aligned}$$

The adjoint approach consist in solving

$$\begin{aligned} \langle F(v(h), h), \phi \rangle &= 0 \\ \langle (\partial_v F)^* \boldsymbol{\lambda}, \phi \rangle &= -\langle \partial_v J, \phi \rangle \end{aligned}$$

and then

$$d_h J = \langle (\partial_h F)^* \lambda, \phi \rangle + \langle \partial_h J, \phi \rangle$$

The direct approach would involve taking the h and λ total derivatives of \mathcal{L} and setting to zero. This would require calculating $d_h J = \partial_v J \partial_h v + \partial_h J$. The tricky part would then be $\partial_h v$, i.e. the sensitivity of velocities with respect to thickness, which we avoid calculating using the adjoint method.

6.16 B inversion using momentum and mass equation

Cost function:

$$J = J_{uv} + J_{\dot{h}} + J_A + J_B + J_C \quad (6.79)$$

Forward models, momentum and mass conservation:

$$\begin{aligned} F_{uv} &= F_{uv}(u, v, h(b), d(b)) && \text{(momentum)} \\ F_{\dot{h}} &= F_{\dot{h}}(u, h(b)) && \text{(mass conservation)} \\ F_b &= F_b(s, S, B) && \text{(floatation)} \end{aligned}$$

where F_{uv} are here the SSA momentum equations, and

$$F_{\dot{h}} = \dot{h} + \partial_x(u(s-b)) - a = 0$$

and b is calculated using the floating condition from s , S and B given ρ and ρ_o as

$$F_b = b - \mathcal{G}B - (1 - \mathcal{G}) \frac{\rho s - \rho_o S}{\rho - \rho_o} \quad (6.80)$$

where

$$\mathcal{G} = \mathcal{H}((s-b) - \rho_o(S-B)/\rho).$$

as explained further in section 6.18 this is a non-linear system and needs to be solved iteratively.

The cost functions are

$$J_{uv} = \frac{1}{2\mathcal{A}} \int \left(((u_s - \tilde{u}_s)/e_u)^2 + ((v_s - \tilde{v}_s)/e_v)^2 \right) d\mathcal{A} \quad (6.81)$$

$$J_{\dot{h}} = \frac{1}{2\mathcal{A}} \int \left((\dot{h} - \tilde{\dot{h}})/e_{\dot{h}} \right)^2 d\mathcal{A} \quad (6.82)$$

and J_B , J_C and J_A are regularisation terms (e.g Eq. 6.41).

The extended cost function becomes

$$\mathcal{L} = J_{uv} + J_{\dot{h}} + J_A + J_B + J_C + (F_{uv}, \lambda_{uv}) + (F_{\dot{h}}, \lambda_{\dot{h}}) + (F_b, \lambda_b)$$

and we wish to determine

$$d_B J = \delta_B J_B + (\delta_B F_{uv}^*, \lambda_{uv}) + (\delta_B F_{\dot{h}}^*, \lambda_{\dot{h}}) + (\delta_B F_b^*, \lambda_b) \quad (6.83)$$

We require

$$\delta_{uv} \mathcal{L} = 0$$

$$\delta_{\dot{h}} \mathcal{L} = 0$$

$$\delta_b \mathcal{L} = 0$$

and we get the adjoint equations are (see also Eq. 6.48)

$$(\delta_{uv} F_{uv}^*, \lambda_{uv}) + (\delta_{uv} F_{\dot{h}}^*, \lambda_{\dot{h}}) + (\delta_{uv} F_b^*, \lambda_b) = -\delta_{uv} J_{uv} - \delta_{uv} J_{\dot{h}} \quad (6.84)$$

$$(\delta_{\dot{h}} F_{uv}^*, \lambda_{uv}) + (\delta_{\dot{h}} F_{\dot{h}}^*, \lambda_{\dot{h}}) + (\delta_{\dot{h}} F_b^*, \lambda_b) = -\delta_{\dot{h}} J_{uv} - \delta_{\dot{h}} J_{\dot{h}} \quad (6.85)$$

$$(\delta_b F_{uv}^*, \lambda_{uv}) + (\delta_b F_{\dot{h}}^*, \lambda_{\dot{h}}) + (\delta_b F_b^*, \lambda_b) = -\delta_b J_{uv} - \delta_b J_{\dot{h}} \quad (6.86)$$

For the cost function Eq. (6.79) and its terms as defined by Eqs. (6.81) and (6.82), $J_{\dot{h}}$ is not an explicit function of either b or u and v , and therefore

$$\begin{aligned}\delta_b J_{uv} &= 0 \\ \delta_{\dot{h}} J_{uv} &= 0 \\ \delta_b J_{\dot{h}} &= 0 \\ \delta_{uv} J_{\dot{h}} &= 0\end{aligned}$$

Also from the definition of F_b by Eq. (6.80) and F_{uv}

$$\begin{aligned}(\delta_{uv} F_b^*, \lambda_b) &= 0 \\ (\delta_{\dot{h}} F_b^*, \lambda_b) &= 0 \\ (\delta_{\dot{h}} F_{uv}^*, \lambda_{\dot{h}}) &= 0\end{aligned}$$

The adjoint system Eqs. (6.84) to (6.86) therefore becomes

$$(\delta_{uv} F_{uv}^*, \lambda_{uv}) + (\delta_{uv} F_{\dot{h}}^*, \lambda_{\dot{h}}) = -\delta_{uv} J_{uv} \quad (6.87)$$

$$(\delta_{\dot{h}} F_{\dot{h}}^*, \lambda_{\dot{h}}) = -\delta_{\dot{h}} J_{\dot{h}} \quad (6.88)$$

$$(\delta_b F_{uv}^*, \lambda_{uv}) + (\delta_b F_{\dot{h}}^*, \lambda_{\dot{h}}) + (\delta_b F_b^*, \lambda_b) = 0 \quad (6.89)$$

Note that if, alternatively, $F_{\dot{h}}$ is included directly in $J_{\dot{h}}$, i.e.

$$J_{\dot{h}} = \frac{1}{2A} \int \left((a - (\partial_x(uh) + \partial_y(vh))) - \tilde{h} \right)^2 dA$$

then $F_{\dot{h}}$ is no longer required to be a part of the extended cost function (the Lagrangian), and the total derivative $d_B J$ can be calculated as

$$d_B J = \delta_B J_B + (\delta_B F_{uv}^*, \lambda_{uv}) + (\delta_B F_b^*, \lambda_b)$$

However, now $J_{\dot{h}}$ is an explicit function of b , so $\delta_b J_{\dot{h}} \neq 0$ and the adjoint system becomes

$$\begin{aligned}(\delta_{uv} F_{uv}^*, \lambda_{uv}) &= -\delta_{uv} J_{uv} - \delta_{uv} J_{\dot{h}} \\ (\delta_b F_{uv}^*, \lambda_{uv}) + (\delta_b F_{\dot{h}}^*, \lambda_{\dot{h}}) + (\delta_b F_b^*, \lambda_b) &= 0\end{aligned}$$

and λ_{uv} is a solution to

$$(\delta_{uv} F_{uv}^*, \lambda_{uv}) = -\delta_{uv} J_{uv} - \delta_{uv} J_{\dot{h}}$$

6.17 Inverting for b using a fixed floating mask

Here we consider the option of inverting only for b for a given flotation mask $\tilde{\mathcal{G}}$. We assume the upper surface (s), is known from measurements \tilde{s} .

Cost function:

$$J = J_{uv} + J_{\dot{h}} + J_A + J_b + J_C \quad (6.90)$$

Forward models, momentum and mass conservation:

$$\begin{aligned}F_{uv} &= F_{uv}(u, b, d(b)) && \text{(momentum)} \\ F_{\dot{h}} &= F_{\dot{h}}(u, b) && \text{(mass conservation)} \\ \mathcal{G} &= \tilde{\mathcal{G}} && \text{(flotation)}\end{aligned}$$

where F_{uv} are here the SSA momentum equations, and

$$F_{\dot{h}} = \dot{h} + \partial_x(u(s - b)) - a = 0$$

The cost functions are

$$J_{uv} = \frac{1}{2\mathcal{A}} \int \left(((u_s - \tilde{u}_s)/e_u)^2 + ((v_s - \tilde{v}_s)/e_v)^2 \right) d\mathcal{A} \quad (6.91)$$

$$J_h = \frac{1}{2\mathcal{A}} \int \left(\left((a - (\partial_x(uh) + \partial_y(vh))) - \tilde{h} \right) / e_h \right)^2 d\mathcal{A} \quad (6.92)$$

and J_b , J_C and J_A are regularisation terms (e.g Eq. 6.41) on the form

$$J_b = \frac{1}{2\mathcal{A}} \int \left((b - \tilde{b}) / e_b \right)^2 d\mathcal{A}$$

Since we here include F_h in the cost function, it does not need to be included in the extended cost function, therefore

$$\mathcal{L} = J_{uv} + J_h + J_A + J_b + J_C + (F_{uv}, \lambda_{uv}).$$

We wish to determine $d_b J$,

$$d_b J = \delta_b J_b + \delta_b J_h + (\delta_b F_{uv}^*, \lambda_{uv}) \quad (6.93)$$

The term $(\delta_b F_{uv}^*, \lambda_{uv})$ accounts for the effect of b on $d_b J$ (see Eq. 6.90) due to the implicit dependency of u and v on b .

We require

$$\delta_{uv} \mathcal{L} = 0$$

and we get the adjoint equation (see also Eq. 6.48)

$$(\delta_{uv} F_{uv}^*, \lambda_{uv}) = -\delta_{uv} J_{uv} - \delta_{uv} J_h \quad (6.94)$$

We assume the floating mask \mathcal{G} is given as an input and we denote the prescribed/measured floating mask as $\tilde{\mathcal{G}}$. We furthermore require that any changes in b do not lead to any changes in the floating mask. Therefore, for the flotation mask not to change during the inversion for b , the ice thickness h must be above the flotation limit where $\tilde{\mathcal{G}} < 1/2$ and below it where $\tilde{\mathcal{G}} > 1/2$, i.e.

$$\begin{aligned} h &> h_f & \text{where } \tilde{\mathcal{G}} \geq 1/2 \\ h &< h_f & \text{where } \tilde{\mathcal{G}} < 1/2 \end{aligned}$$

or

$$\begin{aligned} \rho(s - b) &> \rho_o(S - B) & \text{where } \tilde{\mathcal{G}} \geq 1/2 \\ \rho(s - b) &< \rho_o(S - B) & \text{where } \tilde{\mathcal{G}} < 1/2 \end{aligned}$$

We calculate the bedrock elevation (B) and the draft (d), given ρ and ρ_o , as

$$B = \begin{cases} b & \text{for } \tilde{\mathcal{G}} \geq 1/2 \\ \min(b, \tilde{B}) & \text{otherwise} \end{cases}$$

Since $b = B$ where $\tilde{\mathcal{G}} \geq 1/2$ we have

$$\begin{aligned} b &< \frac{\rho s - \rho_o S}{\rho - \rho_o} & \text{where } \tilde{\mathcal{G}} \geq 1/2 \\ b &> s - \rho_o(S - B)/\rho & \text{where } \tilde{\mathcal{G}} < 1/2 \end{aligned}$$

Provided these constraints on b are enforced, the floating mask (\mathcal{G}) remains unchanged as b is updated during the inversion. All directional derivatives of \mathcal{G} with respect to b are therefore automatically equal to zero. However, as b can change downstream of the grounding line within these constraints, the surface elevation s can change as well according to

$$s = (1 - \rho_o/\rho)b + \frac{\rho_o}{\rho}S, \quad \text{where } \tilde{\mathcal{G}} < 1/2$$

Such changes can be suppressed using an appropriate regularisation on b using as prior

$$\tilde{b} = \frac{\rho \tilde{s} - \rho_o S}{\rho - \rho_o} = \frac{\rho}{\rho_o - \rho}S - \frac{\rho_o}{\rho_o - \rho}\tilde{s} \quad \text{where } \tilde{\mathcal{G}} < 1/2$$

where \tilde{s} are measurements of s , and prescribing errors e_b in b derived from the observational errors e_s of s over floating areas as

$$e_b = e_s / |1 - \rho_o/\rho|$$

Alternatively an additional term J_s to the cost function J can be added as

$$J_s = \frac{1}{2\mathcal{A}} \int \{(1 - \mathcal{G}) [(1 - \rho_o/\rho)b + \rho_o S/\rho - \tilde{s}] / e_s\}^2 d\mathcal{A}$$

The directional derivative of the draft d defined as

$$d = \mathcal{H}(S - B)(S - b)$$

with respect to b is required. Note that where $S = B$, the ice is grounded for any $h > 0$, so therefore $b = B$ and in a weak sense $\int (\delta_b \mathcal{H}(S - b))(s - b) d\mathcal{A} = 0$, hence

$$\delta_b d = -\mathcal{H}(S - B)$$

6.18 Inverting for bedrock elevation B with varying flotation mask

When inverting for bedrock B the elevations of the upper and lower ice surfaces (s and b respectively) need to be recalculated as B is updated. We assume we have reasonably accurate measurements, \tilde{s} , of the surface elevation. When updating b we therefore consider s , S , and B given, and calculate b and h from s , S , and B , i.e.

$$\begin{aligned} b &= b(s, S, B, \rho, \rho_o) \\ h &= h(s, S, B, \rho, \rho_o) \end{aligned}$$

as

$$b = \mathcal{G} B + (1 - \mathcal{G}) \frac{\rho s - \rho_o S}{\rho - \rho_o}, \quad (6.95)$$

$$h = \mathcal{G} (s - B) + (1 - \mathcal{G}) \frac{s - S}{1 - \rho/\rho_o}, \quad (6.96)$$

where

$$\mathcal{G} = \mathcal{H}(h - \rho_o(S - B)/\rho). \quad (6.97)$$

This is a non-linear system because \mathcal{G} depends on h and solving this system is discussed in Sec. 1.15.3

We need to know the directional derivatives of various geometrical variables and quantities with respect to B . These include

$$\begin{aligned} \delta_B \mathcal{G} &= \lim_{\epsilon \rightarrow 0} \frac{d}{d\epsilon} \mathcal{H}(s - (B + \epsilon \delta B) - \rho_o(S - (B + \epsilon \delta B))/\rho) \\ &= \lim_{\epsilon \rightarrow 0} \left(\delta(s - (B + \epsilon \delta B) - \rho_o(S - B - \epsilon \delta B)/\rho) (-\delta B + \frac{\rho_o}{\rho} \delta B) \right) \\ &= \delta(h - h_f) (\rho_o/\rho - 1) \delta B \end{aligned}$$

and

$$\begin{aligned} \delta_B b &= \mathcal{G} \delta B + \delta_B G B - \frac{\rho s - \rho_o S}{\rho - \rho_o} \delta_B \mathcal{G} \\ &= \mathcal{G} \delta B + \left(B - \frac{\rho s - \rho_o S}{\rho - \rho_o} \right) \delta_B \mathcal{G} \\ &= \mathcal{G} \delta B + (\rho_o/\rho - 1) \left(B - \frac{\rho s - \rho_o S}{\rho - \rho_o} \right) \delta(h - h_f) \delta B \end{aligned}$$

and

$$\delta_B h = -\delta_B b$$

Also from

$$d = \mathcal{H}(S - B)(S - b)$$

we have

$$\delta_B d = -\delta(S - B)(S - b) \delta B - \mathcal{H}(S - B) \delta_B b$$

When calculating gradients with the adjoint method we get a term of the form

$$(\delta_B(\partial_x b), \lambda)$$

It's presumably best to use an integral theorem here and write this as

$$(\delta_B(\partial_x b), \lambda) = (\partial_x(\delta_B b), \lambda) = -(\delta_B b, \partial_x \lambda)$$

where $\lambda = 0$ along the boundary, for example something like

$$\begin{aligned} ((\rho h - \rho_o d) \delta_B(\partial_x b), \lambda) &= -(\delta_B b, \partial_x ((\rho h - \rho_o d) \lambda)) \\ &= -(\delta_B b, (\rho \partial_x h - \rho_o \partial_x d) \lambda + (\rho h - \rho_o d) \partial_x \lambda) \end{aligned}$$

6.19 Gradients of objective functions with respect to control variables

In the following we assume that all variables involved, such as A , C , b and λ are represented in the same basis, i.e.

$$\begin{aligned} C &= A_p \phi_p(x, y) \\ A &= A_p \phi_p(x, y) \\ b &= b_p \phi_p(x, y) \\ \lambda &= \lambda_q \phi_q(x, y) \end{aligned}$$

6.19.1 Gradient calculation in 1HD with respect to C

As an example we consider the calculation of the gradient of the objective function J with respect to slipperiness. The only term of the momentum equations containing C is the basal drag term

$$t_b = \mathcal{H}(h - h_f) C^{-1/m} \|v_b\|^{1/m-1} v_b$$

We need to evaluate

$$\begin{aligned} DJ(C)[\phi] &= \langle (\partial_C F)^* \lambda + \partial_C J | \phi \rangle \\ &= \langle \partial_C t_b)^* \lambda + \partial_C J | \phi \rangle \end{aligned}$$

giving

$$DJ(C)[\phi] = \langle \frac{1}{m} \mathcal{H}(h - h_f) C^{-1/m-1} \|v_b\|^{1/m-1} v_b \lambda | \phi \rangle + \langle \partial_C J | \phi \rangle$$

In the above listed expression one needs to form a sum between v_b and λ for each value of C . The adjoint variable λ is a solution of the adjoint equation and is a vector variable with x and y components similarly to v .

6.19.2 Gradient calculation in 1HD with respect to A

The directional derivative can be calculated (see Eq. 6.49) as

$$j'(A) = \partial J(q(p), p) / \partial A + (\partial F / \partial A)^* \lambda \quad (6.98)$$

Focusing on the second term

$$\begin{aligned} (\partial_A F)^* \lambda &= \langle \partial_A \left(2\partial_x(A^{-1/n} h |\partial_x u|^{(1-n)/n} \partial_x u) - t_{bx} - \frac{1}{2} g \partial_x(\rho h^2 - \rho_o d^2) + g \mathcal{H}(h - h_f)(\rho h - \rho_o H^+) \partial_x B \right) | \lambda \rangle \\ &= - \langle 2\partial_A \left(A^{-1/n} h |\partial_x u|^{(1-n)/n} \partial_x u \right) | \partial_x \lambda \rangle \\ &= - \langle \frac{2}{n} A^{-1/n-1} h |\partial_x u|^{(1-n)/n} \partial_x u \delta A, \partial_x \lambda \rangle \end{aligned}$$

where we have omitted writing the boundary term assuming that λ is set to zero along the boundary (or periodic boundary conditions for periodic domains.) Hence

$$\begin{aligned} (\partial_A F)^* \lambda &= \left\langle \frac{2}{n} A^{-1/n-1} h |\partial_x u|^{(1-n)/n} \partial_x u \delta A, \partial_x \lambda \right\rangle \\ &= \left\langle \frac{2}{n} A^{-1/n-1} h |\partial_x u|^{(1-n)/n} \partial_x u \phi_p, \lambda_q \partial_x \phi_q \right\rangle \\ &= \left\langle \frac{2}{n} A^{-1/n-1} h |\partial_x u|^{(1-n)/n} \partial_x u \phi_p, \partial_x \phi_q \right\rangle \lambda_q \end{aligned}$$

or

$$(\partial_A F)^* \lambda = \mathbf{K} \boldsymbol{\lambda}$$

where

$$K = (\partial F / \partial A)^*$$

is

$$K_{pq} = \left\langle \frac{2}{n} A^{-1/n-1} h |\partial_x u|^{(1-n)/n} \partial_x u \phi_p, \partial_x \phi_q \right\rangle \lambda_q$$

however it is more efficient to calculate this matrix-vector product directly without ever forming the matrix as

$$\mathbf{K} \boldsymbol{\lambda} = \left\langle \frac{2}{n} A^{-1/n-1} h |\partial_x u|^{(1-n)/n} \partial_x u \phi_p, \partial_x \lambda \right\rangle$$

6.19.3 Gradient calculation in 1HD with respect to b

The directional derivative can be calculated (see Eq. 6.49) as

$$j'(b) = \partial J(q(p), p) / \partial b + (\partial F / \partial b)^* \lambda \quad (6.99)$$

Simplifying the notation a bit and just considering the grounded ice situation the x term of the SSA equation is

$$F = 2\partial_x \left(A^{-1/n} h |\partial_x u|^{(1-n)/n} \partial_x u \right) - \mathcal{H}(h - h_f) C^{-1/m} \|u\|^{1/m-1} u - \rho g h \partial_x s - \frac{1}{2} g h^2 \partial_x \rho = 0 \quad (6.100)$$

where $h = s - b$.

Considering initially the first term of Eq. (6.100)

$$\begin{aligned} (\partial_b F)^* \lambda &= \left\langle \partial_b \left(2\partial_x (A^{-1/n} h |\partial_x u|^{(1-n)/n} \partial_x u) \right) | \lambda \right\rangle \\ &= - \left\langle 2\partial_b \left(A^{-1/n} (s - b) |\partial_x u|^{(1-n)/n} \partial_x u \right) | \partial_x \lambda \right\rangle \\ &= \left\langle 2A^{-1/n} |\partial_x u|^{(1-n)/n} \partial_x u \delta b, \partial_x \lambda \right\rangle \end{aligned}$$

or

$$[(\partial_b F)^* \lambda]_p = \left\langle 2A^{-1/n} |\partial_x u|^{(1-n)/n} \partial_x u \phi_p, \partial_x \phi_q \right\rangle \lambda_q$$

where we again have omitted writing the boundary term assuming that λ is set to zero along the boundary (or periodic boundary conditions applied for periodic domains.). Using Eq. (1.191)

$$\eta = \frac{1}{2} A^{-1/n} |\partial_x u|^{(1-n)/n}$$

leads to

$$[(\partial_b F)^* \lambda]_p = \left\langle 4\eta \partial_x u \phi_p, \partial_x \phi_q \right\rangle \lambda_q$$

Second term of Eq. (6.100) leads to

$$[(\partial_b F)^* \lambda]_p = \left\langle \delta(h - h_f) C^{-1/m} \|u\|^{1/m-1} u \phi_p, \phi_q \right\rangle \lambda_q$$

(Note: I've ignored here the fact that where the ice is grounded and $b = B$, $h_f = \rho_o H / \rho = \rho_o(S - B) / \rho = \rho_o(S - b) / \rho$ is a function of b)

More generally one can write this as

$$[(\partial_b F)^* \lambda]_p = \langle (\partial_b t_{bx}) \phi_p, \phi_q \rangle \lambda_q$$

And the last two terms of Eq. (6.100) give

$$\begin{aligned} (\partial_b F)^* \lambda &= - \langle \partial_b \left(\rho g h \partial_x s + \frac{1}{2} g h^2 \partial_x \rho \right), \lambda \rangle \\ &= \langle (\rho g \partial_x s + g h \partial_x \rho) \phi, \lambda \rangle \end{aligned}$$

or

$$[(\partial_b F)^* \lambda]_p = \langle (\rho g \partial_x s + g h \partial_x \rho) \phi_p | \phi_q \rangle \lambda_q$$

Usually only the regularisation term is an explicit function of the control variable, i.e.

$$J(F(p, q(p), p) = I(F(p, q(p))) + R(p)$$

and therefore

$$\partial_p J = \partial_p R$$

But if we solve for b and use $\partial_t h$ as a constraint, calculated as $a - \partial_x(uh)$ we now have b explicitly both in the misfit term I and in the regularisation term R , so $\partial_b J$ has now this additional I term.

6.20 Inverting for $\log p$

To lessen the chances of a strictly positive parameter p becoming negative in the course of the inversion we can make a change of variables writing

$$p = 10^\gamma = e^{\gamma \ln(10)}$$

or

$$\log_{10} p = \gamma$$

and invert for γ instead of p . Note that

$$\frac{\partial p}{\partial \gamma} = \ln(10) p .$$

and we find

$$\begin{aligned} \frac{\partial J}{\partial \gamma} &= \frac{\partial J}{\partial p} \frac{\partial p}{\partial \gamma} \\ &= \frac{\partial J}{\partial p} \ln(10) 10^\gamma \\ &= \ln(10) p \frac{\partial J}{\partial p} \end{aligned}$$

showing that the change of variables causes a rescaling of the gradient, making the gradient go to zero as $p \rightarrow 0$. However, for a finite step size this rescaling of the gradient alone does not guarantee that p will not become negative (and $\log p$ complex) during the optimisation. In Ua one therefore also enforces the positivity (non complex) constraint when inverting for $\log p$ of a strictly positive parameter.

For the Hessian we have

$$\begin{aligned} \frac{\partial^2 J}{\partial \gamma^2} &= \frac{\partial}{\partial \gamma} \frac{\partial J}{\partial \gamma} \\ &= \frac{\partial}{\partial \gamma} \left(\frac{\partial J}{\partial p} \frac{\partial p}{\partial \gamma} \right) \\ &= \frac{\partial^2 J}{\partial p \partial \gamma} \frac{\partial p}{\partial \gamma} + \frac{\partial J}{\partial p} \frac{\partial^2 p}{\partial \gamma^2} \\ &= \frac{\partial^2 J}{\partial p^2} \left(\frac{\partial p}{\partial \gamma} \right)^2 + \frac{\partial J}{\partial p} \frac{\partial^2 p}{\partial \gamma^2} \\ &= (\ln(10)p)^2 \frac{\partial^2 J}{\partial p^2} + \ln(10)^2 p \frac{\partial J}{\partial p} \end{aligned}$$

6.21 The form of the adjoint equations for Bayesian approach using Gaussian statistics

We anticipate using a Bayesian approach assuming Gaussian statistics and therefore that the cost function might be on the form

$$\begin{aligned} \min_p I(q(p)) &= \langle q - \hat{q} | K_q^{-1} | q - \hat{q} \rangle + \langle p - \tilde{p} | K_P^{-1} | p - \tilde{p} \rangle \\ &= \langle K_q^{-T/2}(q - \hat{q}) | K_q^{-1/2}(q - \hat{q}) \rangle + \langle K_p^{-T/2}(p - \tilde{p}) | K_p^{-1/2}(p - \tilde{p}) \rangle \end{aligned}$$

where K is a covariance matrix (and therefore positive definite).

Repeating the calculations required in the adjoint approach for this particular case,

$$\begin{aligned} d_p I = d_p \mathcal{L} &= \langle K_q^{-1/2}(q - \hat{q}) | d_p q \rangle + \langle \lambda | \partial_q F d_p q + \partial_p F \rangle + \langle \partial_p \lambda | F \rangle \\ &= \langle K_q^{-1/2}(q - \hat{q}) | d_p q \rangle + \langle \lambda | \partial_q F d_p q + \partial_p F \rangle \\ &= \langle K_q^{-1/2}(q - \hat{q}) + \lambda(\partial_q r)^* | d_p q \rangle + \langle \lambda | \partial_p F \rangle \end{aligned}$$

where we have omitted the $\langle p - \tilde{p} | K_P^{-1} | p - \tilde{p} \rangle$ term for the time being. We now use the flexibility of λ not having been specified and require that

$$\langle K_q^{-1/2}(q - \hat{q}) + \lambda(\partial_q F)^* | \delta p \rangle = 0$$

and therefore

$$d_p I = \langle \lambda | \partial_p F \rangle$$

For a cost function on the form

$$\min_p I(q(p)) = \langle q - \hat{q} | K_q^{-1} | q - \hat{q} \rangle + \langle p - \tilde{p} | K_P^{-1} | p - \tilde{p} \rangle$$

we would arrive at

$$d_p I = \langle \lambda | \partial_p F \rangle + \langle K_p^{-1/2}(p - \tilde{p}) | \delta p \rangle$$

One might ask why we don't just calculate the cost gradient as

$$d_p = \langle K_q^{-1/2}(q - \hat{q}) | d_p u \rangle$$

But this would require calculating $\partial_p q$ which is a pain in the neck and requires N solutions for the forward problem, where $N + 1$ is the number of discrete control parameters. Using the adjoint method we only need to solve the forward problem twice.

6.22 Adjoint equations (Bayesian case with constraints on vertical velocity)

We want to minimise a cost function \tilde{J} on the form

$$\tilde{J}(u, v, w, p) = I(u, v, w) + F(p)$$

where I is a data discrepancy functional, and R a regularisation term

As a misfit function we use

$$I = I_u + I_v + I_o,$$

where each term has the form

$$I_u = \langle C_{uu}^{-1/2} u - \tilde{u} | C_{uu}^{-1/2} u - \tilde{u} \rangle$$

with $C_{uu}^{-1/2}$ being an error covariance matrix.

The regularisation term has the form

$$R = \langle C_{pp}^{-1/2} p | C_{pp}^{-1/2} p \rangle$$

We minimise \tilde{J} subject to the conditions

$$F(u(p), v(p), p) = 0$$

and

$$w_s = f(u, v, h, b)$$

where r are the diagnostic equations, f is a function giving the vertical surface velocity w_o as a function of the variables of the diagnostic equations, and where p stands for some control variable (distributed model parameter) such as the basal slipperiness C or the rate factor A . We therefore consider the extended cost function

$$J(u, v, w, \lambda, \mu, p) = I(u, v, w) + F(p) + < \lambda | F(q(p), v(p), p) \rangle + < \mu | w - f(u, v, h, b) \rangle$$

where λ and μ are Lagrange multipliers.

The directional derivative of J with respect to λ in the direction of $\delta\lambda$ is defined as

$$\frac{d}{d\epsilon} J(\lambda + \epsilon \delta\lambda) |_{\epsilon=0}$$

and is denoted by $\delta J(\lambda, \delta\lambda)$

The directional derivatives of J are

$$\delta J(\lambda, \delta\lambda) = \delta_\lambda J = < \delta\lambda, F(u, v, p) \rangle$$

$$J(\mu, \delta\mu) = < \delta\mu, w - f(u, v, h, b) \rangle$$

$$J(u, \delta u) = < C_{uu}^{-1/2}(u - \tilde{u}, C^{-1/2}\delta u) + < \lambda, \nabla_u r \delta u \rangle - < \mu | \nabla_u f \delta u \rangle$$

6.23 Prognostic equations are formally self-adjoint

The SSTREAM equations are formally⁶ self-adjoint as we will now show.

Define the inner product

$$r = < f_x | \lambda \rangle + < f_y | \mu \rangle$$

where

$$\begin{aligned} f_x &= \partial_x(h\eta(4\partial_x u + 2\partial_y v)) + \partial_y(h\eta(\partial_y u + \partial_x v)) - \mathcal{H}(h - h_f)t_{bx} \\ &\quad - \frac{1}{2}g\partial_x(\rho h^2 - \rho_o d^2) + g\mathcal{H}(h - h_f)(\rho h - \rho_o H^+)\partial_x B \end{aligned} \tag{6.101}$$

$$\begin{aligned} f_y &= \partial_y(h\eta(4\partial_y v + 2\partial_x u)) + \partial_x(h\eta(\partial_x v + \partial_y u)) - \mathcal{H}(h - h_f)t_{by} \\ &\quad - \frac{1}{2}g\partial_y(\rho h^2 - \rho_o d^2) + g\mathcal{H}(h - h_f)(\rho h - \rho_o H^+)\partial_y B \end{aligned} \tag{6.102}$$

or

$$\begin{aligned} r &= \iint \{ (\partial_x(h\eta(4\partial_x u + 2\partial_y v)) + \partial_y(h\eta(\partial_y u + \partial_x v))) - \mathcal{H}(h - h_f)t_{bx} \\ &\quad - \frac{1}{2}g\partial_x(\rho h^2 - \rho_o d^2) + g\mathcal{H}(h - h_f)(\rho h - \rho_o H^+)\partial_x B \} \lambda dx dy \\ &\quad + \iint \{ (\partial_y(h\eta(4\partial_y v + 2\partial_x u)) + \partial_x(h\eta(\partial_x v + \partial_y u))) - \mathcal{H}(h - h_f)t_{by} \\ &\quad - \frac{1}{2}g\partial_y(\rho h^2 - \rho_o d^2) + g\mathcal{H}(h - h_f)(\rho h - \rho_o H^+)\partial_y B \} \mu dx dy \end{aligned}$$

⁶Here 'formally' stands for 'if ignoring boundary conditions'.

The use of Green's theorem gives

$$\begin{aligned}
r = & - \iint_{\Omega} \left\{ h\eta(4\partial_x u + 2\partial_y v)\partial_x \lambda + h\eta(\partial_y u + \partial_x v)\partial_y \lambda + \mathcal{H}(h - h_f)\beta^2 u \lambda \right. \\
& - \frac{1}{2}g(\rho h^2 - \rho_o d^2)\partial_x \lambda + \lambda g \mathcal{H}(h - h_f)(\rho h - \rho_o H^+) \partial_x B \left. \right\} dx dy \\
& + \oint_{\Gamma} (h\eta(4\partial_x u + 2\partial_y v) \lambda n_x + h\eta(\partial_y u + \partial_x v) \lambda n_y - \frac{1}{2}g(\rho h^2 - \rho_o d^2) \lambda n_x) d\Gamma \\
& - \iint_{\Omega} \left\{ h\eta(4\partial_y v + 2\partial_x u)\partial_y \mu + h\eta(\partial_x v + \partial_y u)\partial_x \mu + \mathcal{H}(h - h_f)\beta^2 v \right. \\
& - \frac{1}{2}g(\rho h^2 - \rho_o d^2)\partial_y \mu + \mu g \mathcal{H}(h - h_f)(\rho h - \rho_o H^+) \partial_x B \left. \right\} dx dy \\
& + \oint_{\Gamma} (h\eta(4\partial_y v + 2\partial_x u) \mu n_y + h\eta(\partial_x v + \partial_y u) \mu n_x - \frac{1}{2}g(\rho h^2 - \rho_o d^2) \mu n_y) d\Gamma
\end{aligned}$$

and a second use of Green's theorem gives after some rearrangements

$$\begin{aligned}
r = & \iint_{\Omega} \left\{ \partial_x(h\eta(4\partial_x \lambda + 2\partial_y \mu)) u + \partial_y(h\eta(\partial_y \lambda + \partial_x \mu)) u - \mathcal{H}(h - h_f)\beta^2 u \lambda \right. \\
& + \frac{1}{2}g(\rho h^2 - \rho_o d^2)\partial_x \lambda - \lambda g \mathcal{H}(h - h_f)(\rho h - \rho_o H^+) \partial_x B \left. \right\} dx dy \\
& + \oint_{\Gamma} (h\eta(4\partial_x u + 2\partial_y v) \lambda n_x + h\eta(\partial_y u + \partial_x v) \lambda n_y - \frac{1}{2}g(\rho h^2 - \rho_o d^2) \lambda n_x) d\Gamma \\
& + \iint_{\Omega} \left\{ \partial_y(h\eta(4\partial_x \mu + 2\partial_y \lambda)) v + \partial_x(h\eta(\partial_x \mu + \partial_y \lambda)) v - \mathcal{H}(h - h_f)\beta^2 u \lambda \right. \\
& + \frac{1}{2}cdg(\rho h^2 - \rho_o d^2)\partial_y \mu - \mu g \mathcal{H}(h - h_f)(\rho h - \rho_o H^+) \partial_x B \left. \right\} dx dy \\
& + \oint_{\Gamma} (h\eta(4\partial_y v + 2\partial_x u) \mu n_y + h\eta(\partial_x v + \partial_y u) \mu n_x - \frac{1}{2}g(\rho h^2 - \rho_o d^2) \mu n_y) d\Gamma \\
& - \oint_{\Omega} (uh\eta(4\partial_x \lambda + 2\partial_y \mu)n_x + uh\eta(\partial_y \lambda + \partial_x \mu)n_y) d\Gamma \\
& - \oint_{\Omega} (vh\eta(4\partial_y \mu + 2\partial_x \lambda)n_y + vh\eta(\partial_x \mu + \partial_y \lambda)n_x) d\Gamma
\end{aligned}$$

If we ignore the BCs terms, the equations are clearly self-adjoint.

In Ūa the BCs conditions for the adjoint problem (the boundary terms shown above) are generated automatically from the BCs of the forward problem using some sensible assumptions such as homogenisation of the adjoint BCs if Dirichlet and natural BCs are applied to the forward problem, and periodic BCs for the adjoint problem if periodic BCs are applied to the forward problem. The user can overwrite these assumptions if needed.

The adjoint approach is based on the use of the adjoint of the linearised/tangent forward model around the converged solution of non-linear forward model. The non-linear forward model is

$$F(u) = \mathbf{0}$$

and the tangent model is the directional derivative of the forward model in the direction δu .

$$K = D\mathbf{F}(\mathbf{u})[\delta \mathbf{u}]$$

Often this is simply be written as

$$K = \frac{\partial \mathbf{F}}{\partial \mathbf{u}}$$

Define

$$\langle L \delta U | \Lambda \rangle = \langle U | L \Lambda \rangle$$

where $U = (\delta u, \delta v)^T$ and \mathbf{L} is the operator acting on U as given by the system (1.226) and (1.227).

$$\begin{aligned}
\langle \mathbf{L} \delta u | \Lambda \rangle &= \iint_{\Omega} \left\{ (\partial_x(h\eta(4\partial_x \delta u + 2\partial_y \delta v)) + \partial_y(h\eta(\partial_y \delta u + \partial_x \delta v))) \lambda \right. \\
&\quad \left. + (\partial_y(h\eta(4\partial_y \delta v + 2\partial_x \delta u)) + \partial_x(h\eta(\partial_x \delta v + \partial_y \delta u))) \mu \right\} dx dy \\
&= - \iint_{\Omega} \left\{ h\eta(4\partial_x \delta u + 2\partial_y \delta v) \partial_x \lambda + h\eta(\partial_y \delta u + \partial_x \delta v) \partial_y \lambda \right. \\
&\quad \left. + h\eta(4\partial_y \delta v + 2\partial_x \delta u) \partial_y \mu + h\eta(\partial_x \delta v + \partial_y \delta u) \partial_x \mu \right\} dx dy \\
&\quad + \oint_{\Gamma} \left\{ h\eta(4\partial_x \delta u + 2\partial_y \delta v) \lambda n_x + h\eta(\partial_y \delta u + \partial_x \delta v) \lambda n_y \right. \\
&\quad \left. + h\eta(4\partial_y \delta v + 2\partial_x \delta u) \mu n_y + h\eta(\partial_x \delta v + \partial_y \delta u) \mu n_x \right\} d\Gamma \\
&= \iint_{\Omega} \left\{ (\partial_x(h\eta(4\partial_x \lambda + 2\partial_y \mu)) + \partial_y(h\eta(\partial_y \lambda + \partial_x \mu))) \delta u \right. \\
&\quad \left. + (\partial_y(h\eta(4\partial_x \mu + 2\partial_y \lambda)) + \partial_x(h\eta(\partial_y \lambda + \partial_x \mu))) \delta v \right\} dx dy \\
&\quad + \oint_{\Gamma} \left\{ (h\eta(4\partial_x \delta u + 2\partial_y \delta v) n_x + h\eta(\partial_y \delta u + \partial_x \delta v) n_y) \lambda \right. \\
&\quad \left. + (h\eta(4\partial_y \delta v + 2\partial_x \delta u) n_y + h\eta(\partial_x \delta v + \partial_y \delta u) n_x) \mu \right\} d\Gamma \\
&\quad - \oint_{\Gamma} (h\eta(4\partial_x \lambda + 2\partial_y \mu) n_x + h\eta(\partial_y \lambda + \partial_x \mu) n_y) \delta u d\Gamma \\
&\quad - \oint_{\Gamma} (h\eta(4\partial_y \mu + 2\partial_x \lambda) n_y + h\eta(\partial_x \mu + \partial_y \lambda) n_x) \delta v d\Gamma
\end{aligned}$$

Once the forward model has been solved the velocity field fulfils given the BCs to a high degree of accuracy. The boundary conditions on the δ fields follow from above

6.24 Covariance kernels

$$F(f) = \int \int f(x) \kappa(x, x') f(x') dx dx'$$

where κ is the covariance kernel.

Assuming isotropic, stationary, and translation invariance, i.e.

$$\kappa(x, x') = \kappa(|x - x'|)$$

a multipole expansion of an exponentially decaying covariance is on the form

$$e^{-|x-x_i|^2/4T} = \sum_{n_1, n_2=0}^{\infty} \Theta_{n_1 n_2}(x - c) \dots$$

Chapter 7

Calving

7.1 Level-set method

Level-set methods (LSM) are a conceptual framework for using level sets as a tool for numerical analysis of surfaces and shapes. The advantage of the level-set model is that one can perform numerical computations involving curves and surfaces on a fixed Cartesian grid without having to parameterise these objects.

Wikipedia
Level-set method

The calving rate is a scalar quantity, defined as the difference between the advance/retreat rate of the calving front and the material velocity, \mathbf{v} , of ice at the calving front in normal direction. We use an implicit formulation to describe the position of the calving as the set of points, \mathbf{x}_c fulfilling the condition

$$\varphi(\mathbf{x}_c(t), t) = 0, \quad (7.1)$$

where φ is the *level-set function*. Thus, the calving fronts are the zero levels (zero contour lines) of the level set function φ .

Equation (7.1) holds for any time, t . Thus, if we take the time derivative of φ , for \mathbf{x}_c fixed, we find

$$\begin{aligned} \frac{d}{dt} \varphi(\mathbf{x}(t), t) \Big|_{\mathbf{x}=\mathbf{x}_c} &= \frac{\partial \varphi}{\partial x_k} \frac{\partial x_k}{\partial t} + \partial_t \varphi \\ &= \frac{\partial \varphi}{\partial x_k} u_k + \partial_t \varphi \\ &= \partial_t \varphi + \mathbf{u} \cdot \nabla \varphi \end{aligned}$$

where

$$\mathbf{u}_c = \partial_t \mathbf{x}_c$$

is the calving front velocity. Since, by definition, the value of the level-set function is always equal to zero as we follow a particle confined to the calving front over time, the corresponding time derivative is also equal to zero, that is

$$\frac{d}{dt} \varphi(\mathbf{x}(t), t) \Big|_{\mathbf{x}=\mathbf{x}_c} = \partial_t \varphi + \mathbf{u} \cdot \nabla \varphi = 0 \quad (7.2)$$

While the calving front is the zero level of the level set function, the level set function itself is define throughout the domain. The level set function, φ , is a scalar function of location and time, i.e. $\varphi : \mathbb{R}^2 \times \mathbb{R} \rightarrow \mathbb{R}$, that is

$$\varphi = \varphi(\mathbf{x}, t).$$

Note that the position vector, \mathbf{x} , stands here for any (x, y) location throughout the computational domain. Any point confined to the calving front moves with the velocity, $\mathbf{u}_c = \partial_t \mathbf{x}_c$, in a direction normal to the

calving front. The level set function φ is defined to be positive on one side of the calving front, and negative on the other side. Since it has a constant value (i.e. value of zero) along the calving front, we can find the normal to the calving front as as

$$\hat{\mathbf{n}} = -\frac{\nabla \varphi}{\|\nabla \varphi\|}, \quad (7.3)$$

with

$$\|\nabla \varphi\|^2 = \nabla \varphi \cdot \nabla \varphi.$$

The sign convention used in the definition of the normal in Eq. (7.3) is introduced in the anticipation that φ will be defined as a decreasing function of distance as we travel across the calving front, from the ice covered region to the ice-free region, with the normal $\hat{\mathbf{n}}$ pointing outwards.

The velocity, \mathbf{u}_c , of the calving front is equal to the difference between the material velocity, \mathbf{v} , of ice at the calving front and the calving velocity \mathbf{c} , that is

$$\mathbf{u}_c = \mathbf{v} - \mathbf{c}.$$

As mentioned above, φ does not change for any point along the calving front

$$\varphi(\mathbf{x}_c(t), t) = 0, \quad (7.4)$$

and as above, we have

$$\partial_t \varphi + \mathbf{u}_c \cdot \nabla \varphi = 0,$$

or

$$\partial_t \varphi + (\mathbf{v} - \mathbf{c}) \cdot \nabla \varphi = 0, \quad (7.5)$$

hence

$$\partial_t \varphi + \mathbf{v} \cdot \nabla \varphi = \mathbf{c} \cdot \nabla \varphi, \quad (7.6)$$

The calving velocity vector, \mathbf{c} , is always normal to the calving front itself, and we can write

$$\begin{aligned} \mathbf{c} &= c \hat{\mathbf{n}} \\ &= -c \frac{\nabla \varphi}{\|\nabla \varphi\|}, \end{aligned}$$

where the scalar c is the calving rate, or

$$\partial_t \varphi + \mathbf{v} \cdot \nabla \varphi = -c \|\nabla \varphi\|. \quad (7.7)$$

Eqs. (7.5) and (7.7) are different forms of the *kinematic calving front condition* and it is our evolutionary equation for the level-set function φ for a given material velocity \mathbf{v} of the material particles at the calving front, and a calving rate c . This is a non-linear hyperbolic equation, the non-linearity being due to the dependency of direction of \mathbf{c} on φ . Solving Eqs. (7.5) and (7.7) requires suitable boundary conditions to be prescribed along inflow boundaries.

When used the calculated the evolution of the zero level (which here is a 1-dimensional curve) of a higher-dimensional function φ , (here a 2-dimensional function of x and y) Eq. (7.5) is referred to as the *level-set equation*. In the literature the level-set equation is usually written as

$$\partial_t \varphi + F \|\nabla \varphi\| = 0, \quad (7.8)$$

where the scalar F is the speed in outward normal direction. We can bring Eq. (7.7) to this standard form by defining F as

$$F = \mathbf{v} \cdot \hat{\mathbf{n}} - c.$$

Generally, one finds that the speed function F needs to be both physically and numerically motivated. Examples for the use of the level-set method in glaciology to describe the evolution of glacier surfaces and calving front include [Hossain et al. \(2020\)](#) and [Bondzio et al. \(2016\)](#).

At the beginning of a simulation, the level set needs to be initialised in such a way that its zero level coincides with the initial calving front position, and is positive one one side and negative on the other side of the front. This can be done by, for example, calculating the (signed) distance to the calving front

$$\varphi(\mathbf{r}, t=0) = \min_{\gamma} \|\mathbf{r} - \mathbf{r}(\gamma)\|,$$

where $\mathbf{r} = (x, y)$ and $\mathbf{T}(\gamma)$ is a parameterised vector function giving the x and the y coordinates of the calving front/fronts at $t = 0$. Alternatively, one can solve the Eikonal equation $\|\nabla\varphi\|$ on both sides of the curve. Both approaches ensure that $\|\nabla\varphi\| = 1$ as the curve is crossed.

The level-set equation (7.7) is a non-linear hyperbolic equation. As an example of type of behaviour that can be expected, consider the one-dimensional case where

$$\partial_t \varphi + (v - c) \partial_x \varphi = 0 \quad (7.9)$$

For $u = v - c =$ spatially constant, Eq. (7.9) is a linear advection equation and the solution is a travelling shape-preserving wave

$$\varphi(x, t) = \varphi_0(x - (v - c)t)$$

travelling with the velocity u . However, if $v - c$ is spatially variable, for example if $v - c = \epsilon(x - x_0)$, where ϵ is some (possibly small) constant, then the solution to (7.9) becomes

$$\varphi(x, t) = -(x - x_c) e^{\epsilon(t-t_0)}$$

This example is particularly pertinent because, as mentioned above, the level set is often initialised as a signed distance function, which in this one-dimensional example implies

$$\varphi(x, t = t_0) = x - x_c$$

where here x_c stands for the position of the calving front at $t = t_0$, and $\mathbf{v} - \mathbf{C}$ is generally spatially variable, suggesting that φ may grow without bounds with time. In particular, φ will with time cease being a (signed) distance function with $\|\nabla\varphi\| = 1$. At the same time there are good reasons for wanting φ to be at least approximately a signed distance function at all times. Changes in physical properties as the calving front is crossed can, for example, then be easily parameterised as a function of normal distance to the front using as function of φ .

As shown by Barles et al. (1993) signed-distance function are not solutions to the level-set equation and Barles et al. (1993) gives simple intuitive examples showing that φ can be expected to develop shocks. Determining the level set can, hence, be expected to become increasingly difficult as the gradient of φ grows with time and eventually becomes unbounded.

Several methods have been proposed in the literature to deal with this problem. These include initialisation whereby φ is either periodically reset to be equal to the signed distance function, or where a correction procedure is applied to 'push' the level set towards the signed distance function (e.g. Sussman et al., 1994). Global basis function approach using radial basis function expression for φ is described in Wang et al. (2007).

A level set method based on a variational principle can be derived by adding a perturbation \mathcal{P} to the energy potential (e.g Luo et al., 2019). Minimising this additional potential term involved adding the corresponding directional derivative with respect to φ to the level set equation (Eqs. 7.5 and 7.7), resulting, as I show below, in augmented form of the level-set equation with an additional non-linear diffusion term. The augmented level set equation takes the form

$$\partial_t \varphi + \mathbf{v} \cdot \nabla \varphi - \nabla \cdot (\kappa \nabla \varphi) = -c \|\nabla \varphi\| \quad (\text{scalar form}), \quad (7.10)$$

or, equivalently,

$$\partial_t \varphi + (\mathbf{v} - \mathbf{c}) \cdot \nabla \varphi - \nabla \cdot (\kappa \nabla \varphi) = 0 \quad (\text{vector form}). \quad (7.11)$$

In Eq. (7.10) the calving rate appears as a scalar variable, while in (7.11) as a vector. Eqs. (7.10) and (7.11) are referred to as the scalar and vector forms of the augmented level-set equation, respectively.

Requiring $\|\nabla\varphi\|$ being equal to unity can be achieved by minimising a potential term such as, for example, the the Eikonal functional

$$\mathcal{P} = \frac{1}{2} \int_A (\|\nabla\varphi\| - 1)^2 dA, \quad (7.12)$$

with respect to φ , that is by solving

$$D_{\delta\varphi} \mathcal{P} = 0. \quad (7.13)$$

Adding this directional derivative to the level-set equation is equivalent to imposing it as a weak constraint (weak in the sense that we do not enforce (7.13) to be fulfilled exactly at all times but allow for some deviation of $\|\nabla\varphi\|$ from unity). The resulting augmented level-set equation brings out explicitly the

unavoidable conflict resulting from requiring φ to be a solution to the level-set equation (Eqs. 7.5 and 7.7), while at the same time for $\|\nabla\varphi\|$ to remain close to unity at all times.

The directional derivative of the potential term (7.12) is

$$\begin{aligned} D_{\delta\varphi}\mathcal{P} &= \int_A (\|\nabla\varphi\| - 1) \frac{\nabla\varphi \cdot \nabla\delta\varphi}{\|\nabla\varphi\|} dA \\ &= \int_A \left(1 - \frac{1}{\|\nabla\varphi\|}\right) \nabla\varphi \cdot \nabla\delta\varphi dA \end{aligned}$$

where we have used that¹

$$\begin{aligned} D_{\delta\varphi} \|\nabla\varphi\| &= \lim_{\epsilon \rightarrow 0} \frac{d}{d\epsilon} \|\nabla(\varphi + \epsilon\delta\varphi)\| \\ &= \frac{\nabla\varphi \cdot \nabla\delta\varphi}{\|\nabla\varphi\|}, \end{aligned}$$

or, using the sign convection expressed by Eq. (7.3), that

$$D_{\delta\varphi} \|\nabla\varphi\| = -\hat{\mathbf{n}} \cdot \nabla\delta\varphi. \quad (7.14)$$

This is a weak form of a diffusion term, and in strong form the augmented equation is (7.10) where κ is a diffusion coefficient which we write as $\kappa = \mu k$ where k is non-dimensional and has the form

$$k = 1 - 1/\|\nabla\varphi\|$$

while μ is some suitable selected constant with the dimensions distance² × time⁻¹.² As discussed by Luo et al. (2019) this diffusion term has the undesirable effect that the diffusion rate becomes unbounded for $\|\nabla\varphi\| \rightarrow 0$. Ensuring boundness in this limit seems to have been one of the motivations of Li et al. (2010) and Touré and Soulaïmani (2016) for introducing their modified expressions of κ . and Li et al. (2010) suggested defining

$$\kappa = \mu k(\|\nabla\varphi\|),. \quad (7.15)$$

with

$$k(x) = \begin{cases} 1 - 1/x & \text{for } x \geq 1 \\ \frac{1}{2\pi} \frac{\sin(2\pi x)}{x} & \text{for } x < 1 \end{cases} \quad (7.16)$$

Another approach is to select a perturbation term on the more general form

$$\mathcal{P} = \frac{1}{pq} \int_A (\|\nabla\varphi\|^q - 1)^p dA \quad (7.17)$$

for which

$$\begin{aligned} D_{\delta\varphi}\mathcal{P} &= \int_A (\|\nabla\varphi\|^q - 1)^{p-1} \|\nabla\varphi\|^{q-1} \frac{\nabla\varphi \cdot \nabla\delta\varphi}{\|\nabla\varphi\|} dA \\ &= \int_A (\|\nabla\varphi\|^q - 1)^{p-1} \|\nabla\varphi\|^{q-2} \nabla\varphi \cdot \nabla\delta\varphi dA \end{aligned}$$

¹In more detail:

$$\begin{aligned} D_{\delta\varphi} \|\nabla\varphi\| &= \lim_{\epsilon \rightarrow 0} \frac{d}{d\epsilon} \|\nabla(\varphi + \epsilon\delta\varphi)\| \\ &= \lim_{\epsilon \rightarrow 0} \frac{d}{d\epsilon} ((\partial_x\varphi + \epsilon\partial_x\delta\varphi)^2 + (\partial_y\varphi + \epsilon\partial_y\delta\varphi)^2)^{1/2} \\ &= \lim_{\epsilon \rightarrow 0} \frac{d}{d\epsilon} ((\partial_x\varphi)^2 + (\partial_y\varphi)^2 + 2\epsilon\partial_x\varphi\partial_x\delta\varphi + \epsilon^2(\partial_x\delta\varphi)^2 + 2\epsilon\partial_y\varphi\partial_y\delta\varphi + \epsilon^2(\partial_y\delta\varphi)^2)^{1/2} \\ &= \frac{1}{2} ((\partial_x\varphi)^2 + (\partial_y\varphi)^2)^{-1/2} 2(\partial_x\varphi\partial_x\delta\varphi + \partial_y\varphi\partial_y\delta\varphi) \\ &= \frac{\nabla\varphi \cdot \nabla\delta\varphi}{\|\nabla\varphi\|} \\ &= -\hat{\mathbf{n}} \cdot \nabla\delta\varphi \end{aligned}$$

²Touré and Soulaïmani (2016) suggest setting

$$\mu = \beta \frac{\|\mathbf{u}\| l^2}{2}$$

where β is close to unity, l is the local element length, but this expression appears to have wrong units!

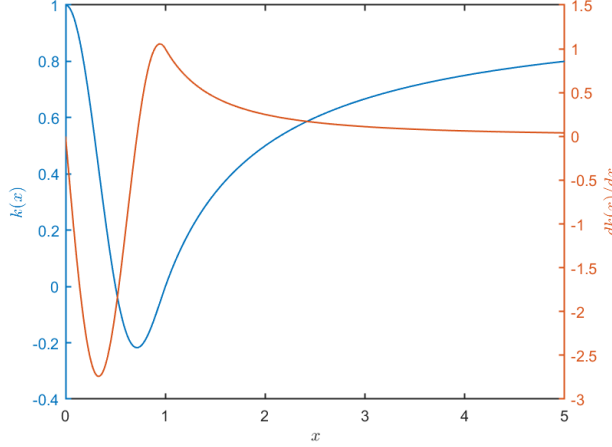


Figure 7.1: The $k(x)$ function suggested by Li et al. (2010), and given by Eq. 7.16. This term introduces forward-and-backward diffusion to Eq. (7.15).

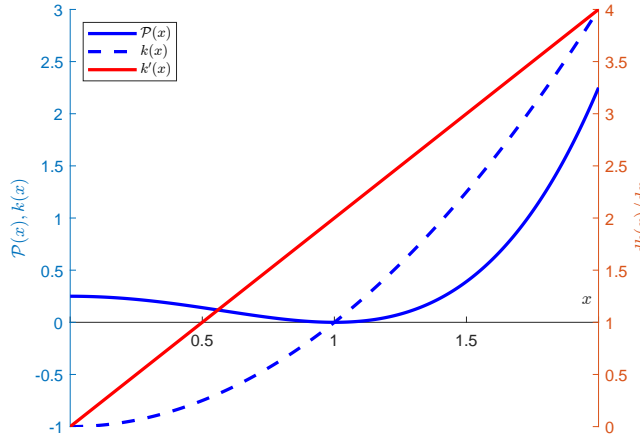


Figure 7.2: The perturbation term \mathcal{P} given by Eq. (7.17) and the corresponding $k(x)$ function given by Eq. (7.18) and the derivative $k'(x)$ used in the Newton-Raphson integration, all shown for $p = 2$ and $q = 2$.

giving a diffusion coefficient

$$\kappa = \mu k(\|\nabla\varphi\|)$$

in Eq. (7.10), where

$$k(x) = (x^q - 1)^{p-1} x^{q-2}, \quad (7.18)$$

which is bounded for $x = \|\nabla\varphi\| \rightarrow 0$, provided $q \geq 2$. For p an even number, the diffusion term defined by Eq. (7.18) can be both negative and positive and is an example of a *forward-and-backward* (FAB) diffusion.

7.1.1 Numerical implementation

In \tilde{U} the level set is evolved by solving the augmented level-set equation either in the c scalar form

$$\partial_t \varphi + \mathbf{v} \cdot \nabla \varphi - \nabla \cdot (\kappa \nabla \varphi) = -c \|\nabla \varphi\|, \quad (7.10)$$

or in its mathematical equivalent \mathbf{c} vector form as

$$\underbrace{\partial_t \varphi}_{\mathcal{T}} + \underbrace{(\mathbf{v} - \mathbf{c}) \cdot \nabla \varphi}_{\mathcal{L}} - \underbrace{\nabla \cdot (\kappa \nabla \varphi)}_{\mathcal{P}} = 0, \quad (7.11)$$

implicitly with respect to φ using the Newton-Raphson method with consistent SUPG weighting.

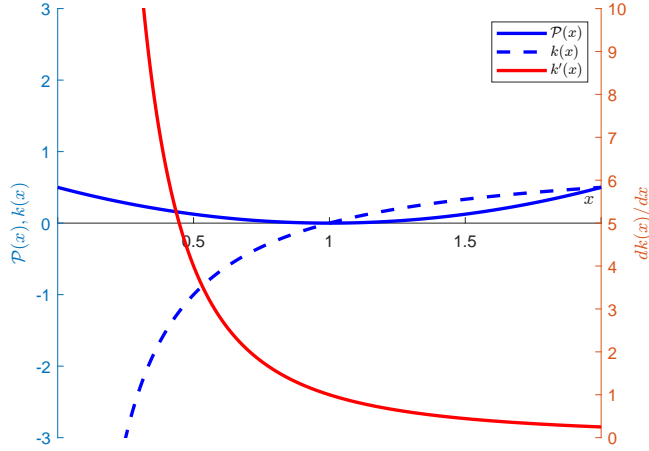


Figure 7.3: Same as Fig. 7.2 but for the Eikonal functional, where $p = 2$ and $q = 1$. In this case the function $k(x)$ is not bounded as $x \rightarrow 0$.

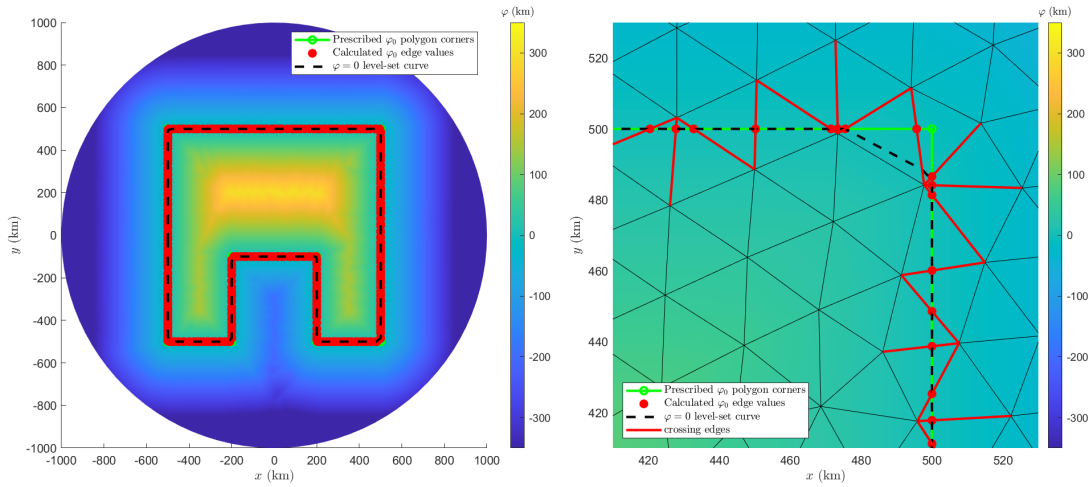


Figure 7.4: Geometric reinitialisation using only crossing points with element edges.

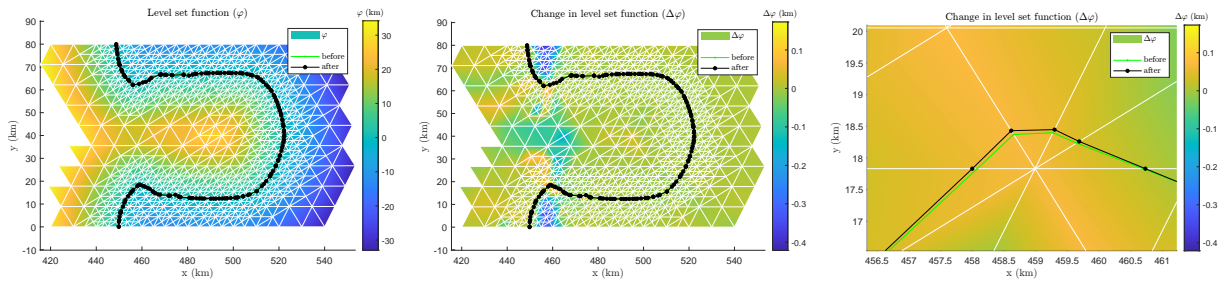


Figure 7.5: Geometrical re-initialisation using additional points along the level set $\varphi = 0$. The leftmost figure shows the level set function φ after re-initialisation, the middle one the change, $\Delta\varphi$, during the re-initialisation, and the rightmost figure is a zoom-in of the middle figure.

This requires linearisation of the non-linear $\|\nabla\varphi\|$ term, and the non-linear FAB diffusivity, $\kappa = \mu k(\|\nabla\varphi\|)$, which in $\bar{U}a$ can have various forms such as

$$k(x) = (x^q - 1)^{p-1} x^{q-2}, \quad (7.18)$$

or

$$k(x) = \begin{cases} 1 - 1/x & \text{for } x \geq 1 \\ \frac{1}{2\pi} \frac{\sin(2\pi x)}{x} & \text{for } x < 1 \end{cases} \quad (7.16)$$

where

$$x = \|\nabla\varphi\|.$$

For the NR formulation all terms involving φ need to be linearised. Linearising the norm of the gradient results in

$$\|\nabla(\varphi + \delta\varphi)\| = \|\nabla\varphi\| - \hat{\mathbf{n}} \cdot \nabla\delta\varphi + O((\delta\varphi)^2).$$

and linearising

$$\kappa = \mu k(\|\nabla\varphi\|),$$

gives

$$\begin{aligned} k(\|\nabla(\varphi + \delta\varphi)\|) &= k(\|\nabla\varphi\|) + \frac{k'(\|\nabla\varphi\|)}{\|\nabla\varphi\|} \nabla\varphi \cdot \nabla\delta\varphi \\ &= k(\|\nabla\varphi\|) - k'(\|\nabla\varphi\|) \hat{\mathbf{n}} \cdot \nabla\delta\varphi \end{aligned}$$

where we used expression (7.14) for the directional derivative $D_{\delta\varphi} \|\nabla\varphi\|$.

Using the (7.11) form furthermore requires linearising $\mathbf{c} \cdot \nabla\varphi$, where

$$\mathbf{c} \cdot \nabla\varphi = -c \frac{\nabla\varphi \cdot \nabla\varphi}{\|\nabla\varphi\|}$$

and we find that³

$$D_{\delta\varphi} (\mathbf{c} \cdot \nabla\varphi) = \mathbf{c} \cdot \nabla\delta\varphi. \quad (7.19)$$

³In more detail:

$$\begin{aligned} D_{\delta\varphi} (\mathbf{c} \cdot \nabla\varphi) &= \nabla\varphi \cdot D_{\delta\varphi} \mathbf{c} + \mathbf{c} \cdot \nabla\delta\varphi \\ D_{\delta\varphi} \mathbf{c} &= -c D_{\delta\varphi} \frac{\nabla\varphi}{\|\nabla\varphi\|} \\ &= -c \left(\frac{\nabla\delta\varphi}{\|\nabla\varphi\|} + (-1)(-1) \frac{\nabla\varphi (\hat{\mathbf{n}} \cdot \nabla\delta\varphi)}{\|\nabla\varphi\|^2} \right) \\ &= -c \left(\frac{\nabla\delta\varphi}{\|\nabla\varphi\|} + \frac{\nabla\varphi (\hat{\mathbf{n}} \cdot \nabla\delta\varphi)}{\|\nabla\varphi\|^2} \right) \\ &= -c \left(\frac{\nabla\delta\varphi}{\|\nabla\varphi\|} - \frac{\hat{\mathbf{n}} (\hat{\mathbf{n}} \cdot \nabla\delta\varphi)}{\|\nabla\varphi\|} \right) \end{aligned}$$

Hence

$$\begin{aligned} \nabla\varphi \cdot D_{\delta\varphi} \mathbf{c} &= -c (-\hat{\mathbf{n}} \cdot \nabla\delta\varphi + 1 \hat{\mathbf{n}} \cdot \nabla\delta\varphi) \\ &= 0 \end{aligned}$$

resulting in,

$$\begin{aligned} D_{\delta\varphi} (\mathbf{c} \cdot \nabla\varphi) &= \nabla\varphi \cdot D_{\delta\varphi} \mathbf{c} + \mathbf{c} \cdot \nabla\delta\varphi \\ &= 0 + \mathbf{c} \cdot \nabla\delta\varphi \\ &= \mathbf{c} \cdot \nabla\delta\varphi \end{aligned}$$

We can also arrive at the result (7.19) more simply as

$$\begin{aligned} D_{\delta\varphi} (\mathbf{c} \cdot \nabla\varphi) &= D_{\delta\varphi} (-c \|\nabla\varphi\|) \\ &= -c D_{\delta\varphi} (\|\nabla\varphi\|) \\ &= c \hat{\mathbf{n}} \cdot \nabla\delta\varphi \end{aligned}$$

showing again that

$$D_{\delta\varphi} (\mathbf{c} \cdot \nabla\varphi) = \mathbf{c} \cdot \nabla\delta\varphi$$

where we have used Eq. (7.14).

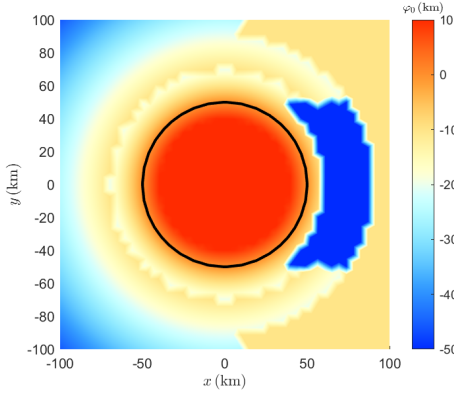


Figure 7.6: Example of level-set re-initialisation by solving only the non-linear diffusion term. This is the initial level set φ_0 .

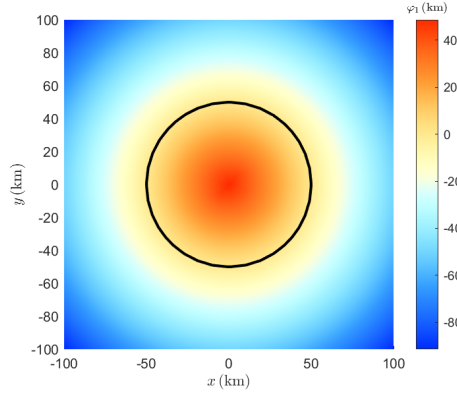


Figure 7.7: And this is φ_1 after solving for the non-linear diffusion term alone, i.e. $\nabla \cdot (\kappa \nabla \varphi_1) = 0$ using φ_0 as an initial guess.

The resulting linearised terms are all added to Eq. (7.20).

For the perturbation in k to be finite as $\|\nabla \varphi\| \rightarrow 0$, we must have

$$\lim_{x \rightarrow 0} \frac{k'(x)}{x} = K$$

where K is some constant. Using $k(x)$ giving by Eq. (7.18) results in

$$\begin{aligned} \frac{k'(x)}{x} &= \frac{(p-1)q(x^q-1)^{p-2}x^{q-1}x^{q-2} + (q-2)(x^q-1)^{p-1}x^{q-3}}{x} \\ &= (p-1)q(x^q-1)^{p-2}x^{2q-4} + (q-2)(x^q-1)^{p-1}x^{q-4} \end{aligned}$$

which is bounded as $x \rightarrow 0$ $p \geq 2$ and for $q = 2$ or $q \geq 4$, in which both the first and the second-order directional derivatives are bounded.

As commonly done in finite-elements, a weak form is obtained by forming the L^2 inner product of the equation to be solved with suitable form functions. The diffusion term is weighted using functions from the same space as used to expand φ (Bubnov-Galerkin method), and the remaining terms are weighted using the streamline-upwind Petrov-Galerkin approach. The diffusion term is integrated by parts, and as a result the natural boundary condition for φ is the free outflow/inflow boundary condition. Generally, a convection-diffusion equation such as (7.10) requires a Dirichlet type boundary condition along the inflow boundary with the (natural) free-outflow boundary condition applied over the remaining parts of the boundary.

The transient solution is formulated using the θ method with consistent streamline-upwind Petrov-Galerkin (SUPG) weighting, giving

$$\langle \varphi_1 - \varphi_0 | N + M \rangle + \Delta t \langle (1-\theta)F_0 \|\nabla \varphi_0\| + \theta F_1 \|\nabla \varphi_1\| | N + M \rangle = 0 ,$$

where

$$\begin{aligned} N(x, y) &= \phi(x, y) \\ M(x, y) &= \tau(\mathbf{v} - \mathbf{c}) \cdot \nabla \phi(x, y) \end{aligned}$$

with φ expanded in the basis $\{\phi(x, y)\}$, i.e. $\varphi(x, y) = \varphi_q \phi_q(x, y)$. See section 2.4 on various options for selecting τ . This non-linear system is then solved using the Newton-Raphson,⁴ where we repeatedly solve for $\delta\varphi$ and update φ_1^i at time step 1 as

$$\varphi_1^{i+1} = \varphi_1^i + \delta\varphi ,$$

where i is the NR iteration number, requires linearisation of all terms.

⁴The explicit form with $\theta = 0$ is clearly a particularly easy option, leading to the simple linear asymmetrical system

$$\langle \varphi_1 | N + M \rangle = \langle \varphi_0 | N + M \rangle + \Delta t \langle F_0 \|\nabla \varphi_0\| | N + M \rangle .$$

This explicit option is available in *Ua* but by default an implicit Newton-Raphson (NR) approach is used.

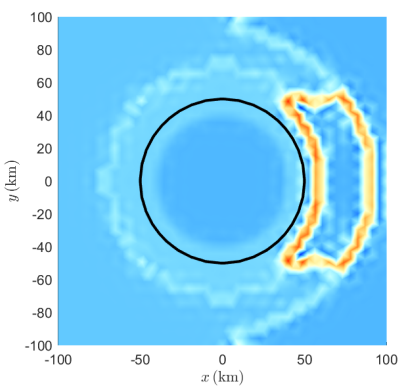


Figure 7.8: Same as in Fig. 7.6, but showing the norm of the gradient, $\|\nabla\varphi_0\|$.

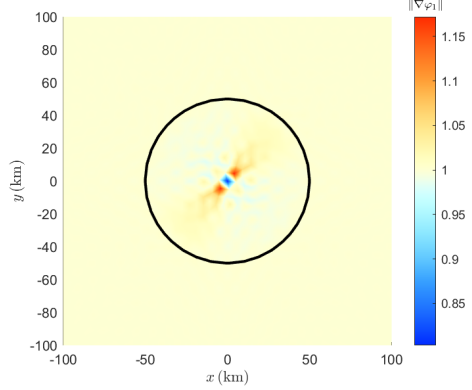


Figure 7.9: Same as in Fig. 7.7, but showing the norm of the gradient, $\|\nabla\varphi_1\|$.

Using the θ method, and after linearisation, Eq. (7.7) is therefore

$$\frac{\varphi_1^i + \delta\varphi - \varphi_0}{\Delta t} + \theta \mathbf{v}_1 \cdot (\nabla\varphi_1^i + \nabla\delta\varphi) + (1 - \theta)\mathbf{v}_0 \cdot \nabla\varphi_0 = \theta(c_1 \|\nabla\varphi_1^i\| - c_1 \hat{\mathbf{n}} \cdot \nabla\delta\varphi) + (1 - \theta)c_0 \|\nabla\varphi_0\| ,$$

which can also be written as

$$\left(1 + \theta\Delta t \left(\mathbf{v} + c \frac{\nabla\varphi_1^i}{\|\nabla\varphi_1^i\|}\right) \cdot \nabla\right) \delta\varphi = \Delta t(\varphi_0 - \varphi_1^i) - \theta\Delta t(\mathbf{v} \cdot \nabla\varphi_1^i + c \|\nabla\varphi_1^i\|) - (1 - \theta)\Delta t(\mathbf{v} \cdot \nabla\varphi_0 + c \|\nabla\varphi_0\|) . \quad (7.20)$$

Here we have yet to include the non-linear diffusion term.

$$\begin{aligned} c \hat{\mathbf{n}} &= \mathbf{c} \\ c \|\nabla\varphi\| &= -\mathbf{c} \cdot \nabla\varphi , \\ \mathbf{c} &= -c \frac{\nabla\varphi}{\|\nabla\varphi\|} \\ \mathbf{c} \cdot \nabla\varphi &= -c \frac{\nabla\varphi \cdot \nabla\varphi}{\|\nabla\varphi\|} = -c \|\nabla\varphi\| \\ \mathbf{c} \cdot \nabla\delta\varphi &= -c \frac{\nabla\varphi \cdot \nabla\delta\varphi}{\|\nabla\varphi\|} \end{aligned}$$

Here the only non-linear contribution stems from the dependence of \mathbf{c}_1 on φ .

Writing (7.11) as

$$\mathcal{L}\varphi = 0$$

where we have defined

$$\mathcal{L}\varphi := \partial_t\varphi + (\mathbf{v} - \mathbf{c}) \cdot \nabla\varphi - \nabla \cdot (\kappa \nabla\varphi)$$

the weak form is

$$\begin{aligned} 0 &= \langle \partial_t\varphi + (\mathbf{v} - \mathbf{c}) \cdot \nabla\varphi | \phi \rangle + \langle \kappa \nabla\varphi | \nabla\phi \rangle - \oint_{\partial\mathcal{A}} \kappa (\nabla\varphi \cdot \hat{\mathbf{n}}) \phi \, d\Gamma \\ &\quad + \sum_{i=1}^{n_{\text{Ele}}} \int_{\mathcal{A}^e} \mathcal{L}\varphi \tau(\mathbf{v} - \mathbf{c}) \cdot \nabla\phi \, d\mathcal{A} \end{aligned}$$

The second spatial derivative in the residual term is calculated using L_2 projection as suggested in Jansen et al. (1999).

Element re-initialisation around calving front

Depending how the calving front is represented graphically, some local element-wise procedure might be required. Fixing the set does this of course, but it ‘freezes’ the level set locally.

$$\begin{aligned}\varphi(\mathbf{p}_1) + \gamma_{12}(\varphi(\mathbf{p}_2) - \varphi(\mathbf{p}_1)) &= 0 \\ \varphi(\mathbf{p}_1) + \gamma_{13}(\varphi(\mathbf{p}_3) - \varphi(\mathbf{p}_1)) &= 0 \\ \frac{\varphi(\mathbf{p}_2) - \varphi(\mathbf{p}_1)}{\|\mathbf{p}_2 - \mathbf{p}_1\|} &= 1 \\ \frac{\varphi(\mathbf{p}_3) - \varphi(\mathbf{p}_1)}{\|\mathbf{p}_3 - \mathbf{p}_1\|} &= 1\end{aligned}$$

or

$$\begin{pmatrix} 1 + \gamma_{12} & -\gamma_{12} & 0 \\ 1 + \gamma_{13} & 0 & -\gamma_{13} \\ -1 & 1 & 0 \\ -1 & 0 & 1 \end{pmatrix} \begin{pmatrix} \varphi_1 \\ \varphi_2 \\ \varphi_3 \end{pmatrix} = \begin{pmatrix} 0 \\ 0 \\ \|\mathbf{p}_2 - \mathbf{p}_1\| \\ \|\mathbf{p}_3 - \mathbf{p}_1\| \end{pmatrix}$$

7.1.2 Ice calving

For a migrating calving front the ice downstream needs to be expunged, i.e. calved away. This can be done in various ways, for example by deactivating the ice-free elements or by applying an additional melt term. The approach that seems to give best results is to use implicit melt-rate parameterisation where additional melt rate is prescribed implicitly as a function of the to-be-calculated ice-thickness. For example as

$$a_c = (1 - \mathcal{H}(\varphi)) (a_1(h - h_{\min}) + a_3(h - h_{\min})^3), \quad (7.21)$$

where \mathcal{H} is the Heaviside step function, φ the level set function, a_c is the additional melt rate, i.e. the calving melt rate, and h_{\min} the desired minimum ice thickness, and a_1 and a_3 are some constants. Setting, for example, $a_1 \neq 0$ and $a_3 = 0$ gives

$$\partial_t h = (h_0 - h_{\min}) e^{a_1 t} + h_{\min},$$

where a_0 is the initial thickness, thereby effectively getting rid of the ice within the time $1/|a_1|$, for $a_1 < 0$. For typical ice-flow situations where the time step is expressed in the unit year, setting $a_1 = -1$ seems reasonable.

‘Implicit melt-rate’ parameterisation, involves including any derivatives of the melt-rate with respect to the solution variables as required in the Newton-Raphson iteration. Since here the melt rate depends on the thickness, h , which together with the velocity is one of the solution variables, we therefore include the term

$$\frac{\partial a_c}{\partial h} = (1 - \mathcal{H}(\varphi)) (a_1 + 3 a_3 (h - h_{\min})^2),$$

in the FE matrix assembly. To obtain the second-order NR convergence in the presence of strong inter-element spatial variation in a_c , this term must be evaluated at the integration points.

7.2 Verification test case

Various technical implementation details:

- During (re)initialisation, when using the fix-point approach (best option) use backward Euler or the φ solution will not be fully reinitialised. Also, as the only term of the equation used is the diffusion term, use standard Galerkin and not the SUPG weighting.

In one dimensional, the position of the calving front x_c is governed by the first-order system

$$\dot{x}_c = f(x_c) \quad (7.22)$$

with

$$f(x) = u(x) - c(x).$$

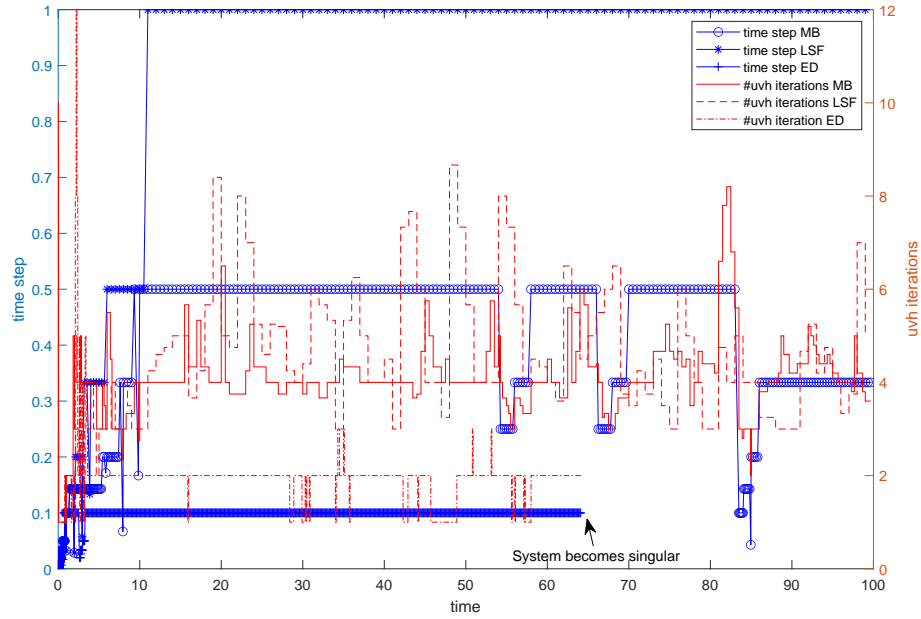


Figure 7.10: This example is based on the MismipPlus setup. Here all floating ice for $x > 500$ km was removed using three different approaches: **MB**, where an additional implicit mass-balance term is added at the nodes, **LSF**, where again an additional implicit mass-balance term is added but prescribed and evaluated directly at the integration points, and **ED**, where floating elements are deactivated. The best performance is obtained by **LSF**. The **LSF** always second order, whereas **MB** loses the second order convergence in the presence of strong spatial gradients in the mass balance.

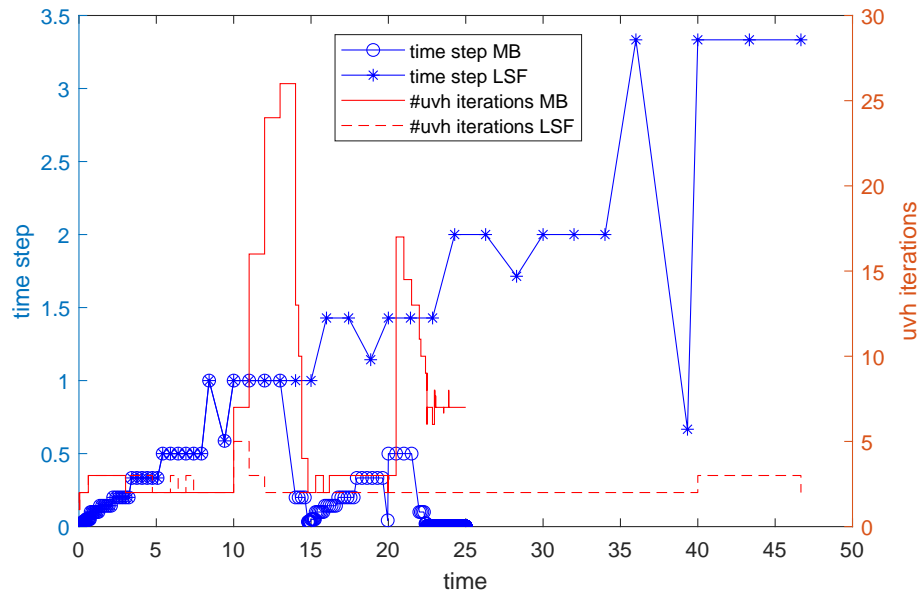


Figure 7.11: This example is based on a one-dimensional ice shelf geometry. Here all floating ice for $x > 500$ km was removed using two different approaches: **MB**, where an additional implicit mass-balance term is added at the nodes, and **LSF**, where again an additional implicit mass-balance term is added but prescribed and evaluated directly at the integration points. The best performance is obtained by **LSF**. Here the lack of second-order convergence when using **MB** severely limits the size of the time step.

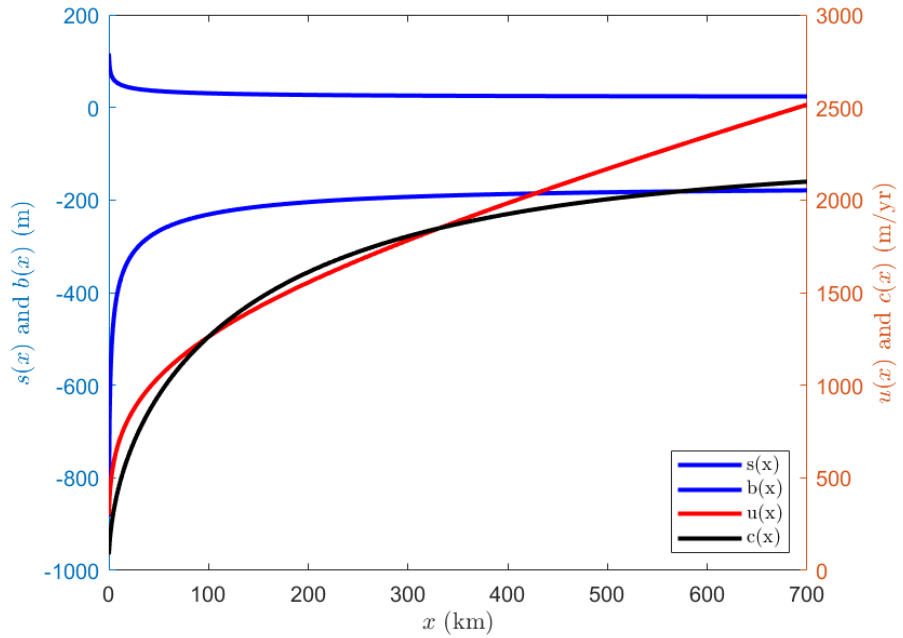


Figure 7.12: Geometry and velocities for a one-dimensional unconfined ice shelf (see Eqs. 11.44 and 11.46). The grounding line is at $x = 0$ and $h_{\text{gl}} = 1000$ m and $u_{\text{gl}} = 300$ m a^{-1} . A calving relationship on the form $c = kh^{-2}$ is shown as a black line with $k = 0.086320 \text{ km}^3 \text{ a}^{-1}$, For this calving relationship and this particular value of k , the ice velocity ($u(x)$) and calving rate ($c(x)$) are equal at $x = x_1 = 100$ km and at $x = x_2 = 331$ km. A calving front is stable at $x = x_1$, and unstable at $x = x_2$. The ice rate factor (A) is set to $A = 1.1461 \times 10^{-8} \text{ a}^{-1} \text{ kPa}^{-3}$ which corresponds to a temperature of -10 degrees Celsius (Smith & Morland, 1982). Ice density $\rho = 910 \text{ kg m}^{-3}$, ocean density $\rho_o = 1030 \text{ kg m}^{-3}$ and gravitational acceleration $g = 9.81 \text{ m s}^{-2}$ and constant surface mass balance of $a_s = 0.3 \text{ m a}^{-1}$.

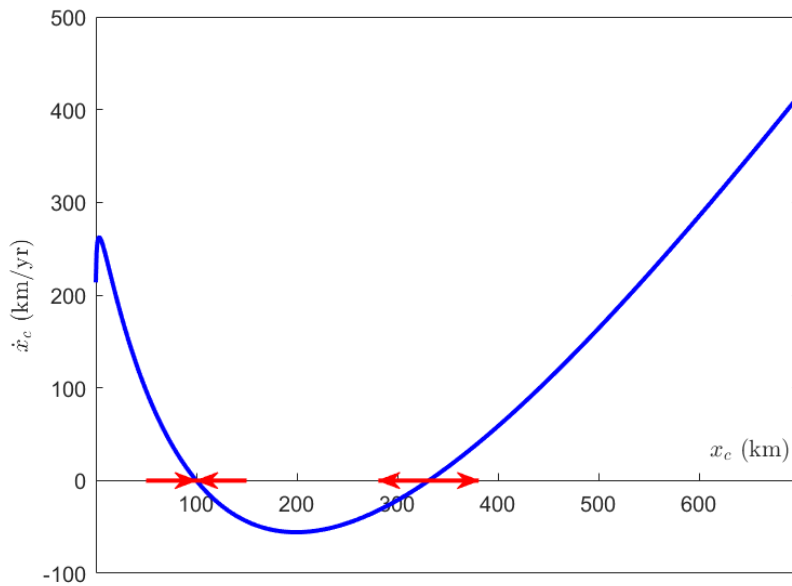


Figure 7.13: Phase portrait for calving law (6.15) with parameter values same as in Fig. 7.12. The steady-state at $x_c = x_1 = 100$ km is stable, and the one at $x_c = x_2 = 331$ km unstable.

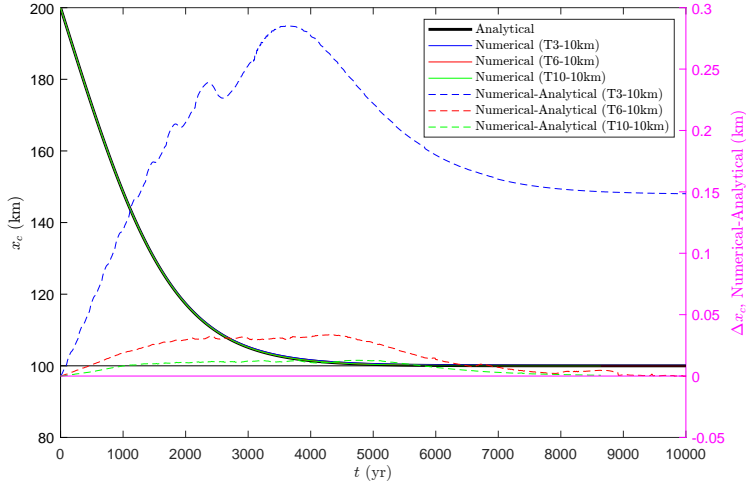


Figure 7.14: Calculated (coloured thin lines) and analytical (thick black line) calving front positions (left y axis) as a function of time, with the difference between the two shown as dashed lines (right y axis). The difference is too small for the analytical solution (black line) to be fully visible under those representing the numerical solution. The calculations were done for linear (T3), quadratic (T6) and cubic (T10) triangular elements. The element partition was in all three cases the same with the overall element diameters set at 10 km, but with finer division for the first 10 km downstream of the grounding line. The calculations were done for an unconfined ice shelf with the calving rate, c , being a function of ice thickness at the calving front as shown in Fig. 7.12. Initially the calving front is at $x = 200$ km and with time the calving front migrates towards the stable steady state solution at $x = 100$ km (see also Fig. 7.13).

A simple test case for the calving implementation can be construed by prescribing the calving rate using the analytical solution for an unconstrained ice shelf.

Solutions for the flow of a one-dimensional un-butressed ice shelf are derived in section 11.5 where it is showed that the velocity is given by

$$u(x) = \left(\frac{K + \gamma (q_{gl} + ax)^{n+1}}{a} \right)^{1/(n+1)} \quad (11.46)$$

and the constants K and γ are given by equations (11.45) and (11.42), respectively. By prescribing the calving rate as a function of thickness, for example as, prescribing

$$c(x) = k h(x)^p \quad (7.23)$$

where k and p are parameters with some suitably selected values, both u and c become known quantities of distance and the position of the calving front and easily be determined from the condition $u(x_c) = c(x_c)$. An example is given in Fig. 7.12 where k and p have been selected to allow two possible steady state calving front positions at x_1 and x_2 .

Since

$$\tau_{xx} = \frac{1}{4} \rho g f \quad (7.24)$$

$$= \frac{\rho g}{4} h \quad (7.25)$$

we can also write the calving rate, c , given by (7.23) as

$$c(x) = k \left(\frac{4\tau_{xx}}{\rho \varrho} \right)^p .$$

A fixed-point of the first-order system (7.22) is stable for $f'(x) < 0$, and unstable for $f'(x) > 0$. In this particular case, we see that a calving front is only stable if, locally around the steady-state position, the calving rate increases faster in along-flow direction than the ice velocity. Any positive perturbation in the calving-front position will then lead to a greater increase in the calving rate than in ice velocity. The calving front therefore retreats until the original steady-state position is found. As evident from the

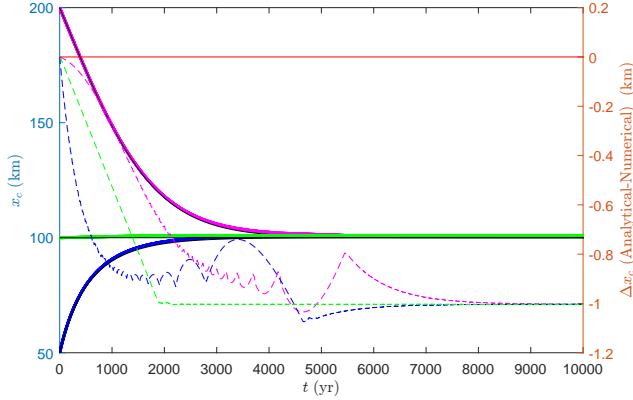


Figure 7.15: Analytical and numerically modelled calving front positions for an unconfined ice shelf (see) with the calving rate, c , being a function of ice thickness at the calving front as shown in Fig. 7.12. The calving front are initially set at $x_c(t = 0) = 50, $x_c(t = 0) = 100, and $x_c(t = 0) = 150 and the numerical solutions are shown as blue, green and magenta lines, respectively. The corresponding analytical solutions are in black. The difference between the analytical and numerical solutions, Δx_c , are shown as dashed lines with the right y -axis as scale. In this particular example, μ was spatially constant and set to $\mu = 1 \times 10^7 \text{ km}^2 \text{ yr}^{-2}$. The resolution of the finite-element mesh was 2 km and the error in the converged solutions about half of that, or 1 km.$$$

phase portrait shown in Fig. 7.13, the calving front position at $x_1 = 100 is therefore stable, while the one to the right at $x_2 = 331$ km is unstable. For $x < x_c \leq x_1$ at $t = t_0$, the calving front will migrate with time and approach $x = x_1$, and for $x_c > x_2$ at $t = t_0$, the calving front will migrate towards infinity at an accelerating rate.$

Stable (steady-state) calving front position requires the calving rate to be equal the ice velocity at that location, and also locally increase slower than the ice velocity in the direction normal to the calving front. For a one-dimensional unbuttressed ice shelf, the ice velocity increases while the ice thickness decreases monotonically with down-stream distance. Hence, for a calving law on the form (7.23) all calving front positions are unstable for any $p > 0$. No steady-state solutions for unconfined ice-shelves are therefore possible where the calving rate increases with ice thickness, or for any calving law based on a quantity that in turns increases with ice thickness, such as (horizontal) strain rates or stresses. In Figs. 7.12 and 7.13, the exponent is set to $p = -2$ to allow for the existence of a least one stable steady state.

The calving-rate expression used in this example is not motivated by any physical considerations and is only selected to allow for a convenient testing of the numerical calving implementation against an analytical solution. It is interesting to note that many experimentally motivated calving laws suggest calving rate to be an increasing function of ice thickness, i.e. with $p > 0$.

$$x_c(t) = \int_{t=t_0}^t (u(x) - c(x)) dx + x_c(t_0)$$

We can express this as

$$\hat{\mathbf{n}} \cdot \nabla(\mathbf{v} - \mathbf{c}) \cdot \hat{\mathbf{n}} < 0 \quad (\text{stable calving front position})$$

where again

$$\hat{\mathbf{n}} = \frac{\nabla \varphi}{\|\nabla \varphi\|}$$

In the particular case of a one-dimensional ice-shelf, and here assumed to align with the x axis, this condition is

$$\frac{\partial(u(x) - c(x))}{\partial x} < 0.$$

7.2.1 Thule

Thule is a synthetic geometry designed to be used as a test case for various ice-sheet modelling experiments. The Thule bedrock, B , is defined as a function of the polar coordinates r and θ , as

$$B = B_a \cos(3\pi r/l) + a$$

Table 7.1

Variable	Description	Units
$g = 9.81$	gravitational acceleration	m s^{-2}
$a_s = 0.3$	surface mass balance	m a^{-1}
$a_s = 0$	basal mass balance	m a^{-1}
$\rho = 917$	ice density	kg m^{-3}
$\rho_o = 1030$	ocean density	kg m^{-3}
$A = 2.9377 \times 10^{-9}$	ice rate factor	$\text{kPa}^{-3} \text{a}^{-1}$
$n = 3$	flow law stress exponent	
$C = 0.001$	basal slipperiness	$\text{m a}^{-1} \text{kPa}^{-3}$
$m = 3$	sliding law stress exponent	
$\text{d2a} = 365.2422$	days in a year	days

where

$$l = R(1 - \cos(2\theta)/2)$$

$$a = B_c - (B_c - B_l) \left(\frac{r - r_c}{R - r_c} \right)^2$$

and $R = 800 \text{ km}$, $B_c = 900 \text{ m}$, $B_l = -2000 \text{ m}$, $B_a = 1100 \text{ m}$, and $r_c = 0 \text{ m}$.

In MATLAB, the bedrock B can be calculated as a function of (x, y) as:

```
B=function(x,y)
% parameters
R=800e3;
Bc=900;
Bl=-2000;
Ba=1100;
rc=0;
% polar coordinates
r=sqrt(x.*x+y.*y);
theta=atan2(y,x);
% B calculation
l=R - cos(2*theta).*R/2 ;
a=Bc - (Bc-Bl)*(r-rc).^2/(R-rc).^2;
B=Ba*cos(3*pi*r./l)+a ;
end
```

The initial calving front is set at $r = r_c = 750 \text{ km}$. The computational domain should obviously be large enough to for the calving front to be within the domain. In the runs done with Uaa a circular computational domain with a radios of 1000 km was used.

The value for rate factor A corresponds to an ice temperature of -20 C° , assuming the Smith & Morland (1982) conversion:

$$A(T) = A_0 f(T)$$

where

$$f(T) = 1.2478766 \times 10^{-39} \exp(0.32769 T) + 1.9463011 \times 10^{-10} \exp(0.07205 T) \quad (f \text{ has no units, } T \text{ in Kelvin})$$

$$A_0 = 5.3 \times 10^{-15} \times 365.25 \times 24 \times 60 \times 60 \quad (\text{units } \text{kPa}^{-3} \text{ a}^{-1})$$

We use Weertman sliding law, often simply written as

$$u_b = C \tau_b^m ,$$

where C is the basal slipperiness and m a stress exponent. Here u_b is the basal sliding velocity and τ_b the bed tangential component of the basal traction. This sliding can also be written more precisely as

$$\mathbf{T}\sigma\hat{\mathbf{n}} + C^{-1/m} \|\mathbf{T}\mathbf{v}\|^{1/m-1} \mathbf{T}\mathbf{v} = 0 \quad \text{for } z = B(x, y)$$

where

$$\mathbf{T} = \mathbf{1} - \hat{\mathbf{n}} \otimes \hat{\mathbf{n}},$$

where \mathbf{T} is the tangential operator, and $\hat{\mathbf{n}}$ unit normal vector to the bed. The sliding law applied over the grounded sections of the ice sheet only. Other formulations for this same sliding law frequently found in the literature are

$$\mathbf{t}_b = \mathcal{G} C^{-1/m} \|\mathbf{v}_b\|^{1/m-1} \mathbf{v}_b, \quad (7.26)$$

$$= \mathcal{G} \beta^2 \mathbf{v}_b, \quad (7.27)$$

where \mathbf{t}_b is the bed-tangential basal traction, β^2 has been defined as,

$$\beta^2 = C^{-1/m} \|\mathbf{v}_b\|^{1/m-1}, \quad (7.28)$$

and where \mathcal{G} is the grounding-floating mask, with $\mathcal{G} = 1$ where grounded, and $\mathcal{G} = 0$ otherwise.

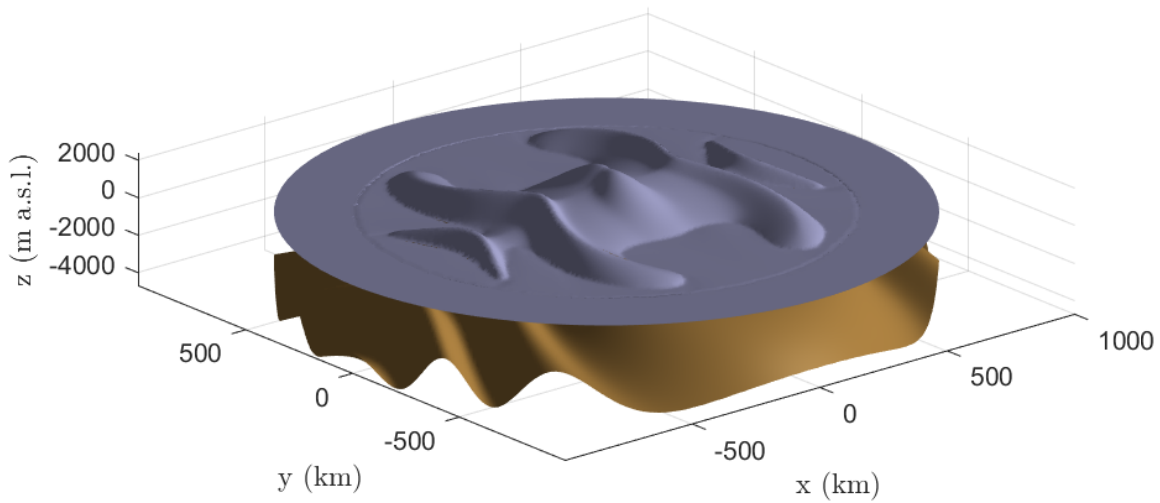


Figure 7.16: Surface and geometry of Thule. This surface geometry is the steady-state solution when starting with zero ice thickness everywhere.

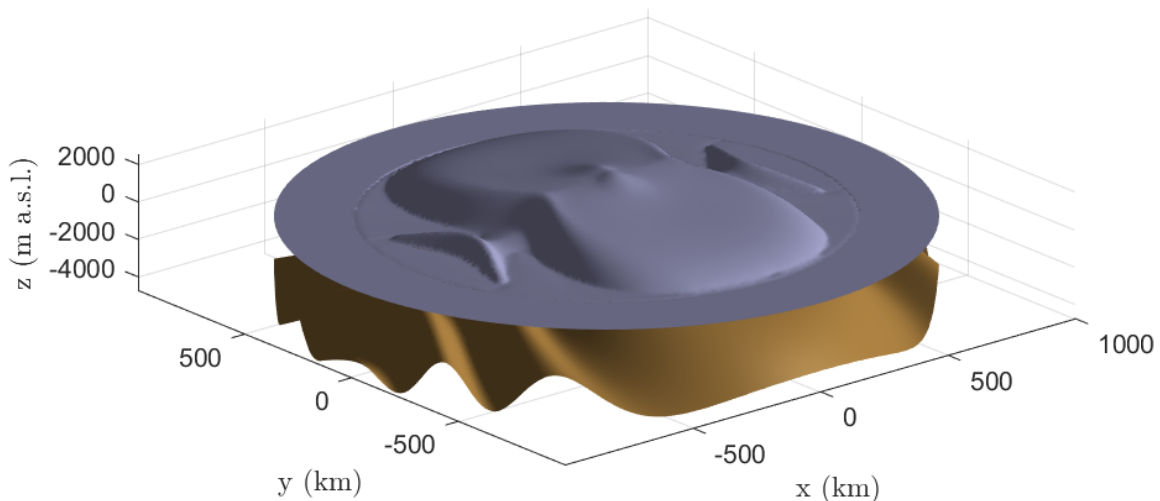


Figure 7.17: Surface and geometry of Thule. This surface geometry is the steady-state solution when starting with a large initial ice thickness where the initial surface geometry is $s = s_0 \sqrt{1 - r/R}$ where $R = 750$ km and $s_0 = 4000$ m, and r is the radial distance from the centre.

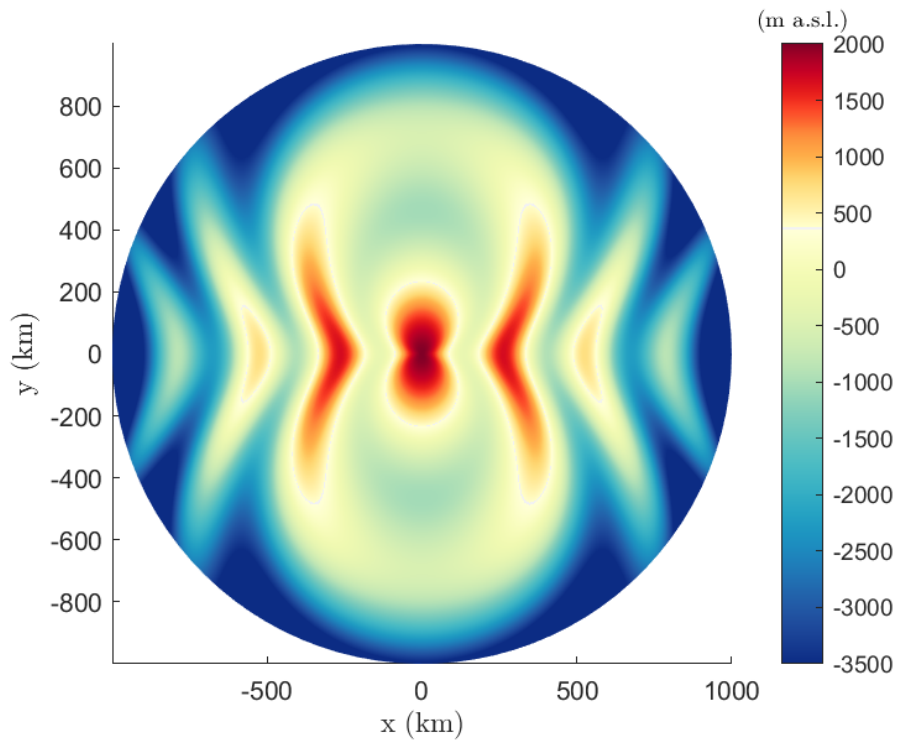


Figure 7.18: Bedrock geometry of Thule

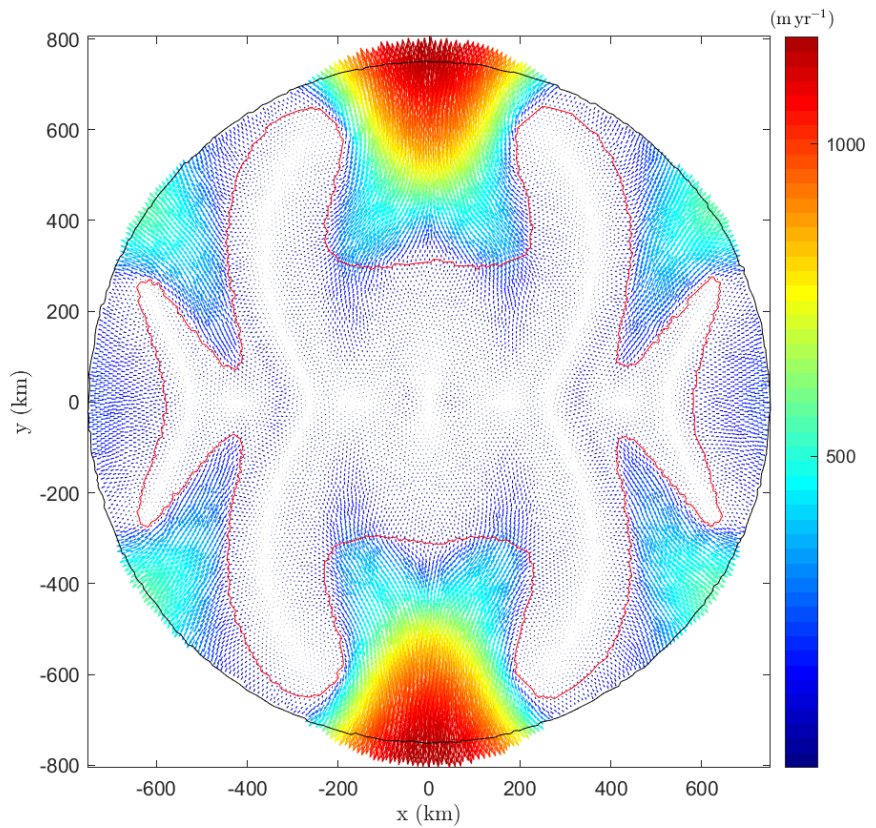


Figure 7.19: Velocities for steady state Thule Min

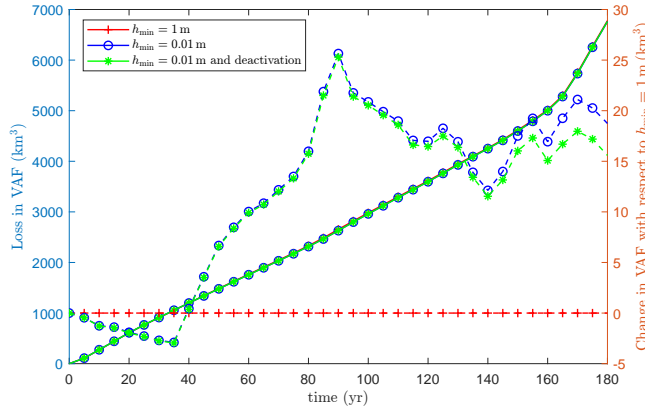
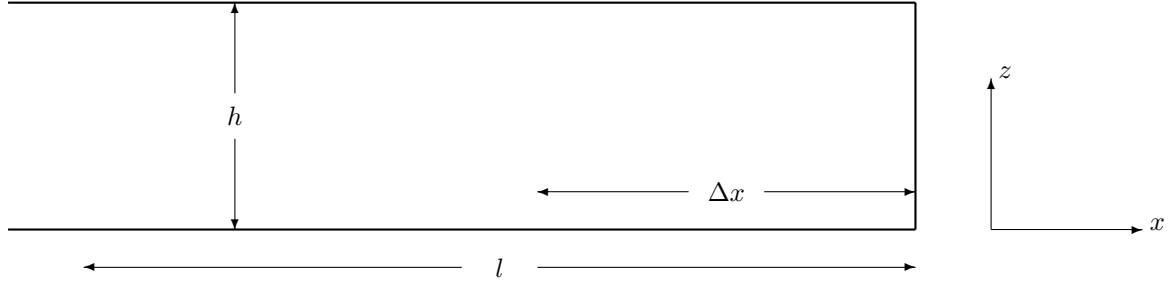


Figure 7.20: Calculated changes in volume above flotation (VAF) for different values of min ice, h_{\min} , thickness downstream of the calving front, as well as automated element deactivation. These experiments were done for a sector WAIS including Pine Island, Thwaites and Pope, Smith and Kohler glaciers. Uniform mesh size of 4.6 km was used. The solid lines showing total VAF loss use the left-hand y axis, and the dashed lines showing difference in calculated VAF with respect to using $h_{\min} = 1$ m use the right-hand y axis.

7.2.2 Thwaites and Pine Island Glacier Calving Experiments

7.3 Calving implemented as surface mass-balance term



Apparently, calving is implemented in some ice-sheet models as an additional surface mass balance term. Here we consider how this fictitious melt term (a_c) relates to calving rate (c), ice thickness (h), and grid size, ($\Delta x, \Delta y$), in a finite difference model. The key idea is for the new surface mass balance term, a_c , to produce the same ice volume loss as that caused by the calving rate c , over the time period Δt .

Over the time step Δt the calving rate c acts to reduce the length by the distance l normal to the ice front where

$$l = c \Delta t .$$

The volume V_c , of ice ‘melted’ through calving is then

$$V_c = l h w ,$$

where w is the (transverse) width, or

$$V_c = c \Delta t h w .$$

Supposing we apply some surface melt a_c over the finite-difference cell $\Delta x \Delta y$, the resulting volume of ice melted will be

$$V_m = a_c \Delta x \Delta y \Delta t$$

By requiring

$$V_m = V_c ,$$

for $w = \Delta y$, that is requiring that the volume of ice we melt, V_m , equals the volume of ice lost through calving, V_c , we find

$$a_c \Delta x \Delta y \Delta t = c \Delta t h \Delta y ,$$

and the applied melt, a_c , required to produce a volume loss equal to that produced through calving is

$$a_c = \frac{c h}{\Delta x} . \quad (7.29)$$

Eq. (7.29) gives the vertically-applied calving melt as a function of the calving rate, ice thickness and the dimensions of the finite difference cell.

This approach will need to be modified somehow should the (remaining) ice thickness of the computational cell be smaller than the desired change in ice thickness, i.e. whenever

$$h \geq a_c \Delta t , \quad (7.30)$$

Should this happen, we run out of ice to melt, and we must start to melt next cell. Using Eq. (7.29), this condition can also be expressed as

$$\begin{aligned} h &\geq a_c \Delta t \\ &= \frac{c h}{\Delta x} \Delta t \end{aligned}$$

giving

$$\Delta x \geq c \Delta t \quad (7.31)$$

Hence, if a_c is defined by Eq. (7.29), condition (7.31) follows from condition (7.30).

Chapter 8

Damage

Material damage, D , can be quantified as

$$D(\hat{\mathbf{n}}) = \frac{A_D}{A}$$

where A is a some cross-sectional area with the unit normal $\hat{\mathbf{n}}$ and A_D is the cross-sectional area of defects or voids within the area A . If there are no voids within the area, then $D = 0$ and the area is undamaged, and for $D = 1$ the area is totally damaged. Other similar definitions are

$$D = \frac{V_D}{V}$$

where V_D is the total number of voids within the volume V .

The stress tensors in the damaged and undamaged material are assumed to be related as

$$\boldsymbol{\tau} = (1 - D)\tilde{\boldsymbol{\tau}}$$

where $\tilde{\boldsymbol{\tau}}$ is the effective deviatoric stress tensor. For scalar damage D , the Glen's flow law (1.188) is then written as

$$\tau_{ij} = (1 - D)A^{-1/n}\dot{\epsilon}^{(1-n)/n}\dot{\epsilon}_{ij}, \quad (8.1)$$

The damage D is a new field variable that is advected with the flow given by the *damage rate equation*

$$\partial_t D + \mathbf{v} \cdot \nabla D = f(D) \quad (8.2)$$

where f is some suitable source term. Wide variety of potential source terms for damage have been proposed.

8.1 Hayhurst criterion and variants thereof

Damage is usually considered initiated once some stress measure is above some threshold stress, σ_{th} , is reached in the damage material. Above that stress, the damage rate is then assumed to increase monotonically above that stress. For example in one-dimension, one could assume damage initiation starts once the stress reaches some threshold stress, i.e. when

$$F(\sigma, \sigma_{\text{th}}) = \tilde{\sigma} - \sigma_{\text{th}} = 0$$

and then provided

$$F \geq 0$$

evolves as

$$\begin{aligned} \partial_t D + \mathbf{v} \cdot \nabla D &= B(\tilde{\sigma}_{xx} - \sigma_{\text{th}})^r \\ &= B \left(\frac{\sigma_{xx}}{1 - D} - \sigma_{\text{th}} \right)^r \end{aligned}$$

where r is some stress exponent and B some constant. For $F < 0$ the damage is unchanged. Note that here the change in D with time is proportional to $1/(1 - D)$, and therefore grows rapidly with D

In the general three-dimensional case we write

$$\partial_t D + \mathbf{v} \cdot \nabla D = B \left(\frac{\Xi}{1 - D} - \sigma_{th} \right)_+^r$$

using the Hayhurst's criterion

$$\Xi = \alpha\sigma_1 - 3\beta p + \sqrt{3}\gamma\sigma_{II}$$

where σ_1 is the maximum principal Cauchy stress, p the pressure, σ_{II} the second invariant of the stress tensor, and

$$\alpha + \beta + \gamma = 1.$$

In glaciological applications, in particular when using the SSA approximation, it has been suggested by several authors, including [Huth et al. \(2021\)](#) and [Keller and Hutter \(2014\)](#), to modify the above Hayhurst criterion somewhat and use instead

$$\Xi = \alpha(\sigma_1 - p_e) + \sqrt{3}\beta\tau - 3\gamma p_e \quad (8.3)$$

where p_e is now the effective pressure, defined as the difference between ice and water pressure,

$$p_e = p - p_w = p - \rho_w g (S - z)_+$$

and τ is the second invariant of the deviatoric stress tensor. Eq.(8.3) is Eq. 16 in [Keller and Hutter \(2014\)](#).

For $\alpha = 1$ and $\beta = \gamma = 0$, damage evolution is related to the principal tensile stress alone. This situation was considered by [Krug et al. \(2014\)](#), who used the evolution law

$$\partial_t D + \mathbf{v} \cdot \nabla D = \left(\frac{\sigma_1}{1 - D} - \sigma_{th} \right)_+^r$$

(their Eq. 11)

In SSA all the horizontal deviatoric stresses are independent of depth and

$$\sigma_{xx} = 2\tau_{xx} + \tau_{yy} + \sigma_{zz}, \quad (17.54)$$

and σ_{zz} is

$$\sigma_{zz} = -\rho g(s - z)$$

or

$$\sigma_{xx} = 2\tau_{xx} + \tau_{yy} - \rho g(s - z).$$

At the base of floating ice shelves

$$\sigma_{zz}(z = b) = -p_w = -(S - b)g\rho_w$$

at the lower ice surface where $z = b$. The vertical variation in stresses for a one-dimensional ice shelf are shown in Fig. 11.1.

See for example Eq.11 in [Mercenier et al. \(2019\)](#) (their Eq. 11)

8.2 Some other damage evolution laws

Gurson:

$$f = \left(\frac{\tau}{\tau_0} \right)^2 + 2f_v \cosh(p/(2\tau_0)) - (1 + f_V) = \leq 0$$

where τ_0 is an effective material yield stress, and f_V the porosity. We therefore also need an evolution of the porosity f_V which can be

$$\dot{f}_V = (1 - f_V)\dot{\epsilon}_{ii}$$

Currently, in glaciology the most commonly used source term appears to be on the form

$$f(D) = B(\chi - \sigma_{th})_+^r$$

where the + bracket subscript indicates we set negative values within the bracket to zero, and where

$$\chi = \alpha\sigma_1 + \beta\tau + \gamma\sigma_I$$

or since for incompressible material such as ice the mechanical pressure is

$$p = -\frac{1}{3}\sigma_I$$

as

$$\chi = \alpha\sigma_1 + \beta\tau - 3\gamma p$$

Here σ_1 is the maximum principal stress, p the pressure and τ the effective stress (i.e. second invariant of the deviatoric stress tensor), and α , β and γ are parameters all having values somewhere between 0 and 1.

8.3 Sainan Sun Damage Model

A vertically averaged damaged, \mathcal{D} , is defined as

$$\mathcal{D} = \frac{d}{h}$$

with $0 \leq \mathcal{D} \leq 1$, where d is a crevasse depth. The effective rate factor, A_{eff} , is then

$$A_{\text{eff}} = \frac{A}{(1 - \mathcal{D})^n}$$

where n is the flow-law exponent. A Nye crevasse depth is estimated, for example as,

$$d_{\text{Nye}} = 2\tau_1/(\rho g)$$

where τ_1 is the maximum tensile deviatoric stress at the surface. The damage field is evolved as

$$\partial_t \mathcal{D} + \nabla(\mathcal{D} \mathbf{v}) = \gamma(\mathcal{D} - \mathcal{D}_{\text{Nye}})$$

where

$$\mathcal{D}_{\text{Nye}} := \frac{d_{\text{Nye}}}{h}$$

Stress is force per area, and we envision the area being reduced as the damage increases. In the presence of damage, the intact load bearing area, \mathcal{A} , is now reduced by the factor $1 - \mathcal{D}$. Correspondingly, the deviatoric stress per intact area, $\tilde{\tau}$ is now

$$\tilde{\tau} = \frac{\tau}{1 - \mathcal{D}}$$

Note that if the stress τ is finite, the stress acting over parts of the area which are undamaged, goes to infinity as the damage field approaches unity. The stress responsible for the deformation of the ice is $\tilde{\tau}$, that is, the stress acting over the area of (still) intact ice. In the stress-balance equations we must use τ , i.e. the force per area, but in the constitutive equation we must use the stress acting on the ice itself, i.e. $\tilde{\tau}$. The flow law is therefore

$$\begin{aligned} \dot{\epsilon} &= A\tilde{\tau}^n \\ &= \frac{A}{(1 - \mathcal{D})^n} \tau^n . \end{aligned}$$

Consider now a uniform ice stream with thickness h and no variation in x direction and zero basal drag. The only non-zero deviatoric stress component is τ_{xy} . The field equation becomes

$$\partial_y(\tau_{xy}) = -\rho g \sin \alpha$$

and

$$2\partial_x \left((1 - \mathcal{D})^{1/n} A^{-1/n} (\dot{\epsilon}_{xy})^{1/n} \right) = \rho g \sin(\alpha) \quad (8.4)$$

where here

$$\mathcal{D} = \frac{2\tau_{xy}}{\rho g h}$$

Using the symmetry condition $\tau_{xy} = 0$ at $y = 0$, the stress is

$$\tau_{xy} = -\rho gy \sin(\alpha)$$

and the maximum principal deviatoric stress is hence

$$\tau_1 = \rho gy \sin(\alpha)$$

and therefore $\tau_1 = \rho gy$ and thus

$$\mathcal{D} = 2 \sin(\alpha) \frac{|y|}{h}$$

Resulting in

$$\partial_y \left((1 - 2 \sin(\alpha) y/h)^{1/n} A^{-1/n} (\dot{\epsilon}_{xy})^{1/n} \right) = \rho g \sin(\alpha) \quad (8.5)$$

Setting $n = 1$, gives

$$(1 - 2 \sin \alpha y/h) \partial_y \dot{\epsilon}_{xy} = A \rho g \sin(\alpha) \quad (8.6)$$

$$\begin{aligned} \dot{\epsilon}_{xy}(y) &= A \rho g \sin(\alpha) \int_0^y \frac{1}{1 - ky'} dy' \\ &= -A \rho g \sin(\alpha) k^{-1} \ln(1 - ky) \\ &= -\frac{1}{2} A \rho g h \ln(1 - ky) \end{aligned}$$

where

$$k := 2 \sin(\alpha)/h$$

and

$$|ky| < 1$$

For $ky \ll 1$ we have the first term in the Taylor series

$$\dot{\epsilon}_{xy}(y) \approx -A \rho g \sin(\alpha) k^{-1} (-ky) = A \rho g \sin(\alpha) y$$

as expected.

Chapter 9

Virtual crack closure technique

The *finite crack extension method*, the *crack closure technique* (CCT), and the closely related *virtual crack closure technique* (VCCT), are some of the more commonly used methods for calculating stress intensity factors (SIF) in finite-elements. Of these, the VCCT is easiest to implement and quite accurate provided the domain at the crack tip is sufficiently well resolved. The methods are all based on the original energy balance proposed by Irwin whereby the energy release is assumed equal to the work (W) required to close the crack. The Irwin expression is

$$W = \frac{1}{2} \int_0^l u(x) \sigma(l - x) dx .$$

Here l is a small crack increment, u the displacement normal to the crack plane (for mode I), σ the stress, and it has been assumed that the crack is aligned with the x direction. The energy release rate, G , is therefore

$$G = \lim_{l \rightarrow 0} \frac{1}{2l} \int_0^l u(x) \sigma(l - x) dx$$

This expression for the energy release rate is sometimes referred to as the *crack-closure integral method* of Irwin. (Note that the 'rate' in the term 'energy release rate', is with respect to changes in crack length. So 'rate' is here not with respect to time but with respect to distance, i.e. the crack increment).

In fracture mechanics G is referred to as the crack driving force, despite not having the units of force. G has the SI units of the product of stress and displacement, or $\text{Pa m} = \text{N/m} = \text{J/m}^2$. The work done by external forces, W is equal to the change in stored deformational energy and therefore G is also equal to the derivative of the potential energy of the body with respect to the crack length.

For purely viscous media we take a very similar viewpoint, but replace displacements and strains with velocities and strain rates, and work and potential energy with rate-of-work and change in potential energy with time. This perfect analogy between elastic and viscous fracture mechanics, whereby

$$\begin{aligned} \epsilon &\rightarrow \dot{\epsilon} \\ d &\rightarrow u \\ J &\rightarrow C^* \end{aligned}$$

where d is displacement and J and C^* are integrals (see below) is discussed in detail by [Gross and Seelig \(2006\)](#).

Calculating the work of external forces in FE is a simple summation exercise

$$\dot{W} = \frac{1}{2} \sum_i (F_x u + F_y v)_i$$

where the sum is over nodes and F_x and F_y the equivalent nodal forces, and now u and v are the x and y velocity components. Most FE programs determine the nodal forces as a part of the matrix assembly (In \tilde{U} these are calculated as the SSA equation is assembled).

In the finite crack extension method, the work W is calculated for several different crack extensions l . For example using central differences the crack driving force is evaluated as

$$\dot{G} \approx \frac{\dot{W}_{+l} - \dot{W}_{-l}}{2l}$$

where here the crack has been extended and closed by the distance l . In principle one can calculate W for a range of l values and plot W as a function of l as done in Antunes et al. (1999) to determine how well the limit $l \rightarrow 0$ is approximated. The SI units of \dot{G} are the same as those of the product of stress and velocity, or $\text{Pa m s}^{-1} = \text{N m}^{-1} \text{s}^{-1}$ and \dot{G} can be thought of as the crack driving force per time unit.

The VCCT method is a clever trick where one uses the (internal) equivalent nodal forces between elements in contact ahead of the crack tip and the relative nodal displacements behind the crack tip to evaluate W . This eliminates the need to open the crack by the distance l (but requires a somewhat different internal estimate of the nodal forces as these will always be close to zero for a structure in mechanical equilibrium). For viscous material we use the jump in velocity across the crack instead of the nodal displacements.

So the general idea is to use the discontinuity in velocity normal to the crack together and the equivalent nodal loads ahead of the crack to estimate the strain-rate energy release rate, \dot{G} , as the crack is extended.

Typically the criteria for crack growth in an elastic medium is

$$G > G^*$$

where G^* is some material parameter. Here I'm not primarily interested in this 'on/off' question and instead write

$$\frac{dl}{dt} = B \left(\frac{\dot{G}}{\dot{G}^*} \right)^q$$

where B , G^* , and q are some parameters.

9.1 J and C^* integrals for elastic and viscous fracture

Elastic J integral

$$J = \int_{\Gamma} (W dy - T_i d_{i,1} dx)$$

where d are displacements, and W the strain energy density

$$W = \int_0^{\epsilon} \sigma_{pq} d\epsilon_{qp}$$

T_i are the components of the traction vector, $T_i = \sigma_{ij} n_j$. The integration path Γ a continuous and differentiable curve surrounding the crack tip, not including the edges of the crack. In the absence of body forces, or if the body forces are acting out of the plane, $J = 0$ for any closed curve. (for prof see: <https://en.wikipedia.org/wiki/J-integral>). Some further details related to the calculation of J integral in FE are found in IPCC (2019).

For creep fracture it is common to use instead the creep C^* integral

$$C^* = \int_{\Gamma} (\dot{W} dy - T_i u_{i,1})$$

where \dot{W} is the stress power

$$\dot{W} = \int_0^{\dot{\epsilon}} \sigma_{pq} d\dot{\epsilon}_{pq}$$

and u_i the velocity components. The C^* is path independent and completely analogous to the J integral, but with displacements replaced by velocities and energy density with energy dissipation rate. C^* is the rate equivalent of the J contour integral.

C represents the power difference as the crack length, l , is increased incrementally

$$C^* = -\frac{1}{w} \frac{dU}{dl}$$

U is the stress-power dissipation rate.

The solution close to the crack tip, for a stationary crack, is given by the HRR-field

$$\begin{aligned}\sigma &\sim \left(\frac{C^*}{Ar}\right)^{1/(n+1)} \\ \dot{\epsilon} &\sim A \left(\frac{C^*}{Ar}\right)^{n/(n+1)} \\ u &\sim A^{1/(n+1)} (C^*)^{n/(n+1)} r^{1/(n+1)}\end{aligned}$$

as $r \rightarrow 0$, where r is the radial distance from the crack tip (Saxena, 1993, 2015; Gross and Seelig, 2006). and C^* can be therefore related to the strength of the stress singularity

$$C^* = \lim_{r \rightarrow 0} \frac{u^{(n+1)/n}}{(Ar)^{1/n}} \quad (9.1)$$

In principle this provides a way of calculating C^* from the SSA by evaluating this limit numerically, or from plotting $\dot{\epsilon}$ and/or u as a function of radial distance, although in practice this may require very finely resolved mesh. Note that Eq. (9.1) has the right physical dimensions, i.e. the dimensions of C^* are those of stress times velocity or Pa m s⁻¹.

Creep crack growth rate is then often assumed to be given by

$$\frac{dl}{dt} = B (C^*)^q$$

where B and q as some material constants.

Chapter 10

Further technical FE implementation details

10.1 Only the (fully) floating condition as a natural boundary condition

Here I am ignoring possible gradients in density and the treatment of the boundary term only includes the fully floated case as a natural condition.

Note that

$$\begin{aligned} \rho gh \partial_x s &= \rho gh \partial_x s + \frac{1}{2} \varrho g \partial_x h^2 - \rho gh(1 - \rho/\rho_o) \partial_x h \\ &= \frac{1}{2} \varrho g \partial_x h^2 + \rho gh \partial_x(s - S - (1 - \rho/\rho_o) h) \end{aligned}$$

hence

$$\rho gh \partial_x s = \frac{1}{2} \varrho g \partial_x h^2 + \rho gh \partial_x s' \quad (10.1)$$

with

$$s' := s - S - (1 - \rho/\rho_o) h$$

and

$$\varrho = \rho(1 - \rho/\rho_o),$$

The field equations can therefore also be written as

$$\begin{aligned} \partial_x(4h\eta\partial_x u + 2h\eta\partial_y v) + \partial_y(h\eta(\partial_x v + \partial_y u)) - \beta^2 u &= \rho gh(\partial_x s' \cos \alpha - \sin \alpha) + \frac{1}{2} \varrho g \cos \alpha \partial_x h^2, \\ \partial_y(4h\eta\partial_y v + 2h\eta\partial_x u) + \partial_x(h\eta(\partial_y u + \partial_x v)) - \beta^2 v &= \rho gh \partial_y s' \cos \alpha + \frac{1}{2} \varrho g \cos \alpha \partial_y h^2 \end{aligned}$$

10.1.1 Remark

To see that the right-hands sides of (1.223) and (10.1) i.e.

$$\begin{aligned} \rho gh \partial_x s &= \frac{1}{2} \varrho g \partial_x h^2 + \rho gh \partial_x s' \\ &= \frac{1}{2} g \partial_x(\rho h^2 - \rho_o d^2) + g(\rho h - \rho_o d) \partial_x b \end{aligned}$$

are equal (ignoring spatial gradients in density) we consider the three cases:

1. Fully floating: In that case $s' = 0$ and $\rho h = \rho_o d$ and both sides are equal.
2. Fully grounded: We have $d = 0$

$$\begin{aligned} \frac{1}{2} g \partial_x(\rho h^2 - \rho_o d^2) + g(\rho h - \rho_o d) \partial_x b &= \frac{1}{2} g \rho \partial_x h^2 + g \rho h \partial_x b \\ &= \rho gh \partial_x s \end{aligned}$$

and

$$\begin{aligned}\frac{1}{2}\varrho g \partial_x h^2 + \rho g h \partial_x s' &= \frac{1}{2}\varrho g \partial_x h^2 + \rho g h \partial_x(s - S - (1 - \rho/\rho_o)h) \\ &= \rho g h \partial_x s\end{aligned}$$

3. Partly floating:

$$\begin{aligned}\frac{1}{2}g\partial_x(\rho h^2 - \rho_o d^2) + g(\rho h - \rho_o d)\partial_x b &= \rho g h \partial_x h - \rho_o g d \partial_x d + g(\rho h - \rho_o d)\partial_x b \\ &= \rho g h \partial_x s - \rho_o g d \partial_x d - \rho_o g d \partial_x b \\ &= \rho g h \partial_x s - \rho_o g d(\partial_x d + \partial_x b) \\ &= \rho g h \partial_x s - \rho_o g d(\partial_x S - \partial_x b + \partial_x b) \\ &= \rho g h \partial_x s\end{aligned}$$

10.1.2 FE formulation

x direction

$$\int_{\Omega} (\partial_x(4h\eta\partial_x u + 2h\eta\partial_y v) - \frac{1}{2}\varrho g \cos \alpha \partial_x h^2 + \partial_y(h\eta(\partial_x v + \partial_y u)) - t_{bx} - \rho g h(\partial_x s' \cos \alpha - \sin \alpha))\phi \, dx \, dy = 0$$

with Weertman type Neumann BC on Γ_2

$$(4h\eta\partial_x u + 2h\eta\partial_y v)n_x + \eta h(\partial_x v + \partial_y u)n_y = \frac{1}{2}\rho(1 - \rho/\rho_o)gh^2n_x$$

Green's theorem used to get rid of second derivatives gives

$$\begin{aligned}- \int_{\Omega} ((4h\eta\partial_x u + 2h\eta\partial_y v)\partial_x \phi - \frac{1}{2}\varrho g \cos \alpha h^2 \partial_x N + h\eta(\partial_x v + \partial_y u)\partial_y N) \, dx \, dy \\ - \int_{\Omega} (t_{bx} + \rho g h(\partial_x s' \cos \alpha - \sin \alpha))\phi \, dx \, dy \\ + \int_{\Gamma} ((4h\eta\partial_x u + 2h\eta\partial_y v - \frac{1}{2}\varrho g \cos \alpha h^2)n_x + h\eta(\partial_x v + \partial_y u)n_y)\phi \, d\Gamma = 0\end{aligned}$$

If the von Neumann boundary condition is of Weertman type, the boundary integral along Γ_2 is equal to zero (for $\alpha = 0$), and zero on the remaining part of the boundary if we set the weight functions to zero and determine the values of the unknowns using Dirichlet boundary conditions.

We are left with

$$\begin{aligned}- \int_{\Omega} (h\eta(4\partial_x u + 2\partial_y v)\partial_x \phi + h\eta(\partial_x v + \partial_y u)\partial_y N) \, dx \, dy - \int_{\Omega} t_{bx}\phi \, dx \, dy \\ = \rho g \int_{\Omega} h((\partial_x s - (1 - \rho/\rho_o)\partial_x h) \cos \alpha - \sin \alpha)\phi \, dx \, dy - \frac{1}{2}\varrho g \cos \alpha \int_{\Omega} h^2 \partial_x \phi \, dx \, dy\end{aligned}$$

y direction

$$\int_{\Omega} \partial_y((4h\eta\partial_y v + 2h\eta\partial_x u) - \frac{1}{2}\varrho g \cos \alpha \partial_y h^2 + \partial_x(h\eta(\partial_y u + \partial_x v)) - t_{by} - \rho g h \partial_y s' \cos \alpha)\phi \, dx \, dy$$

with Weertman type boundary condition

$$\eta h(\partial_x v + \partial_y u)n_x + (4\eta h\partial_y v + 2\eta h\partial_x u)n_y = \frac{1}{2}\rho(1 - \rho/\rho_o)gh^2n_y$$

We have

$$\begin{aligned}- \int_{\Omega} ((4h\eta\partial_y v + 2h\eta\partial_x u)\partial_y \phi - \frac{1}{2}\varrho g \cos \alpha h^2 \partial_y N + h\eta(\partial_y u + \partial_x v)\partial_x N) \, dx \, dy \\ - \int_{\Omega} (t_{by} + \rho g h \partial_y s' \cos \alpha)\phi \, dx \, dy \\ + \int_{\Gamma} ((4h\eta\partial_y v + 2h\eta\partial_x u - \frac{1}{2}\varrho g \cos \alpha h^2)n_y + \eta h(\partial_y u + \partial_x v)n_x)\phi \, d\Gamma = 0\end{aligned} \quad (10.2)$$

Again we can ignore the boundary integral as it is identically equal to zero.

$$\begin{aligned} & - \int_{\Omega} ((4h\eta\partial_y v + 2h\eta\partial_x u)\partial_y \phi + h\eta(\partial_y u + \partial_x v)\partial_x N) dx dy - \int_{\Omega} t_{by}\phi dx dy \\ &= \rho g \cos \alpha \int_{\Omega} h(\partial_y s - (1 - \rho/\rho_o)\partial_y h)\phi dx dy - \frac{1}{2}\varrho g \cos \alpha \int_{\Omega} h^2 \partial_y N dx dy \end{aligned} \quad (10.3)$$

10.1.3 2HD FE diagnostic equation written in terms of h (suitable for fully coupled approach)

Where the ice is afloat, $s - S = (1 - \rho/\rho_o)h$ and $s' = 0$, hence

$$s' = \begin{cases} s - S - (1 - \rho/\rho_o)h, & \text{if } h > h_f \\ 0, & \text{if } h \leq h_f \end{cases}$$

i.e.

$$s' := \mathcal{H}(h - h_f)(s - S - (1 - \rho/\rho_o)h)$$

where

$$h_f := (S - B)\rho_o/\rho$$

We can also write s' as

$$\begin{aligned} s' &= \mathcal{H}(h - h_f)(s - S - (1 - \rho/\rho_o)h) \\ &= \mathcal{H}(h - h_f)(h\rho/\rho_o + s - S - h) \\ &= \mathcal{H}(h - h_f)(h\rho/\rho_o + h + b - S - h) \\ &= \mathcal{H}(h - h_f)(h\rho/\rho_o + h + B - S - h) \\ &= \mathcal{H}(h - h_f)(h\rho/\rho_o + B - S) \\ &= \mathcal{H}(h - h_f)(h\rho/\rho_o - H) \end{aligned}$$

i.e.

$$s'(x) = \mathcal{H}(h - h_f)(\rho/\rho_o h - H) \quad (10.4)$$

where we used the fact that $b = B$ whenever $\mathcal{H}(h - h_f) = 1$. This expression for s' is needed for linearisation around h .

The field equations can therefore be written as before, i.e. as

$$\begin{aligned} \partial_x(4h\eta\partial_x u + 2h\eta\partial_y v) + \partial_y(h\eta(\partial_x v + \partial_y u)) - \beta^2 u &= \rho gh(\partial_x s' \cos \alpha - \sin \alpha) + \frac{1}{2}\varrho g \cos \alpha \partial_x h^2, \\ \partial_y(4h\eta\partial_y v + 2h\eta\partial_x u) + \partial_x(h\eta(\partial_y u + \partial_x v)) - \beta^2 v &= \rho gh\partial_y s' \cos \alpha + \frac{1}{2}\varrho g \cos \alpha \partial_y h^2, \end{aligned}$$

but the linearisation with respect to h needed in a fully coupled approach requires (10.4).

The FE formulation for the prognostic equation is the θ method, i.e.

$$R_p^h = \int_{\Omega} \left\{ \frac{1}{\Delta t} (h_1 - h_0) + \theta \partial_x(u_1 h_1) + (1 - \theta) \partial_x(u_0 h_0) + \theta \partial_y(v_1 h_1) + (1 - \theta) \partial_y(u_0 h_0) - a \right\} N_p dx dy = 0 \quad (10.5)$$

where $0 \leq \theta \leq 1$.

$$a := a_s + a_b$$

10.2 Element integrals

$$x = x_p N_P(\xi, \eta)$$

For 3-node element:

Nodal \mathbf{u} displacement vector of one particular 3-node element

$$\mathbf{u} := \begin{pmatrix} u_1 \\ u_2 \\ u_3 \end{pmatrix}$$

$$\text{fun} := \begin{pmatrix} N_1(\xi, \eta) \\ N_2(\xi, \eta) \\ N_3(\xi, \eta) \end{pmatrix}$$

$$u(x, y) = u_p N_p(x, y) = \mathbf{u}^T \text{fun}$$

$$\text{der} = \begin{pmatrix} \frac{\partial N_1}{\partial \xi} & \frac{\partial N_2}{\partial \xi} & \frac{\partial N_3}{\partial \xi} \\ \frac{\partial N_1}{\partial \eta} & \frac{\partial N_2}{\partial \eta} & \frac{\partial N_3}{\partial \eta} \end{pmatrix}$$

$$\text{coo} = \begin{pmatrix} x_1 & y_1 \\ x_2 & y_2 \\ x_3 & y_4 \end{pmatrix}$$

$$\mathbf{J} = \begin{pmatrix} \frac{\partial x}{\partial \xi} & \frac{\partial y}{\partial \xi} \\ \frac{\partial x}{\partial \eta} & \frac{\partial y}{\partial \eta} \end{pmatrix}$$

$$\mathbf{J}^{-1} = \begin{pmatrix} \frac{\partial \xi}{\partial x} & \frac{\partial \eta}{\partial x} \\ \frac{\partial \xi}{\partial y} & \frac{\partial \eta}{\partial y} \end{pmatrix} = \frac{1}{\det \mathbf{J}} \begin{pmatrix} \frac{\partial y}{\partial \eta} & -\frac{\partial y}{\partial \xi} \\ -\frac{\partial x}{\partial \eta} & \frac{\partial x}{\partial \xi} \end{pmatrix}$$

$$\begin{pmatrix} \frac{\partial}{\partial \xi} \\ \frac{\partial}{\partial \eta} \end{pmatrix} = \mathbf{J} \begin{pmatrix} \frac{\partial}{\partial x} \\ \frac{\partial}{\partial y} \end{pmatrix}$$

$$\begin{pmatrix} \frac{\partial}{\partial x} \\ \frac{\partial}{\partial y} \end{pmatrix} = \mathbf{J}^{-1} \begin{pmatrix} \frac{\partial}{\partial \xi} \\ \frac{\partial}{\partial \eta} \end{pmatrix}$$

$$\mathbf{J} = \begin{pmatrix} \frac{\partial N_1}{\partial \xi} & \frac{\partial N_2}{\partial \xi} & \frac{\partial N_3}{\partial \xi} \\ \frac{\partial N_1}{\partial \eta} & \frac{\partial N_2}{\partial \eta} & \frac{\partial N_3}{\partial \eta} \end{pmatrix} \begin{pmatrix} x_1 & y_1 \\ x_2 & y_2 \\ x_3 & y_4 \end{pmatrix}$$

$$\mathbf{J} = \text{der coo}$$

$$\mathbf{D} = \begin{pmatrix} \frac{\partial N_1}{\partial y} & \frac{\partial N_2}{\partial y} & \frac{\partial N_3}{\partial y} \\ \frac{\partial N_1}{\partial \xi} & \frac{\partial N_2}{\partial \xi} & \frac{\partial N_3}{\partial \xi} \end{pmatrix} = \mathbf{J}^{-1} \begin{pmatrix} \frac{\partial N_1}{\partial \xi} & \frac{\partial N_2}{\partial \xi} & \frac{\partial N_3}{\partial \xi} \\ \frac{\partial N_1}{\partial \eta} & \frac{\partial N_2}{\partial \eta} & \frac{\partial N_3}{\partial \eta} \end{pmatrix}$$

$$\mathbf{D} = \mathbf{J}^{-1} \text{ der}$$

Change of integral, example:

$$\int_{A_e} u_p N_p(x, y) N_q(x, y) dx dy = \int_{\Delta} u_p N_p(\xi, \eta) N_q(\xi, \eta) \det \mathbf{J} d\xi d\eta$$

Example:

$$\int \partial_x u \partial_x \phi dx dy = (\int D_{1p} D_{1q} |\mathbf{J}| d\eta d\xi) u_p$$

10.3 Edge integrals

We have integrals on the form

$$\int_{\Gamma} u(x, y) N(x, y) n_x d\Gamma$$

with

$$\mathbf{n} = \begin{pmatrix} n_x \\ n_y \end{pmatrix}$$

If the boundary is parameterised such that $(x, y) = (x(\gamma), y(\gamma))$ as γ goes from 0 to 1 then

$$\mathbf{n} = \frac{1}{\sqrt{(\partial_{\gamma}x)^2 + (\partial_{\gamma}y)^2}} \begin{pmatrix} -\partial_{\gamma}y \\ \partial_{\gamma}x \end{pmatrix}$$

and

$$d\Gamma = \sqrt{(\partial_{\gamma}x)^2 + (\partial_{\gamma}y)^2} d\gamma$$

and therefore

$$\mathbf{n} d\Gamma = \begin{pmatrix} -\partial_{\gamma}y \\ \partial_{\gamma}x \end{pmatrix} d\gamma$$

Hence

$$\int_{\Gamma} u(x, y) N(x, y) n_x d\Gamma = - \int_0^1 u(x(\gamma), y(\gamma)) N(x(\gamma), y(\gamma)) \partial_{\gamma}y d\gamma$$

10.3.1 Edge 12

For edge 12, $\eta = 0$. I parameterise it as $(\xi, \eta) = (1 - \gamma, 0)$ as this takes me from node 1 to node 2 in clockwise direction (that is how I order the nodes, most FE do it the other way around)

$$x = x_p N_p(1 - \gamma, 0) \quad \text{and} \quad y = y_P N_P(1 - \gamma, 0)$$

The normal is

$$\mathbf{n} d\Gamma = \begin{pmatrix} -\partial_{\gamma}y \\ \partial_{\gamma}x \end{pmatrix} d\gamma$$

and

$$\begin{aligned} \frac{1}{\partial_{\gamma}} &= \frac{1}{\partial\xi} \frac{\partial\xi}{\partial_{\gamma}} + \frac{1}{\partial\eta} \frac{\partial\eta}{\partial_{\gamma}} \\ &= -\frac{1}{\partial\xi} \end{aligned}$$

and therefore

$$\partial_{\gamma}y = -\partial_{\xi}y = -J_{12}$$

and

$$\mathbf{n} d\Gamma = \begin{pmatrix} \partial_{\xi}y \\ -\partial_{\xi}x \end{pmatrix} d\gamma = \begin{pmatrix} J_{12} \\ -J_{11} \end{pmatrix} d\gamma$$

or simply

$$\mathbf{n} d\Gamma = \begin{pmatrix} y_q \partial_{\xi}N_q(\xi, 0) \\ -x_q \partial_{\xi}N_q(\xi, 0) \end{pmatrix} d\gamma$$

For the linear triangle, for example, I get

$$\begin{aligned} x &= x_1\xi + x_2(1 - \xi) + x_3\eta \\ &= x_1(1 - \gamma) + x_2(1 - (1 - \gamma)) + x_30 \\ &= x_1(1 - \gamma) + x_2\gamma \\ y &= y_1(1 - \gamma) + y_2\gamma \end{aligned}$$

and

$$\begin{aligned} \partial_{\gamma}x &= -x_1 + x_2 \\ \partial_{\gamma}y &= -y_1 + y_2 \end{aligned}$$

and a normal

$$\mathbf{n} d\Gamma = \begin{pmatrix} y_1 - y_2 \\ x_2 - x_1 \end{pmatrix} d\gamma$$

10.3.2 Edge 23

For edge 23, $\xi = 0$. I parameterise the edge as $(\xi, \eta) = (0, \gamma)$, this takes me from node 2 to 3 as γ varies from 0 to 1.

$$\mathbf{n} d\Gamma = \begin{pmatrix} -\partial_\gamma y \\ \partial_\gamma x \end{pmatrix} d\gamma$$

$$\partial_\gamma = \partial_\eta$$

and therefore

$$\mathbf{n} d\Gamma = \begin{pmatrix} -\partial_\eta y \\ \partial_\eta x \end{pmatrix} = \begin{pmatrix} -J_{22} \\ J_{21} \end{pmatrix} d\gamma$$

For the linear triangle, for example, I get

$$x = x_1 0 + x_2(1 - \gamma) + x_3 \gamma$$

$$y = y_1 0 + y_2(1 - \gamma) + y_3 \gamma$$

and

$$\partial_\gamma x = -x_2 + x_3$$

$$\partial_\gamma y = -y_2 + y_3$$

and a normal

$$\mathbf{n} d\Gamma = \begin{pmatrix} y_2 - y_3 \\ x_3 - x_2 \end{pmatrix} d\gamma$$

10.3.3 Edge 32

For edge 32 is parameterised as $(\xi, \eta) = (\gamma, 1 - \gamma)$, and

$$\mathbf{n} d\Gamma = \begin{pmatrix} -\partial_\gamma y \\ \partial_\gamma x \end{pmatrix} d\gamma$$

and

$$\begin{aligned} \frac{1}{\partial\gamma} &= \frac{1}{\partial\xi}\frac{\partial\xi}{\partial\gamma} + \frac{1}{\partial\eta}\frac{\partial\eta}{\partial\gamma} \\ &= \frac{1}{\partial\xi} - \frac{1}{\partial\eta} \end{aligned}$$

and therefore

$$\mathbf{n} d\Gamma = \begin{pmatrix} -y_q(\partial_\xi N_q - \partial_\eta N_q) \\ x_q(\partial_\xi N_q - \partial_\eta N_q) \end{pmatrix} d\gamma = \begin{pmatrix} J_{22} - J_{12} \\ J_{11} - J_{21} \end{pmatrix} d\gamma$$

For the linear triangle, for example, I get

$$x = x_1 \gamma + x_2(1 - \gamma - (1 - \gamma)) + x_3(1 - \gamma)$$

or

$$x = x_1 \gamma + x_3(1 - \gamma)$$

$$y = y_1 \gamma + y_3(1 - \gamma)$$

and

$$\partial_\gamma x = x_1 - x_3$$

$$\partial_\gamma y = y_1 - y_3$$

and a normal

$$\mathbf{n} d\Gamma = \begin{pmatrix} y_3 - y_1 \\ x_1 - x_3 \end{pmatrix} d\gamma$$

10.4 Various directional derivatives

10.4.1 Directional derivative of draft with respect to ice thickness

For implicit forward time integration with respect to h using the NR method, various directional derivatives with respect to h must be calculated.

Using Eq. (1.202) we find that the directional derivative of the draft d with respect to h is

$$\begin{aligned} Dd(h)[\Delta h] &= \lim_{\epsilon \rightarrow 0} \frac{d}{d\epsilon} d(h + \epsilon \Delta h) \\ &= \mathcal{H}(h_f - h) \rho \Delta h / \rho_o - \rho h \delta(h_f - h) \Delta h / \rho_o + \mathcal{H}(H) H \delta(h - h_f) \Delta h \\ &= \frac{\rho}{\rho_o} \mathcal{H}(h_f - h) \Delta h + \delta(h - h_f) (H - \frac{\rho}{\rho_o} h) \Delta h \end{aligned}$$

When integrated the second term in the above expression integrates to zero, because where $h = h_f$ we have $H = \rho h / \rho_o$, hence¹

$$Dd(h)[\Delta h] = \frac{\rho}{\rho_o} \mathcal{H}(h_f - h) \Delta h. \quad (10.6)$$

Using Eq. (10.6) the directional derivative of

$$D(\frac{1}{2}g(\rho h^2 - \rho_o d^2))[\Delta h]$$

with respect to perturbation in h is found to be

$$\begin{aligned} D\left(\frac{1}{2}g(\rho h^2 - \rho_o d^2)\right)[\Delta h] &= g(\rho(h \Delta h - \rho_o d \frac{\rho}{\rho_o} \mathcal{H}(h_f - h) \Delta h)) \\ &= \rho g (h - \mathcal{H}(h_f - h) d) \Delta h \end{aligned}$$

The directional derivative of $g(\rho h - \rho_o d) \partial_x b$ with respect to h is found to be

$$D(g(\rho h - \rho_o d) \partial_x b)[\Delta h] = \rho g \mathcal{H}(h - h_f) \partial_x B \Delta h. \quad (10.7)$$

To see this first notice that using Eq. (1.202)

$$\begin{aligned} g(\rho h - \rho_o d) \partial_x b &= g(\rho h - \mathcal{H}(h_f - h) \rho h - \rho_o \mathcal{H}(H) \mathcal{H}(h - h_f) H) \partial_x b \\ &= g(\rho h - (1 - \mathcal{H}(h - h_f)) \rho h - \rho_o \mathcal{H}(H) \mathcal{H}(h - h_f) H) \partial_x b \\ &= g(\rho h + \mathcal{H}(h - h_f)(\rho h - \rho_o H^+) - \rho h) \partial_x b \\ &= g \mathcal{H}(h - h_f)(\rho h - \rho_o H^+) \partial_x b \\ &= g \mathcal{H}(h - h_f)(\rho h - \rho_o H^+) \partial_x B. \end{aligned}$$

Using the above expression we now calculate the directional derivative of $g(\rho h - \rho_o d) \partial_x b$ with respect to h and find

$$\begin{aligned} D(g(\rho h - \rho_o d) \partial_x b)[\Delta h] &= \mathcal{H}(h_f - h) \rho g \partial_x B \Delta h + g \delta(h - h_f) (\rho h - \rho_o H^+) \partial_x B \Delta h \\ &= (\rho \mathcal{H}(h - h_f) + \delta(h - h_f) (\rho h - \rho_o H^+)) g \partial_x B \Delta h \\ &= \rho g \mathcal{H}(h - h_f) \partial_x B \Delta h \end{aligned}$$

where the last step is correct when the expression is evaluated under an integral, thus demonstrating the correctness of Eq. (10.7).

(Not sure where to put this, but keep it here for the time being.) The lower ice surface is related to thickness through

$$b = \mathcal{H}(h - h_f) B + \mathcal{H}(h_f - h) (S - \rho h / \rho_o)$$

and therefore

$$\partial_h b = \delta(h - h_f) B - \delta(h_f - h) (S - \rho h / \rho_o) - \mathcal{H}(h_f - h) \rho / \rho_o$$

¹This argument does not hold if the Heaviside function and the Dirac delta functions are approximated. In that case the full expression must be used. Important for getting quadratic convergence in NR.

and

$$\partial_x b = \partial_h b \partial_x h = \delta(h - h_f) B \partial_x h - \delta(h_f - h)(S - \rho h / \rho_o) \partial_x h - \mathcal{H}(h_f - h) \rho \partial_x h / \rho_o$$

and assuming

$$\frac{\partial^2 b}{\partial h \partial x} = \frac{\partial^2 b}{\partial x \partial h}$$

If $f(x)$ is a test function

$$\partial_x \int \delta(x) \partial_x f(x) dx = -\partial_x \int \mathcal{H}(x) f(x) dx = -f(0) - \int \mathcal{H}(x) \partial_x f(x) dx$$

10.4.2 Linearisation of the 2HD forward problem needed for the adjoint method

For the adjoint method we need

$$\mathbf{K}^{xC} \Delta C_q := -D \mathbf{F}_x(\mathbf{u}_1^i, \mathbf{v}_1^i, \mathbf{h}_1^i)[\Delta C_q]$$

Here ΔC_q is the nodal value itself, the perturbation in C is $\Delta C_q N_q$ (no summation).

$$[\mathbf{K}^{xC}]_{pq} = \frac{1}{m} \int_{\Omega} \mathcal{H}(h - h_f) C^{-1/m-1} \|\mathbf{v}_{xy}\|^{1/m-1} u N_p N_q dx dy \quad (10.8)$$

and

$$[\mathbf{K}^{yC}]_{pq} = \frac{1}{m} \int_{\Omega} \mathcal{H}(h - h_f) C^{-1/m-1} \|\mathbf{v}_{xy}\|^{1/m-1} v N_p N_q dx dy \quad (10.9)$$

where

$$\mathbf{v}_{xy} = \begin{pmatrix} u \\ v \end{pmatrix}$$

and

$$\beta^2 = C^{-1/m} \|\mathbf{v}_{xy}\|^{1/m-1}$$

$$\mathbf{K}^C = \begin{bmatrix} \mathbf{K}^{xC} \\ \mathbf{K}^{yC} \end{bmatrix}$$

is $2N \times n$ where N are degrees of freedom.

If the cost function I is calculated using FE type inner product , then the gradient of the cost function is then given by

$$\begin{aligned} \frac{\partial I}{\partial C_q} &= [\mathbf{K}^C]_{pq} \lambda_p \\ &= \frac{1}{m} \int_{\Omega} \mathcal{H}(h - h_f) C^{-1/m-1} \|\mathbf{v}_{xy}\|^{1/m-1} (u \lambda + v \mu) N_q dx dy \end{aligned}$$

If I is calculated as a discrete sum over values then

$$\frac{\partial I}{\partial C_q} = \frac{1}{m} \mathcal{H}(h - h_f) C^{-1/m-1} \|\mathbf{v}_{xy}\|^{1/m-1} (u \lambda + v \mu)$$

Note: Perturbing on particular nodal value in $C = C_r N_r$ can be written as

$$(C_r + \Delta C \delta_{rp}) N_r$$

$C = C_r N_r$, $\Delta C = \Delta \hat{C} N_q$ with $\Delta \hat{C} = \Delta C_q$

$$\begin{aligned} (C + \Delta C)^m &= (C_r N_r + \Delta \hat{C} N_q)^m \\ &= (C_r N_r + \Delta \hat{C} N_q (C_j N_j) / (C_i N_i))^m \\ &= (C_r N_r)^m (1 + \Delta \hat{C} N_q / (C_i N_i))^m \\ &\approx (C_r N_r)^m (1 + m \Delta \hat{C} N_q / (C_i N_i)) \\ &= (C_s N_s)^m + m (C_s N_s)^{m-1} \Delta \hat{C} N_q \\ &= (C_s N_s)^m + m (C_s N_s)^{m-1} \Delta C \end{aligned}$$

I can write the perturbation as

$$K\Delta\hat{C} = m(C_s N_s)^{m-1} N_q \Delta\hat{C}$$

where

$$K = m(C_s N_s)^{m-1} N_q$$

10.5 FE formulation and linearisation for the 1HD Problem

10.5.1 Field equations and boundary conditions (1HD)

$$4\partial_x(h\eta\partial_x u) - \beta^2 u = \rho gh(\partial_x s \cos \alpha - \sin \alpha)$$

$$\beta^2 = C^{-1/m} \|u\|^{1/m-1}$$

with the sliding law written on the form

$$u = C|t_{bx}|^{m-1} t_{bx}$$

We have

$$t_{bx} = C^{-1/m} |u|^{1/m-1} u.$$

Glen's flow law is

$$\dot{\epsilon}_{ij} = A\tau^{n-1}\tau_{ij},$$

where

$$\tau = \sqrt{\tau_{ij}\tau_{ij}/2}$$

The flow law can also be written as

$$\tau_{ij} = A^{-1/n} \dot{\epsilon}^{(1-n)/n} \dot{\epsilon}_{ij},$$

where

$$\dot{\epsilon} = \sqrt{(\partial_x u)^2} = |\partial_x u|$$

If we write

$$\tau_{ij} = 2\eta\dot{\epsilon}_{ij}$$

then η is the effective viscosity given by

$$\eta = \frac{1}{2}A^{-1/n} \dot{\epsilon}^{(1-n)/n} = \frac{1}{2}A^{-1/n} \|\partial_x u\|^{(1-n)/n}$$

10.6 Linearisation of field equations (1HD)

In the non-linear case using Newton's method I need to linearise the equation.

Linearised with respect to u by writing $u = \bar{u} + \Delta u$, $\eta = \bar{\eta} + \partial_u \eta \Delta u$, and $\beta^2 = \bar{\beta}^2 + \partial_u (\beta^2) \Delta u$

$$4\partial_x(h(\bar{\eta} + \partial_u \eta \Delta u)\partial_x(\bar{u} + \Delta u)) - (\bar{\beta}^2 + D\beta^2(u)[\Delta u])(\bar{u} + \Delta u) = \rho gh(\partial_x s \cos \alpha - \sin \alpha)$$

or

$$4\partial_x(h(\bar{\eta}\partial_x \bar{u} + \partial_x \bar{u} D\eta(u)[\Delta u] + \bar{\eta}\partial_x \Delta u)) - \bar{\beta}^2 \bar{u} - \bar{\beta}^2 \Delta u - \bar{u} D\beta^2(u)[\Delta u] = \rho gh(\partial_x s \cos \alpha - \sin \alpha) \quad (10.10)$$

where

$$\eta = \frac{1}{2}A^{-1/n} \dot{\epsilon}^{(1-n)/n} = \frac{1}{2}A^{-1/n} |\partial_x u|^{(1-n)/n}$$

$$D\eta(u)[\Delta u] = \lim_{\epsilon \rightarrow 0} \frac{d}{d\epsilon} \eta(u + \epsilon \Delta u) \quad (10.11)$$

$$\begin{aligned} &= \lim_{\epsilon \rightarrow 0} \frac{d}{d\epsilon} \frac{1}{2} A^{-1/n} \|\partial_x(u + \epsilon \Delta u)\|^{(1-n)/n} \\ &\stackrel{\partial_x u > 0}{=} \lim_{\epsilon \rightarrow 0} \frac{d}{d\epsilon} \frac{1}{2} A^{-1/n} (\partial_x u + \epsilon \partial_x \Delta u)^{(1-n)/n} \\ &= \lim_{\epsilon \rightarrow 0} \frac{d}{d\epsilon} \frac{1}{2} A^{-1/n} ((\partial_x u)^{(1-n)/n} + (\partial_x u)^{(1-2n)/n} \frac{1-n}{n} \epsilon \partial_x \Delta u + \dots) \\ &= \frac{1}{2} A^{-1/n} ((\partial_x u)^{(1-2n)/n} \frac{1-n}{n} \partial_x \Delta u) \\ &= \frac{1-n}{2n} A^{-1/n} (\partial_x u)^{(1-2n)/n} \partial_x \Delta u \end{aligned} \quad (10.12)$$

Doing the same for $\partial_x u < 0$ shows that

$$D\eta(u)[\Delta u] = \frac{1-n}{2n} A^{-1/n} \|\partial_x u\|^{(1-2n)/n} \text{sign}(\partial_x u) \partial_x \Delta u$$

(old result)

$$\partial_u \eta = \frac{1-n}{2n} A^{-1/n} \|\partial_x u\|^{1/n-2} \text{sign}(\partial_x u)$$

The directional derivative of β^2 is

$$\begin{aligned} D\beta(u)[\Delta u] &= (1/m - 1) C^{-1/m} \|u\|^{(1-3m)/m} u \Delta u \\ &= (1/m - 1) C^{-1/m} \|u\|^{(1-2m)/m} \text{sign}(u) \Delta u \end{aligned}$$

old result

$$\partial_u \beta^2 = (1/m - 1) C^{-1/m} \|u\|^{1/m-2} \text{sign}(u)$$

Inserting into (10.10) gives

$$4\partial_x(h(\bar{\eta}\partial_x\bar{u} + \bar{u}E\partial_x\Delta u + \bar{\eta}\partial_x\Delta u)) - \bar{\beta}^2\bar{u} - \bar{\beta}^2\Delta u - \bar{u}B\Delta u = \rho gh(\partial_x s \cos \alpha - \sin \alpha)$$

where

$$B = (1/m - 1) C^{-1/m} \|u\|^{(1-2m)/m} \text{sign}(u)$$

and

$$E = \frac{1-n}{2n} A^{-1/n} \|\partial_x u\|^{(1-2n)/n} \text{sign}(\partial_x u)$$

which can be written on the form

$$4\partial_x(h(\bar{\eta} + \bar{u}E)\partial_x\Delta u) - (\bar{\beta}^2 + \bar{u}B)\Delta u = \rho gh(\partial_x s \cos \alpha - \sin \alpha) - 4\partial_x(h\bar{\eta}\partial_x\bar{u}) + \bar{\beta}^2\bar{u}$$

10.6.1 Newton Raphson

$$4\partial_x(\eta h\partial_x u) - \mathcal{H}(h - h_f)\beta^2 u = \frac{1}{2} g \cos \alpha \rho (1 - \rho/\rho_o) \partial_x h^2 + \rho gh \cos \alpha \mathcal{H}(h - h_f) \partial_x s' - \rho gh \sin \alpha, \quad (10.13)$$

$$s'(x) = \mathcal{H}(h - h_f)(\rho/\rho_o h - H)$$

where

$$H = S - B,$$

or as

$$4\partial_x(\eta h\partial_x u) - \mathcal{H}(h - h_f)\beta^2 u = \frac{\rho g}{2} \partial_x h^2 \cos \alpha + \rho gh \mathcal{H}(h - h_f) (\rho/\rho_o \partial_x h - \partial_x H) \cos \alpha - \rho gh \sin \alpha \quad (10.14)$$

The FE formulation is

$$\begin{aligned} R_p^u &= \int \{ 4\eta h \partial_x u \partial_x N_p + \mathcal{H}(h - h_f) \beta^2 u N_p \\ &\quad - \frac{\varrho g}{2} h^2 \partial_x \phi \cos \alpha + \rho g h \mathcal{H}(h - h_f) (\rho/\rho_o \partial_x h - \partial_x H) N_p \cos \alpha - \rho g h N_p \sin \alpha \} dx \\ &\quad - h(4\eta \partial_x u - \varrho g h/2) u N_p|_{x_0}^{x_l} = 0 \end{aligned} \quad (10.15)$$

where

$$u = N_p u_p$$

If all von Neumann BC are of Weertman type, the boundary term is zero because at the calving front

$$8\eta \partial_x u = \varrho g h.$$

I also have

$$\partial_t h + \partial_x(uh) = a \quad (10.16)$$

where

$$a = a_s + a_b$$

The FE formulation used is the θ method, i.e.

$$R_p^h = \int \left\{ \frac{1}{\Delta t} (h_1 - h_0) + \theta \partial_x(u_1 h_1) + (1 - \theta) \partial_x(u_0 h_0) - a_s - a_b \right\} N_p dx = 0 \quad (10.17)$$

where $0 \leq \theta \leq 1$.

I go from time $t = t_0$ to time $t = t_1$ where $t_1 > t_0$, and I assume that the values for u at h at $t = t_0$ (i.e. u_0 and h_0) are known. I iteratively solve for corrections to the values at time step $t = t_1$

$$\begin{aligned} u_1 &= \bar{u}_1 + \Delta u \\ h_1 &= \bar{h}_1 + \Delta h \end{aligned}$$

using the Newton-Raphson method.

For Newton-Raphson I need to take the directional derivative of this equation with respect to u and h ,

$$K(\Delta u, \Delta v)^T = \lim_{\epsilon \rightarrow 0} \frac{d}{d\epsilon} \mathbf{R}(\mathbf{v} + \epsilon \Delta \mathbf{v}, \mathbf{h} + \epsilon \Delta \mathbf{h})$$

where I have now ordered the discrete values of u and h into a vector

$$D(\mathcal{H}(h - h_f) \beta^2(u))[\Delta h] = \delta(\bar{h} - h_f) \beta^2(\bar{u}) \Delta h$$

Directional derivative of right-hand term with respect to h .

$$\begin{aligned} D\{\rho g h \partial_x s'\}[\Delta h] &= D\{\rho g h \partial_x (\mathcal{H}(h - h_f)(\rho h/\rho_o - H))\}[\Delta h] \\ &= \lim_{\epsilon \rightarrow 0} \partial_\epsilon (\rho g(h + \epsilon \Delta h) \partial_x(\mathcal{H}(h + \epsilon \Delta h - h_f)(\rho(h + \epsilon \Delta h)/\rho_o - H))) \\ &= \rho g \partial_x(\mathcal{H}(h - h_f)(\rho h/\rho_o - H)) \Delta h \\ &\quad + \rho g h \partial_x(\mathcal{H}(h - h_f) \rho \Delta h/\rho_o) \\ &\quad + \rho g h \partial_x(\delta(h - h_f) \Delta h (\rho h/\rho_o - H)) \quad (= 0) \\ &= \rho g \mathcal{H}(h - h_f)(\rho \partial_x h/\rho_o - \partial_x H) \Delta h \\ &\quad + \frac{\rho^2}{\rho_o} g h \mathcal{H}(h - h_f) \partial_x \Delta h \\ &\quad + \frac{\rho^2}{\rho_o} \delta(h - h_f) h \partial_x h \Delta h \end{aligned}$$

$$\begin{aligned} [\mathbf{K} u h]_{pq} \Delta h_q &= D R_p^u(u, h)[\Delta h_q] = \int \{ 4\bar{\eta} \partial_x \bar{u} \partial_x N_p \\ &\quad + \delta(\bar{h} - h_f) \bar{\beta}^2 \bar{u} N_p \\ &\quad - \varrho g \bar{h} \partial_x N_p \cos \alpha \\ &\quad + \rho g \mathcal{H}(\bar{h} - h_f)(\rho/\rho_o \partial_x \bar{h} - \partial_x H) N_p \cos \alpha \\ &\quad + \rho g \bar{h} \delta(\bar{h} - h_f)(\rho/\rho_o \partial_x \bar{h} - \partial_x H) N_p \cos \alpha \\ &\quad + \rho g \bar{h} \mathcal{H}(\bar{h} - h_f) \rho/\rho_o N_p \cos \alpha \partial_x \\ &\quad - \rho g N_p \sin \alpha \} \Delta h_q dx \end{aligned}$$

$$\begin{aligned} [\mathbf{K}_{uu}]_{pq} \Delta u_q &= DR_p^u(u, h)[\Delta u_q] = \int \{4\bar{h}\partial_u\eta(\bar{u})\partial_x\bar{u}\partial_x N_p\partial_x \\ &\quad + 4\eta(\bar{u})\bar{h}\partial_x N_p\partial_x \\ &\quad + \mathcal{H}(h - h_f)\partial_u\beta^2(\bar{u})N_p \\ &\quad + \mathcal{H}(h - h_f)\beta^2(\bar{u})N_p\} \Delta u_q dx \end{aligned}$$

Linearising (10.17) gives

$$\int \{(\Delta h + \bar{h} - h_0)/\Delta t + \theta\partial_x((\bar{u} + \Delta u)(\bar{h} + \Delta h)) + (1 - \theta)\partial_x(u_0h_0) - a_s - a_b\} N_p dx = 0$$

or

$$\begin{aligned} 0 &= \int \{\Delta h/\Delta t + \theta\partial_x((\bar{u}\Delta h + \bar{h}\Delta u))\} N_p dx + \\ &\quad \int \{(\bar{h} - h_0)/\Delta t + \theta\partial_x(\bar{u}\bar{h}) + (1 - \theta)\partial_x(u_0h_0) - a_s - a_b\} N_p dx \end{aligned} \tag{10.18}$$

or

$$[\mathbf{K}_{hu}]_{pq} \Delta u_q = \theta(\partial_x\bar{h} + \bar{h}\partial_x)\Delta u_q N_p$$

$$[\mathbf{K}_{hh}]_{pq} = (1/\Delta t + \theta(\partial_x\bar{u}N_q + \bar{u}\partial_xN_q))N_p$$

$$\begin{bmatrix} \mathbf{K}_{uu} & \mathbf{K}_{uh} \\ \mathbf{K}_{hu} & \mathbf{K}_{hh} \end{bmatrix} \begin{bmatrix} \Delta \mathbf{v} \\ \Delta \mathbf{h} \end{bmatrix} = \begin{bmatrix} \mathbf{R}^u \\ \mathbf{R}^h \end{bmatrix} \tag{10.19}$$

where

$$\mathbf{r}^h = \mathbf{T}^h - \mathbf{F}^h$$

where \mathbf{T} and \mathbf{F} are the internal and external nodal forces, respectively, and \mathbf{R} is the residual or out-of-balance nodal forces.

$$\mathbf{F}^h = - \int \{a_s + a_b - (\bar{h} - h_0)/\Delta t\} N_p dx$$

and

$$\mathbf{T}^h = \int \{\theta\partial_x(\bar{u}\bar{h}) + (1 - \theta)\partial_x(u_0h_0)\} N_p dx$$

$$T_p^u = \int \{4\eta h\partial_x u\partial_x N_p + \mathcal{H}(h - h_f)\beta^2 u N_p\} dx$$

$$F_p^u = \int \left\{ \frac{\rho g}{2} h^2 \partial_x \phi + \rho g h \mathcal{H}(h - h_f) (\rho/\rho_o \partial_x h - \partial_x H) N_p \right\} dx$$

10.6.2 Connection to Piccard iteration

If instead of writing

$$4\partial_x(h(\bar{\eta}\partial_x\bar{u} + \partial_u\eta\partial_x\bar{u}\Delta u + \bar{\eta}\partial_x\Delta u)) - (\bar{\beta}^2\bar{u} + (\bar{\beta}^2 + \partial_u\beta^2\bar{u})\Delta u) = \rho gh(\partial_x s \cos \alpha - \sin \alpha)$$

we ignore the dependency of η and β^2 on u we get

$$4\partial_x(h(\bar{\eta}\partial_x\bar{u} + \bar{\eta}\partial_x\Delta u)) - (\bar{\beta}^2\bar{u} + \bar{\beta}^2\Delta u) = \rho gh(\partial_x s \cos \alpha - \sin \alpha)$$

or simply

$$4\partial_x(h\bar{\eta}\partial_x(\bar{u} + \Delta u)) - \bar{\beta}^2(\bar{u} + \Delta u) = \rho gh(\partial_x s \cos \alpha - \sin \alpha)$$

which can be solved directly for $\bar{u} + \Delta u$. This is the Piccard iteration, i.e. an incomplete Newton iteration.

10.7 Linearisation in 2HD

10.7.1 Drag-term linearisation (2HD)

Basal drag is generally a function of basal sliding velocity and flotation conditions, i.e.

$$\mathbf{t}_b = f(h, h_f, \mathbf{v})$$

Using Weertman sliding law, basal drag is

$$\mathbf{t}_b = \mathcal{H}(h - h_f) \beta^2 \mathbf{v}_b$$

or

$$\begin{pmatrix} t_{xb} \\ t_{xy} \end{pmatrix} = \mathcal{H}(h - h_f) \beta^2 \begin{pmatrix} u \\ v \end{pmatrix} \quad (10.20)$$

were

$$\beta^2 = C^{-1/m} \|\mathbf{v}_b\|^{1/m-1}$$

$$\mathbf{t}_b = (g(\rho h - \rho_o H))^{q/m} C^{-1/m} \|\mathbf{v}_b\|^{1/m-1} \mathbf{v}_b, \quad (10.21)$$

therefore

$$\tau_b = \tau_b(u, v, h)$$

We therefore need to linearise \mathbf{t}_b with respect to u , v , and h .

We start by linearising β^2 with respect to u and v obtaining²

$$\begin{aligned} \beta(u + \epsilon \Delta u, v + \epsilon \Delta v) &= C^{-1/m} ((u + \epsilon \Delta u)^2 + (v + \epsilon \Delta v)^2)^{(1/m-1)/2} \\ &= C^{-1/m} ((u^2 + v^2 + 2\epsilon(u \Delta u + v \Delta v)))^{(1/m-1)/2} \\ &= C^{-1/m} ((u^2 + v^2)^{(1/m-1)/2} + (1/m-1)(u^2 + v^2)^{(1/m-1)/2-1} \epsilon(u \Delta u + v \Delta v)) \\ &= \beta^2(u, v) + C^{-1/m} (1/m-1)(u^2 + v^2)^{(1/m-3)/2} \epsilon(u \Delta u + v \Delta v)) \end{aligned}$$

The directional derivative is defined as

$$D\beta(\mathbf{v})[\Delta \mathbf{v}_{xy}] = \lim_{\epsilon \rightarrow 0} \frac{d}{d\epsilon} \beta^2(u + \epsilon \Delta u, v + \epsilon \Delta v)$$

and we arrive at³

$$D\beta(\mathbf{v})[\Delta u, \Delta v] = (1/m-1) C^{-1/m} \|\mathbf{v}\|^{(1-3m)/m} (u \Delta u, v \Delta v)$$

and the directional derivatives of \mathbf{t}_b with respect to u and v are therefore

$$\begin{aligned} D\mathbf{t}_{xb}[\Delta u, \Delta v] &= \beta^2 \Delta u + D\beta^2[\Delta u] u + D\beta^2[\Delta v] u \\ &= \beta^2 \Delta u + (1/m-1) C^{-1/m} \|\mathbf{v}\|^{(1-3m)/m} (u^2 \Delta u + uv \Delta v) \\ D\mathbf{t}_{yb}[\Delta u, \Delta v] &= \beta^2 \Delta v + (1/m-1) C^{-1/m} \|\mathbf{v}\|^{(1-3m)/m} (v^2 \Delta v + uv \Delta u) \end{aligned}$$

which can also be written on the form

$$\begin{pmatrix} \Delta t_{xb} \\ \Delta t_{xy} \end{pmatrix} = \mathcal{H}(h - h_f) \begin{pmatrix} \beta^2 + \mathcal{D} u^2 & \mathcal{D} uv \\ \mathcal{D} uv & \beta^2 + \mathcal{D} v^2 \end{pmatrix} \begin{pmatrix} \Delta u \\ \Delta v \end{pmatrix} \quad (10.22)$$

²If $y \ll x$ then $(x+y)^m \approx x^n + m x^{m-1} y$.

³In 1d we get

$$\begin{aligned} D\beta(\mathbf{v})[\Delta \mathbf{v}] &= (1/m-1) C^{-1/m} \|\mathbf{v}\|^{(1-3m)/m} u \Delta u \\ &= (1/m-1) C^{-1/m} \|\mathbf{v}\|^{(1-2m)/m} \text{sign}(u) \Delta u \end{aligned}$$

where we have now added back the $\mathcal{H}(h - h_f)$ factor, and where

$$\mathcal{D} := (1/m - 1) C^{-1/m} \|\mathbf{v}\|^{(1-3m)/m}$$

Note that because of the non-linearity of the sliding law, the basal drag term in x direction depends on both u and v and this is reflected in the directional derivatives above.

In a fully implicit treatment we also must include the effect of grounding/un-grounding the basal drag term, or

$$\begin{aligned} D\mathbf{t}_{xb}[\Delta h] &= \lim_{\epsilon \rightarrow 0} \frac{d}{d\epsilon} \mathbf{t}_{xb}(h + \epsilon \Delta h) \\ &= \lim_{\epsilon \rightarrow 0} \frac{d}{d\epsilon} (\mathcal{H}(h + \epsilon \Delta h - h_f) \beta^2 u) \\ &= \lim_{\epsilon \rightarrow 0} \delta(h + \epsilon \Delta h - h_f) \Delta h \beta^2 u \\ &= \delta(h - h_f) \beta^2 u \Delta h \end{aligned}$$

and therefore for the Weertman sliding law we have:

$$\begin{pmatrix} \Delta t_{bx} \\ \Delta t_{by} \end{pmatrix} = \begin{pmatrix} \mathcal{H}(h - h_f)(\beta^2 + \mathcal{D} u^2) & \mathcal{H}(h - h_f)\mathcal{D} uv & \delta(h - h_f) \beta^2 u \\ \mathcal{H}(h - h_f)\mathcal{D} uv & \mathcal{H}(h - h_f)(\beta^2 + \mathcal{D} v^2) & \delta(h - h_f) \beta^2 v \end{pmatrix} \begin{pmatrix} \Delta u \\ \Delta v \\ \Delta h \end{pmatrix} \quad (10.23)$$

where again

$$\mathcal{D} := (1/m - 1) C^{-1/m} \|\mathbf{v}\|^{(1-3m)/m}$$

For the Budd sliding law (see sec 1.11.2), assuming perfect hydrological connection between the subglacial hydrological system and the ocean,

$$N = \rho g \mathcal{H}(h - h_f) (h - h_f)$$

we have

$$\mathbf{t}_b = N^{q/m} \beta^2 \mathbf{v}_b, \quad (10.24)$$

and linearising with respect to h now gives

$$\begin{aligned} D\mathbf{t}_{xb}[\Delta h] &= \lim_{\epsilon \rightarrow 0} \frac{d}{d\epsilon} \mathbf{t}_{xb}(h + \epsilon \Delta h) \\ &= \lim_{\epsilon \rightarrow 0} \frac{d}{d\epsilon} ((\rho g(h + \epsilon \Delta h - h_f))^{q/m} \beta^2 u) \\ &= \lim_{\epsilon \rightarrow 0} \frac{q}{m} (\rho g(h + \epsilon \Delta h - h_f))^{q/m-1} \rho g \Delta h \beta^2 u \\ &= \rho g \frac{q}{m} (\rho g(h - h_f))^{q/m-1} \beta^2 u \Delta h \end{aligned}$$

and therefore for the Budd sliding law we have:

$$\begin{pmatrix} \Delta t_{bx} \\ \Delta t_{by} \end{pmatrix} = N^{q/m} \begin{pmatrix} N^{q/m} (\beta^2 + \mathcal{D} u^2) & N^{q/m} \mathcal{D} uv & \mathcal{E} \beta^2 u \\ N^{q/m} \mathcal{D} uv & N^{q/m} (\beta^2 + \mathcal{D} v^2) & \mathcal{E} \beta^2 v \end{pmatrix} \begin{pmatrix} \Delta u \\ \Delta v \\ \Delta h \end{pmatrix} \quad (10.25)$$

(10.26)

where

$$\mathcal{E} = \frac{q}{m} N^{q/m-1} \rho g (\delta(h - h_f) (h - h_f) + \mathcal{H}(h - h_f))$$

We see that for example

$$\begin{aligned} \frac{\partial t_{bx}}{\partial h} &= \frac{q}{m} N^{q/m-1} \rho g \beta^2 u \\ &= \frac{q}{m} (\rho g(h - h_f))^{q/m-1} \rho g \beta^2 u \end{aligned}$$

where $h > h_f$, and in the linear case when $q/m = m = 1$, we have

$$\frac{\partial t_{bx}}{\partial h} = \frac{\rho g}{C} u$$

This is the partial derivative with respect to h and as such does not include the effect of changes in h on u . This shows that with Budd sliding law, the basal drag increases with ice thickness everywhere upstream of the grounding line. For Weertman law no similar statement can be made and the basal drag only changes with thickness through the implicit dependency of the velocity on thickness.

Note that for $q/m < 1$, $\Delta t_b \rightarrow \infty$ as $\Delta h \rightarrow h_f$.

Ocean drag term

We add an ocean drag term over the floating section of the form

$$\mathbf{t}_b^o = \mathcal{H}(h_f - h) \beta_o^2 (\mathbf{v}_b - \mathbf{v}_o)$$

with

$$\beta_o^2(u, v) = C_o^{-1/m_o} |\mathbf{v}_b - \mathbf{v}_o|^{1/m_o - 1}$$

The total drag is a sum of that due to basal sliding and ocean currents.

$$\mathbf{t}_b = \mathcal{H}(h - h_f) \beta^2 \mathbf{v} + \mathcal{H}(h_f - h) \beta_o^2 (\mathbf{v} - \mathbf{v}_o)$$

So

$$\begin{aligned} t_{bx}^o &= \mathcal{H}(h_f - h) C_o^{-1/m_o} ((u - u_o)^2 + (v - v_o)^2)^{(1-m)/2m} (u - u_o) \\ t_{yx}^o &= \mathcal{H}(h_f - h) C_o^{-1/m_o} ((u - u_o)^2 + (v - v_o)^2)^{(1-m)/2m} (v - v_o) \end{aligned}$$

and hence

$$\begin{aligned} Dt_{bx}^o[\Delta u] &= \mathcal{H}(h_f - h) C_o^{-1/m_o} \left(\|\mathbf{v}_b - \mathbf{v}_o\|^{(1-m_o)/m_o} + (1/m - 1) \|\mathbf{v}_b - \mathbf{v}_o\|^{(1-3m_o)/m_o} (u - u_o)^2 \right) \Delta u \\ Dt_{bx}^o[\Delta v] &= \mathcal{H}(h_f - h) C_o^{-1/m_o} (1/m - 1) \|\mathbf{v}_b - \mathbf{v}_o\|^{(1-3m_o)/m_o} (v - v_o)(u - u_o) \Delta v \\ Dt_{by}^o[\Delta u] &= \mathcal{H}(h_f - h) C_o^{-1/m_o} (1/m - 1) \|\mathbf{v}_b - \mathbf{v}_o\|^{(1-3m_o)/m_o} (v - v_o)(u - u_o) \Delta u \\ Dt_{by}^o[\Delta v] &= \mathcal{H}(h_f - h) C_o^{-1/m_o} \left(\|\mathbf{v}_b - \mathbf{v}_o\|^{(1-m_o)/m_o} + (1/m - 1) \|\mathbf{v}_b - \mathbf{v}_o\|^{(1-3m_o)/m_o} (v - v_o)^2 \right) \Delta v \\ Dt_{bx}^o[\Delta h] &= -\delta(h_f - h) C_o^{-1/m_o} \|\mathbf{v}_b - \mathbf{v}_o\|^{(1-m_o)/m_o} (u - u_o) \Delta h \\ Dt_{by}^o[\Delta h] &= -\delta(h_f - h) C_o^{-1/m_o} \|\mathbf{v}_b - \mathbf{v}_o\|^{(1-m_o)/m_o} (v - v_o) \Delta h \end{aligned}$$

10.7.2 Flow law linearisation (2HD)

Using Glen's flow law, deviatoric stresses are related to strain rates through Eq. (1.188), i.e.

$$\tau_{ij} = A^{-1/n} \dot{\epsilon}^{(1-n)/n} \dot{\epsilon}_{ij},$$

where

$$\dot{\epsilon} = \sqrt{\dot{\epsilon}_{ij} \dot{\epsilon}_{ij}/2}$$

which in the Shallow Ice Stream Approximation takes the form

$$\dot{\epsilon} = \sqrt{(\dot{\epsilon}_{xx})^2 + (\dot{\epsilon}_{yy})^2 + \dot{\epsilon}_{xx} \dot{\epsilon}_{yy} + (\dot{\epsilon}_{xy})^2} \quad (10.27)$$

$$= ((\partial_x u)^2 + (\partial_y v)^2 + \partial_x u \partial_y v + (\partial_x v + \partial_y u)^2/4)^{1/2}. \quad (10.28)$$

If we write

$$\tau_{ij} = 2\eta \dot{\epsilon}_{ij}$$

where η is the effective viscosity given by

$$\eta = \frac{1}{2} A^{-1/n} \dot{\epsilon}^{(1-n)/n}$$

then, in the Shallow Ice Stream Approximation, η is

$$\eta = \frac{1}{2} A^{-1/n} ((\partial_x u)^2 + (\partial_y v)^2 + \partial_x u \partial_y v + (\partial_x v + \partial_y u)^2 / 4)^{(1-n)/2n}.$$

More generally we can express the stresses as a function of velocities as

$$\tau_{ij} = f(u_q).$$

We now need to linearise each of the stress components with respect to the unknown velocity components u and v velocities. We start with τ_{xx} where we have

$$\tau_{xx} = A^{-1/n} \dot{\epsilon}^{(1-n)/n} \dot{\epsilon}_{xx} \quad (10.29)$$

$$= A^{-1/n} \dot{\epsilon}^{(1-n)/n} \partial_x u \quad (10.30)$$

and we linearise

$$D\tau_{xx}[u; \Delta u] = \lim_{\epsilon \rightarrow 0} \frac{d}{d\epsilon} \tau_{xx}(u; \Delta u) \quad (10.31)$$

$$= \lim_{\epsilon \rightarrow 0} \frac{d}{d\epsilon} (2\eta \partial_x u) \quad (10.32)$$

$$= 2\eta \partial_x \Delta u + (2D\eta[\Delta u]) \partial_x u \quad (10.33)$$

$$\eta = \frac{1}{2} A^{-1/n} ((\partial_x u)^2 + (\partial_y v)^2 + \partial_x u \partial_y v + (\partial_x v + \partial_y u)^2 / 4)^{(1-n)/2n}$$

$$\begin{aligned} & (\partial_x(u + \Delta u))^2 + (\partial_y(v + \Delta v))^2 + \partial_x(u + \Delta u) \partial_y(v + \Delta v) + (\partial_x(v + \Delta v) + \partial_y(u + \Delta u))^2 / 4 \\ &= (\partial_x u)^2 + 2\partial_x u \partial_x \Delta u \\ &+ (\partial_y v)^2 + 2\partial_y v \partial_y \Delta v \\ &+ (\partial_x u + \partial_x \Delta u)(\partial_y v + \partial_y \Delta v) \\ &+ (\partial_x v + \partial_x \Delta v + \partial_y u + \partial_y \Delta u)^2 / 4 \\ &= (\partial_x u)^2 + 2\partial_x u \partial_x \Delta u \\ &+ (\partial_y v)^2 + 2\partial_y v \partial_y \Delta v \\ &+ \partial_x u \partial_y v + \partial_x u \partial_y \Delta v + \partial_y v \partial_x \Delta u \\ &+ (\partial_x v + \partial_y u) / 4 + (\partial_x v + \partial_y u)(\partial_x \Delta v + \partial_y \Delta u) / 2 \\ &= e^2 + \delta de^2 \end{aligned}$$

where

$$\begin{aligned} e^2 &= (\partial_x u)^2 + (\partial_y v)^2 + \partial_x u \partial_y v + (\partial_x v + \partial_y u) / 4 \\ &= \dot{\epsilon}_{xx}^2 + \dot{\epsilon}_{yy}^2 + \dot{\epsilon}_{xx} \dot{\epsilon}_{yy} + \dot{\epsilon}_{xy}^2 \end{aligned}$$

$$\delta e^2 = 2\partial_x u \partial_x \Delta u + 2\partial_y v \partial_y \Delta v + \partial_x u \partial_y \Delta v + \partial_y v \partial_x \Delta u + (\partial_x v + \partial_y u)(\partial_x \Delta v + \partial_y \Delta u) / 2$$

or

$$\begin{aligned} \delta e^2 &= (2\partial_x u + \partial_y v) \partial_x \Delta u + (2\partial_y v + \partial_x u) \partial_y \Delta v + \frac{1}{2} (\partial_x v + \partial_y u) (\partial_x \Delta v + \partial_y \Delta u) \\ &= (2\dot{\epsilon}_{xx} + \dot{\epsilon}_{yy}) \partial_x \Delta u + (2\dot{\epsilon}_{yy} + \dot{\epsilon}_{xx}) \partial_y \Delta v + \dot{\epsilon}_{xy} (\partial_x \Delta v + \partial_y \Delta u) \end{aligned}$$

The directional derivative of η is

$$\begin{aligned} D\eta(u, v)[\Delta u, \Delta v] &= E((2\dot{\epsilon}_{xx} + \dot{\epsilon}_{yy}) \partial_x \Delta u + (2\dot{\epsilon}_{yy} + \dot{\epsilon}_{xx}) \partial_y \Delta v + \dot{\epsilon}_{xy} (\partial_x \Delta v + \partial_y \Delta u)) \\ &= E((2\partial_x u + \partial_y v) \partial_x \Delta u + (2\partial_y v + \partial_x u) \partial_y \Delta v + \frac{1}{2} (\partial_x v + \partial_y u) (\partial_x \Delta v + \partial_y \Delta u)) \end{aligned}$$

where

$$E := \frac{1-n}{4n} A^{-1/n} e^{(1-3n)/n}$$

which I can also write as

$$D\eta(u, v)[\Delta u, \Delta v] = d_u \eta \Delta u + d_v \eta \Delta v \quad (10.34)$$

where

$$d_u \eta = E ((2\dot{\epsilon}_{xx} + \dot{\epsilon}_{yy}) \partial_x + \dot{\epsilon}_{xy} \partial_y)$$

and

$$d_v \eta = E ((2\dot{\epsilon}_{yy} + \dot{\epsilon}_{xx}) \partial_y + \dot{\epsilon}_{xy} \partial_x)$$

where

$$E := \frac{1-n}{4n} A^{-1/n} e^{(1-3n)/n}$$

or as

$$D\eta(u, v)[\Delta u, \Delta v] = d_{xu} \partial_x \Delta u + d_{yu} \partial_y \Delta u + d_{yv} \partial_y \Delta v + d_{xv} \partial_x \Delta v \quad (10.35)$$

where

$$d_{xu} = E (2\dot{\epsilon}_{xx} + \dot{\epsilon}_{yy})$$

and

$$d_{yu} = E \dot{\epsilon}_{xy}$$

and

$$d_{yv} = E (2\dot{\epsilon}_{yy} + \dot{\epsilon}_{xx})$$

and

$$d_{xv} = E \dot{\epsilon}_{xy}$$

$$\begin{pmatrix} D\eta_x \\ D\eta_y \end{pmatrix} = \begin{pmatrix} E(2\dot{\epsilon}_{xx} + \dot{\epsilon}_{yy})\partial_x & E\dot{\epsilon}_{xy}\partial_y & 0 \\ E\dot{\epsilon}_{xy}\partial_x & E(\dot{\epsilon}_{xx} + 2\dot{\epsilon}_{yy})\partial_y & 0 \end{pmatrix} \begin{pmatrix} \Delta u \\ \Delta v \\ \Delta h \end{pmatrix} \quad (10.36)$$

In the 1d case we get

$$\frac{1-n}{4n} A^{-1/n} |\partial_x u|^{(1-3n)/n} 2\partial_x u \partial_x \Delta u = \frac{1-n}{2n} A^{-1/n} |\partial_x u|^{(1-2n)/n} \text{sign}(\partial_x u) \partial_x \Delta u$$

10.7.3 Field-equation linearisation

linearising

$$\begin{aligned} & \partial_x (4h\eta \partial_x u + 2h\eta \partial_y v) + \partial_y (h\eta (\partial_x v + \partial_y u)) - \beta^2 u \\ &= \frac{1}{2} \varrho g \cos \alpha \partial_x h^2 + \rho gh (\partial_x s' \cos \alpha - \sin \alpha) \end{aligned}$$

gives

$$\begin{aligned} & \partial_x (4h(\eta \partial_x u + D\eta \partial_x u + \eta \partial_x \Delta u) + 2h(\eta \partial_y v + D\eta \partial_y v + \eta \partial_y \Delta v)) \\ &+ \partial_y (h(\eta \partial_x v + D\eta \partial_x v + \eta \partial_x \Delta v) + h(\eta \partial_y u + D\eta \partial_y u + \eta \partial_y \Delta u)) \\ &- (\beta^2 u + D\beta^2 u + \beta^2 \Delta u) \\ &= \frac{1}{2} \varrho g \cos \alpha \partial_x h^2 + \rho gh (\partial_x s' \cos \alpha - \sin \alpha) \end{aligned}$$

or

$$\begin{aligned} & \partial_x (4h(D\eta \partial_x u + \eta \partial_x \Delta u) + 2h(D\eta \partial_y v + \eta \partial_y \Delta v)) \\ &+ \partial_y (h(D\eta \partial_x v + \eta \partial_x \Delta v) + h(D\eta \partial_y u + \eta \partial_y \Delta u)) \\ &- (D\beta^2 u + \beta^2 \Delta u) \\ &= \frac{1}{2} \varrho g \cos \alpha \partial_x h^2 + \rho gh (\partial_x s' \cos \alpha - \sin \alpha) - \partial_x (4h\eta(\partial_x u + \partial_y v)) - \partial_y (h\eta(\partial_x v + \partial_y u)) + \beta^2 u \end{aligned}$$

after having done the partial integration I get within the integral

$$\begin{aligned}
 & (4h(D\eta \partial_x u + \eta \partial_x \Delta u) + 2h(D\eta \partial_y v + \eta \partial_y \Delta v)) \partial_x N_i \\
 & + h((D\eta \partial_x v + \eta \partial_x \Delta v) + h(D\eta \partial_y u + \eta \partial_y \Delta u)) \partial_y N_i \\
 & +(D\beta^2 u + \beta^2 \Delta u) N_i \\
 & = +\frac{1}{2} \varrho g \cos \alpha \partial_x h^2 \partial_x N_i - \rho gh(\partial_x s' \cos \alpha - \sin \alpha) N_i - 4h\eta(\partial_x u + 2\partial_y v) \partial_x N_i - h\eta(\partial_x v + \partial_y u) \partial_y N_i - (\text{#0uBS})
 \end{aligned} \tag{10.37}$$

Inserting (10.34)

$$\begin{aligned}
 & (4h(\eta \partial_x \Delta u + \partial_x u(d_u \eta \Delta u + d_v \eta \Delta v)) + 2h(\eta \partial_y \Delta v + \partial_y v(d_u \eta \Delta u + d_v \eta \Delta v))) \partial_x N_i \\
 & + (h(\eta \partial_x \Delta v + \partial_x v(d_u \eta \Delta u + d_v \eta \Delta v)) + h(\eta \partial_y \Delta u + \partial_y u(d_u \eta \Delta u + d_v \eta \Delta v))) \partial_y N_i \\
 & + (\beta^2 \Delta u + u(d_u \beta^2 \Delta u + d_v \beta^2 \Delta v)) N_i \\
 & = +\frac{1}{2} \varrho g \cos \alpha \partial_x h^2 \partial_x N_i - \rho gh(\partial_x s' \cos \alpha - \sin \alpha) N_i - 4h\eta(\partial_x u + 2\partial_y v) \partial_x N_i - h\eta(\partial_x v + \partial_y u) \partial_y N_i - \beta^2 u N_i
 \end{aligned}$$

I take all coefficients in front of Δu and put them in the 11 part of the matrix, and everything in front of Δv and put that in the 12 part of the matrix.

To make this clear insert (10.35) into (10.38)

$$\begin{aligned}
 & 4h(\eta \partial_x \Delta u + \partial_x u(d_{xu} \partial_x \Delta u + d_{yu} \partial_y \Delta u + d_{yv} \partial_y \Delta v + d_{xv} \partial_x \Delta v)) \partial_x N_i \\
 & + 2h(\eta \partial_y \Delta v + \partial_y v(d_{xu} \partial_x \Delta u + d_{yu} \partial_y \Delta u + d_{yv} \partial_y \Delta v + d_{xv} \partial_x \Delta v)) \partial_x N_i \\
 & + h(\eta \partial_x \Delta v + \partial_x v(d_{xu} \partial_x \Delta u + d_{yu} \partial_y \Delta u + d_{yv} \partial_y \Delta v + d_{xv} \partial_x \Delta v)) \partial_y N_i \\
 & + h(\eta \partial_y \Delta u + \partial_y u(d_{xu} \partial_x \Delta u + d_{yu} \partial_y \Delta u + d_{yv} \partial_y \Delta v + d_{xv} \partial_x \Delta v)) \partial_y N_i \\
 & + (\beta^2 \Delta u + u(d_u \beta^2 \Delta u + d_v \beta^2 \Delta v)) N_i \\
 & = +\frac{1}{2} \varrho g \cos \alpha \partial_x h^2 \partial_x N_i - \rho gh(\partial_x s' \cos \alpha - \sin \alpha) N_i - 4h\eta(\partial_x u + 2\partial_y v) \partial_x N_i - h\eta(\partial_x v + \partial_y u) \partial_y N_i - \beta^2 u N_i
 \end{aligned}$$

We have $\Delta u = N_j \Delta u_j$ and $\Delta v = N_j \delta v_j$

$$\left(\begin{array}{cc} K_{11} & K_{12} \\ K_{21} & K_{22} \end{array} \right) \left(\begin{array}{c} \Delta u_j \\ \Delta v_j \end{array} \right)$$

$$\begin{aligned}
 [K_{12}]_{ij} &= h\eta \partial_x N_j \partial_y N_i \\
 &+ 4h\partial_x u d_{yv} \partial_y N_j \partial_x N_i + 4h\partial_x u d_{xv} \partial_x N_j \partial_x N_i \\
 &+ 2h\partial_y v d_{yv} \partial_y N_j \partial_x N_i + 2h\partial_y v d_{xv} \partial_x N_j \partial_x N_i \\
 &+ h\partial_x v d_{yv} \partial_y N_j \partial_y N_j + h\partial_x v d_{xv} \partial_x N_j \partial_y N_i \\
 &+ h\partial_y u d_{yv} \partial_y N_j \partial_y N_i + h\partial_y u d_{xv} \partial_x N_j \partial_y N_i \\
 &= h\eta \partial_x N_j \partial_y N_i \\
 &+ (4h\partial_x u d_{xv} + 2h\partial_y v d_{xv}) \partial_x N_j \partial_x N_i \\
 &+ (h\partial_x v d_{yv} + h\partial_y u d_{yv}) \partial_y N_j \partial_y N_i \\
 &+ (h\partial_x v d_{xv} + h\partial_y u d_{xv}) \partial_x N_j \partial_y N_i \\
 &+ (4h\partial_x u d_{yv} + 2h\partial_y v d_{yv}) \partial_y N_j \partial_x N_i \\
 &= h\eta \partial_x N_j \partial_y N_i \\
 &+ 2Eh(2\dot{\epsilon}_{xx} + \dot{\epsilon}_{yy}) \dot{\epsilon}_{xy} \partial_x N_j \partial_x N_i \\
 &+ Eh2\dot{\epsilon}_{xy}(2\dot{\epsilon}_{yy} + \dot{\epsilon}_{xx}) \partial_y N_j \partial_y N_i \\
 &+ Eh2\dot{\epsilon}_{xy}\dot{\epsilon}_{xy} \partial_x N_j \partial_y N_i \\
 &+ 2Eh(2\dot{\epsilon}_{xx} + \dot{\epsilon}_{yy})(2\dot{\epsilon}_{yy} + \dot{\epsilon}_{xx}) \partial_y N_j \partial_x N_i
 \end{aligned}$$

If we swap u and v and x and y and then i and j (transpose) we get the same matrix, hence

$$K_{12} = K'_{21}$$

$$\begin{aligned}
[K_{11}]_{ij} &= 4h(\eta \partial_x N_j + \partial_x u(d_{xu} \partial_x N_j + d_{yu} \partial_y N_j)) \partial_x N_i \\
&\quad + 2h \partial_y v(d_{xu} \partial_x N_j + d_{yu} \partial_y N_j) \partial_x N_i \\
&\quad + h(\partial_x v(d_{xu} \partial_x N_j + d_{yu} \partial_y N_j)) \partial_y N_i \\
&\quad + h(\eta \partial_y N_j + \partial_y u(d_{xu} \partial_x N_j + d_{yu} \partial_y N_j)) \partial_y N_i \\
&= h(4\eta + (4\partial_x u + 2\partial_y v)d_{xu}) \partial_x N_j \partial_x N_i \\
&\quad + h(\eta + (\partial_y u + \partial_x v)d_{yu}) \partial_y N_j \partial_y N_i \\
&\quad + h(4\partial_x u + 2\partial_y v)d_{yu} \partial_y N_j \partial_x N_i \\
&\quad + h(\partial_x v + \partial_y u)d_{xu} \partial_x N_j \partial_y N_i \\
&= h(4\eta + E2(2\dot{\epsilon}_{xx} + \dot{\epsilon}_{yy})(2\dot{\epsilon}_{xx} + \dot{\epsilon}_{yy})) \partial_x N_j \partial_x N_i \\
&\quad + h(\eta + 2E\dot{\epsilon}_{xy}\dot{\epsilon}_{xy}) \partial_y N_j \partial_y N_i \\
&\quad + Eh2(2\dot{\epsilon}_{xx} + \dot{\epsilon}_{yy})\dot{\epsilon}_{xy} \partial_y N_j \partial_x N_i \\
&\quad + Eh2\dot{\epsilon}_{xy}(2\dot{\epsilon}_{xx} + \dot{\epsilon}_{yy}) \partial_x N_j \partial_y N_i \\
&= 4h\eta \partial_x N_j \partial_x N_i + h\eta \partial_y N_j \partial_y N_i \\
&\quad + 2hE(2\dot{\epsilon}_{xx} + \dot{\epsilon}_{yy})^2 \partial_x N_j \partial_x N_i \\
&\quad + 2Eh\dot{\epsilon}_{xy}^2 \partial_y N_j \partial_y N_i \\
&\quad + 2Eh(2\dot{\epsilon}_{xx} + \dot{\epsilon}_{yy})\dot{\epsilon}_{xy}(\partial_y N_j \partial_x N_i + \partial_x N_j \partial_y N_i)
\end{aligned}$$

so K_{11} and K_{22} are symmetrical.

One might expect that the $ud_u\beta^2 \Delta v$ makes the matrix unsymmetrical, but in fact

$$u d_v \beta^2 = u(1/m - 1)C^{-1/m} \|\mathbf{v}\|^{(1-3m)/m} v = v(1/m - 1)C^{-1/m} \|\mathbf{v}\|^{(1-3m)/m} u = v d_u \beta^2$$

so the contributions to 12 and 21 are equal, and hence this term does not give rise to an unsymmetrical matrix.

The tangent matrix K is symmetrical for non-linear flow including both the non-linear effects of β^2 and η .

Note: In 1D I get

$$\begin{aligned}
&4h(D\eta \partial_x u + \eta \partial_x \Delta u) \partial_x N_i + (D\beta^2 u + \beta^2 \Delta u) N_i \\
&= +\frac{1}{2} \rho g \cos \alpha \partial_x h^2 \partial_x N_i - \rho gh(\partial_x s' \cos \alpha - \sin \alpha) N_i - 4h\eta \partial_x u \partial_x \phi - \beta^2 u N
\end{aligned}$$

10.8 Weak form

x direction

$$\int_{\Omega} (\partial_x(4h\eta \partial_x u + 2h\eta \partial_y v) + \partial_y(h\eta(\partial_x v + \partial_y u)) - t_{bx} - \rho gh(\partial_x s \cos \alpha - \sin \alpha)) \phi \, dx \, dy = 0$$

with von Neumann BC on Γ_2

$$(4h\eta \partial_x u + 2h\eta \partial_y v)n_x + \eta h(\partial_x v + \partial_y u)n_y = \frac{1}{2} \rho gh(h - H)n_x$$

and

$$\eta h(\partial_x v + \partial_y u)n_x + (4\eta h \partial_y v + 2\eta h \partial_x u)n_y = \frac{1}{2} \rho gh(h - H)n_y$$

Green's theorem used to get rid of second derivatives gives

$$\begin{aligned}
&- \int_{\Omega} ((4h\eta \partial_x u + 2h\eta \partial_y v) \partial_x N + h\eta(\partial_x v + \partial_y u) \partial_y w) \, dx \, dy \\
&- \int_{\Omega} (t_{bx} + \rho gh(\partial_x s \cos \alpha - \sin \alpha)N) \, dx \, dy + \int_{\Gamma} ((4h\eta \partial_x u + 2h\eta \partial_y v)n_x + h\eta(\partial_x v + \partial_y u)n_y)N \, d\Gamma = 0
\end{aligned}$$

Using the BC we have

$$\begin{aligned} & - \int_{\Omega} ((4h\eta\partial_x u + 2h\eta\partial_y v)\partial_x N + h\eta(\partial_x v + \partial_y u)\partial_y w) dx dy \\ & - \int_{\Omega} (t_{bx} + \rho gh(\partial_x s \cos \alpha - \sin \alpha))N dx dy + \int_{\Gamma_2} \frac{1}{2}g\rho(1 - \rho/\rho_o)h^2 n_x N d\Gamma = 0 \end{aligned}$$

y direction

$$\int_{\Omega} \partial_y ((4h\eta\partial_y v + 2h\eta\partial_x u) + \partial_x(h\eta(\partial_y u + \partial_x v))) - t_{by} - \rho gh\partial_y s \cos \alpha)N dx dy$$

Green's

$$\begin{aligned} & - \int_{\Omega} ((4h\eta\partial_y v + 2h\eta\partial_x u)\partial_y N + h\eta(\partial_y u + \partial_x v)\partial_x w) dx dy \\ & - \int_{\Omega} (t_{by} + \rho gh\partial_y s \cos \alpha)N dx dy \\ & + \int_{\Gamma} ((4h\eta\partial_y v + 2h\eta\partial_x u)n_y + \eta h(\partial_y u + \partial_x v)n_x)N d\Gamma \end{aligned} \quad (10.39)$$

the von Neumann BC is

$$\eta h(\partial_x v + \partial_y u)n_x + (4h\eta\partial_y v + 2h\eta\partial_x u)n_y = \frac{1}{2}\rho gh(h - H)n_y$$

hence

$$\begin{aligned} & - \int_{\Omega} ((4h\eta\partial_y v + 2h\eta\partial_x u)\partial_y N + h\eta(\partial_y u + \partial_x v)\partial_x N) dx dy \\ & - \int_{\Omega} (t_{by} + \rho gh\partial_y s \cos \alpha)N dx dy + \int_{\Gamma_2} \frac{1}{2}g\rho(1 - \rho/\rho_o)h^2 n_y w d\Gamma = 0 \end{aligned}$$

Ice shelf

$$\int_{\Omega} (\partial_x(4h\eta\partial_x u + 2h\eta\partial_y v) + \partial_y(h\eta(\partial_x v + \partial_y u)) - t_{bx} - \frac{1}{2}\rho(1 - \rho/\rho_o)g\partial_x h^2 N) dx dy = 0$$

On Γ_2 we write the von Neumann BC as

$$(4\eta h\partial_x u + 2\eta h\partial_y v)n_x + \eta h(\partial_x v + \partial_y u)n_y = \frac{1}{2}\rho(1 - \rho/\rho_o)gh^2 n_x$$

and

$$\eta(\partial_x v + \partial_y u)n_x + (4\eta\partial_y v + 2\eta\partial_x u)n_y = \frac{1}{2}\rho(1 - \rho/\rho_o)gh^2 n_y$$

we consider the term

$$\int_{\Omega} (\partial_x(4h\eta\partial_x u + 2h\eta\partial_y v) + \partial_y(h\eta(\partial_x v + \partial_y u)) - \frac{1}{2}\rho(1 - \rho/\rho_o)g\partial_x h^2)N dx dy = \quad (10.40)$$

$$- \int_{\Omega} (4h\eta\partial_x u + 2h\eta\partial_y v + h\eta(\partial_x v + \partial_y u) - \frac{1}{2}\rho(1 - \rho/\rho_o)gh^2)\partial_x N dx dy \quad (10.41)$$

$$+ \int_{\Gamma} ((4h\eta\partial_x u + 2h\eta\partial_y v)n_x + h\eta(\partial_x v + \partial_y u)n_y - \frac{1}{2}\rho(1 - \rho/\rho_o)gh^2 n_x)N d\Gamma \quad (10.42)$$

Along Γ_2 , the path integral disappears and along Γ_1 we set $w^* = 0$, hence

$$- \int_{\Omega} (4h\eta\partial_x u + 2h\eta\partial_y v + h\eta(\partial_x v + \partial_y u) - \frac{1}{2}\rho(1 - \rho/\rho_o)gh^2)\partial_x w - t_{bx}N dx dy = 0 \quad (10.43)$$

10.9 Thoughts about ice shelf von Neumann BC

10.9.1 1d case

Field equation:

$$4\partial_x(\eta h \partial_x u) - t_x - \rho g h \partial_x s \cos \alpha + \rho g h \sin \alpha = 0$$

Boundary condition

$$4\eta \partial_x u = \frac{1}{2} \rho g (1 - \rho/\rho_o) h \quad (10.44)$$

which for $\eta = \frac{1}{2} A^{-1/n} |\partial_x u|^{(1-n)/n}$ can also be written as

$$\partial_x u = A(\rho g f/4)^n$$

where $f = (1 - \rho/\rho_o)h(x_c)$, and x_c is the location of the calving front. We write the field equation as

$$4\partial_x(\eta h \partial_x u) - \beta^2 u - \rho g h \partial_x(s' + (1 - \rho/\rho_o)h) \cos \alpha + \rho g h \sin \alpha = 0$$

with

$$s' := f - (1 - \rho/\rho_o)h = s - S - (1 - \rho/\rho_o)h$$

or as

$$4\partial_x(\eta h \partial_x u) - \frac{1}{2} g \cos \alpha \rho (1 - \rho/\rho_o) \partial_x h^2 - \rho g h \cos \alpha \partial_x s' - \beta^2 u + \rho g h \sin \alpha = 0,$$

using $\partial_x S = 0$. Here S is the elevation of sea level (usually the coordinate system would be defined so that $S = 0$), and s the surface elevation of the upper ice surface.

When deriving the weak form we do integration by terms on the first two terms

$$\begin{aligned} & \int (4\partial_x(\eta h \partial_x u) - \frac{1}{2} g \cos \alpha \rho (1 - \rho/\rho_o) \partial_x h^2 - \rho g h \cos \alpha \partial_x s' - t_x + \rho g h \sin \alpha) N \, dx \\ &= (4\eta h \partial_x u - \frac{1}{2} g \cos \alpha \rho (1 - \rho/\rho_o) h^2) N \Big|_{x_1}^{x_2} \\ & - \int (4\eta h \partial_x u - \frac{1}{2} g \cos \alpha \rho (1 - \rho/\rho_o) h^2) \partial_x N \, dx \\ & - \int (\rho g \cos \alpha h \partial_x s' + t_x - \rho g h \sin \alpha) N \, dx \end{aligned}$$

The neat thing about this formulation is that for the usual BC at the ice-shelf edge, the ‘boundary integral term’ is zero.

The quantity s' is the difference between the actual surface altitude above sea level, and the surface altitude above sea level if floating. On a floating ice shelf s' is equal to zero everywhere.

If all von Neumann boundary conditions are of the type (10.44) we only have to solve

$$\int ((-4\eta h \partial_x u + \frac{1}{2} g \cos \alpha \rho (1 - \rho/\rho_o) h^2) \partial_x w - (\rho g \cos \alpha h \partial_x s' + t_x - \rho g h \sin \alpha) N) \, dx = 0$$

with

$$s' = s - S - (1 - \rho/\rho_o)h$$

or

$$-\int 4\eta h \partial_x u \partial_x N \, dx - \int t_x N \, dx = \rho g \cos \alpha \int h \partial_x s' N \, dx - \frac{1}{2} \rho g \cos \alpha (1 - \rho/\rho_o) \int h^2 \partial_x N \, dx - \rho g \sin \alpha \int h N \, dx$$

10.10 Tracer equation with cross-wind diffusion

$$\partial_t h + \nabla \cdot (\mathbf{v} h) - \nabla \cdot (\boldsymbol{\kappa} \nabla h) = a$$

with

$$\boldsymbol{\kappa} = \epsilon (\mathbf{1} - \hat{\mathbf{n}} \otimes \hat{\mathbf{n}})$$

$$\begin{aligned}
\langle \nabla \cdot (\mathbf{v}h), \phi_q \rangle &= \langle \partial_x(uh) + \partial_y(vh), \phi_q \rangle \\
&= \langle h(\partial_x u + \partial_y v) + u \partial_x h + v \partial_y h, \phi_q \rangle \\
&= \langle \phi_p(\partial_x u + \partial_y v) + u \partial_x \phi_p + v \partial_y \phi_p, \phi_q \rangle h_p
\end{aligned}$$

$$\begin{aligned}
\langle \boldsymbol{\kappa} \nabla h, \nabla \phi_q \rangle &= \langle \epsilon (\mathbf{1} - \hat{\mathbf{n}} \otimes \hat{\mathbf{n}}) \nabla h, \nabla \phi_q \rangle \\
&= \langle \epsilon \mathbf{1} \nabla h, \nabla \phi_q \rangle - \langle \epsilon (\hat{\mathbf{n}} \otimes \hat{\mathbf{n}}) \nabla h, \nabla \phi_q \rangle \\
&= \epsilon h_p \langle \nabla \phi_p, \nabla \phi_q \rangle - \epsilon \langle (\hat{\mathbf{n}} \cdot \nabla h) \hat{\mathbf{n}}, \nabla \phi_q \rangle \\
&= \epsilon h_p (\partial_x \phi_p \partial_x \phi_q + \partial_y \phi_p \partial_y \phi_q) - \epsilon \langle (\hat{\mathbf{n}} \cdot h_p \nabla \phi_p) \hat{\mathbf{n}}, \nabla \phi_q \rangle \\
&= \epsilon h_p (\partial_x \phi_p \partial_x \phi_q + \partial_y \phi_p \partial_y \phi_q) - \epsilon \langle (n_x \partial_x \phi_p + n_y \partial_y \phi_p) h_p \hat{\mathbf{n}}, \nabla \phi_q \rangle \\
&= \epsilon h_p (\partial_x \phi_p \partial_x \phi_q + \partial_y \phi_p \partial_y \phi_q) - \epsilon (n_x \partial_x \phi_p + n_y \partial_y \phi_p) h_p (n_x \partial_x \phi_q + n_y \partial_y \phi_q) \\
&= \epsilon h_p ((\partial_x \phi_p \partial_x \phi_q + \partial_y \phi_p \partial_y \phi_q) - (n_x \partial_x \phi_p + n_y \partial_y \phi_p) (n_x \partial_x \phi_q + n_y \partial_y \phi_q))
\end{aligned}$$

and

$$\begin{aligned}
\epsilon &= \epsilon_i \phi_i \\
n_x &= n_{xi} \phi_i \\
n_y &= n_{yi} \phi_i
\end{aligned}$$

After assembly the system can be written on the form

$$\mathbf{K}\mathbf{h} = \mathbf{b}$$

Test case in cylindrical coordinates

$$\begin{aligned}
\frac{1}{r} \partial_r(r h v_r) &= a \\
r h v_r &= \int_0^r a r' dr'
\end{aligned}$$

Part II

Some aspects of glacier mechanics,
possibly of interest to *Ua* users, but not
specifically related to *Ua*

Here I've put some rather random bits related to glacier mechanics. The selection is based both on what many \tilde{U} a users might find useful, but also reflects somewhat the topics I've covered in previous lectures that I've given on glacier mechanics, especially lectures given at Caltech in 2014.

Chapter 11

An ice shelf in one horizontal dimension (1HD).

We consider an ice shelf in one horizontal dimension (1HD) under plain-strain conditions

$$\dot{\epsilon}_{yy} = 0,$$

and in addition we assume $v = 0$, and that all other transverse gradients to be zero as well. This ice shelf is laterally confined, i.e. it can not spread out in y direction, but there is no friction along the sides. It is free to deform in x direction only.

The vertical stress is, as always in the SSA approximation, given by

$$\sigma_{zz} = -\rho g(s - z), \quad (11.1)$$

where s is the upper surface. The traction at the lower surface, where $z = b$, must equal the ocean pressure giving

$$\rho(s - b) = \rho_o(S - b),$$

from which various other floating relationships follow:

$$h = \rho_o d / \rho = \frac{s - S}{1 - \rho / \rho_o} = \frac{\rho_o}{\rho}(S - b), \quad (11.2)$$

$$b = \frac{\rho s - \rho_o S}{\rho - \rho_o} = S - \frac{\rho}{\rho_o} h, \quad (11.3)$$

$$s = S + (1 - \rho / \rho_o)h = (1 - \rho_o / \rho)b + \frac{\rho_o}{\rho}S, \quad (11.4)$$

$$f = (1 - \rho / \rho_o)h. \quad (11.5)$$

Note that we write $d = S - b$ for the ice shelf draft, $f = S - s$ for the freeboard, and $h = s - b$ and $H = S - B$.

The SSTREAM/SSA equation to be solved is in this case simply

$$4\partial_x(h\eta\partial_x u) = \rho g(1 - \rho / \rho_o)h\partial_x h, \quad (11.6)$$

where the effective viscosity η is given by

$$\eta = \frac{1}{2}A^{-1/n}|\partial_x u|^{(1-n)/n}.$$

Eq. (11.6) is the vertically integrated form of the momentum equation in x direction, and reflects the equilibrium of vertically integrated forces in the horizontal direction. The equation can also be written in terms of the horizontal deviatoric stress τ_{xx} as

$$2\partial_x(h\tau_{xx}) = \rho g(1 - \rho / \rho_o)h\partial_x h, \quad (11.7)$$

or as

$$\partial_x(h\tau_{xx}) = \frac{1}{4}g\varrho\partial_x h^2, \quad (11.8)$$

where

$$\varrho = \rho(1 - \rho/\rho_o).$$

If ϱ is independent of x (an assumption that has already been made in the derivation of Eq. 11.6) then we can integrate (11.8) on both sides, and we find that

$$h\tau_{xx} = \frac{1}{4}g\varrho h^2 + K, \quad (11.9)$$

where K is independent of x .

Note that the freeboard $f = s - S$ is equal to

$$f = (1 - \rho/\rho_o)h, \quad (11.5)$$

so we can also write (11.9) as,

$$h\tau_{xx} = \frac{1}{4}g\rho h f + K. \quad (11.10)$$

The integration constant K follows from the boundary conditions, and we will show below that $K = 0$.

Eq. (11.10) shows that the horizontal deviatoric stresses are directly proportional to the freeboard. In some ways $g\rho f/4$ is the ‘driving stress’ that drives the deformation of the ice shelf, and it plays a similar role to the driving stress $\rho gh\partial_x s$ in the SIA.

Knowing τ_{xx} and σ_{zz} , we can now determine the pressure p from

$$p = \tau_{zz} - \sigma_{zz} = -\tau_{xx} - \sigma_{zz}, \quad (11.11)$$

using the incompressibility condition $\dot{\epsilon}_{xx} + \dot{\epsilon}_{zz} = 0$ and the flow law. The horizontal stress σ_{xx} is then

$$\sigma_{xx} = \tau_{xx} - p = \tau_{xx} - (-\tau_{xx} - \sigma_{zz}) = 2\tau_{xx} + \sigma_{zz}, \quad (11.12)$$

Once we have determined all stresses, we can determine the deformation using the Glen-Steinemann flow law

$$\dot{\epsilon}_{ij} = A\tau^{n-1}\tau_{ij}, \quad (11.13)$$

where A and n are some rheological parameters, and τ is the second invariant of the deviatoric stress tensor given by

$$\tau = (\tau_{pq}\tau_{pq}/2)^{1/2}. \quad (11.14)$$

11.1 Boundary condition at the calving front

Across the (vertical) interface between ice and ocean the traction must be continuous, i.e.

$$(\sigma_{\text{ice shelf}} - \sigma_{\text{ocean}})\hat{n} = 0,$$

where \hat{n} is a unit normal vector pointing horizontally outwards from the calving front. The position of the calving front is given by $x = x_c$.

We ignore bending forces at the calving front and only require continuity of integrated values. Hence we require

$$\underbrace{\int_b^s \sigma_{xx} dz}_{\text{ice shelf}} = \underbrace{\int_b^S \sigma_{xx} dx}_{\text{ocean}} \quad (11.15)$$

The vertically integrated force of the ocean on the ice at $x = x_c$ is given by the integral

$$\underbrace{\int_b^s \sigma_{xx} dx}_{\text{ocean}} = - \int_b^S \rho_o g(S - z) dz = -\frac{1}{2}\rho_o g(S - b)^2, \quad (11.16)$$

where S is the ocean surface.

This integrated force must equal the vertical integrated horizontal stress within the ice shelf along the calving front given by the integral

$$\int_b^s \sigma_{xx} dz,$$

at $x = x_c$. We know σ_{zz} within the ice shelf from Eq. (11.1). Using Eq. (11.12) to express σ_{xx} in terms of σ_{zz} and σ_{xx} , we find

$$\begin{aligned} \underbrace{\int_b^s \sigma_{xx} dz}_{\text{ice shelf}} &= \int_b^s (2\tau_{xx} + \sigma_{zz}) dz \\ &= 2h\tau_{xx} + \rho g \int_b^s (z - s) dz \\ &= 2h\tau_{xx} + \rho g ((s^2 - b^2)/2 - s(s - b)) \\ &= 2h\tau_{xx} - \frac{1}{2}\rho gh^2, \end{aligned} \quad (11.17)$$

where we have made use of the fact that τ_{xx} is independent of z . Hence, equality of vertical integrated horizontal stresses at the calving front requires

$$2h\tau_{xx} - \frac{1}{2}\rho gh^2 = -\frac{1}{2}\rho_o g(S - b)^2, \quad (11.18)$$

Using Eq. (11.18) together with the floating condition (11.2) we find

$$\begin{aligned} 2h\tau_{xx} &= \frac{1}{2}\rho gh^2 - \frac{1}{2}\rho_o g(S - b)^2 \\ &= \frac{1}{2}\rho gh^2 - \frac{1}{2}\rho_o g h(S - b) \frac{\rho}{\rho_o} \\ &= \frac{1}{2}\rho gh(h - S + b) \\ &= \frac{1}{2}\rho gh(s - S) \end{aligned}$$

or

$$h\tau_{xx} = \frac{1}{4}\rho ghf, \quad (11.19)$$

at the calving front where $x = x_c$

Comparing the above boundary condition, valid at the calving front, with expression (11.9), valid anywhere within the ice shelf, we find that integration constant K in Eq. (11.9) is equal to zero, and therefore

$$\tau_{xx} = \frac{1}{4}\rho gf,$$

everywhere.

Note that the (horizontal) boundary condition (11.19) is now identical to the expression for horizontal deviatoric stresses valid everywhere within the ice shelf. Physically this implies that at any given location within the ice shelf, the stresses are identical to stresses imposed by the calving-front boundary condition at that location. In other words, if we were to cut off the ice shelf at any given location, thereby forming a new calving front, the stresses at that newly formed calving front will not be affected. In this respect, the ice shelf downstream of a given point is ‘passive’ and does not affect the flow in upstream direction. In particular, the stresses in the ice shelf downstream from the grounding line do not affect the stresses in the ice shelf at the grounding line.

11.2 The SSA as an expression of horizontal force balance.

Inserting the Glen-Steinemann flow law directly into the boundary condition (11.19) gives

$$A^{-1/n} |\partial_x u|^{(1-n)/n} \partial_x u = \frac{1}{4}\rho gf$$

Since $(s - S) \geq 0$, both τ_{xx} and $\partial_x u$ are positive, and Eq. (11.19) can be written on the form

$$\dot{\epsilon}_{xx} = \partial_x u = A(\rho gf/4)^n, \quad (11.20)$$

at $x = x_c$. Further versions of Eq. (11.19) are

$$2A^{-1/n} h |\partial_x u|^{(1-n)/n} \partial_x u = \frac{1}{2}\rho g(1 - \rho/\rho_o)h^2 \quad (11.21)$$

and

$$8\eta h \partial_x u - \rho g(1 - \rho/\rho_o)h^2 = 0, \quad (11.22)$$

at $x = x_c$.

Note that if we differentiate Eq. (11.22) with respect to x , we find

$$4\partial_x(\eta h \partial_x u) = \rho g(1 - \rho/\rho_o)h \partial_x h. \quad (11.23)$$

which is formally identical to Eq. (11.6) valid for any x . We arrived at (11.23) by considering the vertical integrated force balance along the calving front using 1) the fact that the effective stress τ_{xx} is independent of z , and 2) that the vertical stress component σ_{zz} is equal to the weight of the ice (Eq. 11.1). By simply making these two assumptions, rather than deriving these facts through scaling analysis as we have done, we would have been able to derive Eq. (11.6) in a fairly simple manner.

11.3 Stresses and strains within a one-dimensional plane-strain ice shelf

We now know that

$$\tau_{xx} = \frac{1}{4}\rho g f, \quad (11.24)$$

everywhere within a 1HD ice shelf, where $f = s - S$ is the freeboard given by

$$f = (1 - \rho/\rho_o)h, \quad (11.5)$$

The only non-zero terms of the deviatoric stress tensor are τ_{xx} and τ_{zz} . From (11.14) we find that

$$\tau = |\tau_{xx}| = \frac{1}{4}\rho g f.$$

and using the Glen-Steinemann flow law that

$$\dot{\epsilon}_{xx} = \partial_x u = A(\rho g f / 4)^n, \quad (11.25)$$

or alternatively using (11.5)

$$\dot{\epsilon}_{xx} = \partial_x u = A(\varrho g h / 4)^n, \quad (11.26)$$

where

$$\varrho = \rho(1 - \rho/\rho_o). \quad (1.34)$$

The horizontal stress component can then be calculated as

$$\sigma_{xx} = 2\tau_{xx} + \sigma_{zz} = \frac{1}{2}\rho g f + (z - s)\rho g \quad (11.27)$$

where we have used Eq. (11.1). As can be seen σ_{xx} varies linearly with depth. Along the upper surface where $z = s$, $\sigma_{xx} = \rho g f / 2$ and is positive, and along the lower surface, where $z = b$, $\sigma_{xx} = -\rho(1 - \rho/\rho_o)gh / 2$, and is negative.

The pressure is given by

$$p = \tau_{zz} - \sigma_{zz} = -\frac{1}{4}\rho g f + (s - z)\rho g.$$

Note that the pressure is not hydrostatic.

We write the transverse stress component as

$$\sigma_{yy} = \tau_{yy} - p = \tau_{yy} + \sigma_{zz} - \tau_{zz}.$$

The plane strain conditions implies $\tau_{yy} = 0$ and incompressibility $\tau_{zz} = -\tau_{xx}$, hence

$$\sigma_{yy} = \sigma_{zz} + \tau_{xx} = (z - s)\rho g + \rho g f / 4.$$

11.4 Shear stress

The shear stress τ_{xz} is a first-order quantity (but its vertical derivative enters the equilibrium equations at zeroth order). From

$$\partial_x \sigma_{xx} + \partial_z \sigma_{xz} = 0.$$

we find

$$\partial_z \sigma_{xz} = -\partial_x \sigma_{xx} = \frac{1}{2} \rho g \partial_x s, \quad (11.28)$$

which shows that σ_{xz} also varies linearly with depth and that

$$\tau_{xz} = \frac{1}{2} \rho g \partial_x s z + K, \quad (11.29)$$

where K is an integration constant.

The boundary condition at the upper surface ($z = s$) is

$$\tau_{xz}(z = s) = \sigma_{xx}(z = s) \partial_x s$$

giving

$$\tau_{xz}(z = s) = \frac{1}{2} \rho g s \partial_x s. \quad (11.30)$$

using (11.27). Similarly the boundary condition at $z = b$ gives,

$$\begin{aligned} \tau_{xz}(z = b) &= \rho g h \partial_x b + \sigma_{xx}(z = b) \partial_x b, \\ &= \rho g h \partial_x b + \frac{1}{2} \rho g f \partial_x b - \rho g h \partial_x b, \\ &= \frac{1}{2} \rho g f \partial_x b. \end{aligned} \quad (11.31)$$

From Eq. (11.30) we find can now determine K in (11.29) and find

$$\tau_{xz} = \frac{1}{2} \rho g \partial_x s (z - S). \quad (11.32)$$

It remains to be seen if this expression is consistent with the other boundary condition (11.31) at the lower surface. Inserting $z = b$ into (11.32) gives

$$\tau_{xz} = \frac{1}{2} \rho g \partial_x s (b - S). \quad (11.33)$$

Using the floating condition one can show that

$$\partial_x s (b - S) = \partial_x b (s - S),$$

and therefore that (11.32) fulfils the lower boundary condition also.

From (11.32) we see that σ_{xz}/τ_{zz} is $O(\delta)$ as expected. In contrast to the other stress terms listed above, the shear stress τ_{xz} is a first-order quantity.

Summarising, the stress tensor in an ice shelf where all transverse gradients are zero ($\partial/\partial y = 0$) and $S = 0$, is given by

$$\boldsymbol{\sigma} = -\rho g \begin{pmatrix} s/2 - z & 0 & -\frac{1}{2} z \partial_x s \\ 0 & 3s/4 - z & 0 \\ -\frac{1}{2} z \partial_x s & 0 & s - z \end{pmatrix}, \quad (11.34)$$

and the pressure by

$$p = \rho g (3s/4 - z),$$

and deviatoric stress tensor

$$\boldsymbol{\tau} = \boldsymbol{\sigma} + \mathbf{1} p,$$

is

$$\boldsymbol{\tau} = \rho g \begin{pmatrix} s/4 & 0 & \frac{1}{2} z \partial_x s \\ 0 & 0 & 0 \\ \frac{1}{2} z \partial_x s & 0 & -s/4 \end{pmatrix}. \quad (11.35)$$

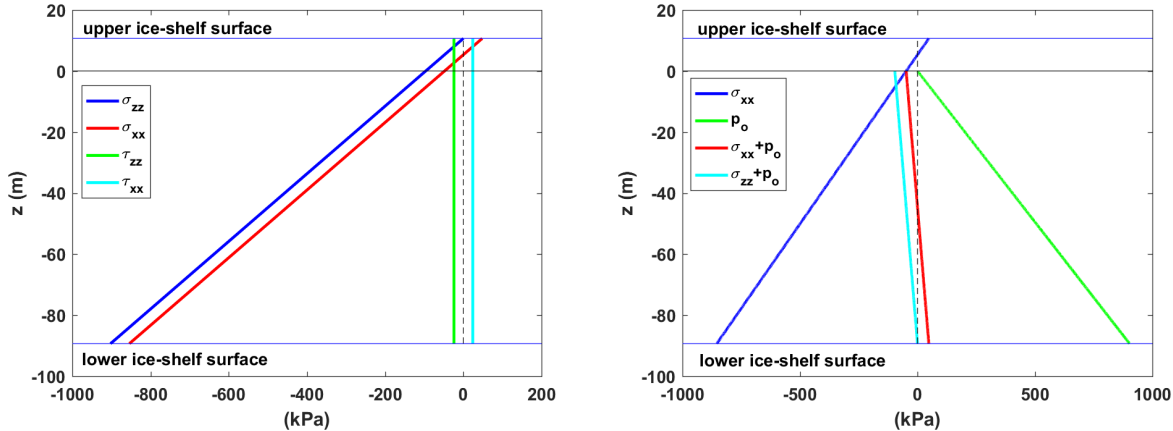


Figure 11.1: Left: Stresses within a one-dimensional ice shelf. Horizontal Cauchy stresses are positive at the surface and negative below $z = d/2$ where d is the ice shelf draft. Horizontal and vertical deviatoric stresses are independent of depth, and horizontal deviatoric stresses positive while vertical deviatoric stresses are negative. Parameters: $\rho = 910 \text{ kg m}^{-3}$, $\rho_o = 1030 \text{ kg m}^{-3}$, $h = 100 \text{ m}$.

Note that the sign of the horizontal stress components (σ_{xx} and σ_{yy}) changes with depth. At the surface ($z = s$) horizontal stresses are positive, at the base ($z = b$) they are negative. The longitudinal horizontal stresses (σ_{xx}) are only positive (extensional stresses) for $z > s/2$ (see Fig. 11.1).

The stresses in the shelf given by Eq. (11.34) are valid everywhere within the ice shelf, in particular the stresses in the ice shelf at the grounding line are also given by Eq. (11.34). As is evident from Eq. (11.34) the stresses, and therefore also the strain rates, are at each location functions of local surface slope and local ice thickness only.

Note that it has here been assumed that $S = 0$, in which case $s = f$, so one could replace s with the freeboard (f) in the above expressions for the stresses.

The ocean pressure, p_o is

$$p_o = \rho_o(S - z)$$

for $z < S$, and therefore

$$\sigma_{xx} + p_o = \rho g(s/2 - z) + \rho_o z$$

for $S = 0$. For $z = -\frac{1}{2} \frac{\rho}{\rho_o} h$ the sum of horizontal stresses and ocean pressure is zero (Fig. 11.1).

11.5 Steady-state geometry of a 1HD plane-strain ice shelf

We will now derive an analytical expressions for steady-state geometry and the velocity of a 1HD plane-strain ice shelf. The surface mass-balance is assumed to be constant. This surface mass balance (a) can be thought of as the sum of the mass fluxes along the upper (a_s) and the lower surface (a_b), i.e. $a = a_s + a_b$.

From Eq. (11.26) we have

$$\partial_x u = A(\varrho g h / 4)^n. \quad (11.36)$$

In a steady state, mass continuity requires

$$\partial_x(uh) = a, \quad (11.37)$$

where we have used that the ice flux q is $q = uh$. Assuming constant accumulation rate we can integrate Eq. (11.37) giving

$$u(x)h(x) - q_{gl} = a(x - x_{gl}) \quad (11.38)$$

where x_{gl} is the grounding line position, and $q_{gl} = q(x_{gl})$ is the flux at the grounding line. We define the origin of the x coordinates so that $x_{gl} = 0$.

We also have from Eq. (11.37)

$$h \partial_x u + u \partial_x h = a \quad (11.39)$$

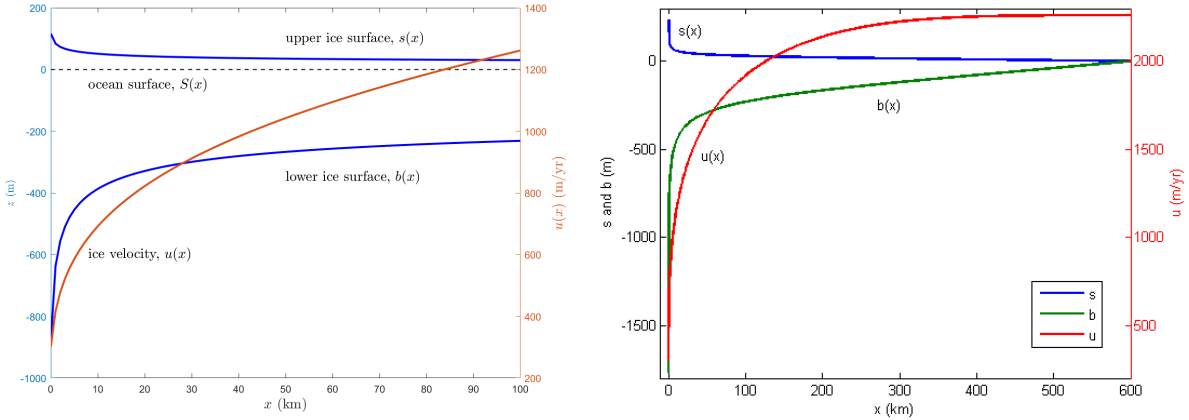


Figure 11.2: Analytical ice shelf profile. The left hand figure is for an accumulation of $a = 0.3 \text{ m a}^{-1}$, while the figure on the right was made for $a = -1 \text{ m a}^{-1}$. All other parameters are the same in both cases. Parameters: $A = 1.14 \times 10^{-8} \text{ kPa}^{-3} \text{ a}^{-1}$, $n = 3$, $h_{gl} = 2000 \text{ m}$, $u_{gl} = 300 \text{ m a}^{-1}$, $\rho = 910 \text{ kg m}^{-3}$, $\rho_o = 1030 \text{ kg m}^{-3}$. The value for A corresponds to an ice temperature of about -10 degrees Celsius.

Replacing u in (11.39) using (11.38) and inserting (11.36) for $\partial_x u$, gives

$$Ah(\varrho gh/4)^n + ((ax + q_{gl})/h)\partial_x h = a, \quad (11.40)$$

which we write as

$$\gamma h^{n+2} + (ax + q_{gl})d_x h = ah, \quad (11.41)$$

with

$$\gamma = A(\varrho g/4)^n, \quad (11.42)$$

where

$$\varrho = \rho(1 - \rho/\rho_o). \quad (11.43)$$

Separating variables

$$\frac{dh}{ah - \gamma h^{n+2}} = \frac{dx}{ax + q_{gl}}, \quad (11.44)$$

integrating both sides and simplifying gives

$$h = \left(\frac{1}{a} \left(\gamma + \frac{K}{(q_{gl} + ax)^{n+1}} \right) \right)^{-1/(n+1)}, \quad (11.45)$$

where K is an integration constant.

We determine K by specifying the thickness at the grounding line, i.e.

$$h(x_{gl} = 0) = h_{gl},$$

and using $q_{gl} = h_{gl}u_{gl}$ which gives

$$K = q_{gl}^{n+1}(a/h_{gl}^{n+1} - \gamma). \quad (11.46)$$

The solution is shown in Fig. 11.2. Possibly the most striking aspect of the solution is how quickly the thickness decreases downstream from the grounding line.

Now that the ice geometry has been determined, the ice velocity can be calculated directly from

$$u = (ax + q_{gl})/h.$$

or

$$u(x) = \left(\frac{K + \gamma(q_{gl} + ax)^{n+1}}{a} \right)^{1/(n+1)} \quad (11.47)$$

For $a > 0$, the ice shelf is infinitely long and approaches asymptotically the thickness $h(x \rightarrow +\infty) = (a/\gamma)^{1/(n+1)}$. For $a < 0$, the ice shelf has a finite length l given by $l = -q_{gl}/a$.

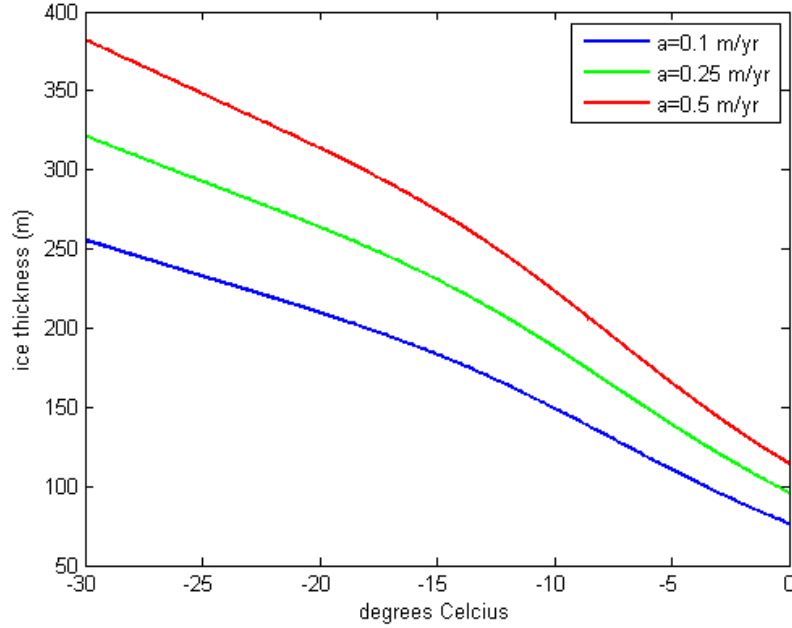


Figure 11.3: Steady-state ice shelf thickness as a function of englacial temperature and surface accumulation. Parameters: $n = 3$, $\rho = 910 \text{ kg m}^{-3}$, $\rho_o = 1030 \text{ kg m}^{-3}$.

The special case $a = 0$ is not covered by the above equations. One finds that for $a = 0$ the thickness distribution is given by

$$h = (h_{gl}^{-(n+1)} + \gamma(n+1)x/q_{gl})^{-1/(n+1)}. \quad (11.47)$$

The above solution describes an ice shelf, with a given ice thickness $h = h_{gl}$ at the grounding line, that spreads out in 1HD without any addition or removal of mass. In the limit $x \rightarrow +\infty$ the ice thickness is zero.

Note that in the above analysis we fixed the flux at the grounding line to q_{gl} . We then determined the ice geometry and velocities down-stream of the grounding line. We are here not in a position to calculate the flux at the grounding line for a given ice thickness (or as a function of any other aspects of the ice geometry that might affect the flux). For a given ice thickness $h = h_{gl}$, and a given ocean bathymetry ($B(x)$), we can however always determine possible positions of the grounding line from the floating condition $\rho h = \rho_o H$, where $H = S - B$ with S the ocean surface and B the ocean bed.

Also note that there are two further possible solutions to the differential equation (11.41). There is the (trivial) solution $h = 0$ and also the somewhat more interesting solution $h = (a/\gamma)^{1/(n+1)}$. For $a < 0$ this solution can be discarded (possible negative or complex valued thickness). However, if $a > 0$ this solution represents an ice shelf with a constant ice thickness that is regenerated through snow fall at the same rate that it spreads out. The ice thickness of such a steady-state ice shelf is shown in Fig. 11.3 as a function of temperature and surface mass balance.

Another interesting fact is that the ice shelf thickness can *increase* with distance downstream from the grounding line. This happens whenever

$$h_{gl} < (a/\gamma)^{1/(n+1)}.$$

This can be seen from an inspection of the solution shown above, or by writing

$$uh = ax + q_{gl},$$

differentiating and inserting Eq. (11.26), giving

$$u\partial_x h + hA(\rho gh/4)^n = a,$$

and then using $u = (ax + q_{gl})/h$ and solving for $\partial_x h$ to arrive at

$$\partial_x h = \frac{a - \gamma h^{n+1}}{(ax + q_{gl})/h},$$

showing that $\partial_x h$ is positive for $h < (a/\gamma)^{1/(n+1)}$.

11.6 Side-drag dominated ice shelf

We are here interested in the limiting case when all the driving stress is balanced by side drag alone, i.e. the term $\partial_x(h\tau_{xx})$ now dropped. This is the opposite limit to the one we considered above where $\partial_x(h\tau_{xx})$ was the dominating term and was $\partial_y(h\tau_{xy})$ was ignored.

The shallow-ice stream (SSTREAM/SSA/Shelfy) equations are

$$\partial_x(h(2\tau_{xx} + \tau_{yy})) + \partial_y(h\tau_{xy}) - t_{bx} = \rho gh\partial_x s \quad (11.48)$$

$$\partial_y(h(2\tau_{yy} + \tau_{xx})) + \partial_x(h\tau_{xy}) - t_{by} = \rho gh\partial_y s \quad (11.49)$$

Over the floating section $t_{bx} = t_{by} = 0$. We assume

$$\dot{\epsilon}_{yy} = \tau_{yy} = 0,$$

$$\partial_y \tau_{xx} = 0,$$

$$\partial_y s = \partial_y h = 0,$$

and ignore longitudinal stretching in the momentum balance, hence Eqs. (11.48) and (11.49) become

$$\partial_y(h\tau_{xy}) = \rho gh\partial_x h, \quad (11.50)$$

$$\partial_x(h\tau_{xy}) = 0. \quad (11.51)$$

We integrate (11.50) with respect to y from the centre-line $y = 0$ to the left-hand margin $y = w$, where the total width of the ice shelf is $2w$, i.e.

$$\tau_m = -\rho gw\partial_x h,$$

where we τ_m is a (positive) shear stress at the margin, i.e. $\tau_m = -\tau_{xy}(y = w)$, and we have used that $\tau_{xy}(y = 0) = 0$. We consider the plastic case when τ_m is a yield stress and independent of ice velocity. This simplification allows us to *calculate the ice thickness directly* as

$$h = h_c - \frac{\tau_m}{\rho gw}(x - x_c),$$

where h_c is the ice thickness at the calving front $x = x_c$. The ice thickness is now a linear function of distance x . For a given location, x_c , of the calving front, the grounding line will simply be located where the ice draft reaches the ocean floor. In this particular case the mass balance upstream of the grounding line has no impact on the position of the grounding line.

Eq. (11.51) remains correct if evaluated along the centre line where $\tau_{xy} = 0$. However, it is unclear if and how this equation can be consistent with the assumption of constant side shear stress and variable ice thickness. But if the ice behaves, as we assume, as a plastic material, then this poses no problem.

Similar to the case where a plastic formulation for basal sliding is used, the geometry is determined directly from the yield stress.¹ The steady-state velocity can then be calculated from the ice thickness distribution using

$$h\partial_x u + u\partial_x h = 0,$$

giving

$$(\lambda - (x - x_c)) \partial_x u - u = 0,$$

where

$$\lambda = \frac{\rho gwh_c}{\tau_m}.$$

The length scale λ is $\rho gh_c/\tau_m$ times the half-width, w , of the ice shelf. I'm guessing a reasonable estimate is $O(\rho gh_c/\tau_m) = 1$ so λ might be similar to the width.

¹For a plastic symmetrical ice sheet on a flat bed

$$\rho gh\partial_x h = \tau_b$$

where τ_b is here the basal yield stress and therefore $\partial_x h^2 = \frac{2\tau_b}{\rho g}$ and hence

$$h^2 = \frac{2\tau_b}{\rho g}|x - x_c|$$

Chapter 12

Simple 1d solutions for an ice-stream

12.1 Problem definition:

Uniform ice thickness h on a constant sloping bed with slope α . The calving front position is at $x = l$. The calving front can be either grounded or floating, and $0 \leq d < \rho h / \rho_o$.

$$4\partial_x(h\eta\partial_x u) - \beta^2 u = \rho gh\partial_x s$$

with

$$\begin{aligned}\eta &= \frac{1}{2} A^{-1/n} |\partial_x u|^{(1-n)/n} \\ \beta^2 &= C^{-1/m} \|u\|^{(1-m)/m}\end{aligned}$$

Boundary conditions:

$$u = C\rho gh\alpha \quad \text{at } x = 0 \tag{12.1}$$

$$\tau_{xx} = \frac{1}{4h} g(\rho h^2 - \rho_o d^2) \quad \text{at } x = l \tag{12.2}$$

Boundary condition (12.2) can also be written as

$$\partial_x u|_{x=l} = A \left(\frac{g(\rho h^2 - \rho_o d^2)}{4h} \right)^n$$

The non-linear case is

$$\frac{2hA^{-1/n}}{n} (\partial_x u)^{1/n-1} \partial_{xx}^2 u - C^{-1/m} u^{1/m} = -\rho gh\alpha$$

which I'm not sure if can be solved. However the linear case

$$\partial_{xx}^2 u - k^2 u = -\frac{A\tau}{2h},$$

has the general solution

$$u = c_1 e^{kx} + c_2 e^{-kx} + C\tau,$$

with

$$k^2 = \frac{A}{2hC},$$

and

$$\tau = \rho gh\alpha$$

BCs (12.1) and (12.2) give

$$\begin{aligned}c_1 + c_2 + C\tau &= C\tau \\ c_1 k e^{kl} - c_2 k e^{-kl} &= K\end{aligned}$$

where

$$K = A \frac{g(\rho h^2 - \rho_o d^2)}{4h}.$$

Hence

$$u = C\tau + \frac{K \sinh kx}{k \cosh kl}.$$

12.1.1 One dimensional uniformly inclined slab with periodic BCs

$$\begin{aligned} 4\partial_x(h\eta\partial_x u) - \beta^2 u &= \rho gh\partial_x s \\ u(0) &= u(l) \\ \partial_x u(0) &= \partial_x u(l) \end{aligned}$$

$$\begin{aligned} \eta &= \eta(x) \\ h &= \bar{h} \end{aligned}$$

$$\begin{aligned} 4h(\partial_x\eta\partial_x u + \eta\partial_{xx}^2 u) - \beta^2 u &= \rho gh\partial_x s \\ u_p &= \beta^{-2}\rho gh\partial_x s \quad (\text{particular solution}) \\ u_h &= C_1 e^{ikx} - C_1 e^{-ikx} \quad (\text{homogeneous solution}) \\ k &= \pm\sqrt{\frac{\beta^2}{\eta h}} \end{aligned}$$

For a periodic solution we find $C_1 = C_2 = 0$. So no dependency of the solution on η !

12.1.2 Two dimensional uniformly inclined slab with periodic BCs

$$\partial_x(4h\eta\partial_x u + 2h\eta\partial_y v) + \partial_y(h\eta(\partial_x v + \partial_y u)) - \beta^2 u = -\rho g \sin \alpha, \quad (1.21)$$

$$\partial_y(4h\eta\partial_y v + 2h\eta\partial_x u) + \partial_x(h\eta(\partial_y u + \partial_x v)) - \beta^2 v = 0. \quad (1.22)$$

$$\begin{aligned} u &= u_0(y) + \epsilon u_1(x, y) \\ v &= \epsilon v_1(x, y) \\ h &= \bar{h} \\ \eta &= \eta_0 + \epsilon \eta_1(x, y) \\ u(-W) &= u(+W) = 0 \\ \partial_y u &= 0 \quad \text{at} \quad y = 0 \\ \beta^2 &= \epsilon \beta_1^2 \end{aligned}$$

Zeroth-order:

$$h\eta_0\partial_{yy}^2 u_0 = -\rho gh \sin \alpha \quad (12.3)$$

$$v_0 = 0 \quad (12.4)$$

First order

$$\partial_x(4\epsilon\eta_0\partial_x u_1 + 2\epsilon\eta_0\partial_y v_1) + \partial_y((\epsilon\eta_0\partial_x v_1) + (\epsilon\eta_1\partial_y u_0 + \epsilon\eta_0\partial_y u_1)) - \epsilon\beta^2 u_1 = 0 \quad (12.5)$$

$$\partial_y(4\eta\partial_y v + 2\eta\partial_x u) + \partial_x(\eta(\partial_y u + \partial_x v)) - \beta^2 v = 0 \quad (12.6)$$

Chapter 13

Grounding-line dynamics

13.1 Ice-Shelf Buttressing

Ice-shelf buttressing is defined as the mechanical impact of the ice shelf on the stress at the grounding line beyond that provided by the ocean. If the vertically integrated horizontal stress state is unaffected by the ice shelf — i.e. if removing the ice shelf does not affect the state of stress at the grounding line — the ice-shelf provides no buttressing.

It is sometimes convenient to define a *buttressing parameter* θ as

$$\theta = \frac{N}{\frac{1}{2}\varrho gh}$$

where

$$N = \hat{\mathbf{n}}_{xy}^T \cdot (\mathbf{R} \hat{\mathbf{n}}_{xy}) \quad (13.1)$$

and

$$\varrho = \rho(1 - \rho/\rho_o), \quad (13.4)$$

and where $\hat{\mathbf{n}}_{xy}$ is a normal vector pointing horizontally outwards from the grounding line. Buttressing is the difference between the normal stress at the grounding line with and without an ice shelf.

In the particular case of a floating ice shelf, the field equations Eq. (1.27) can be written as

$$\nabla_{xy}^T \cdot (h \mathbf{R}) = \frac{1}{2} \nabla_{xy}^T (\varrho g \rho h^2),$$

Using the divergence theorem we find

$$\oint (\mathbf{R} \cdot \hat{\mathbf{n}}_{xy} - \frac{1}{2} \varrho g \rho h \hat{\mathbf{n}}_{xy}) d\Gamma = 0 \quad (13.2)$$

The integrand is identical to the (point wise) expression of the force balance (1.214) at the calving front of a freely floating ice shelf. We can split this path integral into a 1) section along the grounding line, 2) section along the margins, and 3) section along the calving front. If the margins do not contribute, the contribution along the grounding line is equal to that of the calving front. Hence, unbuttressed uniformly-wide ice shelves are passive and don't provide any buttressing.

From Eq. (13.2) it follows that $\theta = 1$ implies no ice-shelf buttressing. This can be taken a bit further by defining normal and tangential buttressing numbers, but the principle is the same.

13.2 Kinematic expression for GL migration

At the grounding line we have the flotation condition

$$\rho h_{gl} = \rho_o H_{gl},$$

that is

$$h_{gl} = h_f,$$

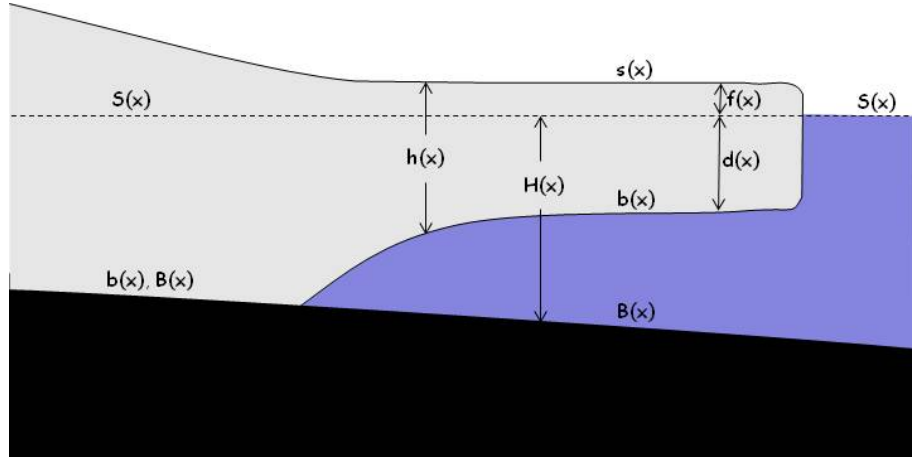


Figure 13.1: Geometrical variables: Glacier surface (s), glacier bed (b), ocean surface (S), ocean floor (B), glacier thickness ($h = s - b$)), ocean depth ($H = S - B$), glacier draft ($d = S - b$), glacier freeboard ($f = s - S$).

where the (maximum) flotation thickness h_f is

$$h_f := \frac{\rho_o}{\rho} H .$$

At any given time t , this condition must always be fulfilled at the grounding line. Note that $H = S - B$, and therefore h_f , are independent of time, whereas $h = s - b$ is a function of time and space, i.e.

$$\begin{aligned} h &= h(x, t) , \\ h_f &= h_f(x) . \end{aligned}$$

Imagine a situation where neither the bedrock, B , or the ocean surface S vary with time. The flotation ice thickness, h_f , is then independent of x , and the grounding line position is located where

$$h(x = x_{gl}, t) = h_f ,$$

is fulfilled.

If ice thickness now changes over the time interval Δt , the grounding line must migrate by a distance Δx_{gl} such that the flotation condition is again fulfilled, that is

$$\begin{aligned} h_f &= h(x = x_{gl} + \Delta x_{gl}, t + \Delta t) \\ &= h(x = x_{gl}, t) + \partial_x h \Delta x_{gl} + \partial_t h \Delta t + O^2 \end{aligned}$$

or

$$\partial_x h \Delta x_{gl} + \partial_t h \Delta t = 0$$

hence,

$$\dot{x}_{gl} = -\frac{\partial_t h}{\partial_x h} .$$

As expected, if ice thickness decreases with distance x , that is $\partial_x h < 0$, the grounding line will advance for $\partial_t h > 0$.

More generally, if we now allow h_f to be a function of x , we solve for the shift in the grounding line position, Δx_{gl} , following a change in the ice thickness profile over the time interval Δt , as follows

$$\begin{aligned} h_f(x = x_{gl}) &= h(x = x_{gl}, t = t_0) \\ h_f(x = x_{gl} + \Delta x_{gl}) &= h(x = x_{gl} + \Delta x_{gl}, t = t_0 + \Delta t) \end{aligned}$$

Taylor expansion gives

$$h_f + \partial_x h_f \Delta x_{gl} + O^2 = h + \partial_x h \Delta x_{gl} + \partial_t h \Delta t + O^2$$

evaluated at $x = x_{gl}$ and $t = t_0$. As as

$$h_f(x_{gl}) = h_f(x_{gl}, t_0),$$

we have

$$\partial_x h_f \Delta x_{gl} = \partial_x h \Delta x_{gl} + \partial_t h \Delta t$$

and therefore arrive at

$$\dot{x}_{gl} = \frac{\partial_t h}{\partial_x(h_f - h)}, \quad (13.3)$$

in the limit $\Delta t \rightarrow 0$.

Eq.(13.3) is a kinematic relationship, and we refer to this equation (13.3) as the *kinematic grounding-line equation*. It contains no additional physics other than the observation that ice thickness at the grounding line is not an explicit function of time. Here this arises because the ice thickness of the grounding line is always given by the flotation condition and is therefore at any location simply a function of the ocean depth H and the density ratio ρ_i/ρ , which both do not depend on time.¹ The kinematic grounding-line equation (13.3) shows how the grounding line migration rate (\dot{x}_{gl}) relates geometrically to temporal thickness changes at the grounding line ($\partial_t h$) and how closely the thickness profile gradient follows the gradient in flotation thickness. If the ice thickness upstream of the grounding line follows the flotation profile $h_f(x)$ closely, a given change in thickens with time requires a large shift in grounding line position to arrive at a new location where flotation is again reached.

At the grounding line $h_f - h = 0$, and with increasing distance directly downstream of the grounding line $h_f - h$ must increase, and hence $\partial_x(h_f - h) \geq 0$. Therefore the grounding line must advance, i.e. $\dot{x}_{gl} > 0$, whenever $\partial_t h > 0$.

One possible issue with using (13.3) might arise if the gradient in thickness ($\partial_x h$) were discontinuous across the grounding line. However, the boundary conditions dictate that $\partial_x u$ approaches the same value at the grounding line from both upstream and downstream directions. Furthermore, if h is continuous across the grounding line, then mass conservation dictates that $\partial_x h$ is also continuous. So under these conditions using (13.3) is justified. As most numerical models do not use the kinematic grounding-line equation (13.3) directly, it can be used to check the internal consistency of calculated grounding-line migration rates and rates of thickness change for a given bedrock geometry. If modelled grounding-line migration is not equal or at least very similar to that predicted by (13.3), then clearly something went wrong somewhere.

Eq. (13.3) has been derived repeatedly in the glaciological literature. The earliest derivation I'm aware of is by Hindmarsh (1996), see his equation (4). In there he makes reference to some earlier work of his (Hindmarsh, 1993) where the formula was also derived (but the source is not easily accessible), and also gives references to further derivations by other authors. The equation was also used by Sam Pegler (which paper?) and Ultee and Bassis (2020) used it, they state, to test calving laws for Greenland outlet glaciers.

13.3 Geometrical grounding-line migration

Changing the sea level (S) causes a shift in the position of the grounding line. This shift is only related to geometrical factors such as ice thickness ($h = s - b$) and ocean depth bedrock ($H = S - B$). To distinguish this shift in grounding-line position from ice-dynamical effects, we refer to this shift as at ‘geometrical grounding-line migration’. This horizontal shift in grounding line position due to time dependent changes in the height of the ocean surface can be determined as follows.

Ocean height (S) changes with time as

$$S(t) = \bar{S} + \Delta S(t),$$

¹Note that the argument leading to the kinematic grounding-line equation (13.3) does not depend on h_f begin

$$h_f = \rho_o H / \rho .$$

If, for example, we had instead

$$h_f = \kappa H$$

where $\kappa \geq 1$ is some number, then we we still arrive at

$$\dot{x} = \frac{\partial_t h}{\partial_x(h_f - h)}$$

but now h_f has a different physical interpretation.

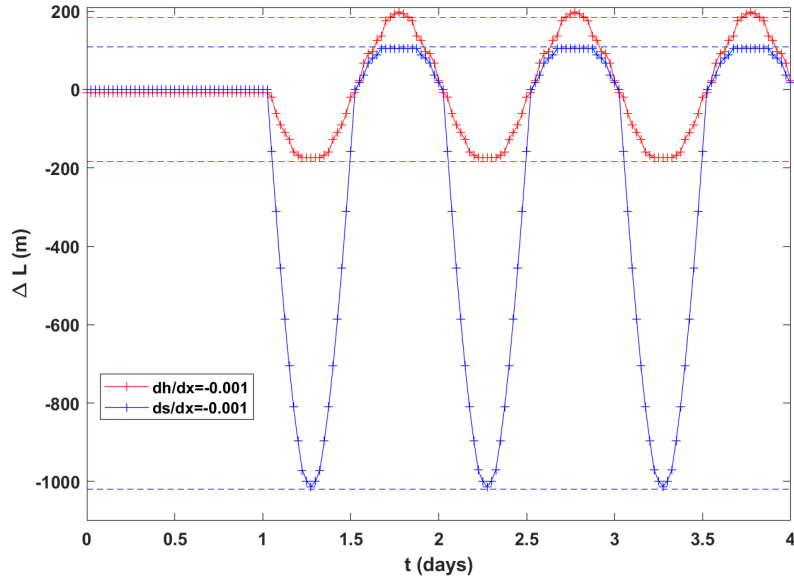


Figure 13.2: Example of grounding line migration in response to tidal forcing using the hydrostatic assumption. The curves were calculated using the flow model \bar{U}_a which is a vertically integrated flow model that calculates grounding line positions using the hydrostatic assumption. The blue curve was calculated for a constant surface slope of $ds/dx = -0.001$ and red curve for a constant thickness gradient of $dh/dx = -0.001$. In both cases the bedrock gradient as $dB/dx = -0.01$. The tidal amplitude was 2 m and the tidal period 1 day. To suppress the effects of ice flow, the flow parameters were set to values that made the ice effectively rigid and basal sliding was enforced to be close to zero. The dashed lines show the upper and lower extent of horizontal grounding-line migration as calculated by Eq. (13.5).

but not spatially (i.e. $\partial_x S(t) = \partial_x \bar{S} = \partial_x \Delta S = 0$)

For $S = \bar{S}$ the grounding line is at $x = x_{gl}$ and

$$\rho(s(x_{gl}) - b(x_{gl})) = \rho_o(\bar{S} - B(x_{gl})). \quad (13.4)$$

For a given perturbation, ΔS , in ocean height, the grounding line moves by some distance ΔL in either up or down-stream direction. At this new grounding line position the floating condition must again hold, and we have

$$\rho(s(x_{gl} + \Delta L) - b(x_{gl} + \Delta L)) = \rho_o(\bar{S} + \Delta S - B(x_{gl} + \Delta L))$$

or

$$\rho(s(x_{gl}) + \partial_x s \Delta L - b(x_{gl}) - \partial_x b \Delta L) = \rho_o(\bar{S} + \Delta S - B(x_{gl}) - \partial_x B \Delta L)$$

(For notational simplicity we have not indicated in the above equation that the derivatives are to be evaluated on both sides of the grounding line and that they are in fact distinct directional derivatives in the up and down-stream directions.) Using (13.4) gives

$$\rho(\partial_x s - \partial_x b) \Delta L = \rho_o(\Delta S - \partial_x B \Delta L)$$

or

$$\Delta L^{+/-} = \frac{\rho_o \Delta S}{\rho(\partial_x s^{+/-} - \partial_x b^{+/-}) + \rho_o \partial_x B^{+/-}} \quad (13.5)$$

Eq. (13.5) is valid even if the derivatives are not constant across the location of grounding line (x_{gl}) at mean tide ($\Delta S = 0$). We have indicated this by adding the superscript $+/-$. Here ΔS is positive for a high tide, and negative for a low tide. At low tide the gradients downstream of x_{gl} are to be used (minus sign), and at high tide the gradients upstream of x_{gl} (positive sign).

If $\partial_x B$ is the same on both sides of the x_{gl} , then it follows from (13.5) that the shifts in grounding line position at high and low tides are only equal in magnitude provided $\partial_x h$ is the same on both sides of $x = x_{gl}$ as well. In other words, for a constant bed slope, a tidally-induced grounding line migration is

symmetrical if, and only if, the thickness gradient does not change across the grounding line. Conversely, if the thickness gradients are not equal on both sides of the grounding line, the grounding line movement will always be asymmetric with respect to the tidal cycle. In the particular case when the ice thickness is constant (and $\partial_x h = 0$) the (horizontal) grounding-line migration is symmetrical with respect to the tide.

Such an asymmetrical grounding line migration takes place if, for example, the upper surface gradient ($\partial_x s$) is constant across the grounding line. In that case the thickness gradient cannot be equal on both sides of $x = x_{\text{gl}}$ as well. There is then a break in thickness gradient at $x = x_{\text{gl}}$ given by

$$\partial_x h = \begin{cases} \partial_x h^+ = \partial_x s - \partial_x B & \text{for } x \leq x_{\text{gl}} \\ \partial_x h^- = \partial_x s / (1 - \rho/\rho_o) & \text{for } x \geq x_{\text{gl}} \end{cases}$$

(There is no need to use the superscripts $+/-$ with $\partial_x s$ and $\partial_x B$ in the above equation because here we are assuming that those derivatives are continuous across the grounding line.) When this expression for the break in thickness gradient is inserted in (13.5) we find that the migration distance ΔL^- at a low tide (when $S = \bar{S} - \Delta L$), is given by

$$\Delta L^- = -\frac{\Delta S}{\frac{\rho/\rho_o}{1-\rho/\rho_o} \partial_x s + \partial_x B},$$

and at a high tide by

$$\Delta L^+ = \frac{\Delta S / (1 - \rho/\rho_o)}{\frac{\rho/\rho_o}{1-\rho/\rho_o} \partial_x s + \partial_x B},$$

and that

$$|\Delta L^-| = (1 - \rho/\rho_o) |\Delta L^+|.$$

In the case of a constant surface gradient, the upstream grounding-line shift at high tide is therefore about 9 times as large as the downstream shift at low tide.

In general we expect neither the thickness nor the surface gradient to be constant across the grounding line. Since the migration is only symmetrical in the particular case of a constant thickness gradient across the grounding line, we expect an asymmetrical grounding line migration in response to tides to be the general rule rather than an exception.

An example of transient hydrostatic grounding-line migration in response to tides is shown in Fig. 13.2. The migration was calculated using the flow model \bar{U}_a . This model, as do most commonly used flow model in glaciology, assumes that the grounding line is always exactly where the hydrostatic floating condition $\rho h = \rho_o(S - b)$ is met. The modelled grounding line displacements are in a good agreement with those calculated using Eq. (13.5). For example, in the case of constant surface slope the modelled values are $\Delta L^- = 105$ m and $\Delta L^+ = -1013$ while those based on Eq. (13.5) are $\Delta L^- = 109$ m and $\Delta L^+ = -1020$. These differences of a few meters are considerably smaller than the spatial dimension of 85 m of the smallest element of the mesh used in this particular run by the FE-model \bar{U}_a .

13.4 Flux at the grounding line

Upstream from the grounding line

$$2\partial_x \left(h A^{-1/n} |\partial_x u|^{1/n-1} \partial_x u \right) - C^{-1/m} \|u\|^{1/m-1} u = \rho g h \partial_x s \quad (13.6)$$

In terms of stresses this equation can also be written as

$$2\partial_x(h\tau_{xx}) - t_{bx} = \rho g h \partial_x s \quad (13.7)$$

Boundary conditions at the grounding line where $x = x_{\text{gl}}$ are

$$\partial_x u = A(\rho g h / 4)^n \quad (13.8)$$

$$h = \rho_o H / \rho. \quad (13.9)$$

Note that boundary condition (13.8) can be rearranged as

$$2A^{-1/n}(\partial_x u)^n = \frac{1}{2} \rho g h$$

If we insert the above expression into (13.6), assuming $\partial_x u > 0$, we arrive at

$$\frac{1}{2}\varrho g\partial_x h^2 - t_{bx} = \rho gh\partial_x s.$$

If we now assume that $\partial_x s \approx \partial_x h$ upstream of the grounding line, for example by setting $s = B + h$ with $\partial_x B = 0$ for $x < x_{gl}$, we obtain

$$[\frac{1}{2}\varrho g\partial_x h^2] - [t_{bx}] = [\frac{1}{2}\rho g\partial_x h^2] \quad (13.10)$$

where the brackets are used to indicate that we are here simply comparing sizes of terms, and where we have written $h\partial_x h = \frac{1}{2}\partial_x h^2$

Since $\varrho \approx \rho/10$ it is clear that the first term on the left-hand side of (13.10) is small compared to the right-hand side, and that the right-hand side must therefore be approximately balanced by the second term on the left-hand side of (13.10), i.e.

$$[t_{bx}] = [-\frac{1}{2}\rho g\partial_x h^2]. \quad (13.11)$$

Note that the key assumption here is that $\partial_x s \approx \partial_x h$ for $x < x_{gl}$.

Downstream of the grounding line, flotation implies that $\partial_x s = \varrho\partial_x h/\rho$ (see Eq. 1.193) and if, for example, $\partial_x s \approx \varrho\partial_x h/\rho$, upstream of the grounding line we instead of (13.10) arrive at

$$[\frac{1}{2}\varrho gh^2] - [t_{bx}] = [\frac{1}{2}\varrho g\partial_x h^2] \quad (13.12)$$

and clearly now it is the first term on the left-hand side that balances the right-hand side.

We will now derive an approximation for the flux at the grounding line as a function of (local) ice thickness, and start by making the assumption that $\partial_x s \approx \partial_x h$ in which case as we have seen

$$t_{bx} \approx -\rho gh\partial_x s,$$

i.e. that the second term on the left-hand sides of (13.6) and (13.7) is now approximately balanced by their respective right-hand sides. Hence, using Weertman sliding law we have

$$u = C(-\rho gh\partial_x h)^m, \quad (13.13)$$

where we have anticipated that $\partial_x h$ will be strictly negative.

In a steady state

$$\partial_x(uh) = a, \quad (13.14)$$

which allows us to write

$$\partial_x h = (a - h\partial_x u)/u. \quad (13.15)$$

Inserting the boundary condition (13.8) into (13.15) gives

$$\partial_x h = (a - hA(\varrho gh/4)^n)/u, \quad (13.16)$$

and then inserting (13.16) into (13.13) and assuming that $a \ll hA(\varrho gh/4)^n$ gives

$$u = C(\rho ghA(\varrho gh/4)^n/u)^m. \quad (13.17)$$

or

$$u^{m+1} = 4^{-nm} CA^m(g\rho)^{m+nm}\delta^{nm} h^{nm+2m},$$

where δ is defined as

$$\delta := 1 - \rho/\rho_o$$

The ice flux $q = uh$ at the grounding line is therefore

$$q = (4^{-nm} CA^m(g\rho)^{m+nm} (1 - \rho/\rho_o)^{nm})^{1/(m+1)} h^{(nm+3m+1)/(m+1)}, \quad (13.18)$$

where² h is the thickness at the grounding line, i.e.

$$h = h_{gl} = \rho_o H/\rho.$$

²For $q = \rho uh$ and keeping the θ term we have

$$q = \rho \left(4^{-n} C^{1/m} A (\varrho g)^{n+1} (1 - \rho/\rho_o)^n \right)^{m/(1+m)} \theta^{nm/(1+m)} h^{(nm+3m+1)/(1+m)}$$

The relationship between flux relationship (13.18) is identical to that of Schoof's 'B' model. We arrived at this flux relationship by assuming that velocity at the grounding line follows from SIA, and that $\partial_x u$ at the grounding line is given by the boundary condition (13.8) for horizontal strain rates. In addition we assumed steady-state conditions and that $a \ll h \partial_x u$.

Note that, as Eq. (13.17) shows, it is possible to express the velocity at the grounding line as a function of the ice thickness h alone, i.e. without any reference to the surface slope $\partial_x h$. This is possible because the surface slope at the grounding line is related to thickness through Eq. (13.16). We were able to use the boundary condition (13.8), the mass conservation equation (13.14), and the simplified momentum equation (13.13) to arrive at Eq. (13.17), giving velocity at the grounding-line as a function of thickness alone. To see this more clearly, inserting (13.13) and (13.8) into

$$u \partial_x h + h \partial_x u = 0$$

gives

$$C(\rho gh \partial_x h)^m \partial_x h + h A(\rho gh/4)^n = 0$$

or

$$\begin{aligned} \partial_x h &= -\left(\frac{h A(\rho gh/4)^n}{C(\rho gh)^m}\right)^{1/(m+1)} \\ &= -\frac{1}{4^{n/(m+1)}} \left(\frac{A}{C}\right)^{1/(m+1)} (\rho g)^{(n-m)/(m+1)} (1 - \rho/\rho_w)^{n/(m+1)} h^{\frac{n+1-m}{m+1}} \end{aligned}$$

showing how the surface slope at the grounding line depends on ice thickness.

13.5 Balance between terms on both side of the grounding line

(What follows is basically a slightly different framing of the argument in section 13.4 used to show that the basal shear traction will balance the driving stress upstream of the grounding line, provided $\partial_x s \approx \partial_x h$.)

Field equation and boundary condition at the grounding line written in terms of velocity are

$$2A^{-1/n} \partial_x \left(h \|\partial_x u\|^{(1-n)/n} \partial_x u \right) - \mathcal{H}(h - h_f) C^{-1/m} \|u\|^{(1-m)/m} u = \rho gh \partial_x s \quad (13.19)$$

$$2A^{-1/n} h \|\partial_x u\|^{(1-n)/n} \partial_x u = \frac{1}{2} \varrho g h^2 \quad \text{at } x = x_{gl} \quad (13.20)$$

$$h = h_f \quad \text{at } x = x_{gl} \quad (13.21)$$

where \mathcal{H} is the Heaviside step function, and where

$$h_f = \rho_o H / \rho$$

and where $\varrho = \rho(1 - \rho/\rho_o)$.

Inserting (13.20) into (13.19) and assuming that over the grounded area $|\partial_x s| \gg |\partial_x b|$, and therefore that $\partial_x h = \partial_x s - \partial_x b \approx \partial_x s$, we arrive at

$$\frac{1}{2} \varrho g \partial_x (h^2) - \mathcal{H}(h - h_f) C^{-1/m} \|u\|^{(1-m)/m} u = \rho gh \partial_x h$$

or

$$\frac{1}{2} \varrho g \partial_x h^2 - \mathcal{H}(h - h_f) C^{-1/m} \|u\|^{(1-m)/m} u = \frac{1}{2} \varrho g \partial_x h^2$$

which immediately shows that the first term on the left hand side is $\varrho/\rho = \rho(1 - \rho/\rho_o)/\rho = (1 - \rho/\rho_o) \approx 0.1$ the size of the right-hand side.

Downstream of the grounding line $s = (1 - \rho_o/\rho)h$ and therefore $\partial_x s = \delta \partial_x b \approx 0.1 \partial_x b$, or $\partial_x s \ll \partial_x h$ and this reversal of the relative sizes of the upper and lower slopes ensures that we now also have the right balance downstream of the grounding line, where the first term on the left-hand side now equals the right-hand side.

13.6 GL scalings (Schoof)

Field equations written in terms of velocity and stresses, respectively, are

$$2A^{-1/n}\partial_x \left(h \|\partial_x u\|^{(1-n)/n} \partial_x u \right) - \mathcal{H}(h - h_f) C^{-1/m} \|u\|^{(1-m)/m} u = \rho g h \partial_x s \quad (13.1)$$

$$2\partial_x(h\tau_{xx}) - \tau_b = \rho g h \partial_x s \quad (13.2)$$

where \mathcal{H} is the Heaviside step function. Boundary conditions at $x = x_{\text{gl}}$ are

$$2A^{-1/n}h \|\partial_x u\|^{(1-n)/n} \partial_x u = \frac{1}{2}\varrho g h^2 \quad (13.3)$$

$$h = h_f \quad (13.4)$$

where

$$h_f = \rho_o H / \rho$$

and where $\varrho = \rho(1 - \rho/\rho_o)$. The above model is only valid for $[z]/[x] \ll 1$ and $u_d/u_b \ll 1$, where u_d is the deformational velocity and u_b the sliding velocity.

Scalings: With $[u]$ and $[x]$ as scales for the horizontal velocity and the span of the ice sheet, the kinematic boundary condition suggests

$$\frac{[u][z]}{[x]} = [a] \quad \text{and} \quad [t] = \frac{[x]}{[u]}$$

We set a scale for C by writing

$$[u]^{1/m}/[C]^{1/m} = \rho g[z][z]/[x]$$

i.e. we balance basal shear stress with the driving stress. We introduce

$$\epsilon = \frac{\tau_{xx}}{\sigma_{xx}} = \frac{A^{-1/n}([u]/[x])^{1/n}}{2\rho g[z]} \quad (13.5)$$

and will consider the case $\epsilon \ll 1$, and we also define

$$\delta = 1 - \rho/\rho_o \quad (13.6)$$

where $\delta \approx 0.1$.

Inserting these scalings into field equation (13.1) and the boundary condition (13.3) gives

$$4\epsilon \partial_x \left(h \|\partial_x u\|^{(1-n)/n} \partial_x u \right) - \|u\|^{(1-m)/m} u = h \partial_x s \quad \text{for } x < x_{\text{gl}} \quad (13.7)$$

$$\|\partial_x u\|^{(1-n)/n} \partial_x u = \frac{\delta h}{8\epsilon} \quad \text{at } x = x_{\text{gl}} \quad (13.8)$$

Summarising the scaled momentum equations are

$$4\epsilon \partial_x \left(h \|\partial_x u\|^{(1-n)/n} \partial_x u \right) - \|u\|^{(1-m)/m} u = h \partial_x s \quad \text{for } x < x_{\text{gl}} \quad (13.9)$$

$$\|\partial_x u\|^{(1-n)/n} \partial_x u = \frac{\delta h}{8\epsilon} \quad \text{at } x = x_{\text{gl}} \quad (13.10)$$

Now we consider the scaled momentum equation (13.7) in the vicinity of the grounding line. As we approach $x \rightarrow x_{\text{gl}}$ from the upstream side we expect the first term on the left-hand side of (13.7) to be given by (13.8). Inserting (13.8) into (13.7) gives

$$\delta h \partial_x h - \|u\|^{(1-m)/m} u = h \partial_x s, \quad (13.11)$$

all quantities evaluated at the grounding line.

Now consider the right-hand side of the above equation. We always have

$$\partial_x s = \partial_x(h + b),$$

Upstream of the grounding line we do not expect $\partial_x b$ to be related (at least not in some simple way) to $\partial_x h$. Consider the case $\partial_x b = 0$ while $\partial_x h$ takes some finite value, then equation (13.2) is

$$\delta h \partial_x h - \|u\|^{(1-m)/m} u = h \partial_x h, \quad (13.12)$$

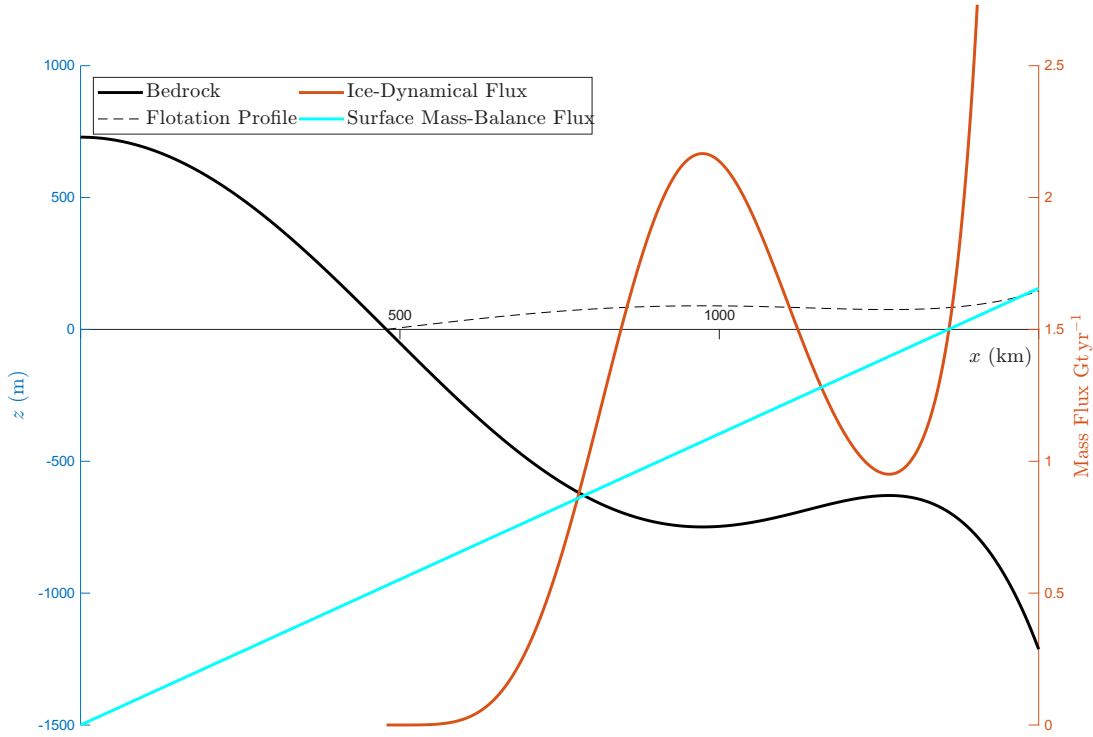


Figure 13.3: Ice flux at a grounding line (red) from Eq. (13.18), and integrated surface mass balance upstream from the grounding line (cyan), for a given bedrock profile (black). Here $A = 1.146 \times 10^{-8} \text{ kPa}^{-3} \text{ a}^{-1}$, $n = 3$, $m = 3$, and $C = 0.8 \times 10^{-3} \text{ kPa}^{-3} \text{ m a}^{-1}$

and since $\delta \ll 1$ (in fact $\delta \approx 0.1$) the second term on the left-hand side approximately balances the right-hand side. We therefore have an approximate balance between basal stress and driving stress.

In physical terms the situation down-stream of the grounding line is clear. There the first term on the left-hand side must balance the term on the right hand side. Here our formulation gives the right balance because since $\partial_x b$ and $\partial_x h$ are related by the floating condition

$$\partial_x s = \partial_x(h + b) = \partial_x(h - (1 - \rho/\rho_o)h) = \delta \partial_x h,$$

and when inserted into

$$\frac{1}{2} \delta \partial_x(hh) = \delta h \partial_x h, \quad (13.13)$$

we arrive, which is the right balance.

Summarising, if h and b are related through the floating condition, the balance is always between the first lhs term and the rhs, but the balance is between the second rhs term and the lhs if

$$|\partial_x b| \ll |\partial_x h|$$

In the particular case $\partial_x b = 0$ the balance is always between the basal shear stress term and the driving stress.

13.7 Grounding-line instability

For a steady state with the grounding line located at $x = x_{\text{gl}}$, mass conservation requires

$$\gamma x_{\text{gl}} + q(x_{\text{gl}}) = 0$$

where we have assumed that the ice divide is at $x = 0$ and the surface mass balance is γ . We assume the surface mass balance is spatially constant and positive, i.e. $\gamma > 0$. Clearly if $\gamma < 0$, no ice sheet is possible.

Perturb x_{gl} by Δx

$$x'_{\text{gl}} = x_{\text{gl}} + \Delta x$$

If

$$\gamma \Delta x - \partial_x q \Delta x < 0$$

then more ice flows across the grounding line than is added over the new surface Δx upstream of the grounding line. The volume of the (grounded) ice sheet must decrease with time and the grounding line must retreat towards the original steady state. (Note that the derivative of q with respect to x is the derivative of q following the grounding-line position.)

Hence, if

$$\partial_x q > \gamma$$

then the grounding line is stable, but

$$\begin{aligned} \frac{\partial q}{\partial x} \Big|_{x=\text{gl}} &= \frac{\partial q_{\text{gl}}}{\partial h_{\text{gl}}} \frac{\partial h_{\text{gl}}}{\partial x} \\ &= \frac{\partial q_{\text{gl}}}{\partial h_{\text{gl}}} \frac{\rho_o}{\rho} \frac{\partial (S_{\text{gl}} - B_{\text{gl}})}{\partial x} \\ &= -\frac{\rho_o}{\rho} \frac{\partial q_{\text{gl}}}{\partial h_{\text{gl}}} \frac{\partial B_{\text{gl}}}{\partial x} \end{aligned}$$

For a prograde bed, $\partial_x B < 0$, and therefore we must have $\partial_h q > 0$ for the grounding line to be stable. Conversely, for a retrograde bed where $\partial_x B > 0$ we must have $\partial_x q < 0$ for the grounding line to be stable.

Chapter 14

Subglacial hydrology

Basal water pressure p_w is expressed as

$$p_w = p_i - N \approx \rho_i g h - N \quad (14.1)$$

where N is the effective water pressure. The argument for introducing the effective water pressure, N , is that we expect the water pressure to be similar to the overburden pressure, $\rho_i g h$ and therefore $|N| \ll \rho_i g h$. If the water pressure is less than the overburden pressure of the ice N is positive, and $N = 0$ when those are equal.

The basal hydraulic potential is defined as

$$\phi = \rho_w g b + p_w \quad (\text{hydraulic potential}) \quad (14.2)$$

The literature of subsurface hydrology often uses instead of the hydraulic potential, the concept of hydraulic head, h_p , defined as

$$h_p := \frac{\phi}{\rho_w g} \quad (\text{hydraulic head}) \quad (14.3)$$

Inserting 14.1 into (14.2)

$$\begin{aligned} \phi &= \rho_w g b + p_w \\ &= \rho_w g b + \rho_i g h - N \\ &= \rho_w g b + \rho_i g (s - b) - N \end{aligned}$$

or

$$\phi = (\rho_w - \rho_i) g b + \rho_i g s - N \quad (14.4)$$

or

$$\phi = \Phi - N \quad (14.5)$$

where

$$\Phi := (\rho_w - \rho_i) g b + \rho_i g s , \quad (14.6)$$

and thus

$$\nabla \phi = (\rho_w - \rho_i) g \nabla b + \rho_i g \nabla s - \nabla N \quad (14.7)$$

showing that, provided $\nabla N \approx 0$, that surface slope is about 10 times more important than bed slope.

In the case of a stagnant water mass, i.e. subglacial lake, for which $\nabla \phi = \mathbf{0}$, and ice at or above flotation, i.e. $N = 0$, the upper and lower glacier surface slopes are related as

$$(\rho_w - \rho_i) \nabla b = -\rho_i g \nabla s .$$

Various approaches to the modelling of subglacial hydrology have been explored. At one end one can use traditional equations of groundwater flow in a confined layer. Another approach is to consider water flow in a thin basal layer of variable thickness.

14.1 Traditional groundwater theory

For a groundwater flow within a layer, the vertically integrated conservation equation of water reads

$$\frac{S_w}{\rho g} \partial_t \phi + \nabla \cdot (\mathbf{q}_w) = a_w . \quad (14.8)$$

The first-term on the left-hand side represents a specific water storage term that is related to the compressibility of the solid phase and its porosity. The dimensionless coefficient, S_w , is the *storativity*, or the *storage coefficient*. The source term, a_w , has the units distance per time. Note that here a_w is in the SI units m/s, and \mathbf{q}_w has the units m²/s.

In terms of the hydraulic head

$$h_p := \frac{\phi}{\rho_w g} \quad (\text{hydraulic head}) \quad (14.3)$$

the Eq. (14.8) reads

$$S_w \partial_t h_p + \nabla \cdot (\mathbf{q}_w) = a_w . \quad (14.9)$$

Assuming a linear Darcy flow law where the horizontal water flux in a confined channel with the thickness h_w , is given as

$$\begin{aligned} \mathbf{q}_w &= -k h_w \nabla \phi \\ &= -k \rho_w g h_w \nabla h_p \end{aligned}$$

where k is the hydraulic conductivity. Since a_w is in the SI units m/s, \mathbf{q}_w the units m²/s, and h_p the units m, k here has the SI units

$$[k] = \frac{m}{s} \frac{1}{[\rho_w][g]}$$

Typically, the hydraulic conductivity k is expressed in the SI units m/s, so we will need to divide values expressed in such units by $\rho_w g$.¹

The groundwater equation becomes

$$\frac{S_w}{\rho g} \partial_t \phi - \nabla \cdot (k h_w \nabla \phi) = a_w . \quad (14.10)$$

or

$$S_w \partial_t h_p - \rho_w g \nabla \cdot (k h_w \nabla h_p) = a_w . \quad (14.11)$$

If we have a confined aquifer, then h_w is constant and does not evolve, that is

$$h_w = \text{fixed} \quad (\text{confined aquifer}) .$$

Our unknown is then the hydraulic pressure head, h_p . Alternatively, we can envision a situation of an unconfined channel where the hydraulic head is the upper boundary itself.

$$h_w = h_p \quad (\text{unconfined aquifer}) .$$

Unconfined aquifers are also referred to as *phreatic aquifers*. For a phreatic aquifer therefore have

$$S_w \partial_t h_w - \rho_w g \nabla \cdot (k h_w \nabla h_w) = a_w . \quad (14.12)$$

and

$$\mathbf{q}_w = -k \rho_w g h_w \nabla h_w = -\frac{1}{2} k \rho_w g \nabla h_w^2 \quad (14.13)$$

again using the linear Darcy law.

The source term, a_w , includes local water sources and leakage rates from above and below the layer.

For confined aquifers we can define

$$K := k h_w \quad (14.14)$$

where K is the transmissivity tensor of the layer, which will depend on the thickness of the layer, for example as $K = h_w k$ where h_w is the thickness of the layer, and k is the hydraulic conductivity tensor. For a fixed layer thickness that does not vary in time, we can however think of K as a constant.

¹Most tables of hydraulic conductivity values are effectively incomprehensible to the average human person as they tend to be provided in the units *darcy*, which definition involves the unit *centipoise*. Glacier till is supposed to have values ranging from 10^{-13} to $10^{-2} \text{ m s}^{-1}/(\rho_w g)$, so it is has been narrowed down to a range covering 11 orders of magnitudes.

14.1.1 Simple analytical steady-state solution of the groundwater equation

Consider the one-dimensional steady-state problem for a confined aquifer, for which Eq. (14.10) has the form

$$\partial_x(kh_w\partial_x\phi) = a_w . \quad (14.15)$$

In terms of the hydraulic (pressure head), h_p , and assuming constant hydraulic conductivity, this can also be written as

$$h_p := \frac{\phi}{\rho_w g} \quad (\text{hydraulic head}) \quad (14.3)$$

or

$$\rho_w g k h_w \partial_{xx}^2 h_p = -a_w$$

with the boundary conditions

$$\begin{aligned} h_p &= h_l \quad \text{at} \quad x = l \\ \partial_x h_p &= 0 \quad \text{at} \quad x = l \end{aligned}$$

The solution is

$$h_p(x) = -\frac{a_w}{\rho_w g k h_w} (x^2/2 + C_1 x + C_2)$$

or

$$h_p(x) = \frac{a_w}{2\rho_w g k h_w} (l-x)^2 + h_l \quad \text{for} \quad x \leq l$$

The solution implies that $h_w \rightarrow +\infty$ as $x \rightarrow -\infty$ so clearly this solution can not be used for infinite aquifers (see also Baer, Hydraulics of Groundwater, 1979).

For a one-dimensional unconfined (phreatic) steady-state aquifer Eq. (14.12) reads where

$$-\frac{\rho_w g k}{2} \partial_x h_w^2 = a_w . \quad (14.16)$$

and the flux is given by Eq. (14.13), which in one-dimension reads

$$q_w = -\rho_w g k h_w \partial_x h = -\frac{\rho_w g k}{2} \partial_x h_w^2 ,$$

where, again, we have assumed a linear Darcy law. Assuming k is not spatially variable, conservation of mass then implies, which is same as Eq. (14.12). Integrating both sides of (14.16)

$$q_x(x) = -\frac{\rho_w g k}{2} \partial_x h_w^2 = a_w x - C_1 , \quad (14.17)$$

and hence

$$\rho_w g k h_w^2(x) = -a_w x^2 + 2C_1 x + C_2 . \quad (14.18)$$

This is the general solution of $h_w(x)$. The constants C_1 and C_2 are then determined by prescribing suitable boundary conditions.

For the boundary conditions, $h_w = h_l$ at $x = l$ and $\partial_x h_w = 0$ at $x = l$

$$\begin{aligned} \partial_x h_w &= 0 \\ \implies \partial_x h_w^2 &= 0 \\ \implies -2a_w l + 2C_1 &= 0 \\ \implies C_1 &= a_w l \end{aligned}$$

and for the BC, that

$$\begin{aligned} h_w(x = l) &= h_l \\ \rho g k h_l^2 &= -a_w l^2 + 2a_w l^2 + C_2 \\ C_2 &= \rho_w g k h_l^2 - a_w l^2 . \end{aligned}$$

Hence

$$\begin{aligned}\rho_w g k h_w^2(x) &= -a_w x^2 + 2C_1 x + C_2 \\ &= -a_w x^2 + 2a_w l x + \rho_w g k h_l^2 - a_w l^2 \\ &= -a_w (x^2 - 2a_w l x + l^2) + \rho_w g k h_l^2 \\ &= -a_w (x - l)^2 + \rho_w g k h_l^2\end{aligned}$$

And the solution is

$$h_w^2 = -\frac{a_w}{\rho_w g k} (l - x)^2 + h_l^2$$

The corresponding flux is

$$q_w(x) = -\frac{\rho_w g k}{2} \partial_x h_w^2 = a_w (x - l)$$

This is a rather odd solution where the flux for $x < l$ is negative and h_w^2 becomes negative for $x \rightarrow -\infty$. However, this is a direct consequence of our prescribed boundary conditions. By setting the flux to zero at $x = l$, the water flux must be directed away from $x = l$ in the negative direction, for $a_w > 0$. This also implies that the water-film thickness must decrease in the negative x direction, and eventually become negative.

Another set of boundary conditions are:

$$\begin{aligned}h_w &= h_l \quad \text{at} \quad x = l \\ h_w &= h_0 \quad \text{at} \quad x = 0\end{aligned}$$

Applying these conditions to

$$\rho_w g k h_w^2(x) = -a_w x^2 + 2C_1 x + C_2 . \quad (14.18)$$

gives

$$\rho_w g k h_0^2 = C_2$$

and

$$\begin{aligned}\rho_w g k h_l^2 &= -a_w l^2 + 2C_1 l + \rho_w g k h_0^2 \\ \implies 2C_1 &= \frac{\rho_w g k}{l} (h_l^2 - h_0^2) + a_w l .\end{aligned}$$

And therefore

$$\begin{aligned}\rho_w g k h_w^2(x) &= -a_w x^2 + 2C_1 x + C_2 \\ &= -a_w x^2 + \left(\frac{\rho_w g k}{l} (h_l^2 - h_0^2) + a_w l \right) x + \rho_w g k h_0^2 \\ &= -a_w (x^2 - l x) + \rho_w g k (h_0^2 + (h_l^2 - h_0^2) x / l)\end{aligned}$$

and from (14.17)

$$q_w(x) = a_w x - \frac{\rho_w g k}{l} (h_l^2 - h_0^2) + a_w l$$

and we note that $q_w(x = 0) \neq 0$.

Now consider the boundary conditions

$$\begin{aligned}q_w &= 0 \quad \text{at} \quad x = 0 \\ h_w &= h_l \quad \text{at} \quad x = l\end{aligned}$$

Applying these conditions to

$$\rho_w g k h_w^2(x) = -a_w x^2 + 2C_1 x + C_2 , \quad (14.18)$$

gives

$$C_1 = 0 ,$$

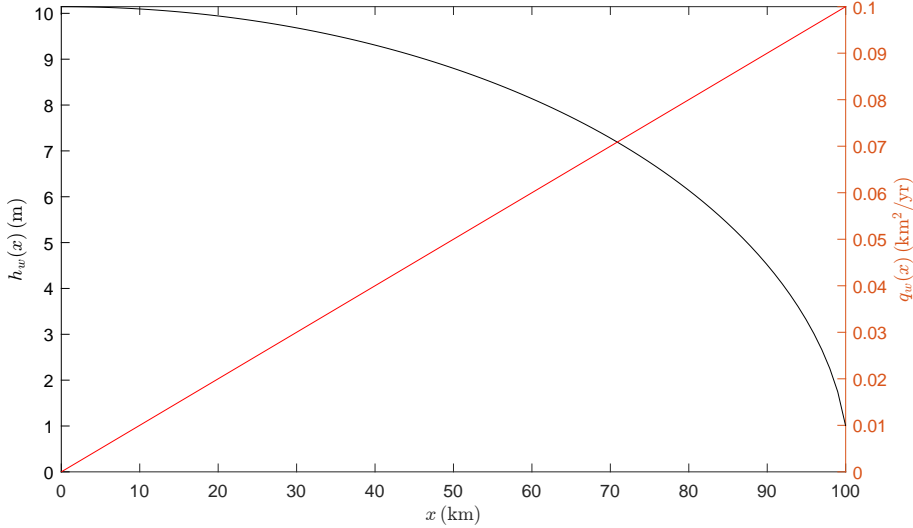


Figure 14.1: The solution to Eq. (14.19) for $h_w(x)$ (black line) and $q_w(x)$ (red line) for an unconfined aquifer. Here $h_w(x = l) = 1 \text{ m}$, $a_w = 1 \text{ m yr}^{-1}$, $l = 100 \text{ km}$ and $k = 1 \times 10^4 \text{ m yr kg}^{-1}$.

and

$$\begin{aligned} \rho_w g k h_l^2 &= -a_w l^2 + C_2 \\ \implies C_2 &= \rho_w g k h_l^2 + a_w l^2 \end{aligned}$$

And therefore

$$\begin{aligned} \rho_w g k h_w^2(x) &= -a_w x^2 + 2C_1 x + C_2 \\ &= -a_w x^2 + \rho_w g k h_l^2 + a_w l^2 \end{aligned}$$

or

$$h_w^2(x) = a_w(l^2 - x^2) + \rho_w g k h_l^2 \quad (14.19)$$

and from (14.17)

$$q_w(x) = a_x x .$$

Note that

$$h_w \partial_x h_w = -a_w l \quad \text{at } x = l$$

and that the slope becomes infinite in the limit where $h_w(x = l) = h_l = 0$. The thickness is in this limit zero, but the flux is finite.

We conclude that if our domain is $0 \leq x \leq l$, and we which to have $q(x = 0) = 0$, this boundary condition must be prescribed at the upper boundary. Prescribing the thickness at $x = 0$, will not provide us with this flux relationship. Also prescribing both the thickness at $h_w(x = l) = h_l$ and a no-flux condition $q_x(x = l) = 0$ results in an unphysical profile with negative (or complex) values for the thickness.

14.1.2 Possible modifications of the groundwater equation for glacier hydrology

There are various reasons why solving Eq. (14.11) my lead to contradictions and conceptual difficulties when applied to glacier flow. For example one might find that the solution my violate

$$\phi(x, y) = \rho_w g b(x, y) + p_w(x, y) < \rho_w g b(x, y)$$

at some locations (x, y) . The water pressure has then become negative. Various approaches have been suggested to address this issue, e.g. [Beyer et al. \(2018\)](#).

If we insert Eqs. (14.4) and (14.7) into Eq. (14.11) we obtain

$$\frac{S_w}{\rho g} \partial_t N - \nabla \cdot (K ((\rho_w - \rho_i) g \nabla b + \rho_i g \nabla s)) - \nabla \cdot (k \nabla N) = m , \quad (14.20)$$

or

$$\frac{S_w}{\rho g} \partial_t N + \nabla \cdot (K \nabla N) = m + \nabla \cdot (K (\rho_w - \rho_i) g \nabla b + \rho_i g \nabla s) . \quad (14.21)$$

In terms of the (constant) water layer thickness we can also write this as

$$\frac{S_w}{\rho g} \partial_t N + \nabla \cdot (k h_w \nabla N) = a_w + \nabla \cdot (k h_w ((\rho_w - \rho_i) g \nabla b + \rho_i g \nabla s)) . \quad (14.22)$$

or

$$\frac{S_w}{\rho g} \partial_t N + \nabla \cdot (k h_w \nabla N) = a_w + \nabla \cdot (k h_w \nabla \Phi) . \quad (14.23)$$

where

$$\Phi := (\rho_w - \rho_i) g b + \rho_i g s , \quad (14.6)$$

This is a linear diffusion equation for N .

Eq. (14.23) requires a boundary condition for ϕ , or N , for those to be fully determined. Otherwise they are only determined within some constant value.

The boundary condition at glacier terminus will be $p_w = 0$ or

$$\phi = \rho_w g b \quad (\text{Boundary condition at terminus})$$

or $p_w = (S - b)\rho g$ at the grounding line, i.e.

$$\phi = \rho_w g b + \rho_w g (S - b) = \rho_w g S \quad (\text{Boundary condition at grounding lines})$$

where S is the ocean surface elevation. At outflow boundaries we might, however, prefer to use the no-flux condition

$$\mathbf{q}_w \cdot \hat{\mathbf{n}} = -K \nabla \phi \cdot \hat{\mathbf{n}} = 0 \quad (\text{No outflow condition})$$

where \mathbf{n} is a unit normal points outwards from the boundary.

When solving (14.22) we might treat s and b as independent of N . However, if $N = 0$, in which case the ice is afloat, we will need to adjust s and b accordingly. For the specific case of a floating ice shelf, where $N = 0$, the ‘water layer’ is the open ocean and we set $S_w = \inf$ and therefore $\partial_t N = 0$. Eq. (14.22) then implies

$$\nabla s = -\frac{\rho_i}{\rho_w - \rho_i} \nabla b$$

as expected.

We have

$$b = B + h_w ,$$

although if h_w is on the order of a few millimetres we might simply write $b = B$.

We solve the transient (14.11) using the θ method, whereby

$$\frac{S_w}{\rho g \Delta t} (\phi_1 - \phi_0) = (1 - \theta)(m_1 + \nabla \cdot (K \nabla \phi_0)) + \theta(m_2 + \nabla \cdot (K \nabla \phi_1)) \quad (14.24)$$

Form the inner products with respect to the basis ψ_p

$$\begin{aligned} \frac{S_w}{\rho g} \langle \phi_1 - \phi_0 | \psi_p \rangle &= (1 - \theta) \Delta t \langle m_0, \psi_p \rangle - \langle K \nabla \phi_0, \nabla \psi_p \rangle \\ &\quad + \theta \Delta t \langle m_1, \psi_p \rangle - \langle K \nabla \phi_1, \nabla \psi_p \rangle \end{aligned}$$

The finite-element formulation is

$$\begin{aligned} \partial_t N - \nabla \cdot (K \nabla \phi) &= a \\ \partial_t N - \nabla \cdot (K \nabla (\Phi - N)) &= a \\ \langle N_1 - N_0, \psi \rangle - \Delta t \langle \nabla \cdot (K \nabla (\Phi - N)), \psi \rangle &= \Delta t \langle a, \psi \rangle \\ \langle N_1 - N_0, \psi \rangle + \Delta t \langle K \nabla (\Phi - N), \nabla \psi \rangle &= \Delta t \langle a, \psi \rangle \\ \langle N_1, \psi \rangle - \theta \Delta t \langle K \nabla N_1, \nabla \psi \rangle &= \langle N_0, \psi \rangle \\ &\quad + \Delta t (1 - \theta) (\langle a_0, \psi \rangle - \langle K \nabla \Phi_0, \nabla \psi \rangle + \langle K \nabla N_0, \nabla \psi \rangle) \\ &\quad + \Delta t \theta (\langle a_1, \psi \rangle - \langle K \nabla \Phi_1, \nabla \psi \rangle) \end{aligned}$$

The last expression is the FE system in the finite form for N_1 , as opposed to an incremental form for ΔN_1 .

14.2 Basal water flow in a film of variable thickness

If we have substantial water thickness, h_w , where

$$b = B + h_w$$

we write this as

$$\phi = \rho_w g(B + h_w) + p_w \quad (\text{hydraulic head}) \quad (14.25)$$

where p_w is the (fixed) water pressure at the top of the water layer. We now have

$$\phi = g(\rho_w - \rho_i)(B + h_w) + g\rho_i s - N, \quad (14.26)$$

and thus

$$\nabla\phi = g(\rho_w - \rho_i)\nabla B + g\rho_i\nabla s + g(\rho_w - \rho_i)\nabla h_w - \nabla N \quad (14.27)$$

We imagine the subglacial water to flow in a film with an effective thickness h_w , for which

$$\partial_t h_e + \partial_t h_w + \nabla \cdot \mathbf{q}_w = a_w \quad (14.28)$$

The h_e terms represents englacial storage, for example a partially filled moulin. For a moulin the englacial storage could be expressed as

$$h_e = A_m(h_p - h_m) = A_m \frac{\phi - \phi_m}{\rho_w g}$$

where A_m is the cross-sectional area of the moulin, and h_m the water level in the moulin.

Water flux in a channel is often described by the empirical Darcy-Weisback law as

$$\mathbf{q}_w = -kh^\alpha \|\nabla\phi\|^{\beta-2} \nabla\phi \quad (14.29)$$

This system (14.4), (14.28) and (14.29), contains h and N as unknowns, and to close the system we need one additional equation, which is provided by an evolutionary law for the water film thickness, h_w . This could, for example, have the form

$$\partial_t h_w = a_b - A|N|^{n-1}N + \gamma\|\mathbf{v}_b\|$$

Assuming, for the moment, linear Darcy flow to keep the notation simple, $\beta = 2$ and $\alpha = 1$, gives

$$\mathbf{q}_w = -kh_w \nabla\phi$$

Inserting into the mass conservation equation, results in

$$\partial_t h_w - \nabla \cdot (kh_w \nabla\phi) = m$$

And then inserting

$$\nabla\phi = \mathbf{d} + \nabla N \quad (14.31)$$

gives

$$\partial_t h_w - \nabla \cdot (kh_w \mathbf{d}) - \nabla \cdot (kh_w \nabla N) = a_w \quad (14.30)$$

and the water sheet thickness evolution is

$$\partial_t h_w = m - A|N|^{n-1}N + \gamma\|\mathbf{v}_b\|$$

The gradient of the hydraulic potential contains terms that are only dependent on the ice geometry, and a term dependent on the effective water pressure N . We write

$$\nabla\phi = \mathbf{d} - \nabla N \quad (14.31)$$

where

$$\mathbf{d} := (\rho_w - \rho_i)g\nabla b + \rho_i g \nabla s \quad (14.32)$$

We note that $k\mathbf{d}$ can be thought of as the velocity of the water in the channel, i.e.

$$\mathbf{v}_w = k\mathbf{d}$$

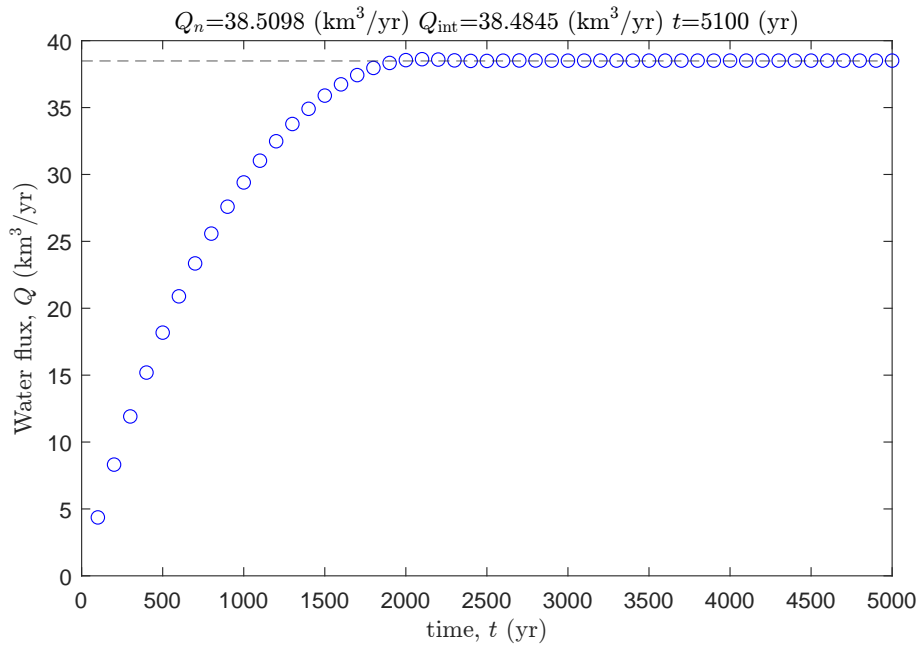


Figure 14.2: Total water flux across a closed circular boundary. In steady state the flux across the boundary must be equal to the total internal water production within the area enclosed by the boundary. The horizontal dashed line is the analytically calculated correct steady state limit $Q_{\text{int}} = \pi r^2 a_w = 38.4845 \text{ km}^3/\text{yr}$

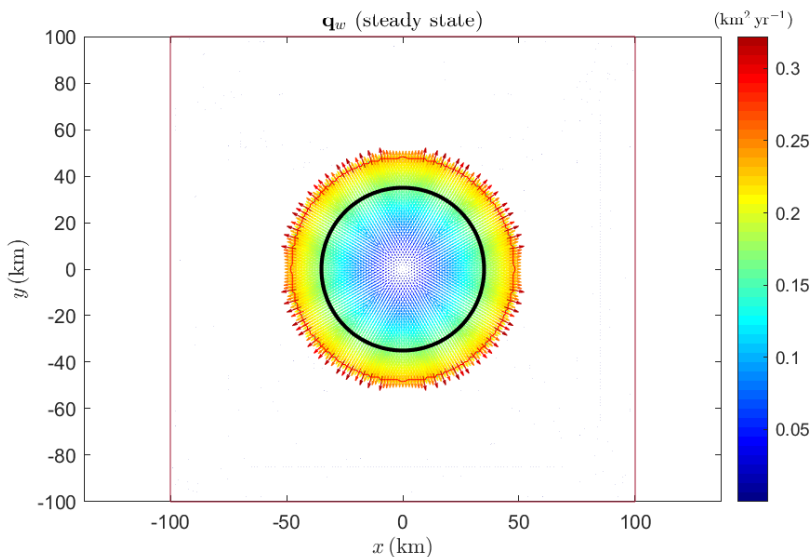


Figure 14.3: Calculated steady state water flux vectors. The thick black line is the circle used in Fig. 14.2 to calculate the water flux shown. The red line is the grounding line. Across the grounded area a uniform water flux of $a_w = 10 \text{ m/yr}$ is prescribed. The radius of the flux gate is $r = 35 \text{ km}$ and the total internal water production within that circle is therefore $Q_{\text{int}} = \pi r^2 a_w = 38.4845 \text{ km}^3/\text{yr}$

14.3 Simplified hydrological model for routing purposes

We have

$$\partial_t h_w + \nabla \cdot (\mathbf{q}_w) = a_w \quad (14.33)$$

where

$$\mathbf{q}_w = -kh_w \nabla \phi \quad (14.34)$$

and

$$\begin{aligned} \phi &= g\rho_w B + g\rho_w h_w + p_w \\ &= g\rho_w B + g\rho_w h_w + g\rho_i h - N \\ &= g\rho_w B + g\rho_w h_w + g\rho_i(s - b) - N \\ &= g\rho_w B + g\rho_w h_w + g\rho_i(s - (B + h_w)) - N \\ &= g(\rho_w - \rho_i)B + g(\rho_w - \rho_i)h_w + g\rho_i s - N \end{aligned}$$

or

$$\phi = \Phi + \Upsilon - N . \quad (14.35)$$

with

$$\Phi := (\rho_w - \rho_i)gB + \rho_i gs , \quad (14.36)$$

and

$$\Upsilon := g(\rho_w - \rho_i)h_w , \quad (14.37)$$

where we have replaced b with B compared to Eq. (14.6). We find that this formulation results in the right answer for a floating ice shelf.² The gradient of the potential is

$$\nabla \phi = \nabla \underbrace{((\rho_w - \rho_i)gB + \rho_i gs)}_{:=\Phi} + \underbrace{g(\rho_w - \rho_i)\nabla h_w}_{:=\Upsilon} - \nabla N \quad (14.38)$$

$$= \nabla \Phi + \nabla \Upsilon - \nabla N \quad (14.39)$$

$$(14.40)$$

We have two unknowns, the water layer thickness h_w and the effective water pressure N . For routing purposes it is common to assume that $N = 0$. Another approach to close the system is to add some additional evolutionary equation for h_w where $h_w = h_w(N)$.

With

$$\mathbf{q}_w = -h_w k \nabla \phi , \quad (14.34)$$

and setting

$$N = 0 ,$$

²For a floating ice shelf $N = 0$ and

$$\phi = g\rho_w(B + H) .$$

Thus

$$\begin{aligned} \rho_w B + \rho_w h_w + \rho_i h &= \rho_w(B + H) \\ \implies \rho_w h_w + \rho_i h &= \rho_w H \\ \implies h_w &= H - \rho_i / \rho_w h \\ \implies h_w &= S - B - \rho_i / \rho_w h \\ \implies h_w + B &= S - \rho_i / \rho_w h \\ \implies b &= S - \rho_i / \rho_w h \end{aligned}$$

which agrees with the flotation relationship Eq. (1.194). We can also check the implications of

$$\mathbf{q}_w = \nabla \phi = \mathbf{0}$$

for a floating ice shelf, i.e.

$$\begin{aligned} \nabla \phi &= \nabla(g(\rho_w - \rho_i)B + g(\rho_w - \rho_i)h_w + g\rho_i s - N) \\ &= \nabla(g(\rho_w - \rho_i)(B + h_w) + g\rho_i s) \\ &= \nabla(g(\rho_w - \rho_i)b + g\rho_i s) \end{aligned}$$

or

$$\nabla s = -(\rho_w / \rho_i - 1) \nabla b$$

and find, as expected, that the basal slope is about 9 times larger and of opposite sign to the surface slope.

our water mass conservation equation (14.33) can then be written as

$$\partial_t h_w - \nabla \cdot (k h_w \nabla(\Phi + \Upsilon)) = a_w \quad (14.41)$$

or as

$$\partial_t h_w - \nabla \cdot (k h_w \nabla \Phi) - \nabla \cdot (\kappa h_w \nabla h_w) = a_w \quad (14.42)$$

where

$$\kappa := g(\rho_w - \rho)k$$

Equation (14.41) is similar (or even identical?) to Eq. (27) in Buehler (2015).

We define the water velocity as

$$\mathbf{v}_w := -k \nabla \Phi \quad (14.43)$$

and write

$$\partial_t h_w + \nabla \cdot (h_w \mathbf{v}_w) - \nabla \cdot (\kappa h_w \nabla h_w) = a_w \quad (14.44)$$

which now has the form of an advection-diffusion equation. The diffusion term is non-linear.

We now have two flux terms, the velocity flux

$$\mathbf{q}_v = k h_w \mathbf{v}_w ,$$

which is related to the ice-sheet potential Φ , and the diffusion flux term

$$\mathbf{q}_D = -\kappa h_w \nabla h_w .$$

Both fluxes depend on the evolving water layer thickness h_w .

There are different possible finite-element formulations possible, depending on whether we use the form pure diffusion form (14.41), or the advection-diffusion from (14.44). Both forms are mathematically equal.

The finite-element formulation of (14.41) is

$$\langle \partial_t h_w | \psi \rangle + \langle k h_w \nabla \Phi + \kappa h_w \nabla h_w | \nabla \psi \rangle = \langle a_w | \psi \rangle \quad (14.45)$$

where integral formula (B.3) has been applied to the two diffusion terms. The natural boundary condition is therefore the no-flux condition.

The finite-element formulation of (14.44) is

$$\langle \partial_t h_w | \psi \rangle + \langle \nabla \cdot (h_w \mathbf{v}_w) | \psi \rangle + \langle \kappa h_w \nabla h_w | \nabla \psi \rangle = \langle a_w | \psi \rangle \quad (14.46)$$

where we have used Eq. B.3, and the additional boundary-integral term is

$$\oint_{\partial\Omega} \psi \kappa h_w (\nabla h_w \cdot \hat{\mathbf{n}}) d\Gamma$$

and

$$h_w (\nabla h_w \cdot \hat{\mathbf{n}}) = 0 ,$$

is therefore the natural boundary condition. Using the natural boundary conditions sets the diffusive flux to zero along the boundary where it is applied. In finite-element context the

$$-\langle \nabla \cdot (k h_w \nabla \Phi) | \psi \rangle$$

either needs to be calculated using at least second-order finite-elements, or either $\mathbf{v}_w := -k \nabla \Phi$ is calculated outside of the element-assembly loop and projected onto the nodes ahead of assembly, and the term is evaluated as

$$\langle \nabla \cdot (h_w \mathbf{v}_w) | \psi \rangle$$

The steady-state solution of the differential equation (14.41) have some properties that might at first appear surprising. For example, if $\mathbf{v}_w = 0$ and $a_w = 0$ then, we must have

$$\nabla \cdot (\kappa h_w \nabla h_w) = 0$$

which requires either $h_w = 0$ or $\nabla h_w = \mathbf{0}$. If we force $h_w > 0$ at the boundary, the diffusive boundary flux out of the boundary is zero despite prescribing finite thickness as a Dirichlet boundary condition.

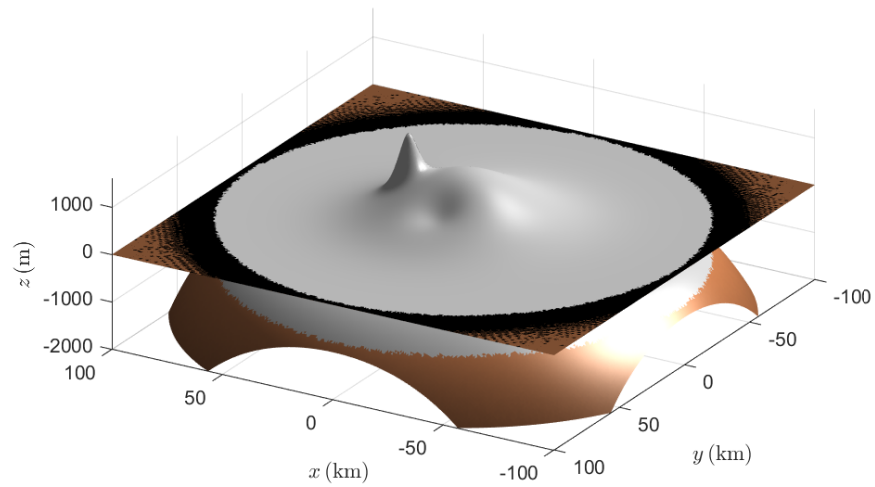


Figure 14.4: Geometry.

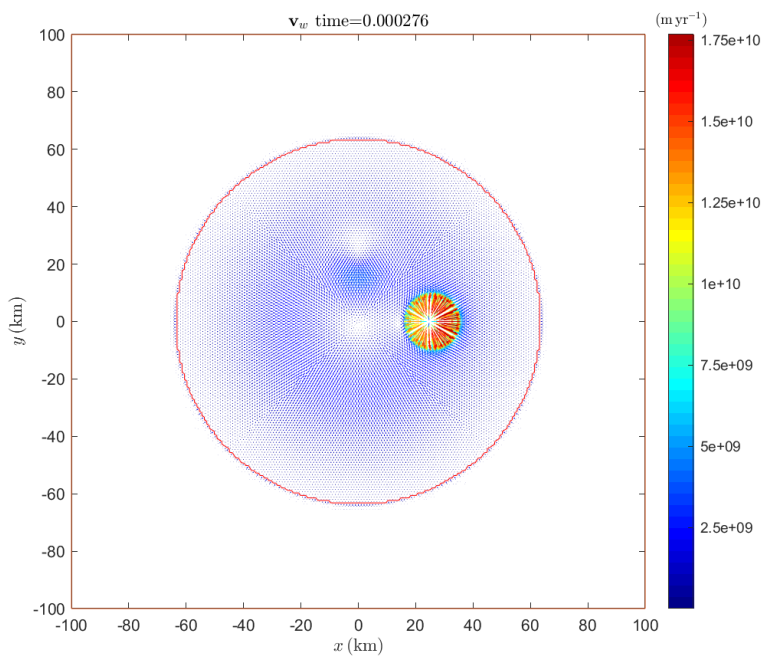


Figure 14.5: Velocities.

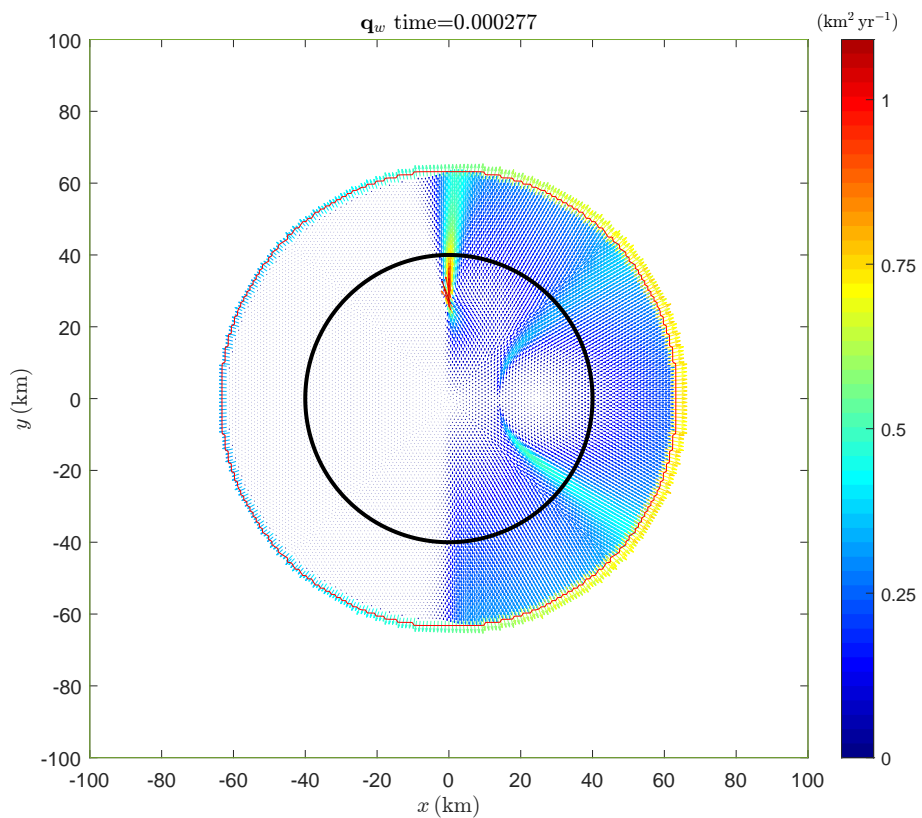


Figure 14.6: Flux. The analytical flux value was $Q = 25.502 \text{ km}^3/\text{yr}$ and numerical steady-state value was $Q = 25.560 \text{ km}^3/\text{yr}$

Chapter 15

Time scales

The *Volume time scale*, t_V is the time it takes to fill the perturbation in steady-state ice volume following a perturbation in, for example, surface mass balance (Jóhannesson, 1992). That is

$$t_V = \frac{\Delta V}{\Delta q}$$

This is a very general concept that can be applied to various situations to provide a lower estimate of the response time t_R . The volume time scale is, hence,

$$t_V = \frac{\text{change in volume following a perturbation}}{\text{change in flux into that volume}}$$

15.1 Alpine glaciers

Here

$$t_V = \frac{\Delta V}{A_0 \Delta a}$$

where A_0 is the original steady state glacier area, Δa is the perturbation in surface mass balance, and ΔV is the change in volume between the initial and final steady states.

In steady state the integrated surface mass balance is zero and therefore to first order

$$\Delta A a_t + A_0 \Delta a = 0$$

where a_t is the mass balance at the terminus. Again to first order

$$\Delta V = \partial_A V \Delta A$$

and therefore

$$\begin{aligned} t_V &:= \frac{\Delta V}{A_0 \Delta a} \\ &= \frac{\partial_A V \Delta A}{A_0 \Delta a} \\ &= -\frac{\partial_A V \Delta A}{\Delta A a_t} \\ &= -\frac{\partial_A V}{a_t} \end{aligned}$$

Jóhannesson's estimate for alpine glaciers is

$$\partial_A V = h_{eq}$$

where h_{eq} is the ice thickness as the equilibrium line, gives Jóhannesson's volume time scale

$$t_V = -\frac{h_{eq}}{a_t}$$

He further showed that

$$t_d, t_p \ll t_V$$

where t_d and t_p are diffusion and propagation time scales associated with local mass redistribution of mass and therefore

$$t_r \approx t_V$$

where t_r is the response time to external perturbation.

15.2 Marine ice sheets

Here we consider a perturbation to surface mass balance being balanced by changes in flux across the grounding line, and therefore to first order

$$\Delta a A_0 + \partial_A q \Delta A = 0$$

where q is the vertically integrated flux across the grounding line (for example $q = uhw$ where u is velocity, h ice thickness, and w the width) or if we consider a flow line

$$\Delta a l_0 + \partial_x q \Delta l = 0$$

Hence, in a flow line situation

$$\begin{aligned} t_V &= -\frac{w \partial_x V \Delta l}{w \Delta l \partial_x q} \\ &= -\frac{\partial_x V}{\partial_x q} \end{aligned}$$

showing that $t_V \rightarrow \infty$ when $\partial_x q \rightarrow 0$ as expected.

Chapter 16

The Shallow Ice Approximation (SIA)

The shallow ice approximation is one of the most commonly used approximations to describe the flow of large ice masses such as ice sheets, ice caps and alpine glaciers. As with other such theories (e.g. the shallow ice shelf approximation), there are two key assumptions, one relating to the geometry of the ice and the other to the stresses within the ice.

16.1 Scaling assumptions

The geometrical assumption is that the horizontal span of the body of ice is large compared to its thickness. This is the assumption of shallowness and we write this as

$$\frac{[z]}{[x]} = \varepsilon \quad (16.1)$$

where $\varepsilon \ll 1$ is some small number, and the square brackets around the symbols denote typical sizes, or scales, of those quantities. For example $[z]$ stands here for a vertical dimension of the ice (ice thickness), and $[x]$ for a typical horizontal dimension (horizontal span). Eq. 16.1 expresses the assumption that typical ice thickness is much smaller than typical horizontal span. These scales also show us how one quantity scales with another. For example, the typical surface slope, $[\alpha]$, must increase with increasing $[z]$ and decrease with decreasing $[x]$. We express this by saying that $[\alpha]$ scales as $[z]/[x]$ and, furthermore, since we have assumed that $[z]/[x]$ is small, we note that $[\alpha]$ will also be small. We write this as

$$[\alpha] = \frac{[z]}{[x]} = \varepsilon$$

The assumption about the stresses is based on our expectation that the stresses will be approximately equal to the stresses we calculated for the uniformly inclined slab in Chapter. (??). There we found that the pressure, p , is $p = \rho g(s - z)$ and $\tau_{xz} = \rho g(s - b) \sin(\alpha)$, where s and b are the upper and lower ice surfaces, respectively.

Note that here, and in contrast to the analysis done in sec. (??), the analysis is done in a basis $\{\hat{\mathbf{e}}_k\}$ where the basis vectors $\hat{\mathbf{e}}_1$ and $\hat{\mathbf{e}}_2$ are in the horizontal, and the $\hat{\mathbf{e}}_3$ is vertical and pointing upwards, i.e. the gravity vector \mathbf{g} is $\mathbf{g} = -g\hat{\mathbf{e}}_3$. Therefore we do not expect these expressions for the pressure and the vertical shear stress to be strictly correct in the more general case where we have a gently undulating bed geometry and spatially variable surface slope. However, we surmise that for sufficiently small surface slopes and slowly undulating bed and surface geometries, the relative sizes between, for example, the pressure p and the shear stress τ_{xz} will scale in the same way, i.e.

$$[\tau_{xz}] = [\alpha][p] .$$

We can also write this as

$$[\tau_{xz}] = \rho g[z][z]/[x] = \rho g[z]\varepsilon = [p]\varepsilon$$

Expressions of this type can be manipulated algebraically to, for example, show that $[z]\rho g = [\tau_{xz}]\varepsilon^{-1}$. Again motivated by the analytical solutions for the uniformly inclined slab, we expect horizontal deviatoric stresses to be smaller than the shear stress τ_{xz} . For the uniformly inclined slab the horizontal deviatoric

stresses were all identical to zero. Here we simply assume that they are much smaller than the vertical shear stresses, and this we can express, as

$$[\tau_{xx}] = \varepsilon [\tau_{xz}] ,$$

and similarly for the other horizontal deviatoric stresses. Note that we are here using the same number ε again, but that we have, at least at this stage, no clear guidance as to how large these horizontal deviatoric stresses can become, or if they do indeed scale linearly with the vertical shear stresses.

Our final scaling assumption relates to the horizontal velocity components u , v and the vertical velocity component w . While we will see below that this scaling relationship can be derived by requiring either the mass conservation or the kinematic boundary condition to be invariant under our scaling, we simply state here that we assume the vertical velocity component to be small in comparison and to scale with the horizontal velocities, i.e.

$$\frac{[w]}{[u]} = \varepsilon .$$

Summarizing, our scaling assumptions so far are:

$$\frac{[z]}{[x]} = \varepsilon \quad \text{and} \quad \frac{[y]}{[x]} = 1 \quad (16.2)$$

$$\frac{[w]}{[u]} = \varepsilon \quad \text{and} \quad \frac{[v]}{[u]} = 1 \quad (16.3)$$

$$\frac{[\tau_{xx}]}{\tau_{xz}} = \varepsilon \quad \text{and} \quad [\tau_{xx}] = [\tau_{yy}] = [\tau_{zz}] = [\tau_{xy}] \quad \text{and} \quad [\tau_{xz}] = [\tau_{yz}] \quad (16.4)$$

$$\frac{[\tau_{xz}]}{[p]} = \varepsilon \quad (16.5)$$

There is one final scaling assumption that we need. Although, this assumptions is possibly more correctly described as a statement about balances. We are here using a rheological law on the form $\dot{\epsilon} = A\tau^n$ (listed in more detail below) and in particular that $\dot{\epsilon}_{xz} = A\tau^{n-1}\tau_{xz}$ and similarly that $\dot{\epsilon}_{yz} = A\tau^{n-1}\tau_{yz}$ and we, again motivated by the solution for the uniformly inclined plane, want vertical shear stresses to balance vertical shear strain rates, i.e.

$$\frac{[u]}{[z]} = [A\tau]^n .$$

This is a statement about the balance between stresses, velocities and distance scales and implies, for example, that

$$\frac{[A\tau^n][x]}{[u]} = \varepsilon^{-1} .$$

16.2 Governing equations

We start with the general form of the mass and momentum equations for incompressible flow at low Reynolds numbers. For completeness we list these here.

$$\partial_x u + \partial_y v + \partial_z w = 0 , \quad (16.6)$$

$$\partial_x \tau_{xx} + \partial_y \tau_{xy} + \partial_z \tau_{xz} = \partial_x p , \quad (16.7)$$

$$\partial_x \tau_{xy} + \partial_y \tau_{yy} + \partial_z \sigma_{yz} = \partial_y p , \quad (16.8)$$

$$\partial_x \tau_{xz} + \partial_y \tau_{yz} + \partial_z \tau_{zz} = \partial_z p + \rho g . \quad (16.9)$$

We assume the upper surface is 'free', i.e. not stresses are applied to the surface and its geometry can evolve with time. The kinematic boundary condition and the stress condition at the upper surface are therefore

$$\begin{aligned} \partial_t s + u \partial_x s + v \partial_y s - w &= a_s, & (\text{at } z = s(x, y)) , \\ \boldsymbol{\sigma} \cdot \hat{\mathbf{n}} &= \mathbf{0} & (\text{at } z = s(x, y)) . \end{aligned}$$

For the lower surface the kinematic boundary condition reads

$$\partial_t b + u \partial_x b + v \partial_y b - w = -a_b, \quad (\text{at } z = s(x, y)).$$

It is often assumed that the geometry of the lower surface does not change with time and that the basal melt can be ignored, in which case $\partial_t b = 0$ and $a_b = 0$. The resulting form of the kinematic boundary condition, $u \partial_x b + v \partial_y b - w = 0$, is then referred to as the 'no-penetration' condition. We assume a power-law relationship between the bed-tangential component of the basal traction

$$\mathbf{t}_b = \boldsymbol{\sigma} \hat{\mathbf{n}} - (\hat{\mathbf{n}}^T \cdot \boldsymbol{\sigma} \hat{\mathbf{n}}) \hat{\mathbf{n}},$$

and basal velocity

$$\mathbf{v}_b = \mathbf{v} - (\hat{\mathbf{n}}^T \cdot \mathbf{v}) \hat{\mathbf{n}},$$

on the form

$$\mathbf{v}_b = c \| \mathbf{t}_b \|^{m-1} \mathbf{t}_b \quad (\text{at } z = s(x, y)), \quad (16.10)$$

where $\hat{\mathbf{n}}$ being a unit normal vector to the bed pointing into the ice. Finally we have the flow law

$$\dot{\epsilon}_{ij} = A \tau^{n-1} \tau_{ij},$$

where A and n are rheological parameters, and

$$\tau^2 = \tau_{kl} \tau_{kl} / 2,$$

is the effective stress.

16.3 Scaling the equations

Scaling the equations involves replacing all physical variables with their non-dimensional counterparts. We use the notation

$$\phi = [\phi] \phi^*,$$

where ϕ is the original dimensional quantity appearing in the governing equations, $[\phi]$ is its scale, and ϕ^* is the non-dimensional scaled counterpart. Generally, by introducing these scales, we expect the non-dimensional scaled variables all to be comparable in sizes and ranges, with the relative sizes of the original dimensional variables expressed through their respective scales. We write for example

$$\begin{aligned} x &= [x] x^*, \\ y &= [y] y^*, \\ z &= [z] z^*. \end{aligned}$$

For ice caps and ice sheets, for example, we can think of $[x]$ and $[y]$ to be on the order of 1000 km, and $[z]$ to be on the order of 1 km, and both x^* and z^* to range from 0 to 1. Hence, x^* and z^* are in this sense comparable in size and range, while $[x]$ and $[z]$ are not.

Scaling the mass-conservation equation (16.6) we find

$$\frac{[u]}{[x]} \frac{\partial u^*}{\partial x^*} + \frac{[v]}{[y]} \frac{\partial v^*}{\partial y^*} + \frac{[w]}{[z]} \frac{\partial w^*}{\partial z^*} = 0$$

or

$$\frac{[u]}{[x]} \frac{\partial u^*}{\partial x^*} + \frac{[u]}{[x]} \frac{\partial v^*}{\partial y^*} + \frac{\varepsilon[u]}{\varepsilon[x]} \frac{\partial w^*}{\partial z^*} = 0$$

and therefore the scaled mass-conservation equation has the same form as the original equation, i.e.

$$\frac{\partial u^*}{\partial x^*} + \frac{\partial v^*}{\partial y^*} + \frac{\partial w^*}{\partial z^*} = 0.$$

Scaling the x component of the momentum equation (16.7) leads to

$$\frac{[\tau_{xx}]}{[x]} \frac{\partial \tau_{xx}^*}{\partial x^*} + \frac{[\tau_{xy}]}{[y]} \frac{\partial \tau_{xy}^*}{\partial y^*} + \frac{[\tau_{xz}]}{[z]} \frac{\partial \tau_{xz}^*}{\partial z^*} = \frac{[p]}{[x]} \frac{\partial p^*}{\partial x^*}$$

or

$$\frac{[\varepsilon \tau_{xz}]}{[x]} \frac{\partial \tau_{xx}^*}{\partial x^*} + \frac{[\varepsilon \tau_{xz}]}{[x]} \frac{\partial \tau_{xy}^*}{\partial y^*} + \frac{[\tau_{xz}]}{\varepsilon[x]} \frac{\partial \tau_{xz}^*}{\partial z^*} = \frac{\varepsilon^{-1} [\tau_{xz}]}{[x]} \frac{\partial p^*}{\partial x^*}$$

and therefore

$$\varepsilon^2 \frac{\partial \tau_{xx}^*}{\partial x^*} + \varepsilon^2 \frac{\partial \tau_{xy}^*}{\partial y^*} + \frac{\partial \tau_{xz}^*}{\partial z^*} = \frac{\partial p^*}{\partial x^*}$$

Scaling the y component, Eq (16.8), similarly gives

$$\varepsilon^2 \frac{\partial \tau_{xy}^*}{\partial x^*} + \varepsilon^2 \frac{\partial \tau_{yy}^*}{\partial y^*} + \frac{\partial \tau_{yz}^*}{\partial z^*} = \frac{\partial p^*}{\partial y^*} .$$

And for the z component of the momentum equation, (16.13), we find

$$\frac{[\tau_{xz}]}{[x]} \frac{\partial \tau_{xz}^*}{\partial x^*} + \frac{[\tau_{yz}]}{[y]} \frac{\partial \tau_{yz}^*}{\partial y^*} + \frac{[\tau_{zz}]}{[z]} \frac{\partial \tau_{zz}^*}{\partial z^*} = \frac{[p]}{[z]} \frac{\partial p^*}{\partial z^*}$$

or that

$$\frac{[\tau_{xz}]}{[x]} \frac{\partial \tau_{xz}^*}{\partial x^*} + \frac{[\tau_{xz}]}{[x]} \frac{\partial \tau_{yz}^*}{\partial y^*} + \frac{[\varepsilon \tau_{xz}]}{\varepsilon [x]} \frac{\partial \tau_{zz}^*}{\partial z^*} = \frac{[p]}{\varepsilon [x]} \frac{\partial p^*}{\partial z^*} + \frac{[\tau_{xz}]}{\varepsilon^2 [x]} \rho g$$

observing that $[\tau_{xz}] = \rho g [z] \varepsilon$ implies $\rho g = \varepsilon^{-2} [\tau_{xz}] [x]$, and therefore

$$\frac{[\tau_{xz}]}{[x]} \frac{\partial \tau_{xz}^*}{\partial x^*} + \frac{[\tau_{xz}]}{[x]} \frac{\partial \tau_{yz}^*}{\partial y^*} + \frac{\varepsilon [\tau_{xz}]}{\varepsilon [x]} \frac{\partial \tau_{zz}^*}{\partial z^*} = \frac{\varepsilon^{-1} [\tau_{xz}]}{\varepsilon [x]} \frac{\partial p^*}{\partial z^*} + \frac{[\tau_{xz}]}{\varepsilon^2 [x]} \rho g$$

giving

$$\varepsilon^2 \frac{\partial \tau_{xz}^*}{\partial x^*} + \varepsilon^2 \frac{\partial \tau_{yz}^*}{\partial y^*} + \varepsilon^2 \frac{\partial \tau_{zz}^*}{\partial z^*} = \frac{\partial p^*}{\partial z^*} + \rho g .$$

Summarizing, the scaled momentum equations are

$$\begin{aligned} \varepsilon^2 \frac{\partial \tau_{xx}^*}{\partial x^*} + \varepsilon^2 \frac{\partial \tau_{xy}^*}{\partial y^*} + \frac{\partial \tau_{xz}^*}{\partial z^*} &= \frac{\partial p^*}{\partial x^*} \\ \varepsilon^2 \frac{\partial \tau_{xy}^*}{\partial x^*} + \varepsilon^2 \frac{\partial \tau_{yy}^*}{\partial y^*} + \frac{\partial \tau_{yz}^*}{\partial z^*} &= \frac{\partial p^*}{\partial y^*} \\ \varepsilon^2 \frac{\partial \tau_{xz}^*}{\partial x^*} + \varepsilon^2 \frac{\partial \tau_{yz}^*}{\partial y^*} + \varepsilon^2 \frac{\partial \tau_{zz}^*}{\partial z^*} &= \frac{\partial p^*}{\partial z^*} + \rho g \end{aligned}$$

Dropping all but the leading terms, the SIA momentum equations are

$$\frac{\partial \tau_{xz}^*}{\partial z^*} = \frac{\partial p^*}{\partial x^*} , \quad (16.11)$$

$$\frac{\partial \tau_{yz}^*}{\partial z^*} = \frac{\partial p^*}{\partial y^*} , \quad (16.12)$$

$$0 = \frac{\partial p^*}{\partial z^*} + \rho g , \quad (16.13)$$

and, as it happens, these are correct to second order, i.e. there are no first-order terms.

Following the same procedure we find that the kinematic boundary condition is unchanged under the scalings, and that the basal sliding law takes the form

$$\begin{aligned} u_b^* &= C \tau^{*m-1} \tau_{xz}^{*m} , \\ v_b^* &= C \tau^{*m-1} \tau_{yz}^{*m} , \end{aligned}$$

where $\tau^{2*} = (\tau_{xz}^{*2} + \tau_{yz}^{*2})$, and the stress condition at the upper surface is

$$\tau_{xz}^* = \tau_{yz}^* = 0 .$$

16.4 SIA solutions

Once we've done the scaling analysis we revert back to our original dimensional variables. The scaling analysis has served its purpose and provided us with the leading-order equations.

The resulting system of equation is so simple that provided the rheological properties of ice are spatially uniform, i.e. A and n do not vary in space, we can solve for both velocities and stresses. From (16.13), which reads

$$0 = \frac{\partial p}{\partial z} + \rho g ,$$

and using the boundary conditions we find that

$$p = \rho g (s - z) ,$$

and inserting this expression for the pressure p into

$$\begin{aligned} \frac{\partial \tau_{xz}}{\partial z} &= \frac{\partial p}{\partial x} , \\ \frac{\partial \tau_{yz}}{\partial z} &= \frac{\partial p}{\partial y} , \end{aligned}$$

and integrating over depth, we find that

$$\begin{aligned} \tau_{xz} &= -\rho g \partial_x s (s - z) \\ \tau_{yz} &= -\rho g \partial_y s (s - z) \end{aligned}$$

and that the effective stress is

$$\tau = \rho g \left((\partial_x s)^2 + (\partial_y s)^2 \right)^{1/2} (s - z) .$$

Using the flow law we can now calculate the strain rates and the deformational velocities through a vertical integration, arriving at

$$(u, v) = -E \|\nabla_{xy} s\|^{n-1} (h^{n+1} - (s - z)^{n+1}) (\partial_x s, \partial_y s) ,$$

where

$$E = \frac{2A}{n+1} (\rho g)^n .$$

These solutions provide us with the stresses and velocities as function of local thickness and surface slope.

Chapter 17

Shallow Ice Stream Approximation (STREAM/SSA)

The shallow ice stream approximation is one of the classical scaling theories in glaciology. It plays a fundamental role in the study of ice stream dynamics. The resulting equations are often referred to as the MacAyeal equations (MacAyeal, 1989) but I will here refer to these equations as the *shallow-ice-stream equations* (STREAM). Other commonly-used names for the resulting approximation of glacier flow are the *shallow ice shelf approximation*(SSA), and *the shelfy approximation*. These equations have been derived numerous times in various papers and doctoral thesis, (e.g. Morland, 1987; Muszynski and Birchfield, 1987; MacAyeal, 1989; Baral, 1999; Schoof, 2006). One will find reading the literature that there are many different ways of deriving the equations.

17.1 Field equations and boundary conditions

The field equations are

$$v_{i,i} = 0 \quad (\text{mass}) \quad (17.1)$$

$$\sigma_{ki,k} + \rho b_i = 0 \quad (\text{linear momentum}) \quad (17.2)$$

$$\sigma_{ij} - \sigma_{ji} = 0 \quad (\text{angular momentum}) \quad (17.3)$$

where v_i are the components of the velocity vector, σ_{ij} the components of the full stress tensor (i.e. the Cauchy stress tensor), and ρ the ice density.

In addition we have the kinematic boundary conditions

$$\frac{\partial s}{\partial t} + u \frac{\partial s}{\partial x} + v \frac{\partial s}{\partial y} - w = a \quad (17.4)$$

valid at the surface $z = s(x, y)$, where a is the accumulation rate, and we have used u , v , and w to denote the x , y , and z components of the velocity vector, respectively. There is a corresponding equation valid at the glacier sole. At the glacier sole both the accumulation rate and the rate of elevation can often be ignored. The kinematic boundary condition is then usually referred to as the ‘no-penetration condition’.

The relation between strain rates and stresses is taken to be

$$\dot{\epsilon}_{ij} = A(T) \tau^{n-1} \tau_{ij}. \quad (17.5)$$

where A is the rate factor and n the stress exponent. Furthermore, τ_{ij} are the deviatoric stress components

$$\tau_{ij} = \sigma_{ij} - \delta_{ij} \sigma_{kk}/3,$$

$\dot{\epsilon}_{ij}$ are the components of the deformation rate tensor (the stretching tensor), and τ is *effective stress* (the square root of the (negative of the) second invariant of the deviatoric stress tensor), i.e.

$$\tau = \sqrt{\tau_{ij} \tau_{ij}/2}.$$

Eq. (17.5) is the well-known Glen-Steinemann law (Steinemann, 1954, 1958a,b; Glen, 1955). Outside of glaciology it is better known as the Norton-Hoff rheology model, or simply as power-law rheology. An increasingly popular alternative description of ice rheology can be found in Goldsby and Kohlstedt (2001).

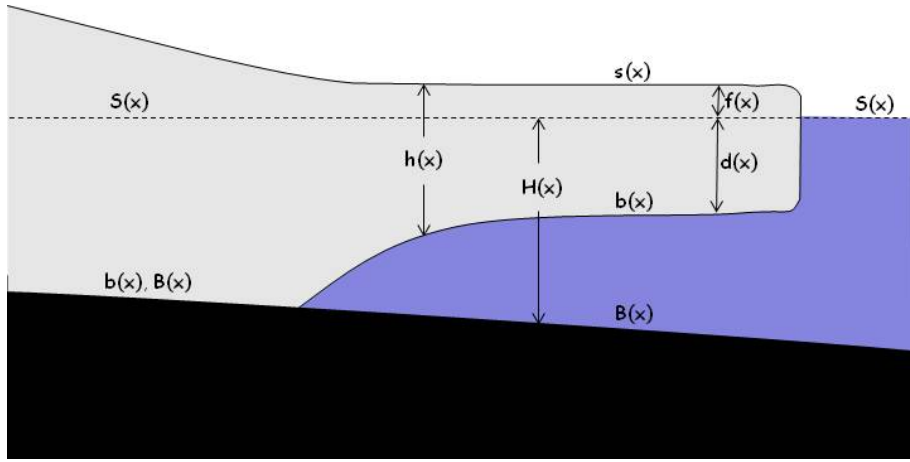


Figure 17.1: Problem geometry.

In the situation when the glacier slides over its bed various theoretical arguments show that we have a mixed-type basal boundary condition to consider of the type

$$\mathbf{t}_b = \mathbf{f}(\mathbf{v}_b)$$

where \mathbf{f} is some function, \mathbf{t}_b is the basal stress vector given by

$$\mathbf{t}_b = \sigma \hat{\mathbf{n}} - (\hat{\mathbf{n}}^T \cdot \sigma \hat{\mathbf{n}}) \hat{\mathbf{n}},$$

with $\hat{\mathbf{n}}$ being a unit normal vector to the bed pointing into the ice, and \mathbf{v}_b is the basal sliding velocity

$$\mathbf{v}_b = \mathbf{v} - (\hat{\mathbf{n}}^T \cdot \mathbf{v}) \hat{\mathbf{n}}.$$

Sometimes a power-law type sliding law

$$\mathbf{v}_b = c |\mathbf{t}_b|^{m-1} \mathbf{t}_b, \quad (17.6)$$

is used, but the correctness of this assumption is debated. The function c is referred to as the basal slipperiness. The sliding law (17.6) is usually referred to as Weertman sliding law. Alternative forms of Weertman sliding law are

$$|\mathbf{v}_b| = c |\mathbf{t}_b|^m,$$

and

$$\mathbf{t}_b = c^{-1/m} |\mathbf{v}_b|^{(1-m)/m} \mathbf{v}_b.$$

17.2 Definition of scales

In the following we will perform scaling analysis of all relevant equations. In general we write for any variable X

$$X = [X] X^*$$

where $[X]$ is the scale and X^* the dimensionless counterpart to X . We do this to all variables entering the problem. The idea is that the sizes of all dimensionless variables are comparable, and that the relative sizes of two variables can be deduced from comparing their respective scales.

The SSTREAM scalings are motivated by three observations:

First, horizontal span is much larger than thickness. The ratio between ice thickness and horizontal span is therefore small compared to unity.

Second, most of the forward motion of ice streams is due to sliding. It is not uncommon for the slip ratio, defined as the ratio between forward motion due to basal motion to forward motion due to shearing throughout the ice, to be on the order of 100 to 1000. Hence, basal and surface velocities are about equal, and one can use the same scale for both of them.

Third, on ice streams and ice shelves vertical shearing is small compared to longitudinal stretching, and vertical shear stresses small compared to horizontal deviatoric stresses. In particular, one can expect

that horizontal strain rates are ‘balanced’ by the horizontal deviatoric stresses.¹ What is meant by ‘balancing’ different quantities will become clear in what follows.

Motivated by these observations we now consider the case of an ice stream with horizontal length scale $[x]$ and vertical length scale $[z]$ where the shallow ice approximation $[z]/[x] = \delta \ll 1$ holds, and write

$$(x, y, z) = [x](x^*, y^*, \delta z^*).$$

where the asterisks denote scaled dimensionless variables.

For the mass conservation equation ($v_{i,i} = 0$) to be invariant we scale the velocity as

$$(u, v, w) = [u](u^*, v^*, \delta w^*). \quad (17.7)$$

If we furthermore require the kinematic boundary condition at the surface

$$\partial_t s + u \partial_x s + v \partial_y s - w = a,$$

where s is the surface to be invariant under the scalings we must have

$$a = \delta[u]a^*,$$

where a is the accumulation rate. Thus the scale for a is $[a] = \delta[u] = [w]$, which seems reasonable as we can expect the vertical velocity to scale with accumulation rate for small surface slopes. We also find, using the same invariant requirement for the surface kinematic boundary condition, that the time must be scaled as

$$t = [x][u]^{-1}t^*.$$

For $[x] \sim 1000$ km, and a vertical dimension of 100 m to 1 km, we have δ in the range of 0.001 to 0.01. Horizontal velocities can be expected to be on the order of a 100 m a^{-1} and w around 0.1 to 1 m a^{-1} , giving the same range of δ . The time scale $[t] = [x][u]^{-1}$ is therefore on the order of 1 to 10 ka.

We assume that the velocity is of same order across the whole ice thickness. In particular we assume that the horizontal components of the basal sliding velocity (u_b and v_b) are of the same order as the surface velocity, i.e.

$$(u_b, v_b) = [u](u_b^*, v_b^*) \quad (17.8)$$

We are considering a situation where the vertical shear components are small compared to all other stress components. A set of scalings for the stresses which reflects this situation is

$$\begin{aligned} &(\sigma_{xx}, \sigma_{yy}, \sigma_{zz}, \tau_{xy}, \tau_{xz}, \tau_{yz}) \\ &= [\sigma](\sigma_{xx}^*, \sigma_{yy}^*, \sigma_{zz}^*, \tau_{xy}^*, \delta\tau_{xz}^*, \delta\tau_{yz}^*). \end{aligned} \quad (17.9)$$

Same scale is used for the pressure, that is $p = [\sigma]p^*$. For the time being, we do not specify how the scale $[\sigma]$ relates to other variables entering the problem.

Note that we are assuming a ratio between vertical and horizontal dimensions equal to that of the vertical and horizontal deviatoric stresses, so for example

$$\delta = \frac{[z]}{[x]} = \frac{[\tau_{xz}]}{[\tau_{xx}]}.$$

In other words, the *aspect ratio*, $[z]/[x]$, is the same as the *stress ratio*, $[\tau_{xz}]/[\tau_{xx}]$.

17.3 Scaling the equations

The analysis is done in a coordinate system which is tilted forward in x direction by the angle α . The equilibrium equations are

$$\begin{aligned} \partial_x \sigma_{xx} + \partial_y \tau_{xy} + \partial_z \tau_{xz} &= -\rho g \sin \alpha, \\ \partial_x \tau_{xy} + \partial_y \sigma_{yy} + \partial_z \sigma_{yz} &= 0, \\ \partial_x \tau_{xz} + \partial_y \sigma_{yz} + \partial_z \sigma_{zz} &= \rho g \cos \alpha. \end{aligned}$$

¹Note that this situation contracts sharply with what is found on most alpine glaciers, ice sheets and ice caps, where rates of ice deformation due to shearing dominate horizontal strain rates (except for the top most layer). In this case normal deviatoric stresses are small compared to the shear stress and the normal stress field close to being isotropic.

The above listed scalings give

$$[\sigma][x]^{-1}\partial_{x^*}\sigma_{xx}^* + [\sigma][x]^{-1}\partial_{y^*}\tau_{xy}^* + [\sigma]\delta[x]^{-1}\delta^{-1}\partial_{z^*}\tau_{xz}^* = -\rho g \sin \alpha,$$

$$[\sigma][x]^{-1}\partial_{x^*}\tau_{xy}^* + [\sigma][x]^{-1}\partial_{y^*}\sigma_{yy}^* + [\sigma]\delta[x]^{-1}\delta^{-1}\partial_{z^*}\sigma_{yz}^* = 0,$$

$$[\sigma][x]^{-1}\delta\partial_{x^*}\tau_{xz}^* + [\sigma][x]^{-1}\delta\partial_{y^*}\sigma_{yz}^* + [\sigma][x]^{-1}\delta^{-1}\partial_{z^*}\sigma_{zz}^* = \rho g \cos \alpha,$$

which can be written as

$$\partial_{x^*}\sigma_{xx}^* + \partial_{y^*}\tau_{xy}^* + \partial_{z^*}\tau_{xz}^* = -\rho g[x][\sigma]^{-1} \sin \alpha, \quad (17.10)$$

$$\partial_{x^*}\tau_{xy}^* + \partial_{y^*}\sigma_{yy}^* + \partial_{z^*}\sigma_{yz}^* = 0, \quad (17.11)$$

$$\delta^2\partial_{x^*}\tau_{xz}^* + \delta^2\partial_{y^*}\sigma_{yz}^* + \partial_{z^*}\sigma_{zz}^* = \rho g\delta[x][\sigma]^{-1} \cos \alpha, \quad (17.12)$$

If we now fix the scale $[\sigma]$ for the stresses as

$$[\sigma] = \rho g[z] = \rho g\delta[x], \quad (17.13)$$

we arrive at

$$\partial_{x^*}\sigma_{xx}^* + \partial_{y^*}\tau_{xy}^* + \partial_{z^*}\tau_{xz}^* = -\delta^{-1} \sin \alpha, \quad (17.14)$$

$$\partial_{x^*}\tau_{xy}^* + \partial_{y^*}\sigma_{yy}^* + \partial_{z^*}\sigma_{yz}^* = 0, \quad (17.15)$$

$$\delta^2\partial_{x^*}\tau_{xz}^* + \delta^2\partial_{y^*}\sigma_{yz}^* + \partial_{z^*}\sigma_{zz}^* = \cos \alpha. \quad (17.16)$$

For the two terms on the right-hand side of the above set of equations to be of order unity we must furthermore require

$$\alpha = O(\delta),$$

i.e. the tilt angle α of the coordinate system must be small. Hence, the angle α is not arbitrary. (As we will see below, and as is to be expected, the shear stress τ_{xz} scales with $\rho g[z] \sin \alpha$ so for it to be small in comparison to the stress scale $\rho g[z]$, α must be small.)

Note that the stress scale must be $[\sigma] = \rho g[z] = \rho g\delta[x]$ for the right-hand side term in Eq. (17.12) to be of order unity for $\alpha = 0$. We could have defined this to be the stress scale from the outset, but doing so would have obscured the fact that this stress scale is required for the vertical gradient of the vertical stresses (i.e. $\partial_z\sigma_{zz}$) to be balanced by the vertical component of the body force (i.e. $-\rho g$) for $\alpha = 0$. Furthermore, note that had we defined the stress scale to be the product of thickness and mean slope, i.e. $[\sigma] = \rho g[z][z]/[x] = \rho g\delta[x]\delta[x]/[x] = \rho g[x]\delta^2$, the right-hand term in Eq. (17.16) would have been on the order of δ^{-1} for $\alpha = 0$, with no term on the left-hand side of that equation to match that term.

If we only consider terms of zeroth order and drop terms of order δ and higher, we arrive at a reduced system where the horizontal gradients of the vertical shear stresses are omitted from the equilibrium equations. There are no first-order terms in the scaled equilibrium equations ((17.14) to (17.16)), and the resulting reduced system is therefore correct to second order. Despite no first-order terms appearing in the scaled equilibrium equations, it does of course not follow that none of the quantities entering these equations are of first order. The vertical shear stresses, τ_{xz} and τ_{yz} , are, for example, of first order.

17.3.1 Sliding law

We assume a power-law relationship between basal shear stress

$$\mathbf{t}_b = \boldsymbol{\sigma} \hat{\mathbf{n}} - (\hat{\mathbf{n}}^T \cdot \boldsymbol{\sigma} \hat{\mathbf{n}}) \hat{\mathbf{n}},$$

and basal velocity

$$\mathbf{v}_b = \mathbf{v} - (\hat{\mathbf{n}}^T \cdot \mathbf{v}) \hat{\mathbf{n}}.$$

or

$$\mathbf{v}_b = c \|\mathbf{t}_b\|^{m-1} \mathbf{t}_b, \quad (17.17)$$

where $\hat{\mathbf{n}}$ being a unit normal vector to the bed pointing into the ice. The scaling of the basal sliding law is done in Appendix A. We find that the components of the scaled basal shear stress vector are given by

$$t_{bx} = [\sigma](\delta\partial_{x^*}b^*(\sigma_{zz}^* - \sigma_{xx}^*) - \delta\partial_{y^*}b^*\tau_{xy}^* + \delta\tau_{xz}^*) + O(\delta^3), \quad (17.18)$$

$$t_{by} = [\sigma](\delta\partial_{y^*}b^*(\sigma_{zz}^* - \sigma_{yy}^*) - \delta\partial_{x^*}b^*\tau_{xy}^* + \delta\sigma_{yz}^*) + O(\delta^3), \quad (17.19)$$

$$t_{bz} = [\sigma](\delta^2((\sigma_{zz}^* - \sigma_{xx}^*)(\partial_{x^*}b^*)^2 + (\sigma_{zz}^* - \sigma_{yy}^*)(\partial_{y^*}b^*)^2 - 2\tau_{xy}^*\partial_{x^*}b^*\partial_{y^*}b^* + \tau_{xz}^*\partial_{x^*}b^* + \sigma_{yz}^*\partial_{y^*}b^*)) + O(\delta^4). \quad (17.20)$$

We see from the above listed equations that the x and y components of the shear stresses vector are of order δ , and that therefore the length of that vector is also of order δ , i.e.

$$\|\mathbf{t}_b\| = O(\delta). \quad (17.21)$$

Hence

$$\begin{aligned} \|\mathbf{t}_b\| &= [\|\mathbf{t}_b\|] |\mathbf{t}_b^*| \\ &= \delta[\sigma] |\mathbf{t}_b^*|. \end{aligned}$$

or

$$[\|\mathbf{t}_b\|] = \delta[\sigma]$$

The scaled basal sliding velocity (\mathbf{v}_b) is

$$\mathbf{v}_b = [u] \begin{pmatrix} u_b^* + O(\delta^2) \\ v_b^* + O(\delta^2) \\ \delta u_b^* \partial_{x^*} b^* + \delta v_b^* \partial_{y^*} b^* + O(\delta^3) \end{pmatrix} \quad (17.22)$$

We have not yet specified the scale $[c]$ for the parameter c in the sliding law but we have already introduced scales for the velocity and the stresses, so by inserting (17.7), (17.13), and (17.24) into (17.17) we arrive at

$$\begin{aligned} [u] u_b^* &= c \|\mathbf{t}_b\|^{m-1} |\mathbf{t}_b^*|^{m-1} [t_{bx}] t_{bx}^* \\ &= c \delta^{m-1} [\sigma]^{m-1} |\mathbf{t}_b^*|^{m-1} \delta[\sigma] t_{bx}^* \\ &= c \delta^m [\sigma]^m |\mathbf{t}_b^*|^{m-1} t_{bx}^* \end{aligned}$$

or

$$u_b^* = c \delta^m [\sigma]^m [u]^{-1} |\mathbf{t}_b^*|^{m-1} t_{bx}^*. \quad (17.23)$$

If we want the sliding velocity to be balanced by the basal shear stress, terms on both side of Eq. (17.23) must be of same order, hence

$$c \delta^m [\sigma]^m [u]^{-1} = O(1).$$

If we write

$$c = [c] c^*, \quad (17.24)$$

then

$$[c] = \delta^{-m} [u] [\sigma]^{-m}. \quad (17.25)$$

Eq. (17.25) shows that c is of the order δ^{-m} . In this sense the slipperiness (c) must be ‘large’ for the theory to be consistent.

The product $c[\sigma]^m$ is the (typical) basal sliding velocity, while $[u]$ is the (typical) surface velocity. Hence, Eq. (17.25) simply reflects the condition that for ‘most’ of the forward motion to be due to basal sliding, the basal slipperiness c must be ‘large’. As an example, if $\partial_x b = \partial_y b = 0$ we find that

$$u^* = c^* \tau_{xz}^{*m}.$$

In principle we could have observed right at the beginning that defining the vertical shear stress components to be of $O(\delta)$ and $u = O(1)$ implies $c = O([u][\sigma]^{-m} \delta^{-m})$ for a basal sliding law of the form $u_b = c \tau_b^m$ if u_b is to be of same order as u .

For the z component of the sliding law obtain using Eq. (17.20) and Eq. (17.22)

$$\begin{aligned} \delta u^* \partial_{x^*} b^* + \delta v^* \partial_{y^*} b^* &= c \|\mathbf{t}_b\|^{m-1} \\ [\sigma] (\delta^2 ((\sigma_{zz}^* - \sigma_{xx}^*) (\partial_{x^*} b^*)^2 + (\sigma_{zz}^* - \sigma_{yy}^*) (\partial_{y^*} b^*)^2 - 2\tau_{xy}^* \partial_{x^*} b^* \partial_{y^*} b^* + \tau_{xz}^* \partial_{x^*} b^* \partial_{y^*} b^* + \sigma_{yz}^* \partial_{y^*} b^*)). \end{aligned} \quad (17.26)$$

Note that the sum of the two terms on the left-hand-side as given by Eqs. (17.18) and (17.19) gives the left-hand side of (17.26), so these equations are consistent. Note furthermore that the vertical component w does not enter the sliding law. The vertical component must be calculated from the basal kinematic boundary condition ($u \partial_x b + v \partial_y b - w = 0$).

Flow law

The flow law can be either written as

$$\dot{\epsilon}_{ij} = A(T) \tau^{n-1} \tau_{ij}, \quad (17.27)$$

or alternatively as

$$\tau_{ij} = A^{-1/n} \dot{\epsilon}^{(1-n)/n} \dot{\epsilon}_{ij},$$

where $\dot{\epsilon} = \sqrt{\dot{\epsilon}_{ij} \dot{\epsilon}_{ij}/2}$ is the *effective strain rate*, and T the englacial temperature.

We have so far not discussed the scalings for the normal deviatoric stresses τ_{xx}^* , τ_{yy}^* , and τ_{zz}^* . These scalings follow directly from the fact that we decided above to scale both the normal stresses (σ_{xx} , σ_{xx} σ_{xx}) and the pressure with $[\sigma]$. Because $\tau_{xx} = \sigma_{xx} + p = [\sigma](\sigma_{xx}^* + p^*) = [\sigma]\tau_{xx}^*$ and similarly for the other components we have

$$(\tau_{xx}, \tau_{yy}, \tau_{zz}) = [\sigma](\tau_{xx}^*, \tau_{yy}^*, \tau_{zz}^*).$$

The square root of the second invariant of the deviatoric stress tensor, or what glaciologist usually refer to as the *effective stress*, is thus

$$\tau = [\sigma] \sqrt{(\tau_{xx}^{*2} + \tau_{yy}^{*2} + \tau_{zz}^{*2})/2 + \tau_{xy}^{*2} + \delta^2(\tau_{xz}^{*2} + \tau_{yz}^{*2})}, \quad (17.28)$$

and therefore

$$[\tau] = [\sigma] \quad (17.29)$$

and

$$\tau = [\sigma]\tau^*$$

where

$$\tau^* = \sqrt{(\tau_{xx}^{*2} + \tau_{yy}^{*2} + \tau_{zz}^{*2})/2 + \tau_{xy}^{*2} + \delta^2(\tau_{xz}^{*2} + \tau_{yz}^{*2})}. \quad (17.30)$$

The effective stress τ is of order unity.

Using the flow law and the incompressibility condition we find

$$0 = v_{i,i} = \dot{\epsilon}_{ii} = \tau_{ii}$$

and

$$\tau_{zz}^2 = (\tau_{xx} + \tau_{yy})^2$$

which can be used to eliminate τ_{zz} from Eq. (17.30).

We now look at the relation between the individual components of the stretching tensor (the strain rates) and the deviatoric stress tensor. We find, for example, that

$$\dot{\epsilon}_{xx} = A\tau^{n-1}\tau_{xx},$$

is in scaled variables

$$[u][x]^{-1}\dot{\epsilon}_{xx}^* = [\sigma]^n A\tau^{*n-1}\tau_{xx}^*.$$

or

$$\dot{\epsilon}_{xx}^* = A[\sigma]^n [x][u]^{-1}\tau^{*n-1}\tau_{xx}^*. \quad (17.31)$$

where

$$\dot{\epsilon}_{xx}^* = \partial_{x^*} u^*$$

If we want the horizontal strain rates ($\dot{\epsilon}_{xx}$, $\dot{\epsilon}_{xy}$, and $\dot{\epsilon}_{yy}$) to be balanced by the corresponding horizontal deviatoric stresses, we must require that both sides of Eq. (17.31) are of same order implying

$$A[\sigma]^n [x][u]^{-1} = O(1).$$

Writing

$$A = [A]A^*,$$

therefore leads to

$$[A] = [u][x]^{-1}[\sigma]^{-n}. \quad (17.32)$$

Next we look at

$$\dot{\epsilon}_{xz} = A\tau^{n-1}\tau_{xz},$$

and find that this gives

$$[u][x]^{-1}(\delta^{-1}\partial_z^* u^* + \delta\partial_{x^*} w^*) = \delta[\sigma]^n A\tau^{*^{n-1}}\tau_{xz}^*,$$

which we can also write as

$$\begin{aligned} \partial_z^* u^* + \delta^2 \partial_{x^*} w^* &= \delta^2 [x][\sigma]^n [u]^{-1} A\tau^{*^{n-1}}\tau_{xz}^* \\ &= \delta^2 A^* \tau^{*^{n-1}}\tau_{xz}^*, \end{aligned}$$

Note that here we are using the scale for A given by (17.32). We must equate terms of same order, and hence find that

$$\partial_z^* u^* = O(\delta^2),$$

and

$$\partial_{x^*} w^* = [x][\sigma]^n [u]^{-1} A\tau^{*^{n-1}}\tau_{xz}^*.$$

We have now reached the important conclusion that the *horizontal velocity component u is independent of depth to second order*. Same argument shows that the other horizontal component v is also independent of depth. Thus, to second order the horizontal velocity components u and v are both independent of z .

We have shown that consistency with the scalings used for stresses requires $\partial_z u$ to be $O(\delta^2)$. Note that we have NOT shown vertical shearing ($\dot{\epsilon}_{xz}$) to be zero. Both $\partial_x w$ and τ_{xz} enter the field equations as first order terms.

The incompressibility conditions states that

$$\partial_{x^*} u^* + \partial_{y^*} v^* + \partial_{z^*} w^* = 0.$$

Differentiating with respect to z , and assuming that the order of differentiation can be changed, gives

$$\partial_{x^* z^*}^2 u^* + \partial_{y^* z^*}^2 v^* + \partial_{z^* z^*}^2 w^* = 0.$$

From which using $\partial_{z^*} u^* = \partial_{z^*} v^* = O(\delta^2)$ it follows that

$$\partial_{z^* z^*}^2 w^* = O(\delta^2)$$

Hence, *to second order $\dot{\epsilon}_{zz}$ is independent of depth and the vertical velocity varies linearly with depth*.

It turns out to be more convenient working with the flow law in the form

$$\tau_{ij} = 2\eta\dot{\epsilon}_{ij}$$

where η is the *effective viscosity* defined as

$$\eta = \frac{1}{2} A^{-1/n} \dot{\epsilon}^{(1-n)/n}.$$

Towards this end we determine the effective strain rate

$$\begin{aligned} \dot{\epsilon} &= \sqrt{(\dot{\epsilon}_{xx}^2 + \dot{\epsilon}_{yy}^2 + \dot{\epsilon}_{zz}^2)/2 + \dot{\epsilon}_{xy}^2 + \dot{\epsilon}_{xz}^2 + \dot{\epsilon}_{yz}^2} \\ &= \sqrt{(\dot{\epsilon}_{xx}^2 + \dot{\epsilon}_{yy}^2 + (\dot{\epsilon}_{xx} + \dot{\epsilon}_{yy})^2)/2 + \dot{\epsilon}_{xy}^2 + \dot{\epsilon}_{xz}^2 + \dot{\epsilon}_{yz}^2}. \end{aligned}$$

Inserting $\dot{\epsilon}_{ij} = (v_{i,j} + v_{j,i})/2$ and using the fact that $\partial_z u = O(\delta^2)$ and $\partial_z v = O(\delta^2)$ we find

$$\begin{aligned} \dot{\epsilon} &= [u][x]^{-1}((\partial_{x^*} u^*)^2 + (\partial_{y^*} v^*)^2 + \partial_{x^*} u^* \partial_{y^*} v^* + (\partial_{x^*} v^* + \partial_{y^*} u^*)^2/4 \\ &\quad + (\delta\partial_{x^*} w^* + O(\delta^2))^2/4 + (\delta\partial_{y^*} w^* + O(\delta^2))^2/4)^{1/2} \\ &= [u][x]^{-1}\sqrt{(\partial_{x^*} u^*)^2 + (\partial_{y^*} v^*)^2 + \partial_{x^*} u^* \partial_{y^*} v^* + (\partial_{x^*} v^* + \partial_{y^*} u^*)^2/4} + O(\delta^2), \end{aligned}$$

or

$$\dot{\epsilon} = \sqrt{(\partial_x u)^2 + (\partial_y v)^2 + \partial_x u \partial_y v + (\partial_x v + \partial_y u)^2/4} + O(\delta^2). \quad (17.33)$$

Slip ratio

We can write the horizontal velocity component u as the sum

$$u = u_b + u_d$$

where u_d is the *deformational velocity*, and u_b the basal sliding velocity. The ratio

$$\gamma := \frac{u_b}{u_d}$$

between the basal sliding velocity and the deformational velocity is the *slip ratio*. Using the relationship for the basal velocity for a uniformly inclined slab with ice thickness h , i.e.

$$u_d = \frac{2A}{n+1} \tau^{n-1} \tau_{xz} h,$$

we find

$$[u_d] = [A][\tau]^{n-1}[\tau_{xy}][z] \quad (17.34)$$

$$= [u][x]^{-1}[\sigma]^{-n}[\sigma]^{n-1}\delta[\sigma]\delta[x] \quad (17.35)$$

$$= \delta^2[u], \quad (17.36)$$

where we have used Eqs. (17.21), (17.25), (17.29), and (17.32). Since $[u_b] = [u]$, we have

$$\gamma = \frac{[u_b]}{[u_d]} = O(\delta^{-2}). \quad (17.37)$$

Note that we did not specify from the outset that the sliding velocity had to be large as compared to the deformational velocity, so (17.37) is a result rather than an assumption. It is worthwhile to think about how we arrived at the conclusion that the slip ratio is of order δ^{-2} . By assuming that the horizontal deviatoric stresses are large compared to vertical shear stresses (see Eq. 17.9), and by balancing the horizontal strain rates with the horizontal deviatoric stresses (see Eq. 17.31), we arrived at a scale for the rate factor A (see Eq. 17.32). We furthermore assumed that the basal sliding velocity was of the same order as the surface velocity (see Eq. 17.8), i.e. of order unity. We then found the basal stress to be of order δ (see Eq. 17.21), and by requiring a balance between the basal sliding velocity and the basal stress implied by the sliding law, we arrived at a scale for the basal slipperiness c (see Eq. 17.25). It then follows, as shown above, that the slip ratio is of order δ^{-2} .

We also have

$$\frac{[c]}{[A]} = \frac{\delta^{-m}[u][\sigma]^{-m}}{[u][x]^{-1}[\sigma]^{-n}} = \delta^{-m}[x][\sigma]^{n-m}.$$

which puts constraints on the numerical value of c with respect to that of A . This can be interpreted as showing that c must be large compared to A . Of course these parameters can not be compared directly, as they have different physical dimensions, but if we, for example consider the case $n = m$, we can write this as

$$\frac{[c]}{[A]} = \delta^{-n-1}[z]$$

showing that $[c] \gg [A]$.

Implications of different balances for the slip ratio

When finding the scale $[u_d]$ (see (17.35)) we used the fact that the effective stress (τ) is of order unity (see Eq. 17.29). In the absence of any significant horizontal deviatoric stresses however, the effective stress would be of order δ and $[u_d]/[u] = O(\delta^{n+1})$. If the ice is not subjected to horizontal deviatoric stresses of order unity, we can still balance horizontal strain rates with the horizontal deviatoric stresses as we did above to arrive at $[A]$. However, in that case it seems more logical to balance the vertical shear strain rates and the vertical shear stresses to arrive at a (different) scale for A .

Furthermore, had we not assumed the aspect ratio and the stress ratio to be equal, but instead written

$$\frac{[z]}{[x]} = \varepsilon \quad \text{and} \quad \frac{[\tau_{xz}]}{[\tau_{xx}]} = \delta,$$

with ε now being the aspect ratio, and δ as ‘stress’ ratio, we would have found that

$$\begin{aligned}[u_d] &= [A][\sigma]^{n-1}\delta[\sigma][z] \\ &= [u][\sigma]^{-n}[x]^{-1}[\sigma]^{n-1}\delta[\sigma]\varepsilon[x] \\ &= [u]\delta\varepsilon,\end{aligned}$$

i.e.

$$\frac{[u_d]}{[u]} = \varepsilon \delta.$$

Remember that the scaling originally introduced for velocity was in terms of the basal sliding velocity, and that therefore in fact

$$\frac{[u_d]}{[u_b]} = \varepsilon \delta,$$

which is the inverse of the slip ratio. We see that for any given aspect ratio ε , the slip ratio ($[u_b]/[u_d]$) becomes small as the stress ratio δ goes to infinity, corresponding to the situation where horizontal deviatoric stresses are small compared to vertical shear stresses.

17.4 The SSTREAM (zeroth-order) equations

Now that we have scaled all equations we can collect terms to the desired order and go back to dimensional quantities.

Note that in the field equations and all the boundary conditions, first order terms are all identically equal to zero. Although we only collect zeroth order terms, the first order correction is zero and the theory is therefore correct to second order in δ .

17.4.1 Boundary conditions

The upper boundary is free. This implies that the surface traction is zero, or

$$\boldsymbol{\sigma}\hat{\mathbf{n}} = \mathbf{0},$$

which to second order reads

$$-\sigma_{xx}\partial_x s - \tau_{xy}\partial_y s + \tau_{xz} = 0, \quad (17.38)$$

$$-\tau_{xy}\partial_x s - \sigma_{yy}\partial_y s + \tau_{yz} = 0, \quad (17.39)$$

$$\sigma_{zz} = 0, \quad (17.40)$$

for $z = s(x, y)$.

Along the lower surface the traction is not zero as the ocean exerts normal stress, but the bed tangential component of the traction is assumed to be

$$\partial_x b(\sigma_{zz} - \sigma_{xx}) - \partial_y b\tau_{xy} + \tau_{xz} = t_{bx}, \quad (17.41)$$

$$\partial_y b(\sigma_{zz} - \sigma_{yy}) - \partial_x b\tau_{xy} + \tau_{yz} = t_{by}. \quad (17.42)$$

$$\sigma_{zz} = -p_w \quad (17.43)$$

for $z = b(x, y)$, where \mathbf{t}_b is provided by a sliding law. This boundary condition along the lower surface is a mixed boundary condition where neither the stresses nor the velocities are prescribed, but rather the relationship between them as

$$u_b = C \|\mathbf{t}_b\|^{m-1} t_{bx}, \quad (17.44)$$

$$v_b = C \|\mathbf{t}_b\|^{m-1} t_{by}, \quad (17.45)$$

We could use the z component of the sliding law to calculate w_b . But since the sliding law is fully consistent with the no-penetration condition (see for example Eq. 17.26), it is easier to determine w_b as a function of u_b and v_b and the bed geometry directly using the no-penetration condition.

17.4.2 Field equations

To zeroth order we obtain from Eq. (17.14) to (17.16)

$$\partial_x \sigma_{xx} + \partial_y \tau_{xy} + \partial_z \tau_{xz} = -\rho g \sin \alpha \quad (17.46)$$

$$\partial_x \tau_{xy} + \partial_y \sigma_{yy} + \partial_z \tau_{yz} = 0, \quad (17.47)$$

$$\partial_z \sigma_{zz} = \rho g \cos \alpha. \quad (17.48)$$

Using $\tau_{ij} = 2\eta\dot{\epsilon}_{ij}$ and $\sigma_{ij} = \tau_{ij} - p\delta_{ij}$ we can also write this system as

$$-\partial_x p + 2\partial_x(\eta\dot{\epsilon}_{xx}) + 2\partial_y(\eta\dot{\epsilon}_{xy}) + 2\partial_z(\eta\dot{\epsilon}_{xz}) = -\rho g \sin \alpha, \quad (17.49)$$

$$-\partial_y p + 2\partial_x(\eta\dot{\epsilon}_{xy}) + 2\partial_y(\eta\dot{\epsilon}_{yy}) + 2\partial_z(\eta\dot{\epsilon}_{yz}) = 0, \quad (17.50)$$

$$-\partial_z p + 2\partial_z(\eta\dot{\epsilon}_{zz}) = \rho g \cos \alpha. \quad (17.51)$$

17.4.3 Vertical integration

We start by considering Eq. (17.48). Integrating from z to $z = s(x, y)$ gives

$$\sigma_{zz}(s) - \sigma_{zz}(z) = -(s - z)\rho g \cos \alpha. \quad (17.52)$$

From (17.40) we find $\sigma_{zz}(s) = 0$ so that

$$\sigma_{zz} = (z - s)\rho g \cos \alpha. \quad (17.53)$$

We now integrate Eq. (17.46) over the depth and use Leibniz' rule

$$\partial_x \int_{b(x)}^{s(x)} f(x, z) dz = \int_{b(x)}^{s(x)} \partial_x f(x, z) dz + f(x, s) \partial_x s - f(x, b) \partial_x b$$

to interchange the order of integration and differentiation, and find

$$\begin{aligned} -\rho g(s - b) \sin \alpha &= \partial_x \int_b^s \sigma_{xx} dz + \partial_y \int_b^s \tau_{xy} dz \\ &\quad - \sigma_{xx}(s) \partial_x s - \tau_{xy}(s) \partial_y s + \tau_{xz}(s) \\ &\quad + \sigma_{xx}(b) \partial_x b + \tau_{xy}(b) \partial_y b - \tau_{xz}(b). \end{aligned}$$

Note that we did not have to specify how τ_{xz} varies across the depth. Because of boundary condition (17.38) the second line is equal to zero. Using (17.41) we find that the third line can be written as $-t_{bx} + \partial_x b \sigma_{zz}(b)$ so that

$$-\rho g(s - b) \sin \alpha = \partial_x \int_b^s \sigma_{xx} dz + \partial_y \int_b^s \tau_{xy} dz - t_{bx} + \partial_x b \sigma_{zz}(b).$$

Since $p = \tau_{zz} - \sigma_{zz}$ and $\tau_{xx} + \tau_{yy} + \tau_{zz} = 0$ because ice is incompressible, we find that σ_{xx} can be written as

$$\begin{aligned} \sigma_{xx} &= \tau_{xx} - p \\ &= \tau_{xx} - \tau_{zz} + \sigma_{zz} \\ &= \tau_{xx} - (-\tau_{xx} - \tau_{yy}) + \sigma_{zz} \\ &= 2\tau_{xx} + \tau_{yy} + \sigma_{zz}. \end{aligned} \quad (17.54)$$

Because u and v are independent of depth it follows that τ_{xy} , τ_{xx} , and τ_{yy} are also all independent of depth. The corresponding vertical integrals are therefore simple to evaluate and we obtain

$$-\rho g h \sin \alpha = \partial_x \int_b^s \sigma_{zz} dz + \partial_x(h(2\tau_{xx} + \tau_{yy})) + \partial_y(h\tau_{xy}) - t_{bx} + \partial_x b \sigma_{zz}(b), \quad (17.55)$$

where $h = s - b$ is the ice thickness. We have already determined σ_{zz} (see Eq. (17.53)) and find that

$$\begin{aligned}\partial_x \int_b^s \sigma_{zz} dz &= \partial_x \int_b^s (z-s)\rho g \cos \alpha dz \\ &= \partial_x \left(-\frac{1}{2}(s-b)^2 \rho g \cos \alpha \right) \\ &= -(s-b)\rho g \cos \alpha (\partial_x s - \partial_x b) \\ &= \sigma_{zz}(b)(\partial_x s - \partial_x b),\end{aligned}$$

which when inserted into Eq. (17.55) gives

$$\partial_x(h(2\tau_{xx} + \tau_{yy})) + \partial_y(h\tau_{xy}) - t_{bx} = \partial_x s h \rho g \cos \alpha - \rho g h \sin \alpha.$$

We can express this result in terms of the components of the velocity vector using $\tau_{ij} = \eta(v_{i,j} + v_{j,i})$ and find that

$$\partial_x(4h\eta\partial_x u + 2h\eta\partial_y v) + \partial_y(h\eta(\partial_x v + \partial_y u)) - t_{bx} = \rho g h (\partial_x s \cos \alpha - \sin \alpha), \quad (17.56)$$

$$\partial_y(4h\eta\partial_y v + 2h\eta\partial_x u) + \partial_x(h\eta(\partial_y u + \partial_x v)) - t_{by} = \rho g h \partial_y s \cos \alpha, \quad (17.57)$$

where we have added the results for the y direction which follow in an identical manner.² The effective viscosity is

$$\eta = \frac{1}{2} A^{-1/n} \dot{\epsilon}^{(1-n)/n},$$

where

$$\dot{\epsilon} = \sqrt{(\partial_x u)^2 + (\partial_y v)^2 + \partial_x u \partial_y v + (\partial_x v + \partial_y u)^2 / 4}.$$

17.4.4 Tensor of restive stresses

In most modeling work the coordinate system is not tilted. For $\alpha = 0$ the vertically integrated form of the momentum equation in x and y directions is

$$\partial_x(h(2\tau_{xx} + \tau_{yy})) + \partial_y(h\tau_{xy}) - t_{bx} = \rho g h \partial_x s, \quad (17.60)$$

$$\partial_y(h(2\tau_{xx} + \tau_{yy})) + \partial_x(h\tau_{xy}) - t_{by} = \rho g h \partial_y s, \quad (17.61)$$

This system can written in a more compact form as

$$\nabla_{xy}^T \cdot (h \mathbf{R}) - \mathbf{t}_{bh} = \rho g h \nabla_{xy}^T s, \quad (17.62)$$

where

$$\mathbf{R} = \begin{pmatrix} 2\tau_{xx} + \tau_{yy} & \tau_{xy} \\ \tau_{xy} & 2\tau_{yy} + \tau_{xx} \end{pmatrix}, \quad (17.63)$$

is sometimes referred to as the *resistive stress tensor*, and

$$\nabla_{xy} = (\partial_x, \partial_y)^T,$$

and

$$\mathbf{t}_{bh} = \begin{pmatrix} t_{bx} \\ t_{by} \end{pmatrix}.$$

Note that as Eq. (17.54) shows

$$2\tau_{xx} + \tau_{yy} = \sigma_{xx} - \sigma_{zz}, \quad (17.64)$$

$$2\tau_{yy} + \tau_{xx} = \sigma_{yy} - \sigma_{zz}, \quad (17.65)$$

²If ρ is a function of x and y then $\partial_x \int_b^s \sigma_{zz} dz = \sigma_{zz}(b)\partial_x h - \frac{1}{2}h^2 g \cos \alpha \partial_x \rho$ and we have

$$\partial_x(4h\eta\partial_x u + 2h\eta\partial_y v) + \partial_y(h\eta(\partial_x v + \partial_y u)) - t_{bx} = \rho g h (\partial_x s \cos \alpha - \sin \alpha) + \frac{1}{2}h^2 g \cos \alpha \partial_x \rho, \quad (17.58)$$

$$\partial_y(4h\eta\partial_y v + 2h\eta\partial_x u) + \partial_x(h\eta(\partial_y u + \partial_x v)) - t_{by} = \rho g h \partial_y s \cos \alpha + \frac{1}{2}h^2 g \cos \alpha \partial_y \rho, \quad (17.59)$$

and the resistive stress tensor can therefore be written as

$$\mathbf{R} = \begin{pmatrix} \sigma_{xx} - \sigma_{zz} & \tau_{xy} \\ \tau_{xy} & \sigma_{yy} - \sigma_{zz} \end{pmatrix}. \quad (17.66)$$

The resistive stress tensor is neither equal to the deviatoric stress tensor or the Cauchy stress tensor. In the Shallow Ice Stream approximation, the deviatoric and the resistive stress tensors are both independent of depth, whereas the Cauchy stress tensor is not.

17.4.5 Weertman sliding law

If we use Weertman sliding law the components of basal shear stress, t_{bx} and t_{by} can be written in terms of the basal velocity as

$$t_{bx} = c^{-1/m} \|\mathbf{v}_b\|^{1/m-1} u, \quad (17.67)$$

$$t_{by} = c^{-1/m} \|\mathbf{v}_b\|^{1/m-1} v. \quad (17.68)$$

The sliding law is sometimes written as

$$t_{bx} = \beta^2 u, \quad (17.69)$$

$$t_{by} = \beta^2 v, \quad (17.70)$$

where

$$\beta = c^{-1/2m} \|\mathbf{v}_b\|^{\frac{1-m}{2m}}.$$

in which case we can also write the field equations as

$$\partial_x(4h\eta\partial_x u + 2h\eta\partial_y v) + \partial_y(h\eta(\partial_x v + \partial_y u)) - \beta^2 u = \rho gh(\partial_x s \cos \alpha - \sin \alpha), \quad (17.71)$$

$$\partial_y(4h\eta\partial_y v + 2h\eta\partial_x u) + \partial_x(h\eta(\partial_y u + \partial_x v)) - \beta^2 v = \rho gh\partial_y s \cos \alpha. \quad (17.72)$$

We now have a system of two partial differential equations that, given appropriate boundary conditions, can be solved for the velocity components u and v . Remember that in general both η and β^2 are functions of the strain rates and the velocity, respectively. The system is therefore non-linear and if solved numerically, some sort of appropriate iterative algorithm (e.g. Newton-Raphson) must be used.

17.5 The shallow ice shelf approximation (SSHELF)

The scaling analysis shown above applies to ice shelves as well. The only change we have to make is setting the basal shear stress to zero. There is no reason to do the analysis in a tilted coordinate system so we also set $\alpha = 0$. Thus for floating ice shelves we have

$$\partial_x(4h\eta\partial_x u + 2h\eta\partial_y v) + \partial_y(h\eta(\partial_x v + \partial_y u)) = \rho gh \partial_x s, \quad (17.73)$$

$$\partial_y(4h\eta\partial_y v + 2h\eta\partial_x u) + \partial_x(h\eta(\partial_y u + \partial_x v)) = \rho gh \partial_y s, \quad (17.74)$$

No stresses act at the upper boundary $z = s(x, y)$, and therefore the stress boundary conditions at the upper surface are (to second order) simply

$$-\sigma_{xx}\partial_x s - \tau_{xy}\partial_y s + \tau_{xz} = 0, \quad (17.75)$$

$$-\tau_{xy}\partial_x s - \sigma_{yy}\partial_y s + \tau_{yz} = 0, \quad (17.76)$$

$$\sigma_{zz} = 0. \quad (17.77)$$

The stress boundary conditions at the lower boundary $z = b(x, y)$ are

$$-\sigma_{xx}\partial_x b - \tau_{xy}\partial_y b + \tau_{xz} = p_w \partial_x b, \quad (17.78)$$

$$-\tau_{xy}\partial_x b - \sigma_{yy}\partial_y b + \tau_{yz} = p_w \partial_y b, \quad (17.79)$$

$$\sigma_{zz} = -p_w, \quad (17.80)$$

where

$$p_w = \rho_w g(S - b),$$

is the ocean pressure acting on the lower boundary of the ice shelf, with ρ_w denoting the ocean density.

We know that

$$\sigma_{zz} = \rho g(z - s), \quad (17.81)$$

and the boundary condition (17.80) therefore implies that

$$\rho g(s - b) = \rho_w g(S - b),$$

or

$$\rho g h = \rho_w g d.$$

One can now work out various other floating relationships, and one finds that where the glacier is afloat the following relations hold:

$$h = \rho_w d / \rho = \frac{s - S}{1 - \rho / \rho_w} = \frac{\rho_w}{\rho} (S - b), \quad (17.82)$$

$$b = \frac{\rho s - \rho_w S}{\rho - \rho_w} = S - \frac{\rho}{\rho_w} h, \quad (17.83)$$

$$s = S + (1 - \rho / \rho_w) h = (1 - \rho_w / \rho) b + \frac{\rho_w}{\rho} S, \quad (17.84)$$

$$f = (1 - \rho / \rho_w) h. \quad (17.85)$$

If $\partial_x S = 0$, the slopes of the upper and the lower boundary are related through

$$b \partial_x s + s \partial_x b = S \partial_x h, \quad (17.86)$$

and also

$$\partial_x s = (1 - \rho / \rho_w) \partial_x h. \quad (17.87)$$

The maximum ice thickness that an ice shelf can have without grounding is

$$h_f := \rho_w H / \rho.$$

Where

$$h \geq h_f,$$

the ice is grounded.

Using (17.87) in (17.73) and (17.74) gives

$$\partial_x (4h\eta\partial_x u + 2h\eta\partial_y v) + \partial_y (h\eta(\partial_x v + \partial_y u)) = \rho g(1 - \rho / \rho_w)h \partial_x h, \quad (17.88)$$

$$\partial_y (4h\eta\partial_y v + 2h\eta\partial_x u) + \partial_x (h\eta(\partial_y u + \partial_x v)) = \rho g(1 - \rho / \rho_w)h \partial_y h. \quad (17.89)$$

Expressed in terms of stresses these equations read

$$\partial_x (h(2\tau_{xx} + \tau_{yy})) + \partial_y (h\tau_{xy}) = \rho g(1 - \rho / \rho_w)h \partial_x h, \quad (17.90)$$

$$\partial_y (h(2\tau_{yy} + \tau_{xx})) + \partial_x (h\tau_{xy}) = \rho g(1 - \rho / \rho_w)h \partial_y h. \quad (17.91)$$

Using the definition of the resisting stress tensor (see Eq. 17.63) the equations can be written on a compact form as

$$\nabla_{xy}^T \cdot (h \mathbf{R}) = \varrho g h \nabla_{xy} h,$$

where

$$\varrho = \rho (1 - \rho / \rho_w).$$

17.5.1 Boundary conditions at the calving front

At the calving front, Γ_s , we require balance of vertically integrated horizontal stresses, i.e.

$$\int_b^s \boldsymbol{\sigma} \hat{\mathbf{n}}_{xy} = - \int_b^S p_w \hat{\mathbf{n}}_{xy} \quad \text{on } \Gamma_c,$$

where p_w is the hydrostatic ocean pressure, and

$$\hat{\mathbf{n}}_{xy} = (n_x, n_y, 0)^T, \quad (17.92)$$

is a unit normal pointing horizontally outward from the ice front. In x and y directions this stress condition is

$$\int_b^s (\sigma_{xx} n_x + \tau_{xy} n_y) dz = - \int_b^S p_w n_x dz \quad \text{on } \Gamma_c, \quad (17.93)$$

$$\int_b^s (\tau_{xy} n_x + \sigma_{yy} n_y) dz = - \int_b^S p_w n_y dz \quad \text{on } \Gamma_c. \quad (17.94)$$

If the draft d at the ice front is zero, i.e. if the ice front is fully grounded, then $S < b$, the right-hand sides of (17.93) and (17.94) are to be set to zero.

Because σ_{xx} can be written as

$$\sigma_{xx} = 2\tau_{xx} + \tau_{yy} + \sigma_{zz},$$

(see Eq. 17.54), and

$$\sigma_{zz} = -\rho g(s - z),$$

within the ice, we find that

$$\begin{aligned} \int_b^s \sigma_{xx} dz &= \int_b^s (2\tau_{xx} + \tau_{yy}) dz - \int_b^s \rho g(s - z) dx \\ &= h(2\tau_{xx} + \tau_{yy}) - \frac{\rho g}{2} h^2 \end{aligned}$$

The x component of the vertically integrated ocean pressure acting on the calving front is

$$\begin{aligned} - \int_b^S p_w n_x dz &= - \int_b^S \rho_w g(S - z) n_x dz \\ &= -\frac{1}{2} \rho_w g (S - b)^2 \\ &= -\frac{1}{2} \rho_w g d^2 \end{aligned}$$

Boundary conditions (17.93) and (17.94) can therefore be written as

$$h(2\tau_{xx} + \tau_{yy}) n_x + h\tau_{xy} n_y = \frac{g}{2}(\rho h^2 - \rho_w d^2) n_x \quad (17.95)$$

$$h(2\tau_{yy} + \tau_{xx}) n_y + h\tau_{xy} n_x = \frac{g}{2}(\rho h^2 - \rho_w d^2) n_y \quad (17.96)$$

or more compactly as

$$\mathbf{R} \hat{\mathbf{n}}_c = \frac{g}{2h}(\rho h^2 - \rho_w d^2) \hat{\mathbf{n}}_c \quad (17.97)$$

where

$$\hat{\mathbf{n}}_c = (n_x, n_y)^T, \quad (17.98)$$

is a unit normal to the calving front.

In arriving at (17.95) and (17.96) we have not specified any particular relationship between ice shelf thickness (h) and ice shelf draft (d). These boundary conditions therefore apply to both grounded and floating ice edges.

If the ice at the calving front is afloat, then h and d are related through the floating condition $\rho h = \rho_w d$. In that case boundary conditions (17.95) and (17.96) take the form

$$h(2\tau_{xx} + \tau_{yy}) n_x + h\tau_{xy} n_y = \frac{1}{2} \varrho g h^2 n_x, \quad (17.99)$$

$$h(2\tau_{yy} + \tau_{xx}) n_y + h\tau_{xy} n_x = \frac{1}{2} \varrho g h^2 n_y, \quad (17.100)$$

where

$$\varrho := \rho(1 - \rho/\rho_w),$$

or again more compactly using the resistive stress tensor as

$$\mathbf{R} \hat{\mathbf{n}}_c = \frac{1}{2} \varrho g h \hat{\mathbf{n}}_c. \quad (17.101)$$

On the other hand if the ice terminates on land then $d = 0$ and

$$h(2\tau_{xx} + \tau_{yy})n_x + h\tau_{xy}n_y = \frac{g}{2}\rho h^2 n_x, \quad (17.102)$$

$$h(2\tau_{yy} + \tau_{xx})n_y + h\tau_{xy}n_x = \frac{g}{2}\rho h^2 n_y. \quad (17.103)$$

or

$$\mathbf{R} \hat{\mathbf{n}}_c = \frac{1}{2}\rho gh \hat{\mathbf{n}}_c. \quad (17.104)$$

Written in terms of the velocity components the boundary conditions along a floating ice front are:

$$\eta h(4\partial_x u + 2\partial_y v)n_x + \eta h(\partial_x v + \partial_y u)n_y = \frac{\varrho gh^2}{2}n_x, \quad (17.105)$$

$$\eta h(\partial_x v + \partial_y u)n_x + \eta h(4\partial_y v + 2\partial_x u)n_y = \frac{\varrho gh^2}{2}n_y. \quad (17.106)$$

17.5.2 Ice Shelf Buttressing

The vertically integrated condition on stresses at the calving front is

$$\int_b^s \boldsymbol{\sigma}_h \hat{\mathbf{n}}_c dz = - \int_b^S p_w \hat{\mathbf{n}}_c dz \quad \text{on } \Gamma_c, \quad (17.107)$$

where the subscript h on the Cauchy stress tensor implies that we are only considering the horizontal stress components, that is

$$\boldsymbol{\sigma}_h = \begin{pmatrix} \sigma_{xx} & \tau_{xy} \\ \tau_{xy} & \sigma_{yy} \end{pmatrix}. \quad (17.108)$$

We denote the left-hand by \mathbf{t}_i (traction on ice side) and those of the right-hand side by \mathbf{t}_o (traction on ocean side), that is

$$\mathbf{t}_i = \int_b^s \boldsymbol{\sigma}_h \hat{\mathbf{n}}_c dz \quad \text{on } \Gamma_c$$

and

$$\mathbf{t}_o = - \int_b^S p_w \hat{\mathbf{n}}_c dz \quad \text{on } \Gamma_c,$$

and find as shown above that

$$\mathbf{t}_i = h\mathbf{R} \hat{\mathbf{n}}_c - \frac{1}{2}\rho gh^2 \hat{\mathbf{n}}_c$$

and

$$\mathbf{t}_o = - \frac{1}{2}\rho_w d^2 \hat{\mathbf{n}}_c = - \frac{1}{2} \frac{\rho}{\rho_w} \rho gh^2 \hat{\mathbf{n}}_c$$

For (17.107) to hold, i.e.

$$\mathbf{t}_i = \mathbf{t}_o$$

it follows that

$$\mathbf{R} \hat{\mathbf{n}}_c = \frac{1}{2}\varrho gh \hat{\mathbf{n}}_c \quad (17.109)$$

Eq. (17.109) is a boundary condition for the resistive stress tensor valid along a floating calving front. Within an ice shelf, and along the grounding line, the resistive stress tensor will in general not fulfill this condition.

We can define ice-shelf buttressing as the impact of the ice shelf on the stress regime along the grounding line. Note that in the absence of an ice shelf, and assuming that the ice front at the grounding line is exactly at flotation, the ice front will be in a direct contact with the ocean. To quantify the impact of the ice shelf on stresses at the grounding line we must therefore compare the stresses along the grounding line to those caused by the ocean pressure. More specifically, if we denote the vertically integrated horizontal traction along the grounding with \mathbf{t}_{gl} , i.e.

$$\mathbf{t}_{gl} = \int_b^s \boldsymbol{\sigma}_h \hat{\mathbf{n}}_c dz \quad \text{on } \Gamma_{gl} \quad (17.110)$$

the buttressing, \mathbf{B} , is by definition

$$\mathbf{B} = \mathbf{t}_o - \mathbf{t}_{gl}. \quad (17.111)$$

The normal and tangential components of the buttressing vector \mathbf{B} are

$$B_n = \hat{\mathbf{n}}_{\text{gl}}^T \cdot (\mathbf{t}_o - \mathbf{t}_{\text{gl}}) \quad (17.112)$$

$$= -\frac{1}{2} \frac{\rho}{\rho_w} \rho g h^2 - h \hat{\mathbf{n}}_{\text{gl}} \cdot (\mathbf{R} \hat{\mathbf{n}}_c) + \frac{1}{2} \rho g h^2 \quad (17.113)$$

$$= \frac{1}{2} \varrho g h^2 - h \hat{\mathbf{n}}_{\text{gl}}^T \cdot \mathbf{R} \hat{\mathbf{n}}_{\text{gl}} \quad (17.114)$$

and

$$B_t = \hat{\mathbf{m}}_{\text{gl}}^T \cdot (\mathbf{t}_o - \mathbf{t}_{\text{gl}}) \quad (17.115)$$

$$= 0 - h \hat{\mathbf{m}}_{\text{gl}}^T \cdot (\mathbf{R} \hat{\mathbf{n}}_{\text{gl}}) + 0 \quad (17.116)$$

$$= h \hat{\mathbf{m}}_{\text{gl}}^T \cdot (\mathbf{R} \hat{\mathbf{n}}_{\text{gl}}) \quad (17.117)$$

where $\hat{\mathbf{m}}_{\text{gl}}$ is a unit vector in the horizontal plane tangential to the grounding line and $\hat{\mathbf{m}}_{\text{gl}}^T \cdot \hat{\mathbf{n}}_{\text{gl}} = 0$.

If we want to non-dimentionalise expressions (17.114) and (17.117) then we can do so in a number of different ways. We could for example normalize with the vertically integrated ocean pressure $|\mathbf{t}_o| = \frac{1}{2} \rho_w g d^2$, or we could normalize using the magnitude of vertically integrated resistive stresses at a calving front, i.e. $h \|\mathbf{R} \hat{\mathbf{n}}_c\| = \frac{1}{2} \varrho g h^2$. In ice shelves, and along grounding lines, horizontal deviatoric stresses are typically on the order of $\varrho g h$ and much smaller than $\rho g d$ and we therefore opt for the second option and define dimensionless normal and tangential buttressing numbers as

$$K_N = \frac{\hat{\mathbf{n}}_{\text{gl}}^T \cdot (\mathbf{t}_o - \mathbf{t}_{\text{gl}})}{h \hat{\mathbf{n}}_c^T \cdot \mathbf{R} \hat{\mathbf{n}}_c} \quad (17.118)$$

$$= \frac{\frac{1}{2} \varrho g h - \hat{\mathbf{n}}_{\text{gl}}^T \cdot \mathbf{R} \hat{\mathbf{n}}_{\text{gl}}}{\frac{1}{2} \varrho g h} \quad (17.119)$$

$$= 1 - \frac{2 \hat{\mathbf{n}}_{\text{gl}}^T \cdot \mathbf{R} \hat{\mathbf{n}}_{\text{gl}}}{\varrho g h} \quad (17.120)$$

and

$$K_T = \frac{\hat{\mathbf{m}}_{\text{gl}}^T \cdot (\mathbf{t}_o - \mathbf{t}_{\text{gl}})}{h \hat{\mathbf{n}}_c^T \cdot \mathbf{R} \hat{\mathbf{n}}_c} \quad (17.121)$$

$$= \frac{2 \hat{\mathbf{m}}_{\text{gl}}^T \cdot \mathbf{R} \hat{\mathbf{n}}_{\text{gl}}}{\varrho g h}. \quad (17.122)$$

These are the same buttressing numbers as used by Gudmundsson (2013).³ Several other ways of quantifying ice-shelf buttressing have been used in the literature. See for example Reese et al. (2018).

³If we normalize with the (absolute value) of the vertically integrated ocean pressure

$$T'_N = \frac{\frac{1}{2} \varrho g h^2 - h \hat{\mathbf{n}}_c^T \mathbf{R} \hat{\mathbf{n}}_c}{\frac{1}{2} \rho_w g d^2},$$

then $T'_N = -1$ for a fully grounded calving front, whereas $T + N = -1/(\rho_w/\rho - 1)$. In general

$$T'_N = (\rho_w/\rho - 1) T_N,$$

so T_N is about 10 times larger than T'_N .

17.6 Scaling the sliding law using SSA/SSTREAM scalings

We start by scaling the unit normal and find

$$\begin{aligned}
\hat{\mathbf{n}} &= \frac{1}{\sqrt{1 + (\partial_x b)^2 + (\partial_y b)^2}} \begin{pmatrix} -\partial_x b \\ -\partial_y b \\ 1 \end{pmatrix} \\
&= \frac{1}{\sqrt{1 + \delta^2(\partial_{x^*} b^*)^2 + \delta^2(\partial_{y^*} b^*)^2}} \begin{pmatrix} -\delta \partial_{x^*} b^* \\ -\delta \partial_{y^*} b^* \\ 1 \end{pmatrix} \\
&= (1 - \delta^2((\partial_{x^*} b^*)^2 + (\partial_{y^*} b^*)^2)/2 + O(\delta^4)) \begin{pmatrix} -\delta \partial_{x^*} b^* \\ -\delta \partial_{y^*} b^* \\ 1 \end{pmatrix} \\
&= \begin{pmatrix} -\delta \partial_{x^*} b^* + O(\delta^3) \\ -\delta \partial_{y^*} b^* + O(\delta^3) \\ 1 - \delta^2((\partial_{x^*} b^*)^2 + (\partial_{y^*} b^*)^2)/2 + O(\delta^4) \end{pmatrix}. \tag{17.123}
\end{aligned}$$

The stress tensor is

$$\boldsymbol{\sigma} = [\sigma] \begin{pmatrix} \sigma_{xx}^* & \tau_{xy}^* & \delta \tau_{xz}^* \\ \tau_{xy}^* & \sigma_{yy}^* & \delta \tau_{yz}^* \\ \delta \tau_{xz}^* & \delta \tau_{yz}^* & \sigma_{zz}^* \end{pmatrix},$$

and the product $\boldsymbol{\sigma} \hat{\mathbf{n}}$ is therefore

$$\begin{aligned}
\boldsymbol{\sigma} \hat{\mathbf{n}} &= [\sigma] \begin{pmatrix} \sigma_{xx}^* & \tau_{xy}^* & \delta \tau_{xz}^* \\ \tau_{xy}^* & \sigma_{yy}^* & \delta \tau_{yz}^* \\ \delta \tau_{xz}^* & \delta \tau_{yz}^* & \sigma_{zz}^* \end{pmatrix} \begin{pmatrix} -\delta \partial_{x^*} b^* + O(\delta^3) \\ -\delta \partial_{y^*} b^* + O(\delta^3) \\ 1 - \delta^2((\partial_{x^*} b^*)^2 + (\partial_{y^*} b^*)^2)/2 + O(\delta^4) \end{pmatrix} \\
&= [\sigma] \begin{pmatrix} -\delta \sigma_{xx}^* \partial_{x^*} b^* - \delta \tau_{xy}^* \partial_{y^*} b^* + \delta \tau_{xz}^* + O(\delta^3), \\ -\delta \tau_{xy}^* \partial_{x^*} b^* - \delta \sigma_{yy}^* \partial_{y^*} b^* + \delta \tau_{yz}^* + O(\delta^3), \\ -\delta^2 \tau_{xz}^* \partial_{x^*} b^* - \delta^2 \tau_{yz}^* \partial_{y^*} b^* + \sigma_{zz}^* (1 - \frac{1}{2} \delta^2((\partial_{x^*} b^*)^2 + (\partial_{y^*} b^*)^2) + O(\delta^4)), \end{pmatrix}, \tag{17.124}
\end{aligned}$$

so that $\hat{\mathbf{n}}^T \cdot \boldsymbol{\sigma}^* \hat{\mathbf{n}}$ where $\boldsymbol{\sigma} = [\sigma] \boldsymbol{\sigma}^*$ is given by

$$\begin{aligned}
\hat{\mathbf{n}}^T \cdot \boldsymbol{\sigma}^* \hat{\mathbf{n}} &= \delta^2 \partial_{x^*} b^* (\sigma_{xx}^* \partial_{x^*} b^* + \tau_{xy}^* \partial_{y^*} b^* - \tau_{xz}^*) + \delta^2 \partial_{y^*} b^* (\tau_{xy}^* \partial_{x^*} b^* + \sigma_{yy}^* \partial_{y^*} b^* - \tau_{yz}^*) \\
&\quad - \delta^2 \tau_{xz}^* \partial_{x^*} b^* - \delta^2 \tau_{yz}^* \partial_{y^*} b^* + \sigma_{zz}^* (1 - \frac{1}{2} \delta^2((\partial_{x^*} b^*)^2 + (\partial_{y^*} b^*)^2) + O(\delta^4)),
\end{aligned}$$

which, if we sort this according to order in δ , is

$$\begin{aligned}
\hat{\mathbf{n}}^T \cdot \boldsymbol{\sigma}^* \hat{\mathbf{n}} &= \sigma_{zz}^* \\
&\quad + \delta^2 \{ (\sigma_{xx}^* - \sigma_{zz}^*) (\partial_{x^*} b^*)^2 + (\sigma_{yy}^* - \sigma_{zz}^*) (\partial_{y^*} b^*)^2 + 2 \tau_{xy}^* \partial_{x^*} b^* \partial_{y^*} b^* - 2 \tau_{xz}^* \partial_{x^*} b^* - 2 \tau_{yz}^* \partial_{y^*} b^* \} \\
&\quad + O(\delta^4).
\end{aligned}$$

It follows that the normal stress vector on the bed, $(\hat{\mathbf{n}}^T \cdot \boldsymbol{\sigma} \hat{\mathbf{n}}) \hat{\mathbf{n}}$, is

$$\begin{aligned}
(\hat{\mathbf{n}}^T \cdot \boldsymbol{\sigma}^* \hat{\mathbf{n}}) \hat{\mathbf{n}} &= \\
&\quad \begin{pmatrix} -\delta \sigma_{zz}^* \partial_{x^*} b^* + O(\delta^3) \\ -\delta \sigma_{zz}^* \partial_{y^*} b^* + O(\delta^3) \\ \sigma_{zz}^* (1 - \delta^2((\partial_{x^*} b^*)^2 + (\partial_{y^*} b^*)^2)/2) + \delta^2 ((\sigma_{xx}^* - \sigma_{zz}^*) (\partial_{x^*} b^*)^2 + (\sigma_{yy}^* - \sigma_{zz}^*) (\partial_{y^*} b^*)^2 + 2 \tau_{xy}^* \partial_{x^*} b^* \partial_{y^*} b^* - 2 \tau_{xz}^* \partial_{x^*} b^* - 2 \tau_{yz}^* \partial_{y^*} b^*) + O(\delta^4) \end{pmatrix}.
\end{aligned}$$

Predictably our insistence on keeping things up to third order is making things look a bit messy.

The shear stress vector (\mathbf{t}_b) can now easily be calculated and is found to be

$$\begin{aligned}
\mathbf{t}_b &= \boldsymbol{\sigma} \hat{\mathbf{n}} - (\hat{\mathbf{n}}^T \cdot \boldsymbol{\sigma} \hat{\mathbf{n}}) \hat{\mathbf{n}} \\
&= [\sigma] \begin{pmatrix} \delta \partial_{x^*} b^* (\sigma_{zz}^* - \sigma_{xx}^*) - \delta \partial_{y^*} b^* \tau_{xy}^* + \delta \tau_{xz}^* + O(\delta^3) \\ \delta \partial_{y^*} b^* (\sigma_{zz}^* - \sigma_{yy}^*) - \delta \partial_{x^*} b^* \tau_{xy}^* + \delta \tau_{yz}^* + O(\delta^3) \\ \delta^2 ((\sigma_{zz}^* - \sigma_{xx}^*) (\partial_{x^*} b^*)^2 + (\sigma_{zz}^* - \sigma_{yy}^*) (\partial_{y^*} b^*)^2 - 2 \tau_{xy}^* \partial_{x^*} b^* \partial_{y^*} b^* + \tau_{xz}^* \partial_{x^*} b^* + \tau_{yz}^* \partial_{y^*} b^*) + O(\delta^4) \end{pmatrix}.
\end{aligned}$$

Hence, the components of the basal shear stress vector are $O(\delta)$ or less.

We now scale the basal velocity vector

$$\mathbf{v}_b = \mathbf{v} - (\hat{\mathbf{n}}^T \cdot \mathbf{v}) \hat{\mathbf{n}}$$

and find

$$\begin{aligned} \mathbf{v}_b &= [u] \begin{pmatrix} u^* \\ v^* \\ \delta w^* \end{pmatrix} \\ &\quad - [u] \left(\begin{pmatrix} -\delta \partial_{x^*} b^* + O(\delta^3) \\ -\delta \partial_{y^*} b^* + O(\delta^3) \\ 1 - \delta^2((\partial_{x^*} b^*)^2 + (\partial_{y^*} b^*)^2)/2 + O(\delta^4) \end{pmatrix}^T \cdot \begin{pmatrix} u^* \\ v^* \\ \delta w^* \end{pmatrix} \right) \left(\begin{pmatrix} -\delta \partial_{x^*} b^* + O(\delta^3) \\ -\delta \partial_{y^*} b^* + O(\delta^3) \\ 1 - \delta^2((\partial_{x^*} b^*)^2 + (\partial_{y^*} b^*)^2)/2 + O(\delta^4) \end{pmatrix} \right) \\ &= [u] \begin{pmatrix} u^* \\ v^* \\ \delta w^* \end{pmatrix} - [u] \begin{pmatrix} \delta^2 u^* (\partial_{x^*} b^*)^2 + \delta^2 v^* \partial_{y^*} b^* \partial_{x^*} b^* - \delta^2 \partial_{x^*} w^* + O(\delta^3) \\ \delta^2 u^* \partial_{x^*} b^* \partial_{y^*} b^* + \delta^2 v^* (\partial_{y^*} b^*)^2 - \delta^2 \partial_{y^*} b^* w^* + O(\delta^3) \\ -\delta u^* \partial_{x^*} b^* - \delta v^* \partial_{x^*} b^* + \delta w^* + O(\delta^3) \end{pmatrix} \\ &= [u] \begin{pmatrix} u^* + O(\delta^2) \\ v^* + O(\delta^2) \\ \delta u^* \partial_{x^*} b^* + \delta v^* \partial_{y^*} b^* + O(\delta^3). \end{pmatrix}. \end{aligned}$$

Hence, to second order

$$\mathbf{v}_b = [u] \begin{pmatrix} u^* \\ v^* \\ \delta u^* \partial_{x^*} b^* + \delta v^* \partial_{y^*} b^* \end{pmatrix}.$$

Chapter 18

Perturbation solutions of the SSTREAM/SSA

18.1 Problem definition

We perform a small-amplitude perturbation analysis of the shallow ice stream (SSTREAM) equations. The discussion is limited to 1d along a flow line in which case the SSTREAM equations are

$$2\partial_x(A^{-1/n} h |\partial_x u|^{(1-n)/n} \partial_x u) - |u/c|^{m-1} u/c = \rho g h \partial_x s \cos(\alpha) - \rho g h \sin \alpha , \quad (18.1)$$

or

$$4\partial_x(h\eta\partial_x u) - |u/c|^{m-1} u/c = \rho g h \partial_x s \cos(\alpha) - \rho g h \sin \alpha , \quad (18.2)$$

with

$$\eta = \frac{1}{2} A^{-1/n} \dot{\epsilon}^{(1-n)/n}$$

where $\dot{\epsilon}$ is the effective strain rate, which here is simply

$$\dot{\epsilon} = |\partial_x u| .$$

Here we will here limit the analysis to linear Newtonian media where $n = 1$, but for a general m . The equaiton we aim to analyse is therefore Eq. (18.2), with η being some positive constant, i.e. linear viscosity.

The horizontal velocity component (u) is constant across the depth, and the vertical velocity component (w) varies linearly with depth. In these equation s is the surface, h is ice thickness, η is the effective ice viscosity, and c is the basal slipperiness. The parameter m and the basal slipperiness c are parameters in the sliding law. We write the basal sliding law on the form

$$\mathbf{u}_b = c(x) \|\mathbf{t}_b\|^{m-1} \mathbf{t}_b , \quad (18.3)$$

where \mathbf{t}_b is the basal stress vector given by $\mathbf{t}_b = \boldsymbol{\sigma}\hat{\mathbf{n}} - (\hat{\mathbf{n}}^T \cdot \boldsymbol{\sigma}\hat{\mathbf{n}})\hat{\mathbf{n}}$, with $\hat{\mathbf{n}}$ being a unit normal vector to the bed pointing into the ice. The function $c(x)$ is referred to as the basal slipperiness.

For a linear viscous media ($n = 1$), in which case the viscosity η in Eq. (18.2) is a material constant and not dependent on the state of stress, and a non-linear sliding law (m arbitrary) this equation can be linearised and solved analytically using standard methods as follows. We write $f = \bar{f} + \Delta f$, where f stands for some relevant variable entering the problem, and look for a zeroth-order solution where \bar{f} is independent of x and y and time t , while the first-order field Δf is small but can be a function of space and time.

The perturbations in bedrock (Δb) and slipperiness (Δc) are step functions of time. They are applied at $t = 0$, i.e. for $t < 0$ we have $\Delta b = 0$ and $\Delta c = 0$ and for $t \geq 0$ both Δb and Δc are some constants. Using this history definition the solutions for the velocity field and the surface geometry become functions of time.

18.1.1 Bedrock perturbations

We start by considering the response to small perturbation in basal topography (Δb). The bedrock perturbation is introduced at $t = 0$, that is

$$b(x, t) = \bar{b} + \mathcal{H}(t) \Delta b(x) \quad (18.4)$$

where $\mathcal{H}(t)$ is the Heaviside step function

$$\mathcal{H}(t) = \begin{cases} 0, & \text{if } t < 0 \\ 1, & \text{if } t \geq 0 \end{cases}$$

We also write

$$\begin{aligned} s(x, t) &= \bar{s} + \Delta s(x, t) \\ u(x, t) &= \bar{u} + \Delta u(x, t) \\ w(x, z, t) &= \Delta w(x, z, t) \\ c &= \bar{c} \\ \eta &= \bar{\eta} \end{aligned}$$

where s is the surface topography, b the bedrock topography, and u and w the x and z components of the velocity vector, respectively, and c is the basal slipperiness. The zeroth-order solution to Eq. (18.2) is

$$\bar{u} = \bar{c} (\rho g \bar{h} \sin \alpha)^m. \quad (18.5)$$

The zeroth-order solution represents a plug flow down an uniformly inclined plane of constant ice thickness.

The first-order field equations are

$$4\eta \bar{h} \partial_{xx}^2 \Delta u - \gamma \Delta u = \rho g \bar{h} \cos(\alpha) \partial_x \Delta s - \rho g \sin(\alpha) \Delta h, \quad (18.6)$$

where

$$\gamma = \frac{\tau_d^{1-m}}{m \bar{c}}, \quad (18.7)$$

and

$$\tau_d = \rho g \bar{h} \sin(\alpha), \quad (18.8)$$

is the driving stress.

The domain of the first-order solution is transformed to that of the zeroth-order problem. Let $f(z)$ be some function of the vertical coordinate z . We have

$$f = \bar{f} + \Delta f$$

where \bar{f} is the zeroth order approximation and Δf the first order perturbation. For $z = \bar{z} + \Delta z$ we write

$$\begin{aligned} f(z) &= \bar{f}(z) + \Delta f(z) \\ &= \bar{f}(\bar{z}) + \partial_z \bar{f}|_{z=\bar{z}}(\bar{z}) \Delta z + \Delta f(\bar{z}) \end{aligned}$$

where terms of second order have been ignored.

For the kinematic boundary condition at the surface

$$\partial_t s + u \partial_x s - w = 0$$

we, for example, get

$$\partial_t(\bar{s} + \Delta s) + (\bar{u} + \Delta u + \partial_z \bar{u}|_{z=\bar{s}} \Delta u) \partial_x(\bar{s} + \Delta s) - (\bar{w} + \Delta w + \partial_z \bar{w}|_{z=\bar{s}} \Delta s) = 0.$$

We have $\partial_z \bar{u} = 0$ and for the particular zeroth-order solution we are using (plug flow) we have $\partial_z \bar{w} = 0$. It follows that to first order the upper and lower boundary kinematic conditions are

$$\partial_t \Delta s + \bar{u} \partial_x \Delta s - \Delta w = 0, \quad (18.9)$$

and

$$\bar{u} \mathcal{H}(t) \partial_x \Delta b - \Delta w = 0, \quad (18.10)$$

respectively. In (18.9) the surface mass-balance perturbation has been set to zero. The jump conditions for the stresses have already been using in the derivation of (18.2) and do not need to be considered further.

This system of equations is solved using standard Fourier and Laplace transform methods. All variables are Fourier transformed with respect to the spatial variables x and y and Laplace transformed with respect to the time variable t . The forward Fourier transform $f(k)$ of a function $f(x)$ is

$$f(k) = \int_{-\infty}^{+\infty} f(x) e^{ikx} dx, \quad (18.11)$$

where i is the imaginary unit. The forward Laplace transform $f(r)$ of a function $f(t)$ is

$$f(r) = \int_{0+}^{+\infty} f(t) e^{-rt} dt. \quad (18.12)$$

The kinematic boundary condition along the lower boundary contains a time-dependent term

$$b(x, t) = \bar{b}(x) + \Delta b(x, t) = \bar{b} + \mathcal{H}(t) \Delta b(x).$$

The Laplace transform of the step function, $\mathcal{H}(t)$, is $1/r$, hence

$$b(k, r) = \bar{b}(k) + \Delta b(k, r) = \bar{b} + \Delta b(k)/r.$$

The Fourier and Laplace transforms of the first-order field Eq. (18.6) is

$$4\eta \bar{h} k^2 \Delta u + \gamma \Delta u = \rho g \sin(\alpha) (\Delta s - \Delta b/r) + ik \rho g \cos(\alpha) \bar{h} \Delta s, \quad (18.13)$$

where γ is defined by Eq. (18.7), and the Fourier transformed mass-conservation equation reads

$$-ik \Delta u + \partial_z \Delta w = 0. \quad (18.14)$$

The transformed linearised kinematic boundary condition at the upper boundary, Eq. (18.9), is then

$$-ik \bar{u} \Delta s + r \Delta s - \Delta s(t=0) - \Delta w = 0 \quad (\text{at } z = \bar{s}) \quad (18.15)$$

and the lower-boundary kinematic condition

$$-ik \bar{u} \Delta b/r - \Delta w = 0 \quad (\text{at } z = \bar{b}). \quad (18.16)$$

In addition we have the initial condition

$$\Delta s_0 := \Delta s(t=0) = 0.$$

We think of Δb and Δs_0 as externally prescribed perturbations, and we want to determine Δu and Δs in terms of Δb and Δs_0 .

The resulting system can be solved in various ways. Note that both u and Δu are constant over the depth, so that

$$\Delta u = \Delta u(k, t) \quad (18.17)$$

and not $u = u(k, z, t)$. From (18.14) we then have

$$\partial_z \Delta w = ik \Delta u, \quad (18.18)$$

which is also independent of depth. Integrating Eq. (18.18) with respect to z therefore gives

$$\Delta w(z) = ik(z - \bar{b}) \Delta u - ik \bar{u} \Delta b/r \quad (18.19)$$

where lower kinematic boundary condition (18.16) has been used to determine the integration constant. Setting $z = \bar{s}$ and using the upper kinematic boundary condition (18.15) gives

$$\Delta w(s) = ik \bar{h} \Delta u - ik \bar{u} \Delta b/r \quad (18.20)$$

$$= -ik \bar{u} \Delta s + r \Delta s - \Delta s_0 \quad (18.21)$$

using $\bar{h} = \bar{s} - \bar{b}$, or

$$k \bar{h} \Delta u = -k \bar{u} (\Delta s - \Delta b/r) - ir \Delta s + i \Delta s_0 \quad (18.22)$$

giving Δu in terms of Δs and Δb . From (18.13) we have

$$(4\eta\bar{h}k^2 + \gamma)\Delta u = \rho g \sin(\alpha) (\Delta s - \Delta b/r) + ik\rho g \cos(\alpha) \bar{h}\Delta s, \quad (18.23)$$

Eqs (18.22) and (18.23) are two equations for two unknowns, i.e. Δs and Δu . We first consider the case $\Delta s_0 = 0$ and solve the system

$$\bar{k}\bar{h}\Delta u = -k\bar{u}(\Delta s - \Delta b/r) - ir\Delta s \quad (18.24)$$

$$\xi\Delta u = \rho g \sin(\alpha) (\Delta s - \Delta b/r) + ik\rho g \cos(\alpha) \bar{h}\Delta s, \quad (18.25)$$

where

$$\xi = \gamma + 4\bar{h}k^2\eta, \quad (18.26)$$

for the (complex) ratio between surface and bedrock amplitude

$$T_{sb}(k, r) := \Delta s(k, r)/\Delta b(k),$$

and find, after some algebraic manipulations, such as

$$\begin{aligned} \frac{k\bar{h}}{\xi} (\rho g \sin(\alpha) (\Delta s - \Delta b/r) + ik\rho g \cos(\alpha) \bar{h}\Delta s) &= -k\bar{u}(\Delta s - \Delta b/r) - ir\Delta s \\ \frac{k\bar{h}}{\xi} (\rho g \sin(\alpha) (T_{sb} - 1/r) + ik\rho g \cos(\alpha) \bar{h}T_{sb}) &= -k\bar{u}(T_{sb} - 1/r) - irT_{sb} \\ \left(\frac{k\bar{h}}{\xi} (\rho g \sin(\alpha) + ik\rho g \cos(\alpha) \bar{h}) + k\bar{u} + ir \right) T_{sb} &= \frac{k}{r}\bar{u} + \frac{k\bar{h}}{\xi}\rho g \sin(\alpha) \\ \left(\frac{k\tau_d}{\xi} (1 + ik\bar{h} \cot \alpha) + k\bar{u} + ir \right) T_{sb} &= \frac{k}{r}(\bar{u} + \tau_d/\xi) \end{aligned}$$

that

$$T_{sb}(k, r) = -\frac{ik(\bar{u} + \tau_d/\xi)}{r(r - p)}, \quad (18.27)$$

where

$$p = i/t_p - 1/t_r, \quad (18.28)$$

and the two timescales t_p (phase time scale) and t_r (relaxation time scale) are given by

$$t_p^{-1} = k(\bar{u} + \tau_d/\xi), \quad (18.29)$$

and

$$t_r^{-1} = \xi^{-1}k^2\tau_d\bar{h} \cot \alpha. \quad (18.30)$$

Note that $t_r > 0$.

The inverse Laplace transform is calculated using the Bromwich integral

$$f(t) = \frac{1}{2\pi i} \int_{\Gamma-i\infty}^{\Gamma+i\infty} e^{rt} f(r) dr, \quad (18.31)$$

where Γ is a real number.

We see from Eq. (18.27) that the $T_{sb}(k, r)$ transfer function has two poles, one at $r = 0$ and another one at $r = p$. The second pole is always in the left-half complex plane and the inverse Laplace transform can be evaluated by contour integration over a semicircle in the left hand plane using the residue theorem. We find that

$$T_{sb}(k, t) = \frac{ik(\bar{u}\xi + \tau_d)}{p\xi} (e^{pt} - 1). \quad (18.32)$$

This transfer function describes the relation between surface and bedrock geometry, where

$$\Delta s(k, t) = T_{sb}(k, t) \Delta b(k).$$

Transfer functions giving the perturbation in velocity can be calculated in the same manner.

Exercise: Calculate $T_{ss_0} := s(k, t)/s(k, t = 0)$ for $\Delta b = 0$ and show that

$$T_{ss_0} = e^{pt}. \quad (18.33)$$

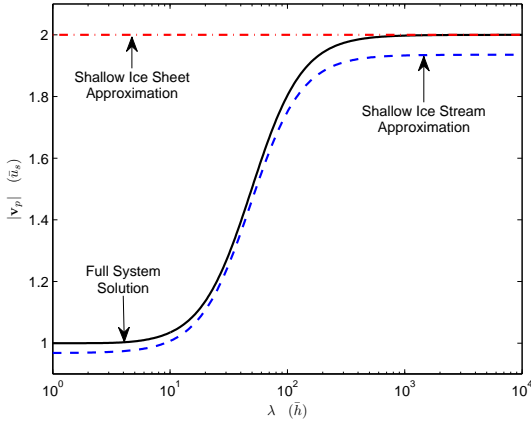


Figure 18.1: The phase speed ($\|\mathbf{v}_p\|$) as a function of wavelength for $\theta=0$. The dashed-dotted curve is based on the shallow-ice-sheet (SSHEET) approximation, the dashed one is based on the shallow-ice-stream (SSTREAM) approximation, and the solid one is a full-system (FS) solution. The surface slope is $\alpha=0.005$ and slip ratio $\bar{C}=30$ and $n = m = 1$. The unit on the y axis is the mean surface velocity of the full-system solution ($\bar{u}=\bar{C}+1=31$).

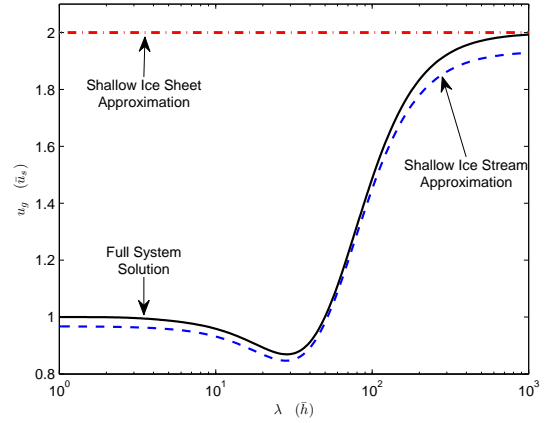


Figure 18.2: The x component of the group velocity (u_g) as a function of wavelength for $\theta=0$. Values of mean surface slope and slip ratio are 0.005 and 30, respectively, and $m = n = 1$.

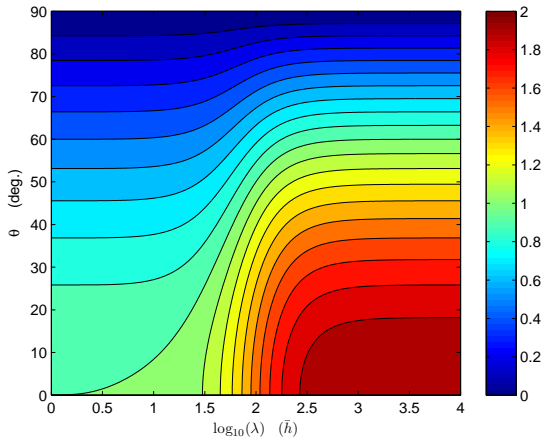


Figure 18.3: The phase speed ($\|\mathbf{v}_p\|$) of the full-system solution as a function of wavelength λ and orientation θ of the sinusoidal perturbations with respect to mean flow direction. The mean surface slope is $\alpha=0.002$ and the slip ratio is $\bar{C}=100$, and $n = m = 1$. The plot has been normalised with the non-dimensional surface velocity $\bar{u}=\bar{C}+1=101$ of the full-system solution.

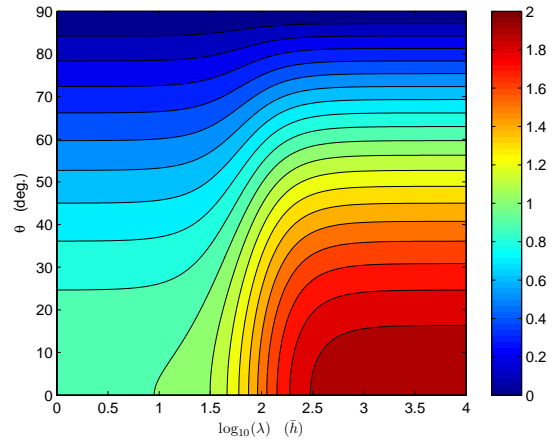


Figure 18.4: The shallow-ice-stream phase speed as a function of wavelength λ and orientation θ . As in Fig. 18.3a the mean surface slope is $\alpha=0.002$ and the slip ratio is $\bar{C}=100$, $n = m = 1$, and the plot has been normalised with the non-dimensional surface velocity $\bar{u}=\bar{C}+1=101$ of the full-system solution.

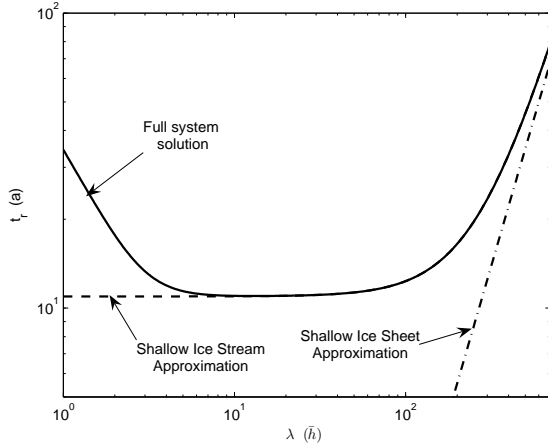


Figure 18.5: The relaxation time scale (t_r) as a function of wavelength λ . The wavelength is given in units of mean ice thickness (\bar{h}) and t_r is given in years. The mean surface slope is $\alpha=0.002$, the slip ratio is $\bar{C}=999$, and $n = m = 1$. For these values t_r is on the order of 10 years for a fairly wide range of wavelengths. Lowering the slip ratio will reduce the value of t_r . It follows that ice streams will react to sudden changes in basal properties or surface profile by a characteristic time scale of a few years.

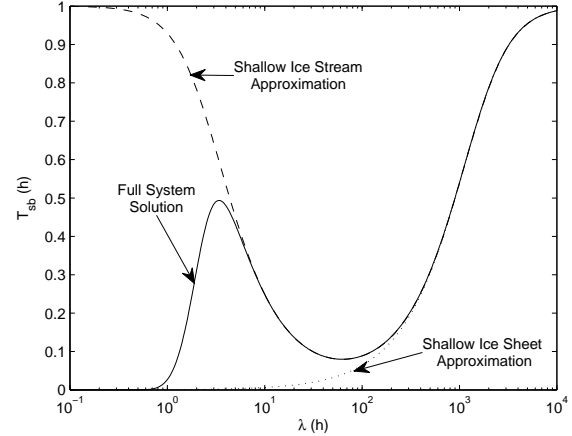


Figure 18.6: Steady-state response of surface topography (Δs) to a perturbation in bed topography (Δb). The surface slope is 0.002, the mean slip ratio $\bar{C}=100$, and $n = m = 1$. Transfer functions based on the shallow-ice-stream approximation (dashed line, Eq. 18.32), the shallow-ice-sheet approximation (dotted line), and a full system solution (solid line) are shown.

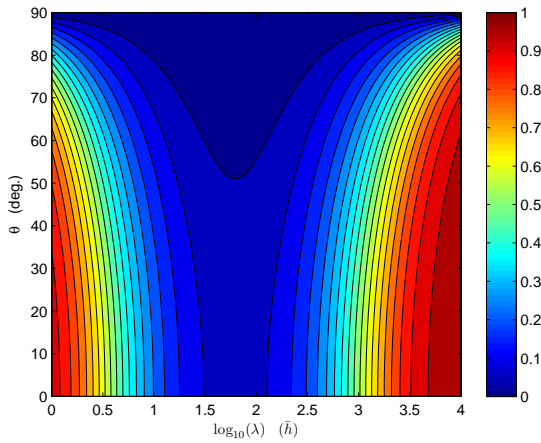


Figure 18.7: (a) The SSTREAM amplitude ratio ($|T_{sb}|$) between surface and bed topography (Eq. 18.32). Surface slope is 0.002, the slip ratio $\bar{C}=99$, and $n = m = 1$. λ is the wavelength of the sinusoidal bed topography perturbation and θ is the angle with respect to the x axis, with $\theta=0$ and $\theta=90$ corresponding to transverse and longitudinal undulations in bed topography, respectively.

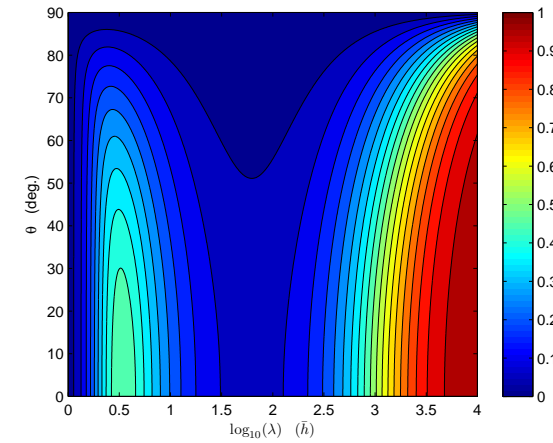


Figure 18.7: (b) The FS amplitude ratio between surface and bed topography ($|T_{sb}|$). The shape of the same transfer function for the same set of parameters based on the SSTREAM approximation is shown in Fig. 18.7a.

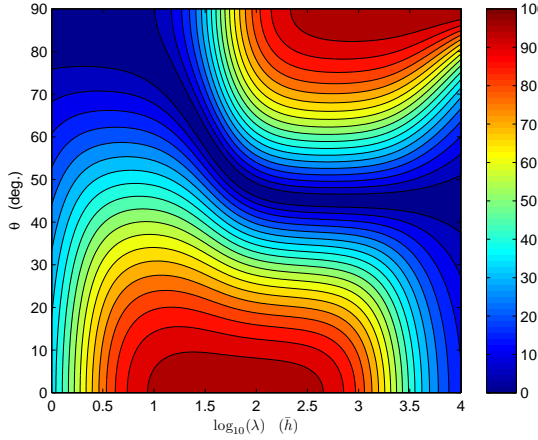


Figure 18.8: (a) The steady-state amplitude ratio ($|T_{ub}|$) between longitudinal surface velocity (Δu) and bed topography (Δb) in the shallow-ice-stream approximation. Surface slope is 0.002, the slip ratio is 99, and $n = m = 1$.

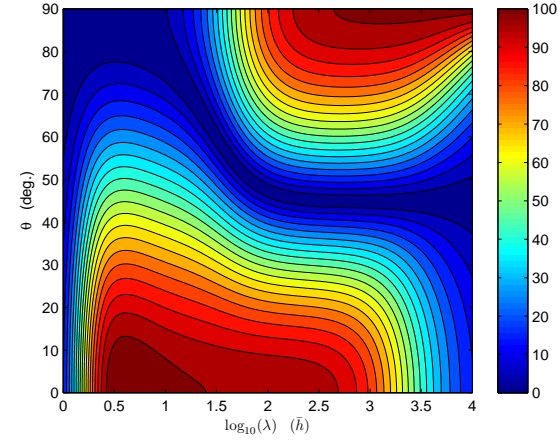


Figure 18.8: (b) The steady-state amplitude ratio ($|T_{ub}|$) between longitudinal surface velocity (Δu) and bed topography (Δb). The shape of the same transfer function for the same set of parameters, but based on the shallow-ice-stream approximation, is shown in Fig. 18.8a.

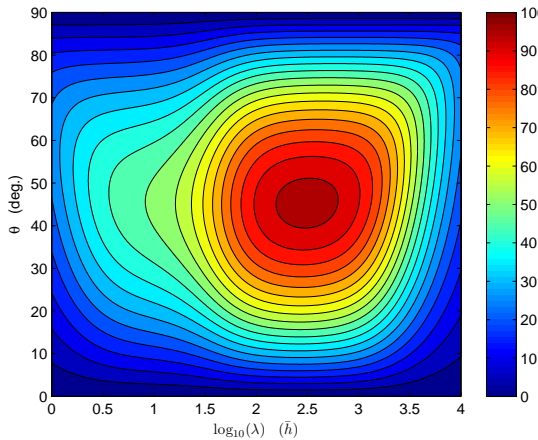


Figure 18.9: (a) The steady-state amplitude ratio ($|T_{vb}|$) between transverse velocity (Δv) and bed topography (Δb) in the shallow-ice-stream approximation. Surface slope is 0.002, the slip ratio is 99 and $n = m = 1$.

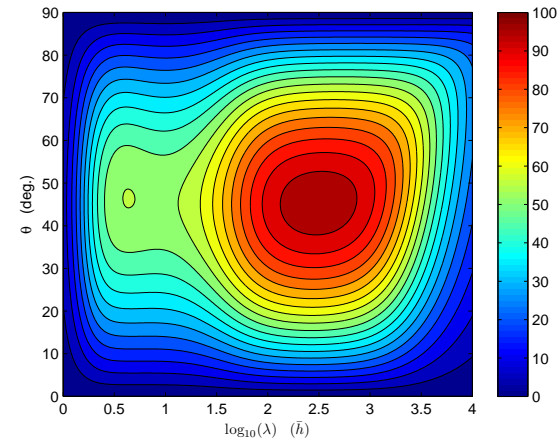


Figure 18.9: (b) The steady-state amplitude ratio ($|T_{vb}|$) between transverse velocity (Δv) and bed topography (Δb). The shape of the same transfer function for the same set of parameters, but based on the shallow-ice-stream approximation, is shown in Fig. 18.9a.

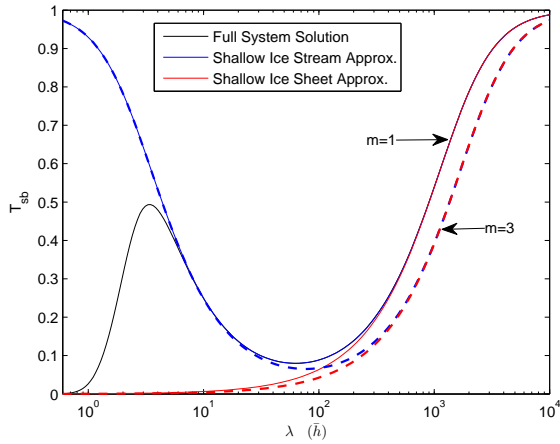


Figure 18.9: Steady-state response of surface topography to a perturbation in bed topography for linear and non-linear sliding. All curves are for linear medium ($n=1$). The solid lines are calculated for linear sliding ($m=1$) and the dashed lines for non-linear sliding ($m=3$). The red lines are SSHEET solutions, the blue ones are SSTREAM solutions, and the black line is a FS solution which is only available for $m=1$. Mean surface slope is 0.002 and slip ratio is equal to 100.

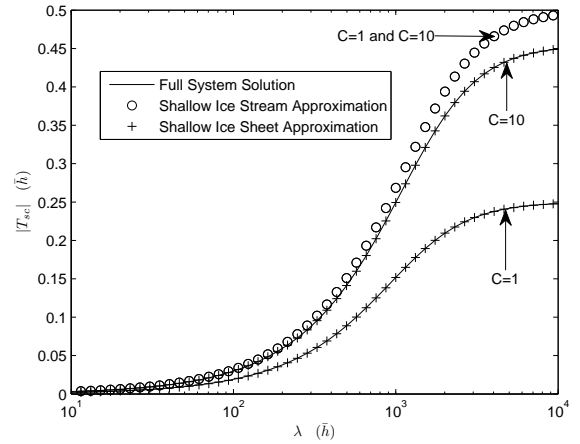


Figure 18.9: Steady-state response of surface topography to a basal slipperiness perturbation. Shown are FS (solid line), SSTREAM (circles), and SSHEET (crosses) transfer amplitudes for both $\bar{C}=1$ and $\bar{C}=10$. In the plot the SSTREAM curves for $\bar{C}=1$ and $\bar{C}=10$ are too similar to be distinguished. The surface slope is 0.002.

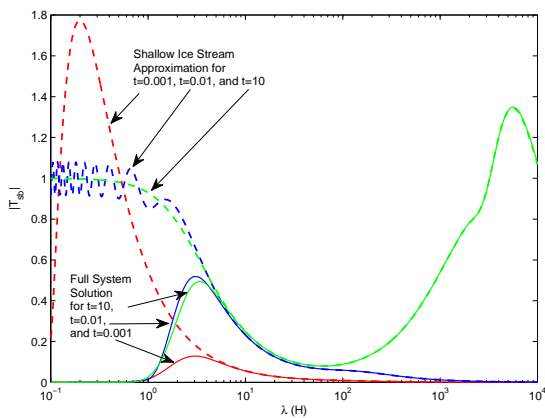


Figure 18.10: Transient surface topography response to a sinusoidal perturbation in bed topography applied at $t=0$. Shown are the amplitude ratios between surface and bed topography ($|T_{sb}|$) as a function of wavelength for $\alpha=0.002$, $\theta=0$, $C=100$, and $n = m = 1$ for $t=0.001$ (red), $t=0.01$ (blue), and $t=10$ (green).

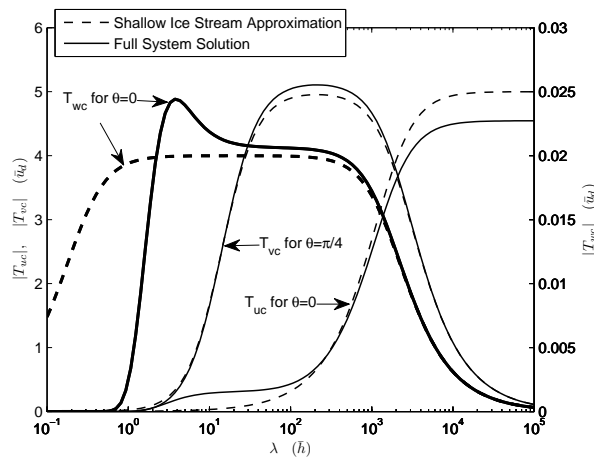


Figure 18.10: Steady-state response of surface longitudinal (u), transverse (v), and vertical (w) velocity components to a basal slipperiness perturbation. The surface slope is 0.002 and the slip ratio $\bar{C}=10$. The T_{uc} and T_{wc} amplitudes are calculated for slipperiness perturbations aligned transversely to the flow direction ($\theta=0$). For T_{vc} , $\theta=45$ degrees. Of the two y axis the scale to the left is for the horizontal velocity components (T_{uc} and T_{wc}), and the one to the right is the scale for T_{uc} .

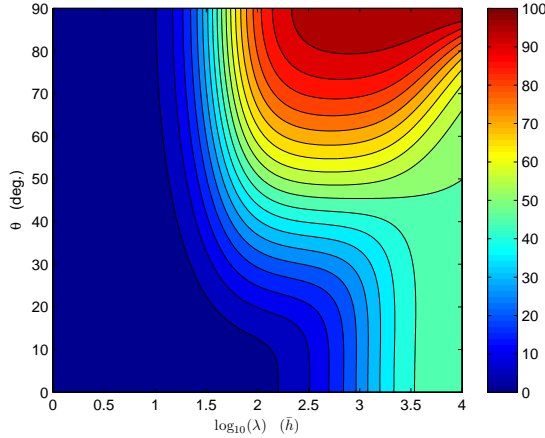


Figure 18.11: Steady-state response of the surface longitudinal (Δu) velocity component to a basal slipperiness perturbation in the shallow-ice-stream approximation. The surface slope is 0.002 and the slip ratio $\bar{C}=99$.

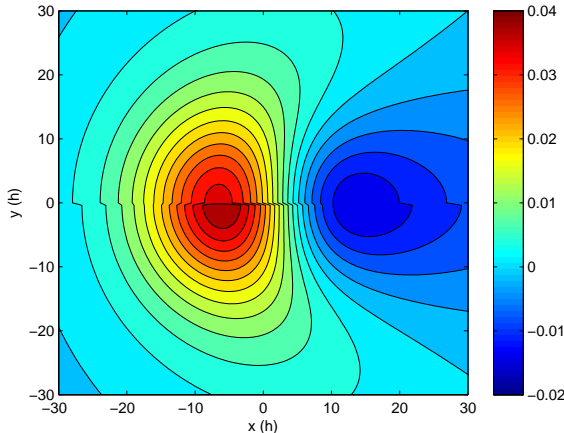


Figure 18.12: (a) Surface topography response to a flow over a Gaussian-shaped bedrock disturbance as given by a FS (lower half of figure) and a SSTREAM solution (upper half of figure). The mean flow direction is from left to right. Surface slope is 3 degrees and mean basal velocity equal to mean deformational velocity ($\bar{C}=1$). The spatial unit is one mean ice thickness (\bar{h}). The Gaussian-shaped bedrock disturbance has a width of $10 \bar{h}$ and it's amplitude is $0.1 \bar{h}$. The problem definition is symmetrical about the x axis ($y=0$) and any deviations in the figure from this symmetry are due to differences in the FS and the SSTREAM solutions.

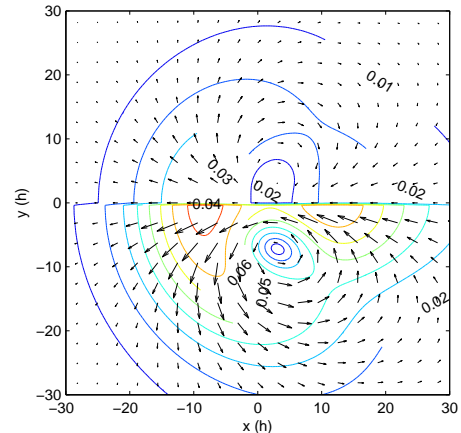


Figure 18.13: (b) Response in surface velocity to a Gaussian-shaped bedrock perturbation. All parameters are equal to those in Fig. 18.12a. The contour lines give horizontal speed and the vectors the horizontal velocities. The velocity unit is mean-deformational velocity (\bar{u}_d). The slip ratio is equal to one, and the mean surface velocity is $2\bar{u}_d$. The upper half of the figure is the SSTREAM solution and the lower half the corresponding FS solution.

18.1.2 Slipperiness perturbations

We now consider the response to small perturbation in basal slipperiness. We write the slipperiness perturbation on the form

$$c(x, t) = \bar{c} (1 + \mathcal{H}(t) \Delta c(x))$$

where Δc is the fractional perturbation in basal slipperiness. The total perturbation is $\bar{c}\Delta c$. As before we write $h = \bar{h} + \Delta h$, $s = \bar{s} + \Delta s$, $u = \bar{u} + \Delta u$, and $w = \Delta w$. Since there is no perturbation in basal topography we have $b = \bar{b}$ and $h = \bar{h} + \Delta s$.

For the zeroth-order problem we get the plug-flow solution as before

$$\bar{u} = \bar{c} \rho g \bar{h} \sin(\alpha). \quad (18.34)$$

$$\partial_t \Delta s + \bar{u} \partial_x \Delta s - \Delta w = 0, \quad (18.35)$$

and

$$\bar{u} \partial_x \Delta b - \Delta w = 0, \quad (18.36)$$

To first order the upper and lower boundary kinematic conditions are

$$\partial_t \Delta s + \bar{u} \partial_x \Delta s - \Delta w = 0, \quad (18.37)$$

as before, while the basal boundary conditions are

$$\Delta w = 0, \quad (18.38)$$

In the field equation (18.2) we have, among other terms, the term $(u/c)^{1/m}$. For $u = \bar{u} + \Delta u$ and $c = \bar{c}(1 + \Delta c)$ we find

$$\left(\frac{u}{c}\right)^{1/m} = \left(\frac{\bar{u} + \Delta u}{\bar{c}(1 + \Delta c)}\right)^{1/m} = \bar{c}^{1/m} ((\bar{u} + \Delta u)(1 - \Delta c))^{1/m} = \left(\frac{\bar{u}}{\bar{c}}\right)^{1/m} - \gamma \bar{u} \Delta c + \gamma \Delta u$$

where

$$\gamma = \frac{1}{\bar{u}m} \left(\frac{\bar{u}}{\bar{c}}\right)^{1/m} = \frac{\tau_d^{1-m}}{m\bar{c}}$$

where

$$\gamma = \frac{\tau_d^{1-m}}{m\bar{c}}, \quad (18.39)$$

and

$$\tau_d = \rho g \bar{h} \sin(\alpha), \quad (18.40)$$

is the driving stress.

We then find that the first-order field equations are

$$4\eta \bar{h} \partial_{xx}^2 \Delta u - \gamma \Delta u = \rho g \bar{h} \cos(\alpha) \partial_x \Delta s - \rho g \sin(\alpha) \Delta h, \quad (18.41)$$

and these can be solved using standard Fourier and Laplace transformation methods as done above for the case of bedrock perturbation.

Part III

Appendices

Appendix A

Calculating vertical surface velocity

The sign convention for upper- and lower-surface mass balance is such that the kinematic boundary conditions at the upper and lower surfaces read, respectively,

$$\partial_t s + u \partial_x s + v \partial_y s - w_s = a_s, \quad (\text{A.1})$$

$$\partial_t b + u \partial_x b + v \partial_y b - w_b = -a_b, \quad (\text{A.2})$$

i.e. adding ice is always defined as positive surface mass balance.

Subtracting (A.2) from (A.1) gives

$$\partial_t h + u \partial_x h + v \partial_y h - w_s + w_b = a_s + a_b,$$

where it has been used that u does not change with depth. Now using (A.5) gives

$$\partial_t h + u \partial_x h + v \partial_y h + h(\dot{\epsilon}_{xx} + \dot{\epsilon}_{yy}) = a_s + a_b,$$

or

$$\partial_t h + \partial_x(uh) + \partial_y(vh) = a_s + a_b, \quad (\text{A.3})$$

hence, in the flux-conservation equation both upper and lower mass balance terms have the same sign.

A.1 grounded part

On the grounded part $\partial_t s = \partial_t h$ and the kinematic boundary condition gives

$$w_s = \partial_t h + u \partial_x s + v \partial_y s - a_s, \quad (\text{A.4})$$

but this requires $\partial_t h$ to be known before we can calculate w_s . An alternative approach is to integrate the vertical strain rate $\dot{\epsilon}_{zz}$ over the thickness, use the mass conservation equation and the fact that horizontal strain rates do not change across the thickness, to arrive at

$$w_s = w_b - h(\dot{\epsilon}_{xx} + \dot{\epsilon}_{yy}). \quad (\text{A.5})$$

We now calculate w_b from the kinematic boundary condition at the lower surface as

$$w_b = a_b + u \partial_x b + v \partial_y b,$$

and insert into (A.5) arriving at

$$w_s = a_b + u \partial_x b + v \partial_y b - h(\dot{\epsilon}_{xx} + \dot{\epsilon}_{yy}), \quad (\text{A.6})$$

which represents a convenient way of calculation w_s once the horizontal velocity field has been determined.

A.2 floating part

Where the ice is afloat

$$s = S + (1 - \rho/\rho_o) h$$

i.e.

$$\partial_t s = (1 - \rho/\rho_o) \partial_t h$$

The kinematic boundary condition at the surface gives

$$w_s = \partial_t s + u \partial_x s + v \partial_y s - a_s$$

and therefore

$$w_s = (1 - \rho/\rho_o) \partial_t h + u \partial_x s + v \partial_y s - a_s \quad (\text{A.7})$$

If $\partial_t h$ is known (A.7) can be used to calculate w_s , otherwise we use (A.3) and find that

$$w_s = (1 - \rho/\rho_o) (a_s + a_b - \partial_x q_x - \partial_y q_y) + u \partial_x s + v \partial_y s - a_s \quad (\text{A.8})$$

An alternative way of calculating w_s is to insert the floating condition

$$s = (1 - \rho_o/\rho) b$$

into (A.1) and to use (A.2) to get rid of $\partial_t b$

$$(1 - \rho_o/\rho)(w_b - a_b - u \partial_x b - v p_y b) + (1 - \rho_o/\rho)(u \partial_x b + v \partial_y b) - w_s = a_s \quad (\text{A.9})$$

to arrive at the simple and intuitive expression

$$(1 - \rho_o/\rho)(w_b - a_b) = a_s + w_s \quad (\text{A.10})$$

and then to use the (A.5) to get rid of w_b leading to

$$w_s = -(1 - \rho/\rho_o) (h(\dot{\epsilon}_{xx} + \dot{\epsilon}_{yy}) - a_b) - a_s \rho/\rho_o \quad (\text{A.11})$$

The above expression shows that adding ice to the surface ($a_s > 0$) over a floating ice shelf gives rise to neg. vertical surface velocity, as does horizontal divergent flow ($\dot{\epsilon}_{xx} + \dot{\epsilon}_{yy} > 0$), and basal melting ($a_b < 0$).

Appendix B

Integral theorem

If f and g are scalar functions then in x and y directions we have

$$\int_{\Omega} f \partial_x g \, d\Omega = - \int_{\Omega} \partial_x f g \, d\Omega + \oint_{\partial\Omega} f g n_x \, d\Gamma \quad (\text{B.1})$$

$$\int_{\Omega} f \partial_y g \, d\Omega = - \int_{\Omega} \partial_y f g \, d\Omega + \oint_{\partial\Omega} f g n_y \, d\Gamma \quad (\text{B.2})$$

If we write $g = g_x$ in the upper one and $g = g_y$ in the lower one, add them together and define $\mathbf{g} = (g_x, g_y)^T$ and $\hat{\mathbf{n}} = (n_x, n_y)^T$ then we arrive at

$$\int_{\Omega} f \nabla_{xy} \cdot \mathbf{g} \, d\Omega = - \int_{\Omega} \nabla_{xy} f \cdot \mathbf{g} \, d\Omega + \oint_{\partial\Omega} f \mathbf{g} \cdot \hat{\mathbf{n}} \, d\Gamma \quad (\text{B.3})$$

Appendix C

Finite-Element equations derived from a minimisation problem

Consider the minimisation problem

$$\min_{\phi} I$$

where

$$I = \int_{\mathcal{A}} \left(\frac{1}{2} (g\phi^2 + k_x(\partial_x \phi)^2 + k_y(\partial_y \phi)^2) - f\phi \right) d\mathcal{A} \\ + \oint_{\partial\mathcal{A}} \left(\frac{1}{2} \alpha(s)\phi^2 - \gamma(s)\phi \right) ds$$

for

$$\phi = \phi(x, y)$$

and the given functions $k_x(x, y)$, $k_y(x, y)$, $f(x, y)$, and $g(x, y)$, with the Dirichlet boundary condition along the sub-section $\partial\mathcal{A}_1$ of the boundary $\partial\mathcal{A} = \partial\mathcal{A}_1 + \partial\mathcal{A}_2$, that is

$$\phi = \varphi \quad \text{on } \partial\mathcal{A}_1.$$

As we show below, the stationary value of I with respect to a variation in ϕ is found when $\phi(x, y)$ is a solution to

$$g\phi - \partial_x(k_x \partial_x \phi) - \partial_y(k_y \partial_y \phi) = f, \quad (\text{C.1})$$

and ϕ fulfils both

$$\phi = \varphi \quad \text{on } \partial\mathcal{A}_1,$$

and

$$(\mathbf{k}\nabla\phi) \cdot \hat{\mathbf{n}} + \alpha(s)\phi = \gamma(x) \quad \text{on } \partial\mathcal{A}_2,$$

where

$$\partial\mathcal{A} = \partial\mathcal{A}_1 + \partial\mathcal{A}_2.$$

To see that this is indeed the case, we note that for ϕ to be the minimum, the first variation of I with respect to ϕ must be zero, i.e.

$$\delta_{\phi} I = 0$$

The variation of I with respect to ϕ is

$$\delta_{\phi} I = \int_{\mathcal{A}} (g\phi \delta\phi + k_x \partial_x \phi \partial_x \delta\phi + k_y \phi_y \partial_y \delta\phi - f \delta\phi) d\mathcal{A} \quad (\text{C.2})$$

$$+ \oint_{\partial\mathcal{A}} (\alpha(s)\phi \delta\phi - \gamma(s) \delta\phi) ds \quad (\text{C.3})$$

We now use partial integration to get rid of the $\partial_x \delta\phi$ and $\partial_y \delta\phi$ terms as follows

$$\int_{\mathcal{A}} (k_x \partial_x \phi \partial_x \delta\phi + k_y \phi_y \partial_y \delta\phi) d\mathcal{A} = - \int_{\mathcal{A}} (\partial_x(k_x \partial_x \phi) \delta\phi + \partial_y(k_y \phi_y) \delta\phi) d\mathcal{A} + \int_{\partial\mathcal{A}} (k_x \partial_x \phi n_x + k_y \phi_y n_y) \delta\phi ds$$

Hence

$$\begin{aligned}\delta_\phi I = & - \int_{\mathcal{A}} (g\phi + \partial_x(k_x \partial_x \phi) + \partial_y(k_y \partial_y \phi) - f) \delta\phi \, d\mathcal{A} \\ & + \oint_{\partial\mathcal{A}} (k_x \partial_x \phi n_x + k_y \phi_y n_y + \alpha\phi - \gamma) \delta\phi \, ds\end{aligned}\quad (\text{C.4})$$

For the first variation to be zero, i.e.

$$\delta_\phi I = 0 \quad (\text{C.5})$$

for any $\delta\phi$ we conclude that

$$g\phi - \partial_x(k_x \partial_x \phi) - \partial_y(k_y \partial_y \phi) = f, \quad (\text{C.1})$$

at any location (x, y) within the domain \mathcal{A} , and

$$k_x \partial_x \phi n_x + k_y \phi_y n_y + \alpha\phi - \gamma = 0,$$

along the boundary, except for $\partial\mathcal{A}_1$ where we have

$$\phi = \varphi \quad \text{on} \quad \partial\mathcal{A}_1,$$

where we must add the condition

$$\delta\phi = 0 \quad \text{on} \quad \partial\mathcal{A}_1.$$

From (C.2) and (C.3) we see that Eq. (C.5) can be written on the form

$$\langle g\phi | \delta\phi \rangle + \langle k_x \partial_x \phi | \partial_x \delta\phi \rangle + \langle k_y \partial_y \phi_y | \partial_y \delta\phi \rangle - \langle f | \delta\phi \rangle = 0, \quad (\text{C.6})$$

where the inner product is defined as

$$\langle f | g \rangle = \int_{\mathcal{A}} f(x, y) g(x, y) \, d\mathcal{A} \quad (\text{C.7})$$

with the natural boundary condition being

$$k_x \partial_x \phi n_x + k_y \phi_y n_y + \alpha\phi - \gamma = 0.$$

The FE equations are exactly Eq. (C.6) with the basis functions being ϕ . The FE-equations are, thus, derived directly from a minimisation problem.

In the finite element method, functions are expanded with respect to a set of basis functions $\phi_p(x)$ with $p = 1 \dots N$ as

$$f(x) = \sum_{i=1}^N a_i \phi_i(x)$$

Here a_i are the coefficients in the expansion, and in a given basis the function $f(x)$ can be considered to be a function of those set of coefficients $\{a_i\}$, where the curly bracket indicates that the whole set of coefficients is included

$$f = f(a_i)$$

$$\begin{aligned}Df(\{a_i\})[a_q] &= \lim_{\epsilon \rightarrow 0} \frac{d}{d\epsilon} f(a_1, a_2, \dots, a_q + \epsilon, \dots, a_N) \\ &= \lim_{\epsilon \rightarrow 0} \frac{d}{d\epsilon} \left(\sum_{i=1}^N a_i \phi_i(x) + \epsilon \phi_q(x) \right) \\ &= \phi_q(x)\end{aligned}$$

Appendix D

Definition of gradients in terms of directional derivatives and inner products

The directional derivative of the scalar function $J(p)$ in the direction ϕ is denoted by $Df(p)[\phi]$ and defined as

$$\begin{aligned} Df(p)[\phi] &= \lim_{\epsilon \rightarrow 0} \frac{d}{d\epsilon} f(p + \epsilon\phi) \\ &= \lim_{\epsilon \rightarrow 0} \frac{f(p + \epsilon\phi) - f(p)}{\epsilon} \end{aligned}$$

The directional derivative is sometimes written as $\delta f(p, \phi)$ or as $f'(p, \phi)$ i.e.

$$Df(p)[\phi] = f'(p, \phi) = \delta f(p, \phi)$$

are different ways of writing the directional derivative, all commonly found in the literature.

We define the gradient through

$$Df(p)[\phi] = \langle \nabla f(p) | \phi \rangle_H \quad (\text{D.1})$$

where H is a Hilbert space and $f : H \rightarrow \mathbb{R}$. Here $\nabla f(p)$ is the gradient of f , and the expression above defines the gradient in terms of the (directional) derivative for a given inner product. In other words, for a function $f : H \rightarrow \mathbb{R}$ the gradient is defined as the Riez-representation for the directional derivative $Df(p)[\phi]$ through (D.1). The directional derivative depends on the inner product $\langle \cdot, \cdot \rangle_H$ and the gradient is not defined without specifying the inner product.

Example: Consider the case $H = \mathbb{R}^n$ with the inner product

$$\langle \mathbf{x} | \mathbf{y} \rangle = \mathbf{x}^T \mathbf{M} \mathbf{y}$$

where \mathbf{M} is symmetric and positive definite (for example the mass matrix or any covariance matrix.)

The directional derivative is

$$Df(p)[\phi] = \frac{\partial f}{\partial p_q} \phi_q = \langle \mathbf{M}^{-1} \partial f / \partial p_q | \phi_q \rangle$$

and therefore

$$[\nabla f]_p = [\mathbf{M}^{-1}]_{pq} \partial f / \partial \phi_q$$

Had we instead used the Euclidean inner product as $\langle \mathbf{x} | \mathbf{y} \rangle = \mathbf{x}^T \mathbf{y}$ the elements of the corresponding (Euclidean) gradient are

$$[\nabla_E f]_p = \partial f / \partial \phi_p \quad (\text{D.2})$$

or

$$\nabla f = \mathbf{M}^{-1} \nabla_E f \quad (\text{D.3})$$

where the subscript E denotes the Euclidean gradient. This distinction becomes important in the application of the adjoint method where we obtain a gradient that is dependent on the natural FE inner product

$$\begin{aligned}\langle f|g \rangle &= \int f g dA \\ &= \int f_p \phi_p g_q \phi_q dA \\ &= \mathbf{f} \mathbf{M} \mathbf{g}\end{aligned}$$

Hence in FE the dual pairing is

$$\langle f|g \rangle = \mathbf{f}^T \mathbf{M} \mathbf{g}.$$

The adjoint L^* of a given operator L is defined as

$$\langle L^* f|g \rangle = \langle f|Lg \rangle$$

for any f and g .

If we are working in $H_1 = \mathbb{R}^{d_1}$ and the dual space is $H_2 = \mathbb{R}^{d_2}$ and

$$\langle f|g \rangle_{H_1, H_2} = \mathbf{f}^T \mathbf{g}$$

and

$$\langle L^* f|g \rangle_{H_1, H_2} = \langle f|Lg \rangle_{H_1, H_2}$$

and we denote by \mathbf{L} and \mathbf{L}^* the matrix representations of the continuous linear operators L and L^* , respectively, then

$$\mathbf{L}^* = \mathbf{L}^T.$$

But if the dual pairing is

$$\langle f|g \rangle_{H_1, H_2} = \mathbf{f}^T \mathbf{M} \mathbf{g}$$

where \mathbf{M} is a positive definite matrix, then

$$\mathbf{L}^* = \mathbf{M}^{-T} \mathbf{L}^T \mathbf{M}^T$$

as can be seen as follows

$$\begin{aligned}\langle M^* f|g \rangle_{H_1, H_2} &= \langle f|Lg \rangle_{H_1, H_2} \\ &= \mathbf{f}^T \mathbf{M} (\mathbf{L} \mathbf{g}) \\ &= \mathbf{f}^T \mathbf{M} \mathbf{L} \mathbf{M}^{-1} \mathbf{M} \mathbf{g} \\ &= (\mathbf{M}^{-T} \mathbf{L}^T \mathbf{M}^T \mathbf{f})^T \mathbf{M} \mathbf{g} \\ &= \langle \mathbf{M}^{-T} \mathbf{L}^T \mathbf{M}^T \mathbf{f}|g \rangle_{H_1, H_2}\end{aligned}$$

We can generalise this a bit further and consider the case where the dual space has a different dimension with

$$\begin{aligned}\langle f|f \rangle_{H_1 H_1} &= \mathbf{f}^T \mathbf{M}_1 \mathbf{f} \\ \langle g|g \rangle_{H_2 H_2} &= \mathbf{g}^T \mathbf{M}_2 \mathbf{g}\end{aligned}$$

and find that

$$\mathbf{L}^* = \mathbf{M}_1^{-T} \mathbf{L}^T \mathbf{M}_2^T$$

Bibliography

- Antunes, F. V., Ferreira, J. M., and Byrne, J. (1999). Stress intensity factor calculation based on the work of external forces. *International Journal of Fracture*, 98(1):1–14.
- Asay-Davis, X. S., Cornford, S. L., Durand, G., Galton-Fenzi, B. K., Gladstone, R. M., Gudmundsson, G. H., Hattermann, T., Holland, D. M., Holland, D., Holland, P. R., Martin, D. F., Mathiot, P., Pattyn, F., and Seroussi, H. (2016). Experimental design for three interrelated marine ice sheet and ocean model intercomparison projects: MISMIP v. 3 (MISMIP +), ISOMIP v. 2 (ISOMIP +) and MISOMIP v. 1 (MISOMIP1). *Geoscientific Model Development*, 9(7):2471–2497.
- Bank, R., Coughran, W., Fichtner, W., Grosse, E., Rose, D., and Smith, R. (1985). Transient Simulation of Silicon Devices and Circuits. *IEEE Transactions on Computer-Aided Design of Integrated Circuits and Systems*, 4(4):436–451.
- Baral, D. R. (1999). *Asymptotic theories of large scale motion, temperature and moisture distributions in land based polythermal ice shields and in floating ice shelves. A critical review and new developments.* PhD thesis, Technische Universität Darmstadt.
- Barles, G., Soner, H. M., and Souganidis, P. E. (1993). Front Propagation and Phase Field Theory. *SIAM Journal on Control and Optimization*, 31(2):439–469.
- Bathe, K.-J. (2007). Conserving energy and momentum in nonlinear dynamics: A simple implicit time integration scheme. *Computers & Structures*, 85(7-8):437–445.
- Beyer, S., Kleiner, T., Aizinger, V., Rückamp, M., and Humbert, A. (2018). A confined-unconfined aquifer model for subglacial hydrology and its application to the Northeast Greenland Ice Stream. *Cryosphere*, 12(12):3931–3947.
- Blatter, H. (1995). Velocity and stress fields in grounded glaciers: a simple algorithm for including deviatoric stress gradients. *Journal of Glaciology*, 41(138):333–344.
- Bondzio, J. H., Seroussi, H., Morlighem, M., Kleiner, T., Rückamp, M., Humbert, A., and Larour, E. Y. (2016). Modelling calving front dynamics using a level-set method: application to Jakobshavn Isbræ, West Greenland. *The Cryosphere*, 10(2):497–510.
- Boyd, S. and Vandenberghe, L. (2004). *Convex optimization*. WORLD SCIENTIFIC.
- Budd, W. (1970). The Longitudinal Stress and Strain-rate Gradients in Ice Masses. *Journal of Glaciology*, 9(55):19–27.
- Budd, W. F. (1969). The dynamics of ice masses. Australian National Antarctic Research Expedition, Scientific Report 108, Melbourne, Australia.
- Caciopoli, L. D. (2015). *application-of-multirate-TR-BDF2-method-to-the-time-discretization-of-nonlinear-conservation-laws*. PhD thesis, Politecnico Milano.
- Chan, T. F. C. and Keller, H. B. (1982). Arc-Length Continuation and Multigrid Techniques for Nonlinear Elliptic Eigenvalue Problems. *SIAM Journal on Scientific and Statistical Computing*, 3(2):173–194.
- Cliffe, K. A., Spence, A., and Tavener, S. J. (2000). The numerical analysis of bifurcation problems with application to fluid mechanics. *Acta Numerica*, 9:39–131.

- Cornford, S. L., Martin, D. F., Graves, D. T., Ranken, D. F., Le Brocq, A. M., Gladstone, R. M., Payne, A. J., Ng, E. G., and Lipscomb, W. H. (2013). Adaptive mesh, finite volume modeling of marine ice sheets. *Journal of Computational Physics*, 232(1):529–549.
- Cornford, S. L., Seroussi, H., Asay-Davis, X. S., Gudmundsson, G. H., Arthern, R., Borstad, C., Christmann, J., Dias dos Santos, T., Feldmann, J., Goldberg, D., Hoffman, M. J., Humbert, A., Kleiner, T., Leguy, G., Lipscomb, W. H., Merino, N., Durand, G., Morlighem, M., Pollard, D., Rückamp, M., Williams, C. R., and Yu, H. (2020). Results of the third Marine Ice Sheet Model Intercomparison Project (MISMIP+). *The Cryosphere*, 14(7):2283–2301.
- Dharmaraja, S. (2007). *An analysis of the TR-BDF2 integration scheme*. PhD thesis, MIT.
- Doedel, E. (2013). An Introduction to Numerical Continuation Methods with Application to some Problems from Physics Persistence of Solutions. (May).
- Dukowicz, J. K., Price, S. F., and Lipscomb, W. H. (2010). Consistent approximations and boundary conditions for ice-sheet dynamics from a principle of least action. *Journal of Glaciology*, 56(197):480–496.
- Dukowicz, J. K., Price, S. F., and Lipscomb, W. H. (2011). Incorporating arbitrary basal topography in the variational formulation of ice-sheet models. *Journal of Glaciology*, 57(203):461–467.
- Echelmeyer, K. A., Kamb, B., and Kamb, B. (1986). Stress-Gradient Coupling in Glacier Flow: II. Longitudinal Averaging in the Flow Response to Small Perturbations in Ice Thickness and Surface Slope. *Journal of Glaciology*, 32(111):285–298.
- Glen, J. W. (1955). The creep of polycrystalline ice. *Proceedings of the Royal Society of London, Ser A*, 228(1175):519–538.
- Goldberg, D. N. (2011). A variationally derived, depth-integrated approximation to a higher-order glaciological flow model. *Journal of Glaciology*, 57(201):157–170.
- Goldsby, D. L. and Kohlstedt, D. L. (2001). Superplastic deformation of ice: Experimental observations. *Journal of Geophysical Research*, 106(B6):11,017–11,030.
- Gross, D. and Seelig, T. (2006). *Fracture Mechanics*. Mechanical Engineering Series. Springer Berlin Heidelberg, Berlin, Heidelberg.
- Gudmundsson, G. H. (2013). Ice-shelf buttressing and the stability of marine ice sheets. *The Cryosphere*, 7(2):647–655.
- Hindmarsh, R. C. A. (1993). Qualitative Dynamics of Marine Ice Sheets. In *Ice in the Climate System*, pages 67–99. Springer Berlin Heidelberg, Berlin, Heidelberg.
- Hindmarsh, R. C. A. (1996). Stability of ice rises and uncoupled marine ice sheets. *Annals of Glaciology*, 23:105–115.
- Hindmarsh, R. C. A. (2004). A numerical comparison of approximations to the Stokes equations used in ice sheet and glacier modeling. *Journal of Geophysical Research: Earth Surface*, 109(F1):1–15.
- Hosea, M. and Shampine, L. (1996). Analysis and implementation of TR-BDF2. *Applied Numerical Mathematics*, 20(1-2):21–37.
- Hossain, M. A., Pimentel, S., and Stockie, J. M. (2020). Modelling dynamic ice-sheet boundaries and grounding line migration using the level set method. *Journal of Glaciology*, 66(259):766–776.
- Huth, A., Duddu, R., and Smith, B. (2021). A Generalized Interpolation Material Point Method for Shallow Ice Shelves. 2: Anisotropic Nonlocal Damage Mechanics and Rift Propagation. *Journal of Advances in Modeling Earth Systems*, 13(8):1–26.
- IPCC (2019). IPCC Special Report on the Ocean and Cryosphere in a Changing Climate [H.-O. Pörtner Roberts, D.C. Masson-Delmotte, V. Zhai, P. Tignor, M. Poloczanska, E. Mintenbeck, K. Nicolai, M. Okem, A. Petzold, J. B. Rama, N. Weyer (eds.)]. *In press*, (September).

- Jansen, K. E., Collis, S. S., Whiting, C., and Shaki, F. (1999). A better consistency for low-order stabilized finite element methods. *Computer Methods in Applied Mechanics and Engineering*, 174(1-2):153–170.
- Jia, D. and Esmaily, M. (2023). A time-consistent stabilized finite element method for fluids with applications to hemodynamics. *Scientific Reports*, 13.
- Jóhannesson, T. (1992). *Landscape of Temperate Ice Caps*. PhD thesis, Univ. of Washington.
- Joughin, I., Smith, B. E., and Schoof, C. G. (2019). Regularized Coulomb Friction Laws for Ice Sheet Sliding: Application to Pine Island Glacier, Antarctica. *Geophysical Research Letters*, 46(9):4764–4771.
- Kamb, B. and Echelmeyer, K. A. (1986). Stress-gradient coupling in glacier flow: I. Longitudinal averaging of the influence of ice thickness and surface slope. *Journal of Glaciology*, 32(4091):267–284.
- Keller, A. and Hutter, K. (2014). Conceptual thoughts on continuum damage mechanics for shallow ice shelves. *Journal of Glaciology*, 60(222):685–693.
- Krug, J., Weiss, J., Gagliardini, O., and Durand, G. (2014). Combining damage and fracture mechanics to model calving. *The Cryosphere*, 8(6):2101–2117.
- Kuznetsov, Y. A. (1998). Elements of Applied Bifurcation Theory, Second Edition. 112:614.
- Li, C., Xu, C., Gui, C., and Fox, M. D. (2010). Distance regularized level set evolution and its application to image segmentation. *IEEE Transactions on Image Processing*, 19(12):3243–3254.
- Lindgren, F., Rue, H., and Lindström, J. (2011). An explicit link between Gaussian fields and Gaussian Markov random fields: the stochastic partial differential equation approach. *Journal of the Royal Statistical Society: Series B (Statistical Methodology)*, 73(4):423–498.
- Luo, K., Shao, C., Chai, M., and Fan, J. (2019). Level set method for atomization and evaporation simulations. *Progress in Energy and Combustion Science*, 73:65–94.
- MacAyeal, D. R. (1989). Large-scale ice flow over a viscous basal sediment: Theory and application to ice stream B, Antarctica. *Journal of Geophysical Research: Solid Earth*, 94(B4):4071–4087.
- Manzan, M; Oñate, E. (2000). Stabilization Techniques for Finite Element Analysis of Convection-Diffusion Problems of convection-diffusion problems. *International Center Fot Numerical Methods in Engineering*, (February):1–43.
- Mercenier, R., Lüthi, M. P., and Vieli, A. (2019). A Transient Coupled Ice Flow Damage Model to Simulate Iceberg Calving From Tidewater Outlet Glaciers. *Journal of Advances in Modeling Earth Systems*, 11(9):3057–3072.
- Morland, L. W. (1987). Unconfined ice-shelf flow. In van derVeen, C. J., , and Oerlemans, J., editors, *Dynamics of the West Antarctic Ice Sheet*, pages 99–116. Springer, New York.
- Morlighem, M., Rignot, E., Binder, T., Blankenship, D., Drews, R., Eagles, G., Eisen, O., Ferraccioli, F., Forsberg, R., Fretwell, P., Goel, V., Greenbaum, J. S., Gudmundsson, H., Guo, J., Helm, V., Hofstede, C., Howat, I., Humbert, A., Jokat, W., Karlsson, N. B., Lee, W. S., Matsuoka, K., Millan, R., Mouginot, J., Paden, J., Pattyn, F., Roberts, J., Rosier, S., Ruppel, A., Seroussi, H., Smith, E. C., Steinhage, D., Sun, B., van den Broeke, M. R., van Ommen, T. D., van Wessem, M., and Young, D. A. (2020). Deep glacial troughs and stabilizing ridges unveiled beneath the margins of the Antarctic ice sheet. *Nature Geoscience*, 13(2):132–137.
- Muszynski, I. and Birchfield, G. E. (1987). A coupled marine ice-stream-ice – shelf model. *Journal of Glaciology*, 33(113):3–14.
- Nye, J. F. (1969). The effect of longitudinal stress on the shear stress at the base of an ice sheet. *Journal of Glaciology*, 8(53):207–213.
- Pacaud, F., Schanen, M., Maldonado, D. A., Montoisson, A., Churavy, V., Samaroo, J., and Anitescu, M. (2022). Batched Second-Order Adjoint Sensitivity for Reduced Space Methods. In *Proceedings of the 2022 SIAM Conference on Parallel Processing for Scientific Computing (PP)*, pages 60–71. Society for Industrial and Applied Mathematics, Philadelphia, PA.

- Papadimitriou, D. I. and Giannakoglou, K. C. (2008). Direct, adjoint and mixed approaches for the computation of Hessian in airfoil design problems. *International Journal for Numerical Methods in Fluids*, 56(10):1929–1943.
- Pattyn, F. (2003). A new three-dimensional higher-order thermomechanical ice sheet model: Basic sensitivity, ice stream development, and ice flow across subglacial lakes. *Journal of Geophysical Research*, 108(B8):2382.
- Raphson, J. (1702). *Analysis Aequationum Universalis*. BiblioBazaar.
- Reese, R., Gudmundsson, G. H., Levermann, A., and Winkelmann, R. (2018). The far reach of ice-shelf thinning in Antarctica. *Nature Climate Change*, 8(1):53–57.
- Rheinboldt, W. C. (1988). Lectures on Numerical Methods in Bifurcation Problems (Herbert B. Kelley). *SIAM Review*, 30(4):677–677.
- Salinger, A. A. G., Bou-Rabee, N. M., Pawlowski, R. P., Wilkes, E. D., Burroughs, E. A., Lehoucq, R. B., and Romero, L. A. (2002). LOCA 1.0 Library of continuation algorithms: theory and implementation manual. *Sandia National Laboratories, SAND2002-0396*, (October).
- Saxena, A. (1993). Fracture Mechanics Approaches for Characterizing Creep-Fatigue Crack Growth. *JSME international journal. Ser. A, Mechanics and material engineering*, 36(1):1–20.
- Saxena, A. (2015). Creep and creep–fatigue crack growth. *International Journal of Fracture*, 191(1-2):31–51.
- Schelpe, C. A. O. and Gudmundsson, G. H. (2023). Incorporating Horizontal Density Variations Into Large-Scale Modeling of Ice Masses. *Journal of Geophysical Research: Earth Surface*, 128(2):1–39.
- Schoof, C. (2006). A variational approach to ice stream flow. *Journal of Fluid Mechanics*, 556:227.
- Schoof, C. (2010). Coulomb Friction and Other Sliding Laws In a Higher-Order Glacier Flow Model. *Mathematical Models and Methods in Applied Sciences*, 20(01):157–189.
- Schoof, C. and Hindmarsh, R. C. A. (2010). Thin-Film Flows with Wall Slip: An Asymptotic Analysis of Higher Order Glacier Flow Models. *The Quarterly Journal of Mechanics and Applied Mathematics*, 63(1):73–114.
- Steinemann, S. (1954). Results of preliminary experiments on the plasticity of ice crystals. *Journal of Glaciology*, 2:404–413.
- Steinemann, S. (1958a). Experimentelle Untersuchungen zur Plastizität von Eis. Geotechnische Serie Nr. 10, Beiträge zur Geologie der Schweiz.
- Steinemann, S. (1958b). Résultats expérimentaux sur la dynamique da la glace et leurs correlations avec le mouvement et la pétrographie des glaciers. *International Association of Scientific Hydrology*, 47:184–198.
- Touré, M. K. and Soulaïmani, A. (2016). Stabilized finite element methods for solving the level set equation without reinitialization. *Computers and Mathematics with Applications*, 71(8):1602–1623.
- Tsai, V. C., Stewart, A. L., and Thompson, A. F. (2015). Marine ice-sheet profiles and stability under Coulomb basal conditions. *Journal of Glaciology*, 61(226):205–215.
- Ultee, L. and Bassis, J. N. (2020). SERMeQ Model Produces a Realistic Upper Bound on Calving Retreat for 155 Greenland Outlet Glaciers. *Geophysical Research Letters*, 47(21).
- Van Der Veen, C. J. and Whillans, I. M. (1989). Force Budget: I. Theory and Numerical Methods. *Journal of Glaciology*, 35(119):53–60.
- Wagner, T. J. W., Dell, R. W., and Eisenman, I. (2017). An Analytical Model of Iceberg Drift. *Journal of Physical Oceanography*, 47(7):1605–1616.
- Wang, S., Lim, K., Khoo, B., and Wang, M. (2007). An extended level set method for shape and topology optimization. *Journal of Computational Physics*, 221(1):395–421.
- Weertman, J. (1961). Stability of ice-age ice sheets. *Journal of Geophysical Research*, 66(11):3783–3792.
- Whittle, P. (1954). On Stationary Processes in the Plane. *Biometrika*, 41(3/4):434.